NOVA MEDICAL SCHOOL FACULDADE DE CIÊNCIAS MÉDICAS

UNIVERSIDADE NOVA DE LISBOA

HIP DEFORMITIES and FEMOROACETABULAR IMPINGEMENT

VASCO MIGUEL VOGADO TORRES MASCARENHAS

Tese para obtenção do grau de Doutor em Medicina
na Especialidade de Medicina da Imagem (Cirurgia e Morfologia Humana)
na Faculdade de Ciências Médicas | NOVA Medical School da Universidade NOVA de Lisboa

SETEMBRO, 2019

HIP DEFORMITIES and FEMOROACETABULAR IMPINGEMENT

Vasco Miguel Vogado Torres Mascarenhas

Orientador: Professor Doutor José Guimarães Consciência,
Professor Associado c/ Agregação
Faculdade de Ciências Médicas – Nova Medical School

Co-orientador – Professor Doutor Rui Mateus Marques,
Professor Associado
Faculdade de Ciências Médicas – Nova Medical School

Tese para obtenção do grau de Doutor em Medicina
na Especialidade de Medicina da Imagem (Cirurgia e Morfologia Humana)

“Twenty years from now you will be more disappointed by the things
that you didn’t do than by the ones you did do, so throw off the bowlines,
sail away from safe harbor, catch the trade winds in your sails.
Explore, Dream, Discover.”

MARK TWAIN

Aos meus pais, Artur e Maria de Jesus, por estarem sempre presentes,
pelos valores que me transmitiram, e por me terem ensinado
a acreditar que nenhum sonho é impossível.
Aos meus filhos, José Maria e Verinha, o meu maior e melhor sonho.
À minha mulher, Bárbara, por, simplesmente, tudo.

TABLE OF CONTENTS

INDEX

FIGURE INDEX

TABLE INDEX

LIST OF ABBREVIATIONS

AcCartil	Acetabular cartilage
Accov	Acetabular coverage
ACinc	Acetabular inclination
Acvers	Acetabular version
α°	Alpha angle
ASIS	Anterior superior iliac spine
AIIS	Anterior inferior iliac spine
AP	Anteroposterior
AUC	Area under the curve
AI	Artificial intelligence
CCD	Cervicodiaphyseal angle
CT	Computed tomography
CFA	Conflito femoroacetabular
CR	Conventional plain radiograph
COS	Cross-over sign
DHD	Developmental hip dysplasia
DD	Developmental hip disorders
FABER	Flexion, abduction, external rotation
FADIR	Flexion, adduction, internal rotation
FGP	Femoral growth plate
FAI	Femoroacetabular impingement
FAIS	Femoroacetabular impingement syndrome
FH	Femoral head
FHN	Femoral head-neck
Gd	Gadolinium
HA	Hip arthroscopy
HPS	Hip preserving surgery
LCEA	Lateral center-edge angle
LT	*Ligamentum teres*
MR	Magnetic resonance
MRI	Magnetic resonance imaging

MFCA	Medial femoral circumflex artery
NAHS	Non arthritic hip score
Ω°	Omega angle
OA	Osteoarthritis
PI	Pelvic incidence
PT	Pelvic tilt
PSIS	Posterior superior iliac spine
PWS	Posterior wall sign
PD	Proton density
ROM	Range of motion
ROC	Receiver operating characteristic
RefInt	Reference intervals
ROI	Region of interest
TR	Repetition time
RM	Ressonância magnética
SS	Sacral slope
SI	Signal intensity
SNR	Signal to noise ratio
SCFE	Slipped *capitis femoris* epiphysis
SE	Spin echo
SP	Spinopelvic
SPP	Spinopelvic parameters
SD	Standard deviation
SHD	Surgical hip dislocation
TE	Time of echo
TC	Tomografia computorizada
THA	Total hip arthroplasty
3D	Three-dimensional or tridimensional
TRC	Triradiate cartilage
TSE	Turbo spin echo
US	United States
Y.O.	Years of age
ZO	*Zona orbicularis*

ACKNOWLEDGEMENTS

I would like to express my gratitude to those who have contributed to the accomplishment of this work and have encouraged me throughout this journey.

To Professor José Guimarães Consciência, I am truly thankful for accepting to be my Tutor in a Thesis in the field of Medical Imaging. I am also extremely grateful for his important role mentoring this project and for integrating me into the field of research. Moreover, I express my immense gratitude for sharing all his knowledge on these subjects. I do not have enough words to thank him for his admirable generosity and for all that he has taught me over these years.

To Professor Rui Mateus Marques for having encouraged me throughout the Doctoral Thesis. I express my gratitude for having trusted me.

To Professor Paulo Rego for believing in me, sharing generously his knowledge and projects. I am extremely grateful for his patience with my concerns, for welcoming my urgent ideas and requests, despite his numerous tasks and responsibilities, for guiding me through the knowledge of hip preserving sciences. Furthermore, I thank him for the friendship which grew along this journey.

To Pedro Patricio, as General Imaging manager at Luz-Saúde, and Dr. Augusto Gaspar, as Director of the Imaging Department of the Hospital da Luz Lisboa, for always believing in me and (really) giving me the opportunity to grow professionally. Without that support nothing would have been possible!

To the Supervisor Radiographer of the Imaging Department, Ruben Teixeira, for all the support to my research project, since the beginning of my Thesis. And to the Radiographers of the Imaging Department of the Hospital da Luz: João Novo, Rogério Lopes, Sara Gonçalves, Ana Graça, Angela Valério, Tiago Castela. I do not have enough words to thank them for all the support and for being always available to perform the examinations to the recruited patients, at any time of the day (and also at night!). You are the best team of Radiographers I could have worked with and you know that I will always be grateful for your effort and dedication.

Again, I would like to thank Professor Paulo Rego and also to Dr. Pedro Dantas and Dr. Olufemi Ayeni for their kindness and commitment in answering all my doubts regarding hip preserving surgery.

To Dr. Reto Sutter and Professor Lennart Jans for their collaboration and the precious help they gave me by critically reviewing all papers.

To my colleagues from Hospital da Luz, either from Radiology or other Departments, whose list of names would not fit this page, with whom it is a pleasure to collaborate. Work with you made me a better radiologist and a better researcher. I really appreciate all the words of encouragement during the past few years.

To the Administration Board of Luz-Saúde, to its President Engª Isabel Vaz, and to the Clinical Director, Professor José Roquette, I am grateful for your outstanding support which was fundamental for my Thesis.

To my brothers, to my family and friends, for being always present, for celebrating with me the happiest moments and each victory and for encouraging me in all the difficult moments.

To my father, my dearest friend and teacher, for having taught me the beauty of science and knowledge, and for being always so demanding with myself. He also influenced me to be a perfectionist (for better or worst!), taught me to always work hard and never ever be satisfied with a "no". I can imagine him, from where he is now, with a proud smile while watching over me.

Also, to both my parents, to whom I owe everything. I cannot express all my gratitude for your unconditional love, for always being there for me. For encouraging me to give always my best in everything, without losing focus on what is really important, for supporting me when I fall and for giving me confidence to get up and move on. And, of course, for teaching me that being honourable is invaluable.

Finally, to my children for enriching my life with love and for making me feel always the best Father, even at times when I was overloaded with work.
And to my wife Bárbara for all her love and friendship. Over the past 20 years we have grown together, we got married, raised a beautiful family, and we were able to accomplish so many things together.

DISCLAIMER

1) This thesis was performed in accordance with the applicable legal decrees published in "*Diário da República,* 2ª série – Nº 153 – 7 de Agosto de 2015", namely "Regulamento nº 519/2015" and "Capítulo V Artigo 26º (Regime transitório)";

2) The research hereby presented has obtained approvals from the "Comissão Nacional de Proteção de Dados" (nº 7301/2016), "Comissão de Ética da NOVA Medical School – CEFCM" (nº61/2014/CEFCM), the "Conselho Científico da NOVA Medical School" (nº000869/2015), the "Comissão de Ética do Hospital da Luz" and the "Conselho Científico do Hospital da Luz";

3) This work was performed in the Imaging Centre of Hospital da Luz, Lisboa, with the co-operation of several other departments within the same institution;

4) Financing for the prosecution of all the research work including software analysis, graphic design and statistical analysis are the author's sole responsibility;

5) This thesis has been written in English and reviewed according to the United Kingdom Oxford dictionary;

6) Photographs and manual illustrations presented in this thesis are either from the author's personal database, from Prof. Dr. Paulo Rego's database (with permission) or from other authors (with permission);

7) References, images and tables are numbered in order of appearance throughout the thesis, excluding published papers, according to the format of the "American Medical Association". Published papers are embedded in the thesis, although retaining their original referencing style and numbering (in accordance to the guidelines of the corresponding journal).

PUBLICATIONS

In accordance with "Regulamento nº 519/2015, Capítulo V Artigo 26º (Regime transitório) e Capítulo III, Artigos 18º a 21º, publicado em *Diário da República*, 2ª série – Nº 153 – 7 de Agosto de 2015", this thesis contains materials and results from the following papers, which were all published. The author of this dissertation has contributed actively in the conceptualization, execution, interpretation and writing of these works (in order of appearance throughout the thesis).

I. Mascarenhas VV, Caetano A. **Imaging the Young Adult Hip in the Future**. Ann Joint 2018; 3:47. doi: 10.21037/aoj.2018.04.10.

II. Mascarenhas VV, Rego P, Dantas P, Morais F, McWilliams J, Collado D, Marques H, Gaspar A, Soldado F, Consciência JG. **Imaging prevalence of femoroacetabular impingement in symptomatic patients, athletes, and asymptomatic individuals: A systematic review.** Eur J Radiol. 2016 Jan;85(1):73-95. doi: 10.1016/j.ejrad.2015.10.016. Epub 2015 Nov 2. Review. PubMed PMID: 26724652.

III. Mascarenhas VV, Rego P, Dantas P, Castro M, Jans L, Marques RM, Gouveia N, Soldado F, Ayeni OR, Consciência JG. **Hip shape is symmetric, non-dependent on limb dominance and gender-specific: implications for femoroacetabular impingement. A 3D CT analysis in asymptomatic subjects.** Eur Radiol. 2018 Apr;28(4):1609-1624. doi: 10.1007/s00330-017-5072-9. Epub 2017 Nov 6. PubMed PMID: 29110047.

IV. Mascarenhas VV, Rego P, Dantas P, Gaspar A, Soldado F, Consciência JG. **Cam deformity and the omega angle, a novel quantitative measurement of femoral head-neck morphology: a 3D CT gender analysis in asymptomatic subjects.** Eur Radiol. 2017 May;27(5):2011-2023. doi: 10.1007/s00330-016-4530-0. Epub 2016 Aug 30. PubMed PMID: 27578045.

v. Rego PR, Mascarenhas V, Oliveira FS, Pinto PC, Gaspar A, Ovídio J, Collado DG. **Morphologic and angular planning for Cam resection in femoroacetabular impingement: value of the omega angle.** Int Orthop. 2016 Oct;40(10):2011-2017. Epub 2015 Nov 18. PubMed PMID: 26578079.

vi. Rego P, Mascarenhas VV, Collado D, Coelho A, Barbosa L, Ganz R. **Arterial topographic anatomy near the femoral head-neck perforation with surgical relevance.** J Bone Joint Surg Am. 2017 Jul 19;99(14):1213-1221. doi:10.2106/JBJS.16.01386. PubMed PMID: 28719561.

vii. Lopes DS, Pires S, Mascarenhas VV, Silva T, Jorge JA. **On a "Columbus' Egg" for the shape of asymptomatic, dysplastic and impinged hip joints**, Medical Engineering and Physics 2018, https://doi.org/10.1016/j.medengphy.2018.07.001.

viii. Mascarenhas VV, Rego P, Dantas P, Caetano A, Jans L, Marques RM, Ayeni OR, Consciência JG. **Can we discriminate symptomatic hip patients from asymptomatic volunteers based on anatomical predictors? A 3D MRI study on Cam, pincer and spinopelvic parameters.** Am J Sports Med. 2018 Nov;46(13):3097-3110. doi: 10.1177/0363546518800825.

ix. Marin-Peña O, Lund B, Ayeni OR, Dantas P, Griffin D, Khanduja V, Said HG, Tey M, Dickenson E, Kay J, Mascarenhas VV, Sadakah GG, Sunil Kumar KH, and Tahoun M. **Basic Concepts in Hip Arthroscopy.** ESSKA 2018 45 G.M.M.J. Kerkhoffs et al. (eds.), ESSKA Instructional Course Lecture Book, https://doi.org/10.1007/978-3-662-56127-0_4.

x. Rego PA, Mascarenhas VV, Oliveira FS, Pinto PC, Sampaio E, Monteiro J. **Arthroscopic versus open treatment of Cam-type femoroacetabular impingement: retrospective cohort clinical study.** Int Orthop. 2018 Apr;42(4):791-797. doi:10.1007/s00264-017-3735-4. Epub 2018 Jan 3. PubMed PMID: 29299653.

This thesis only includes published results.

ABSTRACT

Conceptually, the preservation of a human anatomical structure makes more sense than its replacement. This concept is even more striking in the case of human joints due to the multitude of unsolved problems related to implants used in orthopaedic surgery. With respect to the hip, joint preservation assumes an increased technical complexity when compared to other joints; this is due to two main reasons: the intra-articular epiphyseal circulation of the femur and the proximity of large neurovascular structures.

Femoroacetabular impingement (FAI) and acetabular dysplasia (DHD) in young adults are two common but poorly characterised pathological entities. If undiagnosed and untreated, dysplasia in childhood may lead to residual DHD in young adults, as diagnosed on radiographs, and may also give rise to symptoms such as hip pain and restricted range of motion. The diagnosis of FAI in adults is based on clinical and imaging criteria. The most frequently noticed symptoms of FAI include hip pain and restricted function. Radiologically, two main subtypes of FAI are recognised: The Cam-type, with the pathoanatomical mechanism located on the femoral side, and the Pincer-type on the acetabular side. Although with different pathological patterns, both types cause pain and articular damage of the labrum and cartilage. While Cam-type FAI is believed to be a major contributing factor to the early onset of hip osteoarthritis (OA), which eventually requires a total hip replacement, the relationship of other shapes and morphologies with OA are still under debate.

Despite the initial promising reports on outcomes following surgical management of these conditions, the best approach to diagnose and manage them still remains controversial. Although for some patients there are unambiguous clinical and imaging findings of FAI, for a substantial number of patients there are minimal or intermediate findings. Moreover, several studies have reported a high prevalence of FAI morphology among the "normal" population and in asymptomatic healthy individuals. At present, there is no adequate imaging tool to facilitate the reliable allocation of all patients into the correct diagnostic group or to confidently rule out diagnosis. However, imaging parameters can be used to describe different hip morphological characteristics and additionally confirm or preclude the diagnosis of FAI.

This thesis focuses on assessing hip morphology in different populations by investigating which specific joints are more prone to developing symptoms and by evaluating treatment outcomes of a FAI cohort. Specifically, this research concentrates on the following: 1) examining population-specific (symptomatic and non-symptomatic) characteristics of hip morphology; 2) developing an anatomic-based model to establish "at-risk" hip joints, incorporating subject-specific hip geometries and spinopelvic parameters and 3) investigating treatment outcomes in a Cam-type FAI cohort.

In our clinical progression in imaging and in this particular area of pathology, we became aware of the existence of several gaps that we sought to fill with the now published research hereby described. The systematisation by chapters precisely reflects the need to address the issue in simultaneously distinct and complementary areas of knowledge.

This thesis consists of six chapters, which cover the entire spectrum from the diagnosis to treatment of the young hip. To present the aims of this thesis in a sequential manner from general morphology to more specific FAI-related topics, the analysis of the asymptomatic hip will be presented first, followed by how joint morphology is associated with symptoms and, finally, will conclude with treatment.

In **PART I**, we introduce the topics that are relevant to understand the full scope of our thesis; we aim to accomplish this by addressing the relevance and contemporariness of the "FAI" theme and by describing the general and vascular anatomy of the hip. **Chapter 1** is devoted to hip development and morphogenesis. In **Chapter 2**, we address the importance of imaging by conducting a thorough review of current and future perspectives on this topic (Paper I). In **Chapter 3**, we perform a systematic review of the literature to write a state-of-the-art overview, focussing on asymptomatic and symptomatic FAI morphology prevalence and highlighting the multiple gaps in knowledge regarding the role of hip morphology in the pathogenesis of FAI (Paper II).

Building on the first part, we address the rationale and aims of this thesis in **PART II**.

In **PART III**, we describe the original research that was performed and published. **Chapter 4** focusses on the detailed characterisation of hip morphology, both osseous and vascular. Bony hip morphology was quantified using a semi-automated software, which allows to robustly study in detail shape variants in an asymptomatic population and their relationship with sex, side and limb dominance (Paper III). Cam morphology was further defined by developing a novel quantitative parameter, with diagnostic and treatment planning capabilities using a cohort of both asymptomatic individuals (Paper IV) and patients undergoing surgery (Paper V). Moreover, we felt the need to better characterise the topography of the deformity and its relationship with the nourishing arteries of the femoral head, as Cam morphology frequently has a posterior extension that overlaps the retinacular vascular structures. However, its arterial origin has never been described or confirmed in the literature. For this reason, the importance of the aforementioned parameter has been outlined by the cadaveric arterial topographic study of the proximal femur (Paper VI). In **Chapter 5**, we test multiple parameters and their associated shape variants to detect which ones allow identifying a risk-increased joint in various populations. To this end, we use both advanced computing for shape modelling (Paper VII) and three dimensional (3D) magnetic resonance imaging (MRI) (Paper VIII). **Chapter 6** describes the various treatment options (Paper IX) and outcomes in a cohort clinical study, comparing open surgery with arthroscopic surgery in terms of treating Cam deformities (Paper X).

The results of the aforementioned chapters are summarised in **PART IV**, presenting the general synthesis, discussing the results in the light of current literature and detailing the conclusions of this thesis. The scope of potential future research within this field is also presented in this chapter.

In brief, this thesis suggests the following:

First, detailed imaging assessment of hip morphology is paramount to better understanding both the hip joint and pelvic morphology (Paper I).

Second, the case definitions of different morphologies and clinical entities are missing as far as FAI and related disorders are concerned. Qualitative and quantitative radiographic findings thought to be associated with Cam- and Pincer-type FAI, as well as the coexistence between them, are quite common among different populations (Paper II).

Third, in adult asymptomatic populations, sex-specific reference intervals for hip measurements for DHD and FAI morphology are wider than currently accepted values (Paper III). Moreover, femoral morphology with distinct Cam magnitudes and epicentres is also sex-specific, with higher mean alpha angle ($\alpha°$) and omega angle ($\Omega°$) values seen in males (Paper IV).

Forth, Cam deformity frequently overlaps with the retinacular vascular structures seen in an MRI; this finding has practical surgical relevance. Additionally, the radial extension of the Cam deformity ($\Omega°$) is more significantly associated with the patients' symptoms prior to surgery than the $\alpha°$ (paper V). The origin of the vascular structures seen in the retinacular fold is unequivocally arterial in nature, and these structures have a more anterior distribution than classically assumed (Paper VI).

Fifth, ovoid geometries are more representative of both articular surfaces of the hip joint as well as of Cam, Pincer and mixed impinged hips when compared to spherical or ellipsoidal shapes (Paper VII). Individuals with larger Cam deformities, decreased acetabular coverage and increased pelvic anteflexion are more likely to experience hip symptoms (Paper VIII). This provides clinicians with indications of how the pathology exacerbates, allowing them to perform the correct clinical assessments and proceed with the correct form of care. From a patient's perspective, an early and accurate diagnosis could prevent cartilage degradation and progression to OA.

Sixth, similar outcomes and significant functional improvement are observed when comparing open and arthroscopic surgery in the treatment of Cam deformities (follow-up time of two years). It should be noted that the female gender was associated with poor hip function in the preoperative evaluation (papers IX and X).

Looking ahead, imaging and hip preserving surgery (HPS) will evolve hand-in-hand in the face of new and greater challenges. The increasing number of analytic parameters describing hip joint pathomorphologies as well as new sophisticated 3D imaging-analysis together with emerging artificial intelligence-based technologies have transported us beyond simple classification systems. Moreover, more reliable diagnostic and treatment guidelines that go beyond differentiation into pure FAI and dysplasia are paramount. The largely unknown natural course of both hips with symptomatic FAI and asymptomatic individuals continues to present research opportunities as far as diagnosis, treatment and prognosis are concerned.

Keywords: hip, femoroacetabular impingement, imaging, hip dysplasia, Cam, computed tomography, magnetic resonance, surface fitting, alpha angle, omega angle, prevalence, anatomy, spinopelvic, reference value, normal value.

RESUMO

Conceptualmente, a conservação de uma estrutura anatómica é mais benéfica do que a sua substituição. No caso das articulações humanas, este conceito é particularmente importante face aos múltiplos problemas, ainda não resolvidos, relacionados com próteses e materiais usados na cirurgia ortopédica. Na articulação coxofemoral, o conceito de preservação, melhorando os parâmetros biomecânicos, assume uma complexidade técnica acrescida maioritariamente pelo facto de a circulação epifisária do fémur ser intra-articular e dada a proximidade de importantes estruturas neurovasculares.

O conflito femoroacetabular (CFA) e a displasia acetabular no adulto jovem, são duas entidades patológicas comuns embora com múltiplas áreas ainda por investigar. A displasia infantil, não diagnosticada e não tratada, pode originar displasia acetabular residual na idade adulta e consequente sintomatologia e limitação funcional. O diagnóstico de CFA no adulto é baseado em critérios clínicos e radiográficos. Clinicamente apresenta-se igualmente com dor e limitação funcional. Radiologicamente, dois subtipos de CFA são habitualmente reconhecidos, o tipo Cam (mecanismo patológico decorrente de asfericidade femoral) e o tipo Pincer (por hipercobertura acetabular). Embora com padrões diferentes de envolvimento articular, os dois mecanismos de conflito condicionam dor, lesão estrutural do labrum e condropatia.

Atualmente, a morfologia Cam é considerada como um dos principais fatores de risco morfológico que contribuem para o desenvolvimento de osteoartrose precoce da coxofemoral, eventualmente com necessidade de recurso a prótese total da anca.

Apesar de a investigação inicial na área da cirurgia conservadora da anca ter documentado bons resultados cirúrgicos, atualmente a controvérsia é francamente superior ao consenso relativamente à melhor abordagem diagnóstica e terapêutica.

Caracteristicamente, apesar de em muitos casos os achados clínicos e radiológicos serem inequívocos para o diagnóstico de CFA, um número substancial de doentes apresenta achados frustes ou equívocos. Por outro lado, múltiplos estudos descreveram uma alta prevalência de morfologia compatível com CFA na população adulta e em indivíduos saudáveis assintomáticos. Atualmente, não existe uma ferramenta de imagem ideal que facilite a alocação fidedigna de todos os doentes

a um grupo patológico específico ou, por outro lado, exclua com confiança o diagnóstico de conflito. No entanto, os parâmetros de imagem podem ser utilizados para analisar e descrever as diferentes características morfológicas da anca e adicionalmente confirmar o diagnóstico de CFA. Esta tese enfoca, por um lado, a avaliação da morfologia coxofemoral em diferentes populações, investigando quais articulações estão mais predispostas ao desenvolvimento de sintomas e, por outro, os resultados do tratamento cirúrgico de uma coorte com o diagnóstico de CFA tipo Cam. Especificamente, a investigação efetuada: 1) examinou características morfológicas específicas da coxofemoral em diferentes populações (sintomáticas ou não sintomáticas); 2) desenhou um modelo estatístico baseado em preditores anatómicos no sentido de estabelecer as articulações em risco de desenvolvimento sintomático, incorporando geometrias articulares específicas e parâmetros espinhopélvicos; e 3) analisou os resultados de terapêutica cirúrgica numa coorte de doentes com o diagnóstico CFA tipo Cam.

Durante a progressão clínica na área da imagiologia e nesta área patológica em particular, apercebemo-nos da existência de múltiplas lacunas de conhecimento que procurámos colmatar com a investigação agora publicada e descrita nesta tese. A sistematização por capítulos reflete precisamente a necessidade de abordar a questão em áreas de conhecimento, simultaneamente distintas e complementares.

Os seis capítulos desta tese abrangem o espectro clínico desde o diagnóstico até ao tratamento da anca jovem. De modo a apresentar os objetivos desta tese numa sequência lógica, desde a anatomia geral até à morfologia e tratamento específicos do CFA, a análise da anca assintomática será descrita em primeiro lugar seguida pela análise da relação anatomoclínica entre morfologia articular e sintomas. Por último será abordada a terapêutica do doente sintomático.

Na **PARTE I**, apresentamos os tópicos essenciais para compreender a abrangência do espectro da presente tese, designadamente a relevância e a contemporaneidade do tema "CFA" e adicionalmente o enquadramento anatómico, morfológico e vascular desta articulação. O **Capítulo 1** é dedicado ao desenvolvimento e morfogénese da anca. No **Capítulo 2**, sublinhamos a importância e o papel da imagem através de uma revisão enfocada nas perspetivas atuais e futuras sobre este tópico (Artigo I). No **Capítulo 3**, realizamos uma revisão sistemática da literatura no sentido de descrever o estado da arte com foco na prevalência da morfologia de CFA em populações assintomáticas e sintomáticas. Este capítulo destaca as múltiplas lacunas de conhecimento relativas ao papel da morfologia da articulação coxofemoral na patogénese do CFA (Artigo II).

Com base nesta parte introdutória, abordamos seguidamente os objetivos da presente tese, gerais e específicos, na **PARTE II**.

Na **PARTE III**, descrevemos o corpo da investigação clínica original efetuada. O **Capítulo 4** é dedicado à caracterização detalhada da morfologia da anca, designadamente óssea e vascular. A morfologia coxofemoral foi quantificada utilizando *software* com capacidade de semi-automatização analítica, permitindo estudar a prevalência e relação entre as diferentes morfologias articulares e o género, dominância e simetria articular (Artigo III). A morfologia Cam foi ainda alvo de caracterização mais aprofundada, através do desenvolvimento de um novo parâmetro quantitativo com potencialidade diagnóstica e de planeamento cirúrgico/ /prognóstico, primariamente testado numa coorte assintomática (Artigo IV) e seguidamente também em doentes com indicação cirúrgica (Artigo V).
Na nossa atividade clínica diária apreciámos a necessidade urgente de melhor caracterizar a topografia da deformidade Cam e a respetiva relação com as artérias nutritivas da epífise femoral. A impressão clínica referida sugeria que a morfologia Cam frequentemente se estendia posteriormente ao quadrante póstero-superior, intersectando a região retinacular vascular. No entanto, por imagem a natureza arterial destas estruturas nunca havia sido confirmada. Por esta razão, a importância do parâmetro mencionado foi sublinhada e comprovada no estudo cadavérico com avaliação topográfica vascular do fémur proximal (Artigo VI).
No **Capítulo 5** testámos múltiplos parâmetros imagiológicos e respetivas variações/relações com diferentes morfologias coxofemorais, no sentido de identificar as articulações com risco clínico aumentado de desenvolvimento sintomático. Para este fim efetuámos estudos baseados em computação avançada com modelação estatística (Artigo VII) e também em ressonância magnética (RM) tridimensional (Artigo VIII).
O **Capítulo 6** descreve as opções de tratamento (Artigo IX) e os resultados clínicos num estudo clínico de uma coorte com *follow-up* mínimo de 2 anos, comparando a abordagem cirúrgica aberta e artroscópica (Artigo X).

Os resultados dos diferentes capítulos estão sumarizados na **PARTE IV**, onde apresentamos a síntese geral, a discussão crítica dos resultados obtidos à luz da literatura atual e finalmente as conclusões relevantes. As oportunidades futuras de investigação são igualmente abordadas neste capítulo.

Em resumo o trabalho constante da presente tese sugere:

> **Primeiro**, que a avaliação imagiológica detalhada da morfologia coxofemoral é essencial no sentido de compreender aprofundadamente não só a própria articulação como também a morfologia pélvica (Artigo I).
>
> **Segundo**, paradoxalmente, a definição clínica de um caso patológico e das diferentes entidades relacionadas, é ainda inexistente. Os parâmetros quantitativos e qualitativos que comummente estão associados com CFA tipo Pincer e Cam são francamente frequentes em diferentes populações (sintomáticas e assintomáticas) (Artigo II).

Terceiro, em populações assintomáticas adultas, os intervalos de referência específicos para os parâmetros quantitativos associados a morfologia de CFA e displasia são mais latos e com limites superiores mais elevados do que os atualmente utilizados na prática clínica (Artigo III). A morfologia femoral bem como os epicentros/magnitudes das deformidades Cam são específicos de género, observando-se maiores valores de ângulo alfa e ómega em indivíduos do sexo masculino (Artigo IV).

Quarto, é frequente a interseção entre a extensão póstero-superior da deformidade Cam e a convergência epifisária das estruturas vasculares retinaculares observadas em RM, aspetos que se revestem de primordial importância no planeamento cirúrgico. Adicionalmente a extensão radial da deformidade Cam (ângulo ómega) está significativamente mais relacionada com a sintomatologia clínica pré-cirúrgica do que o parâmetro mais comummente utilizado na prática clínica (ângulo alfa) (Artigo V). A origem das estruturas vasculares observadas por RM na prega retinacular é inequivocamente arterial, sendo que abrange uma extensão mais anterior do que classicamente assumido (Artigo VI).

Quinto, as geometrias ovalares (em detrimento das morfologias esféricas e elipsoides) são melhor representativas de ambas as superfícies articulares da coxofemoral, designadamente do fémur e acetábulo, bem como das ancas sintomáticas que clinicamente exibem sinais de CFA (Pincer, Cam e misto) (Artigo VII). Indivíduos com maiores deformidades Cam, aspetos de hipocobertura acetabular e acentuação da anteflexão pélvica apresentam uma maior probabilidade de desenvolverem sintomas articulares (Artigo VIII). Esta observação é crítica, dado que fornece, na prática clínica, informação essencial acerca da potencial predisposição para fenómenos de exacerbação sintomática futura, permitindo desta forma instituição de medidas terapêuticas/preventivas adequadas. Na perspetiva do doente, um diagnóstico precoce e preciso, pode conceptualmente prevenir, numa primeira fase, alterações condropáticas articulares e, numa segunda instância, progressão para artrose estabelecida.

Sexto, documentamos resultados clínicos e funcionais significativamente favoráveis quando comparamos a abordagem artroscópica e aberta no tratamento cirúrgico da deformidade Cam, sendo de observar que o género feminino está associado a menor *score* funcional na avaliação pré-operatória (Artigos IX e X).

Futuramente, a imagiologia e a cirurgia conservadora da anca irão desenvolver-se conjuntamente e em paralelo com novos e maiores desafios. A descrição de novos parâmetros analíticos para avaliação da patoanatomia coxofemoral, associada à inovação tecnológica crescente e à implementação da inteligência artificial, impõem uma evolução clínica oposta à assunção de classificações patológicas demasiadamente simplistas. Nesse sentido a existência de *guidelines* de

diagnóstico e terapêutica mais efetivas e baseadas na evidência, que nos levem além da pura diferenciação entre CFA e displasia, são urgentes. A história natural das deformidades Cam e Pincer, sintomáticas ou assintomáticas, é ainda grandemente desconhecida, assumindo-se como uma área determinante de investigação no que concerne ao diagnóstico, terapêutica e prognóstico.

Palavras-Chave: coxofemoral; conflito femoroacetabular; imagem; displasia; Cam; tomografia computorizada; ressonância magnética; *surface fitting*; ângulo alfa; ângulo ómega; prevalência; anatomia; espinho-pélvico; valores de referência; valores normais.

part 1

INTRO-DUCTION

Part of **Chapter 2** is based on the following publication:
"Imaging the Young Adult Hip in the Future"
Ann Joint 2018; doi: 10.21037/aoj.2018.04.10

Part of **Chapter 3** is based on the following publication:
"Imaging prevalence of femoroacetabular impingement in symptomatic patients, athletes, and asymptomatic individuals: A systematic review."
European Journal of Radiology 2016 Jan;85(1):73-95

chapter 1

HIP ONTOGENESIS AND MORPHOGENESIS

1.1 HIP DEVELOPMENT AND ONTOGENESIS

1.1.1 The Hip Joint

The skeleton provides protection, maintains body shape, and enables movement. The movement of body parts is possible due to the coupling of bones in joints and the bony anatomy of each joint adapting to its specific function[1]. The human hip joint, for example, can be simplified as a weight bearing ball (femoral head) and socket (acetabulum) joint[1], but it functions as part of a complex anatomic unit that consists of the femur, the pelvis and the lumbosacral spine. However, it should be noted that this unit greatly varies among different species of animals[1].

The articular surfaces of the femoral head (FH) and the acetabulum are covered by a layer of shock-absorbing hyaline cartilage, which enables them to move smoothly. However, the FH and acetabulum have intrinsic shortcomings that lead to some instability; hence, they are additionally supported by soft tissue structures[1-3]. The relatively shallow acetabulum is surrounded by a ring of fibrocartilage (labrum) that deepens the acetabulum. Moreover, it has been found that the labrum increases the acetabular contact surface area from 28.8 cm^2 to 36.8 cm^2, thereby extending acetabular coverage[2,4]. The stability of the hip is further enhanced by a capsule, which consists of multiple ligaments that run from the pelvis to the femoral neck. Within this capsule, the synovial membrane produces a fluid that lubricates the cartilage, thereby virtually eliminating friction during movement of the hip[4].

1.1.2 Aspects of Evolution (Phylogeny)

1.1.2.1 From developing bone to locomotion

A combination of fossil anatomy and genetic information from modern species has improved our understanding of bone evolution[3]. Mineralised tissues (bone) were a major breakthrough in evolution. Calcium carbonate, the common constituent of rock, started being used as reinforcement in organisms approximately half a billion years ago[1,3]. Since then, fossils have been used to study the calcified remains of life's evolution. However, it was genetic studies that revolutionised our understanding of the early stages of evolution of these tissues[5]. For example, a related family of genes, which likely arose from a common ancestor, produces the mineralised tissues for teeth (enamel, dentine) and skeletons (bone extra-cellular matrix)[6] (Figure 1).

Bone is specific to vertebrates; it originated as a result of mineralisation around the basal membrane of the throat or skin, resulting in tooth-like structures and protective shields in animals with a soft cartilage-like endoskeleton[1].

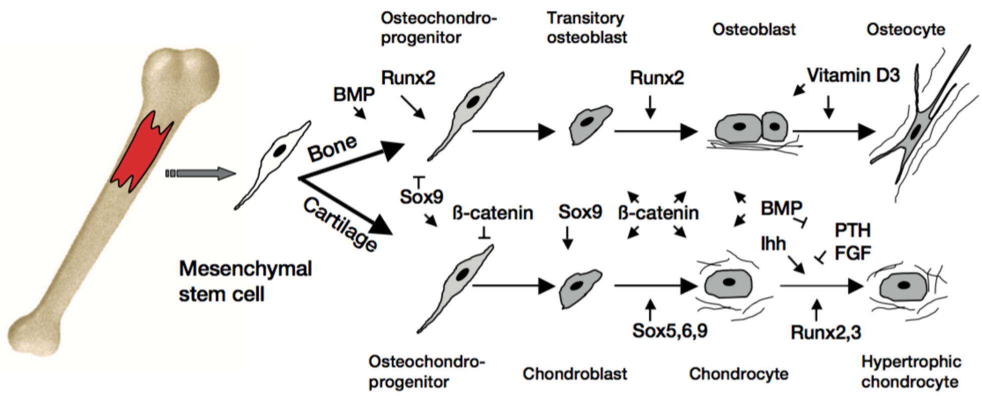

FIGURE 1 – Major gene networks thought to govern skeletal evolution. The arrows indicate positive interactions while the horizontal lines indicate negative interactions. The scheme depicts signalling pathways as they are currently understood, but most of the processes are under intensive investigation. Information has been collected from multiple sources cited throughout the text (reprinted with permission from Wagner et al., *Acta Orthopaedica* 2011; 82 (4): 393–398).

The existence of an endo- and exoskeleton imparts major differences to function. Although the exoskeleton quickens the speed of evolution of animal life, it also imposes limitations, which are mostly associated with limited body size, lack of surface sensory organs and locomotion constraints; therefore, the next major change to the endoskeleton during the process of evolution proved to be a major adaptive advantage[7]. These changes encouraged the development of a strong muscular system and added further adaptive values to animal life, such as greater overall mobility and the appearance of a regenerative and environment-sensitive dermis[7]. Moving from aquatic to terrestrial environments, further developments improved locomotion.

1.1.2.2 From initial locomotion to bipedestrial gait

The development of terrestrial life forms hinged on the evolution from paired fins to limbs that could eventually bear weight. Molecular genetic studies now show that the fin can transform to a limb through subtle changes in a relatively small number of genetic switches[3].
With evolution, amphibians started walking with a sprawling gait, with the limbs still perpendicular to the long axis of the body (similar to the paired fins in fish). As much heavier loads can be carried by vertical limbs than those that are horizontal (Figure 2), the emergence of vertical positioning and rounding of the hip joint increased stride length, increased loading of the limbs and decoupled walking from breathing. These developments, in turn, increased stamina, as running no longer counteracted breathing[2,7].

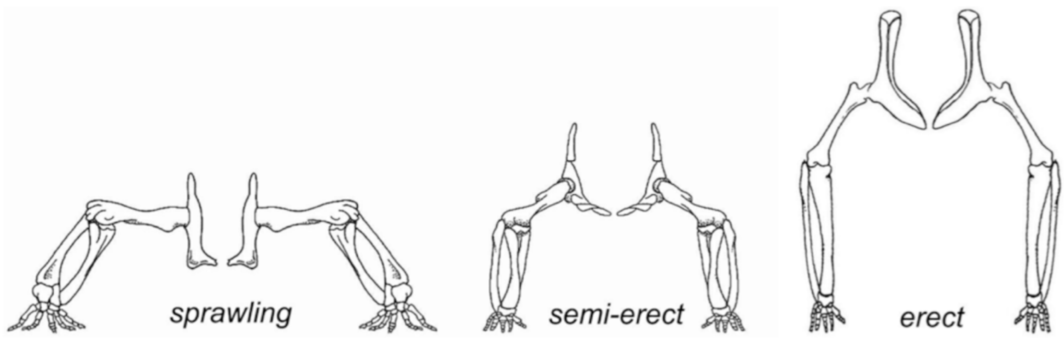

FIGURE 2 – Posture types: sprawling (e.g., reptiles), semi-erect and erect (e.g., cursorial mammals). Adapted from Hogervorst et al.[2,7] (reprinted with permission. McCarthy JC et al. *Hip Joint Restoration*. Springer; 2016).

1.1.2.3 Evolution of the mammal and human hip

The most striking feature of the first three million years of human evolution (i.e., from about 7–6 to about 3.5 million years ago) is the compacting of the pelvis. More importantly, the ilium became much shorter, and the sacrum enlarged in all dimensions[1,7-9] (Table 1). This development made the female pelvis the only bone frame capable of conveying information about the two most peculiar traits of human evolution – bipedestrial gait and encephalisation (development of a disproportionately enlarged brain) – as the female pelvis exhibits both the adaptations that developed to facilitate permanent bipedestrial gait and, at the same time, accommodate the birth of a large-brained baby[1].

SPECIES	*Chimpanzee*	*Ardipithecus ramidus*	*Australopithecus afarensis*	*Australopithecus africanus*	*Homo erectus*	*Homo sapiens*
Age	5 million years ago to present	4.4 million years ago	3.2 million years ago	2.7 million years ago	1.5 million years ago	Current date
Pelvis AP View					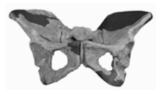	
Pelvis Axial view			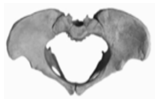		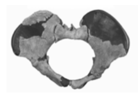	

TABLE 1 – Photographs showing the evolution of the shape and orientation of the female pelvis (from chimpanzee to man). Note that the birth canal first widens transversely, but from *Au. Afarensis* to *H. sapiens*, only AP deepening occurs (adapted from Hogervorst et al.[2,7] with permission).

The first trait of evolution that was found in hominids (early human ancestors) was the ability to walk upright; it was later that they developed a large brain. Furthermore, hominids developed an exclusive bipedal gait within 2–3 million years of evolution.

Extensive osseous adaptations of the lumbar spine, pelvis, hip and femur characterise the emergence of the human bipedal gait with its "double extension" of the lumbar spine and hip[2,3,9]. The now "compacted" pelvis and extension of the hip joint along with the elongation of the femur effectively increased leg length (improving energy efficiency) and influenced concavity at the femoral head-neck (FHN) junction and femoral neck anteversion[1,8].

The changes in the proximal femur reflect the increased bipedism (Figures 3 and 4). The human hip has a thicker femoral neck (decreased FHN ratio) and reduced concavity compared to the non-human apes. Furthermore, while variability can be observed in the proximal femoral morphology of humans, the same is not observed in non-human apes. This difference can be explained through evolution. Proximal femoral concavity was more important for the non-human apes, such as for climbing, than for modern humans because the latter experiences high loading of the hip due to activities such as running[10,11].

FIGURE 3 – Superior view of a gorilla femur (A), chimpanzee femur (C), modern human femur with *coxa recta* (B) and modern human femur with *coxa rotunda* (D) (adapted from Hogervorst et al.[7,12] with permission).

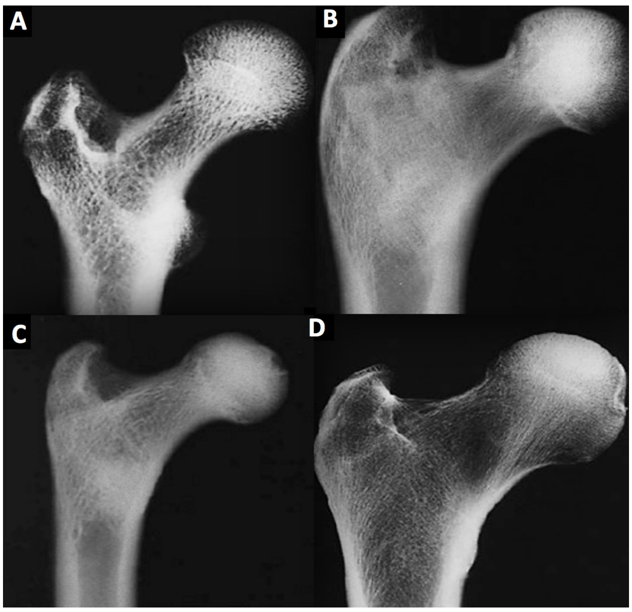

FIGURE 4 – Radiographs of hominid hips with head-neck ratios (largest head diameter divided by smallest neck width). The human hip has the thickest neck and decreasing offset. Note the thicker cortical bone in the superior femoral neck of the apes (A) orangutan (B) gorilla (C) chimpanzee (D) *homo sapiens*. The AP view is not to scale. Information has been collected from multiple sources cited throughout the text (adapted from Hogervorst et al.[7,12] with permission).

Mammals exhibit a large variation in hip morphology. However, conceptually, only two types of hips (based on differences in the proximal concavity of the femur) can describe the majority of femurs[6,12]. C*oxa recta* and *coxa rotunda* relate to the ossification pattern of the proximal femur and are typical to locomotor categories[12-14] (Table 2). It has been hypothesised that when hominids evolved into bipedal runners, their FH morphology began to evolve from a *coxa rotunda* to a less spherical *coxa recta*[1,10]. The morphology of the FH is probably functionally related to locomotion and habitat. Furthermore, it should be noted that both genetics and biomechanics (loading history) play a role in the development of the hip morphotype (ontogeny)[3,6] although, currently, this variability has no proper explanation (yet it is important, as certain morphotypes are associated with osteoarthritis (OA))[10,15].

	SHAPE	POSITION	OSSIFICATION	EXAMPLES
COXA RECTA	✓ non-spherical head and/or a straight section on the superior FH/FHN	✓ head is positioned eccentrically on a short femoral neck and is shifted antero-inferiorly.	✓ evolves from a single secondary osseous epiphysis (coalesced)	Most mammals
COXA ROTUNDA	✓ round femoral head (spherical)	✓ the femoral neck is relatively long and narrow	✓ FH and the greater trochanter emerge from two separate secondary ossification centres	Few mammals (orangutans, chimpanzees and gorillas)

TABLE 2 – Summarising differences between *coxa recta* and *coxa rotunda* with respective shape, position and ossification. Information has been collected from multiple sources cited throughout the text.

1.2 HUMAN HIP MORPHOGENESIS (ONTOGENY)

Hip ontogenesis, or morphogenesis, describes the development of the hip from its foetal origin to the adult form. Understanding the sequential steps of the hip's development is critical to elucidate the pathobiology mechanisms of disease and deformity[3,12].

A normal child's hip develops from an intricate balance between a growing acetabulum, a growing proximal femur and the vasculature that adapts to the bony changes. The program for hip development begins with a genetic template that is actuated by a cascade of cell signalling factors. Within the outline provided by the genetic code, embryonic, foetal and childhood development of the hip continue and keep changing in accordance with various environmental and biologic factors[8,10].

1.2.1 In the Uterus

Pre-natal development is divided into two stages: a) the embryonic stage in the first two months of life, beginning with the fertilisation of the oocyte, followed by b) the foetal stage, which encompasses the period from the eighth week of life to birth. Tissue differentiation predominantly occurs during the embryonic phase, whereas the foetal period is marked by growth and development[10,16]. In the last phase of pre-natal development, the limbs and joints grow and mature in relative proportions and pre-established spatial orientations.

During development, the foetus assumes an upright position inside its mother. It has a very large head and long legs and, in the last trimester, the uterus wall tends to hyperflex the hip, levering the femur against the prominent anterosuperior iliac spine[12] (interestingly, non-human apes do not have prominent anterior iliac spines, have smaller heads/shorter legs and no known dysplasia). This hyper flexed position may act as a mechanical factor in explaining the decrease in relative acetabular depth and increase in femoral anteversion with increasing gestation, predisposing to a neonatal/infant hip dysplasia[12,17]. The cervicodiaphyseal angle (CCD) in foetal development appears to decrease with foetal age, further decreasing with age postnatally. Femoral anteversion, on the other hand, has been noted to increase with increasing foetal age; however, this is accompanied by a steady decrease during postnatal development[17]. Moreover, although the acetabulum increases in depth and grows in all dimensions in the uterus, its orientation does not change in any significant manner[18].

1.2.2 Post-natal Development

A delicate balance can be observed between the growing proximal femur, the acetabular and triradiate cartilages and adjacent bones that allow the acetabulum to develop. However, it is not fully understood what controls this balance, but it is likely that genetics is involved in maintaining this balance to a certain extent. There is also evidence to suggest that an adverse intrauterine environment may play a role in the genesis of hip pathology[17].

Developmental changes in either hip component affect the responsive growth of its companion. The normal pressure of the FH in the acetabulum maintains a balance in the proliferation of triradiate and acetabular growth cartilage. Secondary deformities result from the failure of head-acetabular relationships, such as congenital dislocation of the hip and primary epiphysiodesis of the triradiate cartilage (TRC). Anatomically, the proximal femur adapts to the growth of the primary epiphyses and associated biomechanical forces[1].

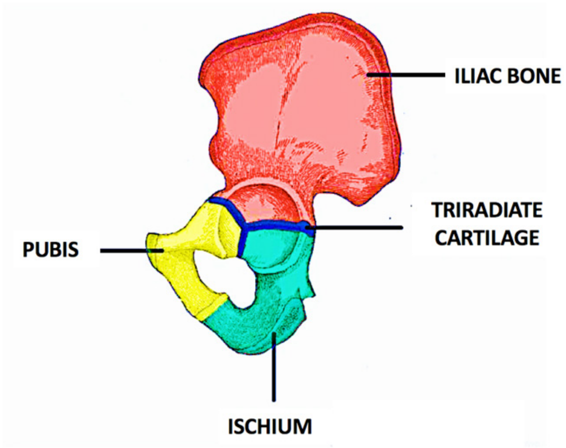

FIGURE 5 – Illustration of the main components of the acetabulum.

1.2.2.1 Acetabulum

At birth, the acetabular cartilage (AcCartil) complex comprises the saucer-shaped AcCartil laterally and the Y-shaped TRC medially (Figure 5). These two components of the AcCartil complex are anatomically continuous, and their coordinated growth results in the final acetabular shape[16]. Eventually, the TRC goes on to form the non-articular medial wall of the acetabulum while the AcCartil forms the cup-shaped rim of the acetabulum. At the periphery of the AcCartil is a fibrocartilagenous structure or labrum, which adds depth to the acetabulum. The capsular insertion is continuous with the labrum and the periosteum covering the pelvic bones[19].

The AcCartil complex undergoes interstitial growth within the cartilage and appositional growth under the perichondrium. The TRC, which is composed of the hyaline cartilage, represents the conjoined physeal plates of the three pelvic bones[16,19].

The three main acetabular ossification centres, which have been listed as follows, develop in the AcCartil[16]: 1) the *os acetabuli* (eventually forms the anterior wall of the acetabulum); 2) the iliac acetabular cartilage centre (forms the superior acetabular bone and joint surface); 3) the ischial acetabular centre (develops to form the posterior acetabulum). All ossification centres appear by 8 to 9 years of age (y.o.) and fuse by 17 to 18 y.o. As most of the acetabular shape is determined by 8 y.o., this age is important for prognosis of several paediatric hip disorders[16,20,21]. The growth of acetabular height and width depends on the interstitial growth of the TRC. However, growth in depth and the construction of the final acetabular shape are extremely reliant on the interaction with a spherical femoral head. Moreover, other factors, such as periosteal new bone formation, must come into play in the adjacent pelvic bones to allow the acetabulum to develop normally during growth[8,14,16].

1.2.2.2 Femur

In infants, the entire proximal femur is composed of cartilage. The proximal femoral (secondary) ossification centre appears between 4–7 months after birth. Following its appearance, it continues to enlarge until adulthood, when only a thin layer of articular cartilage remains. The enlargement of the FH and greater trochanter is facilitated by appositional growth, and their subjacent growth plates contribute to the length and width of the neck, respectively[19]. Their concurrent function not only yields growth along their respective axis but also a common vector of growth directed along the axis of the femoral shaft. The contact pressures exerted on the FH cartilage by the tight-fitting acetabulum result in its spherical appositional growth, as increasing pressure inhibits growth[22].

It should be noted that any disturbance in these growth plates can lead to angular abnormalities of the proximal femur[14,19,23]. For instance, the *varus* and *valgus* angulation of the neck is controlled by the contributions to the lateral growth of the neck by the three growth plates, which have been listed as follows (Figure 6):

I. Femoral head growth plate (FGP): This initially contributes to the maintenance of its sphericity. As the neck elongates, the geographic centre of the head moves proximally until the FGP achieves its final position at the FHN junction.
II. Greater trochanter growth plate (TGP): This primarily contributes to the longitudinal growth of the proximal femur and the lateral width of the femoral neck.
III. Femoral neck isthmus growth plate (FNI): This connects the trochanteric and femoral neck plates along the lateral border of the femoral neck. The FNI dynamically contributes to the lateral width of the neck, maintaining pace with the TGP and FGP.

An understanding of the interrelationships of the growth zones of the proximal femur and their alterations that result from genetic, environmental and developmental influences permits early diagnosis of growth deformities[13,23,24].

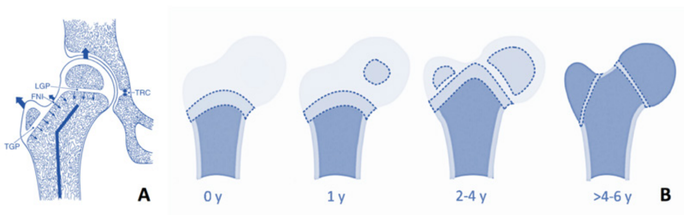

FIGURE 6 – (A) Illustration of the three femoral growth plates and TRC. The arrows represent the resultant main vectors of force in these growth plates. *(B)* Schematic representation of the growing human hip region, showing the primary femoral and secondary ossification centres and proximal diaphyseal growth plate at ages 0, 1 year, 2–4 years and > 4 to 6 years. The panels represent normal development, showing an isthmic interruption of the chondroepiphysis prior to trochanteric osseous expansion, normal orientation of the capital growth plate and normal head-neck offset.

1.2.3 Factors that influence growth and shape

Child hip development is an ordered pathway of processes that result from the delicate interplay of cellular and mechanical influences. Cell signalling, intrauterine differentiation and postnatal growth with the maturation of its accompanying blood supply are critical to hip development. Central to this process is the necessary contact between the FH and acetabulum to enable congruent development.

Developmental hip disorders (DDs), such as developmental dysplasia of the hip (DHD), slipped *capitis femoris* epiphysis (SCFE) and femoroacetabular impingement (FAI), have been viewed by some as morphological variants of the normal hip[1,25]. The sequelae of these diseases and their treatments may be understood in the context of the growth history of the joint[19]. The femoroacetabular morphology of DD is believed to induce OA through local cumulative mechanical overload acting on genetically controlled patterning systems and subsequent damage of joint structures[3].

However, it remains unclear why hip morphology differs between individuals with seemingly comparable load histories and why certain hips with DD progress to symptomatic OA, whereas others do not. Furthermore, genetic factors most likely act through multiple genes, each with modest effect sizes. Therefore, single genes that explain a DD are unlikely to be found. Apparently, the interplay between genes and load history not only determines hip morphotype but also joint cartilage robustness ("cartilotype") and resistance to symptomatic OA[3]. Integrating observations from several fields that have recently provided an explanation to hip morphology (i.e., imaging, evolution and genetics) can improve our understanding of hip ontogeny, DD and OA development (Figure 7).

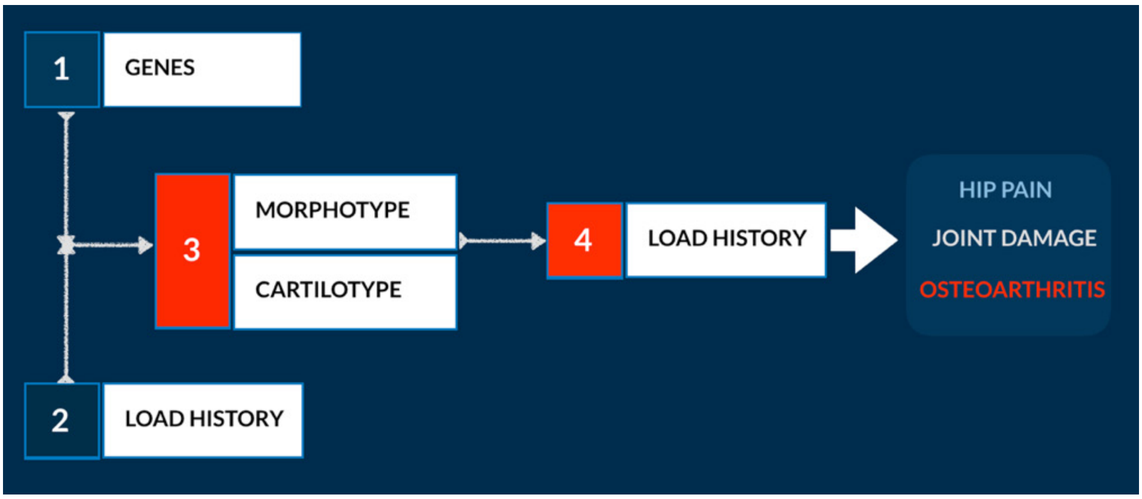

FIGURE 7 – Schematic illustration of currently proposed factors and fluxogram of hip pathology. Information has been collected from multiple sources and has been cited throughout the text.

1.2.3.1 Genetic background

Genes may account for some of these morphological differences and increased susceptibility to disease. They have only recently been linked to hip morphology[3,5,26] as genetic architecture for hip morphogenesis is apparently complex and polygenic (i.e., no genes specific for each DD have been found). OA susceptibility genes that are involved in endochondral ossification influence the effect of joint shape on OA. These genes might either affect the shape itself or moderate how the shape affects the cartilage[26].

OA has a considerable hereditary component and is considered to be a polygenic disease[27], reflecting the result of multiple interacting genes with small effects that tend to be related to the process of synovial joint development. Early-onset OA has been linked to mutations in matrix molecules that are often associated with chondrodysplasias, whereas less destructive structural abnormalities or mutations confer increased susceptibility to injury or malalignment, which can result in middle-age onset. Finally, mutations in molecules that regulate subtle aspects of joint development and structure lead to late-onset OA[5]. As such, they could also determine the age at which OA becomes apparent, the joint sites involved, the severity of the disease and how rapidly it progresses[5].

1.2.3.2 Mechanical factors

More than a century ago, Roux and Wolff already observed that bone is capable of adapting itself to its mechanical environment. This has been well illustrated by the trabecular structure of the proximal femur, which is aligned along main loading directions. This has led to the idea that external forces as a result of sport activities, specifically during the period of skeletal growth, influence bone architecture and bone morphology[7,23,24,28]. Observations from recent literature showed that:

1. **Bone and growth plates are adaptive tissues**

Bone has the ability to constantly renew itself. This is realized by osteoclasts and osteoblasts working together in structural basic multicellular units[5]. During growth, remodelling also takes place to adapt bone structure to changing mechanical loads, which is then referred to as modelling. Bone and cartilage adapt to their mechanical environment, and the cartilaginous growth plate is likely affected in its differentiation and ossification process by mechanical loads. Cam deformity on radiographs gradually develop from approximately 13 years of age until the closure of the growth plate[23]. Accordingly, finite element models showed high mechanical stress on impact loading in the open growth plate and surrounding bone, exactly where the Cam deformity usually develops[24], particularly in a position of flexion and external rotation[24,29].

II. Load history

The prevalence of the *coxa reta* deformity (commonly referred to as Cam morphology) seems especially high in weight-bearing sports that require high flexion with rotational movements of the hip (e.g., soccer, basketball and ice hockey require these hip-loading patterns). Ice hockey players were 4.5 times more at risk for having a Cam deformity than skiiers[30]. In boys between the ages of 12–13 y.o., the adolescent growth spurt occurs[19] and the skeleton is especially responsive to mechanical *stimuli*. This might be a critical period, since subtle mechanical triggers might interact with molecular *stimuli* and easily lead to bone formation[31].

Further, a dose-response relationship is apparent, as elite soccer players who practiced more than 3 times per week before the age of 12 years were 2.6 times more likely to have a Cam deformity than elite soccer players that practiced three times or less before the age of 12[6,32]. Finite element analysis revealed that the orientation of the growth plate, combined with certain loading scenarios, modulates bone formation. This means that a specific orientation of the growth plate with extension towards the femoral neck can result in a synergistic effect on bone formation in the anterolateral head-neck junction[24,31].

1.3 HIP MORPHOLOGY

Classically, the hip has been described as one morphologically simple loading joint, although the recent description of some anatomical features has remarkably enriched this apparent simplicity. The interpretation of the function of anatomical structures by "layers", with specific and complementary functional levels, has contributed to the explanation of symptomatic pathological *phenomena*.

The basic anatomy around the hip consists of the superficial surface anatomy and deep bony, muscular and neurovascular anatomy. The clinically relevant surface anatomy consists of several superficial, palpable bony prominences. The anterior landmarks consist of the prominent anterior superior iliac spine (ASIS) and anterior inferior iliac spine (AIIS), which serve as insertion points for the *sartorius* and direct head of the *rectus femoris*, respectively. The greater trochanter and posterior superior iliac spine (PSIS) are also easily identifiable. They are important landmarks for imaging diagnosis and incision planning. Understanding the relationship of these structures with the deeper anatomy is a critical, clinical anatomic principle. Accurate identification and palpation of these structures are vital to all surgical hip planning.

Presently there is no detailed knowledge about the combined function of the pelvic/abdominal muscle girdle and the mobility of the hip, but there is a clear relationship between these two anatomical regions in the sense that an alteration of the global spinopelvic structure influences the hip and vice versa[33]. Therefore, evaluating these structures by functional layers more closely parallels clinical significance[4,33–35].

1.3.1 Structural Layer

This bony structural layer essentially consists of the proximal femur, the acetabulum, the hyaline cartilage that lines the two articular surfaces and the acetabular labrum. The hip is a diarthrodial joint and is defined by the constrained bony articulation of the proximal femur and acetabulum.

1.3.1.1 Femur

The FH has a spherical shape, in continuity with the femoral neck, which usually has a cylindrical shape flattened from front to back. In *coxa rotunda*, there is continuity between its spherical shape and the periphery of the FHN. Although this is the normal anatomy classically described, we now know that in up to 7-100% of humans there are variants of this morphology, with the presence of a non-spherical sector at the FNH junction[14] (Figure 8).

Usually, the articular cartilage covers about ⅔ of the FH and presents a variable thickness, higher in its central region and in the loading zone. Its lateral borders correspond to the FHN transition, except in the upper areas where the cartilage is bordered by the postero-superior synovial fold covering the retinacular arteries that nourish the epiphysis[37]. The average distance that separates the lateral border of the cartilage from the nourishing arterial orifices is not known. During this thesis, we describe the methodology used to obtain the value of this distance. This knowledge is important because osteoplasty of the FHN junction often extends near these nourishing holes. The *fovea capitis* is a small area devoid of cartilage in the FH, and it is located slightly posterior and inferior to the centre of the FH cartilage (Figure 8).

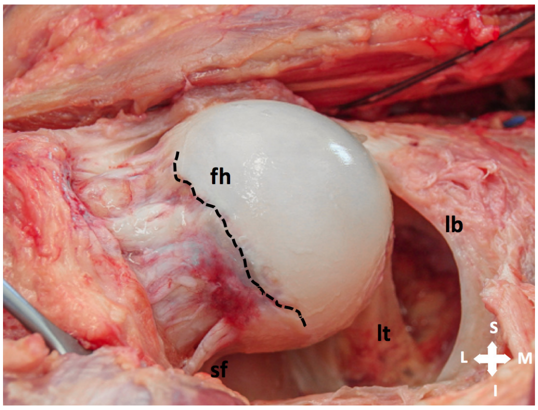

FIGURE 8 – Dissection photography of the right hip. Femoral head with the typical spherical shape of a *coxa rotunda* and the hyaline articular cartilage lining slightly lateral to the equatorial region and with an irregular border (dashed line). fh: femoral head; lb: labrum; lt: *ligamentum teres*; sf: synovial fold; S: superior; I: inferior; M: medial; L: lateral.

1.3.1.2 Acetabulum

The acetabular cavity has a concave hemispherical shape[38] that results from the contributions of the 3 bones of the pelvis, the ilium, ischium and pubis. It is orientated approximately 45° caudally (abduction) and 15° anteriorly (anteversion)[20]. Its hemispherical shape covers 170° of the femoral head[20,38]. The acetabular fossa is located in the inferior region of the acetabulum and is surrounded by the horseshoe-shaped lunate surface (non-articular surface of the acetabulum, covered by synovia). The transverse ligament limits the inferior margin of the fossa and is in continuity with the anterior and the posterior labrum[39] (Figure 9).

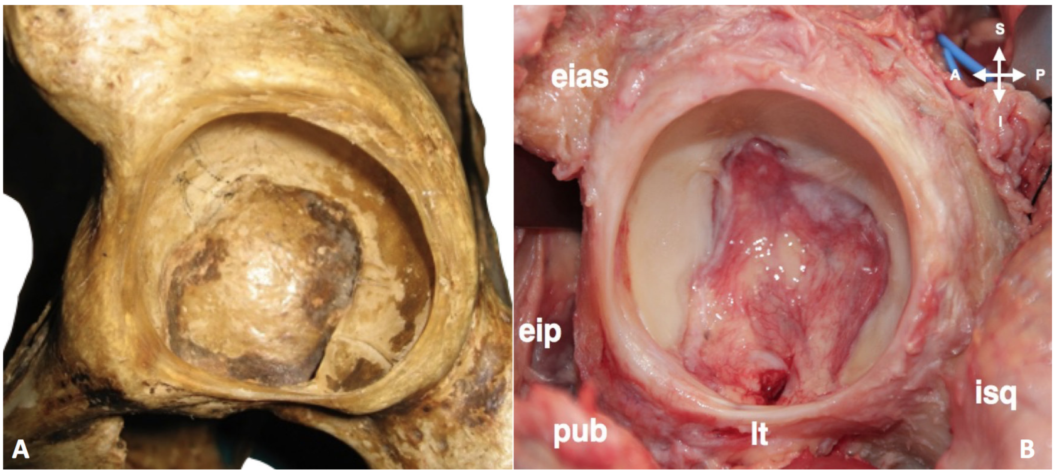

FIGURE 9 – (A) Bony pelvis cadaveric specimen, representing the anatomy of the acetabulum. (B) Soft tissue cadaveric specimen of the acetabulum (eias): anterosuperior iliac spine; (eip): eminence iliopectineus; (pub): pubis; (lt): transverse ligament; (isq): isquion. S: superior; I: inferior; A: anterior; P: posterior.

1.3.1.3 Labrum

The labrum is a fibrocartilage with a triangular cross section, although its morphology can vary widely[38]. Its base is inserted in the osseous acetabular rim; the articular or internal surface is in continuity with the acetabular cartilage and the capsular or external surface is attached to the articular capsule. The labrum is in continuity with the transverse ligament, antero-inferiorly and postero-inferiorly. The labral vascular supply arises from a periacetabular vascular ring with radial branches that course over the capsular surface of the labrum, terminating in its free edge. Kalhor et al.[37] did not show vessels entering the labrum from the adjacent subchondral bone. The clinical relevance of this fact is that the majority of the labral lesions are located in the chondrolabral junction with preservation of the vascularity tree (surgical labral detachment may interfere with its blood supply) (Figure 10).

As it has its own innervation (coming from the obturator nerve), the labrum can be an important source of pain when it is subjected to an abnormal tension or when it presents structural changes or discontinuity with the bone or cartilage[38]. It has free nerve endings with both proprioceptors and nociceptors, which may explain the decreased proprioception and pain in an athlete with a torn acetabular labrum. These changes very rarely occur in isolation and are frequently associated with changes in bone morphology such as in DHD or FAI[41,42]. Like the knee meniscus, the labrum may have the greatest healing potential at the peripheral capsulo-labral junction[38].

The sublabral sulcus (Figure 10) is an anatomic variant that should not be confused with a labral tear. In arthroscopy, it is a well-defined cleft between the labrum and the acetabular hyaline cartilage with smooth edges, no signs of inflammation and no labral instability on probing. Its most frequent location is the postero-inferior (48%) quadrant[43]. There is a normal concavity in the anterior acetabular rim in relation to the iliopsoas tendon (psoas "U"). It is universally present, and its superior aspect is a reliable arthroscopic landmark for the 3 o'clock position[44].

Because the labrum appears to enhance joint stability and preserve joint congruity, there is a significant concern about the potential for rotational instability or hypermobility of a labral deficient hip. This instability may result in redundant capsular tissue and create a potential abnormal load distribution due to a transient incongruous joint resulting from subtle subluxation[45,46]. Presently, known labrum functions include the following[2,47]:

- **I.** acting as a load-bearing structure containing the FH in extreme ranges of motion (ROM), especially flexion;
- **II.** acting as a tension band to limit expansion during motion between the anterior and posterior columns during loading in the gait cycle;

III. contributing significantly to decrease tension on the cartilage during dynamic trans articular compression;

IV. joint sealing function by limiting fluid leakage from the joint space, thus protecting the cartilage layers.

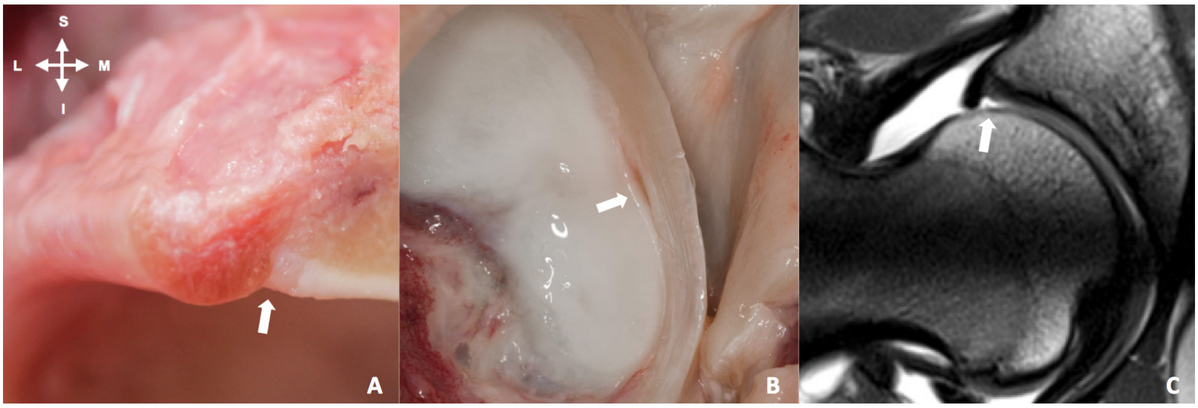

FIGURE 10 – (A) Macrophotography of the acetabular labrum section. There is a normal depression in the chondrolabral transition and the continuity of the labral tissue with the bone and cartilage surface (arrow). (B) Detail of the anterior articular surface where we frequently observe a more pronounced depression in the chondrolabral continuity (arrow). (C) Arthrography magnetic resonance image of the same groove as in (A) (arrow). This variant should not be confused with labrum rupture. S: superior; I: inferior; M: medial; L: lateral.

1.3.2 Capsulo-ligamentous Layer

1.3.2.1 Capsule and peripheral compartment

The anatomical structure that most influences the peripheral space is the joint capsule. It is a thick and tense fibrous sleeve extending from the outer neck to the acetabular rim. The inner surface is entirely covered with synovia. Some portions of the capsule have an increased thickness or are reinforced. Namely, (a) the superolateral part is reinforced by the reflected tendon of the *rectus femoris*, (b) the anterolateral part by the ilio-femoral ligament (y-shaped ligament of Bigelow), (c) the anteromedial part by the pubo-femoral ligament and (d) the posterior capsule by the ischio-femoral ligament[4].

The *zona orbicularis* (ZO) is a major hip stabilizer and represents a circumferential thickening of the capsule, forming a ring around the FHN. It consists of a thicker layer of annular fibres crossing the above-mentioned longitudinal ligaments and, thus, strengthening the capsule. Just cranial to the ZO, close to the anterior capsular recess, lies the psoas tendon[48].

The iliopsoas bursa is located beneath the myotendinous portion of the iliopsoas muscle, anterior to the hip joint capsule and lateral to the femoral vessels. The bursa separates the iliopsoas tendon from the articular capsule, and it may directly communicate with the peripheral compartment in 15–20% of cases. This finding may bear clinical relevance and can increase the risk of fluid extravasation during hip arthroscopy[39] (Figure 11).

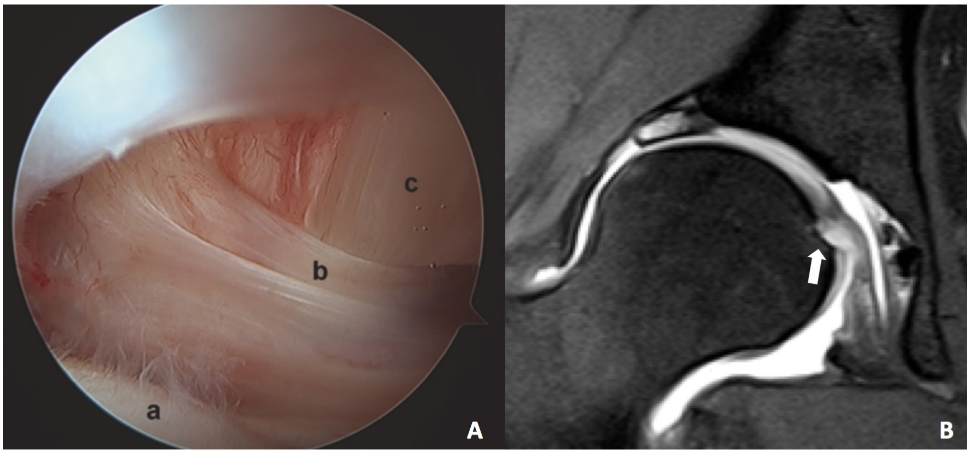

FIGURE 11 – (A) Arthroscopic image of the peripheral compartment of a right hip with an articular communication with the iliopsoas tendon. The femoral head (**a**), the anterior capsule (**b**) and the iliopsoas tendon (**c**). (B) Arthrography magnetic resonance image of the hip. *Fovea capitis* with *ligamentum teres* insertions are shown (arrow).

The spiral orientation of the capsular ligaments provides a "screw" effect in full extension. The ligaments tighten or coil with maximal extension, making this a position of maximal soft tissue stability. Interestingly, the position of maximal articular congruency is not with the hip in an extended position but in a flexed position[39]. The position of optimal articular contact (FABER: flexion, abduction, external rotation) is actually a position of soft tissue laxity with the ligaments uncoiled. Thus, the position of maximal instability, from both soft tissue and osseous perspectives, is flexion and adduction[4]. The formation of adhesions of the capsule to the labrum caused by recurrent synovitis or after surgery[49] can also be a source of pain.

1.3.2.2 Ligamentum teres

The *ligamentum teres* (LT) has traditionally been viewed as an embryonic remnant with no role in the biomechanics or vascularization of adult hips (Figure 11). However, the LT is a strong intraarticular ligament that is anatomically and biochemically similar to the anterior cruciate ligament of the knee. It arises from the transverse ligament and the ischial and pubic margins of the acetabular fossa and has a fascicular appearance with an anterior and posterior bundle.

The ligament is trapezoidal at its base and runs to the FH, where it becomes progressively round or oval shaped and inserts into the *fovea capitis* (Figure 12). During dynamic clinical evaluation, the ligament is tight in hip external rotation[50]. The exact function of the LT is not yet clear and different theories have been proposed as follows[50-53]:

- **I.** Intrinsic stabilizer that resists joint subluxation forces;
- **II.** May play a role in nociception and coordination of movements;
- **III.** Provides blood supply to the developing FH;
- **IV.** May help to distribute synovial fluid within the hip joint via a "windshield wiper effect"[50-52];
- **V.** Patients with LT tears develop hip microinstability. When combined with sporting activities, this results in damage to the labrum and cartilage (explaining the high association rate between tears of the LT, labral tears and cartilage lesions)[53].

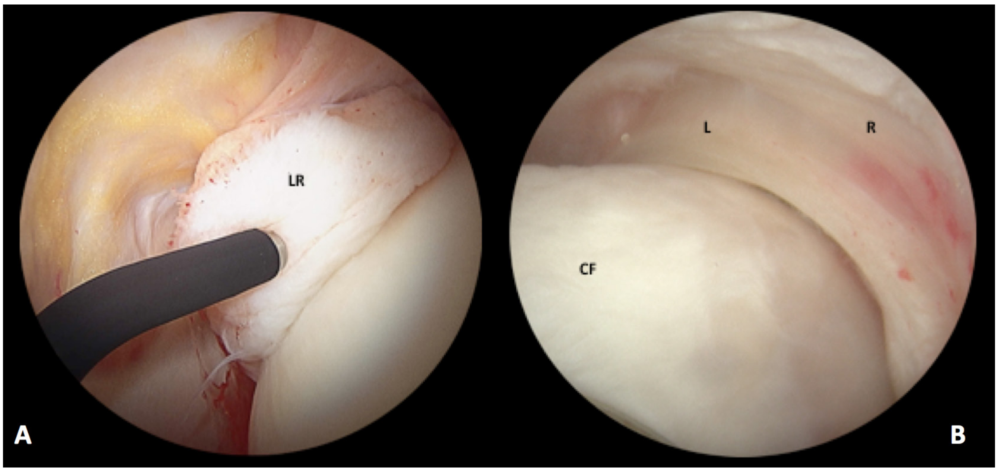

FIGURE 12 – Hip arthroscopic images (A) *ligamentum teres* (LR), (B) anterior perillabral recess (R); Femoral head (CF); Labrum (L). CF: femoral head; L: labrum; R: perilabral recess.

1.3.3 Muscular Layer

The muscular attachments surrounding the hip are extensive, with a total of 27 muscles crossing the hip joint. A detailed understanding of the muscular attachments and innervations are critical for safe open surgical procedures[54]. They can be broadly broken down by their main function[4,39] (Table 3):

- **I.** Primary flexors: the iliac, psoas, *iliocapsularis*, *pectineus*, *rectus femoris* (direct and indirect heads) and *sartorius*;
- **II.** Extensors: The *gluteus maximus*, *semimembranosus*, *semitendinosus*, *biceps femoris* (long and short heads) and *adductor magnus* (ischiocondyle part);

III. Abductors: The *gluteus medius*, *gluteus minimus*, *tensor fascia lata*, and iliotibial band;

IV. Adductors: The *adductor brevis*, *adductor longus*, *gracilis* and the anterior part of the *adductor magnus*;

V. External rotators: The *piriformis*, *quadratus femoris*, *inferior gemellus*, *superior gemellus*, *obturator externus* and *obturator internus*.

	MUSCLE	FUNCTION	IMPORTANT SPECIFICITES
DEEP LAYER	***Piriformis*** ***Quadratus femoris*** ***Gemellus*** ***Obturator externus*** ***Obturator internus***	- Active: External rotator. - Passive: Hip stabilizers.	- Intimate relation with the deep branch of the posterior femoral circumflex artery that penetrates the capsule below the terminal portion of its tendon. - Between the muscular bodies of the *piriformis* and the *gemellus* superior, the large sciatic nerve emerges to its extra pelvic path.
	Gluteus minimus[55] **(GM)**	- Mainly abductor, but also internal and external rotator.	- During hip surgery, the posterior border of the *gluteus minimus* serves as a reference for the dissection of the joint capsule and for the location of anastomotic vascular branches.
	Iliocapsularis	- Hip stabilizer preventing lateral and superior head migration.	- The ratio of the transverse section of the *iliocapsularis* to the iliopsoas muscle in MRI can be a marker of instability.
INTERMEDIATE LAYER	***Gluteus medius***[56]	- Mainly abductor.	- Lateral surgical approaches: Its posterior border can serve as a reference for the location of the tendon of the piriformis.
SUPERFICIAL LAYER	***Gluteus maximus***[57]	- Extensor and external rotator.	- Forms a vast fan that covers the deep and superficial planes of the hip.
	Tensor fascia lata	- Hip abductor.	- 2nd most important abductor.
THIGH MUSCLES	**Iliopsoas**[20,58,59]	- Hip flexion and external rotation. - The most important hip flexor[4].	- Proximity to the acetabular border and to the iliopectine eminence explains symptoms of snapping or mechanical instability in situations of increased femoral anteversion or insufficiency of the anterior acetabulum[59]. - Controversy regarding its involvement in impingement pathology with the acetabular labrum[58].
	Adductors	- Adduction. - Extension of their proximal insertion around the obturator orifice makes them extensors or hip flexors as a function of the relative position of the joint (inversion of their muscular actions).	- The proximal insertion of the adductors can be a cause of symptoms when there is muscle hyperactivity in order to transversely balance the pelvis[60]. - Important in maintaining the transverse balance of the pelvis and during bipedal gait.
	Hamstrings	- Hip extensors. - Contribute to AP muscular balance of the pelvis.	- The proximal insertion of the hamstrings can be a frequent cause of symptoms due to tendinopathy or ruptures[61].
	Rectus femoris* (direct and indirect heads) and *sartorius	- Hip flexor. - With the TFL, antagonize hamstring action.	- The proximal insertion of the *rectus femoris* is a frequent site of rupture or avulsion[61].

TABLE 3 – Summarising functions and specificities of the pelvic and hip muscles.

1.3.4 Neuromechanical Layer

This is a theoretical concept that integrates multiple interlinked anatomical structures, physiological events and kinematic changes that depend on the proprioception and pain sensitivity of the periarticular structures. Locally, this layer is formed by the neurovascular structures, mechanoreceptors and nociceptors present in LT, capsule, labrum and tendons. On a broader view, this level refers to the relative pelvic position in relation to the femur. Postural balance may be affected by changes in lumbar kinesis.

The FH and the acetabulum have a reciprocal interaction where proximal femoral morphology can compensate for acetabular morphology and vice versa. To exemplify, a large Cam deformity would impinge later on a shallow acetabulum than on a *protrusio acetabulum*[62]. The principle of "reciprocal interaction" explains the difficulty to set threshold values for morphologic parameters predisposing to impingement, with only extreme values being strongly predictive for the development of impingement or instability[33]. Sagittal pelvic kinematics and spinopelvic angular parameters are new parameters under investigation for their relationship with the development of symptomatic FAI[34].

1.3.5 Vascular anatomy of the hip

Detailed knowledge of the extra osseous vascularization of the proximal femur and iliac allowed the development of hip preserving surgery (HPS) techniques[63]. The overall vascularization of the hip joint will be described with particular detail for the proximal femur.

The primary vascular pathways are extensions from the internal and external iliac vessels. From the internal iliac system, the superior and inferior gluteal arteries and obturator artery supply most of the surrounding hip musculature (laterally and medially respectively) and periacetabular region[37]. From the external iliac system, the medial and lateral femoral circumflex arteries anastomoses around the proximal femur.

1.3.5.1 Proximal femur

The learning curve of the technique of hip surgical dislocation is facilitated by the visualization of anatomical structures, particularly vascular structures, and by the direct visualization of the mechanism of impingement[63,64]. However, in more extensive deformities requiring a wider resection, visualization of the posterior region of the FHN may be impossible. In these cases, preoperative imaging information on the spatial location of vascular structures has definite added value.

In advanced HPS, the possibility of a circumferential approach of the FHN, generating a flap of soft parts containing the external rotators and the deep branch of the medial femoral circumflex artery (MCFA), allows the performance of realignment osteotomies at the level of the femoral neck. Similarly, knowledge of the location of the posterior border of the superior retinacular fold may be relevant and may contribute to the safety of the procedure[65].

- **I.** The MFCA has 3 main branches: The ascending, deep and trochanteric. The deep branch of the MFCA is the primary blood supply to the FH[66];
- **II.** The lateral femoral circumflex artery, metaphyseal artery and the medial epiphyseal artery all give small contributions to the vascularisation of the FH, with the medial epiphyseal artery providing most of the perfusion to the peri foveolar area.[66]

Course of the MCFA: The course of its deep branch is quite predictable. It usually originates from the deep femoral artery and starts medial between the pectineus and iliopsoas tendon along the inferior border of the *obturator externus*. Here, a trochanteric branch sprouts off at the proximal border of the *quadratus femoris* to the lateral trochanter (Figure 13). Posteriorly, the deep MFCA enters between the proximal border of the *quadratus femoris* and the inferior *gemellus*. It then travels anteriorly along the conjoint tendon of the inferior *gemellus*, *obturator internus* and superior *gemellus* and perforates the capsule at the level of the superior *gemellus*. It then originates 2–5 superior retinacular vessels intracapsularly[67]. Doppler laser studies clearly show that the superior retinacular arteries alone are sufficient to ensure perfusion of the FH, and conversely, when their flow is interrupted, the remaining systems are not sufficient to maintain arterial perfusion[68] (Figure 14).

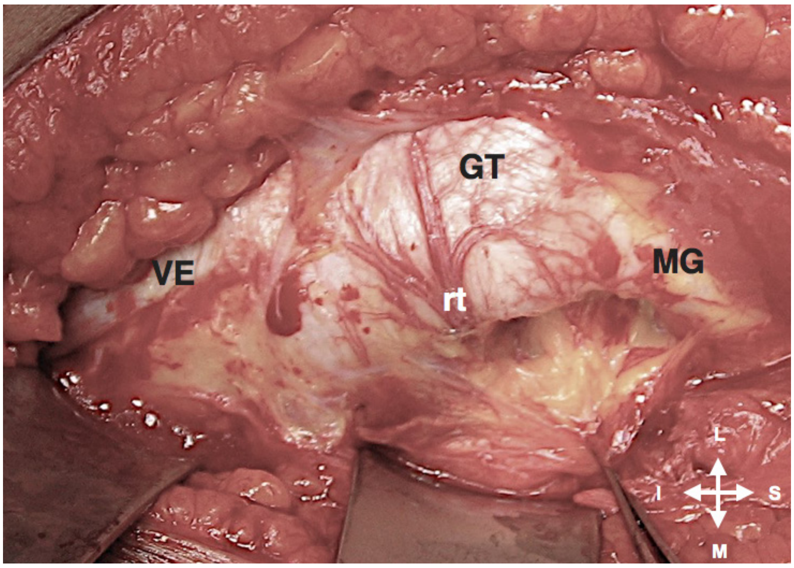

FIGURE 13 – Open dislocation surgical procedure. Notice the location of the trochanteric branch of the posterior circumflex artery. VE: *vastus lateralis*; GT: great tuberosity; MG: *gluteus medius*; rt: trochanteric branch; S: superior; I: inferior; L: lateral; M: medial.

Anastomosis: The deep branch of the MFCA has multiple anastomoses[66,67,69]:

I. The descending branch of the lateral femoral circumflex artery joins the deep MCFA at the base of the neck of the femur;
II. The deep branch of the superior gluteal artery joins it at the insertion of *gluteus medius*;
III. The inferior gluteal artery anastomoses with the deep MFCA along the inferior border of the *piriformis*, posterior to the conjoined tendon;
IV. The internal pudendal artery joins it near the retro acetabular space.

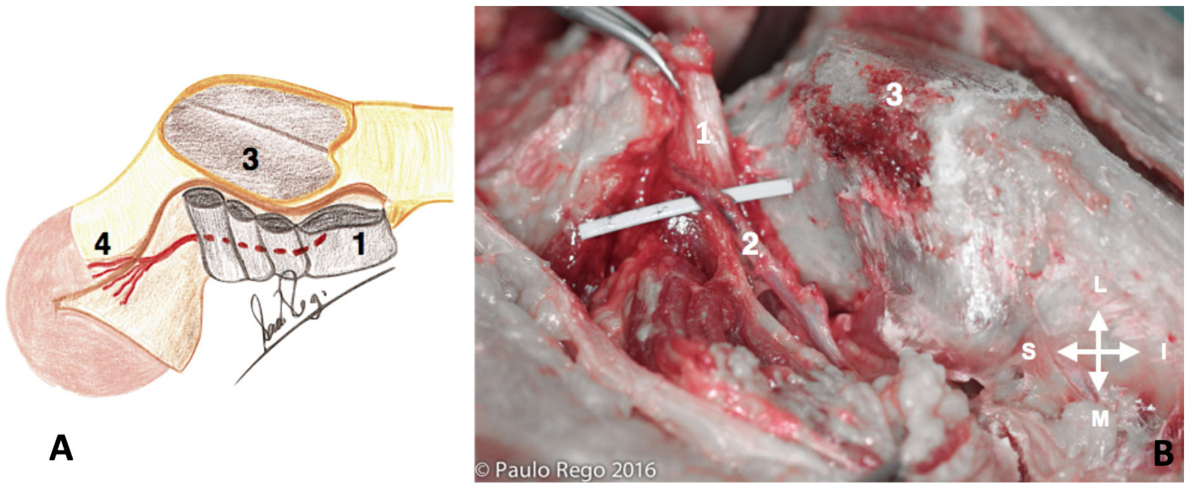

FIGURE 14 – (A) Schematic drawing of the external rotators' flap containing the deep branch of the posterior circumflex artery (posterior view). (B) Representative cadaveric photograph of the same anatomy. 1: external rotators; 2: deep branch of the posterior circumflex artery; 3: great trochanter; S: superior; I: inferior; L: lateral; M: medial. (adaptation from Prof. Dr. Paulo Rego's illustration and photography, with permission).

1.3.5.2 Acetabulum and peri-articular soft-tissues

The periacetabular region is nourished by several branches of the internal iliac artery that extensively anastomose to form a periacetabular circle on the outer and inner face of the iliac bone (contributions from superior gluteal, inferior gluteal, obturator, 4^{th} lumbar artery and iliolumbar artery)[70]. In its anterior region, this anastomotic circle is connected to the ascending branch of the anterior circumflex artery (Figure 15). Detailed knowledge of this vascular anatomy is very important in surgical procedures of acetabular reorientation for the preservation of the vascularization of the acetabular fragment[37,63,70].

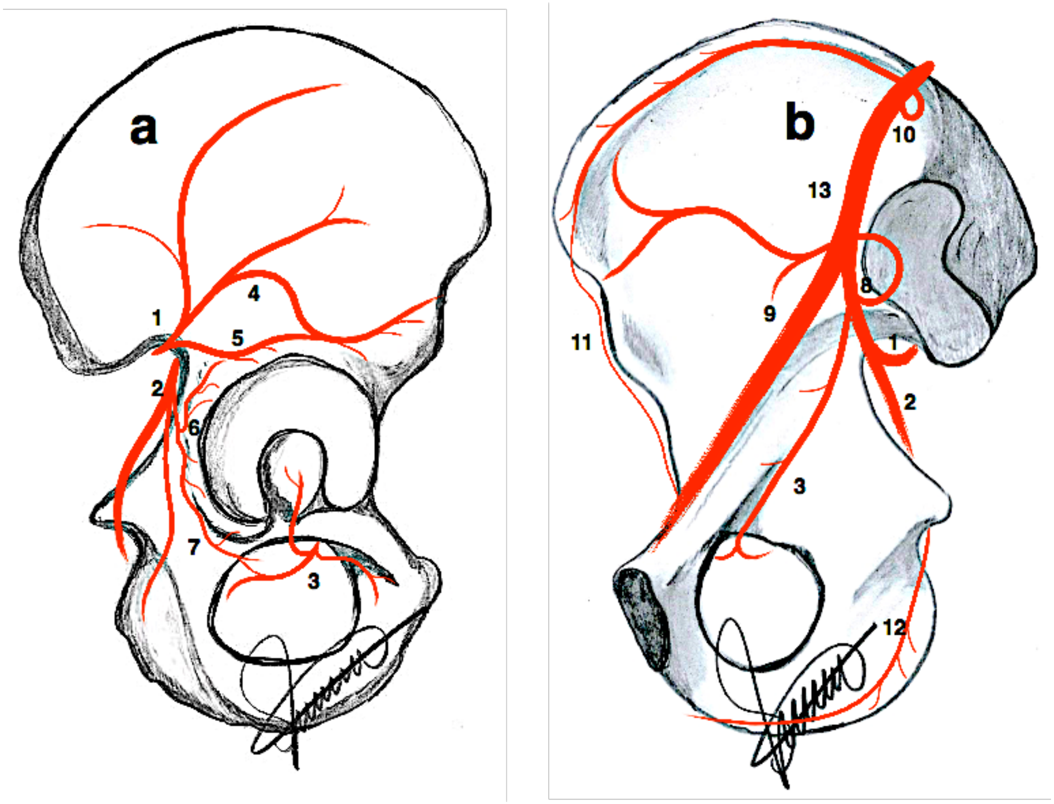

FIGURE 15 – Illustration of the lateral (a) and medial (b) facets of the iliac with the respective arterial anastomotic network of the peri-acetabular region. 1: upper gluteal artery; 2: gluteal inferior artery; 3: obturator artery; 4: supra-acetabular a.; 5: acetabular a.; 6: acetabular branch of gluteal inferior a.; 7: anastomosis between inferior gluteal a. and obturator a.; 8: iliolumbar a.; 9: nourishing branch of iliolumbar a.; 10: 4th lumbar a.; 11: deep iliac circumflex a.; 12: medial pudendal a.; 13: common iliac a. (adaptation from Prof. Dr. Paulo Rego's illustration, with permission).

chapter 2

CLINICAL EVALUATION

2.1 IMAGING ANATOMY

The hip joint is classically described as having spherical surfaces[4], with the FH having a ⅔-shape of a sphere in continuity with the FHN. The acetabular cavity corresponds to a concave sphere segment in all its extension and is covered with cartilage in its more peripheral zones (horseshoe-shaped) with a central, non-articular zone[4].

Conventional plain radiograph (CR) remains the standard imaging modality to assess the hip despite modern three-dimensional (3D) computed tomography (CT) or magnetic resonance imaging (MRI). In clinical practice, we quantify hip morphology using angles and lines that are usually visible in an anteroposterior (AP) radiograph with standardized acquisition of the entire pelvis with additional views according to each clinical situation[71-76]. As such, knowing the technical principles of radiographic imaging is essential for the correct interpretation of CR. In contrast to CT or MRI, a CR is a two-dimensional projection of a 3D reality.

Given the enormous individual variability, it is difficult to precisely define the thresholds between what is normal or pathological regarding the shape of the hip, with extensive research having been done on the subject since the last century[77,78]. To better understand the variants of normal and what is considered to be the pathological deviation, it is paramount to describe and quantify imaging parameters that can guide us throughout this dissertation.

2.1.1 General technical considerations

For the pelvis AP radiograph, the legs must be 15° internally rotated to compensate for femoral antetorsion. The central beam is centred to the midpoint between the upper border of the symphysis and a line connecting the two ASIS. Other technical aspects are paramount to adequately understand pelvic imaging. The main factors include (Figure 16):

I. ***Conical projection***[79]***:*** CR is based on a point-shaped X-ray source with conical projection. Therefore, distortion of the pelvic anatomy is unavoidable. Typically, the closer an object is located to the X-ray source, the more lateral it will be projected;

II. ***Film-tube distance***[80,81]***:*** This distance affects hip anatomy on the radiograph. For e.g., by increasing film-tube distance the apparent acetabular anteversion increases (should be around 120 cm);

III. ***Centring and direction of the X-Ray beam***[80]***:*** Centring is one of the most important factors influencing the anatomy of the hip on CR. To avoid distortion, the craniocaudal angle of the beam is standardized such that the sacrococcygeal joint is 1 to 3 cm from the superior aspect of the pubic symphysis. This is particularly important as it ensures adequate representation of the intrinsic properties of the acetabulum (coverage, orientation and depth). By lowering the centre of the X-ray beam (low-centred AP pelvic radiograph) or by moving the central beam to the centre of the hip, the apparent acetabular anteversion increases;

IV. ***Pelvic orientation***[71,79]***:*** Orientation can vary in three dimensions: Obliqueness, rotation and tilt. While variations in pelvic obliqueness and rotation can be decreased by a standardized acquisition technique, pelvic tilt can vary substantially. Pelvic tilt mainly affects the apparent anteversion of the acetabulum (with increasing pelvic tilt, the apparent acetabular anteversion decreases and vice versa).

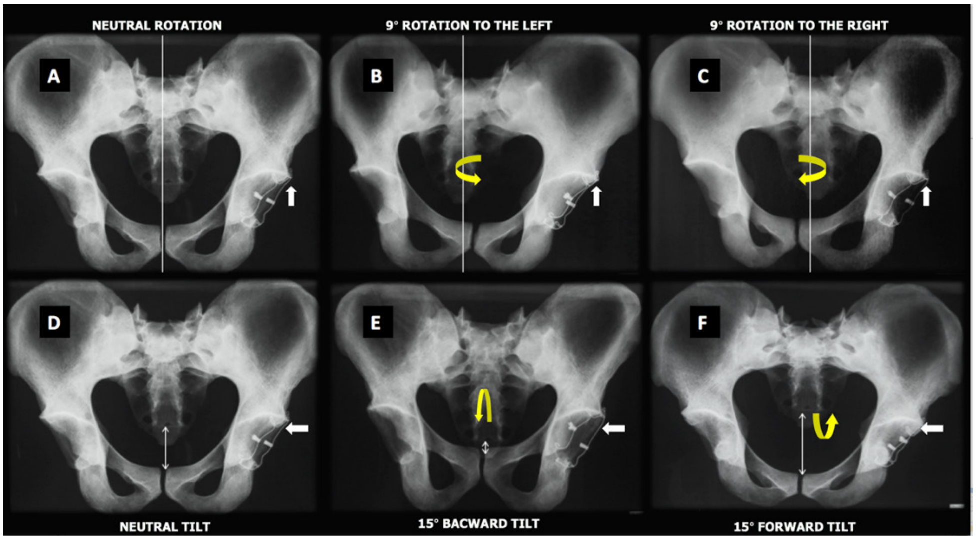

FIGURE 16 – Pelvic orientation during radiograph acquisition affects the projected hip anatomy. (A) A cadaver pelvis in neutral position. Both acetabula are anteverted. (B) Rotation of 9° towards the left, results in a cranial retroversion of the left acetabulum and an increased anteversion on the right. (C) A rotation of 9° towards the right, results in a cranial retroversion of the right acetabulum and increased anteversion on the left. Ideally, the rotation should be 0°. (D) Pelvic tilt during radiograph acquisition is estimated by the vertical distance between the sacrococcygeal joint and symphysis (white vertical double-headed arrow). (E) By a 15° backward pelvic tilt, both acetabula show increased anteversion (white horizontal arrow). (F) By a 15° forward pelvic tilt, both acetabula show a cranial retroversion (positive crossover signs indicated by white horizontal arrow) (adapted from Tannast et al.[80] with permission).

Proper positioning on an AP pelvic radiograph is recognized when: i) femur – the greater trochanter is seen laterally and the lesser trochanter is partially superimposed on the femoral neck, ii) the obturator rings and acetabular teardrops are symmetric and iii) midsacral line aligns with the pubic symphysis.

2.1.2 Views and basic technique

Pelvic radiographs performed in the supine position are preferred by some authors because they can be directly compared to CR performed intraoperatively or at follow-up during early rehabilitation and restricted weight bearing[80]. On the other hand, in clinical entities where acetabular evaluation is of paramount importance (such as Pincer FAI and DHD), weight bearing AP pelvic radiographs should be obtained given that they reflect functional anatomical positioning[82] and also account for the differences in pelvic flexion-extension and acetabular version variations.

Different techniques have been described for the axial/lateral view of the hip[83] and also for the AP view of the hip/pelvis (Figure 17 and 18), which are performed to answer specific questions (Table 4).

PROJECTION	TECHNIQUE	FEATURES
AP PELVIS	Patient supine or standing, legs 15° internally rotated. X-ray centred to midpoint between the upper border of symphysis and a line connecting both ASIS.	Basic radiographic evaluation of the hip for HPS, total hip arthroplasty or trauma surgery.
AP HIP	Patient supine or standing, legs 15° internally rotated. Hip-centred X-ray beam.	Performed in total hip arthroplasty; not recommended for HPS due to different X-ray centring and altered morphology of the hip.
AXIAL CROSS-TABLE	Patient supine, ipsilateral leg 15° internally rotated, contralateral hip flexed and elevated.	Depicts the anterior and posterior FHN contour.
DUNN-RIPPSTEIN	Patient supine, hips in 90° flexion and 20° abduction, knees in 90° of flexion, legs in holding device.	Femoral antetorsion, anterior and posterior femoral head-neck contour.
DUNN 45°	Patient supine, hips in 45° flexion and 20° abduction.	Increased sensitivity to detect Cam deformities in the anterosuperior head-neck area.
LAUENSTEIN	Patient supine, hip-centred X-ray beam, hip and knee flexed, and hip in maximal abduction.	Anterior and posterior femoral head-neck contour.
FROG-LEG LATERAL	Patient supine, pelvis-centred X-ray beam, both hips and knee flexed, and the leg abducted so the soles of the feet contact.	Anterior and posterior femoral head-neck contour.
FALSE PROFILE	Patient standing, hip-centred x-ray beam, contralateral hip is tilted backward by 25°, ipsilateral foot remains parallel to radiographic table.	Anterior acetabular coverage, anterosuperior subluxation, quantification of posteroinferior joint space.
TRUE LATERAL	Patient supine, horizontal X-ray beam from lateral and centred to the hip.	Pelvic inclination; concomitantly performed with AP pelvis view to correlate pelvic inclination with vertical distance from symphysis to sacrococcygeal joint on AP pelvis view.
FUNCTIONAL (ABDUCTION/ /ADDUCTION)	Patient positioning and centring of X-ray for AP pelvis view; additional abduction or adduction of the hip, possible combination of abduction, internal rotation and flexion.	Abduction view to differentiate between subluxation and true joint space narrowing in dysplastic hips, to simulate acetabular coverage following acetabular reorientation or femoral osteotomy.

TABLE 4 – Radiographic projections of the hip.

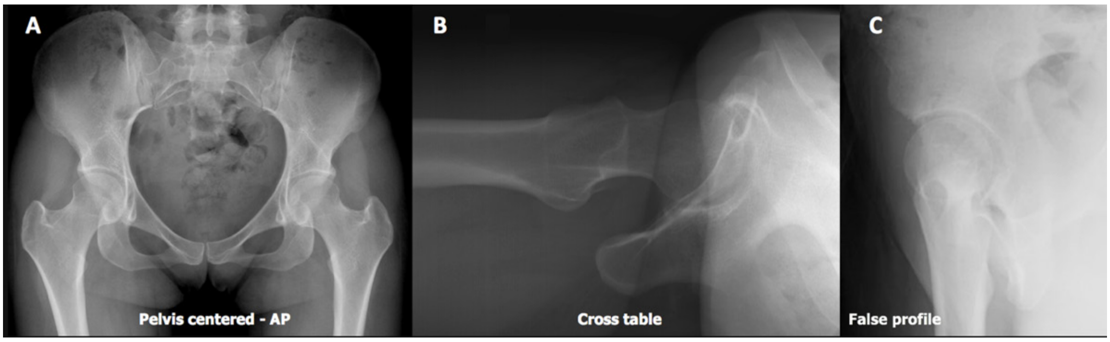

FIGURE 17 – Radiographic views: Standing anteroposterior pelvic (A), cross table lateral (B) and false profile (C).

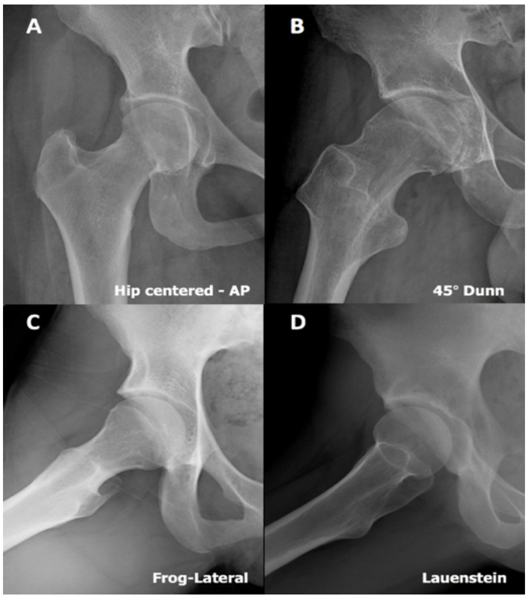

FIGURE 18 – Radiographic views: Anteroposterior hip centred (A), Dunn 45° (B), frog-leg lateral (C) Lauenstein (D).

2.1.3 Femoral head and neck evaluation

Considering the 3D geometry of the hip, in addition to the classically described parameters that relate the femoral shaft and the FHN and their thresholds (CCD angle = 130–135°[84] and femoral neck anteversion = 10°[85,86]), it is important to consider the relation between the FH itself with the neck (Table 5).

FEMUR AND JOINT	PARAMETER	VALUES	RADIOGRAPH	DEFINITION	NORMAL FINDINGS
FEMUR SPHERICITY	ALPHA (BETA) ANGLE[87] (Figure 20)	(°)	Axial and AP pelvis	Angle formed by the FHN axis and line through the centre of the FH and the point where the anterior (posterior) head-neck contour exceeds the head radius.	<50 (42±7)
	PISTOL-GRIP DEFORMITY[95,96]	Qualitative	Axial and AP pelvis	Seen as a "bump" to the FHN junction.	Absent
	FLATTENING OF THE LATERAL ASPECT OF THE FEMORAL HEAD[80,91]	Qualitative	Axial and AP pelvis	The head was said to be aspherical if the femoral epiphysis extended more than 2 mm outside the reference circle corresponding to a spherical head.	Absent
	GAMMA (DELTA) ANGLE[85] (Figure 19)	(°)	AP pelvis	Angle formed by the femoral head-neck axis (a) and line through the centre of the femoral head (C) and the point where the cranial (caudal) head-neck contour exceeds the head radius.	53±13 (43±5)
	OFFSET[96,97]	(mm)	Axial and AP pelvis	Difference (o) between the femoral head radius (r) and the neck radius.	>10
	OFFSET RATIO[98]	na	Axial and AP pelvis	Ratio of offset (o) to the femoral head radius (r). If the ratio is <0.17, a Cam deformity is likely present.	>0.20
	FEMORAL DISTANCE[99]	(mm)	Axial and AP pelvis	The perpendicular distance between a tangent along the cortex of the femoral neck and the point of the largest osseous deformity at the FHN junction.	2.2 to 3.6
	TRIANGULAR INDEX[100]	na	AP pelvis	A perpendicular line (p) is drawn at half the head radius (r). Distance (R) is measured from the femoral head centre (C) to the point where (p) intersects the anterior femoral head-neck contour. The triangular index is positive if R = r + 2 mm.	Negative
JOINT CONGRUENCY	SHENTON'S LINE [101]	(intact/ interrupted)	AP pelvis	Interrupted if the caudal femoral head-neck contour and the superior border of the obturator foramen do not form a harmonic arc.	Intact
	LATERALIZATION OF FEMORAL HEAD OR POSITION OF THE HIP CENTRE [81]	(mm)	AP pelvis	Shortest distance between the medial aspect of the femoral head (FH) and the ilioischial line (IIL). Lateralized if greater than 10 mm.	<10
ADDITIONAL FINDINGS	CERVICODIAPHYSEAL ANGLE[84]	(°)	AP pelvis	Angle formed by the FHN axis (C) and the femoral shaft axis (D).	129–135
	FOVEA ANGLE DELTA[12]	(°)	AP pelvis	Angle formed by a line through the medial edge of the acetabular roof (M) and the centre of the FH (C) and a line through the lateral border of the fovea capitis (F) and the centre of the FH (C).	26 ± 10
	JOINT SPACE WIDTH (JSW)[102]	(mm)	AP Pelvis standing	Measured radially at three locations within the joint: Medially (at the medial margin of the weight bearing surface), centrally (determined by a vertical line through the centre of the FH), and laterally (at the lateral margin of the subchondral sclerotic line).	≥4
	FEMORAL TORSION[103]	(°)	Transverse images over proximal and distal femur	The angle between the longitudinal axis of the femoral neck and the tangent at the condyles of the distal femur.	10–25

TABLE 5 – Imaging parameters to describe the proximal femoral morphology (see Figure 21 for illustration). na: not applicable; (°): degrees; (mm): milimeters.

In 2009, Toogood et al.[85] published an anatomical study on 375 femurs stated as a representative sample of the human population considering the following important parameters (Figure 19 and 20):

- **I.** Translation – examined through four offset FHN measurements (anterior, posterior, superior, inferior);
- **II.** Concavity of the FHN junction – measured from four angles; two in the horizontal plane (α-alpha and β-beta, respectively anterior and posterior), and two in the coronal plane (γ-gamma and δ-delta, respectively upper and lower);
- **III.** Rotation of the head in relation to the axis of the femoral neck (based on the orientation of the growth cartilage scar);
- **IV.** Neck-shaft relationship – assessed using neck version and CCD.

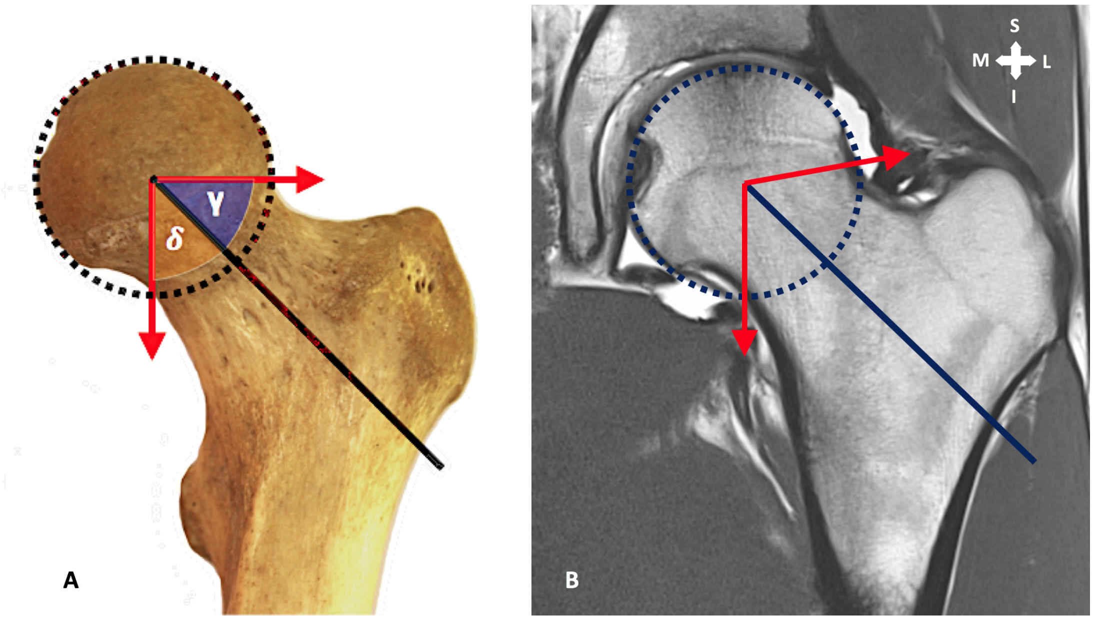

FIGURE 19 – (A) Photography of a cadaveric specimen with illustrated angles and lines; (B) direct arthrography magnetic resonance, coronal plane (proton density; TR:2300ms, TE:32ms). The represented angles respectively exemplify the measurement of the concavity at the transition between the neck and the head. They are formed by the axis line of the femoral neck and the line that intercepts it in the geometric centre of the femoral head and passes simultaneously at the point of the circumference of the femoral head when it meets the neck. The alpha angle is a measure of focal, two-dimensional, asphericity. In the population studied by Toogood, averages for gamma and delta angles were ɣ = 41.85°; δ = 42.95° respectively.

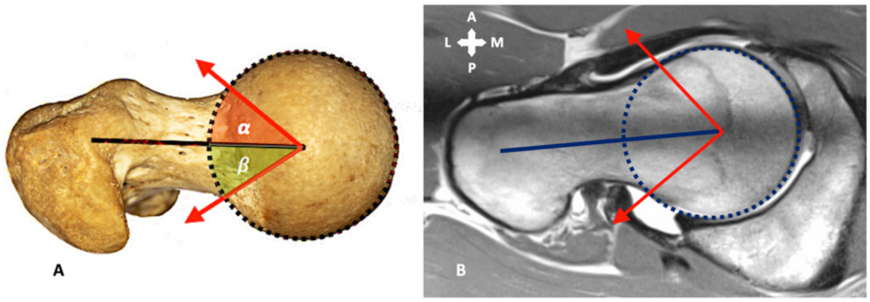

FIGURE 20 – (A) Photography of a cadaveric specimen with illustrated angles and lines; (B) direct arthrography magnetic resonance, axial oblique plane (proton density; TR:2500ms, TE:37ms). The represented angles respectively exemplify the measurement of the concavity at the FHN (in the population studied by Toogood, averages for α/β were 45.6°/41.8° respectively).

The angles measuring concavity of the FHN are an adaptation of the alpha angle (α°)[87], initially described on an axial oblique MRI as the measure to quantify the sphericity of the FHN junction. The α° is clinically applied to quantify the sphericity of the FH and it has been used with other imaging techniques[61,88-93] and in other locations of the FH[90,93] to characterise the deformity from a 3D perspective[93,94].

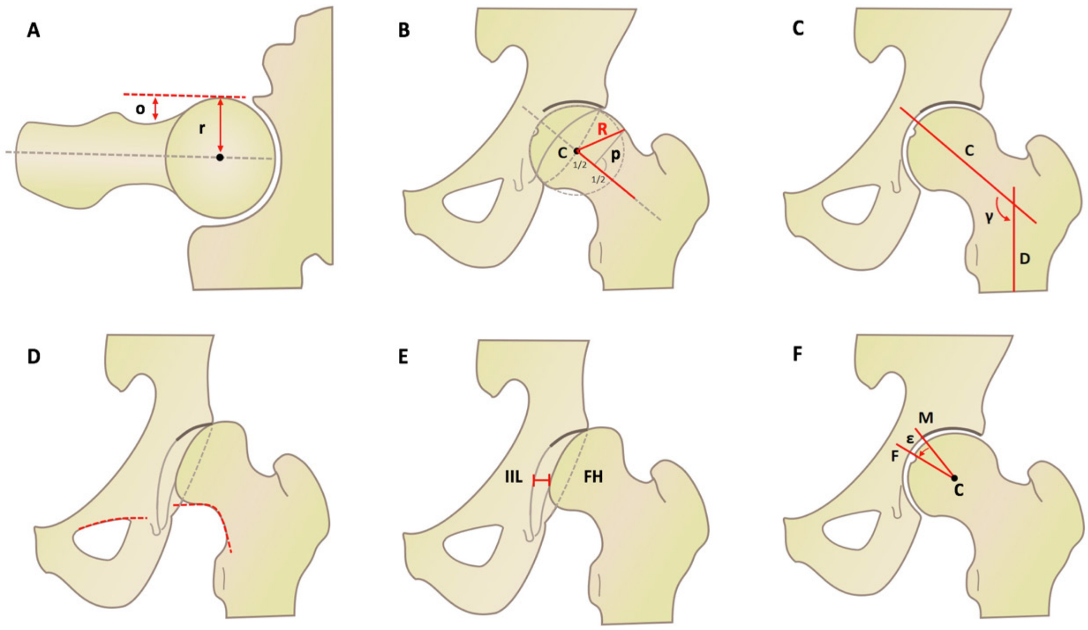

FIGURE 21 – Imaging parameters to describe proximal femoral morphology. See Table 5 for definitions. (A) offset and offset ratio; (B) triangular index; (C) cervicodiaphyseal (CCD) angle; (D) Shenton's line; (E) lateralization of femoral head; (F) fovea angle delta.

2.1.4 Acetabular evaluation

The morphology of the acetabulum has been described as a horseshoe-like articular surface, incompletely surrounding a quadrangular non-articular surface referred to as the acetabular fossa[104]. The quantifiable aspects of the acetabular morphology are defined in two parameters: Size and orientation (Table 6 and Figures 22–25).

I. The size depends on the i) depth, ii) the extent of the articular cartilage-lined area and the iii) size of the non-articular central region;
II. The orientation depends mainly on the dynamic pelvic orientation itself. In some cases, there may be poor spatial orientation of the cavity relative to the hemi pelvis itself[89].

ACETABULUM	PARAMETER	VALUES	RADIOGRAPH	DEFINITION	NORMAL FINDINGS
DEPTH	***COXA PROFUNDA***[12]	Qualitative	AP pelvis	Acetabular fossa (AF) touches or crosses the ilioischial line (IIL).	Absent
	PROTRUSIO ACETABULI[12]	Qualitative	AP pelvis	Femoral head (FH) touches or crosses the ilioischial line (IIL).	Absent
	ACETABULAR DEPTH[12]	(mm)	CT/MRI – transverse oblique image through the centre of the femoral neck	Distance between centre of FH and a line connecting the anterior/posterior acetabular rim. Positive if the centre of the FH is lateral to that line.	>3
COVERAGE	**LATERAL CENTER-EDGE**[105]	(°)	AP pelvis CT/MRI	Angle formed by a vertical line (v) and a line through the centre of the FH (C) and the lateral edge of the bone dense area (L).	20–39
	REFINED CENTER EDGE ANGLE OF OGATA[106]	(°)	AP pelvis	Lateral end of the sourcil, i.e., the weight bearing area of the acetabulum, rather than the lateral rim of the acetabulum.	15–35
	ACETABULAR ROOF ANGLE OF TÖNNIS OR SOURCIL ANGLE[78]	(°)	AP pelvis CT/MRI	Angle formed by a horizontal line (h) and a line through the medial (M) and lateral edge (L) of the acetabular roof.	0–14
	EXTRUSION INDEX[81]	(%)	AP pelvis	Percentage of the FH width (B) which is not covered by the acetabulum (A).	17–27
	SHARP ANGLE[101]	(°)	AP pelvis	Angle between a horizontal line (hL) and a line connecting the acetabular teardrop (TD) with the lateral edge of the acetabulum (LEA).	33–38
	ACETABULAR DEPTH-WIDTH RATIO[101]	na	AP pelvis	The depth of the acetabulum divided by the width of the acetabulum, multiplied by 1000, presented as a ratio: (A/B) * 1000.	Not described
	ANTERIOR CENTER-EDGE[12]	(°)	False profile CT/MRI	Angle formed by vertical line (V) and a line through the centre of FH (C) and the anterior edge of acetabulum (E)	>25

ACETABULUM	PARAMETER	VALUES	RADIOGRAPH	DEFINITION	NORMAL FINDINGS
COVERAGE	**COVERAGE** [107]	(%)	CT/MRI	Measures the % cover of the FH by the weight-bearing zone, with the position of the pelvis standardised in relation to a specific anatomical plane.	Posterior (35-43%) Anterior (30-38%) Total (66-81%)
	ACETABULAR VERSION[103] **(1, 2 AND 3 O'CLOCK)**	(°)	CT/MRI	Angle formed by the intersection of the line perpendicular to the line between the posterior pelvic margins and the line connecting the acetabular anterior/ posterior rim.	At the centre of the FH: 10–25. Abnormal at 3 o´clock if >30.
	AASA[108]	(°)	Axial CT slice through the centre of the FH	Lines through the centre of the FH and contralateral FH and tangential to the anterior lip of the acetabulum.	>60 (mean 63-64)
	PASA[108]	(°)	Axial CT slice through the centre of the femoral heads	Lines through the centre of the FH and contralateral FH and tangential to the posterior lip of the acetabulum.	>90 (mean 105)
	HASA[108]	(°)	Axial CT slices through the centre of the femoral heads	Lines through the anterior lip of the acetabulum, through the centre of the FH and the posterior lip of the acetabulum.	>140
ORIENTATION	**POSTERIOR WALL SIGN**	Qualitative	AP pelvis	Positive if the posterior wall (PW) runs medially to the centre of the FH (C).	Absent
	ANTERIOR AND POSTERIOR ACETABULAR WALL INDEX[12]	na	AP pelvis	Ratio of the width of the anterior (AW)/ posterior acetabular wall (PW) measured along the femoral head-neck axis (a), divided by the femoral head radius (r).	AWI: 0.41 (Range: 0.30–0.51) PWI: 0.91 (Range: 0.81–1.14)
	CROSSOVER SIGN[12]	Qualitative	AP pelvis	Anterior wall (AW) crosses the posterior wall (PW).	Absent
	RETROVERSION INDEX[12]	(%)	AP pelvis	Percentage of the retroverted acetabular opening (a) divided by the entire opening (b).	0
	ISCHIAL SPINE SIGN[12]	Qualitative	AP pelvis	Positive if the ischial spine (IS) is projected medially to the pelvic brim (PB).	Absent
OTHERS	**AIIS WIDTH**[12]	cm	CT/MRI		1
	DISTAL BASE OF AIIS TO ACETABULAR RIM[12]	cm	CT/MRI		≥0.5
	MCKIBBIN INDEX or COTAV[109]	na	CT/MRI	Sum of the femoral version angle and the acetabular version angle measured at 3 o'clock.	30–40

TABLE 6 – Radiographic parameters to describe acetabular morphology (see Figure 22 for illustration). AF: acetabular fossa; IIL: ilioischial line; FH: femoral head; COTAV: combined femoral torsion-acetabular version index; AIIS: anterior inferior iliac spine; AASA: anterior acetabular sector angle; PASA: posterior acetabular sector angle; HASA: horizontal acetabular sector angle; AWI: anterior acetabular wall index; PWI: posterior acetabular wall index; na: not applicable; (°): degrees; (mm): milimeters.

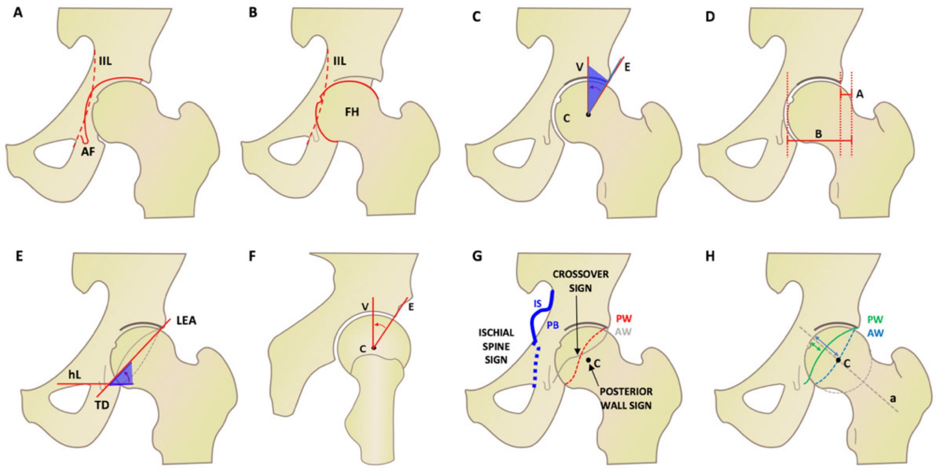

FIGURE 22 – Imaging parameters to describe acetabular morphology. See Table 6 for definitions and abbreviations. (A) *Coxa profunda*; (B) *protrusio*; (C) lateral center-edge angle; (D) extrusion index; (E) Sharp angle; (F) anterior center-edge angle; (G) posterior wall sign, ischial spine sign and crossover sign; (H) anterior and posterior acetabular wall index.

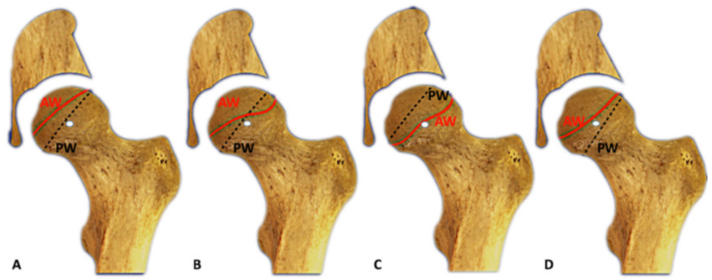

FIGURE 23 – Illustration of the normal projection of the anterior and posterior acetabular margin (which quantifies the acetabular version): The posterior projection (black line) should cross the centre of rotation of the femoral head and the anterior (red line) should lie more medial (A). When the posterior wall is normal and the anterior is more lateral, intersecting the posterior, we have a retroversion, with an "excess" of the antero-superior wall (B); when the posterior wall is more medial and the anterior wall more lateral, the acetabulum is overall retroverted (C); when the anterior wall is large and the posterior wall is lateral to the centre of rotation of the head, there is usually global acetabular hypercoverage (D). PW: posterior wall; AW: anterior wall.

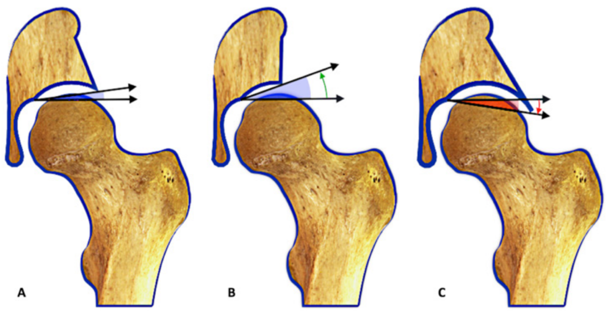

FIGURE 24 – Acetabular roof angle, between a horizontal line and a line that is tangent to the edge of the acetabular border, intersecting the inner border of the acetabular roof (loading area). The normal value is 0 to 10° (A); if > 10° (B), there is acetabular hypocoverage or dysplasia; if <0° (C), there is acetabular overcoverage that predisposes to Pincer-type impingement.

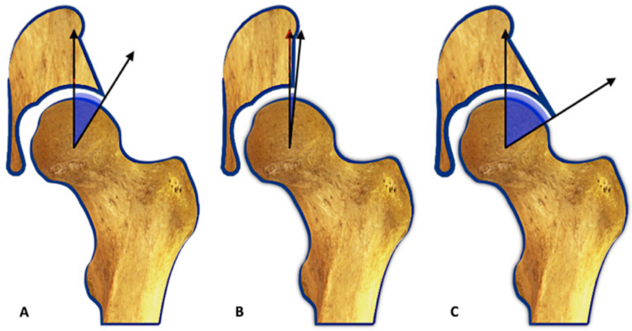

FIGURE 25 – Lateral center-edge angle (LCEA) coverage between a vertical line and a line that is tangent to the margin of the acetabular border, intersecting the geometric centre of the femoral head. The normal value is 25 to 30° (A); if <20° (B), there is acetabular undercoverage or dysplasia; if> 35° (C), there is acetabular overcoverage that predisposes to Pincer-type impingement.

2.1.5 Other Relevant Measurements

2.1.5.1 Femoral Torsion

In the first decade after the discovery of FAI, Cam- and Pincer-type deformities were considered the two main osseous abnormalities. Subsequently, abnormal femoral torsion (version) was recognized as an additional factor in the development of FAI[42,110]. In the last few years, its significance has been confirmed, and it is believed that torsion abnormalities are one of the three major osseous factors in the development of impingement, together with Cam/Pincer-type morphology[63,80]. Femoral torsion is the angle between the longitudinal axis of the femoral neck and the tangent at the condyles of the distal femur[12]. Usually, the femoral neck is pointing in an anterior direction compared to the femoral condyles, termed femoral antetorsion (or anteversion).

2.1.5.2 Spinopelvic parameters

The hip joint does not act in isolation. The pelvis moves around the bicoxofemoral axis, leading to various amount of tilt in different functional positions[33]. Accordingly, the spinopelvic (SP) morphology is thought to affect hip function and pathology. Pelvic tilt influences acetabular orientation, degree of femoral head coverage and impingement-free ROM[34]. In line with this, each individual is characterised by his/her pelvic incidence[111].

The measurements of interest included Pelvic Incidence (PI), Sacral Slope (SS) and Spinopelvic Tilt (PT), according to previously described methods[33] (Figure 26 and Table 7). PT and SS are dynamic parameters that change with hip motion and pelvic position. PI, in contrast, is a fixed parameter for each individual. In brief, PT and SS depend on posture (SS is higher when supine and lower when standing) and conjointly compose PI, which is an individual position-independent angle. With regard to pathology, there is a direct relationship between lumbar lordosis and SS, and a strong positive correlation between PI and sacral kyphosis. Han et al. concluded that a high PI value in patients with degenerative lumbar scoliosis might be associated with the high prevalence of degenerative lumbar spondylolisthesis. Also, in patients with isthmic spondylolisthesis, greater SP values are associated with a greater slip grade[33, 112-113].

Thus, the pelvic tilt is closely connected to the sagittal balance of the spine. In a patient with increased anterior PT, there is an increase of acetabular coverage when compared with a normal pelvic tilt[112]. This can be measured on standing lateral radiographs of the pelvis or with 3D imaging. A normal pelvic tilt is thought to be around 5.2±6.5°[113]. An increased anterior pelvic tilt results in a reduced internal rotation of the hip and can be a contributing factor to FAI[71]. The impact of the acetabular and SP morphologies in FAI and OA remains inadequately characterised. Amazingly, in current clinical practice for evaluating patients with suspected FAI, these are not regularly used.

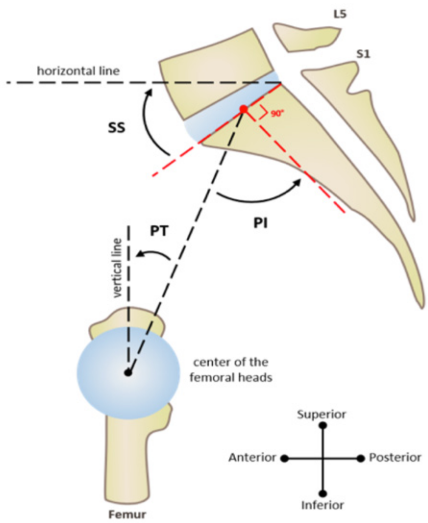

FIGURE 26 – Illustration representing spinopelvic parameters. See table 7 for definitions. Pelvic Incidence (PI), Sacral Slope (SS) and Pelvic Tilt (PT).

SPINOPELVIC PARAMETERS	PARAMETER	VALUES	RADIOGRAPH	DEFINITION
	Pelvic incidence	(°)	Standing sagittal lumbosacral	Angle between the line perpendicular to the sacral plate at its midpoint and a line from the mid-point between the axis of the two femoral heads to the center of the surface of the sacrum. PI = SS + PT
	Sacral slope	(°)	Standing sagittal lumbosacral	Angle formed by a line drawn parallel to the end plate of the sacrum to a horizontal reference line.
	Pelvic tilt	(°)	Standing sagittal lumbosacral	Angle formed by a line from the midpoint of the sacral end plate to the center femoral heads and a vertical reference line.

TABLE 7 – The spinopelvic parameters. Definition of pelvic incidence, sacral slope and pelvic tilt. PI: pelvic incidence; SS: sacral slope; PT: pelvic tilt; (°) degrees.

2.2. CURRENT AND FUTURE PERSPECTIVES ON IMAGING

“Imaging the Young Adult Hip in the Future”

Mascarenhas VV, Caetano A. Ann Joint 2018; 3:47. doi: 10.21037/aoj.2018.04.10

Imaging the young adult hip in the future

Vasco V. Mascarenhas[1], **António Caetano**[2]

[1]MSK Imaging Center (UIME), Hospital da Luz, Lisboa, Portugal; [2]Radiology Department, Hospital Curry Cabral, Lisboa, Portugal

Contributions: (I) Conception and design: All authors; (II) Administrative support: All authors; (III) Provision of study materials or patients: All authors; (IV) Collection and assembly of data: All authors; (V) Data analysis and interpretation: All authors; (VI) Manuscript writing: All authors; (VII) Final approval of manuscript: All authors.

Correspondence to: Vasco V. Mascarenhas. MSK imaging center (UIME), Hospital da Luz, Av. Lusiada 100, 1500-650 Lisboa, Portugal. Email: mascarenhas.vasco@gmail.com.

Abstract: The past fifty years have transformed diagnostic imaging of the hip joint. Innovation has been the catalyst for the transformation of radiology, as the arrival of new imaging modalities and the introduction of magnetic resonance imaging, resulted in a paradigm shift from bone morphology analysis to integrated soft tissue, joint and cartilage assessment. Hip pathology in general and the concept of femoroacetabular impingement (FAI) has come to the forefront of imaging and orthopedics. In just a few years, MRI findings that were in the past ascribed to degenerative change or normal variation must now be integrated in different entities, such as cam impingement or subspine impingement. Understanding the pathophysiology through the visualization of osseous structures and detailed depiction of soft tissue structures has become part of routine clinical imaging and has had a major impact on therapeutic decision-making. The purpose of this article is to provide a historical perspective on the utility of various types of imaging techniques for the hip joint, including cutting-edge clinical applications and topics at the forefront of musculoskeletal research. The current limitations as well as future directions of biochemical imaging will be outlined. Finally, emerging trends that will shape the field of hip imaging in the years to come will be discussed.

Keywords: Hip; imaging; femoroacetabular impingement (FAI); magnetic resonance

Received: 23 February 2018; Accepted: 20 April 2018; Published: 26 May 2018.
doi: 10.21037/aoj.2018.04.10
View this article at: http://dx.doi.org/10.21037/aoj.2018.04.10

Introduction

Musculoskeletal (MSK) imaging has undergone a major transformation over the past five decades. Advancements in orthopaedic surgery and arthroscopy have developed in unison with imaging techniques, which has led to improvements in clinical diagnosis, therapeutic interventions and patient prognostication.

With recent major developments of magnetic resonance imaging (MRI), attention has turned to the unique capability of defining bone morphology and soft tissue abnormalities. Additionally, the development of state-of-the-art quantitative MRI techniques has allowed for the depiction of early stage cartilage lesions (1). However, MRI is still limited in its ability to provide static morphological diagnosis. In the future, we will likely see all-in-one patient-centric examinations based on MRI, which can provide valuable information on joint morphology, biochemical function and dynamic "*in vivo*" assessment.

Imaging

The past

Conventional radiography (XR) remains the cornerstone of hip imaging (2), and continues to have a role in screening, diagnosis and post-operative surveillance. The advent of computed tomography (CT), represented a transformation in clinical practice from XR to cross-sectional imaging. Initially, only low-quality axial two-dimensional images were available and examination times were even longer than current MRI acquisition times. Only with the establishment

Table 1 Timeline of major achievements in imaging and hip orthopedics

Timeline	Authors	Findings or procedure	Event
1933	Elmslie (4)	"many patients who develop OA at a comparatively early age – for example from 40 to 50- will be found to have a pre-existing deformity of the joint"	Landmark on research to determine the cause of hip OA
1958	Wiles (5)	Precedent of the modern genre arthroplasties	First prosthetic total hip replacement
1965	Murray (6)	Concept that secondary OA also derives from cases with subtler morphologic hip deformities. OA secondary to the "tilt deformity"	OA described as secondary if associated to a pre-existing deformity
1974	Ambrose and Hounsfield (7,8)	The first description of a Computerized axial tomography in the radiology literature by Hounsfield and colleagues in the British Journal of Medicine	First clinical application of computerized axial tomography
1975	Murray and Stulberg (6,9)	"pistol grip deformity" first described as a finding similar to the "tilt deformity", including a flattened lateral femoral neck with widening and shortening of the FHN	Cam deformity first described
1976	Mansfield (10)	Finger image of the Dr. Maudsley	First-ever human MRI image
1987	Hajek (11)	To enhance the efficacy of MRI in evaluating articular soft-tissue structures, arthrography was performed before imaging in 45 fresh cadaveric specimens	First study of direct magnetic resonance arthrography with gadopentetate dimeglumine/saline mixture into cadaveric shoulder joints
1993	Langen (12)	Image quality improved with substantial radiation dose reduction	Introduction of digital radiography
1998	–	Simultaneous acquisition of four interweaving helices or spiral paths where previously there had been only one had a profound effect on the volume and spatial resolution of imaging	First multidetector (four-detector row) scanner CT
2001	Ganz (13)	Safe hip surgical dislocation	Understanding the pathophysiology of FAI

FHN, femoral head-neck; OA, osteoarthritis.

of multiplanar reconstructions based on 3D data sets was the use of CT in MSK imaging transformed (3), allowing for accurate and improved surgical planning (*Table 1*).

MRI allows for a more comprehensive analysis of the articular cartilage, capsulolabral tissue, soft-tissue and osseous structures (14). Thirty years ago, MRI examinations were technically difficult and resulted in low resolution images. The development of MR arthrography (MRA) had a major impact on treatment decisions, particularly in the evaluation of cartilage and labral integrity (2). In the mid-1990s MRA was the examination of choice for the evaluation of labral disruption, and remains the imaging gold-standard for patients with femoroacetabular impingement (FAI) (15).

The present

The hip joint has gained particular attention in the last decade in parallel with significant advances in MSK imaging. Ganz developed a revolutionary technique that allowed for safe dislocation of the hip and direct visualization of the joint, which provided fundamental insights into the pathogenesis of early osteoarthritis (OA) (3,13). New biomechanical concepts were recognized such as the depiction of FAI as a major cause of secondary OA in non-dysplastic hips (14-18).

Crucial questions still remain to be answered. For instance:

(I) What morphological factors, beside cam-type FAI and dysplasia contribute to hip OA (19)?
(II) During disease progression, what is the exact discriminative point when cartilage damage becomes irreversible (20)?
(III) Why are some patients with FAI morphology asymptomatic and never develop OA (21-23)?

Accurately determining the amount of articular cartilage injury is important as it has a direct impact on the clinical decision-making between hip preservation surgery and total hip replacement (24). The workup of the young patient with hip pain generally follows specific algorithms (25)

(*Figures 1,2*). The primary goals of diagnostic imaging are to accurately identify osseous morphology and characterize the amount of chondrolabral damage. However, it is important to understand the limitations and strengths of each imaging modality, as for example, both XR and CT lack accuracy for assessing articular cartilage pathology (2), whereas specific MRI sequences and advanced technologies can be useful (26).

New technical and imaging innovations are presently available in routine clinical setting, bringing important implications to the study of the young hip (21). The diagnostic performance of these techniques may therefore improve the ability to predict an individual patient-specific outcome (2,22).

1	HISTORY and EXAMINATION	CLINICAL ASSESSMENT
2	MORPHOLOGY	PELVIC RADIOGRAPH MRI
3	ARTICULAR DAMAGE	MRI
4	DIFFERENTIAL DIAGNOSIS	MRI
5	FINAL DIAGNOSIS	CLINICAL ASSESSMENT
6	TREATMENT	CLINICAL ASSESSMENT
7	FOLLOW-UP	CLINICAL ASSESSMENT MRI

Figure 1 Algorithm for evaluation of FAI used at Hospital da Luz in Lisbon. First, the diagnosis of FAI is suspected based on patient history and clinical findings. Next, the hip is assessed on an anteroposterior pelvic radiograph (acetabulum and pincer morphology) and on a 45° Dunn view. Using MRI, the morphology of the femur is assessed (cam deformities, femoral torsion) and damage to the cartilage and labrum is evaluated. Lastly, all data are combined to reach a diagnosis, define appropriate course of treatment and follow-up.

Radiography

After history and clinical examination, XR is useful to assess for OA, including evaluation of bone morphology, joint space width as well as to exclude other hip pathology (23). XR should include a standing anteroposterior (AP) view of the pelvis, and a lateral view of the affected hip. Nonetheless the utility and accuracy of the various types of radiographs remains controversial (25,27).

Ultrasound, arthrography and CT

Conventional arthrography is seldomly performed as it has been replaced by MRA. However, the origin of the referred hip pain might still be confirmed by intra-articular anesthetic injection (28). Ultrasound is not routinely used in the workup of FAI, although ultrasound-guided injection procedures can be helpful to exclude pain derived from periarticular structures such as trochanteric pathology, iliopsoas bursitis and other myotendinous elements (29). CT can be helpful in the characterization of fractures and unusual bony anatomy. Further, it is helpful to evaluate bony morphology of the pelvis, version, the anterior inferior iliac spine and extra-articular causes of impingement, as well as, building 3D models (30-32). Regarding FAI, pincer-type morphology is currently well addressed with standard

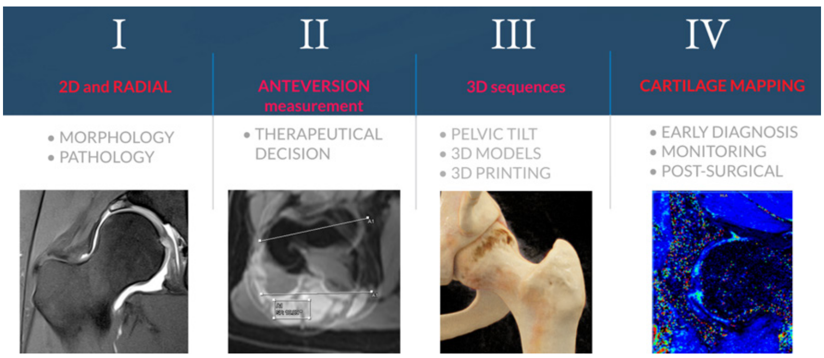

Figure 2 Schematic figure representing proposed complete MRI protocol for the assessment of the young hip. 2D sequences with radial imaging are used for the assessment of morphology and pathology. Version assessment of the femoral neck is performed. 3D sequences to allow for correction of pelvic tilting, 3D modelling, 3D printing and virtual ROM simulations. Finally, a sequence that allows for cartilage biochemical mapping.

pelvic XR (25), while for cam morphology, CT or MRI can offer a clear advantage since the complexity of the three-dimensional femoral shape can be thoroughly evaluated (33). Furthermore, measuring femoral version is only feasible with cross-sectional imaging (25).

Magnetic resonance imaging

MRI is an all-in-one imaging method as it depicts joint and periarticular pathology, including stress fractures, myotendinous injuries, bursitis and signs of ischiofemoral impingement (26). MRI can accurately assess bone morphology associated with FAI syndrome and detect chondrolabral damage. While conventional MRI can only detect macroscopic chondral damage (34), the presence of subchondral edema and cystic changes, have been shown to be indirect signs of advanced cartilage changes in the hip joint at the time of arthroscopy (35).

MRI techniques include (23,36):

(I) Conventional MRI;

(II) Magnetic resonance arthrography (direct/indirect; with or without traction);

(III) Quantitative biochemical MRI: T2/T2* mapping, delayed gadolinium-enhanced of cartilage (dGEMRIC) and T1rho (T1ρ).

Technical advances in MSK MRI are emerging with potential for implementation into clinical practice, namely (37,38):

(I) High-resolution 3D sequences for imaging of cartilage (23);

(II) Biochemical imaging of cartilage;

(III) 7.0 Tesla MRI (39);

(IV) Imaging of metal prosthetics with novel MRI pulse sequences (22).

New quantitative MRI imaging is encouraging for early detection of chondral and labrum injuries (40), as it probes changes in cartilage properties and biochemical composition, which represents an early stage of the degenerative cascade (41).

High-Resolution MRI

In order to obtain high-resolution MRI, a compromise between time and resolution is mandatory given that technical details are optimized (42,43). As such, some factors must be warranted:

(I) Time: maintain patient throughput with short examination times (around 30 minutes);

(II) Magnet: 3.0Tesla MRI has been widely adopted for hip evaluation. The theoretical doubling of signal-to-noise ratio can be used to obtain high-resolution (hR) imaging and/or shorter scan acquisition times;

(III) Coils: dedicated hip coils for optimal image quality (44). Improved coil geometry will further improve image quality;

(IV) Advanced morphological sequences (37):

- ❖ Implementation of parallel imaging allowing scan time to be accelerated;
- ❖ Compressed sensing;
- ❖ Isotropic MR images allowing for multiplanar reformats and 3D imaging.

MR arthrography

MRA can be performed by introduction of contrast material either (I) intra-articularly, as in direct MRA (dirMRA) or (II) intravenously, as in indirect MRA (indMRA) (45).

A detailed and comprehensive protocol for dirMRA should be strictly followed to achieve maximum quality (*Figures 2-6*). MRA of the hip plays a major role in:

(I) Diagnosing internal derangements of the joint (46);

(II) Evaluating symptomatic improvement following administration of anesthetic, helpful to confirm that symptoms and joint changes are related.

Several studies have compared the performance of these different protocols with variably reported accuracies (47-49). Previously, MRA has shown to be more accurate in detecting minor acetabular cartilage defects than non-contrast MRI (50,51). Diagnostic test accuracy was shown to be better for dirMRA when compared with conventional MRI for detection of labral and cartilage injury, in specific chondral lesions. Concerning indMRA, good results were also obtained, although more studies are needed to fully assess its accuracy (52). In patients with suspected FAI, MRA may still be considered the gold standard of imaging for the evaluation of the chondrolabral injury (25,49,53).

MR arthrography with leg traction

The rationale behind traction MRA (traMRA) is centered on the separation of the acetabular and femoral surfaces allowing a better assessment of the chondrolabral interface and central compartment (54,55). Recently, a study correlating traMRA with arthroscopy assessed the utility of this technique for the diagnosis of chondrolabral damage (55). Traction was well tolerated by most patients and consistently achieved separation of cartilage layers, enabling accurate detection of chondral and labral lesions (55).

Procedure: prior to the application of traction with the hip slightly flexed, a conventional arthrography injection

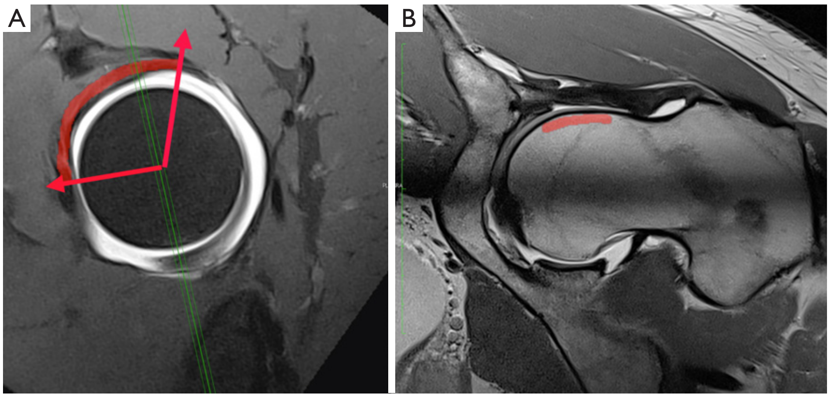

Figure 3 Direct arthro-magnetic resonance examination. Sagittal fat-suppressed proton-density sequence (A) and corresponding radial cut in Proton-Density (B). Red curved line represents CAM morphology assessed on the radial cut at 1:00 o'clock (B) and corresponding deformity in the sagittal plane extending from 11:30 to 3:00.

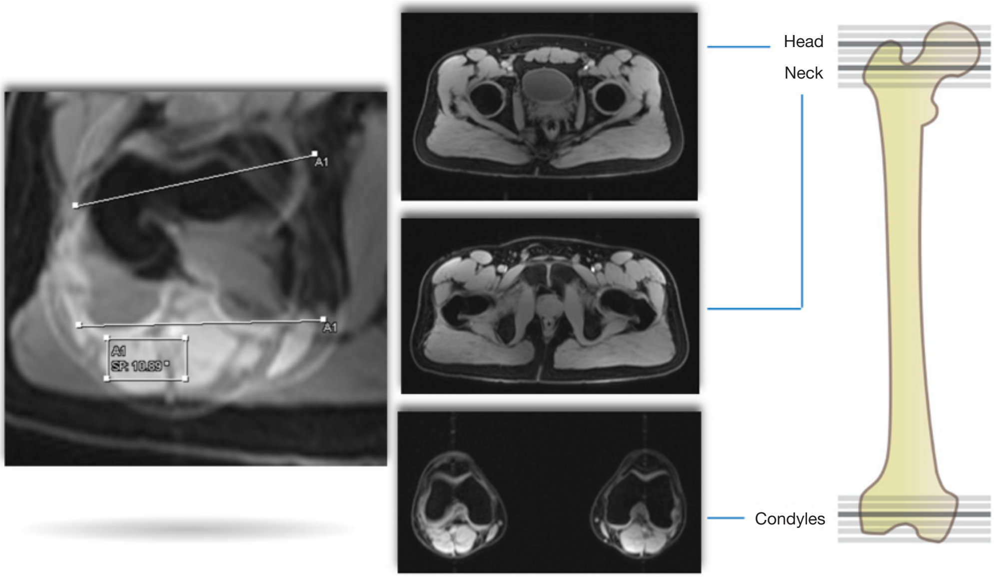

Figure 4 Measuring femoral torsion by MRI as a routine part of general hip workup. Femoral version is determined by the angle between the femoral neck axis and an axis parallel to the posterior aspect of the femoral condyles, measured in the transverse plane.

(10–27 mL) is performed and MR-compatible traction devices are routinely used for continuous traction during the examination. Traction devices consist of a weight connected to a pulley system, a cable or rope connected to the leg either with an ankle brace or with adhesive straps for skin traction. The amount of traction varies between 6 and 23 kg for a period ranging between 3 and 19 min among different studies (51,54,55).

Schmaranzer *et al.* (55) reported detection of acetabular/femoral chondral injury with a sensitivity of 85–88%/81–86% and specificity of 78–96%/91–94%, respectively (*Table 2*). The combination of contrast agent and additional space from distraction allows for improved visualization of the cartilage surfaces of the femoral head and acetabulum as

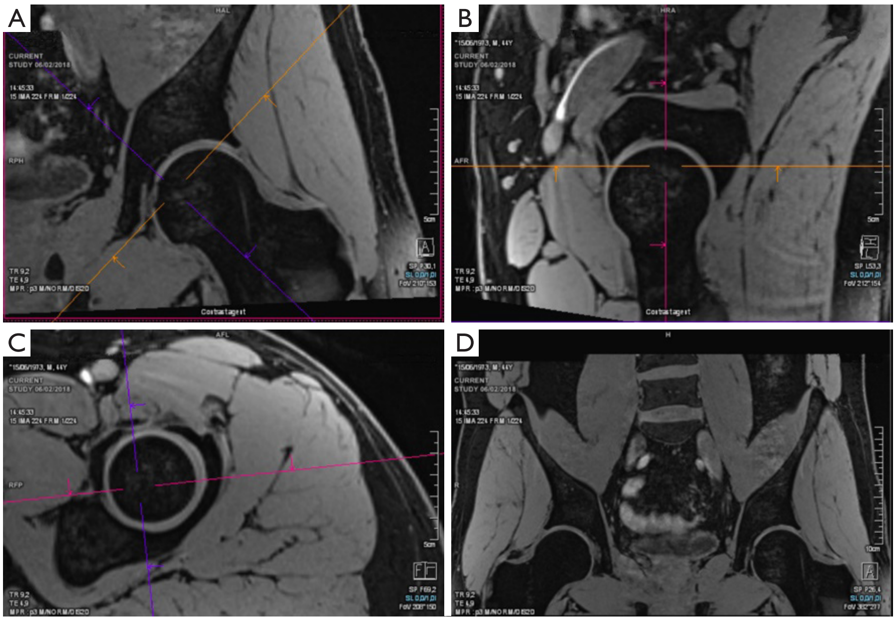

Figure 5 A 44-year-old male undergoing hip preserving surgery. Multiplanar reformats based on isotropic T1-VIBE sequence of the whole pelvis. (A) Coronal reformat of the hip. A Cam morphology is depicted on the transition of the superior quadrants with an intact chondrolabral junction; (B) oblique axial reformat (long axis of the neck), showing normal offset of the femoral head-neck junction; (C) short neck axis reformat; (D) coronal pelvic reformat.

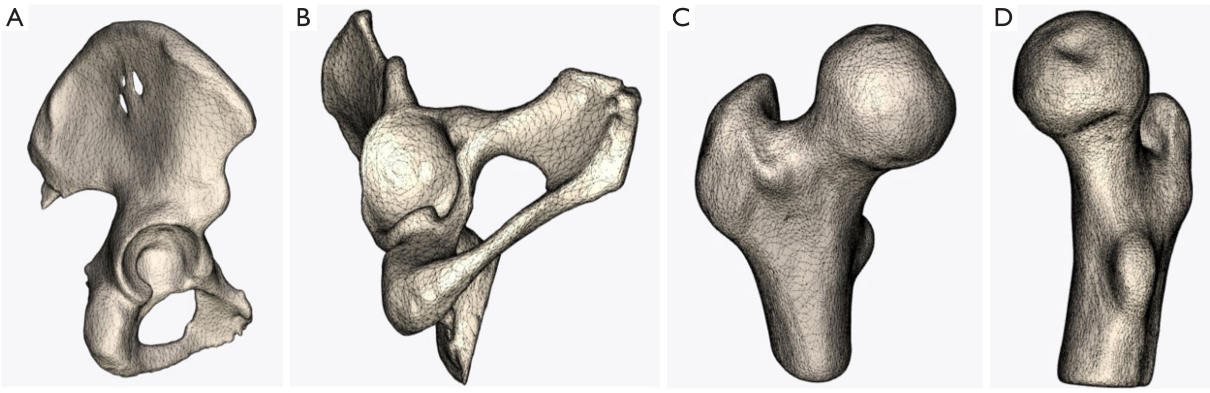

Figure 6 A 23-year-old female undergoing hip preserving surgery. 3D Model reconstructed based on volumetric MRI sequence of the pelvis. (A) Lateral view of the acetabulum; (B) inferior view of the acetabulum, showing normal pelvic morphology; (C) femoral 3D model anterosuperior view, showing discrete convexity of the femoral head neck junction; (D) medial view of the same model.

Table 2 Sensitivity and specificity for detection of chondral damage according to different studies using magnetic resonance

MRI techniques	Sensitivity (%)	Specificity (%)
MRA (53,56,57)	40–83	41–91
MRA with traction (55)	81–88	78–96

distinct entities.

Advanced cartilage imaging

Improved evaluation of articular cartilage status is imperative to allow both assessment of patients who may benefit from FAI surgery, as well as, long-term evaluation of clinical outcomes (26). Recognition of pre-existing degenerative changes at an early stage is therefore crucial. Although large defects can be confidently detected by conventional MRI, morphologic sequences lack crucial (quantitative) information on the pathophysiology of cartilage degeneration (36). Prior to structural damage of the cartilage, early changes can be evaluated using functional MRI techniques (1). This field remains an ongoing subject of research and future developments are necessary to allow its widespread use (1). Currently the main limitations include the narrow applicability of normative threshold standards (as they are dependent on multiple factors) and current indefinite clinical correlation. Challenges in quantitative imaging (17,23,41,58) presently include:

- (I) Hardware related:
  - (i) Need for dedicated cartilage-specific sequences and high-MR field strengths;
  - (ii) High signal-to-noise (SNR) ratio and high-spatial resolution;
  - (iii) Technical variations (changes in acquisition parameters can lead to limited comparability).
- (II) Anatomy related:
  - (i) Hip joint cartilage (deep location, thickness and its spherical shape);
  - (ii) Hip susceptibility to artifacts and volume averaging;
  - (iii) Mapping values represent the sum of the signal of joint fluid and both chondral surfaces;
  - (iv) Standard regional/sectorial differences in the biochemical composition of hip cartilage.
- (III) Patient related:
  - (i) Cartilage loading (has an influence on the extracellular matrix). Current recommendation is that this technique should be performed in the unloaded state at the end of the MR scan;
  - (ii) Inter-subject anatomic variations (can lead to misinterpretations with added limited comparability; patient-driven normalization can compensate for deviations caused by technical changes and variations related to age and individual cartilage configuration).

Quantitative MRI techniques (1) can probe the depletion and/or disorganization of proteoglycan and collagen/water (*Table 3*):

Delayed gadolinium-enhanced MRI of cartilage (dGEMRIC)

Glycosaminoglycan (GAG) are negatively charged polysaccharides (consist of NH and OH groups) that highly attract water and serve to resist compressive forces. High contents are found in the extracellular matrix of healthy cartilage (1). The dGEMRIC is used for assessing typical features of early-onset OA, namely GAG loss and collagen breakdown (41). It is based on the use of a contrast agent named gadopentetate dimeglumine [$Gd(DTPA)^2$]. $Gd(DTPA)^{2-}$ is an anionic molecule and is negatively charged. In the case of depletion of GAGs due to arthritis, these GAG's are replaced by $Gd(DTPA)^{2-}$ within the cartilage if given time. Consequently, the measurable $Gd(DTPA)^{2-}$ concentration is relatively low in native cartilage and relatively high in case of arthritis. The distribution of $Gd(DTPA)^{2-}$ in the cartilage can be measured by a T1 weighted sequence. By measuring the spatial variations between $Gd(DTPA)^{2-}$ and GAGs, the quality of cartilage can be determined (75,76).

This technique can either be used with direct intra-articular or intravenous injection of a contrast agent (75), and a time delay separating contrast agent administration and image acquisition is used (intravenous: 30–90 min; intra-articular: 15–30 min) (76). The most widely used protocol of Burstein recommends 10–20 minutes of exercise (e.g., walking, climbing stairs, and cycling) immediately after the contrast administration. No exercise is recommended after intra-articular based protocol. It has been suggested that isolated T1Gd assessment of the hip joint cartilage is sufficient for the evaluation without the need for time consuming pre-contrast imaging (except in the setting of post-operative cartilage repair) (77). Baseline dGEMRIC was shown to be able to predict the development of radiographic OA (40). Similarly, the size and position of cam morphology determined the severity and location of progressive cartilage damage, supporting the

Table 3 Main characteristics of MRI compositional techniques

Technique	Target	Sequences	Normal	Pathology	Pros	Cons
dGEMRIC (34,59-63)	Cartilage GAGs (concentration of negatively charged contrast molecules of Gd-DTPA is inversely proportional to the local proteoglycan concentration)	Intravenous or direct intra-articular application of contrast agent. T1 weighted sequence. Time frame between contrast agent administration and T1Gd relaxation time measurement	Higher T1Gd values toward the superior zone reflecting a high-GAG concentration at this weight-bearing region	Higher T1Gd relaxation time values will be measured in healthier cartilage, whereas low T1Gd values will be observed in degenerated, GAG-depleted cartilage. Lower T1Gd values in asymptomatic hips with cam deformities compared with morphologically normal hips. Severity of the GAG loss correlates with the magnitude of the cam deformity	Most studied and standardized methods Effectiveness in histological and biochemical evaluation of repair tissue at early stage after allograft chondrocyte implantation. May predict development of OA	2D-based technique. Longer acquisition time. Risk of motion artifacts. Regional differences in GAG concentration. Pharmacokinetic-related contrast agent uptake variations owed to age, sex, body
T1 ρ (64-66)	GAG (sensitive to the protons of hydrogen molecules attached to proteoglycans in the extracellular matrix)	"Spin lock" pulses to lock the transverse magnetization and drive the recovery of longitudinal magnetization	T1ρ relaxation time is inversely correlated with the GAG content in cartilage regions with normal T2 relaxation time	T1ρ values are increased with progressive joint degeneration	Seems to be more sensitive for the detection of early cartilage degeneration than T2 mapping. Does not require contrast. No time frame between contrast agent and MRI	Involves high-RF energy which can result in tissue heating. May not be specific to any one inherent tissue parameter, as concentration of other molecules beside collagen fibers produce changes in T1ρ values. Not commercially available and still requires post-processing. SNR ratio constraints associated with the thin cartilage layers and hip deeper location. Application in the hip joint relatively limited due to SNR constraints
T2 mapping (67-69)	Collagen and Water (sensitive to collagen and water content and collagen fiber orientation in the extracellular matrix)	Multi-echo spin-echo sequences	T2 values decrease progressively from surface layer to deep layer (because of anisotropy in different layers)	Damage to the extracellular matrix is associated with increased T2 relaxation times. Normal cartilage T2 gradient pattern becomes less apparent (pre-arthritic patients) or disappeared (early-arthritic patients)	Easy to implement. No contrast agent. No time frame needed. Well documented reproducibility and validity of T2 quantification	Long-acquisition times that typically exceed 10 min. Constraint on 2D acquisitions (magic angle effect). Less sensitive for detecting early stages of cartilage lesions. High degree of structural variation of the cartilage tissue with respect to location of the joint

Table 3 (*continued*)

Table 3 *(continued)*

Technique	Target	Sequences	Normal	Pathology	Pros	Cons
T2* mapping (70-74)	Collagen and water (bulk water content and interactions between water molecules and collagen fibers within cartilage)	Multi-echo gradient-echo sequences	Higher values in superficial zone (due to high-water content and superior molecule mobility), and lower T2* values in the cartilage-bone interface. Topographical T2* variations (low values posterior-superior and anterior-inferior at the periphery of the acetabulum)	Negative correlation between the histological grading of degenerated cartilage (Mankin grading) and T2*. Correlated T2* maps of acetabular cartilage (superficial, deep, and full-thickness cartilage) with intra-operative arthroscopic cartilage assessment (cartilage degeneration grading according to a modified Beck scale). Lower T2* values were noted for superficial, deep, and full-thickness cartilage in regions with intra- operatively identified cartilage damage	Easy to implement in clinical routine. Shorter acquisition times and higher resolution compared to T2 mapping. Ability to carry out isotropic 3D cartilage evaluation. Ultrashort echo-time enhanced T2* mapping of cartilage has the potential to visualize deep cartilage characteristics better than standard T2 mapping	Magic angle effects. Not fully validated for clinical diagnostics. More susceptible to artefact (Difficult mapping of articular cartilage in postoperative studies)

biomechanical etiology of FAI (18,78).

T2 and T2* mapping (*Figures* 7,*8*)

T2/T2* mapping have been shown to correlate with chondral matrix hydration and collagen integrity (1). Each tissue has a similar transverse relaxation time (T2) at a specified MR strength. Relaxation times are correlated to the speed by which nuclei lose phase after magnetic excitation. An additional de-phasing effect comes into play if gradient-echo MRI is performed, referred to as T2* mapping. T2 mapping is a well proven imaging modality (79). However, the orientation of collagen fibres influences the estimation of T2 relaxation values and reduces the accuracy of T2 mapping in certain regions of articular cartilage (magic angle effect). Due to the magic angle effect, T2 values of cartilage are influenced by its orientation relative to the static magnetic field (B0). Secondly, the acquisition times are relatively long. Thirdly, T2 mapping appears less sensitive for detecting early stages of cartilage lesions (80). T2* mapping has shorter acquisition times and higher resolution compared to T2 mapping although it is more prone to magic angle effects and is more susceptible to artifact (70).

T1ρ (T1 rho)

Similar to dGEMRIC, T1rho (T1ρ) relaxation time mapping is sensitive to the GAG content of hyaline cartilage. In a T1ρ sequence the spins in the direction of the B0 magnetization are first flipped into the transverse plane by a 90-degree radiofrequency (RF) pulse. A second RF pulse, better known as spin-lock pulse, is applied parallel to the magnetization vector. This spin-locked magnetization will relax with a time constant T1ρ and is dependent on the frequency and duration of the spin-lock pulse (TSL). The spin-lock pulse is applied with variable TSLs, at least two, at certain intervals which are also depended on the spin-lock frequency.

T1ρ—like T2 mapping—is founded on the motion of water molecules. T1ρ is widely considered to be sensitive to the protons of hydrogen molecules attached to proteoglycans of cartilage due to the second spin-lock pulse (64). Nevertheless, correlation with other factors, such as extracellular matrix, collagen content and collagen orientation were found too. The general consensus is that T1ρ may provide an imaging biomarker for the detection of cartilage degradation, based on the tissue's macromolecular content (41). In the FAI setting, it has been shown that early femoral and acetabular chondral changes can be detected before macroscopic lesions are apparent, and displays differences in distribution patterns across the deeper and

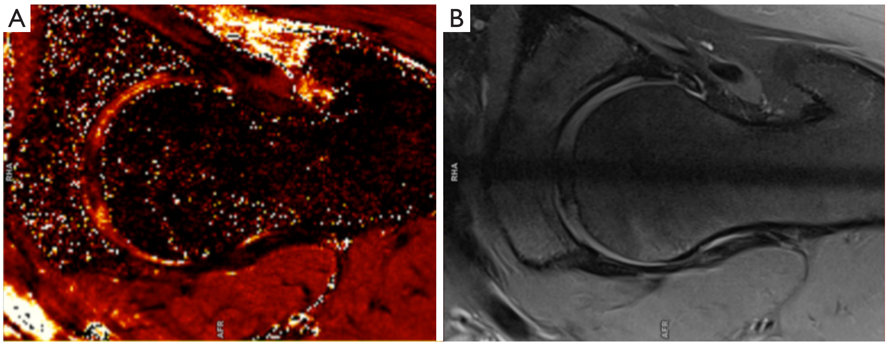

Figure 7 Pre-operative imaging of a 35-year-old female with mixed type FAI. (A) Radial T2 mapping measurements at 3.0 Tesla show decreased T2 relaxation times in the central compartment; (B) on the corresponding proton density radial cut morphological sequence, no obvious cartilage lesions are depicted.

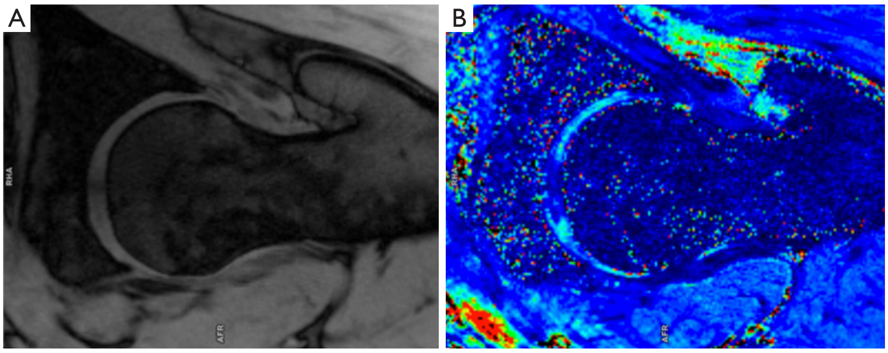

Figure 8 Pre-operative imaging of a 25-year-old male with CAM type FAI. (A) T2* radial cut morphological sequence; (B) radial T2* mapping measurements at 3.0 Tesla show decreased T2* relaxation times in the central compartment.

superficial cartilage layers (64,81).

gagCEST

gagCEST has been used in the knee joint and conceptually is the only technique that directly measures GAG cartilage content (82). It is based on an asymmetry in the z-spectrum of cartilage created by hydroxyl groups in the GAG molecule. The application of this method in the hip has not yet been demonstrated.

Sodium

Sodium (^{23}Na) cartilage imaging can be also performed in this setting. The rationale behind its use centers on the negatively charged GAG molecules in the cartilage binding of positively charged Na^+ maintaining the electroneutrality of the extracellular matrix (83). Na molecules conceptually distribute in proportion to the GAG molecules in degenerated articular cartilage. As such, proteoglycan cartilage loss caused by cartilage degeneration can be visualized (84). 3D-Isotropic MRI mapping sodium using a 7.0 Tesla system was used for the assessment of the knee, showing promise as a feasible alternative for evaluating OA (39). Limitations of sodium mapping include the need for a high-field MRI and dedicated hardware as well as anatomical constraints due to the deep location of the hip chondral surfaces.

Near future perspectives

Knowledge of biomechanics and physiopathology of the hip evolves in parallel with the need for non-invasive strategies to further assess the joint. As such, it is imperative for simultaneous advances in both static and dynamic automated imaging techniques. Currently, the acquisition

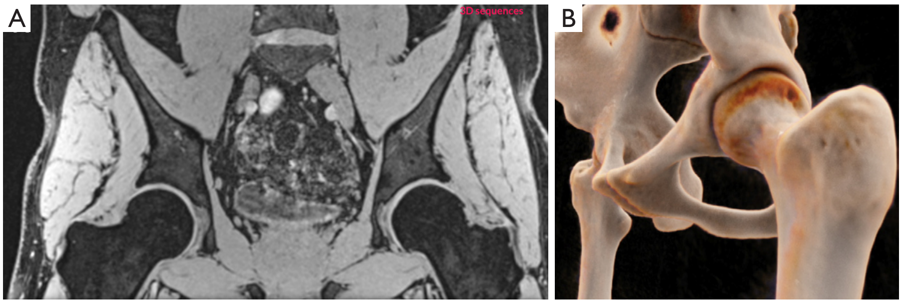

Figure 9 A 25-year-old female with hip pain undergoing MRI work-up examination, showing discrete osteophytes of the left femoral head. (A) Coronal volumetric MRI based sequence; (B) corresponding 3D Model with cinematic rendering quality.

of XR and MRA are the cornerstone of hip imaging. Computer-assisted (CompAssist) techniques have been based on data derived from isotropic CT images, while some studies based segmentation of those datasets on alternative tools such as MRI (85,86). However, MRI-based automated segmentation (AutSeg) has not yet reached the clinical standard due to relatively low contrast differences between bone and soft tissues (85).

The ideal future gold standard comprehensive all-in-one examination would comprise (23,87,88):

(I) Tools for accurate diagnosis and cartilage mapping;
(II) Pre-operative treatment planning and virtual treatment performance;
(III) AutSeg algorithms as well as intra-operative non-invasive registration methods such as statistical shape models (SM);
(IV) Intra-operative navigation (OpNav).

Developing OpNav tools to execute the pre-operative plan is currently a focus of expanding research, which has already seen clinical applications in hip and knee arthroplasty. These advances will hopefully lead to improved accuracy of intra-operative decision-making for both open and arthroscopic FAI procedures (89-91).

3D modeling (Figure 9)

Traditionally, surgeons have relied on 2D imaging to pre-operatively assess the hip, before evaluating areas of impingement by means of intra-operative dynamic visualization and fluoroscopy. However, subject-tailored surgical planning is developing on the basis of 3D hip modeling (92).

Patients with FAI have abnormal complex 3D bone and soft-tissues morphology. As such, routine 3D modeling may provide the surgeon a better understanding of the abnormal bony pathomorphology that would otherwise be difficult to visualize on 2D images. Models based on biplanar (92), 3D CT (30) or MRI (93) data sets (*Figure 9*) have been used to simulate specific individual bone morphology, define impingement-free range of motion (ROM), and to perform virtual functional analysis with different degrees of function (88). However, further clinical applicability and validation of these models for clinical diagnostics is still needed.

Automated image analysis

Most of the previous AutSeg work has been performed using XR (92) or CT (94-96). Advances in image processing have helped automate measurements, as well as, bone segmentation, thereby improving objectivity and reproducibility. Adding 3D anatomical information to the AutSeg (97) may be useful in reaching better imaging results that are less dependent on other parameters such as patient positioning.

MR imaging enables noninvasive, all-in-one, 3D assessment of the joint structure including biochemical changes with no ionizing radiation and optimal soft tissue contrast. Automated analysis using MR image sets (*Figure 10*) includes (85):

(I) An SM-based algorithm allows building 3D femoral and acetabular reconstructions;
(II) A coordinate system of the joint is generated to build a 2D shape map to project femoral head sphericity for calculation of specific parameters (for instance alpha angles);
(III) Automatically reformatted images using the constructed coordinate system;

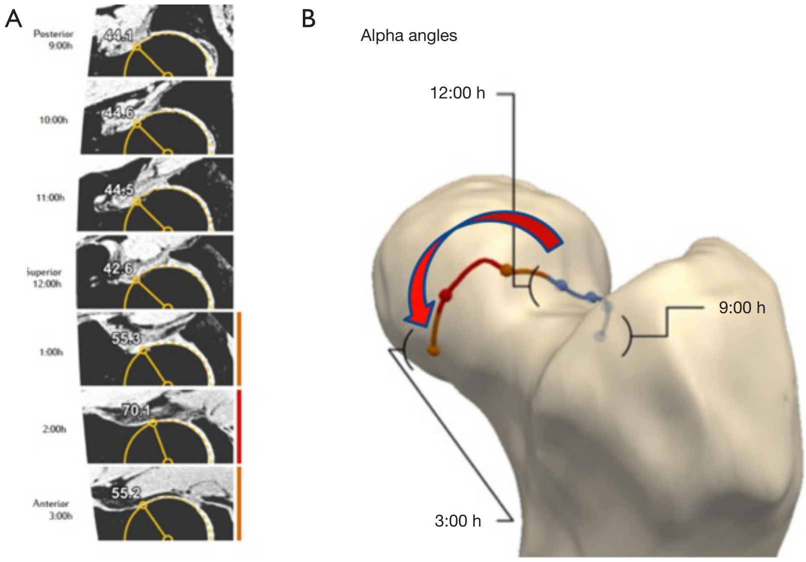

Figure 10 Volumetric semi-automated MR evaluation of the femoral head-neck junction with corresponding 3D model. (A) Automated alpha-angle (α°) measurements made at different points around the femoral head-neck junction in steps of 1° starting at 9 o'clock (posterior); 10, 11, and 12 o'clock (superior); and 1, 2, and 3 o'clock (anterior) (B). 3D Hip model (showing extension and location of a cam lesion represented on the corresponding 3D model (red arrow). Red and orange lines correspond to abnormal α°s; blue line represent normal α°s for a given α threshold.

(IV) Automated evaluation of desired parameters according to specified algorithm (*Figure 10*).

Advantages of 3D method analyzed MR images of the hip joint include (85,96,98):

(I) Allows for large-scale morphometric and clinical MR investigations of the hip region;
(II) High reliability and reproducibility;
(III) Improved analyses of cam-type morphology.

Imaging-based dynamic ROM simulations and virtual surgery

3D data sets of volumetric imaging bear high potential for the dynamic assessment of FAI allowing to perform pre-operative simulation of ROM, collision detection and accurate visualization of impingement areas. In addition to virtual 3D reconstruction of the hip joint, dynamic manipulation of the image may be useful to the surgeon, when pre-operatively assessing the deformity and planning for surgical correction (90) (*Figure 11*).

(I) "HipMotion" (86) constructs 3D representations of the femur and pelvis from CT. In addition, the model can be manipulated by the user, and pre-operative virtual ROM for patients with FAI can be calculated based on contact or interference occurring at the point of impingement.
(II) 3D software package Mimics (94) (Materialise, NV, Heverlee, Belgium). Automated morphologic analysis of the cam lesion can be conducted by MATLAB (Math Works, Natick, MA) and used to measure the clinical ROM of the hip joint. Measured motions are imposed on the 3D reconstructed anatomy, and the size and location of the abutting portion of the cam lesion are defined for each motion.
(III) "Dionics PLAN Hip Impingement Planning System" (Smith & Nephew, Andover, MA) is a tool used to analyze patient-specific CT images. After automatic 3D rendering of the hip, dynamic ROM can be analyzed and areas of bony impingement defined on both the proximal femur and acetabular rim/pelvis. In addition, virtual surgical correction can be performed and dynamic impingement-free ROM reassessed. This tool also provides a platform for intra-operative assistance by performing virtual correction and creating an *in vivo* comparative

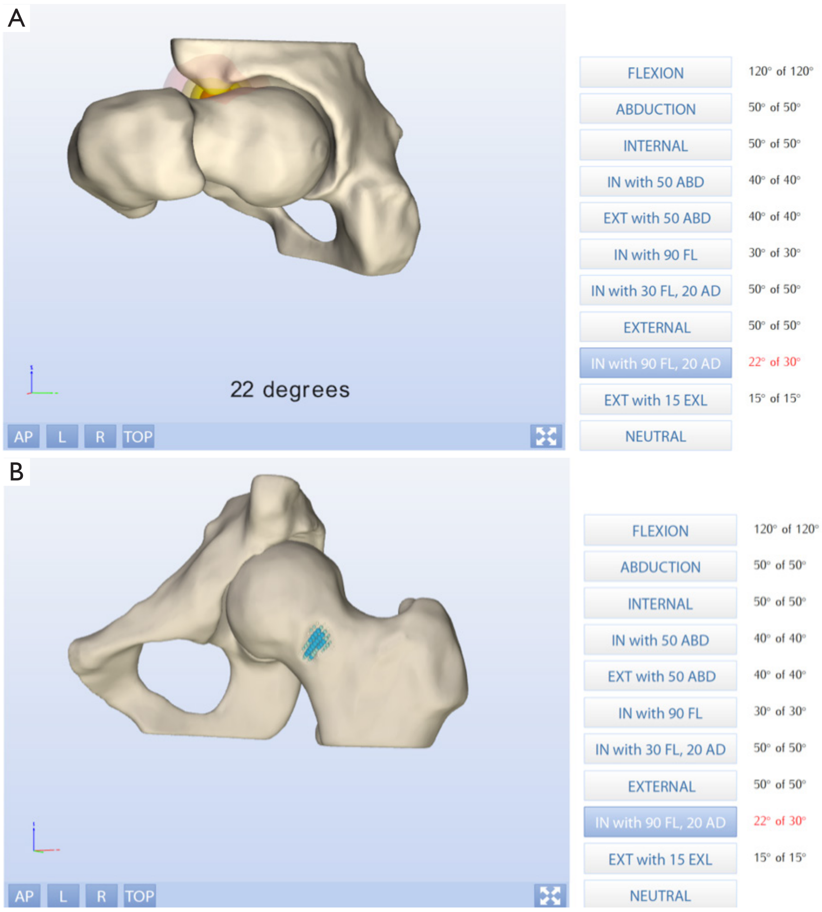

Figure 11 MRI based 3D modelling and dynamic virtual assessment. (A) Virtual ROM detects impingement areas at specific degrees of motion represented on the right. In this 30-year-old male with a cam deformity there was impingement noted at 22° of internal rotation with 90° of flexion and 20° adduction; (B) pre-operative planning allows depiction of areas of impingement on the virtual model (blue and green dots on the femoral head-neck junction).

virtual fluoroscopic image.

(IV) Hip Analysis/semi-AutSeg using "Articulis™" (Clinical Graphics, The Netherlands) has been validated and tested for reliability (30). Multiple studies have successfully used this software for research and clinical purposes in asymptomatic and symptomatic populations from CT and MRI data sets (22,23,99,100).

Computer-based navigation

3D imaging and computer navigation could play a major role in the planning of HPS. Furthermore, these advances could improve patient outcomes and lessen intra-operative and postoperative complications, such as under resection and over resection (88). For instance, it has been used in different hip pathologies, such has:

(I) FAI (88): a modified version of BrainLAB Hip-CT, which has primarily been used to assist with total hip arthroplasty (91) has been applied to arthroscopic FAI surgery. A C-arm adapter (Fluoro 3D, Vector Vision) can be used to synchronize the 3D CT dataset with intra-operative fluoroscopy allowing real-time feedback of surgical instrument placement in relation to the FHN (101). Planning and conduction of navigated osteochondroplasty using a surgical milling device was feasible and accurate (91).

(II) PAO (89): Pflugi *et al.* used two measurement units attached to the pelvis and peri-acetabular fragment. Registration of the patient was obtained with a pre-operatively acquired SM (considering the anterior pelvic plane) and a specific device used to include that orientation in the reference coordinate system. After registration, the two sensors are applied and orientation is displayed. A patient-SM generated from a pre-operatively acquired 3D data-set is used to monitor in real-time the re-orientation of the peri-acetabular fragment to improve femoral coverage.

Real-time functional imaging

Biomechanical knowledge on hip impingement has been limited from research using intra-operative observation (13) and computer models (86,102). Real-time *in vivo* impingement under conditions of physiologic joint loading would be ideal and hopefully lead to an improved understanding of which hips and morphologies become symptomatic.

Open MRI with ROM testing *in vivo* has significant advantages compared to computer simulations, image-based model tracking, intra-operative observation, and *ex vivo* studies as it permits (103):

(I) Assessment of impingement in hips during functional postures;
(II) Evaluating the effect of posture and cam/pincer morphology size on clinically meaningful impingement;
(III) Visualization of differences in cam morphology "behavior" between symptomatic and non-symptomatic cohorts.

Having virtual simulations as a starting point, one can easily appreciate the advantage of combined *in vivo* imaging and real time functional analysis.

3D printing

A long way was seen from radiographs to 3D printing (3Dpr), but undoubtedly computerization of radiology and orthopedics is an inescapable fact. 3D imaging and printing might be a step forward for patient-centric tailored approach, from individual anatomy to treatment planning and building specific hardware needed for each patient (99). 3Dpr might be applied in subject-specific tools and surgical device building (100,104), as well as, in complex clinical settings such as pelvic osteotomies (105).

A combination of 3Dpr and CompAssist virtual surgical planning has also been used for pre-operative planning of acetabular fracture reduction (106). The authors stated that 3Dpr technology combined with virtual surgery for acetabular fractures is feasible, accurate, and effective leading to improved patient-specific pre-operative planning and outcome of real surgery.

Future trends in MSK radiology

MRI in 2050

In brief, the future of MRI will include comprehensive 3D joint imaging, done within fractions of the time currently spent and multiparametric in nature, allowing for automated biochemical cartilage analysis. Undoubtedly MRI trends include:

(I) Field strengths greater than 3.0 Tesla will be the new standard;
(II) 3D MRI acquisitions with potential for secondary multiplanar reconstructions performed in any desired sequence weighting;
(III) hR non-contrast imaging will replace MRA, with improved hR 3D cartilage assessment;
(IV) Implementation of quantitative imaging biomarkers in clinical routine imaging;
(V) Semiautomated or fully automated diagnostic examinations (with the aid of artificial intelligence algorithms to diagnose and automatically quantify specific parameters).

Magnetic resonance fingerprinting (MRF) (107)

MRF uses a pseudorandomized acquisition that prompts the characteristics from different tissues to have a unique signal or "fingerprint" that is dependent of the unique multi-dimensional material properties under analysis. This technique permits a noninvasive quantification of multiple properties of a material or tissue simultaneously through a new approach to data acquisition, post-processing and visualization. These can then be translated into quantitative maps of the MR parameters of interest. This technique would be useful to:

(I) Provide a novel approach to analyze, quantify and diagnose simple and complex changes that can represent disease surrogates on early/preventable disease;
(II) Accurately identify the presence of targeted molecules/tissue-specific material, which will increase the diagnostic and prognostic capability of MRI;
(III) Substantially decrease measurement errors and improve accuracy when coupled with a specific pattern recognition algorithm.

Big data and artificial intelligence

Understanding the advantages and limitations associated with large databases, particularly in the era of value-based health care is paramount. The implementation of standardized national orthopedic registries in conjunction with readily programmable and adaptable programs tailored to radiologists and orthopedic surgeons will ultimately improve patient outcomes while minimizing the economic burden (108,109).

One promising new technology with the potential to launch the next stage of progress in medical image is artificial intelligence (AI), which is the science of engineering intelligent machines and computer programs. Machine learning (ML) derives from AI and is defined as a set of methods that automatically detect patterns in data, and then utilize those patterns to predict future data or enable decision making under uncertain conditions (110). Applications in medical imaging include (111) (I) automatic labeling and captioning; (II) image segmentation and registration; (III) computer-aided detection and diagnosis; (IV) acting as a reading assistant and automatic dictation; (V) integration with healthcare big data.

Personalized medicine and biobanks

Personalized medicine will transform radiology and the health system within the next 50 years. The original concept of precision medicine involves the prevention and implementation of treatment strategies that consider individual variability by assessing large sets of data, including patient information, medical imaging, and genomic sequences (112). Patient-based imaging data will be implemented and cross-linked to population based–data already acquired in biobanks. These biological databanks are designed to identify early environmental and genetic causes of normal and abnormal growth, development and health from fetal life until young adulthood. They are already well underway and established as a comprehensive population-based health knowledge (112).

Conclusions

Technological innovation was essential for the recent transformation of MSK imaging. State-of-the-art contemporary joint imaging has allowed for improved diagnostic accuracy of most conditions that affect the hip and surrounding structures. Imaging the hip in the future will permit an ultra-fast, near perfect, noninvasive automated quantification of clinically relevant bone and soft tissue pathology through data acquisition, post-processing and visualization. Conceptually, this will involve a personalized approach and population-specific matching to standardize data from healthy and diseased individuals.

Acknowledgements

The authors would like to thank José Roquette, João Sá, Isabel Vaz and Pedro Patrício for their continuing and enthusiastic support of clinical research at Hospital da Luz.

Footnote

Conflicts of Interest: The authors have no conflicts of interest to declare.

References

1. Oei EH, van Tiel J, Robinson WH et al. Quantitative radiologic imaging techniques for articular cartilage composition: toward early diagnosis and development of disease-modifying therapeutics for osteoarthritis. Arthritis Care Res (Hoboken) 2014;66:1129-41.
2. Sutter R, Zanetti M, Pfirrmann CWA. New Developments in Hip Imaging. Radiology 2012;264:651-67.
3. McEnery KW, Wilson AJ, Murphy WA. Comparison of spiral computed tomography versus conventional computed tomography multiplanar reconstructions of a fracture displacement phantom. Invest Radiol 1994;29:665-70.
4. Elmslie RC. Remarks on aetiological factors in osteo-arthritis of the hip-joint. Br Med J 1933;1:1-46.1.
5. Wiles P. The surgery of the osteo-arthritic hip. Clin Orthop Relat Res 2003;(417):3-16.

6. Murray RO. The aetiology of primary osteoarthritis of the hip. Br J Radiol 1965;38:810-24.
7. Ambrose J. Computerized transverse axial scanning (tomography). 2. Clinical application. Br J Radiol 1973;46:1023-47.
8. Hounsfield GN. Computerized transverse axial scanning (tomography). 1. Description of system. Br J Radiol 1973;46:1016-22.
9. Stulberg SDC, Harris LD, Ramsey WH, et al. Unrecognized childhood hip disease: a major cause of idiopathic osteoarthritis of the hip. The hip Proceedings of the third open scientific meetings of the hip society 1975.
10. Mansfield P, Maudsley AA. Medical imaging by NMR. Br J Radiol 1977;50:188-94.
11. Hajek PC, Baker LL, Sartoris DJ, et al. MR arthrography: anatomic-pathologic investigation. Radiology 1987;163:141-7.
12. Langen HJ, Klein HM, Wein B, et al. Comparative evaluation of digital radiography versus conventional radiography of fractured skulls. Invest Radiol 1993;28:686-9.
13. Ganz R, Gill TJ, Gautier E, et al. Surgical dislocation of the adult hip a technique with full access to the femoral head and acetabulum without the risk of avascular necrosis. J Bone Joint Surg Br 2001;83:1119-24.
14. Polak JF, Jolesz FA, Adams DF. Magnetic resonance imaging of skeletal muscle. Prolongation of T1 and T2 subsequent to denervation. Invest Radiol 1988;23:365-9.
15. Hodler J, Yu JS, Goodwin D, et al. MR arthrography of the hip: improved imaging of the acetabular labrum with histologic correlation in cadavers. AJR Am J Roentgenol 1995;165:887-91.
16. Ganz R, Parvizi J, Beck M, et al. Femoroacetabular impingement: a cause for osteoarthritis of the hip. Clin Orthop Relat Res 2003;(417):112-20.
17. Riley GM, McWalter EJ, Stevens KJ, et al. MRI of the Hip for the evaluation of femoroacetabular impingement; past, present, and future. J Magn Reson Imaging 2015;41:558-72.
18. Khan M, Bedi A, Fu F, et al. New perspectives on femoroacetabular impingement syndrome. Nat Rev Rheumatol 2016;12:303-10.
19. Thomas GE, Palmer AJ, Batra RN, et al. Subclinical deformities of the hip are significant predictors of radiographic osteoarthritis and joint replacement in women. A 20 year longitudinal cohort study. Osteoarthritis Cartilage 2014;22:1504-10.
20. Agricola R, Weinans H. Femoroacetabular impingement: what is its link with osteoarthritis? Br J Sports Med 2016;50:957-8.
21. Li AE, Jawetz ST, Greditzer HG 4th, et al. MRI Evaluation of Femoroacetabular Impingement After Hip Preservation Surgery. AJR Am J Roentgenol 2016;207:392-400.
22. Khodarahmi I, Fritz J. Advanced MR Imaging after Total Hip Arthroplasty: The Clinical Impact. Semin Musculoskelet Radiol 2017;21:616-29.
23. Sutter R, Stoel BC, Buck FM, et al. Internal Derangements of Joints-Past, Present, and Future. Invest Radiol 2015;50:601-14.
24. Ganz R, Leunig M, Leunig-Ganz K, et al. The Etiology of Osteoarthritis of the Hip. Clin Orthop Relat Res 2008;466:264-72.
25. Sutter R, Pfirrmann CWA. Update on Femoroacetabular Impingement: What Is New, and How Should We Assess It? Semin Musculoskelet Radiol 2017;21:518-28.
26. Li AE, Jawetz ST, Greditzer HG, et al. MRI for the preoperative evaluation of femoroacetabular impingement. Insights Imaging. Insights Imaging 2016;7:187-98.
27. Griffin DR, Dickenson EJ, O'Donnell J, et al. The Warwick Agreement on femoroacetabular impingement syndrome (FAI syndrome): an international consensus statement. Br J Sports Med 2016;50:1169-76.
28. Khan W, Khan M, Alradwan H, et al. Utility of Intra-articular Hip Injections for Femoroacetabular Impingement: A Systematic Review. Orthop J Sports Med 2015;3:2325967115601030.
29. Buck FM, Hodler J, Zanetti M, et al. Ultrasound for the evaluation of femoroacetabular impingement of the cam type. Diagnostic performance of qualitative criteria and alpha angle measurements. Eur Radiol 2011;21:167-75.
30. Röling MA, Visser MI, Oei EHG, et al. A quantitative non-invasive assessment of femoroacetabular impingement with CT-based dynamic simulation--cadaveric validation study. BMC Musculoskelet Disord 2015;16:50.
31. Weber AE, Jacobson JA, Bedi A. A review of imaging modalities for the hip. Curr Rev Musculoskelet Med 2013;6:226-34.
32. Kraeutler MJ, Chadayammuri V, Garabekyan T, et al. Femoral Version Abnormalities Significantly Outweigh Effect of Cam Impingement on Hip Internal Rotation. J Bone Joint Surg Am 2018;100:205-10.
33. Mascarenhas VV, Rego P, Dantas P, et al. Cam deformity and the omega angle, a novel quantitative measurement of

femoral head-neck morphology: a 3D CT gender analysis in asymptomatic subjects. Eur Radiol 2017;27:2011-23.
34. Bittersohl B, Steppacher S, Haamberg T, et al. Cartilage damage in femoroacetabular impingement (FAI): preliminary results on comparison of standard diagnostic vs delayed gadolinium-enhanced magnetic resonance imaging of cartilage (dGEMRIC). Osteoarthritis Cartilage 2009;17:1297-306.
35. Krych AJ, King AH, Berardelli RL, et al. Is Subchondral Acetabular Edema or Cystic Change on MRI a Contraindication for Hip Arthroscopy in Patients With Femoroacetabular Impingement? Am J Sports Med 2016;44:454-9.
36. Gold SL, Burge AJ, Potter HG. MRI of hip cartilage: joint morphology, structure, and composition. Clin Orthop Relat Res 2012;470:3321-31.
37. Ai T, Morelli JN, Hu X, et al. A historical overview of magnetic resonance imaging, focusing on technological innovations. Invest Radiol 2012;47:725-41.
38. Tao H, Shang X, Lu R, et al. Quantitative magnetic resonance imaging (MRI) evaluation of cartilage repair after microfracture (MF) treatment for adult unstable osteochondritis dissecans (OCD) in the ankle: correlations with clinical outcome. Eur Radiol 2014;24:1758-67.
39. Wang L, Wu Y, Chang G, et al. Rapid isotropic 3D-sodium MRI of the knee joint in vivo at 7T. J Magn Reson Imaging 2009;30:606-14.
40. Palmer A, Fernquest S, Rombach I, et al. Diagnostic and prognostic value of delayed Gadolinium Enhanced Magnetic Resonance Imaging of Cartilage (dGEMRIC) in early osteoarthritis of the hip. Osteoarthritis Cartilage 2017;25:1468-77.
41. Oei EH. Quantitative musculoskeletal imaging biomarkers. Quant Imaging Med Surg 2016;6:621-2.
42. Kuo R, Panchal M, Tanenbaum L, et al. 3.0 Tesla imaging of the musculoskeletal system. J Magn Reson Imaging 2007;25:245-61.
43. Shapiro L, Harish M, Hargreaves B, et al. Advances in musculoskeletal MRI: Technical considerations. J Magn Reson Imaging 2012;36:775-87.
44. Potter HG, Schachar J. High resolution noncontrast MRI of the hip. J Magn Reson Imaging 2010;31:268-78.
45. Ghebontni L, Roger B, El-khoury J, et al. MR arthrography of the hip: normal intra-articular structures and common disorders. Eur Radiol 2000;10:83-8.
46. Petchprapa CN, Rybak LD, Dunham KS, et al. Labral and cartilage abnormalities in young patients with hip pain: accuracy of 3-Tesla indirect MR arthrography. Skeletal Radiol 2015;44:97-105.
47. Leunig M, Podeszwa D, Beck M, et al. Magnetic resonance arthrography of labral disorders in hips with dysplasia and impingement. Clin Orthop Relat Res 2004;(418):74-80.
48. Perdikakis E, Karachalios T, Katonis P, et al. Comparison of MR-arthrography and MDCT-arthrography for detection of labral and articular cartilage hip pathology. Skeletal Radiol 2011;40:1441-7.
49. Smith TO, Hilton G, Toms AP, et al. The diagnostic accuracy of acetabular labral tears using magnetic resonance imaging and magnetic resonance arthrography: a meta-analysis. Eur Radiol 2011;21:863-74.
50. Waldt S, Burkart A, Lange P, et al. Diagnostic performance of MR arthrography in the assessment of superior labral anteroposterior lesions of the shoulder. AJR Am J Roentgenol 2004;182:1271-8.
51. Cerezal L, Carro LP, Llorca J, et al. Usefulness of MR arthrography of the hip with leg traction in the evaluation of ligamentum teres injuries. Skeletal Radiol 2015;44:1585-95.
52. Saied AM, Redant C, El-Batouty M, et al. Accuracy of magnetic resonance studies in the detection of chondral and labral lesions in femoroacetabular impingement: systematic review and meta-analysis. BMC Musculoskelet Disord 2017;18:83.
53. Sutter R, Zubler V, Hoffmann A, et al. Hip MRI: How Useful Is Intraarticular Contrast Material for Evaluating Surgically Proven Lesions of the Labrum and Articular Cartilage? AJR Am J Roentgenol 2014;202:160-9.
54. Llopis E, Cerezal L, Kassarjian A, et al. Direct MR arthrography of the hip with leg traction: feasibility for assessing articular cartilage. AJR Am J Roentgenol 2008;190:1124-8.
55. Schmaranzer F, Klauser A, Kogler M, et al. Diagnostic performance of direct traction MR arthrography of the hip: detection of chondral and labral lesions with arthroscopic comparison. Eur Radiol 2015;25:1721-30.
56. Schmid MR, Nötzli HP, Zanetti M, et al. Cartilage lesions in the hip: diagnostic effectiveness of MR arthrography. Radiology 2003;226:382-6.
57. Neumann G, Mendicuti AD, Zou KH, et al. Prevalence of labral tears and cartilage loss in patients with mechanical symptoms of the hip: evaluation using MR arthrography. Osteoarthritis Cartilage 2007;15:909-17.
58. Bittersohl B, Hosalkar HS, Hesper T, et al. Advanced Imaging in Femoroacetabular Impingement: Current State and Future Prospects. Front Surg 2015;2:34.

59. Mamisch TC, Kain MSH, Bittersohl B, et al. Delayed gadolinium-enhanced magnetic resonance imaging of cartilage (dGEMRIC) in Femoacetabular impingement. J Orthop Res 2011;29:1305-11.
60. Domayer SE, Mamisch TC, Kress I, et al. Radial dGEMRIC in developmental dysplasia of the hip and in femoroacetabular impingement: preliminary results. Osteoarthritis Cartilage 2010;18:1421-8.
61. Bittersohl B, Hosalkar HS, Apprich S, et al. Comparison of pre-operative dGEMRIC imaging with intra-operative findings in femoroacetabular impingement: preliminary findings. Skeletal Radiol 2011;40:553-61.
62. Guermazi A, Alizai H, Crema MD, et al. Compositional MRI techniques for evaluation of cartilage degeneration in osteoarthritis. Osteoarthritis Cartilage 2015;23:1639-53.
63. Zilkens C, Miese F, Krauspe R, et al. Symptomatic Femoroacetabular Impingement: Does the Offset Decrease Correlate With Cartilage Damage? A Pilot Study. Clin Orthop Relat Res 2013;471:2173-82.
64. Anwander H, Rakhra KS, Melkus G, et al. T1q Hip Cartilage Mapping in Assessing Patients With Cam Morphology: How Can We Optimize the Regions of Interest? Clin Orthop Relat Res 2017;475:1066-75.
65. Subburaj K, Valentinitsch A, Dillon AB, et al. Regional variations in MR relaxation of hip joint cartilage in subjects with and without femoralacetabular impingement. Magn Reson Imaging 2013;31:1129-36.
66. van Tiel J, Kotek G, Reijman M, et al. Is T1ρ Mapping an Alternative to Delayed Gadolinium-enhanced MR Imaging of Cartilage in the Assessment of Sulphated Glycosaminoglycan Content in Human Osteoarthritic Knees? An in Vivo Validation Study. Radiology 2016;279:523-31.
67. Watanabe A, Boesch C, Siebenrock K, et al. T2 mapping of hip articular cartilage in healthy volunteers at 3T: a study of topographic variation. J Magn Reson Imaging 2007;26:165-71.
68. Nishii T, Shiomi T, Tanaka H, et al. Loaded Cartilage T2 Mapping in Patients with Hip Dysplasia. Radiology 2010;256:955-65.
69. Yamamoto S, Watanabe A, Nakamura J, et al. Quantitative T2 mapping of femoral head cartilage in systemic lupus erythematosus patients with noncollapsed osteonecrosis of the femoral head associated with corticosteroid therapy. J Magn Reson Imaging 2011;34:1151-8.
70. Hesper T, Neugroda C, Schleich C et al. T2*-Mapping of Acetabular Cartilage in Patients With Femoroacetabular Impingement at 3 Tesla: Comparative Analysis with Arthroscopic Findings. Cartilage 2018;9:118-26.
71. Bittersohl B, Hosalkar HS, Hughes T, et al. Feasibility of T2*mapping for the evaluation of hip joint cartilage at 1.5T using a three-dimensional (3D), gradient-echo (GRE) sequence: A prospective study. Magn Reson Med 2009;62:896-901.
72. Bittersohl B, Miese FR, Hosalkar HS, et al. T2* mapping of acetabular and femoral hip joint cartilage at 3 T: a prospective controlled study. Invest Radiol 2012;47:392-7.
73. Apprich S, Mamisch TC, Welsch GH, et al. Evaluation of articular cartilage in patients with femoroacetabular impingement (FAI) using T2* mapping at different time points at 3.0 Tesla MRI: a feasibility study. Skeletal Radiol 2012;41:987-95.
74. Siebenrock KA, Kienle KP, Steppacher SD, et al. Biochemical MRI Predicts Hip Osteoarthritis in an Experimental Ovine Femoroacetabular Impingement Model. Clin Orthop Relat Res 2015;473:1318-24.
75. Zilkens C, Miese F, Kim YJ, et al. Direct comparison of intra-articular versus intravenous delayed gadolinium-enhanced MRI of hip joint cartilage. J Magn Reson Imaging 2014;39:94-102.
76. Zilkens C, Tiderius CJ, Krauspe R, et al. Current knowledge and importance of dGEMRIC techniques in diagnosis of hip joint diseases. Skeletal Radiol 2015;44:1073-83.
77. Lattanzi R, Petchprapa C, Glaser C, et al. A new method to analyze dGEMRIC measurements in femoroacetabular impingement: preliminary validation against arthroscopic findings. Osteoarthritis Cartilage 2012;20:1127-33.
78. Liu Q, Wang W, Thoreson AR, et al. Finite element prediction of contact pressures in cam-type femoroacetabular impingement with varied alpha angles. Comput Methods Biomech Biomed Engin 2017;20:294-301.
79. Matzat SJ, van Tiel J, Gold GE, et al. Quantitative MRI techniques of cartilage composition. Quant Imaging Med Surg 2013;3:162-74.
80. Hesper T, Hosalkar HS, Bittersohl D, et al. T2* mapping for articular cartilage assessment: principles, current applications, and future prospects. Skeletal Radiol 2014;43:1429-45.
81. Nozaki T, Kaneko Y, Yu HJ, et al. T1rho mapping of entire femoral cartilage using depth- and angle-dependent analysis. Eur Radiol 2016;26:1952-62.
82. Ling W, Regatte RR, Navon G, et al. Assessment of glycosaminoglycan concentration in vivo by chemical exchange-dependent saturation transfer (gagCEST). Proc

Natl Acad Sci U S A 2008;105:2266-70.
83. Binks DA, Hodgson RJ, Ries ME, et al. Quantitative parametric MRI of articular cartilage: a review of progress and open challenges. Br J Radiol 2013;86:20120163.
84. Bangerter NK, Tarbox GJ, Taylor MD, et al. Quantitative sodium magnetic resonance imaging of cartilage, muscle, and tendon. Quant Imaging Med Surg 2016;6:699-714.
85. Xia Y, Fripp J, Chandra SS, et al. Automated 3D quantitative assessment and measurement of alpha angles from the femoral head-neck junction using MR imaging. Phys Med Biol 2015;60:7601-16.
86. Tannast M, Kubiak-Langer M, Langlotz F, et al. Noninvasive three-dimensional assessment of femoroacetabular impingement. J Orthop Res 2007;25:122-31.
87. Albers CE, Wambeek N, Hanke MS. Imaging of femoroacetabular impingement-current concepts. J Hip Preserv Surg 2016;3:245-61.
88. Albers CE, Hanke MS, Ecker TM, et al. Computer Assisted Diagnosis and Treatment Planning of Femoroacetabular Impingement (FAI). In: Lecture Notes in Computational Vision and Biomechanics. Cham: Springer International Publishing, 2015:173-96.
89. Pflugi S, Liu L, Ecker TM, et al. A cost-effective surgical navigation solution for periacetabular osteotomy (PAO) surgery. Int J Comput Assist Radiol Surg 2016;11:271-80.
90. Kuhn AW, Ross JR, Bedi A. Three-dimensional Imaging and Computer Navigation in Planning for Hip Preservation Surgery. Sports Med Arthrosc 2015;23:e31-8.
91. Ecker TM, Puls M, Steppacher SD, et al. Computer-assisted femoral head-neck osteochondroplasty using a surgical milling device an in vitro accuracy study. J Arthroplasty 2012;27:310-6.
92. Schumann S, Liu L, Tannast M, et al. An Integrated System for 3D Hip Joint Reconstruction from 2D X-rays: A Preliminary Validation Study. Ann Biomed Eng 2013;41:2077-87.
93. Xia Y, Fripp J, Chandra SS, et al. Automated bone segmentation from large field of view 3D MR images of the hip joint. Phys Med Biol 2013;58:7375-90.
94. Audenaert EA, Baelde N, Huysse W, et al. Development of a three-dimensional detection method of cam deformities in femoroacetabular impingement. Skeletal Radiol 2011;40:921-7.
95. Masjedi M, Azimi DY, Nightingale CL, et al. A method of assessing the severity of cam type femoro-acetabular impingement in three dimensions. Hip Int 2012;22:677-82.
96. Chandra SS, Xia Y, Engstrom C, et al. Focused shape models for hip joint segmentation in 3D magnetic resonance images. Med Image Anal 2014;18:567-78.
97. Heimann T, Meinzer HP. Statistical shape models for 3D medical image segmentation: a review. Med Image Anal 2009;13:543-63.
98. Chu C, Chen C, Liu L, et al. FACTS: Fully Automatic CT Segmentation of a Hip Joint. Ann Biomed Eng 2015;43:1247-59.
99. Flecher X, Migaud H. From radiographs to 3D printing: How can new surgical planning technologies contribute to hip surgery? Orthop Traumatol Surg Res 2017;103:323-4.
100. Rankin TM, Giovinco NA, Cucher DJ, et al. Three-dimensional printing surgical instruments: are we there yet? J Surg Res 2014;189:193-7.
101. Brunner A, Horisberger M, Herzog RF. Evaluation of a computed tomography-based navigation system prototype for hip arthroscopy in the treatment of femoroacetabular cam impingement. Arthroscopy 2009;25:382-91.
102. Khanduja V, Baelde N, Dobbelaere A, et al. Patient-specific assessment of dysmorphism of the femoral head-neck junction: a statistical shape model approach. Int J Med Robot 2016;12:765-72.
103. Buchan LL, Zhang H, Konan S, et al. Open-MRI measures of cam intrusion for hips in an anterior impingement position relate to acetabular contact force. J Orthop Res 2016;34:205-16.
104. Brown GA, Milner B, Firoozbakhsh K. Application of computer-generated stereolithography and interpositioning template in acetabular fractures: a report of eight cases. J Orthop Trauma 2002;16:347-52.
105. Upex P, Jouffroy P, Riouallon G. Application of 3D printing for treating fractures of both columns of the acetabulum: Benefit of pre-contouring plates on the mirrored healthy pelvis. Orthop Traumatol Surg Res 2017;103:331-4.
106. Zeng C, Xing W, Wu Z, et al. A combination of three-dimensional printing and computer-assisted virtual surgical procedure for preoperative planning of acetabular fracture reduction. Injury 2016;47:2223-7.
107. Ma D, Gulani V, Seiberlich N, et al. Magnetic resonance fingerprinting. Nature 2013;495:187-92.
108. Anoushiravani AA, Patton J, Sayeed Z, et al. Big Data, Big Research: Implementing Population Health-Based Research Models and Integrating Care to Reduce Cost and Improve Outcomes. Orthop Clin North Am

2016;47:717-24.
109. Aphinyanaphongs Y. Big Data Analyses in Health and Opportunities for Research in Radiology. Semin Musculoskelet Radiol 2017;21:32-6.
110. Mayo RC, Leung J. Artificial intelligence and deep learning - Radiology's next frontier? Clin Imaging 2017;49:87-8.
111. Lee JG, Jun S, Cho YW, et al. Deep Learning in Medical Imaging: General Overview. Korean J Radiol 2017;18:570-84.
112. Kooijman MN, Kruithof CJ, van Duijn CM, et al. The Generation R Study: design and cohort update 2017. Eur J Epidemiol 2016;31:1243-64.

doi: 10.21037/aoj.2018.04.10
Cite this article as: Mascarenhas VV, Caetano A. Imaging the young adult hip in the future. Ann Joint 2018;3:47.

chapter 3

PATHOLOGY: IMPINGEMENT, HIP DYSPLASIA AND OSTEOARTHRITIS

Due to the main focus of this thesis, we will mainly refer to FAI and only briefly to dysplasia.

3.1 HISTORICAL PERSPECTIVE

The concept of FAI resulting from abnormal contact between two joint structures was first published in 1936 by Smith Peterson[114], who simultaneously described an osteotomy of the femoral neck and acetabular margin in order to improve symptoms. The idea was further developed as a combination of various mechanical hip disorders and multi-factorial failure processes. A relationship was initially established between proximal femoral "head-tilt" abnormalities with the onset of hip OA[115], where, subsequently correlations were established between FH deformities following SCFE. However, the early theories and relationships were not yet supported with clinical evidence.
The "pistol grip" term was also used to describe the shape of the FHN junction from AP radiographs, in comparison with a pistol handle[116]. These abnormal geometric configurations showed signs of early cartilage degeneration, but no direct correlations were evident between the deformity and end-stage OA. At this point, the observations were based on visual interpretations of radiographic evidence, and no work was done to determine the attainable motions in a "pistol grip" joint[95].
Subsequent works noted that impingement was experienced at high amplitudes of hip motions. Based on a combination of radiographic and preliminary physical examinations, general terms were used to describe the impingement, referring to the deformity as "head-tilt"[115] or "post-slip"[117], epiphyseal displacement[115,117,118], acetabular rim syndrome[80,119] and cervicoacetabular impingement[80] (Figure 27).
It was then introduced that anterior hip impingement could also be due to peri-acetabular osteotomy[120], proposing that impingement was secondary to surgical repositioning of dysplastic acetabula. Variable degrees of groin pain and limited ROM were now observed in patients,

explaining the ossification of the anterior rim. An additional follow-up study investigated the presence of protrusions after femoral neck fractures[121]. Similar consequences of secondary anterior FAI were observed. The focus was on the FH, where an oversized bony protrusion was formed at the site of the anterior fracture, bridging the femoral head and neck. The intention of these combined studies was to explain the mechanisms that initiated FAI, proposing that a deformity was formed at the femoral neck or acetabular rim due to trauma or surgery.

The continuing research led Ganz et al.[118] to recognize FAI as a pathomechanical process and a contributor to early adult hip pain and OA[118]. The intention of their research was to link FAI as a hip deformity, with the pathogenesis of idiopathic OA. With extensive open surgical dislocations, they proposed that FAI was a mechanism for the development of early OA for most non-dysplastic hips[118]. It was suggested that FAI was no longer just a resolute hip deformity, but rather, a failure process initiated by a multitude of possible biological and mechanical mechanisms that would eventually provoke the onset of OA.

This notion of FAI-related OA focused more on dynamic motion as opposed to directional axial loading of the hip. The theory of axial hip overload to provoke OA was disputed, further justifying that the development of OA in young adults, with normal hip configurations, cannot be correctly justified with solely concentric and eccentric overload. Research thus far was unable to discuss mechanisms that initiate FAI or justify the aetiology of the deformity, but it provided significant groundwork for clinical and radiographic assessments to distinguish FAI types.

Recently, FAI has been deemed to be a pathomechanical process by which a human hip can fail[122] rather than a disease, with emerging clinical evidence and ongoing biomechanical studies continuing to support the idea that FAI provokes hip OA[118,123-126]. Active adults with groin pain may now be successfully treated with early detection[118,127-130].

From the review of literature on FAI, a great extent of past research focused on recognizing the correct pathology and deformity originating from OA, leading to subsequent treatment and surgical solutions for FAI[123,131-133].

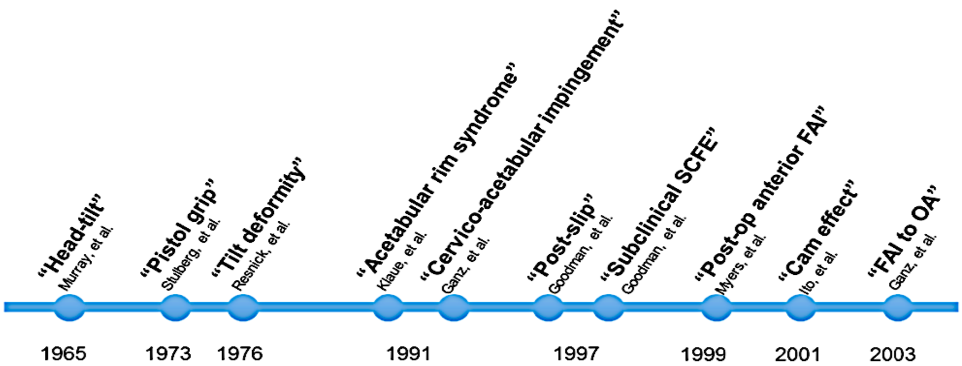

FIGURE 27 – Timeline of terminology from previous studies leading up to the association of FAI to OA (adapted from Beaule et al.[134], with permission).

3.2. PATHOLOGY

Morphological shapes of the hip give rise to a continuous spectrum of disease ranging from isolated instability to impingement with decreased mobility. Located at one end of this spectrum is acetabular dysplasia and, on the other, FAI. In many situations, however, there is a combination of several morphological changes that may have greater or lesser clinical expression and determine the predominance of a mechanism of chondral and labral injury: instability or impingement[42].

3.2.1 Dysplasia

At one end of the spectrum, DHD, seen as an insufficiency of contact between the articular surfaces[135], is characterised by an increase in the inclination of the acetabular roof (acetabular index angle or acetabular inclination angle) and a decrease in lateral and/or anterior coverage (decreased lateral center-edge angle (LCEA) and anterior center-edge angle). Additionally, it may or may not be associated with an increase in the CCD (*coxa valga*), anteversion of the femoral neck and retroversion of the acetabulum[42]. This combination usually results in a static overload of the acetabular roof and an instability or inability to maintain the centre of rotation of the joint fixed, resulting in lateral, superior and anterior migration of the head. Clinically, DHD may be quite symptomatic[135] and has been reported as a risk factor for early-onset OA[136].

The diagnosis of dysplasia has historically been based on assessments of acetabular anatomy on the AP pelvic radiography, most commonly using the LCEA. Recent advances in imaging of the dysplastic hip with CT scans have demonstrated that hip dysplasia is, in fact, a 3D deformity of the acetabulum and that multiple patterns of acetabular instability exist that may not be completely assessed on two-dimensional imaging, allowing an evolution away from vague terms such as "*borderline* dysplasia"[137].

3.2.2 Femoroacetabular impingement

FAI is a motion-related clinical disorder of the hip. It represents symptomatic premature contact between the proximal femur and the acetabulum[138] (Table 8). Based on the location of the shape abnormality, two types of FAI can be distinguished: Cam impingement (femoral side) and Pincer impingement (acetabular side) (Figures 28 and 29).

	PATIENT CHARACTERISTICS					INTRA-ARTICULAR DAMAGE	
	SEX	**AGE**	**ACTIVITY**	**DEFORMITY**	**MECHANISM**	**EARLY DAMAGE**	**LATE DAMAGE**
Cam FAI	Mainly male	Young	High-level athletes; High-impact sports	"Cam-type deformity": Eccentric femoral head with laterally increasing radius	Sheering forces inside the joint and damage to the acetabular cartilage; "inclusion injury"	Acetabular cartilage delamination; Outside-in acetabular cartilage lesions	Large, full thickness anterosuperior acetabular cartilage defects; Labral damage with undersurface tears; Femoral head cartilage lesions
Pincer FAI	Mainly female	Middle aged	Recreational athletic activity	"Overcoverage" of the femoral head: *coxa profunda*, *protrusio acetabuli*, acetabular retroversion	Linear impact between acetabular rim and FHN junction; "impaction injury"	Labral damage ranging from subtle shortening and rounding to extensive labral damage	Ossified bony rim with partially ossified labrum; Cartilage damage at acetabular rim; "Contrecoup" posteroinferior acetabular damage

TABLE 8 – Summarizing table of the clinical, epidemiological and joint damage characteristics of femoroacetabular impingement.

3.2.2.1 Cam mechanism

Cam impingement is caused by extra bone formation – a Cam morphology – in the antero-lateral FHN junction[97] (resulting in flattening or convexity). This deformity may cause impingement against the acetabular rim, especially during flexion and internal rotation of the hip[139]. This type of impingement has classically been described to occur in young athletic males[140], although this preference of subpopulation has not been proven.

The abnormal contact results in shear forces at the acetabular rim[2] and is typically accompanied by labral tears[141] and detachment of the acetabular cartilage from the subchondral bone[139,142]. This biomechanically based hypothesis of Cam impingement has been supported by studies showing an association between a Cam deformity and limited internal hip rotation[87] as well as hip pain[143] (Figure 28).

Furthermore, the explanation of how soft-tissue damage and subsequent OA is caused by Cam impingement is also supported by intra-operative findings in symptomatic patients with Cam morphology[144,145]. Acetabular cartilage delamination[146] has been found in the anterosuperior quadrant of the joint, corresponding to the site where the deformity is forced into the acetabulum ("inclusion injury"). These observations suggest a relationship between Cam FAI and OA[125], but again, epidemiological evidence is scarce and mostly retrospective studies are available. These studies do generally show an association between a Cam deformity and OA, though the strength of association varies between studies. One of the major limitations of these studies is that no conclusions on causality can be drawn, as a non-spherical FH can also be a result of the advanced OA process itself. When the pathophysiological mechanism between a Cam morphology and pain, limited function, and hip OA holds true, a theoretically plausible explanation for development of hip OA is provided. Interestingly, a Cam deformity might develop during skeletal maturation of the hip as a result of high-impact sporting activities, which would be a promising preventative opportunity for the formation of a Cam morphology and subsequent hip OA[23].

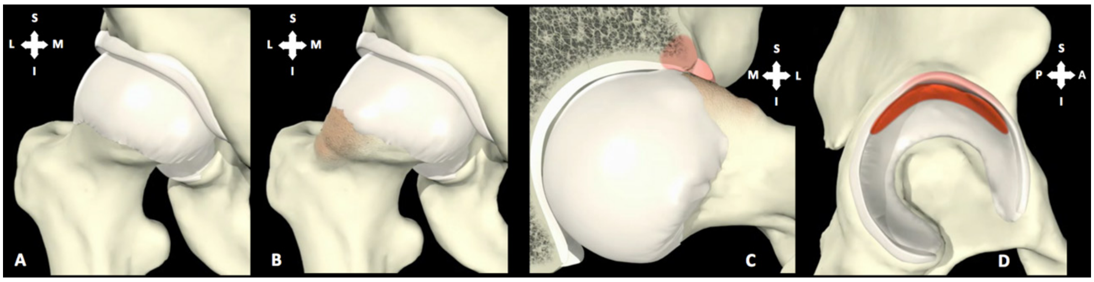

FIGURE 28 – A schematic representation of the hypothesized mechanism of Cam femoroacetabular impingement. (A) Normal spherical femoral head and acetabulum, which is congruent with the femoral head provides the hip a wide range of motion. A Cam deformity (B) can cause Cam impingement against the acetabular rim, especially during flexion and internal rotation of the hip (C) leading to a typical pattern of acetabular chondrolabral damage anterosuperiorly (D).

3.2.2.2 Pincer mechanism

Pincer impingement is caused by overcoverage of the acetabulum relative to the FH (either global or focal overcoverage). The hypothesis proposed by Ganz et al.[118] states that the femoral neck causes an abnormal linear contact against the acetabulum during terminal motion of the hip. It has classically been described to occur primarily in middle-aged women[147], though no longitudinal studies are available to confirm this.

Initially, labral damage is the main characteristic as the cartilaginous labrum might be crushed between the acetabular rim and the femoral neck (Figure 29). When there are repetitive episodes of impingement, chondral damage might gradually develop, conceptually leading to hip OA. It was therefore suggested that Pincer impingement progresses relatively slow towards hip OA. This hypothesis is supported by intra-operative findings in symptomatic patients with a Pincer morphology, where acetabular damage was found throughout the acetabulum in a small, thin marginal strip[123]. However, only low-evidence and sometimes conflicting studies exist that investigate the relationship between Pincer FAI and OA[126,146,148-151]. In fact, even when symptomatic, some research reports that overcoverage seems to be protective in relation to chondral aggression[126].

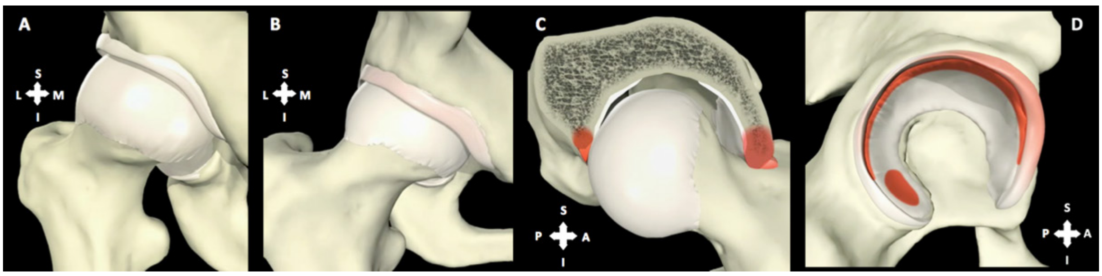

FIGURE 29 – Schematic representation of the hypothesized mechanism of Pincer FAI. (A) Normal spherical femoral head and acetabulum, which is congruent with the femoral head provides the hip a wide range of motion. A Pincer deformity (B) can cause Pincer impingement against the femoral neck, especially during terminal flexion of the hip (C) leading to a typical pattern of circumferential acetabular cartilage damage (D).

3.2.2.3 Diagnosis

FAI syndrome (FAIS) has been recently defined as a triad of symptoms, clinical signs and imaging findings[118,138,152]. This term and its definition build on the definitions of FAI from Ganz et al.[118] and Sankar et al.[153]. To ensure that there is a distinction between patients with FAIS and those with Cam or Pincer morphology, but no symptoms, clinical signs and imaging findings must be present to diagnose FAIS.

3.2.2.3.1 Symptoms: The primary symptom of FAIS is motion-related or position-related pain in the hip or groin[118], although it may also be felt in the back, buttock or thigh. In addition to pain, patients may also describe clicking, catching, locking, restricted ROM or "giving way"[154-156].

3.2.2.3.2 Signs: Diagnosis of FAIS does not depend on a single clinical sign (many have been described and are used in clinical practice[154]). When FAIS is suspected, it is important to examine gait, leg control, muscle tenderness and ROM, including internal rotation in flexion and the FABER sign (flexion abduction external rotation). Hip impingement tests usually reproduce the patient's typical pain, although the most commonly used test, flexion adduction internal rotation (FADIR), is sensitive but not specific[157]. With further and gradual internal rotation, hip pain is elicited[158]. There is often a limited ROM, typically restricted internal rotation in flexion[159].

3.2.2.3.3 Diagnostic injections: A common clinical problem lies in determining whether pain (or surrogate symptoms) is really arising from the hip or from other structures in the groin and hip region. Frequently, image-guided (X-ray or ultrasound) local anaesthetic injections are useful in helping to resolve this situation[160,161], as they have both diagnostic and therapeutic value. Pain relief following a local anaesthetic injection would support a FAIS diagnosis, when the other diagnostic criteria are met[138]. Byrd et al., demonstrated that relief with an intraarticular injection was 90% accurate for predicting the presence of intraarticular findings during arthroscopy[162]. Interestingly, in a prospective study by Ayeni et al., no relief from an injection was a negative predictor of short-term outcome following FAI surgery[163].

3.2.2.3.4 Imaging: Morphological assessment of the hip is paramount in order to diagnose FAIS. Imaging is best achieved as previously described and firstly identifies normal, dysplasia, Cam or Pincer morphology. Additionally, it may exclude other alternative pathological conditions. These morphologies however, in the absence of appropriate symptoms and clinical signs, do not constitute a diagnosis of FAIS. In fact, a substantial proportion of people in the general population have Cam or Pincer morphology[36].

Many radiographic measures of FAI morphology have been described, including the $\alpha°$ (Cam), cross-over sign (COS) and LCEA (Pincer)[80]. In a large ongoing clinical trial (FASHIoN)[164] addressing treatment for FAIS, patients were included with an α°>55° at any FHN junction position (to define Cam morphology) and a positive COS or LCEA>39° (to define Pincer morphology). Considering previously mentioned parameters and ongoing questions, some authors try to define what is normal and what is abnormal, also suggesting possible combinations of morphology that characterise classically and recently described pathological entities[94] (Table 9).

	Normal	Dysplasia	Cam FAI	Pincer FAI
Acetabular inclination	0–10°	>10°	Variable	<0°
Lateral center-edge	25–30°	<20°	Variable	>35°
Alpha angle	<55°	Variable	>55°	Variable
Retroverted acetabulum	Absent	Up to 1/3 of patients	Variable	Frequent
Femoral version	15-20°	Mostly anteverted	Variable	Variable

TABLE 9 – Possible combinations of morphology and angular parameters that characterise pathological entities.

Nötzli at al.[87] established that impingement was associated with an α° greater than 50° (measured on an oblique-axial MRI plane). Later on, other authors referenced 50°[80,165] (oblique axial MRI plane) and 50.5°[166-168] as an indicator of an abnormally shaped femoral in their cohorts (to define Cam morphology). The modification of the imaging views, to observe the α° in different radiographic planes[166] and multiple radial views[90,93,167-170] around the clock-face of the FH, improved the assessment of the Cam deformity.[93,167,170]

Recognizing that the Cam deformity was statistically prevalent at the anterosuperior FH, a higher α° value greater than 60° in the radial 1:30 plane was suggested as a threshold and predictor of hip pain[93,167,168,170]. Individuals with a higher α°, thus with a more severe deformity, had prevalent labral and cartilage lesions at the anterosuperior acetabular cartilage[171,172], which was confirmed with open SHD[63,118] and imaging[80,123].

The main problems with the α° angle are: i) only moderate reproducibility[173]; ii) incomplete quantification of Cam morphology[166,174,175]; iii) suboptimal accuracy in distinguishing patients with FAIS from healthy individuals as there is a substantial overlap in α° measurements between these groups[93]. This further suggested that both views, axial and radial, must be considered, and perhaps in conjunction with 3D model analysis, to provide clinicians with another perspective to analyse a deformity[170,176].

3.2.2.4 Treatment

Treatment strategies for FAIS include conservative care, rehabilitation, surgery and post-surgery care. Each of these may have a role in different patients, but there is little evidence to compare their effectiveness[164]. There is currently no high-level evidence to support the choice of a definitive treatment[177,178]. This is best done in a shared decision-making process, supporting the individual patient to make an informed preference decision on the best treatment option[179].

Conservative care of patients with FAIS is poorly described but includes patient education, activity and lifestyle modification, oral analgesia including non-steroidal anti-inflammatory drugs, intra-articular steroid injection and watchful waiting[180]. There are no reports of what effect such an approach, in isolation, has on FAIS symptoms. Similar conservative strategies are recommended in other musculoskeletal disorders such as OA[181]. Physiotherapist-led rehabilitation aims to reduce patients' symptoms by improving hip stability, neuromuscular control and movement patterns. However, details of what should be incorporated in such a programme have not been well tested, and it would appear that different physiotherapists are delivering different treatments[180].

Surgery aims to correct hip morphology to achieve impingement-free motion and treat intra-articular damage[63,118,182]. Cam morphology can be reshaped, and femoral torsion or neck angle adjusted; the acetabulum can be reoriented, or its rim trimmed. Where there is damage to the labrum or articular cartilage, this can be resected, repaired or reconstructed. Often, these procedures can be done by either arthroscopic or open surgery[183,184].

Initially, the SHD pioneered by Ganz was the gold standard of treatment[63]. This technique involved a controlled surgical dislocation of the hip while preserving blood supply to the FH[63]. However, hip arthroscopy is increasingly being utilized to successfully treat FAI. Recent studies have also documented that arthroscopy is associated with fewer complications, less pain and less resource utilization[185].

Overall, the surgical efficacy of FAI treatment, regardless of surgical approach, is supported by clinical evidence that is limited to case series and cohort studies, as reported by a recent systematic review[186]. Nevertheless, the potential of this intervention to improve pain and conceptually prevent the development of OA has led to rapid adoption of global surgical interventions. Postoperative physiotherapy protocols have been described, but their value is also uncertain[187-189].

3.2.2.5 Prognosis

Asymptomatic individuals: The risk for developing symptoms or OA in asymptomatic populations with FAI-like morphology is unknown when compared to other individuals with normal morphology. There is no evidence that treating asymptomatic people who have FAI morphology will alter the risk of developing FAIS or OA, and so, it is seldom indicated to offer surgery. Preventive physiotherapy-led rehabilitation strategies may be appropriate in professional athletes where the prevalence of Cam morphology is high, such as professional football teams[190]. In exceptional circumstances, and in a shared decision-making process with a patient, surgery may occasionally be appropriate for high-risk patients. An example of such a patient could be an active young adult who has had surgery for FAIS in one hip and in whom chondrolabral injury is seen developing in the other (painless) hip[191].

FAIS: Patients with FAI syndrome who are not treated probably experience a gradual deterioration of symptoms[192]. In patients who are treated for FAIS, symptoms frequently improve and return to full activity, including sports[193]. Physiotherapy-led rehabilitation seems to be associated with an improvement in symptoms for at least 2 years[180]. However, evidence supporting this action is restricted to only a few observational studies with small sample sizes and important methodological weaknesses. Reports of surgery results are more numerous and describe significant improvement up to 5 years[132,194-196], but they suffer similar issues of poor design and therefore, a high-risk of bias. Longer-term results have been reported for SHD, including improved symptoms persisting in most patients for at least 10 years[197,198]. The long-term outlook for patients with FAIS is unknown. It is currently unknown whether treatment for FAIS prevents hip OA. All prospective cohort studies available demonstrate an association between Cam morphology and hip OA[124,125,199,200], however, there is no established association with Pincer morphology[15]. Presently, it is unknown whether FAIS is associated with a higher risk of OA than isolated Cam morphology or evidence that treatment for FAIS alters the risk of subsequent OA[138].

3.2.3 Hip Osteoarthritis

OA is the most frequently occurring chronic joint disease worldwide[201]. It is symptomatically characterised by pain, stiffness and loss of function[201], and on a tissue level by loss of cartilage, osteophyte formation, subchondral sclerosis and cyst formation[202].

OA has a detrimental impact on quality of life and forms an increasing economic burden[203] (both direct and indirect costs). Direct cost is the cost of medical care due to OA and associated comorbidities, and this has been estimated to exceed $100 billion per year for hip OA alone in the United States (US). Indirect costs are those as a result of OA, but not associated directly with treatment. They include, for example, productivity loss and might be 1.5 times the direct cost of OA. The latter is exemplified by the fact that OA is the second cause of work disability after ischaemic heart disease in males over 50 years in the US[201]. The cost of hip OA in Portugal is unknown.

The lack of a precise definition of the disease has made difficult to determine the prevalence of OA. There is often a discrepancy between the clinical presentation and the radiographic evidence of OA. In research, the commonly used definitions of hip OA include i) “symptomatic OA” (quantified by the ACR criteria)[204]; ii) “radiographic OA” (quantified by the Kellgren and Lawrence scale (K&L)[205]); or iii) total joint replacement as a result of OA[204].
OA can affect any synovial joint, but the joints most affected by OA are in order of decreasing prevalence: The spine (cervical and lumbar), phalanges (distal interphalangeal joint and the first carpometacarpal joint), the knee, and the hip[206]. Besides the definition used, the reported prevalence of hip OA depends largely on the characteristics of the study population such as age, gender and ethnicity. In the US, the prevalence of radiographic hip OA (K&L>1) in population-based studies ranges from 11.9–27.6%[207].

In Portugal, the “Instituto Nacional de Saúde Dr. Ricardo Jorge”, in a report on the most prevalent chronic diseases, identified that 24% of the participants reported suffering from some form of rheumatic disease (Branco J, Nogueira P, Contreira T. *Uma observação sobre a prevalência de algumas doenças crónicas, em Portugal Continental*. Lisboa: Instituto Nacional de Saúde Dr. Ricardo Jorge; 2005). As far as OA is concerned, general data presented by the “Liga Portuguesa Contra as Doenças Reumáticas” estimates that probably 6% of the portuguese population has the disease (LPCDR. Liga Portuguesa Contra as Doenças Reumáticas. Estatísticas das Doenças Reumáticas 2013; [Consulted 2018 Jan 08]; available in: http://www.lpcdr.org.pt/index.php?option=com_content&view=cate gory&id=69&Itemid=128).

The portuguese “Direção Geral da Saúde”, in a report from 2003, described that the prevalence of OA was approximately 3.8% in the knee and 1.3% in the hip. Other important data, presented by the portuguese “Observatório Nacional das Doenças Reumáticas” (ONDOR), estimated radiographic hip OA, in subjects older than 40 years, to be approximately 54.8% in men and 24.5% in women; hip symptomatic disease is estimated to be 2.4% in men and 2.2% in women (Lucas R, Monjardino MT. *O Estado da Reumatologia em Portugal: Observatório Nacional da Doenças Reumáticas*. Lisboa: ONDOR; 2010).

The projected number of older adults with arthritis or other chronic musculoskeletal joint symptoms is expected to nearly double from 21.4 million in 2005 to 41.1 million by 2030 in the US. The burden of hip OA is increasing due to the aging population and the obesity crisis; as a result, the need for total hip arthroplasty (THA) is expected to grow 174%, to 572,000 primary THAs per year by 2030 in the US[207].

3.3. MORPHOLOGY AND THE SYMPTOMATIC STATE

3.3.1 Systematic review of FAI morphology prevalence

"Imaging prevalence of femoroacetabular impingement in symptomatic patients, athletes, and asymptomatic individuals: A systematic review."

Mascarenhas VV, Rego P, Dantas P, Morais F, McWilliams J, Collado D, Marques H, Gaspar A, Soldado F, Consciência JG.
Eur J Radiol. 2016 Jan;85(1):73-95. doi: 10.1016/j.ejrad.2015.10.016.
Epub 2015 Nov 2. Review. PubMed PMID: 26724652.

European Journal of Radiology 85 (2016) 73–95

Contents lists available at ScienceDirect

European Journal of Radiology

journal homepage: www.elsevier.com/locate/ejrad

Imaging prevalence of femoroacetabular impingement in symptomatic patients, athletes, and asymptomatic individuals: A systematic review

Vasco V. Mascarenhas*, Paulo Rego, Pedro Dantas, Fátima Morais, Justin McWilliams, Diego Collado, Hugo Marques, Augusto Gaspar, Francisco Soldado, José G. Consciência

Hospital da Luz, Lisbon, Portugal

ARTICLE INFO

Article history:
Received 9 June 2015
Received in revised form
29 September 2015
Accepted 25 October 2015

Keywords:
Hip
Femoroacetabular impingement
Anatomy
Imaging
Reference Value
Normal value
Prevalence

ABSTRACT

Background: There is a wide discrepancy in reported prevalence rates for cam, pincer, and mixed femoroacetabular impingement (FAI), particularly among distinct populations, namely asymptomatic or symptomatic subjects and athletes. No systematic analysis to date has yet compared studies among these groups to determine differences in radiographic signs of FAI.
Methods: A systematic review of existing literature was performed to determine the prevalence of radiographic signs of FAI among athletes, asymptomatic subjects, and symptomatic patients. Preferred Reporting Items for Systematic Reviews and Meta-Analyses (PRISMA) guidelines were applied to systematically search PubMed, MEDLINE, CINAHL, and Cochrane databases.
Results: We identified 361 studies in our literature search. After considering the exclusion criteria, 60 were included in this systematic review: 15 in athletes, 10 in purely asymptomatic patients, and 35 in symptomatic, non-athlete populations. Cam impingement was significantly ($p = 0.0003$) more common in athletes versus asymptomatic subjects but not compared to symptomatic patients ($p = 0.107$). In addition, cam FAI was significantly more common in symptomatic versus asymptomatic cases ($p = 0.009$). The percentage of patients with cam-type FAI showed significant differences across groups ($p = 0.006$). No significant differences were found between pincer-type FAI morphology prevalence when comparing athletes to symptomatic patients. However, mixed-type FAI was significantly more common in athletes versus asymptomatic subjects ($p = 0.03$) and in asymptomatic versus symptomatic subjects ($p = 0.015$). The percentage of patients with mixed-type FAI showed significant differences across groups ($p = 0.041$). The mean alpha angle was significantly greater in the symptomatic group versus either the asymptomatic or athlete group ($p < 0.001$). Significant differences in mean alpha angles were noted across groups ($p = 0.0000$).
Conclusions: Imaging suspicion of FAI is common among athletes, asymptomatic, and symptomatic populations. However, significant differences in type and imaging signs of FAI exist among these groups that need to be considered in patients' decision making.

1. Introduction

Femoroacetabular impingement (FAI) refers to the conflicting movement of the femoral head-neck junction and acetabular rim against one another [1]. This abnormal contact eventually results in hip joint damage and may progress to functional limitation and pain causing conditions, such as osteoarthritis [2–4]. FAI is a common cause of hip pain and restricted range of motion [1]. There are two types of FAI. Cam-type generally involves a femoral head-neck bony deformity, while pincer-type exhibits acetabular overcoverage [1]. In some patients a cam and pincer impingement mixed-type combination might also be detected [5].

Diagnosis of FAI is based on a combination of clinical and radiological testing [5]. Radiological examinations using conventional X-rays have been tested in different views, including the Dunn, anterior–posterior (AP), and frog-leg lateral views [5,6]. Magnetic resonance imaging (MRI) has been recently used to enable visualization of intra-articular pathology [7–9]. However, there is a wide discrepancy in reporting prevalence rates for cam, pincer, and

* Corresponding author at: Rua Artilharia Um, 71-77 Lt 6 Bloco A 3, 1250-039 Lisbon, Portugal.
E-mail address: mascarenhas.vasco@gmail.com (V.V. Mascarenhas).

http://dx.doi.org/10.1016/j.ejrad.2015.10.016

Table 1
Characteristics of studies involving athletes (number of studies = 15).

Ref.	Level of evidence	Population type	No. participants	No. of hips	Demographics	Imaging	Major findings reported
12	III	Semi-professional (n = 22) and amateur (n = 22) soccer players	44	88	All males from Germany; median 23.3 years (range 18–30 years); amateurs were students at Ruhr-University Bochum; semi-professionals played in first league of Westphalia/Germany	MRI	Cam: 13/22 (59%) vs 9/22 (40%) of semi-professional players vs amateur players (p = 0.228) Pincer: none reported Mean alpha angle in kicking leg: 57.3° ± 8.2° vs 51.7° ± 4.8° (semi-professional vs amateur players) (p = 0.008) CEA: right hip, 35.8° ± 4.03 in semi-professionals vs 32.1° ± 2.45 in amateurs (p < 0.001); left hip, 35.0 ± 3.51 vs 32.0 ± 3.28 in semi-professionals vs amateurs (p = 0.003) Chondral defect: 2/22 (9.1%) vs 1/22 (4.5%) of semi-professional vs amateur players (p = 1.0) Acetabular labral tear: 3/22 (13.6%) vs 1/22 (4.5%) of semi-professional vs amateur players (p = 0.616)
13	III	Asymptomatic youth ice hockey players (n = 61), age-matched youth skiers (controls; n = 27)	88		All males; median age: hockey players, 14.5 ± 2.7 years; skiers, 15.2 ± 2.7 years; age range, 10–18 years	MRI	Cam: 79% of ice hockey players vs 40% of skiers (p < 0.005); significant correlation between age and alpha angle in ice hockey players Mean alpha angle: 60.1° ± 7.4° in hockey players vs 55.2° ± 7.0° in skiers (p = 0.05) Pincer: none reported; CEA: none reported Chondral defect: 5/61(8.2%) hockey vs no skiers Acetabular labral tear: 42/61 (68.8%) of hockey vs 19/27 (70.4%) of skiers

Table 1 (*Continued*)

Ref.	Level of evidence	Population type	No. participants	No. of hips	Demographics	Imaging	Major findings reported
14	III	Non-athletes ($n = 20$) versus elite ice hockey players ($n = 20$)	40		18 females, 22 males; age range, 16–30 years; mean: 20.1 years for non-athletes, 20.6 years for athletes; athletes from Ontario	MRI	Cam: 5/20 (25%) non-athletes vs 11/20 (55%) athletes; odds ratio of cam based on alpha angle >50° was 3.35 for athletes vs non-athletes Mean alpha angle: 43.2° ± 9.7° in non-athletes vs 54.2° ± 12.0° in athletes ($p = 0.003$) Pincer: no significant difference between groups LCEA: 2/20 non-athletes vs 2/20 athletes Labral tear: 12/20 non-athletes vs 12/20 athletes Osseous bump: 4/20 non-athletes vs 4/20 athletes
15	III	Youth actively involved in a variety of sports activities	35		30 females, 5 males; age range, 13–18 years; mean age, 16 years	MRI	Cam only: 2/35 (6%); Mixed cam and pincer: 18/35 (51%); Pincer only: 15/35 (43%) Median alpha angle: 53° for all patients; Positive COS: 33/35 patients (94.3%) Labral tear: 16/28 evaluated patients (57% of evaluated patients)
16	III	Semi-professional ($n = 14$) versus amateur ($n = 14$) soccer players	28		All males; median age: semi-pro, 22.2 ± 2.3 years; amateur, 22.7 ± 2.9 years	MRI	Median alpha angle: semi-pro, 55.16° ± 6.58°; amateur, 51.65° ± 4.43° ($p = 0.11$) COS, labral tears, chondral defects not reported

Table 1 (*Continued*)

Ref.	Level of evidence	Population type	No. participants	No. of hips	Demographics	Imaging	Major findings reported
17	III	Capoeira (Brazilian martial art) players	24	48	10 females, 14 males; mean age: 31.5 ± 4.4 years (range, 25–42 years)	X-ray	Cam: 44/48 hips; 22/48 alpha angle >60°, associated with groin pain ($p = 0.002$) Pincer: 18/48 hips; Mixed: 16/48 hips Mean alpha angles: AP, 50.7° ± 7.7°; frog-leg lateral, 57.4° ± 7.1°; HNO: 6.3 ± 1.7 mm. Reduced head-neck offset ($p < 0.001$) and increased alpha angle ($p = 0.008$) were significantly associated with higher Tonnis grade LCEA: 34.7° ± 2.8°; Acetabular index, 4.5 ± 2.4; Positive COS in 16/48 hips (33.3%)
18	III	College football players at National Football League Scouting Combine; mixed asymptomatic (164 hips) and pain (75 hips)	125	239	All males	AP pelvic and frog-leg lateral X-rays	90% of players (87% of hips) had radiographic signs of cam, pincer, or mixed FAI Cam defined as alpha angle >55°: 94/125 players (75.2%) or 156/239 hips (65.3%) Pincer: 97/125 players (77.6%) or 173/239 hips (72.4%) Mixed-type FAI: 79/125 (63.2%) or 124/239 hips (51.9%) Acetabular retroversion: 59/125 players (47.2%) or 97/239 hips (40.6%); *Coxa profunda*: 5/125 players (4.0%) or 6/239 hips (2.5%); COS: 89/125 players (71.2%) or 154/239 hips (64.4%); Labral ossification: 19/125 players (15.2%) or 22/239 hips (9.2%) Increased alpha angle was the only independent predictor of pain; radiographic signs of cam and mixed-type correlated with presence of symptoms

Table 1 (*Continued*)

Ref.	Level of evidence	Population type	No. participants	No. of hips	Demographics	Imaging	Major findings reported
19	III	Symptomatic or asymptomatic adult female professional ballet dancers ($n=30$; 59 hips) versus asymptomatic non-dancer adult women ($n=14$; 28 hips; controls)	44	87	All females; mean age of dancers, 24.6 years (range, 18–39 years); mean age of controls, 27.1 years (range, 20–34 years)	MRI	Acetabular cartilage lesions: dancers, 17/59 hips (28.8%) >5 mm; controls, 2/28 hips (7.1%) >5 mm ($p=0.026$) Mean alpha angles: anterior, dancers: 45.5° ± 5.3°, controls, 47.5° ± 4° ($p=0.018$); anterosuperior, dancers: 46.7° ± 6.7°, controls, 46.0° ± 4.9° ($p=0.863$); superior, dancers: 40.2° ± 4.8°, controls, 46.6° ± 4.4° ($p<0.001$) Labral lesions: degeneration in 24 hips (40.7%) of dancers and 12 hips (42.9%) of controls ($p=0.847$); ≥2 lesions in 11 hips (18.6%) vs 1 (3.6%) of dancers vs controls; tears in 28 hips (47.5%) of dancers and 8 hips (28.6%) of controls for OR:2.3 dancers vs controls ($p=0.095$); Low prevalence of FAI in dancers, but the presence of other lesions suggests pincer-like impingement
20	III	College football players	65	130	All males on University of Utah football team; mean age: 21 ± 1.9 years	AP pelvic and frog-leg lateral X-rays	123 hips (95%) with ≥1 radiographic abnormality: 74 hips (55%) with alpha angle >50°; 86 hips (64%) with HNO <8 mm; acetabular over-coverage: 10 hips (7%) with LCEA >40°; 21 hips (16%) with acetabular index less than 0°; COS in 82 hips (61%). Tönnis grade 1: 22 hips (17%); Tönnis grade 0:0 Alpha angle and head–neck offset significantly correlate with internal rotation

Table 1 (*Continued*)

Ref.	Level of evidence	Population type	No. participants	No. of hips	Demographics	Imaging	Major findings reported
21	III	50 high-level soccer players (25 females, 25 males) versus 50 controls (25 females, 25 males)	100	200	50 females, 50 males; age range, 18–30 years	AP and frog-leg lateral X-rays	Cam: 15/25 male players (60%) vs 14/25 male controls (56%) ($p = 0.774$); 9/25 female players (36%) vs 8/25 female controls (32%) ($p = 0.765$) Alpha angle: right hip, 57.5° in male players vs 55.4° in male controls ($p = 0.242$); 50.0° in female players vs 48.5° in female controls ($p = 0.244$); left hip, 55.1° in male players vs 54.4° in male controls ($p = 0.676$); 49.2° in female players vs 49.1° in female controls ($p = 0.938$) Between gender groups: Cam deformity, 29/50 males (58%) vs 17/50 females (34%) ($p = 0.016$); alpha angle, right hip, 56.4° in males vs 49.3° in females ($p = 0.001$); alpha angle, left hip, 54.7° in males vs 49.1° in females ($p = 0.001$) Between players and controls: Cam deformity, 24/50 players (48%) vs 22/50 controls (44%) ($p = 0.688$); alpha angle, right hip, 53.8° in players vs 52.0° in controls ($p = 0.126$); alpha angle, left hip, 52.1° in players vs 51.7° in controls ($p = 0.717$)
22	III	Elite soccer players from the U.S. Men's National Soccer Team and the Women's Professional Soccer Team	95		20 females, 75 males; mean age: 25.4 ± 4.2 years	AP and frog-leg lateral X-rays	Cam: 61/95 (64.2%); males, 51/75 (68%); females, 10/20 (50%) Pincer: 22/95 (23.2%); males, 20/75 (26.7%); females, 2/20 (10%) Males: average alpha angle, 65.6°; cam-positive hips, average alpha angle, 70.7°; 72% (54/75) showed radiographic evidence of FAI Females: average alpha angle, 52.9°; cam-positive hips, average alpha angle, 60.8°; 50% (10/20) showed radiographic evidence of FAI Overall, 64/95 (67.4%) radiographic sign of FAI.

Table 1 (*Continued*)

Ref.	Level of evidence	Population type	No. participants	No. of hips	Demographics	Imaging	Major findings reported
23	III	College football players	67	134	All males; mean age: 21 ± 1.9 years	AP and frog-leg lateral X-rays	Mean alpha angle: frog-leg lateral, 52° ± 10°; AP, 55° ± 12°; 72% of players with increased alpha angle; >50° in 54% by frog-lateral and 55% by AP X-ray Mean lateral center edge angle: 30° ± 6.6°; 7% of players with increased lateral center edge angle >40° Acetabular index: 4.9° ± 5.4°; 16% with decreased AI; 61% with positive COS Head-neck offset: 6.5 ± 3.1 mm; 64% with decreased (<8 mm) femoral HNO 95% of hips with at least one sign of cam or pincer impingement; 21% with only one sign of cam FAI, and 52% with only one sign of pincer FAI
24	III	National Football League players with history of hip pain or injury	107	123	50 males, 50 females; mean age: females, 31.4 years (range, 16–49 years); males, 28.7 years (range, 14–49 years); all patients at Washington University School of Medicine, St. Louis, Missouri	AP and frog-leg lateral X-rays	Cam and/or pincer in 116/123 hips (94.3%). Cam only in 12 hips (9.8%). Cam deformity detected in 88% females and 100% males ($p = 0.027$) Pincer: 28 hips (22.8%); Mixed-type: 76 hips (61.8%) COS >10 mm (28% females, 47% males) ($p = 0.113$) LCEA >40° and/or acetabular index <0 in 25% females and 21% males ($p = 0.669$) Max alpha angle: females, 57.6°; males, 70.8° ($p < 0.001$); alpha angle <50° (30% females vs 6% males; $p = 0.002$) Mean alpha angles (females vs males) ($p < 0.001$): AP, 49.0° vs 64.9°; Dunn, 53.1° vs 65.3°; frog-leg, 45.7° vs 56.9° HNO ratio: minimum, 0.16 vs 0.14 mm in females vs males ($p < 0.001$); >0.17 mm in 22% females and 4% males ($p = 0.007$)

Table 1 (*Continued*)

Ref.	Level of evidence	Population type	No. participants	No. of hips	Demographics	Imaging	Major findings reported
25	III	Butterfly-style (n = 44 players; 68 hips) versus positional (n = 26 players; 34 hips) ice hockey players	70	102	high school, collegiate, and professional butterfly-style hockey goalies; average age, 21.1 ± 5.7 years (range, 14–43 years) positional players; average age, 21.0 ± 7.2 years (14–49 years)	AP and Dunn lateral X-rays, CT	Butterfly players had larger alpha angle and increased prevalence of FAI Values below compare butterfly vs positional players: AP: LCEA, 27.3° ± 5.5° vs 29.6° ± 4.5° (p = 0.03); alpha angle 61.3° ± 16.7° vs 54.0° ± 13.5° (p = 0.02); positive crossover sign: n = 40 (58.8%) vs n = 15 (44.1%) (p = 0.16) Modified Dunn lateral: alpha angle, 63.4° ± 11.1° vs 60.4° ± 10.6° (p = 0.20); HNO ratio, 0.16 ± 0.03 vs 0.15 ± 0.02 (p = 0.10) CT: Femoral anteversion, 14.2° ± 9.2° vs 12.9° ± 6.8° (p = 0.43); maximum alpha angle, 80.9° ± 10.2° vs 68.6° ± 11.3° (p < 0.0001); LCEA, 27.6° ± 5.3° vs 30.0° ± 5.4° (p = 0.04); positive COS in 52.9% vs 44.1% (p = 0.40)
26	III	Adolescent athletes (n = 226)	226	452	high school students participating in sports; 12–18 years (mean age, 15 years)	MRI, X-rays	Mean alpha angle (radial sequence), 44.3° (p < 0.001); Cam lesion (alpha angle of 55°), OR = 14.4; Mean acetabular version:17.9 (p < 0.001); Labral lesion 38%;

CEA—center edge angle; LCEA—lateral center edge angle; HNO—Head–neck offset; COS—crossover sign.

Table 2
Characteristics of studies involving asymptomatic subjects (number of studies = 10).

Ref.	Level of evidence	Population type	No. of participants	No. of hips	Demographics	Imaging type	Major findings reported
27	III	Volunteers	200	400	111 females, 89 males; mean age: 29.4 years (range, 21.4 to 50.6 years); race: 158 (79%) were white	MRI	Cam prevalence was 14%; more common in males (24.7% compared with 5.4% in females) Mean alpha angle: Anterior: right hip, 40.94° ± 7.00°; left hip, 40.62° ± 7.11°; overall, 40.78° ± 7.05°; Anterosuperior: right hip, 50.23° ± 8.01°; left hip, 50.07° ± 8.27°; overall, 50.15° ± 8.13° Mean alpha angle by gender: Anterior: males, 44.02° ± 7.82°; females, 38.19° ± 5.06°; Anterosuperior: males, 54.09° ± 8.54°; females, 46.99° ± 6.19°
28	III	Asymptomatic volunteers	82	164	54 females, 28 males; mean age: 50.4 years (range, 40–60 years)	X-ray	Cam: alpha angle >50° in 41/164 hips (one-fourth of hips); average alpha angle: 45° ± 8.6° (range, 32°–74°); average alpha angle by gender: males, 47.52°; females, 43.85° ($p = 0.028$); male predominance: 19/56 (34%) vs 12/108 (11.11%) female hips Mixed type: 6 cases (3.7%) Radiographic alterations: deep thigh, 120 hips (76.0%); COS, 20 hips (12.6%); posterior wall sign, 58 hips (36.7%); ischial spine sign, 47 hips (29.7%); average CEA: 33.85° ± 7.10°; average AI: 2.27° ± 5.28°; average angle of anterior acetabular coverage: 34.25° ± 8.3°; average anterior offset: 9.22° ± 2.46°; minimum articular space: 3.8°

Table 2 (*Continued*)

Ref.	Level of evidence	Population type	No. of participants	No. of hips	Demographics	Imaging type	Major findings reported
29	III	Asymptomatic hips of patients who previously received CT for thoracic, urogenital, or abdominal indications	94	188	45 females, 49 males; mean age: 49.0 ± 16.6 years	CT	Upper limits for alpha angles (at 90°/45°) were 68°/83° (men) and 69°/84° (women) compared to literature (50°, 55°, or 60°) Cam: mean alpha angle, 51° ± 9° at 90°, 59° ± 13° at 45°; mean femoral HNO: 9 ± 2 mm Pincer: mean acetabular version angle, 19° ± 6°; LCEA, 32° ± 6°; mean AI, 6° ± 5°
30	III	Asymptomatic volunteers	170	340	93 females, 77 males; average age: 29.5 years (range, 25.7–54.5 years)	MRI	11 patients (14 hips) reported pain; 7/14 hips showed cam deformity; 37/318 non-painful hips showed cam deformity (significantly associated with development of hip pain) Mean alpha angle at 3:00: 38.3° vs 41.1° (p = 0.004); Mean alpha angle at 1:30: 48.0° versus 50.4° (p = 0.04) Comparing group with pain (14) vs without pain (318): mean alpha angle at 3:00: 44.1° vs 40.9° (p = 0.03); at 1:30: 54.4° vs 50.9° (p = 0.01); Hips with alpha angle >60° at 1:30, 6 hips with pain (42.8%) vs 30 hips without pain (9.4%) (p = 0.001)
31	III	Volunteers from general population	83		44 females, 39 males; Mean age: females, 44 ± 11 y (range, 22–67 year); males, 48 ± 12 year (range, 28–69 year)	AP pelvic and cross-table lateral X-rays	95% reference intervals for alpha angle and anterior offset ratio were higher than normally reported: 32°–62° and 0.14–0.24, respectively Mean alpha angle: males, 48° ± 8°; females, 47° ± 8°

Table 2 (*Continued*)

Ref.	Level of evidence	Population type	No. of participants	No. of hips	Demographics	Imaging type	Major findings reported
32	III	Asymptomatic	201	402	96 females, 105 males; 99 white (58 males, 41 females), 102Chinese (47 males, 55 females)	CT	Significantly higher percentage (53%) of hips in white subjects showed ≥2 radiographic signs of FAI compared to 41% of Chinese subjects Significant differences: alpha angle at 1:30 in 15% vs 32% (Chinese vs white women) ($p = 0.004$); COS in 12% vs 41% (Chinese vs white males)($p < 0.001$) and 2% vs 16% (Chinese vs white females)($p < 0.001$); CEA in 3% vs 13% (Chinese females vs white females)($p = 0.005$);
36	III	Healthy 19-year olds; all born at Haukeland University Hospital in Norway in 1989	1,152		480 males, 672 females; age: 19 years	AP and frog-leg X-rays	FAI detected in 35 of 480 (7.3%) male subjects and 32 of 672 (4.8%) female subjects Cam: increased alpha in males: right 114 (24%), left hips, 99 (21%); females: right, 101 (15%), left, 111 (16%); COS: males: right 213 (46%), left, 228 (49%); females: right, 271 (41%), left, 273 (41%)
33	III	Subjects from Osteoporotic Fractures in Men study	4,140		All males >65 years old from 6 clinics in United States; mean age: 77 ± 5 years; non-white: 395 (10%)	AP X-ray	Pincer, cam, or mixed-types of radiographic FAI prevalence of 57% (1748/3,053), 29% (886/3,053), and 14% (419/3,053), respectively; pincer and mixed-type associated with hip pain; impingement angle <70° associated with less pain versus larger angles

Table 2 (*Continued*)

Ref.	Level of evidence	Population type	No. of participants	No. of hips	Demographics	Imaging type	Major findings reported
34	III	Patients who lacked apparent hip problems and had X-rays due to trauma	339		169 females, 170 males; mean age: males, 47 ± 17 years; females, 55 ± 19 years	AP and frog-lateral X-rays	Significantly lower alpha angle and higher head-neck offset ratio in females; upper limit of 95% reference interval for alpha angle was 70° for males and 61° (AP) or 66° (lateral) for females; Males: HNO ratio: AP, 0.15 ± 0.03 mm, lateral, 0.17 ± 0.04 mm; females:; mean alpha angle: males, AP, 49.4° ± 10.5°, lateral, 49.1° ± 10.6°; females, AP, 45.0° ± 8.0°, lateral, 46.1° ± 9.9°
35	III	Sumiswald Cohort of young men being evaluated during recruitment to the Swiss Army	244		All males; mean age of those with cam: 20.0 ± 0.7 years, for those without cam: 19.9 ± 0.7 years	MRI	67/244 (27.5%) cases of cam; Associated with labral lesions, impingement pits. Labral lesions: 57 (85%) of cam and 118 (67%) without cam, OR: 2.77 Intralabral signal alterations in 32 (48%) with cam and 54 (31%) without cam, OR: 2.12 Labral avulsions present in 51 (76%) with cam and 102 (58%) without cam, OR: 2.24

CEA—center edge angle; LCEA—lateral center edge angle; HNO—Head–neck offset; COS—crossover sign

Table 3
Characteristics of studies involving symptomatic subjects (number of studies = 35).

Ref.	Level of evidence	Population type	No. of participants	No. of hips	Demographics	Imaging type	Major findings
37	III	68 patients with clinical symptoms of FAI, 25 normal volunteers	93	118 (68 symptomatic hips, 50 control hips)	32 females (23 symptomatic, 18 control); 61 males (45 symptomatic, 32 control); mean age of symptomatic patients: 28 ± 6.6 years; mean age of control: 29 ± 3.9 years	MRI	Epiphyseal torsion angles increased in patients with symptoms of FAI compared to normal volunteers; No correlation between increased epiphyseal torsion angles and increased alpha angles; 51/68 patients (75%) with labral defects: no difference between epiphyseal torsion angle values in patients with labral abnormalities and patients with an intact labrum Acetabular cartilage defects in 25/68 patients (36.8%).
38	III	63 patients with FAI, 63 asymptomatic volunteers	126		60 females, 66 males; mean age: asymptomatic, 34.4 years; patients with FAI, 35.3 years	MRI	33/63 (52%) cam, 10/63 (16%) pincer, 20/63 (32%) with mixed-type FAI. Femoral antetorsion similar in asymptomatic and those with FAI. Both groups: female had significantly higher antetorsion angles vs male. Significantly greater antetorsion for pincer vs cam or pincer vs cam plus mixed-type.
40	III	Patients with all types of FAI (cam, pincer and mixed)	66	69	Gender not reported; age not reported	MRI	MRI detection of labral tears in 39 hips, but arthroscopy showed tears in only 13: sensitivity, 81%; specificity, 51%; accuracy, 58%; positive predictive value, 33%; negative predictive value, 90% MRI detection of chondral damage: sensitivity, 17%; specificity, 100%; accuracy, 55%; positive predictive value of MRA was 100% and negative predictive value was 51%.
7	III	Patients with clinical symptoms of cam FAI	50	50	Gender breakdown and mean age not reported	frog-leg lateral X-ray, MRI	Frog-leg lateral X-ray detected cam FAI, but MRI needed to detect other conditions. Mean triangular index: radiograph (2.9 ± 1.2) vs MRI (2.6 ± 0.8). Mean alpha angles (AP radiograph): less than 50 years, 82° ± 22°; greater than 50 years of age, 75° ± 13°; females, 73° ± 9°; males, 75° ± 10° Mean alpha angles (lateral radiograph): less than 50 years, 83° ± 19°; greater than 50 years 77° ± 13°; females, 73° ± 9°; males, 75° ± 10° Mean alpha angles (MRI): less than 50 year 85° ± 21°; greater than 50 years, 80° ± 16°; females, 85° ± 21°; males, 84° ± 20°
41	III	Patients with clinically suspected FAI	41	25 right and 16 left hips	23 females, 18 males; age range, 17–60 years; mean, 39 ± 11 years	MRI	Alpha angle measured in oblique axial vs radial plane MR images; alpha angle <55° on oblique axial images in 22/41 hips (54%), but these same patients showed alpha angles of 55° or greater on radial plane images; mean alpha angles: Oblique axial 53.4° ± 11.1°; Maximal radial 70.5° ± 14° ($p < 0.001$)

Table 3 (*Continued*)

Ref.	Level of evidence	Population type	No. of participants	No. of hips	Demographics	Imaging type	Major findings
42	III	Subjects retrieved from database of patients receiving joint-preserving surgery	68	68	37 females, 31 males; mean age of 38 years (range, 17–60 years)	Supine AP pelvic, cross-table, Dunn X-rays; MRI	MRI: 43/68 hips were cam-positive (alpha angle >50.5°); of these, cam-positivity detected in 30 on AP pelvis, 39 on cross-table lateral, and 42 on Dunn X-ray; 25/68 with isolated labral tears; mean alpha angle: AP, 65°, crosstable, 63°, Dunn, 61°, MRI, 59°
43	III	Patients referred for hip pain and/or labral tears	42	42	23 females, 19 males; mean age of 39 years (range 18–78 years)	MRI	Borderline association of herniation pits with high AFA (corresponding to pincer). Labral tear was more common with a low AFV, and cartilage loss was usually posterior if high AFA but not statistically significant correlation
39	III	53 patients and 53 age- and gender-matched asymptomatic volunteers	106	106	42 females, 64 males (20–50 years age)	MRI	33/53 cam, 20/53 mixed Volunteers and patients with cam showed overlapping alpha angle measurements; alpha angles >55° in 20/53 (38%) volunteers by reader 1 and 33/53 (62%) volunteers by reader 2; Mean alpha angles: 65.4° ± 11.5° and 65.2° ± 7.3° for readers 1 and 2 in patients and 53.3° ± 9.6° and 55.0° ± 8.8° in volunteers, respectively (p = 0.001, patients vs. volunteers).
44	III	36 non-dysplastic, painful hips; 20 asymptomatic hips of volunteers	42 (30 patients, 12 controls)	56 (36 hips from patients, 20 control hips)	18 females, 24 males (symptomatic: 13 females, 17 males); mean age of symptomatic group, 40.7 years; mean age of control group, 37 years	CT, MRI	Mean alpha angle, 66.4° in patients vs 43.8° in control; labral tear in all but one symptomatic hip; 61% of symptomatic hips had cartilage damage; mean alpha angle significantly greater in the symptomatic vs control group: 66.4 ± 17.2 vs 43.8 ± 4.46 (p = 0.001); Males had significantly greater alpha angles vs females in the symptomatic group: 73.3 vs v.7 (p = 0.009) but not in the control group: 43.7 vs 43.8 (p = 0.22). Symptomatic females had significantly greater alpha angles vs control (p = 0.01).
45	III	Patients with clinical FAI	40	42	18 females, 22 males; mean age of 36.5 years (range, 17–67 years)	MRI	Abnormal alpha angle in 39/42 hips (93%); 40/42 (95%) with anterosuperior cartilage abnormality; 42/42 with anterosuperior labral tear; 37/42 hips (88%) showed this triad on MRI; mean alpha angle: 69.7° (range, 40.8°–91.3°)
46	III	10 cam, 10 asymptomatic, 10 healthy control	30		All males; age range, 18–35 years	CT	Mean alpha angle (p < 0.01): healthy group, 49.4°; asymptomatic, 65.2°; symptomatic, 74.5°; mean anterior offset ratio in the patient group was 0.15 compared to 0.17 in the asymptomatic control group with radiographic features specific to FAI (P = 0.05) and 0.21 in the healthy control group (P = 0.001). CEA: cam, 35.2 ± 7.3; asymptomatic, 32.7 ± 5.5; symptomatic, 35.4 ± 4.6; Acetabular anteversion (degrees): cam, 16.2 ± 3.4; asymptomatic, 15.74 ± 2.6; symptomatic,16 ± 3.1; Positive COS (number of patients): cam, 5; asymptomatic, 2; symptomatic, 0;

Table 3 (*Continued*)

Ref.	Level of evidence	Population type	No. of participants	No. of hips	Demographics	Imaging type	Major findings
47	III	No prior surgery, prospectively recruited based on clinical symptoms	46		20 females, 26 males; age range, 21–45 years; mean age, 32.3 years	MRI	37/38 (97%) showed labral-chondral transition zone lesions; 7/38 showed labral tears; Separate acetabular cartilage abnormality was surgically identified in 39% of cases, and femoral cartilage lesions were found in 20%. The acetabular chondral lesions were correctly identified in 89–94% of cases.
48	II	Non-arthritic adult patients with hip pain	46	50	25 females, 21 males; average patient age was 32.8 years (range, 18–49 years)	Supine and weight-bearing AP pelvic X-rays	Weight-bearing X-rays resulted in reduced acetabular coverage.
49	III	Recruited due to hip pain	50			MRI	Significant variability between readers of MRI alpha angle; subjective assessment of alpha angle was suboptimal unless a bone abnormality was suspected
50	III	Recruited based on clinical symptoms	49	60	age range 13–50 years, mean age 28 ± 10.2 years	Cross-table lateral, Dunn X-rays; MRI	Radial MRI detected cam in 45/60 (75%) and in 40/60 by X-ray; Dunn view more sensitive than cross-table lateral view; Cam deformity in radiographs: 48.3% (26/60) of the AP views vs 58.3% (35/60) in Dunn/cross-table lateral views. Both views: 88.8% (40/45) of the cam lesions could be detected. Range of alpha angles: 36.3–96.7° for AP view, 35.6–89.4° for Dunn, 38.0–114° for cross-table lateral view. Mean alpha angle: MRI, 64.1° ± 11.9°; mean LCE: 23.3 ± 6.96°. 28 cases had positive COS.
51	III	24 cam, 23 normal	47		Mean age of "normal" subjects: 55 ± 21 years; ratio of female:male of 13:10. Mean age of cam hips: 54 ± 17 years with a female:male ratio: 13:11	CT	Larger femoral head detected in those with cam deformity versus normal
52	II	Surgical patients	41		28 females, 13 males	CT; AP pelvic, Dunn, frog-leg lateral, and cross-table X-rays	37/41 alpha angle >50° by X-ray vs 30/41 by CT; maximum angle was greater on X-rays than CT in 25/41 (61%); three-view X-ray (AP pelvic, Dunn, and frog-leg lateral) effectively detects abnormal cam; radiograph (all views), mean alpha angle: 61.9°; CT, mean alpha angle: 59.8°
53	III	75 patients (96 hips), 50 asymptomatic controls (100 hips)	125	196	37 females, 88 males; mean age: FAI, 38.0 years; controls, 36.2 years	Frog-leg lateral X-ray	Frog-leg lateral X-ray reproducibly detected cam FAI with threshold of alpha angle >58° in females and >63° in males; Mean values in the controls and FAI patients were: alpha angle, 49.3° vs. 73.9° ($p < 0.0001$); HNO, 7.6 mm and 2.5 mm ($p < 0.0001$);

Table 3 (*Continued*)

Ref.	Level of evidence	Population type	No. of participants	No. of hips	Demographics	Imaging type	Major findings
54	III	Patients scheduled for surgery due to symptomatic FAI	100		50 females, 50 males; mean age of the female cohort was 31.4 years (range, sixteen to forty-nine years), and the mean age of the male cohort was 28.7 years (range, fourteen to forty-nine years)	AP pelvic, Dunn, and frog-leg lateral X-rays	Females vs. males: Isolated cam (femoral based): radiographic, 47% vs. 44%, clinical, 68% vs. 38%; mixed: Radiographic, 41% vs. 56%, clinical, 32%vs. 62%; Isolated pincer (acetabular based): radiographic, 6% vs. 0%, clinical, 0% vs. 0%; females vs. male for all values: Pincer deformity: 47% vs. 56% ($p = 0.464$); COS >10 mm: 28% vs. 47% ($p = 0.113$); LCEA >40° and/or AI <0°: 25% vs. 21% ($p = 0.669$); Cam deformity: 88% vs. 100% ($p = 0.027$); Alpha angle (max.) 57.6° vs. 70.8° ($p < 0.001$); HNO (min.): 0.16 vs. 0.14 ($p < 0.001$); Posterior wall sign (<0 mm) 56% vs. 85% ($p = 0.009$)
55	III	Patients presenting with groin-based pain	50		Age range 17–40 years	Supine frog-leg lateral X-rays	Radiographic evidence of increased alpha angle may not be best measure of functional impingement
56	III	26 symptomatic patients, 19 asymptomatic, healthy controls	45		Patients: 10 female, 16 male; mean age was 39 ± 10.7 (range,17–58); controls: 7 female, 12 male; mean age: 39 ± 11.7 (range, 16–56)	X-ray, CT	Alpha angle >50° in all patients and 2/19 controls; mean alpha angle: CT, 65.8°; radiographic, 63.9° ($p < 0.05$); Mean radiographic alpha angle in patients was 63.3° and 44.9° in controls ($p < 0.001$). Mean acetabular center edge angle was 32.8° on false-profile view
57	III	15 patients with cam FAI, 15 control femurs from cadaver database	30	30	Mean age: patients, 26 ± 7; controls, 27 ± 8 years	CT, X-ray	Significantly larger alpha angle in patients vs controls; asphericity of cam FAI patient femurs was 4.99 ± 0.39 mm (significantly greater than controls at 2.41 ± 0.31 mm) ($p < 0.001$); mean alpha angle for control vs. cam: Frog-leg Lateral 45.7 ± 7.0 vs. 68.1 ± 15.4; AP, 50.2 ± 8.8 vs. 73.1 ± 19.6; crosstable lateral, 44.1 ± 7.5 vs. 63.7 ± 11.7
58	III	Elderly patients who previously received internal fixation for femoral neck fracture	187		All patients ≥50 years	Frog-leg lateral X-ray	157/187 with cam-type impingement; Mean alpha were 67 (SD 14.5. Mean HNO: 5.2 (SD 4.8), and the mean head diameter was 47.4 (SD 14.2). The mean HNO ratio: 0.11 with a standard deviation of 0.08.
59	III	Patients who received pelvic radiography at single institution and did not have clinically diagnosed FAI	262	522	162 females, 100 males	Supine AP X-ray	Cam impingement: 40 hips (7.7%) with male predominance; pincer impingement: 330 hips (63.2%) with female predominance; mixed-type impingement: 82 hips (15.7%) with male predominance; no correlation with pain; 58 hips (11.1%), no radiographic sign of FAI; Coxa profunda affected more female than male ($p < 0.0001$). Prevalence of acetabular retroversion decreased with progressive age for both genders ($p < 0.0001$). No parameter found to be significantly more present in patients with pain when compared with patients without pain

Table 3 (*Continued*)

Ref.	Level of evidence	Population type	No. of participants	No. of hips	Demographics	Imaging type	Major findings
60	III	consecutive patients presenting with hip pain in 6-month timespan	33	66	17 females, 16 males; age range, 21–40 years; mean age, 33 years	AP pelvic	64/66 previously reported normal hips (33/34 female, 31/32 male) with ≥1 radiographic sign of FAI; COS: 12 hips (8 male, 4 female), and in 5 patients (3 men, 2 women). Coxa profunda: 49 (31 female, 18 male), and in 24 patients these were bilateral (15 women, 9 men). Protrusio acetabuli: no cases. Prominent posterior wall sign: 49 (18 female, 9 male), bilaterally in nine patients (7 women, 2 men). Acetabular index: range −8.8–12.38 (mean, 3.98; median, 5.28). LCEA: range, 27–588 (mean 38.38, median 37.58).
61	III	39 with cam FAI versus 45 controls	84	84	51 females (18 cam, 35 control), 33 males (23 cam, 10 control); age range of cam patients, 17 to 84 years, with a mean of 57.6 years; controls, 54 to 101 years, mean: 67 years	cross-table lateral	Mean alpha angle: control group, 56°; FAI group, 81.1°
62	III	Patients receiving surgery for FAI: 516 unilateral, 132 bilateral	648		unilateral group: 514 (248 female; 266 male), and bilateral group: 132 (46 female, 86 male); 294 females, 354 males total; mean age of unilateral: 30.3 years and 27.6 years for bilateral patients	MRI, CT	OR:1.7 for males with bilateral vs females; significantly larger mean alpha angle for bilateral patients (63.8°) vs unilateral group (59.8°); larger alpha angle and reduced acetabular anteversion were significant risk factors for bilateral surgery; LCEA: unilateral, 428 patients, 34.42° ± 14.59°, bilateral, 101 patients, 32.75° ± 6.81° (p = .907); Acetabular version At 1 O'clock unilateral, 2.97 ± 9.44, bilateral, −0.06 ± 9.14 (p = 0.003)
63	III	Patients with clinical diagnosis of FAI	41		17 females, 24 males	MRA	100% sensitivity for cam deformities and os acetabuli; significant sensitivity for detecting labral tears
64	III	Consecutive patients with symptomatic FAI in one hip	100	200	56 females, 44 males; Age range was 13–61 years, with a mean of 34.3 years (±11.3) years.	MRI	43 cam, 37 pincer, and 20 mixed; 95% of symptomatic hips showed ≥1 radiographic sign of FAI; radiographic signs poor predictors of hip pain; Symptomatic vs. asymptomatic: Neck shaft angle (degrees) 132.18 vs. 133.07 (p = 0.005); Male vs. female: Joint space narrowing 29% vs. 11% (p = 0.02); femoral osteophytes 22% vs. 2% (p = 0.002); Number of patients with non-sphericity femoral head in AP or lateral images 25 vs. 16 (p = 0.006); Alpha angle (degree) 88° vs. 68.1°(p < 0.001);
65	III	122 symptomatic patients, 100 asymptomatic	222	222	Symptomatic, mean age of 41 years; asymptomatic, mean age of 31 years (p < 0.0001)	AP and Dunn X-rays	Femoral bump significantly more frequent and alpha and Lequesne anteversion angles and femoral offset significantly larger in symptomatic vs asymptomatic; mean alpha angle for asymptomatic vs. symptomatic (p = 0.0001): AP: 53 ± 11.6 vs. 72.7 ± 9.1; Dunn 59.8 ± 10.9 vs. 71.6 ± 7; Dunn 45° 67.5 ± 8.1 vs. 72.7 ± 6.4

Table 3 (*Continued*)

Ref.	Level of evidence	Population type	No. of participants	No. of hips	Demographics	Imaging type	Major findings
66	III	Patients with unilateral hip/groin pain	269	538	121 males (age, 35.7 ± 9.6 years) and 148 females (age, 37.6 ± 9.6 years)	AP pelvic X-ray	Cam or pincer detected in 38 painful hips and in 7 non-painful hips; prevalence of FAI in painful hips (14.1%) was significantly higher than that of non-painful hips (2.6%); males had higher prevalence of FAI in the painful hip; AP angle a: males: cam, 96.7° (5.1) vs. non-cam, 50.2° (7.8); females: cam, 87.7° (11.4)° vs. 43.5° (5.0)
67	III	Patients who received scans prior to surgery for FAI	8		1 female, 7 males; 19–46 years (mean, 28.6 years)	AP and frog-lateral X-rays, MRA	All patients had hip pain, bump appearance, labral tears, and osteoarthritis; Acetabular retroversion in 5/8 (62.5%); 3/8 with cam based on alpha angle, and 5/8 with mixed-type; no pincer based on lack of crossover sign; alpha angle (range, 48°–84°), mean alpha angle: 62.9° ± 12.2°; Subchondral edema, herniation pit, and paralabral cyst were not observed.
68	II	Males presenting with hip-related complaints	155		All males; mean age, 32 years; range, 18–50 years	AP or lateral X-rays	135/155 (87%) with ≥1 radiographic sign of FAI; 94 patients had adequate pelvic/hip AP films: 88/94 (94%) with ≥1 radiographic finding of FAI; 57/94 (65%) with mixed-type, 15/94 (17%) with cam only, 16/94 (18%) with pincer only; Tonnis grade: 0 in 93 of the 155 (61%), 1 in 44 patients (28%), 2 in 10 (6%), and 3 in 5 patients (3%).
69	III	Non-surgical patients diagnosed with FAI	50		20 females, 30 males; mean age, 28.8 years (cam FAI: mean age, 28.8 years ± 6.5; pincer FAI: mean age, 28.8 years ± 9.4)	MRI	33 cam, 17 pincer; alpha angles larger in cam vs pincer (68° vs 54°); acetabulum ($p < 0.001$) deeper in pincer FAI group (mean depth, 4.8 mm) vs cam (mean depth, 0.7 mm); Cartilage lesions in cam larger at anterosuperior ($p = 0.001$) and superior ($p = 0.018$) positions than in pincer. Cartilage lesions in pincer ($p = 0.017$) larger at the posteroinferior position than in cam; ($p = 0.047$) more labral lesions at the posterior and posteroinferior positions in Pincer;
70	II	56 patients (61 cam hips) and 24 controls (24 asymptomatic hips)	80	85 (61 hips treated for cam and 24 asymptomatic control)		Frog-lateral, AP, cross-table X-rays	Larger femoral head sphericity and alpha angle and smaller HNO in symptomatic vs controls; X-ray views differed; frog-lateral detected highest% of sphericity among patients (88%); average alpha angles in symptomatic hips: cross-table lateral, 58.8°; AP, 71.5°; frog-lateral, 65.2°; average HNO for symptomatic hips: cross-table lateral, 9.6 mm; AP, 7.6 mm; frog-lateral, 6.6 mm; mean alpha angle: 65° for hips with impingement vs 47° control

CEA—center edge angle; LCEA—lateral center edge angle; HNO—Head–neck offset; COS—crossover sign mixed FAI, particularly among distinct populations, such as groups of asymptomatic or symptomatic subjects and athletes [10]. No systematic analysis to date has compared studies of asymptomatic, symptomatic, and athlete groups to determine differences in radiographic signs of FAI. The purpose of this study was to systematically review the existing literature to determine the prevalence of cam, pincer, and mixed FAI based on imaging of athletes, asymptomatic volunteer subjects, and symptomatic patients.

2. Methods

We performed a systematic review using the Preferred Reporting Items for Systematic Reviews and Meta-Analyses (PRISMA) guidelines and a PRISMA checklist [11]. The literature search was performed by one reviewer in March 2015 using the search terms ((((femoroacetabular impingement [Title/Abstract])) AND ((((radiograph[Title/Abstract]) OR radiographic[Title/Abstract]) OR imaging [Title/Abstract]) OR X-ray[Title/Abstract]) AND (English[lang]))). The PubMed, MEDLINE, CINAHL, and Cochrane databases were searched. Among the studies that were identified, we included those reporting radiographic, computed tomographic, and/or MRI findings indicative of FAI in athletes, symptomatic patients, and/or asymptomatic volunteers. FAI with cam, pincer, and mixed-type conditions were included. References within the included studies were also examined for potential inclusion. Articles were excluded if they involved participants who received total joint arthroplasty or other hip surgery, pathologic conditions other than FAI, such as osteoarthritis, dysplasia, slipped capital femoral epiphysis, or Legg–Calve–Perthes disease, the use of other imaging modalities, such as ultrasound or bone-scan imaging, or joints other than the hip. In addition, non-English language articles, letters to the editor, topic reviews, and meeting abstracts were excluded. The search algorithm is shown in Fig. 1. The number of participants, mean age, gender breakdown (if reported), type of deformity (cam, pincer, or mixed), chondral or labral defects, race (if reported), mean alpha angle, center edge angle, head–neck offset, crossover sign, and type(s) of imaging were noted for each study. The alpha angle and additional radiologic signs of FAI were recorded for each study.

Descriptive statistics were calculated for each study and parameter or variable analyzed. Continuous variable data were reported as mean standard deviation (weighted means when applicable). Categorical data were reported as frequencies with percentages. For all statistical analysis, $p < 0.05$ was deemed statistically significant. Statistical analysis between all groups was performed by two-tailed Student's t-test; comparisons across all groups were performed by one-way analysis of variance (ANOVA).

3. Results

The literature search identified 361 studies. After considering the inclusion and exclusion criteria, 60 studies were included. These consisted of 15 studies of athletes [12–26] (Table 1), 10 studies of purely asymptomatic patients [27–36] (Table 2), and 35 studies of symptomatic, non-athlete populations [7,37–70] (Table 3).

3.1. Athletes (Table 1)

The studies involving athletes included 958 subjects and 1389 hips. Cam-type impingement was found in 66.4 ± 23.5% of athletes, whereas pincer-type impingement was found in 51.2 ± 20.3% (Table 4). The average percentage of athletes that showed radiographic signs of mixed-type FAI was calculated as 57.1 ± 6.1% from the two studies that reported this finding. The mean alpha angle was 55.7° ± 3.6° (Table 5). Two studies reported chondral defects

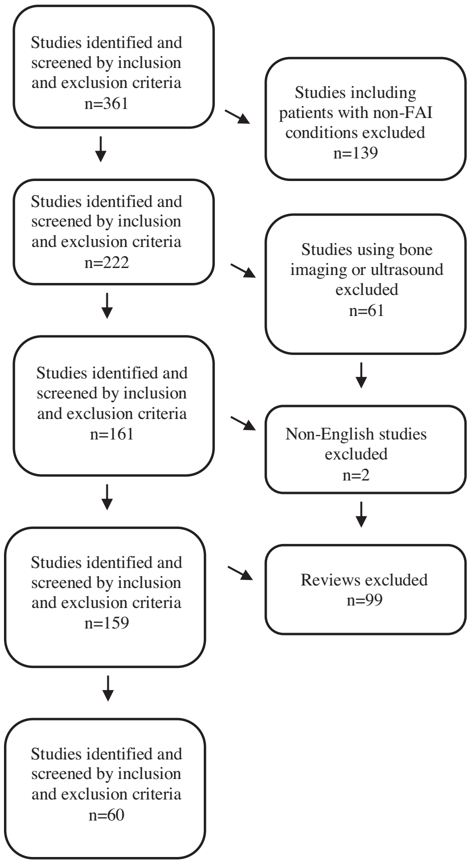

Fig. 1. Systematic search and identification of studies in the PubMed, MEDLINE, CINAHL, and Cochrane databases based on the Preferred Reporting Items for Systematic Reviews and Meta-analyses (PRISMA) guidelines.

Table 4
Percentage of subjects with cam versus pincer FAI.

	Cam[a], (%)	Pincer, (%)	Mixed[g], (%)
Athletes	66.4 ± 23.5[b]	51.2 ± 20.3[c]	57.1 ± 6.1[e]
Asymptomatic	22.4 ± 6.2[d]	57 (1 study)	8.8 ± 5.1[f]
Symptomatic	49.0 ± 21.2	28.5 ± 19.2	40.2 ± 18.0

[a] $p = 0.006$ across groups for cam, one-way ANOVA.
[b] $p = 0.0003$ compared to asymptomatic, $p = 0.107$ compared to symptomatic, two-tailed student's t-test.
[c] $p = 0.169$ compared to symptomatic group, two-tailed student's t-test.
[d] $p = 0.009$ compared to symptomatic, two-tailed student's t-test.
[e] $p = 0.03$ for athletes versus asymptomatic and $p = 0.144$ for athletes versus symptomatic, two-tailed student's t-test.
[f] $p = 0.015$ compared to symptomatic group, two-tailed student's t-test.
[g] $p = 0.041$ across groups for mixed-type, one-way ANOVA.

in an average of 8.6 ± 0.4%, and labral tears were reported in 49.8 ± 21.4% of athletes. Positive crossover sign was reported in 64.5 ± 18.6% of athletes.

The most commonly represented sport was football [18,20,23,24] (364 players), which was followed by soccer [12,16,21,22] (217 players) and ice hockey [13,14,25] (Table 6). The majority (>90%) of football players showed radiologic evidence of FAI regardless of whether symptoms existed [18,20,23,24]. Mixed-type FAI, which shows evidence of cam and pincer impingement, was the most common among these. The alpha angle was an important independent predictor of pain among football players [18]. In contrast to these, studies involving soccer players showed

Table 5
Mean radiographic values.

Alpha angles[b]	
Athletes[a]	55.7° ± 3.6°
Asymptomatic[a]	47.0° ± 2.0°
Symptomatic[a]	67.4° ± 8.0°
Chondral defects	
Athletes	8.6 ± 0.4%
Asymptomatic	NR
Symptomatic	NR
Labral tears	
Athletes[d]	49.8 ± 21.4
Asymptomatic	NR
Symptomatic	27.6 ± 9.2
Positive crossover sign	
Athletes[c]	64.5 ± 18.6
Asymptomatic	28.5 ± 15.8
Symptomatic	18.2 (1 study)

[a] *P*-values show significant difference ($p < 0.001$) for this group versus any one of the other groups by two-tailed student's *t*-test.
[b] ANOVA shows $p = 0.000$ across groups.
[c] $p = 0.206$ for athletes versus asymptomatic, two-tailed student's *t*-test.
[d] $p = 0.226$ compared to symptomatic by two-tailed student's *t*-test.

greater variability in their findings. For example, one study concluded that semi-professional soccer players had significantly larger alpha angles than amateur players [12] while another study [16] showed no significant difference. Two studies that compared high-level male and female soccer players noted that males had greater alpha angles compared to those of female players [21,22]. Consistent with this finding, a higher percentage of males showed radiologic evidence of FAI compared to that of females [21,22] as well as a higher percentage of bilateral hip involvement (44% vs 20%) [21]. Studies on ice hockey players pointed out an increased radiologic evidence of FAI depending on the style of ice hockey [25] and in comparison to non-athletes [14] as well as skiers [13]. Interestingly, cam impingement was common among those who practiced Capoeira [17], whereas adult ballet dancers showed little sign of FAI on radiographs [19]. However, these same dancers did exhibit significantly more cartilage lesions and herniation pits, which may be indicative of pincer-like impingement [19].

3.2. *Asymptomatic population (Table 2)*

Among studies that included only asymptomatic subjects, there were 6705 individuals and 7282 hips. Cam-type impingement was found in 22.4 ± 6.2% of all asymptomatic subjects, whereas pincer-type impingement was found in 57% (Table 4) and a mixed-type was detected in 8.8 ± 5.1%. The mean alpha angle was 47.0° ± 2.0° (Table 5) and a positive crossover sign was reported in 28.5 ± 15.8%. Radiologic evidence of FAI was fairly common among these populations, although substantially lower than the one observed in athletes. One study showed a 14% prevalence of cam impingement [27] and two other studies showed 27–29% prevalence of cam-type FAI [33,35]. Alpha angles >50° or cam deformities were detected in 12–25% [28,30] with male predominance [28,33]. A study that included a large cohort of asymptomatic patients noted a high prevalence of pincer impingement (57%) [33]. Importantly, the reference intervals for alpha angles were in several studies higher than those used in most literature. Similarly, in Nardos' study [33] alpha angles smaller than 70° were less likely to cause pain.

3.3. *Symptomatic population (Table 3)*

There were 3472 patients and 4169 hips included in the symptomatic group. The vast majority of studies found ≥1 radiographic sign of FAI. The prevalence of cam or mixed-type FAI ranged from 63% to 94% and the prevalence of pincer-type FAI ranged from 18% to 51%. Cam-type impingement was found in an average of 49.0 ± 21.2%, whereas pincer-type impingement was found only in 28.5 ± 19.2% (Table 4) and a mixed-type occurred in 40.2 ± 18.0%. The mean alpha angle was 67.4° ± 8.0° (Table 5). Labral tears were reported in 27.6 ± 9.2% of patients, and a positive crossover sign was reported in 18.2% in one study.

Multiple studies compared symptomatic and asymptomatic populations. A higher percentage of symptomatic hips demonstrated increased alpha angles, labral tears, and epiphyseal torsion angles compared to asymptomatic normal volunteers [37,44,46,56,61,65,70]. Similar to findings reported in studies of asymptomatic subjects, cam-type impingement showed male predominance among symptomatic patients [59] and interestingly, this was also documented in mixed-type FAI. Additionally this study suggested that pincer-type occurred primarily in females [59], whereas another study [54] showed a slightly higher prevalence among males. In males with symptomatic hips compared to those of females there was a tendency to show significantly larger alpha angles [53] as well as evidence of FAI in painful hips [66], and bilateral hip involvement [62].

3.4. *Findings across groups*

Cam impingement was significantly ($p = 0.0003$) more common in athletes compared to asymptomatic but not to symptomatic subjects (Table 4). In addition, cam FAI was significantly ($p = 0.009$) more common in symptomatic versus asymptomatic cases. Comparisons of the percentage of patients with cam-type FAI showed significant ($p = 0.006$) differences across groups. No significant differences were found between pincer-type FAI morphology prevalence when comparing athletes to symptomatic patients; however there were insufficient numbers of cases of pincer FAI reported in the studies of asymptomatic subjects. Comparisons of the percentage of patients with mixed-type FAI showed significant ($p = 0.041$) differences across groups. Mixed-type FAI was significantly ($p = 0.03$) more common in athletes versus asymptomatic subjects and in asymptomatic versus symptomatic subjects ($p = 0.015$). Significant differences were also noted across groups for mean alpha angle. The mean alpha angle was significantly ($p < 0.001$) greater in the symptomatic group versus either the asymptomatic or athlete group. Additional imaging signs of FAI, such as labral tears and chondral defects were noted for each study if reported (Tables 1–3); however, there were no significant differences in labral tears or positive crossover sign.

FAI can be assessed using a variety of imaging techniques. Among the 15 studies that included athletes, seven used MRI, seven

Table 6
Characteristics of studies involving athletes by type of activity.

	Number of participants	Female	Male	Mean age (years)
Soccer [12,16,21,22]	217	45	172	24.02 ± 3.1
Ice hockey [13,14,25]	151	9	142	18.02 ± 2.5
American Football [18,20,23,24]	364	50	314	23 ± 3.4
Capoeira [17]	24	10	14	31.5 ± 5.5
Ballet [19]	30	30		24.6 ± 3.4
Non-specified [15,26]	261	56	205	16 ± 5.5

used frog-leg lateral and AP X-ray views, and one used CT. In asymptomatic populations, there were more studies that used X-rays ($n = 5$) compared to MRI ($n = 3$) and CT ($n = 2$). Symptomatic populations were most commonly imaged using MRI-based techniques, including MRI ($n = 11$), magnetic resonance arthrography (MRA) ($n = 1$) and combined X-rays and either MRI or MRA ($n = 4$). Another two used combined CT and MRI, whereas three studies used CT and X-rays. There were 12 studies that imaged symptomatic patients exclusively by X-ray.

4. Discussion

The purpose of this study was to determine the prevalence of FAI and associated lesions across different groups, namely asymptomatic, symptomatic patients and athletes. The prevalence of imaging signs of cam-type impingement, including mixed-type FAI, varied greatly among studies and specific populations. The prevalence of cam FAI was lowest in the asymptomatic population, highest in symptomatic populations, and was most variable among athletes. In fact, the prevalence of cam deformity is known to be sex-dependent, associated with pain, activity dependent and develops gradually in adolescents and probably only during skeletal growth [54,75].

Radiographic evidence of pincer-type impingement was not noted in all studies and those that reported cases of pure pincer FAI also showed variability. The relatively high prevalence of pincer FAI in an asymptomatic population is consistent with the reported results in Frank et al. [10], which showed a 67% prevalence of pincer FAI among asymptomatic individuals. Furthermore, our finding that in asymptomatic populations a pure pincer FAI was more common than cam or mixed-type FAI was again consistent with the reported data [10]. In fact its pathological implications as well as its association with hip osteoarthritis are unclear and yet to be defined [71]. Also crossover and posterior wall signs might be a normal variant [72]. Overall, studies on asymptomatic patients demonstrate that radiologic signs of FAI are common regardless of whether pain is present.

These findings emphasize that FAI syndrome should be considered a clinical diagnosis and that patient history and physical examination are the cornerstone of hip evaluation. Reliance on imaging diagnosis of FAI syndrome is thus unwise and this study should be considered in clinical decision making for hip pain patients.

FAI morphology can be assessed using a variety of imaging techniques and detection of FAI may vary depending on imaging type selection; thus, differences in imaging modality may partially explain the substantial variability noticed in FAI prevalence rates. CT was used less frequently than X-ray or MRI. In addition, among the available X-ray views, frog-leg lateral was a common choice in detecting typical radiographic signs of FAI, including femoral sphericity, head–neck offset, and increased alpha angle. MRI was a popular choice for imaging hips in all populations, which is likely due to its ability to evaluate bone and soft tissues [50]. Radial MRI was more sensitive than any X-ray view alone, and was thus considered critical for diagnosing FAI [50].

Our systematic review found a male predominance for cam and mixed-type deformities, which is consistent with findings reported in another systematic review [10]. The overall male:female distribution of cam FAI has been estimated to be 14:1 [5]. In contrast, pincer FAI is reported to exhibit a male:female distribution of 1:3 [5], which is consistent with findings reported in one of the studies included in our review [59]. Interestingly, bilateral cam FAI seems to be more prevalent in males. One study showed an almost 2:1 male:female distribution whereas another showed a 3:1 distribution for bilateral hip involvement [21,62]. These findings reflect sex-dependent disease patterns, particularly with symptomatic FAI. Female have more pronounced symptomatology and milder morphologic abnormalities, while males have generally higher activity levels, larger morphological abnormalities and more extensive articular disease [54]. Also, there are age-dependent radiographic patterns, namely higher prevalence of *coxa vara* with increasing age and lower prevalence of acetabular retroversion with decreasing age [59].

Imaging signs of FAI did not necessarily correlate with the presence of symptoms. This was highlighted by the 14–29% prevalence of radiographic evidence of cam FAI among asymptomatic subjects. However, the presence of hip pain appears to be a predictive factor for the presence of FAI, as at least one radiographic sign of FAI was found in the majority of symptomatic hips. Nevertheless, one study found that the only independent predictor of pain was an increased alpha angle [18]. Development of symptomatic FAI is dependent on the type, intensity and frequency of individual activities [75], which partially explains the fact that cam impingement was significantly more common in athletes compared to asymptomatic populations. Thus, imaging should be performed in patients who report hip pain to carefully evaluate the presence of deformities and joint abnormalities.

The alpha angle is a commonly used radiographic measure to define cam FAI. Generally it is considered abnormal if greater than 50–55° [73]. In a recent review it was noted that asymptomatic patients might have borderline values of mean alpha angle (54°) [10]. However, other studies on asymptomatic populations showed that the reference interval upper limit was actually greater than 62° [29,31,33], which might suggest that the upper threshold at which an alpha angle is considered to demonstrate FAI may need to be re-assessed. It has also been noted that alpha angles poorly discriminate symptomatic and non-symptomatic population [39]. This review illustrates that purely asymptomatic population had mean normal alpha angles (47.0° ± 2.0°) whereas symptomatic subjects had mean pathologic alpha angles (67.4° ± 8.0°). Increasing alpha angles have been shown to be associated with decreased function, pain, vigorous activity and to be highly predictive for development of osteoarthritis [2,75,76]. Other radiographic measures can be used to characterize cam conditions, namely head–neck offset and offset ratio. However these measures were inconsistently reported in the reviewed studies.

A recent systematic review has shown that approximately two thirds of asymptomatic individuals have pincer morphologic characteristics on imaging studies [10]. However, this high prevalence may be confounded in several ways. In fact we came across similar prevalence in asymptomatic population but disproportionally higher prevalence in the athletes. Unfortunately, pincer morphologic characteristics were poorly defined among the studies. The report of pincer deformity included the presence of radiographic parameters such as the crossover sign and posterior wall sign, with poor reliability for the diagnosis of this morphologic condition.

Furthermore, the included studies used mainly radiography rather than computed tomography for measuring pincer deformity, which is highly affected by several parameters such as pelvic tilt and rotation.

Labral injury is a well-documented cause of hip pain in FAI syndrome, with MRI proving a sensitive modality for establishing the diagnosis [74]. Both MRI and MRA have moderate sensitivity and specificity (sensitivity 66%, 87%; specificity 79%, 64%), but diagnostic accuracy of MRA appears to be superior to MRI in detecting acetabular labral tears [77]. A recent study documented that more than two thirds of asymptomatic patients had MRI findings suggestive of a labral tear [10]. Our review reported an overall mean prevalence of 60% (49.8 ± 21.4 %) in athletes and a lower mean prevalence in symptomatic population, not exceeding 37% (27.6 ± 9.2). Once more lack of standardization of diagnostic criteria and different study methodologies has to be considered for this paradox of labral tears being more frequent in the asymptomatic population. Furthermore arthroscopic correlation of imaging findings is the gold standard for confirmation of labral injury; however, this was lacking in the included studies.

Regarding treatment, the strong association between a cam deformity and osteoarthritis led to the assumption that hip pathology could be prevented. Surgical removal of the deformity has been undertaken, however no long term data exists concerning the structural joint preservation gain following surgery and the optimal timing for this action. The severity of chondropathy is associated with worse outcomes, conversely early stage surgery in undesirable as not every symptomatic cam deformity develops osteoarthritis. Additionally definitive long-term benefit of surgery over physical therapy hasnít been established.

There were several potential limitations in our analysis. Generally the limitations of a systematic review are usually based on the limitations of the analyzed studies. Limitations introducing selection bias are reflected by the variability in the threshold values used to detect radiographic signs of FAI, such as the cut-off value for alpha angle. Several studies suggested that the most commonly applied values for differentiating normal versus abnormal alpha angles may need to be re-evaluated and possibly increased [29,31,33,34], as our study points out. Other sources of selection bias include participantís age, sex, geography, activity level, race and sports engaged. There were more males versus females represented in the studies included in our analysis, and some including only males. There was also a tendency for most studies to be limited to a single institution or geographic region, which decreases the ability to generalize findings. Radiographic techniques and quality introduce detection bias as these are highly variable. Assignment of FAI morphologic features was made by both radiography and MRI on different radiographic views or MRI protocols and with different threshold values to determine pathological and non-pathological conditions.

5. Conclusions

Although imaging suspicion of FAI was detected in all populations, there was substantial variability in the prevalence of cam, pincer, and mixed-type FAI among the populations included in this review. Imaging detected at least one sign of FAI in the majority of symptomatic patients and athletes, whereas asymptomatic patients showed the lowest prevalence of radiographic signs of FAI, as expected. FAI is a clinical diagnosis with patient history and physical examination being the cornerstone of hip evaluation. Overall, imaging becomes an indispensable tool for evaluating the presence of FAI, especially among athletes and patients reporting pain, however reliance on imaging diagnosis of FAI seems to be unwise. This study might be used to assist general practitioners and surgeons in clinical decision making for hip pain patients.

References

[1] L.M. Tibor, M. Leunig, The pathoanatomy and arthroscopic management of femoroacetabular impingement, Bone Joint Res. 1 (10) (2012) 245–257.
[2] R. Agricola, M.P. Heijboer, S.M.A. Bierma-Zeinstra, J.A.N. Verhaar, H. Weinans, J.H. Waarsing, Cam impingement causes osteoarthritis of the hip: a nationwide prospective cohort study (CHECK), Ann. Rheum. Dis. 72 (6) (2013) 918–923.
[3] S. Glyn-Jones, A.J.R. Palmer, R. Agricola, et al., Osteoarthritis, Lancet (2015) 1–12.
[4] M. Tannast, D. Goricki, M. Beck, S.B. Murphy, K.A. Siebenrock, Hip damage occurs at the zone of femoroacetabular impingement, Clin. Orthop. Relat. Res. 466 (2) (2008) 273–280.
[5] M. Tannast, K.A. Siebenrock, S.E. Anderson, Femoroacetabular impingement: radiographic diagnosis—what the radiologist should know, AJR Am. J. Roentgenol. 188 (6) (2007) 1540–1552.
[6] J.C. Clohisy, A Systematic approach to the plain radiographic evaluation of the young adult hip, J. Bone Joint Surg. (American) 90 (Suppl. 4) (2008) 47.
[7] R. Kumar, A. Aggarwal, V. Krishnan, N. Gopinathan, S. Chakraborty, Femoroacetabular impingement and comparison of radiological indexes: a study on 50 cases, Musculoskelet. Surg. 97 (2) (2013) 153–158.
[8] R. Lattanzi, C. Petchprapa, D. Ascani, et al., Detection of cartilage damage in femoroacetabular impingement with standardized dGEMRIC at 3T, Osteoarthritis Cartilage 22 (2014) 447–456.
[9] F.R. Miese, C. Zilkens, A. Holstein, et al., MRI morphometry, cartilage damage and impaired function in the follow-up after slipped capital femoral epiphysis, Skeletal Radiol. 39 (6) (2010) 533–541.
[10] Frank, J.M., Harris, J.D., Erickson, B.J., et al., Prevalence of femoroacetabular impingement imaging findings in asymptomatic volunteers: a systematic review. YJARS [Internet] (2015), 1–6. Available from: http://eutils.ncbi.nlm.nih.gov/entrez/eutils/elink.fcgi?dbfrom=pubmed&id=25636988&retmode=ref&cmd=prlinks. (2015).
[11] D. Moher, A. Liberati, J. Tetzlaff, D.G. Altman, PRISMA Group. Preferred reporting items for systematic reviews and meta-analyses: the PRISMA Statement, Open Med. 3 (3) (2009) e123–e130.
[12] M. Lahner, P.A. Walter, C. Schulze Pellengahr von, M. Hagen, L.V. Engelhardt von, C. Lukas, Comparative study of the femoroacetabular impingement (FAI) prevalence in male semiprofessional and amateur soccer players, Arch. Orthop. Trauma Surg. 134 (8) (2014) 1135–1141.
[13] M.J. Philippon, C.P. Ho, K.K. Briggs, J. Stull, R.F. LaPrade, Prevalence of increased alpha angles as a measure of cam-type femoroacetabular impingement in youth ice hockey players, Am. J. Sports Med. 41 (6) (2013) 1357–1362.
[14] O.R. Ayeni, K. Banga, M. Bhandari, et al., Femoroacetabular impingement in elite ice hockey players, Knee Surg. Sports Traumatol. Arthrosc. 22 (4) (2013) 920–925.
[15] E.L. Sink, J. Gralla, A. Ryba, M. Dayton, Clinical presentation of femoroacetabular impingement in adolescents, J. Pediatr. Orthop. 28 (8) (2008) 806–811.
[16] M. Lahner, C. Schulze Pellengahr von, P.A. Walter, et al., Biomechanical and functional indicators in male semiprofessional soccer players with increased hip alpha angles vs. amateur soccer players, BMC Musculoskelet. Disord. 15 (1) (2014) 1–6.
[17] M. Mariconda, A. Cozzolino, F. Di Pietto, M. Ribas, V. Bellotti, A. Soldati, Radiographic findings of femoroacetabular impingement in capoeira players, Knee Surg. Sports Traumatol. Arthrosc. 22 (4) (2014) 874–881.
[18] C.M. Larson, R.S. Sikka, M.C. Sardelli, et al., Increasing alpha angle is predictive of athletic-related hip and groin pain in collegiate national football league prospects, YJARS 29 (3) (2013) 405–410.
[19] F.C. Kolo, C. Charbonnier, C.W.A. Pfirrmann, et al., Extreme hip motion in professional ballet dancers: dynamic and morphological evaluation based on magnetic resonance imaging, Skeletal Radiol. 42 (5) (2012) 689–698.
[20] A.L. Kapron, A.E. Anderson, C.L. Peters, et al., Hip internal rotation is correlated to radiographic findings of cam femoroacetabular impingement in collegiate football players, YJARS 28 (11) (2012) 1661–1670.
[21] A.C. Johnson, M.A. Shaman, T.G. Ryan, Femoroacetabular impingement in former high-level youth soccer players, Am. J. Sports Med. 40 (6) (2012) 1342–1346.
[22] M.B. Gerhardt, A.A. Romero, H.J. Silvers, D.J. Harris, D. Watanabe, B.R. Mandelbaum, The prevalence of radiographic hip abnormalities in elite soccer players, Am. J. Sports Med. 40 (3) (2012) 584–588.
[23] A.L. Kapron, A.E. Anderson, S.K. Aoki, et al., Radiographic prevalence of femoroacetabular impingement in collegiate football players: AAOS exhibit selection, J. Bone Joint Surg. 93 (19) (2011) e111 (1–10).
[24] J.J. Nepple, R.H. Brophy, M.J. Matava, R.W. Wright, J.C. Clohisy, Radiographic findings of femoroacetabular impingement in National Football League Combine athletes undergoing radiographs for previous hip or groin pain, Arthroscopy 28 (10) (2012) 1396–1403.
[25] J.R. Ross, A. Bedi, R.M. Stone, E. Sibilsky, E. nselman, B.T. Kelly, C.M. Larson, Characterization of symptomatic hip impingement in butterfly ice hockey goalies, Arthroscopy (2014).
[26] B.J. Yuan, R.B. Bartelt, B.A. Levy, J.R. Bond, R.T. Trousdale, R.J. Sierra, Decreased range of motion is associated with structural hip deformity in asymptomatic adolescent athletes, Am. J. Sports Med. 41 (7) (2013) 1519–1525.
[27] K. Hack, G. Di Primio, K. Rakhra, P.E. Beaulé, Prevalence of cam-type femoroacetabular impingement morphology in asymptomatic volunteers, J. Bone Joint Surg. 92 (14) (2010) 2436–2444.
[28] R.B. Scheidt, C.R. Galia, C.V. Diesel, R. Rosito, C.A.S. Macedo, Prevalence of radiographic markers of femoroacetabular impingement in asymptomatic adults, Rev. Col. Bras. Cir. 41 (1) (2014) 36–42.
[29] M. Lepage-Saucier, C. Thiéry, A. Larbi, F.E. Lecouvet, B.C. Vande Berg, P. Omoumi, Femoroacetabular impingement: normal values of the quantitative morphometric parameters in asymptomatic hips, Eur. Radiol. 24 (7) (2014) 1707–1714.
[30] V. Khanna, A. Caragianis, G. DiPrimio, K. Rakhra, P.E. Beaulé, Incidence of hip pain in a prospective cohort of asymptomatic volunteers: is the cam deformity a risk factor for hip pain? Am. J. Sports Med. 42 (4) (2014) 793–797.
[31] T.C.B. Pollard, R.N. Villar, M.R. Norton, et al., Femoroacetabular impingement and classification of the cam deformity: the reference interval in normal hips, Acta Orthop. 81 (1) (2010) 134–141.
[32] J. Van Houcke, W.P. Yau, C.H. Yan, et al., Prevalence of radiographic parameters predisposing to femoroacetabular impingement in young asymptomatic chinese and white subjects, J. Bone Joint Surg. Am. 97 (4) (2015) 310–317.

[33] Osteoporotic Fractures in Men (MrOS) Research Group, L. Nardo, N. Parimi, et al., Femoroacetabular impingement: prevalent and often asymptomatic in older men: the osteoporotic fractures in men study, Clin. Orthop. Relat. Res. (2015).
[34] C.R. Fraitzl, T. Kappe, F. Pennekamp, H. Reichel, C. Billich, Femoral head–neck offset measurements in 339 subjects: distribution and implications for femoroacetabular impingement, Knee Surg. Sports Traumatol. Arthrosc. 21 (5) (2012) 1212–1217.
[35] S. Reichenbach, M. Leunig, S. Werlen, et al., Association between cam-type deformities and magnetic resonance imaging-detected structural hip damage: a cross-sectional study in young men, Arthritis Rheum. 63 (12) (2011) 4023–4030.
[36] L.B. Laborie, T.G. Lehmann, I.Ø. Engesæter, L.B. Engesæter, K. Rosendahl, Is a positive femoroacetabular impingement test a common finding in healthy young adults? Clin. Orthop. Relat. Res. 471 (7) (2013) 2267–2277.
[37] C. Schaeffeler, M. Eiber, K. Holzapfel, H. Gollwitzer, E.J. Rummeny, K. Woertler, The epiphyseal torsion angle in mr arthrography of the hip: diagnostic utility in patients with femoroacetabular impingement syndrome, Am. J. Roentgenol. 198 (3) (2012) W237–W243.
[38] R. Sutter, T.J. Dietrich, P.O. Zingg, C.W.A. Pfirrmann, Femoral antetorsion: comparing asymptomatic volunteers and patients with femoroacetabular impingement, Radiology 263 (2) (2012) 475–483.
[39] R. Sutter, T.J. Dietrich, P.O. Zingg, C.W.A. Pfirrmann, How useful is the alpha angle for discriminating between symptomatic patients with cam-type femoroacetabular impingement and asymptomatic volunteers? Radiology 264 (2) (2012) 514–521.
[40] D.B.A. Banks, R.A. Boden, R. Mehan, M.J. Fehily, Magnetic resonance arthrography for labral tears and chondral wear in femoroacetabular impingement, Hip 22 (4) (2012) 387–390.
[41] K.S. Rakhra, A.M. Sheikh, D. Allen, P.E. Beaulé, Comparison of MRI alpha angle measurement planes in femoroacetabular impingement, Clin. Orthop. Relat. Res. 467 (3) (2008) 660–665.
[42] C. Barton, M.J. Salineros, K.S. Rakhra, P.E. Beaulé, Validity of the alpha angle measurement on plain radiographs in the evaluation of cam-type femoroacetabular impingement, Clin. Orthop. Relat. Res. 469 (2) (2010) 464–469.
[43] E.C. Kavanagh, P. Read, F. Carty, A.C. Zoga, J. Parvizi, W.B. Morrison, Three-dimensional magnetic resonance imaging analysis of hip morphology in the assessment of femoral acetabular impingement, Clin. Radiol. 66 (8) (2011) 742–747.
[44] P.E. Beaulé, E.J. Zaragoza, K. Motamedi, N. Copelan, F.J. Dorey, Three-dimensional computed tomography of the hip in the assessment of femoroacetabular impingement, J. Orthop. Res. 23 (6) (2005) 1286–1292.
[45] A. Kassarjian, L.S. Yoon, E. Belzile, S.A. Connolly, M.B. Millis, W.E. Palmer, Triad of MR arthrographic findings in patients with cam-type femoroacetabular impingement 1, Radiology 236 (2) (2005) 588–592.
[46] E.A. Audenaert, I. Peeters, L. Vigneron, N. Baelde, C. Pattyn, Hip morphological characteristics and range of internal rotation in femoroacetabular impingement, Am. J. Sports Med. 40 (6) (2012) 1329–1336.
[47] S.L.J. James, K. Ali, F. Malara, D. Young, J. O'Donnell, D.A. Connell, MRI findings of femoroacetabular impingement, Am. J. Roentgenol. 187 (6) (2006) 1412–1419.
[48] W.M. Pullen, A. Henebry, T. Gaskill, Variability of acetabular coverage between supine and weightbearing pelvic radiographs, Am. J. Sports Med. 42 (11) (2014) 2643–2648.
[49] M.R. Nouh, M.E. Schweitzer, L. Rybak, J. Cohen, Femoroacetabular impingement can the alpha angle be estimated? Am. J. Roentgenol. 190 (5) (2008) 1260–1262.
[50] S.E. Domayer, K. Ziebarth, J. Chan, S. Bixby, T.C. Mamisch, Y.J. Kim, Femoroacetabular cam-type impingement: diagnostic sensitivity and specificity of radiographic views compared to radial MRI, Eur. J. Radiol. 80 (3) (2011) 805–810.
[51] M. Masjedi, C.S. Marquardt, I.M.H. Drummond, S.J. Harris, J.P. Cobb, Cam type femoro-acetabular impingement: quantifying the diagnosis using three dimensional head–neck ratios, Skeletal Radiol. (2012).
[52] J.J. Nepple, J.M. Martel, Y.-J. Kim, I. Zaltz, J.C. Clohisy, ANCHOR study group. Do plain radiographs correlate with CT for imaging of cam-type femoroacetabular impingement? Clin. Orthop. Relat. Res. 470 (12) (2012) 3313–3320.
[53] A. Espié, B. Chaput, J. Murgier, X. Bayle-Iniguez, F. Elia, P. Chiron, 45°–45°–30° Frog-leg radiograph for diagnosing cam-type anterior femoroacetabular impingement: reproducibility and thresholds, Orthop. Traumatol. Surg. Res. : OTSR 100 (8) (2014) 843–848.
[54] J.J. Nepple, C.N. Riggs, J.R. Ross, J.C. Clohisy, Clinical presentation and disease characteristics of femoroacetabular impingement are sex-dependent, J. Bone Joint Surg. 96 (20) (2014) 1683–1689.
[55] M. Khan, A. Ranawat, D. Williams, et al., Relationship between the alpha and beta angles in diagnosing CAM-type femoroacetabular impingement on frog-leg lateral radiographs, Knee Surg. Sports Traumatol. Arthrosc. (2014).
[56] G.A. Odri, R. Frioux, H. Redon, et al., Reliability of a new hip lateral view to quantify alpha angle in femoroacetabular impingement, Orthop. Traumatol. Surg. Res.: OTSR 100 (4) (2014) 363–367.
[57] M.D. Harris, A.L. Kapron, C.L. Peters, A.E. Anderson, Correlations between the alpha angle and femoral head asphericity: Implications and recommendations for the diagnosis of cam femoroacetabular impingement, Eur. J. Radiol. 83 (5) (2014) 788–796.
[58] On behalf of the FAITH Investigators, G. Mathew, M. Kowalczuk, et al., Radiographic prevalence of CAM-type femoroacetabular impingement after open reduction and internal fixation of femoral neck fractures, Knee Surg. Sports Traumatol. Arthrosc. 22 (4) (2014) 793–800.
[59] F. de Bruin, M. Reijnierse, V. Farhang-Razi, J.L. Bloem, Radiographic signs associated with femoroacetabular impingement occur with high prevalence at all ages in a hospital population, Eur. Radiol. 23 (11) (2013) 3131–3139.
[60] C. Sullivan, J. Chakraverty, K. Foley, S. Narayanaswamy, S. Kamath, Femoroacetabular impingement: presence of FAI-like features on conventional radiography in young patients presenting to primary care with hip pain, Acta Radiol. 54 (6) (2013) 690–697.
[61] Y. Yamamoto, Y. Hiejima, Usefulness of cross-table lateral view radiograph for the diagnosis of cam-type femoroacetabular impingement, Eur. J. Orthop. Surg. Traumatol. 24 (3) (2013) 365–369.
[62] G.G. Klingenstein, R.M. Zbeda, A. Bedi, E. Magennis, B.T. Kelly, Prevalence and preoperative demographic and radiographic predictors of bilateral femoroacetabular impingement, Am. J. Sports Med. 41 (4) (2013) 762–768.
[63] A. Aprato, A. Massè, C. Faletti, et al., Magnetic resonance arthrography for femoroacetabular impingement surgery: is it reliable? J. Orthopaed. Traumatol. 14 (3) (2013) 201–206.
[64] A.S. Ranawat, B. Schulz, S.F. Baumbach, M. Meftah, R. Ganz, M. Leunig, Radiographic predictors of hip pain in femoroacetabular impingement, HSS J. 7 (2) (2011) 115–119.
[65] O.F. Miguel, H.B. Cabrita, M.B. Rodrigues, A.T. Croci, A comparative radiographic investigation of femoroacetabular impingement in young patients with and without hip pain, Clinics 67 (5) (2012) 463–467.
[66] G.X. Chen, Y. Zhang, W.B. Wang, et al., An alternative radiographic measure for cam-type FAI in patients with idiopathic hip pain, Hip 21 (2) (2011) 146–153.
[67] S.-J. Hong, W.Y. Shon, C.Y. Lee, J.S. Myung, C.H. Kang, B.H. Kim, Imaging findings of femoroacetabular impingement syndrome: focusing on mixed-type impingement, J. Clin. Imaging 34 (2) (2010) 116–120.
[68] L.M. Ochoa, L. Dawson, J.C. Patzkowski, J.R. Hsu, Radiographic Prevalence of femoroacetabular impingement in a young population with hip complaints is high, Clin. Orthop. Relat. Res. 468 (10) (2010) 2710–2714.
[69] C.W.A. Pfirrmann, B. Mengiardi, C. Dora, F. Kalberer, M. Zanetti, J. Hodler, Cam and pincer femoroacetabular impingement: characteristic MR. arthrographic findings in 50 patients, Radiology 240 (3) (2006) 778–785.
[70] J.C. Clohisy, R.M. Nunley, R.J. Otto, P.L. Schoenecker, The frog-leg lateral radiograph accurately visualized hip cam impingement abnormalities, Clin. Orthop. Relat. Res. 462 (2007) 115–121.
[71] R. Agricola, M.P. Heijboer, R.H. Roze, et al., Pincer deformity does not lead to osteoarthritis of the hip whereas acetabular dysplasia does: acetabular coverage and development of osteoarthritis in a nationwide prospective cohort study (CHECK), Osteoarthritis Cartilage 21 (10) (2013) 1514–1521.
[72] C.M. Larson, A. Moreau-Gaudry, B.T. Kelly, et al., Are normal hips being labeled as pathologic? A CT-based method for defining normal acetabular coverage, Clin. Orthop. Relat. Res. 473 (4) (2014) 1247–1254.
[73] H.P. Nötzli, T.F. Wyss, C.H. Stoecklin, M.R. Schmid, K. Treiber, J. Hodler, The contour of the femoral head–neck junction as a predictor for the risk of anterior impingement, J. Bone Joint Surg. (Br. vol.) 84 (4) (2002) 556–560.
[74] G.M. Riley, E.J. McWalter, K.J. Stevens, M.R. Safran, R. Lattanzi, G.E. Gold, MRI of the Hip for the evaluation of femoroacetabular impingement; past, present, and future, J. Magn. Reson. Imaging (2014).
[75] R. Agricola, M.P. Heijboer, A. Ginai, P. Roels, A. Zadpoor, J. Verhaar, H. Weinans, J. Waarsing, A cam deformity is gradually acquired during skeletal maturation in adolescent and young male soccer players: a prospective study with minimum 2-year follow-up, Am. J. Sports Med. 42 (4) (2014) 798–806.
[76] R. Agricola, et al., Cam impingement: defining the presence of a cam deformity by the alpha angle, Osteoarthritis Cartilage (2013) http://dx.doi.org/10.1016/j.joca.2013.11.007.
[77] T.O. Smith, G. Hilton, A.P. Toms, S.T. Donell, C.B. Hing, The diagnostic accuracy of acetabular labral tears using magnetic resonance imaging and magnetic resonance arthrography: a meta-analysis, Eur. Radiol. 21 (4) (2011) 863–874, http://dx.doi.org/10.1007/s00330-010-1956-7, Epub Sep. 22.

3.3.2 Concepts on population models

Presently, the question remains of how reliable clinical assessment and imaging measurements are to differentiate between overall symptomatic and asymptomatic populations. From the epidemiological standpoint, one can think of at least 6 distinct populations:

I. Asymptomatic individuals
   a. Normal morphology (without Cam and Pincer morphology);
   b. FAI morphology;
   c. Other "abnormal" morphologies.
II. Symptomatic patients
   a. Normal morphology;
   b. FAI morphology (FAIS);
   c. Other "abnormal" morphologies.

For some patients there is a clear-cut diagnosis of FAIS, but a large number of patients have intermediate or minimal findings. Further, a substantial number of studies describe a high prevalence of FAI morphology in the normal population and in asymptomatic healthy individuals[36,88,93,110,148,167]. Population models may help elucidate this situation (Figure 30):

I. Model A: With relatively distinct groups of healthy individuals and patients;
II. Model B: With a substantial overlap between the healthy and the diseased group.

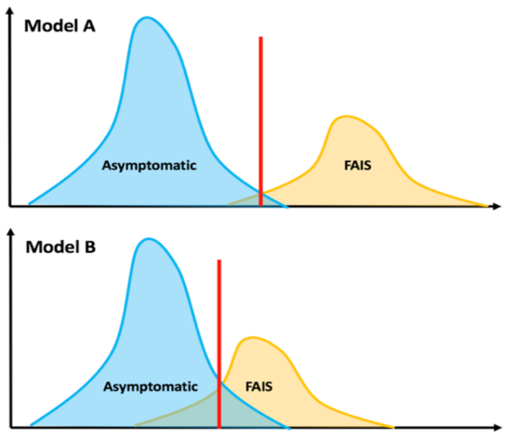

FIGURE 30 – Theoretical model of distribution of Cam, Pincer morphology and FAIS in the population. If the distribution of measurement values for FAI deformities and measurement values in healthy individuals is spread as in the model A (upper row), a diagnostic test can be found that distinguishes between healthy individuals and patients with FAI with a good reliability, as shown by the red vertical threshold. However, as shown in the bottom row, if there is a large overlap between measurements in healthy individuals and FAI patients, it is not possible to reliably distinguish between healthy individuals and patients with FAI based on simple morphological measurements because any chosen threshold results in a substantial lack of sensitivity and specificity (large number of false-positive and false-negative).

In model A, it should be possible to distinguish relatively well between healthy and diseased individuals by choosing an appropriate test and threshold. If, however, the reality better resembles the second overlapping model (B), then the measurements and thresholds we apply will result in a large number of false-positive and false-negative findings. Therefore, imaging findings are only one of several puzzle pieces in the diagnostic process and need to be correlated with the patient's clinical history, symptoms and clinical findings to reach a correct diagnosis.

At the current time, there is no magic tool of imaging that facilitates the reliable allocation of all patients into the correct diagnostic group or confidently rules out the diagnosis. Nevertheless, imaging can be used to describe the various morphological characteristics of the hip and can be beneficial in confirming or precluding the diagnosis of FAI in many patients. This is certainly an area of needed original research, in order to correctly classify individuals.

part II

RATIONALE and AIMS

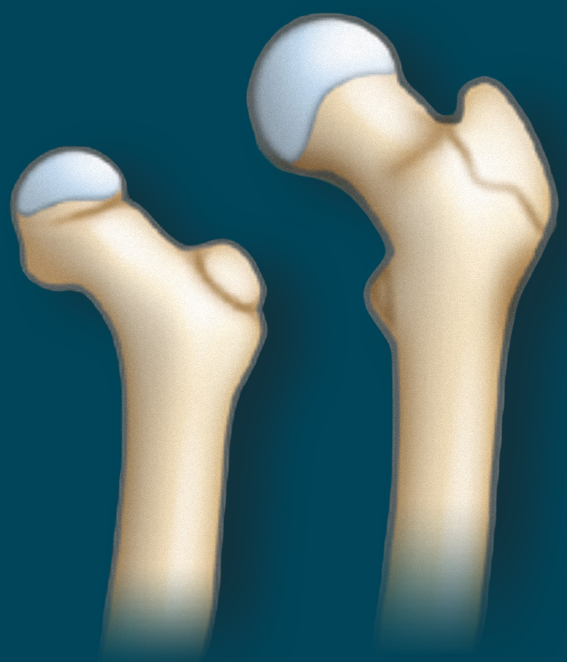

RATIONALE

Pathological hip deformities leading to mechanical joint failures constitute a substantial proportion of ongoing challenges in radiology and orthopaedics. Both imaging and surgical approaches are now used routinely by a growing number of providers to address injuries to the cartilage and labrum within the hip and to correct abnormalities of coverage and version of the joint itself. Advances in our understanding of hip pathology, better imaging, and improved surgical technique have all contributed to this exponential rise. Along with this increase in the number of surgical cases, however, comes an increased responsibility to make sure that we make the correct clinical diagnosis. In other words, not every patient who presents to a doctor's office with hip pain requires advanced imaging or surgery. Based on a recent cost analysis in the US, by Kahlenberg et al.[208], FAI patients visited up to four health care providers, underwent more than three diagnostic imaging tests, and tried three different treatments, all prior to receiving a correct diagnosis of joint damage due to FAI. The duration between the initial onset of symptoms and diagnosis for these patients lasted approximately 32 months with an approximate average cost per patient of $2,500 USD.

Hip impingement has received a great extent of clinical and biomechanical interest, with an exponentially increasing rate of scientific publications in recent years[122]. Paradoxically, the concept of FAI remains elusive and sometimes wrongly associated with other hip morphologies[80,114,117], with plenty of still unanswered questions regarding aetiology[134], prevalence[36], diagnosis[209], treatment[130] and prognosis[210].
There are indications that the shape of the hip is associated with development of hip pain[136,168] and OA[15,124,125], though it is unknown which specific shape variants in non-OA hips will lead to hip damage. Recent evidence on this topic points towards an important role of specific shape variants of the acetabulum (Pincer deformity) and proximal femur (Cam deformity) which may lead to joint damage via a motion dependent process known as FAI[138]. Although the hip can remain functional, the deformities may lead to early anatomical and functional adaptations, resulting in progressive cartilage degradation.

The morphology leading to mechanical FAI occurs when the anterosuperior aspect of the femoral head impacts the acetabulum during combined motions in hip flexion and rotation[211], as well as during squatting[211,212]. Typically, a Cam deformity is indicated by an α° greater than 50.5° or 60° in the oblique-axial or radial plane, respectively[87,93,167,170]. Although several studies demonstrated that the severity of the Cam deformity (thus, elevated α°) were associated with hip pain and joint degeneration, other common radiographic measures and anatomical features of the FHN junction and acetabulum have been mentioned as potential factors for symptomatic FAI[88,151,213]. It remains unclear which combination of anatomical parameters can predict which patients are at risk of developing symptoms.

Although the pathomechanism of FAI involves a complex spectrum of anatomical and functional parameters, the detection protocols to recognize the symptomatic morphology remains an ongoing and critical challenge. Improving the evaluation of hip joint pathomorphologies including through the use of 3D analysis is paramount. Too often we confuse the presence of a Cam deformity (a morphological finding) with symptomatic Cam-type impingement (a pathophysiological finding), which can lead to either the overtreatment of these deformities and/or insufficient management of other underlying abnormalities. Our systematic review[214] and also a recent report by Frank et al.[36] reported that the prevalence of an asymptomatic Cam morphology ranged from 7% to 100% between studies (mean of 22,4 ± 6,2%[214]), depending on the imaging method used and the population included (athletes or non-athletes). The mean α° in those asymptomatic hips was 47° (±2.0°)[214] and 54.1° (±5.1°)[36], respectively (again regardless of type of population, imaging method or measurement location around the femoral head). The prevalence of asymptomatic hips with Pincer deformity ranged from 57%[214]-76%[36] between studies, again with Pincer morphology poorly defined.

Hip morphology analysis became more complex when we included torsional deformities of the femur and the acetabulum, as well as malorientation of the femur into the 3D concept of FAI or hip instability. While this information is helpful, it has mainly been gathered from low-evidence evaluations of procedures that did not improve patients' symptoms and/or function in the ways we had hoped. Also, knowing that both symptomatic and asymptomatic individuals with a similar Cam deformity may experience joint deterioration which conceptually would lead to OA, it is imperative to delineate the differences of the asymptomatic group from the symptomatic patients in efforts to establish a better detection protocol and explain the risk of symptoms.

High quality prospective studies are needed to help us determine which abnormalities are most important to correct, and which ones can be safely left alone. Cam deformity found in a patient with slight dysplasia may be asymptomatic and of little importance, but it may cause accelerated arthritis in a patient who also has femoral retrotorsion.

AIMS AND OBJECTIVES

With current literature on FAI focusing primarily on surgical methods, outcomes and subsequent comprehensive literature reviews, very little research has been performed to examine the paradox of the high prevalence of the so-called abnormal hip morphologies.

In the first part of this thesis we discuss general diagnostic, anatomical and developmental issues. The imaging prevalence of different hip shapes is addressed by performing a systematic review of the literature. In the second part, we characterise hip morphology using 3D advanced imaging, by developing a novel quantitative methodology and also by studying the arterial supply to the femoral head. In the third part we investigate and bridge the gap between the asymptomatic and the symptomatic hip. Finally, the last part will address treatment of the symptomatic hip.

With the ultimate goal to better understand the pathomorphology of FAI, the purpose of this research will be to address the question at large: "what represents normal morphology and how to differentiate it from pathological hip shapes".

In this sense, we aim to specifically evaluate the following <u>primary</u> items:

1) Investigate the prevalence of different hip morphologies in different populations, by systematically reviewing the existing literature:

- **a)** to determine the reported prevalence of Cam, Pincer, and mixed FAI morphology based on imaging of asymptomatic subjects, symptomatic patients and athletes.
- **b)** to determine the reported prevalence and values of parameters of FAI morphology, namely $\alpha°$ and COS, based on imaging of asymptomatic subjects, symptomatic patients and athletes.

  ARTICLE: "Imaging prevalence of femoroacetabular impingement in symptomatic patients, athletes, and asymptomatic individuals: A systematic review." *European Journal of Radiology 2016 Jan;85(1):73-95*

2) Develop the imaging approach and reference intervals of hip morphology, in asymptomatic subjects:

a) Characterising femoral and acetabular morphology using quantitative measurements taken from 3D CT in asymptomatic subjects.

I. Estimate the overall normative ranges as well as sex- and side-specific quantitative parameters for hip measurements.

II. Establish the relationship between hip shape and side, limb dominance and age.

ARTICLE: "Hip shape is symmetric, non-dependent on limb dominance and gender-specific: implications for femoroacetabular impingement. A 3D CT analysis in asymptomatic subjects." *Eur Radiol. 2018 Apr;28(4):1609-1624. doi: 10.1007/s00330-017-5072-9. Epub 2017 Nov 6.*

b) Characterisation of the Cam morphology:

I. Implementing a new parameter for morphology quantification of the FHN junction (omega angle (Ω°)).

II. Use 3D measurements, namely the Ω°, to quantify the location, extent and sex-dependence of Cam morphology.

ARTICLE: "Cam deformity and the omega angle, a novel quantitative measurement of femoral head-neck morphology: a 3D CT gender analysis in asymptomatic subjects". *Eur Radiol. 2017 May;27(5):2011-2023. doi: 10.1007/s00330-016-4530-0. Epub 2016 Aug 30.*

3) Investigate if and how we can predict an "at-risk" hip joint by comparing asymptomatic and symptomatic hips and addressing:

a) hip morphology normative measurements and shapes (by 3D-MRI and advanced computational frameworks) with objective comparison of the pathoanatomy in these populations.

b) spinopelvic parameters normative measurements (by 3D-MRI) in both populations.

c) potential distinguishing threshold values to differentiate these populations, by ascertaining which parameters are most useful and how they should be used to achieve best results.

ARTICLE: "Can we discriminate symptomatic hip patients from asymptomatic volunteers based on anatomical predictors? *A 3D MRI Study On Cam, Pincer and Spinopelvic Parameters". Am J Sports Med. 2018 Nov;46(13):3097-3110. doi: 10.1177/0363546518800825.*

ARTICLE: "Modelling the shape of asymptomatic, dysplastic and impinged hip joints". *Med Eng Phys. 2018 Sep; 59:50-55. doi: 10.1016/j.medengphy.2018.07.001. Epub 2018 Jul 29.*

As additional secondary aims, we investigated:

4) The vascular anatomy of the proximal femur, assessing the extension of the lateral retinaculum near the FHN junction, the distribution of the arterial vascular *foramina* and initial intracapital course of these vessels (a MRI study in cadaver specimens).

ARTICLE: "Arterial topographic anatomy near the femoral head-neck perforation with surgical relevance". *J Bone Joint Surg Am. 2017 Jul 19;99(14):1213-1221. doi:10.2106/JBJS.16.01386.*

5) Treatment techniques and outcomes, by analysing:

a) the clinical and surgical planning usefulness of Ω° by determining the relationship between the extension of Cam deformities and the location of the retinacular fold at the FHN junction.

b) the compared results of two different surgical techniques —open and arthroscopic— in cam resection over the posterosuperior retinacular *foramina* area.

ARTICLE: "Morphologic and angular planning for Cam resection in FAI: value of the omega angle." *Int Orthop. 2016 Oct;40(10):2011-2017. Epub 2015 Nov 18.*

c) evaluate and compare clinical and radiographic results of Cam FAI surgery using both hip arthroscopy (HA) and surgical hip dislocation (SHD) techniques, with an average follow-up time of 59 months, intending to ascertain:

I. which variables were significantly associated with the functional pre-operative score and which were predictive of the functional outcome after surgery.

II. if there were significant differences in the outcomes between HA and SHD;

ARTICLE: "Arthroscopic versus open treatment of cam-type femoroacetabular impingement: retrospective cohort clinical study". *Int Orthop. 2018 Apr;42(4):791--797. doi:10.1007/s00264-017-3735-4. Epub 2018 Jan 3.*

The six chapters of this thesis cover the spectrum from the diagnosis to treatment of the symptomatic young hip. In order to present the aims of this thesis in a logical sequence of general morphology to more specific FAI related morphology and treatment, the analysis of the asymptomatic hip will be presented first followed by how morphology relates with symptoms, and finally treatment.

In **PART I,** we introduced the topics that are relevant to understand the full scope of our thesis. **Chapter 1** is devoted to hip development and morphogenesis. In **Chapter 2** we addressed imaging anatomy and performed a thorough review of current and future perspectives on this topic. In **Chapter 3**, we performed a systematic review of the literature to write a state-of-the-art overview focusing on asymptomatic and symptomatic FAI morphology prevalence. This seminar highlights the gap in knowledge regarding hip morphology role in the pathogenesis of FAI.

Building on the first part of the thesis we hereby address the rationale and aims for this thesis in **PART II**.

In **PART III** we focus on the original research performed. **Chapter 4** is focused on the detailed characterisation of hip morphology, both osseous and vascular. Bony hip morphology was quantified using a semi-automated software, which allows to robustly study in detail shape variants within a population and their relationship with sex, side and limb dominance. Cam morphology was further defined by developing a novel quantitative measure, with diagnostic and treatment planning capabilities. Finally, the importance of this parameter is outlined by the arterial topographic study of the proximal femur. In **Chapter 5** we tested multiple parameters and their associated shape variants to find which ones allows to identify a risk-increased joint in various populations. To this end we have used both advanced computing for shape modelling and 3D-MRI. **Chapter 6** described treatment options and outcomes in a cohort clinical study.

The results of the above-mentioned chapters are summarised in **PART IV**, presenting the general synthesis, discusses the results of the work performed in the light of the current literature, and comes to the conclusions of this thesis. Potential future research topics within this field and limitations are also presented in this chapter.

part III

BODY of WORK

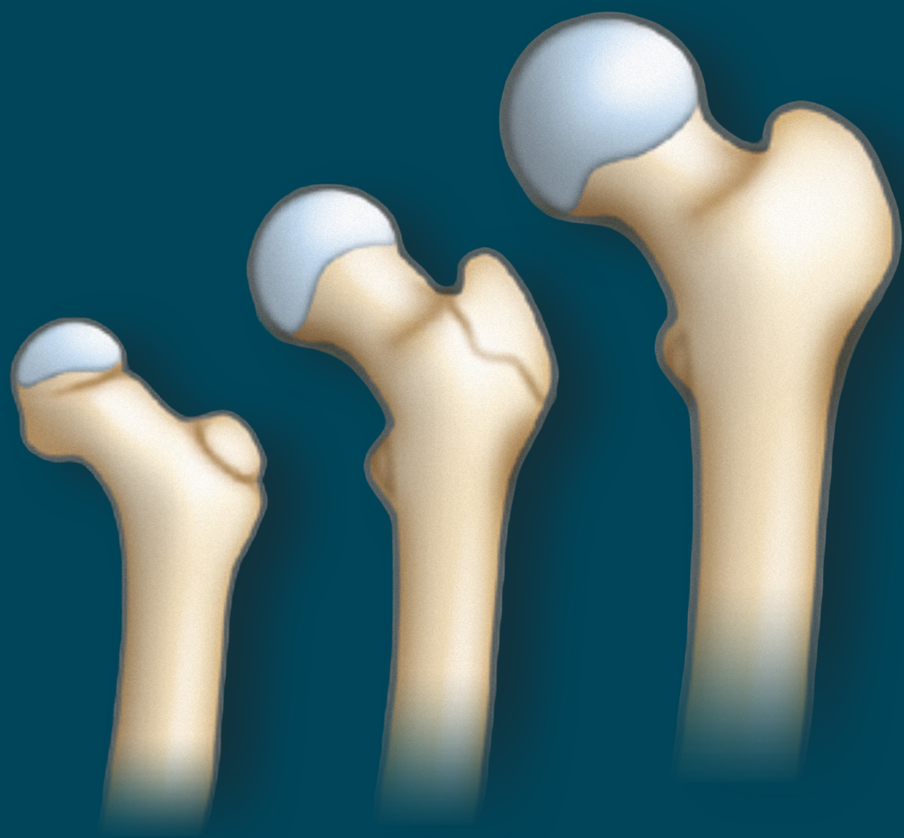

chapter 4

CHARACTERISATION OF HIP MORPHOLOGY

Chapter IV is based on the following publications:

"Hip shape is symmetric, non-dependent on limb dominance and gender-specific: implications for femoroacetabular impingement. A 3D CT analysis in asymptomatic subjects"
European Radiology 2018 Apr;28(4):1609-1624

"Cam deformity and the omega angle, a novel quantitative measurement of femoral head-neck morphology: a 3D CT gender analysis in asymptomatic subjects"
European Radiology 2017 May;27(5):2011-2023.

"Morphologic and angular planning for cam resection in femoroacetabular impingement: value of the omega angle"
International Orthopedics. 2016 Oct;40(10): 2011-2017.

"Arterial Topographic Anatomy Near the Femoral Head-Neck Perforation with Surgical Relevance"
The Journal of Bone and Joint 2017 99(14): 1213-1221

CHAPTER 4.1

This chapter is based on the following paper:

"Hip shape is symmetric, non-dependent on limb dominance and gender-specific: implications for femoroacetabular impingement. A 3D CT analysis in asymptomatic subjects"
European Radiology 2018 Apr;28(4):1609-1624

Eur Radiol
DOI 10.1007/s00330-017-5072-9

MUSCULOSKELETAL

Hip shape is symmetric, non-dependent on limb dominance and gender-specific: implications for femoroacetabular impingement. A 3D CT analysis in asymptomatic subjects

Vasco V. Mascarenhas[1] · Paulo Rego[2] · Pedro Dantas[3] · Miguel Castro[4] · Lennart Jans[5] · Rui M. Marques[6] · Nélia Gouveia[6] · Francisco Soldado[7] · Olufemi R. Ayeni[8] · José G. Consciência[6]

Received: 29 March 2017 / Revised: 6 August 2017 / Accepted: 11 September 2017

Abstract

Objective To determine the reference intervals (RefInt) of the quantitative morphometric parameters of femoroacetabular impingement (FAI) in asymptomatic hips with computed tomography (CT) and determine their dependence on age, side, limb dominance and sex.

Methods We prospectively included 590 patients and evaluated 1111 hips with semi-automated CT analysis. We calculated overall, side- and sex-specific parameters for imaging signs of cam [omega and alpha angle (α°)] and pincer-type morphology [acetabular version (ACvers), lateral centre-edge angle (LCEA) and cranio-caudal coverage].

Results Hip shape was symmetrical and did not depend on limb dominance. The 95% RefInt limits were sex-different for all cam-type parameters and extended beyond current abnormal thresholds. Specifically, the upper limits of RefInt for α° at 12:00, 1:30 and 3:00 o'clock positions were 56°, 70° and 58°, respectively, and 45° for LCEA. Acetabular morphology varied between age groups, with a trend toward an LCEA/ACvers increase over time.

Conclusion Our morphometric measurements can be used to estimate normal hip morphology in asymptomatic individuals. Notably they extended beyond current thresholds used for FAI imaging diagnosis, which was most pronounced for cam-type parameters. We suggest the need to reassess α° RefInt and consider a 60° threshold for the 12:00/3:00 positions and 65-70° for other antero-superior positions.

Key Points

- *Hip shape is symmetrical regardless of limb dominance.*
- *Pincer/cam morphology is frequent in asymptomatic subjects (20 and 71%, respectively).*
- *LCEA and acetabular version increases with age (5-7° between opposite age groups).*
- *Femoral morphology is stable after physeal closure (in the absence of pathology).*

Electronic supplementary material The online version of this article (https://doi.org/10.1007/s00330-017-5072-9) contains supplementary material, which is available to authorized users.

✉ Vasco V. Mascarenhas
mascarenhas.vasco@gmail.com

1 MSK imaging Unit (UIME), Imaging Centre, Hospital da Luz, Lisbon, Portugal
2 Department of Orthopaedic Surgery, Hospital da Luz, Lisbon, Portugal
3 Hospital CUF Descobertas, Lisbon, Portugal
4 Centro Hospitalar do Algarve, Faro, Portugal
5 Department of Radiology, Ghent University Hospital, Gent, Belgium
6 NOVA Medical School, Lisbon, Portugal
7 Paediatric Hand Surgery and Microsurgery, Hospital Sant Joan De Deu, Universitat De Barcelona, Barcelona, Spain
8 Division of Orthopaedic Surgery, Department of Surgery, McMaster University, Hamilton, ON, Canada

Published online: 06 November 2017

• *Alpha and omega angle thresholds should be set according to sex.*

Keywords Hip · Femoroacetabular impingement · Multidetector computed tomography · Reference value · Normal value

Abbreviations

ACcov	Acetabular cranio-caudal coverage
ACinc	Acetabular inclination (Tönnis angle or Sourcil angle)
ACvers	Acetabular version
Alpha angle	α°
BMI	Body mass index
CDA	Cervico-diaphyseal angle
CT	Computed tomography
DICOM	Digital Imaging and Communications in Medicine
FAI	Femoroacetabular impingement
FHN	Femoral head-neck
LCEA	Lateral centre-edge angle
MRI	Magnetic resonance Imaging
Omega angle	Ω°
OA	Osteoarthritis
RefInt	Reference intervals
SD	Standard deviation

Introduction

Femoroacetabular impingement (FAI) syndrome is a motion-related clinical disorder with a triad of symptoms, clinical signs and imaging findings [1], has been associated with hip pain and functional impairment, and can ultimately lead to osteoarthritis (OA) [2].

The prevalence of FAI morphology in the general population is not known and estimates vary widely likely owing to the disparity in the case definition of FAI and in the populations sampled [3, 4]. Furthermore, the presence of shape abnormalities does not always lead to hip OA, suggesting that there are other intervening factors than just joint morphology [5]. Conversely, development of symptomatic FAI in the presence of morphological abnormalities is co-dependent on the type and intensity of activities that one undertakes associated with the individual vulnerability [6].

Distinguishing normal and abnormal morphology has proved a difficult task [7]. The presence of a cam/pincer morphology is a prerequisite for defining cam-type/pincer-type FAI. Although an obvious cam deformity is not difficult to recognise, there may be more subtle differences that might be clinically important [8]. Objective methods to quantify these morphologies are, therefore, mandatory. For cam morphology several objective measures have been proposed [9–11] but still the α angle (α°) [12] is most commonly used. For anteroposterior pelvic radiographs, a threshold of 60° could distinguish between normal and abnormal α° in two large cohorts [13]. For other planes, views and modalities, a threshold between 55°-60° seems appropriate [7, 12], although more research is required to validate the presence of a cam deformity in other modalities [10, 14–17].

A pincer deformity includes a variety of acetabular morphological and/or orientation abnormalities and its quantification is, therefore, challenging. Similarly multiple quantitative measures [14, 17] have been proposed to capture these specificities; however the most appropriate ones and accompanying threshold values remain to be determined.

In previous reports on normal hip morphology, sex differences in orientation such as greater acetabular anteversion [16, 18–20], acetabular inclination [18, 19] and femoral sphericity in females were described [4, 10]. However large-scale reports are missing in this regard, specifically using reproducible 3D imaging methods. Similarly, regarding age, symmetry and limb dominance, the literature specifically addressing their relationship with hip shape is scarce [16, 21–23].

To our knowledge, no previous study in a large cohort of asymptomatic individuals using cross-sectional imaging has (1) determined the reference intervals (RefInt) of the quantitative morphometric parameters associated with FAI; (2) evaluated the relationship among sex, side, age, limb dominance and hip shape.

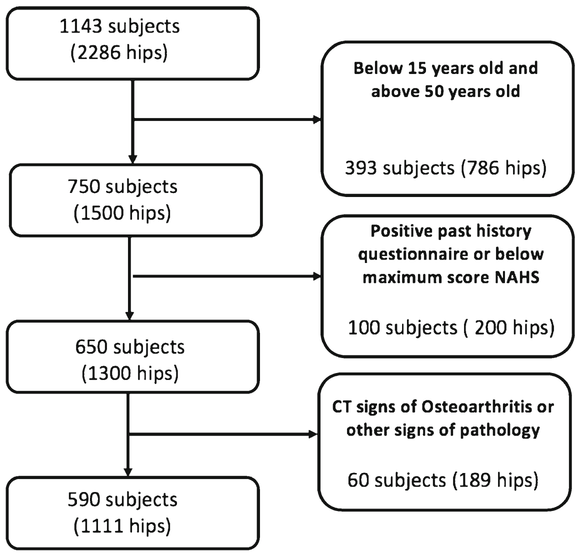

Fig. 1 Flow of subjects from cohort inclusion to the final study population

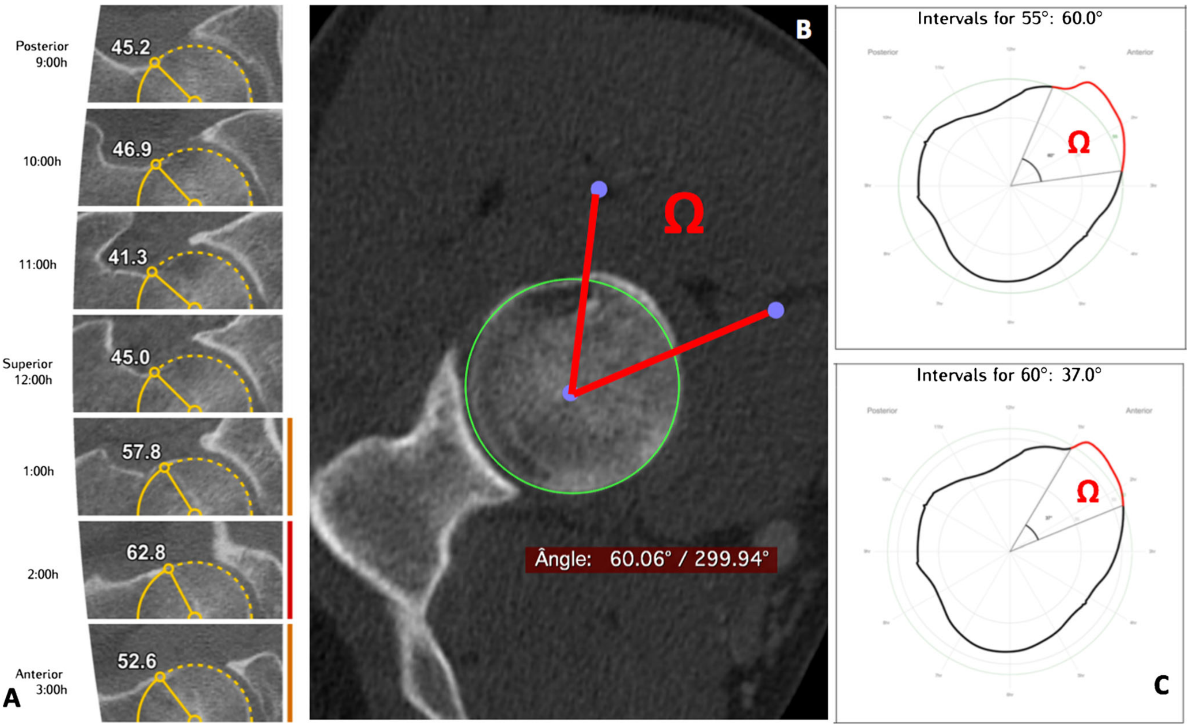

Fig. 2 **A** Alpha-angle (α°) measurements made at different points around the femoral head/neck junction starting at 9 o'clock (posterior); 10, 11 and 12 o'clock (superior); and 1, 2 and 3 o'clock (anterior). **B** Femoral neck short-axis computed tomography (CT) reformats show the bone contour abnormality from 1 to 2 o'clock [omega angle (Ω°) of 60°]. The Ω° is formed by two lines intersecting the centre of the femoral neck at the level of the head/neck junction. The most posterior line posteriorly intersects the point at which the α° begins to be abnormal beyond a best-fitting circle and the anterior line at the point where the α° returns to normal. **C** Polar plot (2D) of the 360° α°, representing the Ω° angle (*red symbol*) for different α° thresholds [55° (upper right), 60° (lower right)]. *Red lines* represent increased α°s for a given threshold

The purpose of this study was to (1) characterise femoral and acetabular morphology using quantitative measurements taken from 3D CT; (2) estimate the overall normative ranges as well as sex- and side-specific parameters for 3D measurements of the hip; (3) establish the relationship between hip shape and side, limb dominance and age.

Methods

Patient population

Institutional ethics committee approval was obtained prior to beginning this study. All participants provided written informed

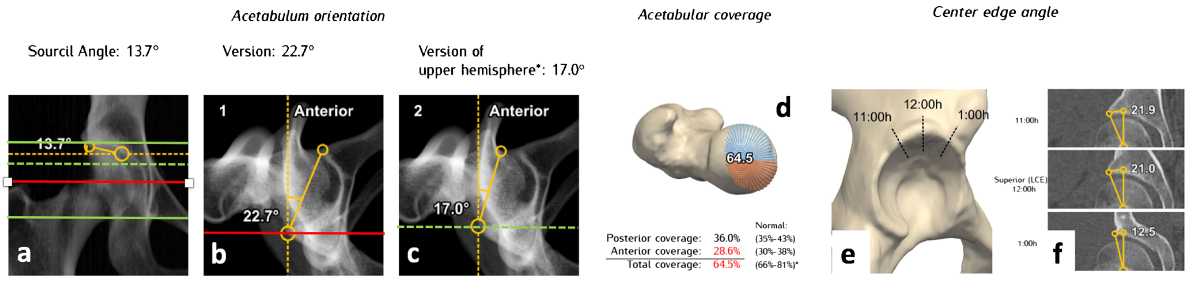

Fig. 3 CT-based MIP reconstructions of the right hip corrected for pelvic flexion and lateral tilt, with corresponding measurements of (**a**) the sourcil angle or acetabular inclination (*solid* and *dashed yellow lines*); (**b**) acetabular version at the axial plane of the centre of the femoral head (center ACvers) (corresponding to the *solid red line* in **a**), determined by measuring the angle between the transverse axis and the acetabular axis, which is the axis orthogonal to the acetabular plane; (**c**) acetabular version of the upper hemisphere (upper ACvers), measured on the axial slice corresponding to the upper quarter (*dashed green line* in **a**) between the acetabular roof (*solid green line*) and the inferior axial plane of the tear drop (*solid green line*]; (**d**) 3D representation of the cranio-caudal acetabular coverage (anterior coverage represented in *orange*; posterior coverage represented in *blue*); (**e** and **f**) 3D representation of the lateral centre edge angle and corresponding 2D CT measurements at 1:00, 12:00 and 11:00 o'clock

Table1 Characterisation of recruited patients (sex and limb dominance)

		n*	%
Sex	Male	271	45.9%
	Female	319	54.1%
	Total	590	100%
Dominance	Left	53	9%
	Right	537	91%
	Total	590	100%

*Data expressed as absolute count

Table 3 Region of origin of recruited patients (absolute count and percentage of total)

Region of origin	Total	% of total
Total	590	100%
European	537	93.6%
Non-European	53	6.4%
Africa	27	4.5%
America	17	2.8%
Asia	6	1%
Oceania	3	0.05%

consent. We prospectively recruited consecutive adult patients undergoing CT at multiple centres from our health group (hospitals with a large population disperse all over the country) for abdominal/urogenital indications from January 2015 to June 2016 (including a fraction of patients from a previous published cohort [10]). All eligible participants completed the nonarthritic hip score (NAHS) questionnaire [24] and another questionnaire regarding demographics, limb dominance and clinical history (including current/past hip/groin pain, orthopaedic conditions, childhood hip pathology and/or hip trauma) (Fig. 1).

Exclusion criteria included: (1) subjects over 50 and less than 15 years old (y.o.); (2) all subjects with less than the maximum NAHS [24] possible score (100); (3) positive answer to one or more of the other hip-related questions; (4) CT signs of OA (defined as the presence of at least one of the following findings [16]: joint-space narrowing, osteophytes, subchondral bone changes (including sclerosis/cysts), fracture, posttraumatic deformity, Perthes disease, osteonecrosis, slipped capital femoral epiphysis or bone lesions).

CT imaging and three-dimensional model

CT imaging was performed using a 16- or 64-slice CT scanner (Siemens, Erlangen, Germany). Patients were positioned in a standard supine position with legs parallel in neutral rotation and received no additional radiation beyond that required for the CT ordered to evaluate their medical condition. The pelvis was reconstructed with 1 mm thickness from the antero-superior iliac spine to the lesser trochanters.

Table 2 Characterisation of recruited patients (age breakdown in groups, body mass index, weight and height)

	Mean*	SD		Min*		Max*
Weight**	73	17		46		124
Height***	171	10		146		198
BMI	24	4,8		16.4		40
Age	33	8		14		45
	<20 yo	21-25 yo	26-30 yo	31-35 yo	36-40 yo	41-45 yo
	68*	50*	86*	124*	148*	114*

Bottom two rows represent age breakdown in subgroups

*Data expressed as absolute count; ** in kilograms; *** in centimeters

SD, standard deviation; BMI, body mass index; Min, minimum; Max, maximum

Images were uploaded for analysis and semi-automatically segmented using Articulis™ (Clinical Graphics, The Netherlands), which was previously validated for reliability and accuracy [25]. Two musculoskeletal radiologists (VVM and MC, with 12 and 9 years of experience) certified that each segmentation contained all osseous contours and accurate CT measurements.

Alpha angle, omega angle and cervicodiaphyseal angle

To determine the omega angle (Ω°) (Fig. 2), we calculated the clockwise 360° $\alpha°$ (according to Nötzli et al. [12]) by using a regression sphere fit of the femoral head-neck (FHN) junction [26]. The first angle was obtained using a measurement plane defined by the femoral neck axis and a vector perpendicular to this axis pointing upward to define a superior 12 o'clock position [27] (Fig. 2a). Next, projecting the 360 $\alpha°$ in a polar plot (Fig .2b and c), we found the Ω° according to Mascarenhas et al. [10]. The head/neck femoral diameters and the cervicodiaphyseal angle (CDA) [28] were semi-automatically measured.

Cam-type morphology was defined as an $\alpha° > 55°$ at any location around the femoral neck [7], although we also considered additional thresholds in line with previous reports (namely 50° and 60°) [7, 12].

Acetabular inclination, acetabular version, cranio-caudal coverage and lateral centre-edge angle

Acetabular inclination (ACinc) (Fig. 3a) and version at the centre and upper hemisphere (centre and upper ACvers) (Fig. 3b and c) were derived from the coordinate frame by the software comparing it with the pelvic plane [29]. Acetabular cranio-caudal coverage (ACcov) was calculated and determined as a percentage of the femoral head surface [30] (Fig. 3d).

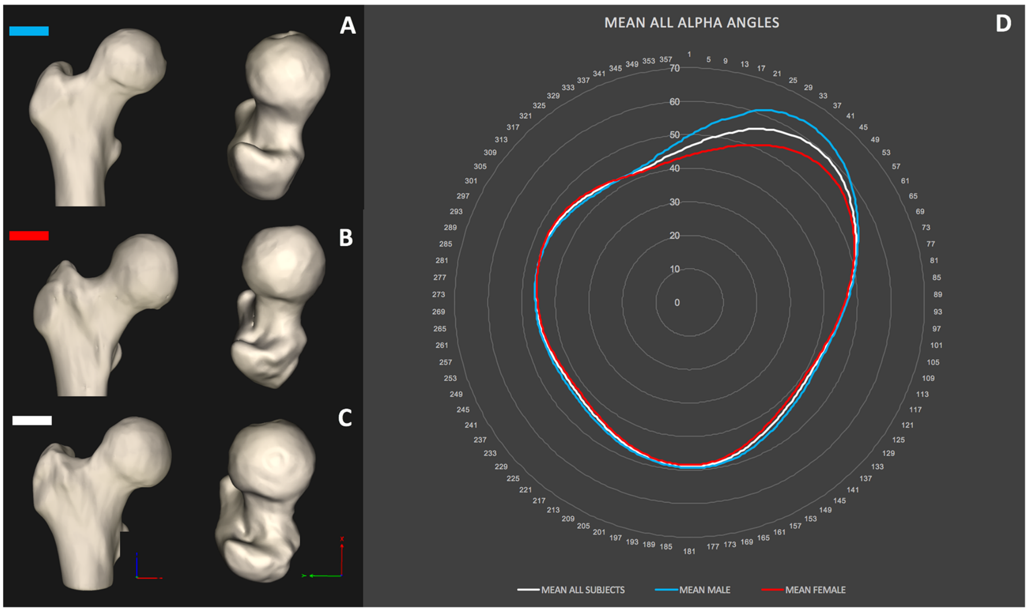

Fig. 4 Evaluation of the femoral head/neck morphology. Three-dimensional model in two projections (*left* to *right*: anterior and superior views). **a** Top row: male 3D model; **b** middle row: female 3D model; **c** bottom row: mean 3D model comprising all subjects; **d** corresponding 2D map of mean circumferential alpha angles (α°) at every degree for all participants (*white line*), for male subjects (*blue line*) and female subjects (*red line*): 0 corresponds to 12-o'clock position; 89° corresponds to 3-o'clock position

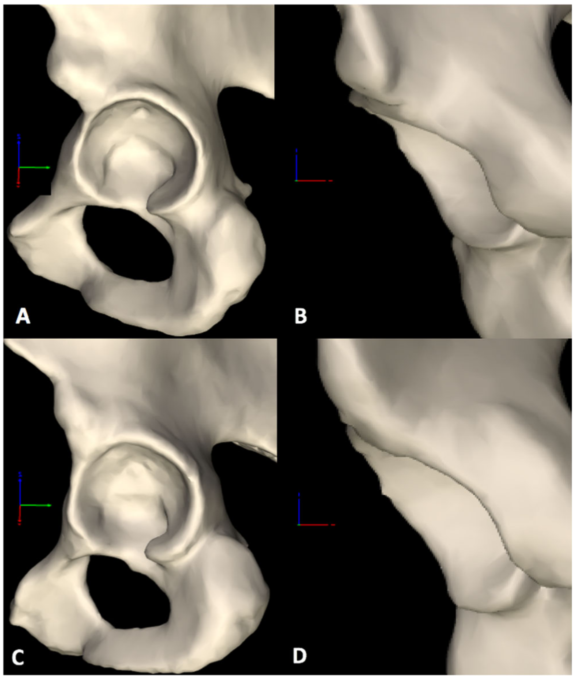

Fig. 5 Evaluation of the acetabular morphology. Three-dimensional model in two projections, lateral and strict anterior views. *Top row* (**a** and **b**): male 3D model. *Bottom row* (**c** and **d**): female 3D model. Female acetabulum has a shorter AP diameter and a shallower anterior wall

The lateral centre-edge angle (LCEA) was measured between the plane of the y-axis of the pelvis and a line from the centre of a regression sphere in the acetabulum to the osseous acetabular rim [17], performed in 30° steps from the 1:00-11:00 positions (Fig. 3e and f).

Pincer-type morphology was considered positive when we observed: (1) acetabular depth ≥ 3 mm (*coxa profunda*), and/or (2) LCEA>39°, and/or (3) centre ACvers < 10° and/or (4) upper ACvers < 0° (acetabular retroversion, which also defined the focal pincer subgroup). Acetabular dysplasia was defined as LCEA ≤ 20° [17, 31, 32].

Statistical analysis

For all morphometric parameters, mean values, SD (standard deviation) and double-sided 95% RefInt were calculated. Quantitative parameters are described by their mean and SD. Qualitative parameters are described in numbers and percentage. For the mean comparisons, Student's *t* test was implemented to compare quantitative variables (if test conditions were not met, a nonparametric test was used). To evaluate correlation between two quantitative parameters, Pearson or Spearman coefficients were computed. A *p* value of 0.05 was considered statistically significant for all analyses. Statistical analyses were performed using dedicated software (MedCalc Software version 11.6; Belgium).

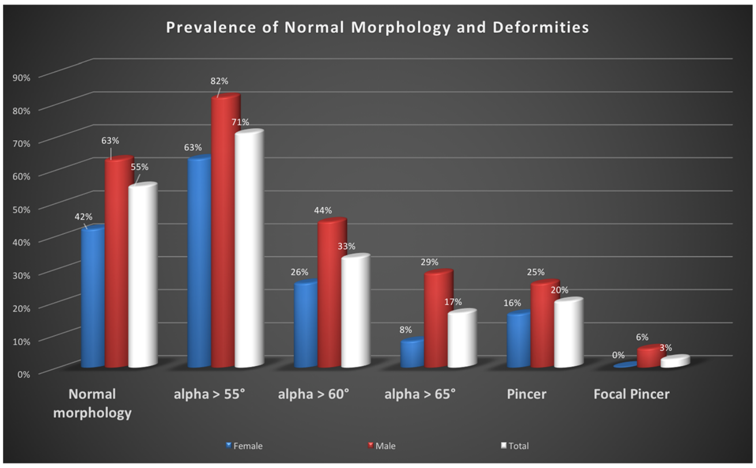

Fig. 6 Prevalence of "normal" morphology (considering all subjects with alpha angles inferior to 55° and no acetabular abnormalities), cam morphology (considering alpha angle thresholds of 55°, 60° and 65°) and pincer morphology (global and focal). Breakdown by sex and categories of pathology (percentage of total asymptomatic subjects)

Results

Population information

Of the initial 2286 hips in 1143 patients, a total of 553 patients were excluded according to the exclusion criteria (mean age: 63.2 ± 11.8 y.o.) (Fig. 1). In total, 1111 hips in 590 patients, all with closed physes, met the criteria for inclusion in the final analysis (271 males; 319 females; $p = 0.07$) (Tables 1, 2 and 3). Left-handers accounted for 9% of individuals indicating a similar prevalence to previous reports [23].

Overall

For the femoral morphotype (Fig. 4), the mean values of α° were 58° ± 7°/56° ± 7° at 1:30/1:00 o'clock and 35° ± 29° for the Ω° considering a threshold of α° 55°. The magnitude of the mean differences of α° was higher at 1:00 followed by the 00:30 o'clock position (males had more 9.5-10°).

For the acetabular morphotype (Fig. 5), the means were 21° ± 5° for ACvers (centre), 35° ± 6° for the LCEA and 3.4° ± 5.4° for ACinc. Concerning acetabular coverage, the mean was 74% ± 5% for the total ACcov (anterior ACcov: 41% ± 3%; posterior ACcov 33% ± 4%).

Cam morphology prevalence varied between 17%, 33% and 71% according to different α° thresholds (65°, 60° and 55°, respectively). Conversely, 20% of all subjects had pincer-type morphology (*coxa profunda*: 18.5%; LCEA > 39°: 12.2%; acetabular retroversion: 3%) (Fig. 6) and 2.6% acetabular dysplasia.

Sex

Sex differences were observed in several parameters at the femoral and acetabular sides (Tables 4 and 5). Pincer and cam morphology was significantly more prevalent in males [pincer: 25% vs. 16% ($p = 0.005$); cam: 44% vs. 26% for a 60° α° threshold ($p < 0.0001$)] (Fig. 6).

At the *femoral* side (Table 4 and Fig. 4), in males, we noticed higher mean values of Ω° ($p < 0.001$) and for all α° from 11:30 to 2:00 o'clock ($p < 0.001$) and for femoral head/neck diameters ($p < 0.001$). Conversely, females showed higher mean values of α° at 10:30 and of the CDA ($p < 0.001$). Different sex mean α° measurements were notably significant at 1:30/1:00 (males vs. females: 60° vs. 56° and 60° vs. 53°, respectively; $p < 0.001$) and paradoxically at 10:30 o 'clock (males vs. women: 43° vs. 45°; $p < 0.001$).

At the *acetabular* side (Table 5 and Fig. 5), in males, we noticed higher mean values of acetabular cup diameter and LCEA at 1:00 (estimated difference of 3°; $p < 0.001$), and in other cases where there was a statistically significant difference, the values were higher in females, namely in total/anterior ACcov and ACvers ($p < 0.001$). The magnitude of mean differences was greater for acetabular cup diameter and ACvers.

True retroversion (upper ACvers < 0°) was observed only in the upper hemisphere and no true global retroversion was identified. The prevalence of focal acetabular retroversion was 5.9% (16 of 271) for males and 0.9% (2 of 319) for females ($p = 0.04$).

Side and limb dominance (paired and unpaired)

Concerning femoral parameters, mean values did not differ between left/right sides. On the acetabular side, mean values of anterior ACcov differed between sides only on the unpaired analysis, being superior on the right sides ($p = 0.047$; mean differences of +0.5%), which can be considered not clinically important. All other parameters were symmetric.

Considering limb dominance, there was no difference between sides. Only when we paired dominant/non-dominant limbs did we find that mean ACinc was 1.1° higher on the dominant side ($p < 0.029$).

Table 4 Femoral side morphometric quantitative measurements (overall mean, SD, range and 95% reference intervals) and breakdown by sex and side (with corresponding mean differences and *p* values)

	Mean	SD	Min	Max	95% reference intervals	*p*	Mean difference
Femoral head diameter (mm)	43	3.8	37.2	53.1	38-52		
Male	47.6	2.5	41.7	53.1	43-52	<0.001	6.2
Female	41.4	2.2	37.3	47.6	38-46		
Left	44	3.9	37.2	52.9	38-52	NS	-
Right	44	3.8	37.6	53.1	38-52		
Femoral neck diameter (mm)	30.4	3.4	24.3	39.6	25-37		
Male	33.4	2.2	28.7	39.6	29-37	<0.001	5.5
Female	28.2	2.0	24.3	34.2	25-33		
Left	30.4	3.4	24.3	37.8	25-37	NS	-
Right	30.3	3.3	24.9	39.6	25-37		
Cervicodiaphyseal angle (°)	130.5	5.4	113	156	120-141		
Male	129	5	113	144	118-139	<0.001	-2.7
Female	132	6	118	156	122-142		
Left	130.6	5.2	113	147	120-139	NS	-
Right	130.4	5.5	115	147	120-142		
Omega angle 55 (°)	34	29	0	186	0-80		
Male	42	24	0	186	0-88	<0.001	19.8
Female	28	24	0	129	0-72		
Left	32.3	23	0	121	0-74	NS	-
Right	35.5	25	0	186	0-85		
Omega angle 60 (°)	14	19	0	164	0-59		
Male	21	21	0	164	0-72	<0.001	20
Female	10	16	0	80	0-54		
Left	13.4	18	0	100	0-55	NS	-
Right	15.4	20	0	164	0-60		
Alpha angle 9:00 (°)	45.2	4.8	32.1	64.3	36-55		
Male	45.5	4.5	34.5	64.3	37-55	NS	-
Female	45	4.9	32.1	56.9	35-54		
Left	45.2	4.9	33.9	56.9	35-55	NS	-
Right	45.3	4.6	32.1	64.3	37-55		
Alpha angle 10:00 (°)	45.9	4.8	31.3	61.5	36-55		
Male	45.3	4.2	31.3	58.5	36-54	NS	-
Female	46.5	5	32.9	61.5	36-57		
Left	45.9	4.8	34.9	61.5	36-58	NS	-
Right	46	4.8	31.3	57.9	36-54		
Alpha angle 10:30 (°)	44.1	4.7	30.4	61.2	36-55		
Male	43.2	4	30.4	54.7	35-52	<0.001	-1.7
Female	44.8	5	30.6	61.2	36-56		
Left	44	4.5	35.7	61.2	37-55	NS	-
Right	44.1	4.9	30.4	56.8	34-54		
Alpha angle 11:00 (°)	42.2	4.2	28.6	60.5	35-51		
Male	42	3.8	30.7	59.1	35-49	NS	-
Female	42.3	4.9	28.6	60.5	35-51		
Left	42.3	3.9	34.3	60.5	35-50	NS	-
Right	42	4.5	28.6	59.1	33-51		
Alpha angle 12:00 (°)	45.2	5.4	30.3	87.9	37-56		
Male	47.4	6.3	37.8	87.9	39-66	<0.001	5.8
Female	43.5	4	30.3	57.2	36-51		
Left	45.2	4.9	35.1	87.9	37-55	NS	-
Right	45	5.9	30.3	82.2	36-56		
Alpha angle 1:00 (°)	55.9	6.9	36.2	89.7	43-72		
Male	59.8	7.7	40.2	89.7	47-74	<0.001	10.3

Table 4 (continued)

	Mean	SD	Min	Max	95% reference intervals	*p*	Mean difference
Female	53.1	6.2	36.2	80.7	42-67		
Left	56.1	7.3	41.2	89.7	44-74	NS	-
Right	55.6	7.9	36.2	89.5	43-72		
Alpha angle 1:30 (°)	58	6.5	40	84.2	46-70		
Male	60.3	6.5	42.7	84.2	46-71	<0.001	5.9
Female	56.5	5.9	40	78.3	44-70		
Left	58.2	6.2	42	84.2	47-71	NS	-
Right	57.9	6.7	40	81.1	44-70		
Alpha angle 2:00 (°)	55.3	5.8	37.5	82.2	42-66		
Male	55.8	6	40.1	82.2	43-67	<0.001	2.5
Female	54.9	5.6	37.5	70.5	41-66		
Left	55	5.7	37.5	76.8	42-67	NS	-
Right	55.5	5.8	40.1	82.2	42-65		
Alpha angle 3:00 (°)	46.2	5.8	30.8	65.7	36-58		
Male	46.1	5.9	30.8	65.7	34-63	NS	-
Female	46.2	5.7	33.3	65.4	36-57		
Left	45.4	5	34.4	65.1	36-55	NS	-
Right	46.8	6.3	30.8	65.7	35-63		

SD, standard deviation; Min, minimum; Max, maximum; NS, non-significant. *T-test for independent samples

Age

$\alpha°$ measurements had weak correlations to age and were only observed from 10:00-12:00 (Table 6 in supplemental data). On the subgroup analysis only the 10:30 position revealed significant differences between groups, namely between < 20 y.o. and all other groups (by a mean difference of 3-4°). Concerning $\Omega°$, age groups did not differ (Table 6 in supplemental data).

There were differences between age groups concerning anterior ACcov (p = 0.013) and ACvers (p < 0.0001). Concerning centre ACvers, there were differences between the 36-40 group and both the under 20 y.o./21-25 groups [mean differences: +4.5° (p = 0.004) and +4.2° (p = 0.035), respectively]. Therefore, the ACcov and ACvers increased with age (estimated in 4% and 6-7°, respectively, between age opposites) (Table 6 in supplemental data).

Concerning LCEA at 12:00, differences were noted between the under 20 y.o. and the 36-40/41-45 groups (mean differences: -6.2°/-5.1°; p = 0.001/p = 0.012, respectively), meaning that LCEA increased with age, approximately 5-7° between opposite age groups.

Discussion

Prior studies have primarily used plain radiographic (XR) parameters to characterise the acetabulum and femur [33–38]. However, several other studies reported poor reliability for defining hip pathomorphology with XR and improved accuracy with CT scans (Tables 7 and 8), raising concerns on defining hip disorders and anatomy based on XR alone [33, 38, 52]. It is possible that clinicians are not only overdiagnosing and overtreating these conditions, but also paradoxically missing the diagnosis entirely [53]. Specifically, clinical advantages of this methodology have been addressed in a recent report [10], including (1) accurate spatial visualisation of hip morphology, (2) improved diagnosis and monitoring through the use of quantitative 3D morphometric assessment and (3) standardising and reducing variability in clinical research.

Our study provides both normative hip data and a reproducible method for evaluating hip morphology as the sample size is the largest reported using cross-sectional imaging.

The RefInt limits were beyond abnormal thresholds found in the literature for cam morphology, providing additional insights into the evolving understanding of the $\alpha°$ and its associated reference standards. Increasing the threshold of abnormal $\alpha°$ would improve its specificity, prevent overdiagnosis of FAI and consequently decrease the number of unneeded surgeries. Therefore, we suggest rethinking the threshold of abnormal $\alpha°$. We propose an $\alpha°$ upper-limit RefInt of 60° for the 12:00/3:00 positions and 65-70° for the 1:00/1:30 o'clock positions. Although higher than the previously published threshold of 50° to 55° [12], the results are in agreement with several authors (Tables 7 and 8), namely with Agricola et al.

Table 5 Acetabular side morphometric quantitative measurements (overall mean, SD, range and 95% reference intervals) and breakdown by sex and side (with corresponding mean differences and *p* values)

	Mean	SD	Min	Max	95% reference intervals	*P**	Mean difference
Acetabular coverage anterior (%)	40.8	2.5	34.3	46.6	36-45		
Male	40.2	2.4	34.3	46.4	36-46	<0.001	-1.3
Female	41.2	2.4	35.2	46.6	36-44		
Left	40.5	2.5	34.3	46.6	36-45	0.047	+0.5% (superior on the right)
Right	41.1	2.4	34.6	46.6	36-45		
Acetabular coverage posterior (%)	33	3.5	22.5	41.9	27-40		
Male	33.2	3.3	22.5	41.9	27-40	NS	-
Female	32.9	3.5	24.6	41.5	26-40		
Left	33	3.4	25.8	41.5	27-40	NS	-
Right	32.9	3.5	22.5	41.9	26-40		
Acetabular coverage total (%)	74	5	58.6	87.5	64-84		
Male	73.4	4.9	58.6	84.8	63-84	0.028	-1.3
Female	74.1	5.2	61.1	87.5	64-83		
Left	74	5	58.5	84.8	64-84	NS	-
Right	74	5	58.6	83.8	63-83		
Acetabular version (centre) (°)	21	5.1	4.7	33.2	12-31		
Male	18.2	4.8	4.7	29.7	8-27	<0.001	-5.2
Female	22.9	4.4	12.7	33.2	14-32		
Left	21	4.8	7.8	32.4	10-30	NS	-
Right	20.9	5.4	4.7	33.2	12-32		
Acetabular version (upper) (°)	21	7.3	-7.2	37	6-34		
Male	18.5	7.7	-7.2	33.8	1-32	<0.001	-5.2
Female	22.6	6.6	2.2	37	8-34		
Left	20.9	7	0.9	35.3	5-33	NS	-
Right	20.8	7.6	-7.2	37	6-34		
Acetabular cup diameter (mm)	47.8	3.9	40.2	57.1	41-55		
Male	51.3	2.4	45.3	57.1	47-56	<0.001	6.1
Female	45.3	2.6	40.2	51.6	41-51		
Left	47.6	4	40.2	56.3	41-56	NS	-
Right	47.9	3.7	40.8	57.1	41-55		
Acetabular inclination (°)	3.4	5.4	-13.3	15.5	-8 – 14		
Male	2.4	5.4	-12.5	15.5	-9 – 14	NS	-
Female	4	5.3	-13.3	14.5	-6 -13		
Left	3	5.4	-13.3	13.6	-8 - 12	NS	-
Right	3.6	5.4	-12.5	15.5	-7 - 14		
Lateral CEA 1:00 (°)	25.6	7.4	2.8	47.6	10-40		
Male	27.4	7.1	2.8	47.6	13-41	0.001	2.9
Female	24.3	7.3	8.1	42.3	10-39		
Left	25.2	7.3	8.4	45.7	9-38	NS	-
Right	25.9	7.4	2.8	47.6	10-41		
Lateral CEA 12:00 (°)	35	5.8	18.8	55.5	22-45		
Male	35.8	6	20.3	50.7	24-47	NS	-
Female	34.4	5.7	18.8	55.5	22-45		
Left	34.8	6	18.8	55.5	22-45	NS	-
Right	35.2	5.7	20.3	51	22-46		
Lateral CEA 11:00	32.5	6.4	14.6	52.8	21-45		
Male	32.6	7.2	14.6	48.3	20-46	NS	-
Female	32.4	5.7	16.7	52.8	19-42		
Left	32.2	6.6	16.7	51.2	18-44	NS	-
Right	32.8	6.1	14.6	52.8	21-45		

SD, standard deviation; Min, minimum; Max, maximum; NS non-significant. *T-test for independent samples

Table 6 Acetabular and femoral morphotype breakdown by age groups (mean and SD). Correlation of femoral and acetabular quantitative parameters with age

		Age						Correlation coefficient (p) (a)
		<20 Mean (SD)	21-25 Mean (SD)	26-30 Mean (SD)	31-35 Mean (SD)	36-40 Mean (SD)	41-45 Mean (SD)	
Omega angle	55	35.5 (33.4)	31.6 (24)	38.5 (27.9)	42.2 (26.8)	36.2 (27.3)	43.3 (26.8)	NS
	60	20.7 (29)	11.5 (18.6)	21.7 (25)	21.3 (24.3)	16.9 (22.8)	23.6 (25.5)	NS
Alpha angle	9:00	45.4 (6.4)	44.4 (5.4)	46.2 (4.9)	45 (5.1)	45.88 (4.1)	45.9 (4.7)	NS
	10:00	43.9 (5.6)	45.7 (5.2)	46.9 (5.4)	46.1 (4.7)	46.3 (3.5)	46.6 (5)	0.038 *
	10:30	40.9 (4.7)	44.8 (5.3)	44.9 (5.5)	44.4 (4.3)	44.3(3.9)	44.7 (4.6)	0.011*
	11:00	40.1 (4.7)	42.8 (4.4)	42.6 (4.6)	42.5 (4)	42.6 (3.7)	42.6 (4.2)	0.042*
	12:00	45.3 (6.4)	44.4 (4.9)	45.7 (6.7)	46.2 (6.4)	46.4 (5.4)	48.2 (10.4)	0.026*
	1:00	58 (11.8)	54.2 (8.1)	57.4 (10.1)	58.7 (9.6)	57.8 (8.9)	59.2 (10.2)	NS
	1:30	59.6 (10.4)	56.2 (5.8)	60 (8.2)	60.6 (7.9)	57.7 (6.2)	60.3 (6.8)	NS
	2:00	57.1 (9.9)	54.1 (5.7)	57.4 (7.6)	56.7 (6.3)	54.5 (5.6)	56.9 (5.5)	NS
	3:00	45.8 (7.6)	45.2 (6.7)	47.1 (6.6)	47 (6.1)	46.8 (5.9)	47.5 (6)	NS
Femoral diameter	Head	44.1 (3.8)	42.8 (3.1)	44 (4.8)	43.8 (3.6)	44.9 (3.7)	45.1 (4)	0.036*
	Neck	30.4 (3.7)	29.3 (2.7)	30.38 (4.4)	30.3 (3.1)	31.4 (3.2)	31.4 (3.6)	0.022*
CDA		131.8 (5.6)	131.7 (4.8)	132.5 (6.1)	130.2 (4.5)	130.5 6.7)	129.2 (5.5)	0.009*
Acetabular coverage	Anterior	39.7 (2.5)	40.2 (2.7)	40.7 (2)	40.7 (2.4)	41.4 (2.9)	41.4 (2.6)	0.000**
	Posterior	33.2 (3.5)	33.9 (3.7)	33 (3.5)	32.8 (3.4)	33 (3.6)	33.6 (3.3)	NS
	Total	73 (5.1)	74.1 (5.8)	73.8 (4.7)	73.5 (5)	74.4 (5.8)	75 (5.1)	NS
Acetabular version	Center	18.5 (5.7)	18.8 (5.7)	20.2 (4.5)	31.4 (5)	23 (5.5)	20.6 (4.7)	0.000**
	Upper	16.1 (7.5)	17 (8.5)	19.9 (6.3)	20.6 (7.1)	23.5 (7.2)	22.2 (7.6)	0.000**
Acetabular diameter		47.5 (3.8)	46.5 (2.9)	47.9 (4.7)	47.4 (3.8)	49 (3.8)	49 (3.9)	0.007*
Acetabular inclination		3.7 (4.7)	3.4 (5.8)	2.8 (4.5)	3.4 (5.6)	3 (6.2)	2.3 (5.7)	NS
LCEA	1:00	24.9 (7.3)	26.7 (6.5)	26.4 (7.8)	25.6 (7.4)	25.8 (8)	28.6 (7.8)	NS
	12:00	32.4 (6.2)	34.5 (5.5)	35 (5)	35.5 (6.4)	36.4 (6.7)	37.6 (6.1)	0.000**
	11:00	28.7 (6.2)	30.4 (5.6)	31.9 (4.7)	32.7 (6.4)	35 (7.5)	35.8 (6.8)	0.000**

SD, standard deviation; Min, minimum; Max, maximum; NS, non-significant. *T-test for independent samples. (a) Pearson or Spearman correlation coefficients *inferior to 0.200 (weak); **0.200 -0.400 (moderate); ***0.400 -0.600 (strong)

[13] (who also measured the 12:00 position $\alpha°$) and similar to a recent report using MRI [54] that suggested increasing the threshold to 63°/66° at 3:00/1:30 o'clock, respectively. The sample size used in our study was significantly larger than that of previous studies, demonstrating higher statistical power. However large multicentre studies will provide more definitive data on this concept.

Sex differences arise in the natural physiological growth namely in the development of the FHN junction [55] but also in joint orientation, including acetabular anteversion and coverage [41]. Interestingly, other studies found sex-dependent disease patterns in patients with symptomatic FAI. Females had milder morphological abnormalities, while males had larger morphological abnormalities and more extensive joint disease [56–60].

At the femoral side, in males, we noticed lower mean CDA [40] and higher mean $\Omega°$ and $\alpha°$ from 11:30-2:00 o'clock ($p < 0.001$). Magnitudes of cam morphology and RefInt for $\alpha°$ were significantly sex-different, consistent with the majority of previous results [10, 13, 15, 61] but divergent from some studies [16, 62]. Specifically, overall mean $\alpha°$ at 3/1:30/12:00 o'clock was 46°/58°/45°, 46°/60°/47° for males and 46°/56°/43° for females. Mean $\alpha°$ was significantly sex-different at 1:00/1:30 (more 8-10° in males) and conversely females revealed higher mean values for $\alpha°$ at 10:30. We hypothesise that this latter finding [10] results from constitutional development during adolescence where cam morphology results from bone adaptation in response to vigorous hip loading. In fact, it has been determined that during the growth spurt in boys (around 12–13 y.o.), the skeleton is particularly responsive to mechanical stimuli [63]. This might also account for other sex differences since girls' growth spurt occurs about 1.5 years earlier [64] apart from the fact that more boys typically engage in higher intensity sports [65].

For the pincer morphotype, there is also controversy as prior studies have shown that women have more acetabular

Table 7 Femoral morphotype reference intervals with comparison to relevant literature (asymptomatic populations)

	Mean	SD	Mean ± 2 SD	95% reference intervals	Reference limits in the literature
Cervico-diaphyseal angle (°)	130.5	5.4	120-141	120-141	Mean*: 128.8° (range: 98–180°) [39] Mean**: 130.7° (range 107.1–151.9°; SD:6.5°) [40] Mean**: 125.1° (SD: 4.9°) [41]
Male	129	5	119-139	118-139	Mean**: 129.6° (range: 113°–148°; SD 5.9°) [40] Mean**: 124.3° (SD: 4.8°) [41]
Female	132	6	120-144	122-142	Mean**: 131.9° (range: 107°–151.9°; SD 6.8°) [40] Mean**: 125.5°; SD: 4.9° [41]
Omega angle 60 (°)	14	19	0-52	0-59	Mean**: 17° (range: 0–84°) [10]
Omega angle 55 (°)	34	29	0-92	0-97	Mean**: 35° (range: 0–89°) [10]
Alpha angle 9:00 (°)	45.2	4.8	36-55	36-55	Mean**: 44.9° (SD: 4.3°; range: 23.2–53.9°) [10]
Alpha angle 10:30 (°)	44.1	4.7	35-54	36-55	Mean**: 43.8° (SD: 3.7°; range: 35.7–52.5°) [10] Mean***: 49.2° (SD: 9.6°) [7]
Alpha angle 12:00 (°)	45.2	5.4	34-56	37-56	Mean**: 47.8 (SD: 6.7; range: 37.1–77°) [10] Mean**: 47.7° (range: 31–71°) [42] Mean***: 51.8° (SD: 9.9°) [7]
Alpha angle 1:00 (°)	55.9	6.9	42-70	43-72	Mean**: 58.9° (SD: 8.8°; range: 41.6–80.3°) [10] Mean**: 52.5° (range: 36–72°) [42]
Alpha angle 1:30 (°)	58	6.5	45-71	46-70	Mean**: 58.9° (SD: 6.8; range: 46.4–76.4°) [10] Mean**: 59° (SD: 13°) [16] Mean***: 50.9° [43] Mean***: 53.3 (SD: 9.6°) [7]
Alpha angle 2:00 (°)	55.3	5.8	44-67	42-66	Mean**: 54.9° (SD: 5.5°; range: 39.3–71) [10] Mean**: 47.9° (range: 30–65°) [42]
Alpha angle 3:00 (°)	46.2	5.8	37-58	36-58	Mean**: 45.8° (SD: 4.9; range: 35–59.1) [10] Mean**: 45.57° (range: 30° to 70°) [44] Mean**: 51° (SD: 9) [16] Mean**: 46° (range: 34–74°) [42] Mean***: 49.8° (SD: 7.2) [7] Mean***: 40.9° [43]

*CR; **CT; ***MRI

SD, standard deviation; 95% RI, 95% reference interval

anteversion and a greater prevalence of global acetabular overcoverage [20, 66–68]. The mean values found for LCEA (35°±6°), ACinc (3°±5°) and craniocaudal coverage (74% ± 5) were in accordance with the results of large-scale studies [69], namely regarding the upper thresholds for the LCEA [22, 44, 50, 69, 70] and discordant with other studies [17] on small observational groups.

Of the examined acetabuli, cranial retroversion (crossover sign) was a uncommon finding (3%), divergent with a previous study [14] and coherent with Tannenbaum et al. [48] (15% vs. 3.8%, respectively). Acetabular retroversion and anterior overcoverage were not more prevalent in women in the anterosuperior acetabulum, consistent with previous reports [48]. In fact, males had a higher prevalence of retroversion with a clear tendency to have a more prominent anterosuperior wall (anteversion angles were on average 5° lower in males compared to 2.7° in a previous study [19]). Women had more ACcov and a smaller anterior wall, in line with previous reports [21, 41, 48, 51].

Concerning limb dominance, given that more than 85% of individuals are right-handed, we sought to investigate the association between dominance side and hip shape as in the development of OA one is significantly more likely to require hip arthroplasty on their dominant side [23]. However dominant/non-dominant limbs were globally symmetric, suggesting that this predisposition cannot be explained by differences in hip shape alone. Conceptually, as varying tasks are attributed to each of the lower limbs, the dominant limb for forward propulsion and non-dominant limb for postural stabilisation, this may influence the dominant hip in the progression of degenerative disease.

Similarly, there were no differences in hip shape analysis between sides. Our RefInt were similar between right/left hips, comparable with previous reports [16, 71, 72]. Interestingly, also in a symptomatic cohort there were no differences in cam deformity parameters, femoral torsion, acetabular version and LCEA between affected/unaffected hips. A decreased CDA was hypothesised as the only diagnostic

Table 8 Acetabular morphotype reference intervals with comparison to relevant literature (asymptomatic populations)

	Mean	SD	Mean ± 2 SD	95% reference intervals	Reference limits in the literature
Acetabular coverage total (%)	74%	5	64-84	64-84	Mean**: 71% (range: 62-78) [45] Mean**: 73% (SD 4; range: 66-81) [30]
Male	73.4	4.9	64-83	63-84	Mean**: 73% (SD 4; range: 67-79) [30]
Female	74.1	5.2	64-84	64-83	Mean**: 73% (SD: 4; range: 66-81) [30]
Acetabular version (centre) (°)	21°	5.1	11-31	12-31	Range*: 15-20° [46, 47]; Mean**: 18° (range 8-30°) [45] Mean**: 23° (SD: 5, range 12-39) [19] Mean**: 21.1 (range: 11-36°) [42] Mean**: 18.85°; 95% RI: 5° - 29° [44] Mean**: 20° (SD: 6.8) [41] Mean**: 19° (SD: 6) [16]
Male	18.2	4.8	9-27	8-27	Mean**: 15° (SD: 7; range: 1 – 24) [30] Mean**: 22° (SD: 6, range: 12-39) [19] Mean**: 20.2° [48] Mean**: 16.8° [44] Mean**: 17.5° (SD: 6.1) [41] Mean**: 17° (SD: 5; 95% RI: 7-27) [16]
Female	22.9	4.4	14-32	14-32	Mean**: 18° (SD: 8; range: 2-31) [30] Mean**: 23° (SD: 5; range 15-35) [19] Mean**: 24.3° [48] Mean**: 19° [44] Mean**: 21.3° (SD: 6.8) [41] Mean**: 21° (SD: 6; RI 95%: 10-32) [16]
Acetabular version (upper)	21	7.3	7-35	6-34	Mean**: 15.7° (SD 8.0°) [49]
Male	18.5	7.7	3-34	1-32	Mean**: 15.5° [48]
Female	22.6	6.6	9-36	8-34	Mean**: 18.3° [48]
Acetabular inclination (°)	3.4	5.4	-7 -14	-8– 14	Mean*: 4.4° (95 % RI: −6.9° - 14.9°) [50] Mean**: 6° (SD: 5) [16]
Male	2.4	5.4	-8 - 13	-9 -14	Mean*: 4.4° (95% RI: −6.9-14.4°) [50] Mean**: 6° (SD: 5; 95% RI: -3 -14°)[16]
Female	**4**	**5.3**	**-6 - 15**	**-6 - 13**	Mean*: 3.48° (95% RI: −8.8-13.8°) [50] Mean**: 6° (SD: 4; 95% RI: -1 – 16°) [16]
Lateral CEA 12:00 (°)	**35**	**5.8**	**23-47**	**22-45**	Mean**: 37°; 95% RI: 28-47° [45] Mean*: 33.6° (95% RI: 18.1°-48°) [50] Mean*:32.8°(Range: 13.7°-58.8°) [22] Mean*: 36.3° (95% RI: 24.9–47.8°) [51] Mean**: 34.84° (95% RI: 21°-46°) [44] Mean**: 35.8° (SD: 6) [41] Mean**: 32° (SD: 6) [16]
Male	35.8	6	24-48	24-47	Mean*: 32.43° (95% RI: 17 - 46.5) [50] Mean*: 37.7° (95% RI: 26.9–48.5°) [51] Mean**: 36.09° [44] Mean**:37.9° SD: 5.3° [41] Mean**: 35°; SD: 6°; 95% RI: 22-47° [16]
Female	34.4	5.7	23-46	22-45	Mean*: 33.94° (95 % RI: 17.9-49.7°) [50] Mean*: 34.9° (95% RI: 23.5–46.3°) [51] Mean**: 33°[44] Mean**: 34.7° (SD: 6.1°) [41] Mean**: 32° (SD: 6°; 95% RI: 21-46°) [16]

*CR; **CT; ***MRI

SD, standard deviation; 95% RI, 95% reference interval

predictor to determine which hip may be at a greater risk of developing early symptoms [5, 73] or OA [74]. These findings have important associated implications. First, hip symmetry questions the concept that only small morphological variations, namely the CDA and ACinc, could alter the interplay between the femoral and acetabular side. Second, questions remain about the aetiology of hip OA, which may be more prevalent on the dominant side, and as such we hypothesise that causation might be related to other non-morphological dynamic causes. Third, for study design and clinical trials purposes, one can safely assume that both hips are alike.

Regarding age, femoral parameters were stable after physeal maturity. In contrast, LCEA increased with age (approximately 5-7° between opposite age groups), coherent with previous reports that estimated that the LCEA was positively correlated with age, increasing annually by 0.78° before adulthood and by 0.07° in adults [22].

Similarly, anterior ACcov and ACvers increased with age (respectively 4%/6-7° between age opposites) in accordance with Stem et al. [19], who estimated an increase of 0.7° in anteversion for every 10-year age increase. This finding to the best of our knowledge has not been further addressed in the literature and suggests that pelvic orientation and version probably change during adulthood. We hypothesise that osseous apposition, cumulative degenerative changes and pregnancy might contribute to this upward coverage and anteversion tendency.

This study has several limitations. First, our RefInt were derived from a limited sample of 590 individuals. Second, selecting a protocol for this study may have been subject to several biases. Specifically, our participants were not selected from healthy volunteers. In addition, we used patient survey information to exclude hip pathology but did not perform a clinical hip examination. However, we prospectively included patients presenting for non-orthopaedic pathology and excluded all patients with any reported history of hip pathology or symptoms. Additionally, we excluded any patients with signs of hip pathology on CT so that our cohort comprised asymptomatic individuals only. Third, this study did not include correlation of semi-automated measurements and traditional manual measurements; such comparison between 2D and 3D CT methods would be useful but was not an objective of our study, apart from the fact that the software used had already been validated for this purpose. Lastly, measurements of torsional abnormalities, which are a known cause of pain and osteoarthritis [46], could not be performed for ethical reasons.

To develop more generalisable RefInt, larger individual cohort studies with more varied demographics are needed. Further investigations are also needed to incorporate 3D measurements of the hip in symptomatic patients for a complete comparison between these populations to get a better picture of hip biomechanics in cases of FAI.

Conclusions

Hip morphometric measurements in this cohort of asymptomatic individuals extended beyond current thresholds used for the clinical diagnosis of FAI, which was especially true for cam-type parameters, suggesting that symptomatic FAI likely reflects a complex dynamic interaction of morphology and other factors and thus cannot be explained by differences in hip shape alone.

Our results, although preliminary, suggest the need for consideration of redefining the current morphometric parameters used in FAI diagnosis. Therefore, we suggest considering an $\alpha°$ threshold of 60° as an upper limit for the 12:00/3:00 positions and 65-70° for other antero-superior positions.

Acknowledgements The authors would like to thank José Roquette, João Sá, Isabel Vaz and Pedro Patrício for their continuing and enthusiastic support of clinical research at Hospital da Luz and Rúben Teixeira, Ana Filipa Graça, Rogério Lopes, Diogo Corrente, João Novo and Tiago Castela for their efforts toward optimising technical issues and providing patient care.

Funding The authors state that this work has not received any funding.

Compliance with ethical standards

Guarantor The scientific guarantor of this publication is Prof. Dr. José Roquette.

Conflict of interest The authors of this manuscript declare no relationships with any companies, whose products or services may be related to the subject matter of the article.

Statistics and biometry One of the authors has significant statistical expertise. No complex statistical methods were necessary for this paper.

Informed consent Written informed consent was obtained from all subjects (patients) in this study.

Ethical approval Institutional Review Board approval was obtained.

Study subjects or cohorts overlap Ninety-four of the 590 patients of the current cohort were previously studied and published [Mascarenhas VV, Rego PA, Dantas P, et al (2016) Cam deformity and the omega angle, a novel quantitative measurement of femoral head-neck morphology: a 3D CT gender analysis in asymptomatic subjects. Eur Radiol. doi: 10.1007/s00330-016-4530-0]. Substantially and important different objectives, statistical power and conclusions are therefore withdrawn from this cohort.

Methodology
• prospective
• cross-sectional study
• multicentre study

References

1. Griffin DR, Dickenson EJ, O'Donnell J et al (2016) The Warwick Agreement on femoroacetabular impingement syndrome (FAI syndrome): an international consensus statement. Br J Sports Med 50: 1169–1176. https://doi.org/10.1136/bjsports-2016-096743
2. Agricola R, Waarsing JH, Arden NK et al (2013) Cam impingement of the hip: a risk factor for hip osteoarthritis. Nat Publ Group 9:630–634. https://doi.org/10.1038/nrrheum.2013.114

3. Hunter DJ, Marin-Pena O (2016) Striving for multidisciplinary consensus on the diagnosis and management of patients with femoroacetabular impingement: more evidence is needed. Br J Sports Med. https://doi.org/10.1136/bjsports-2016-096830
4. Mascarenhas VV, Rego P, Dantas P et al (2016) Imaging prevalence of femoroacetabular impingement in symptomatic patients, athletes, and asymptomatic individuals: A systematic review. Eur J Radiol 85:73–95. https://doi.org/10.1016/j.ejrad.2015.10.016
5. Ng KCG, Lamontagne M, Beaulé PE (2016) Differences in anatomical parameters between the affected and unaffected hip in patients with bilateral cam-type deformities. Clin Biomech (Bristol, Avon) 33:13–19. https://doi.org/10.1016/j.clinbiomech.2016.01.007
6. Agricola R, Weinans H (2015) What causes cam deformity and femoroacetabular impingement: still too many questions to provide clear answers: Figure 1. Br J Sports Med bjsports–2015–094773. doi: https://doi.org/10.1136/bjsports-2015-094773
7. Sutter R, Dietrich TJ, Zingg PO, Pfirrmann CWA (2012) How useful is the alpha angle for discriminating between symptomatic patients with cam-type femoroacetabular impingement and asymptomatic volunteers? Radiology 264:514–521. https://doi.org/10.1148/radiol.12112479
8. Thomas GER, Palmer AJR, Batra RN et al (2014) Subclinical deformities of the hip are significant predictors of radiographic osteoarthritis and joint replacement in women. A 20 year longitudinal cohort study. Osteoarthritis and cartilage / OARS. Osteoarthr Res Soc 22:1504–1510. https://doi.org/10.1016/j.joca.2014.06.038
9. Ehrmann C, Rosskopf AB, Pfirrmann CWA, Sutter R (2015) Beyond the alpha angle: Alternative measurements for quantifying cam-type deformities in femoroacetabular impingement. J Magn Reson Imaging. https://doi.org/10.1002/jmri.24861
10. Mascarenhas VV, Rego PA, Dantas P et al (2016) Cam deformity and the omega angle, a novel quantitative measurement of femoral head-neck morphology: a 3D CT gender analysis in asymptomatic subjects. Eur Radiol. https://doi.org/10.1007/s00330-016-4530-0
11. Rego PRA, Mascarenhas V, Oliveira FS, et al (2015) Morphologic and angular planning for cam resection in femoro-acetabular impingement: value of the omega angle. Int Orthop (SICOT) 1–7. doi: https://doi.org/10.1007/s00264-015-3053-7
12. Nötzli HP, Wyss TF, Stoecklin CH et al (2002) The contour of the femoral head-neck junction as a predictor for the risk of anterior impingement. J Bone Joint Surg Br Vol 84:556–560
13. Agricola R, Waarsing JH, Thomas GE et al (2014) Cam impingement: defining the presence of a cam deformity by the alpha angle: data from the CHECK cohort and Chingford cohort. Osteoarthritis Cartil/OARS, Osteoarthr Res Soc 22:218–225. https://doi.org/10.1016/j.joca.2013.11.007
14. Larson CM, Moreau-Gaudry A, Kelly BT et al (2014) Are Normal Hips Being Labeled as Pathologic? A CT-based Method for Defining Normal Acetabular Coverage. Clin Orthop Relat Res 473:1247–1254. https://doi.org/10.1007/s11999-014-4055-2
15. Hack K, Di Primio G, Rakhra K, Beaulé PE (2010) Prevalence of cam-type femoroacetabular impingement morphology in asymptomatic volunteers. J Bone Joint Surg 92:2436–2444. https://doi.org/10.2106/JBJS.J.01280
16. Lepage-Saucier M, Thiéry C, Larbi A et al (2014) Femoroacetabular impingement: normal values of the quantitative morphometric parameters in asymptomatic hips. Eur Radiol 24:1707–1714. https://doi.org/10.1007/s00330-014-3171-4
17. Tannast M, Hanke MS, Zheng G et al (2015) What are the radiographic reference values for acetabular under- and overcoverage? Clin Orthop Relat Res 473:1234–1246. https://doi.org/10.1007/s11999-014-4038-3
18. Murtha PE, Hafez MA, Jaramaz B, DiGioia AM (2008) Variations in acetabular anatomy with reference to total hip replacement. J Bone Joint Surg Br Vol 90:308–313. https://doi.org/10.1302/0301-620X.90B3.19548
19. Stem ES, O'Connor MI, Kransdorf MJ, Crook J (2006) Computed tomography analysis of acetabular anteversion and abduction. Skelet Radiol 35:385–389. https://doi.org/10.1007/s00256-006-0086-4
20. Hildebrand F, Shin H-O, Flötotto L et al (2012) The prevalence of reduced acetabular anteversion in asymptomatic patients: a retrospective analysis. Z Orthop Unfall 150:601–606. https://doi.org/10.1055/s-0032-1327795
21. Peterson JB, Doan J, Bomar JD et al (2014) Sex Differences in Cartilage Topography and Orientation of the Developing Acetabulum: Implications for Hip Preservation Surgery. Clin Orthop Relat Res. https://doi.org/10.1007/s11999-014-4109-5
22. Shi YY, Liu TJ, Zhao Q et al (2010) The normal centre-edge angle of Wiberg in the Chinese population: a population-based cross-sectional study. J Bone Joint Surg Br Vol 92:1144–1147. https://doi.org/10.1302/0301-620X.92B8.23993
23. Cawley DT, Guerin SJ, Walsh J et al (2015) The significance of hand dominance in hip osteoarthritis. Semin Arthritis Rheum 44:527–530. https://doi.org/10.1016/j.semarthrit.2014.11.001
24. Christensen CP, Althausen PL, Mittleman MA et al (2003) The nonarthritic hip score: reliable and validated. Clin Orthop Relat Res:75–83. https://doi.org/10.1097/01.blo.0000043047.84315.4b
25. Röling MA, Visser MI, Oei EHG et al (2015) A quantitative non-invasive assessment of femoroacetabular impingement with CT-based dynamic simulation–cadaveric validation study. BMC Musculoskelet Disord 16:50. https://doi.org/10.1186/s12891-015-0504-7
26. Klenke FM, Hoffmann DB, Cross BJ, Siebenrock KA (2015) Validation of a standardized mapping system of the hip joint for radial MRA sequencing. Skelet Radiol 44:339–343. https://doi.org/10.1007/s00256-014-2026-z
27. Philippon MJ, Stubbs AJ, Schenker ML et al (2007) Arthroscopic Management of Femoroacetabular Impingement: Osteoplasty Technique and Literature Review. Am J Sports Med 35:1571–1580. https://doi.org/10.1177/0363546507300258
28. Toogood PA, Skalak A, Cooperman DR (2008) Proximal Femoral Anatomy in the Normal Human Population. Clin Orthop Relat Res 467:876–885. https://doi.org/10.1007/s11999-008-0473-3
29. Köhnlein W, Ganz R, Impellizzeri FM, Leunig M (2009) Acetabular Morphology: Implications for Joint-preserving Surgery. Clin Orthop Relat Res 467:682–691. https://doi.org/10.1007/s11999-008-0682-9
30. Dandachli W, Kannan V, Richards R et al (2008) Analysis of cover of the femoral head in normal and dysplastic hips: new CT-based technique. J Bone Joint Surg Br Vol 90:1428–1434. https://doi.org/10.1302/0301-620X.90B11.20073
31. Leunig M, Jüni P, Werlen S et al (2013) Prevalence of cam and pincer-type deformities on hip MRI in an asymptomatic young Swiss female population: a cross-sectional study. Osteoarthr Cartil 21:544–550. https://doi.org/10.1016/j.joca.2013.01.003
32. Nho J-H, Lee Y-K, Kim HJ et al (2012) Reliability and validity of measuring version of the acetabular component. J Bone Joint Surg Br Vol 94-B:32–36. https://doi.org/10.1302/0301-620X.94B1.27621
33. Clohisy JC, Carlisle JC, Trousdale R et al (2008) Radiographic Evaluation of the Hip has Limited Reliability. Clin Orthop Relat Res 467:666–675. https://doi.org/10.1007/s11999-008-0626-4
34. Jamali AA, Mak W, Wang P et al (2013) What Is Normal Femoral Head/Neck Anatomy? An analysis of radial CT reconstructions in adolescents. Clin Orthop Relat Res 471:3581–3587. https://doi.org/10.1007/s11999-013-3166-5
35. Monazzam S, Bomar JD, Agashe M, Hosalkar HS (2012) Does femoral rotation influence anteroposterior alpha angle, lateral center-edge angle, and medial proximal femoral angle? A pilot

study. Clin Orthop Relat Res 471:1639–1645. https://doi.org/10.1007/s11999-012-2708-6
36. Nepple JJ, Brophy RH, Matava MJ et al (2012) Radiographic findings of femoroacetabular impingement in National Football League Combine athletes undergoing radiographs for previous hip or groin pain. Arthroscopy 28:1396–1403. https://doi.org/10.1016/j.arthro.2012.03.005
37. Siebenrock KA, Kalbermatten DF, Ganz R (2003) Effect of pelvic tilt on acetabular retroversion: a study of pelves from cadavers. Clin Orthop Relat Res:241–248. https://doi.org/10.1097/01.blo.0000030508.43495.79
38. Zaltz I, Kelly BT, Hetsroni I, Bedi A (2012) The crossover sign overestimates acetabular retroversion. Clin Orthop Relat Res 471: 2463–2470. https://doi.org/10.1007/s11999-012-2689-5
39. Boese CK, Dargel J, Oppermann J et al (2015) The femoral neck-shaft angle on plain radiographs: a systematic review. Skelet Radiol 45:19–28. https://doi.org/10.1007/s00256-015-2236-z
40. Boese CK, Jostmeier J, Oppermann J et al (2015) The neck shaft angle: CT reference values of 800 adult hips. Skelet Radiol 45:455–463. https://doi.org/10.1007/s00256-015-2314-2
41. Nakahara I, Takao M, Sakai T et al (2010) Gender differences in 3D morphology and bony impingement of human hips. J Orthop Res 29:333–339. https://doi.org/10.1002/jor.21265
42. Chakraverty JK, Sullivan C, Gan C et al (2013) Cam and pincer femoroacetabular impingement: CT findings of features resembling femoroacetabular impingement in a young population without symptoms. AJR Am J Roentgenol 200:389–395. https://doi.org/10.2214/AJR.12.8546
43. Khanna V, Caragianis A, DiPrimio G et al (2014) Incidence of hip pain in a prospective cohort of asymptomatic volunteers: is the cam deformity a risk factor for hip pain? Am J Sports Med 42:793–797. https://doi.org/10.1177/0363546513518417
44. Kang ACL, Gooding AJ, Coates MH et al (2010) Computed tomography assessment of hip joints in asymptomatic individuals in relation to femoroacetabular impingement. Am J Sports Med 38: 1160–1165. https://doi.org/10.1177/0363546509358320
45. Dandachli W, Najefi A, Iranpour F et al (2012) Quantifying the contribution of pincer deformity to femoro-acetabular impingement using 3D computerised tomography. Skelet Radiol. https://doi.org/10.1007/s00256-012-1389-2
46. Tönnis D, Heinecke A (1999) Acetabular and femoral anteversion: relationship with osteoarthritis of the hip. J Bone Joint Surg Am 81: 1747–1770
47. Reikeras O, Bjerkreim I, Kolbenstvedt A (1983) Anteversion of the acetabulum and femoral neck in normals and in patients with osteoarthritis of the hip. Acta Orthop Scand 54:18–23
48. Tannenbaum EP, Zhang P, Maratt JD et al (2015) A computed tomography study of gender differences in acetabular version and morphology: implications for femoroacetabular impingement. Arthrosc: J Arthrosc Relat Surg 31:1247–1254. https://doi.org/10.1016/j.arthro.2015.02.007
49. Dandachli W, Ul Islam S, Tippett R et al (2011) Analysis of acetabular version in the native hip: comparison between 2D axial CT and 3D CT measurements. Skelet Radiol 40:877–883. https://doi.org/10.1007/s00256-010-1065-3
50. Werner CML, Ramseier LE, Ruckstuhl T et al (2012) Normal values of Wiberg's lateral center-edge angle and Lequesne's acetabular index–a coxometric update. Skelet Radiol. https://doi.org/10.1007/s00256-012-1420-7
51. Fowkes LA, Petridou E, Zagorski C et al (2011) Defining a reference range of acetabular inclination and center-edge angle of the hip in asymptomatic individuals. Skelet Radiol 40:1427–1434. https://doi.org/10.1007/s00256-011-1109-3
52. Wassilew GI, Heller MO, Diederichs G et al (2012) Standardized AP radiographs do not provide reliable diagnostic measures for the assessment of acetabular retroversion. J Orthop Res 30:1369–1376. https://doi.org/10.1002/jor.22086
53. Ayeni OR, Chan K, Whelan DB et al (2014) Diagnosing femoroacetabular impingement from plain radiographs: do radiologists and orthopaedic surgeons differ? Orthop J Sports Med 2: 2325967114541414. https://doi.org/10.1177/2325967114541414
54. Golfam M, Di Primio LA, Beaulé PE et al (2017) Alpha angle measurements in healthy adult volunteers vary depending on the MRI plane acquisition used. Am J Sports Med 45:620–626. https://doi.org/10.2214/AJR.06.0921
55. Vo A, Beaulé PE, Sampaio ML et al (2015) The femoral head-neck contour varies as a function of physeal development. Bone Joint Res 4:17–22. https://doi.org/10.1302/2046-3758.42.2000356
56. Nepple JJ, Riggs CN, Ross JR, Clohisy JC (2014) Clinical presentation and disease characteristics of femoroacetabular impingement are sex-dependent. J Bone Joint Surg 96:1683–1689. https://doi.org/10.2106/JBJS.M.01320
57. Lindner D, Bitar El YF, Jackson TJ et al (2014) Sex-based differences in the clinical presentation of patients with symptomatic hip labral tears. Am J Sports Med 42:1365–1369. https://doi.org/10.1177/0363546514532226
58. Joseph R, Pan X, Cenkus K et al (2016) Sex differences in self-reported hip function up to 2 years after arthroscopic surgery for femoroacetabular impingement. Am J Sports Med 44:54–59. https://doi.org/10.1177/0363546515610535
59. Frank RM, Lee S, Bush-Joseph CA et al (2016) Outcomes for hip arthroscopy according to sex and age: a comparative matched-group analysis. J Bone Joint Surg 98:797–804. https://doi.org/10.2106/JBJS.15.00445
60. Malviya A, Raza A, Jameson S et al (2015) Complications and survival analyses of hip arthroscopies performed in the National Health Service in England: A review of 6,395 cases. Arthroscopy. https://doi.org/10.1016/j.arthro.2014.12.013
61. Gosvig KK, Jacobsen S, Sonne-Holm S, Gebuhr P (2008) The prevalence of cam-type deformity of the hip joint: a survey of 4151 subjects of the Copenhagen Osteoarthritis Study. Acta Radiol 49:436–441. https://doi.org/10.1080/02841850801935567
62. Pollard TCB, Villar RN, Norton MR et al (2010) Femoroacetabular impingement and classification of the cam deformity: the reference interval in normal hips. Acta Orthop 81:134–141. https://doi.org/10.3109/17453671003619011
63. Agricola R, Heijboer MP, Ginai AZ et al (2014) A cam deformity is gradually acquired during skeletal maturation in adolescent and young male soccer players: a prospective study with minimum 2-year follow-up. Am J Sports Med 42:798–806. https://doi.org/10.1177/0363546514524364
64. MacKelvie KJ, Khan KM, McKay HA (2002) Is there a critical period for bone response to weight-bearing exercise in children and adolescents? a systematic review. Br J Sports Med 36:250–257 discussion 257
65. Agricola R, Bessems JHJM, Ginai AZ et al (2012) The development of cam-type deformity in adolescent and young male soccer players. Am J Sports Med 40:1099–1106. https://doi.org/10.1177/0363546512438381
66. Hetsroni I, Torre Dela K, Duke G et al (2013) Sex differences of hip morphology in young adults with hip pain and labral tears. Arthroscopy 29:54–63. https://doi.org/10.1016/j.arthro.2012.07.008
67. Atkinson HD, Johal KS, Willis-Owen C et al (2010) Differences in hip morphology between the sexes in patients undergoing hip resurfacing. J Orthop Surg Res 5:76. https://doi.org/10.1186/1749-799X-5-76
68. Larson CM, Sikka RS, Sardelli MC et al (2013) Increasing alpha angle is predictive of athletic-related "hip" and "groin" pain in collegiate national football league prospects. YJARS 29:405–410. https://doi.org/10.1016/j.arthro.2012.10.024

69. Scheidt RB, Galia CR, Diesel CV et al (2014) Prevalence of radiographic markers of femoroacetabular impingement in asymptomatic adults. Rev Col Bras Cir 41:36–42
70. Gosvig KK, Jacobsen S, Sonne-Holm S et al (2010) Prevalence of malformations of the hip joint and their relationship to sex, groin pain, and risk of osteoarthritis: a population-based survey. J Bone Joint Surg Am 92:1162–1169. https://doi.org/10.2106/JBJS.H.01674
71. Laborie LB, Lehmann TG, Engesaeter IO et al (2011) Prevalence of radiographic findings thought to be associated with femoroacetabular impingement in a population-based cohort of 2081 healthy young adults. Radiology 260:494–502. https://doi.org/10.1148/radiol.11102354
72. Laborie LB, Lehmann TG, Engesaeter IO et al (2014) The alpha angle in cam-type femoroacetabular impingement: new reference intervals based on 2038 healthy young adults. Bone Joint J 96-B: 449–454. https://doi.org/10.1302/0301-620X.96B4.32194
73. Ranawat AS, Schulz B, Baumbach SF et al (2011) Radiographic predictors of hip pain in femoroacetabular impingement. HSS Jrnl 7:115–119. https://doi.org/10.1007/s11420-010-9192-x
74. Bardakos NV, Villar RN (2009) Predictors of progression of osteoarthritis in femoroacetabular impingement: a radiological study with a minimum of ten years follow-up. J Bone Joint Surg Br Vol 91:162–169. https://doi.org/10.1302/0301-620X.91B2

CHAPTER 4.2

This chapter is based on the following paper:

"Cam deformity and the omega angle, a novel quantitative measurement of femoral head-neck morphology: a 3D CT gender analysis in asymptomatic subjects"

European Radiology 2017 May;27(5):2011-2023.

Eur Radiol
DOI 10.1007/s00330-016-4530-0

MUSCULOSKELETAL

Cam deformity and the omega angle, a novel quantitative measurement of femoral head-neck morphology: a 3D CT gender analysis in asymptomatic subjects

Vasco V. Mascarenhas[1] · Paulo Rego[2] · Pedro Dantas[3] · Augusto Gaspar[1] · Francisco Soldado[4] · José G Consciência[5]

Received: 25 April 2016 / Accepted: 21 July 2016

Abstract

Objective Our objectives were to use 3D computed tomography (CT) to define head–neck morphologic gender-specific and normative parameters in asymptomatic individuals and use the omega angle (Ω°) to provide quantification data on the location and radial extension of a cam deformity.

Methods We prospectively included 350 individuals and evaluated 188 asymptomatic hips that underwent semiautomated CT analysis. Different thresholds of alpha angle (α°) were considered in order to analyze cam morphology and determine Ω°. We calculated overall and gender-specific parameters for imaging signs of cam morphology (Ω° and circumferential α°).

Results The 95 % reference interval limits were beyond abnormal thresholds found in the literature for cam morphology. Specifically, α° at 3/1 o´clock were 46.9°/60.8° overall, 51.8°/65.4° for men and 45.7°/55.3° for women. Cam prevalence, magnitude, location, and epicenter were significantly gender different. Increasing α° correlated with higher Ω°, meaning that higher angles correspond to larger cam deformities.

Conclusion Hip morphometry measurements in this cohort of asymptomatic individuals extended beyond current thresholds used for the clinical diagnosis of cam deformity, and α° was found to vary both by gender and measurement location. These results suggest that α° measurement is insufficient for the diagnosis of cam deformity. Enhanced morphometric evaluation, including 3D imaging and Ω°, may enable a more accurate diagnosis.

Key Points

- *95% reference interval limits of cam morphotype were beyond currently defined thresholds.*
- *Current morphometric definitions for cam-type morphotype should be applied with care.*
- *Cam prevalence, magnitude, location, and epicenter are significantly gender different.*
- *Cam and alpha angle thresholds should be defined according to sex/location.*
- *Quantitative 3D morphometric assessment allows thorough and reproducible FAI diagnosis and monitoring.*

Keywords Hip · Femoroacetabular impingement · Multidetector computed tomography · Reference value · Variant

Abbreviations

FAI	Femoroacetabular impingement
FHN	Femoral head/neck
OA	Osteoarthritis
CT	Computed tomography
MRI	Magnetic resonance imaging
CR	conventional X-ray

✉ Vasco V. Mascarenhas
mascarenhas.vasco@gmail.com

1 MSK imaging Unit (UIME), Imaging Center, Hospital da Luz, Lisbon, Portugal

2 Department of Orthopaedic Surgery, Hospital da Luz, Lisbon, Portugal

3 Hospital CUF Descobertas, Lisbon, Portugal

4 Hospital Sant Joan De Deu, Universitat De Barcelona, Barcelona, Spain

5 NOVA Medical School, Campo Mártires Pátria, Lisbon, Portugal

Published online: 30 August 2016

Ω°   Omega angle
α°   Alpha angle

Introduction

Femoroacetabular impingement (FAI) is a common cause of hip pain and refers to the abnormal conflicting movement of the femoral head–neck (FHN) junction against the acetabular rim [1], eventually resulting in hip damage and osteoarthritis (OA) [2–4]. The cam type generally involves an FHN deformity and the pincer-type acetabular overcoverage [1]. There is a wide discrepancy in reported prevalence rates between cam and pincer FAI among asymptomatic and symptomatic and athletes [5, 6].

The diagnosis of FAI is made using a combination of clinical and imaging findings [7]. Different radiographic views using conventional X-rays (CR) have been tested for diagnostic utility in FAI [7, 8]. However, the reliability of two-dimensional (2D) measurements has been questioned [9], since FHN morphology cannot be fully characterized using a single CR [9, 10].

Magnetic resonance imaging (MRI) [11] and computed tomography (CT) [12] allow reconstructions in multiple planes, providing a better understanding of the magnitude of the femoral morphology. However, CT/MRI standard techniques for measuring cam-type FAI still provide only a 2D characterization of FHN morphology, since measurements are made on a limited series of slices [13–15]. Morphological studies have demonstrated that the femoral head may be elliptical in shape with important interindividual variability. This variability may further contribute to significant variations in alpha angle (α°) measurements and to related diagnostic limitations of oblique axial and multiple radial-plane imaging protocols [15, 16].

The α°, the most frequently used parameter to grade cam morphology and describe the FHN junction, has been suggested as a predictor for the risk of anterior impingement and extent of cartilage defects [17, 18]. However, an α° measurement is performed in only one plane and so is highly dependent on the position at which it is measured [19]. Several authors have questioned the diagnostic accuracy and relevance of the α° [20, 21], as abnormally high α° values have been reported in asymptomatic individuals [6] and amazingly normal threshold values to diagnose cam deformities may range from 50° to 82° [17, 21–24]. Studies using these reference intervals to identify cam deformities have demonstrated a risk for false-positive results when applying these thresholds [15, 25, 26].

Accurately understanding the 3D spatial characteristics of cam deformities is of paramount importance not only for diagnosis but also for optimal treatment planning. Current 2D imaging protocols for FAI do not permit complete consideration of these features. The radial extension of cam deformity has been described using MRI to compare bone resection using different surgical techniques [27], but 3D imaging might provide more accurate estimates. However, the optimal method for using 3D CT in this setting has not been well defined. In addition, we lack normative data with regard to 3D morphology of the FHN in asymptomatic individuals. A predictable and accurate method for evaluating femoral morphology is needed to optimize surgical results and minimize complications [28].

To our knowledge, no previous study has evaluated 3D radial circumference of the FHN in a cohort of young, asymptomatic patients. The purpose of this study in a cohort of asymptomatic individuals was to:(a) characterize FHN morphology using angular measurements taken from 3D CT images; (b) estimate overall and gender-specific normative ranges for 3D angular measurements of the FHN junction; and (c) use 3D angular measurements, namely, the omega angle (Ω°), to quantify the location and extent of cam lesions.

Methods

Study population

Institutional ethics committee approval was obtained prior to beginning this study, and all participants provided written informed consent. We prospectively recruited consecutive adult patients undergoing pelvic CT at our institution for thoracic, abdominal, or urogenital indications from August to December 2015. All eligible participants completed a questionnaire regarding their clinical history, including current or past hip/groin pain, medical or surgical hip-joint conditions, history of childhood hip pathology, and/or hip trauma. Patients who gave a positive answer to one or more of these questions were excluded. Additionally, all patients completed the nonarthritic hip score (NAHS) questionnaire [29]. Any patient with less than the maximum possible score was also excluded.

In all, 350 hips were potentially eligible for analysis. We then excluded all patients with CT signs of OA, defined as the presence of at least one of the following findings [30]: joint-

Table 1 Characteristics of included and excluded individuals

	Number[a]	Age ± SD (years–old)[b]	Range
Total included patients	94	34.8 ± 7.2	18–44
Male	49	35.0 ± 8.2	18–44
Female	45	34.4 ± 5.2	23–44
Total excluded patients	256	40.0 ± 4.2	18–46

[a] Absolute count

[b] Mean ± standard deviation (SD)

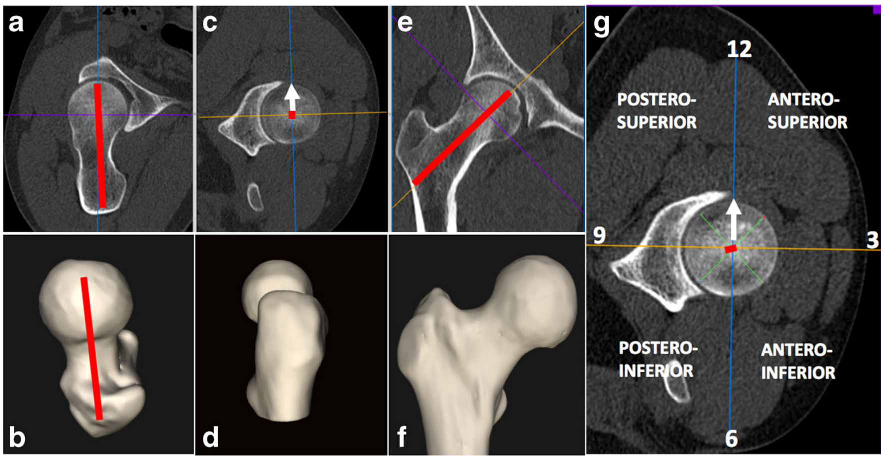

Fig. 1 Reformatted 3D computed tomography (CT) images and corresponding 3D hip model in a 36-year-old man. Oblique axial (**a**, **b**), short-axis image at femoral head/neck junction (**c**, **d**), and oblique coronal (**e**, **f**) imaging used to determine 12-o'clock position according to the protocol proposed by Philippon et al [33] (**g**). *Red line* represents central neck axis

space narrowing, osteophytes, or subchondral bone changes, including sclerosis or cysts. Finally, we excluded hips with any other diagnosed abnormalities on CT: fracture, posttraumatic deformity, Perthes disease, osteonecrosis, slipped capital femoral epiphysis, dysplasia (lateral center-edge angle <20°), or bone lesions (Table 1). In total, 188 hips in 94 patients met criteria for inclusion in the final analysis.

CT imaging

CT imaging was performed using a Somatom Sensation 64-slice CT scanner (Siemens, Erlangen, Germany). Patients were positioned in a standard supine position with legs parallel in neutral rotation and patellae pointing directly upward. The pelvis was reconstructed from the anterior superior iliac

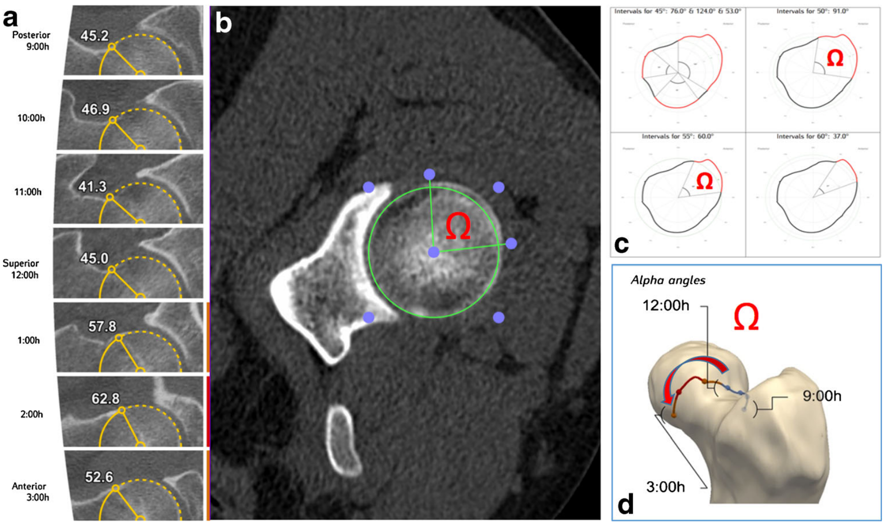

Fig. 2 Alpha-angle (α°) measurements made at different points around the femoral head/neck junction in steps of 1° starting at 9 o'clock (posterior); 10, 11, and 12 o'clock (superior); and 1, 2, and 3 o'clock (anterior) (**a**).Femoral short-axis computed tomography (CT) reformat derived from Fig. 1 shows bone contour abnormality from 12- to 3-o'clock [omega angle (Ω°) of 91°]. The Ω° is formed by *two lines* intersecting the center of the femoral neck at the level of the head/neck junction. The most *proximal line* intersects peripherally the point at which the α° begins to be abnormal beyond a best-fitting circle and the *distal line* at the point where the α° returns to normal (**b**). Polar plot (2D) of the 360° α°, representing the Ω° angle (*red symbol*) for different α° thresholds [45° (upper left), 50° (upper right), 55° (lower left), 60° (lower right)]. *Red lines* represent increased α°s for a given threshold (**c**). Hip model (3D) showing extension and location of a cam lesion represented on the corresponding 3D model (*red arrow*). The Ω° measures the amount of linear radial extension of a cam deformity corresponding to the angular measurement of the *red arrow. Red and orange lines* correspond to abnormal α°s; *blue line* represent normal α°s for a given α threshold

Table 2 Mean alpha angles (α°), standard deviation (SD), and upper limit of 95 % of confidence interval (CI) at each clock-face position (all participants)

	Plane orientation by clock face	All alpha angles[a]	SD	Upper limit of 95 % CI[a]
Posterosuperior	9	44.9	4.3	45.8
	9:30	45.6	3.5	46.3
	10	45.2	3.7	46.0
	10:30	43.8	3.7	44.6
	11	42.6	3.4	43.3
	11:30	43.4	3.4	44.1
Anterosuperior	0	47.8	6.7	49.2
	0:30	54.1	9.2	56.0
	1	58.9	8.8	60.8
	1:30	58.9	6.8	60.3
	2	54.9	5.5	56.1
	2:30	50.8	4.9	51.2
Anteroinferior	3	45.8	4.9	46.9
	3:30	42.7	4.4	43.6
	4	41.7	3.6	42.4
	4:30	42.8	3.5	43.5
	5	45.2	3.6	46.0
	5:30	48.2	3.5	48.9
Posteroinferior	6	49.3	3.3	50.0
	6:30	48.1	3.5	48.9
	7	46.0	3.7	46.8
	7:30	44.2	3.9	45.0
	8	43.8	4.2	44.7
	8:30	44.5	4.2	45.4

[a] Mean

spines to the lesser trochanters, with 1- mm thickness. Patients received no additional radiation during imaging beyond that required for the CT studies ordered to evaluate their specific medical conditions.

Three-dimensional model

Digital Imaging and Communications in Medicine (DICOM) images were uploaded for analysis using Articulis (Articulis[TM]; Clinical Graphics, Delft, The Netherlands) and semiautomatically segmented using this software, which had been previously validated for reliability and accuracy [31]. For each hip, nonradiodense structures were digitally subtracted, rendering a 3D image of a hemipelvis containing the left or right hip. Two experienced radiologists (VVM and AG) checked whether each segmentation contained all osseous contours of the CT scan.

Omega angle

To determine the Ω° (Figs. 1 and 2), we calculated the clockwise 360°, α° by using a regression sphere fit of the FHN junction [32]. The α° was calculated according to method 1 described by Nötzli et al. [17]. The first angle was obtained using a measurement plane defined by the femoral neck axis and a vector perpendicular to this axis pointing upward to define a superior 12 o'clock position [33] (Fig. 1). For subsequent measurement planes, this vector was rotated around the femoral neck in steps of 1°, leading to measurement of the 360° α°. An automated algorithm based on radial sequences was then used to determine the maximum α° and its location (Fig. 2a). Two radiologists (VVM and AG) reviewed the images to confirm plausibility of computer-determined measurements. Next, projecting the 360 α° in a polar plot (Fig. 2c), we found the Ω° by measuring the angle corresponding to the three points formed by the center of the femoral head, the point where the α° exceeds a determined threshold value and the last one where the α° returns to a normal value (Figs. 2b and c). We used 45, 50, 55, and 60° as α° thresholds for measuring different Ω° values (Fig. 2c). This automated analysis yielded measurements of cam magnitude (determined by the 360° α° and Ω°) and cam location (mapped on the previously defined clock face system, both in 2D maps and 3D models) (Fig. 2c and d).

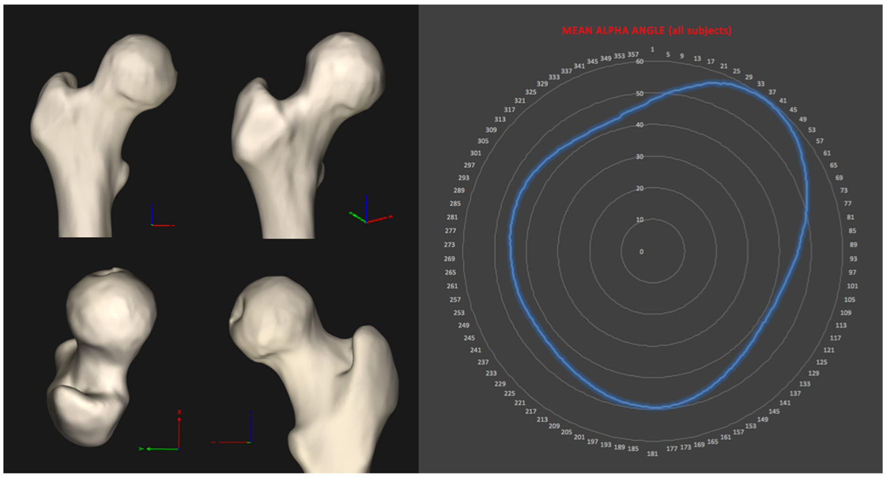

Fig. 3 Evaluation of femoral head/neck (FHN) morphology. Three-dimensional model in four projections: *top row* (left to right), anterior and anterosuperior views; *bottom row* (left to right), superior and posterior views. Corresponding 2D map of mean circumferential alpha angles (α°) at every degree for all participants: *0* 12-o'clock position; *89°* 3-o'clock position

Statistical analysis

For all morphometric parameters, mean values, standard deviations (SD), and double-sided 95 % reference intervals were calculated. Quantitative parameters are described by their average and SD. Qualitative parameters are described in numbers and percentage. For the average comparison, Student's *t* test was implemented to compare quantitative variables. If test conditions were not met, a nonparametric test was used. To evaluate correlation between two quantitative parameters, Pearson or Spearman coefficients were computed. A *p* value of 0,05 was considered statistically significant for all analyses. Statistical analyses were performed using dedicated software (MedCalc Software version 11.6; Belgium).

Results

Images were obtained for 188 hips from 94 patients (age range 18–44; 49 men and 45 women) (Table 1). Measured α° ranged from 45° to 75°, with an overall mean maximal α° of 59.5° at 1:14 o'clock. Of the 188 hips, 182 demonstrated at least one elevated α° value at any single clock-face segment when using an α° threshold of 50°. The mean elevated α° measurement was 60.5° (range 50.1–80.3°) (Table 2 and Fig. 3).

The presence of a cam deformity was defined as an increased α° for at least three consecutive points of measurement. Applying α° thresholds of 50°, 55°, and 60°, cam deformity was identified in 182, 148, and 90 hips, respectively, out of 188 (Fig. 4).

The clock-face position at which α° was most frequently elevated was 1 and 1:30 o´clock (respectively: frequency of raised α° = 82 and 87; frequency of location of largest α° = 32 vs 35). The involved clock-face segments ranged between 0 and 6; mean of the α° measurements at each clock-face position was greatest at the 1:30 position (58.9° ± 6.8; range 46.4–76.4°) and at 1 o´clock (58.9° ± 8.8; range 41.6–80.3°) (Table 3).

Sex differences were observed by the presence, magnitude, and location of cam deformities. Overall cam prevalence was higher in men for any threshold of α° ($p < 0{,}01$), as was maximal mean α° (63.63° vs 55.74°; $p < 0{,}001$). Sex-different α° measurements were notably significant at 1:30 (men vs women 61.79° vs 55.73°, $p < 0.001$), at 1:00 (men vs women 63.5° vs 53.3°, $p < 0.001$), and at 10–10:30 o´clock ($p = 0.042$) (Table 4 and Fig. 5)

Mean cam magnitude, defined by the radial extension of the deformity, was significantly greater in men (from 0–2 h 32 min vs 0 h 36 min–2 h 28 min; $p = 0.01$). Mean epicenter of the cam deformity was located significantly more superiorly in the anterosuperior quadrant for men compared with women (1 h 04 min vs 1 h 32 min; $p < 0.001$) (Table 5 and Fig. 6).

Mean angular range of radial extension of involved segments was translated by a mean Ω°. The Ω° for a 50° and 55°, α° threshold was, respectively, 65° ± 25 (men vs women 71° vs 57°, $p = 0.02$) and 35° ± 24 (men vs women 43° vs 25°, $p = 0{,}03$) (Table 5). Significant positive correlations were seen

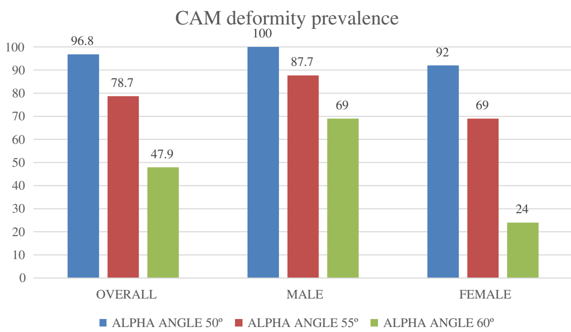

Fig. 4 Cam deformity prevalence: overall participants and gender-specific breakdown by different alpha angle (α°) thresholds (50, 55, and 60°)

Table 3 Frequency and mean increased alpha angles (α°) at each clock-face position in 188 hips. Location of largest alpha angles recorded at each position, mean range of deformity (radial extension), and mean epicenter (point of highest α°) also shown

	Plane orientation by clock-face position	Increased alpha angle[a] (for 50° threshold)	Range [a]	Frequency of raised alpha angle[b]	Location of largest alpha angle[b]	Range of deformity [a] (radial extension)	Epicenter of deformity[c]
Posterosuperior	9	51	50.3–53.9	10	0	0:10'–2:30'	1:14' ± 6'
	9:30	51.4	50.1–52.2	10	0		
	10	51.5	50.2–55.3	12	0		
	10:30	51.3	50.2–52.5	12	0		
	11	51	51–51	2	0		
	11:30	52	50.4–52	10	0		
Anterosuperior	0	56.4	50.1–77	40	2		
	0:30	58.2	50.2–81.9	122	8		
	1	60.5	50.1–80.3	164	35		
	1:30	58.9	46.4–76.4	174	36		
	2	55	39.3–71	154	11		
	2:30	53.9	50.1–65.3	92	1		
	3	53.8	50.2–59.1	30	1		

[a] Mean

[b] Absolute count

[c] Mean ± standard deviation

between Ω° and α° for all thresholds of Ω° and locations of α° measurements (increasing values of α° significantly corresponded to higher values of Ω°) (Table 6).

Discussion

There is a need for improved techniques and criteria to identify and treat FAI [34]. Considering the strong association between cam FAI and OA [2], the ongoing debate in the literature on criteria for an imaging diagnosis of FAI is of paramount importance. Prior studies have used different cutoff values for morphometric parameters of cam FAI [7, 17, 21, 23–25, 30, 35–44,] (Table 7). Accordingly, recent studies have pointed out the high prevalence of radiographic findings suggestive of FAI in asymptomatic populations [6] when applying currently used diagnostic thresholds, emphasizing the need for re-evaluation of these cutoffs [36, 45–47].

In our asymptomatic cohort, we found that the measured cam morphometry values extended beyond commonly used

Table 4 Mean of all alpha angles (α°), range, and standard deviation (SD) at each clock-face position in 188 hips. Mean male/female α° and corresponding statistical difference recorded at each position also shown

	Plane orientation by clock face	All alpha angles[a] ± SD	Range [a]	Male [a]	Female [a]	*P* value (*t* test)
Posterosuperior	9	44.9 ± 4.3	23.2—53.9	44.6	45.1	NS
	9:30	45.6 ± 3.5	36.5–52.2	45.2	46	NS
	10	45.2 ± 3.7	35.5–55.5	44.4	46.1	0.043
	10:30	43.8 ± 3.7	35.7–52.5	42.7	45.1	0.042
	11	42.6 ± 3.4	34.7–51	42.1	43.1	NS
	11:30	43.4 ± 3.4	35.4–52	44	42.7	NS
Anterosuperior	0	47.8 ± 6.7	37.1–77	50.4	44.8	<0.001
	0:30	54.1 ± 9.2	36.9–81.9	58.6	49.1	<0.001
	1	58.9 ± 8.8	41.6–80.3	63.5	53.3	<0.001
	1:30	58.9 ± 6.8	46.4–76.4	61.8	55.7	<0.001
	2	54.9 ± 5.5	39.3–71	56.2	53.6	0.032
	2:30	50.8 ± 4.9	38.2–65.3	50.4	49.9	NS
	3	45.8 ± 4.9	35–59.1	45.9	45.8	NS

NS not significant

[a] Mean

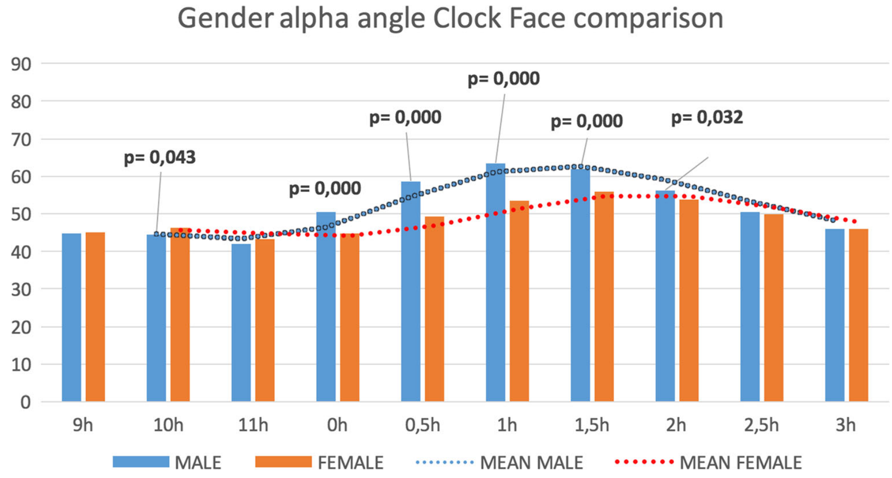

Fig. 5 Alpha angle (α°) measurement comparison by gender at each clock-face position. Statistically significant differences are marked by the corresponding *p* value

thresholds for the diagnosis of cam deformity. For example, upper limits of reference intervals calculated for α° at 3/1:30 were 46.8°/60.3°. Previously, Sutter et al. [21] found the highest α° measurements at the anterosuperior quadrant to be 55.0° ± 8.8, and α° >55° in 38–62 % of asymptomatic volunteers. Our study found the highest α° measurements to be 58.9° ± 6.8, and almost 78 % were found to have an α° >55°.

Also, we found normative data similar to the 50° thresholds previously proposed at 3 o'clock by Nötzli et al. [17] and at 1:30 by Lepage-Saucier et al. [30], but our measurements were globally higher at the anterosuperior quadrant compared with most other studies [21, 35]. In a recent review, cam-type morphology was found in 22.4 ± 6.2 % of all asymptomatic individuals [6]. In contrast, in this study, we found a higher prevalence of cam morphology, reaching 78.7 %/48.9 % for 55°/60° α° thresholds, respectively. Similarly to findings in our study, however, in a study using radial MRI, Reichenbach et al. [45] found that 73.3 % of asymptomatic cases showed some evidence of a cam-type deformity.

In regards to cam location and magnitude, our study confirms that in an asymptomatic cohort, the deformity was most prominent in the anterosuperior FHN junction and extended around a significant radial extent. The most common position in which we found the largest α° and a raised α° coincided with 1 and 1:30 o'clock on the clock face. These results are generally consistent with findings of other studies [11, 48], although slightly superior to the anterosuperior quadrant 2 o'clock position defined by Khan et al. [49].

Including measurement of Ω° to define cam radial location and extension permits better characterization of cam deformity. In this study, greater α° was found to correlate with increasing Ω°. We found a mean increase in α° measurements of 60.5° (50.1–80.3°) compared with 64.6° (50.8–86°) in a symptomatic cohort using a similar methodology [49]. In that study, the arc of cam deformity ranged between 60° and 90° [49], but our study found lower magnitudes (mean Ω° 65°), as would be expected in an asymptomatic cohort. This is an area for further application of the Ω° technique, enabling detailed subgroup analysis.

Some variation between our results and previously reported values might be explained by the heterogeneity of imaging methods employed, different locations of α° measurements,

Table 5 Overall evaluation and by gender of magnitude and location of cam deformities: mean omega angles for different alpha-angle thresholds (range in brackets), mean range of deformity, and mean epicenter (peak location of cam deformity). Significant gender differences are marked with an asterisk (*)

	Omega angle (50° alpha angle threshold)	Omega angle (55° alpha angle threshold)	Omega angle (60° alpha angle threshold)	Range of cam deformity ± SD (50° alpha angle threshold)	Epicenter position (mean alpha angle at epicenter)
Overall	65° (0–179°)	35° (0–89°)	17° (0–84°)	0:10'–2:30' ±6'	1:14' (59.5°)
Male	71° (24–179°)*	43° (0–89°)**	27° (0–84)***	0:00–2:32' ±9'****	1:04' (63.6°)*****
Female	57° (0–107°)*	25° (0–66°)**	5° (0–44)***	0:36'–2:28' ±4'****	1:32' (55.7°)*****

SD standard deviation

*p = 0,02, **p = 0.03, ***p = 0.04,****p = 0.01, ***** $p < 0.001$

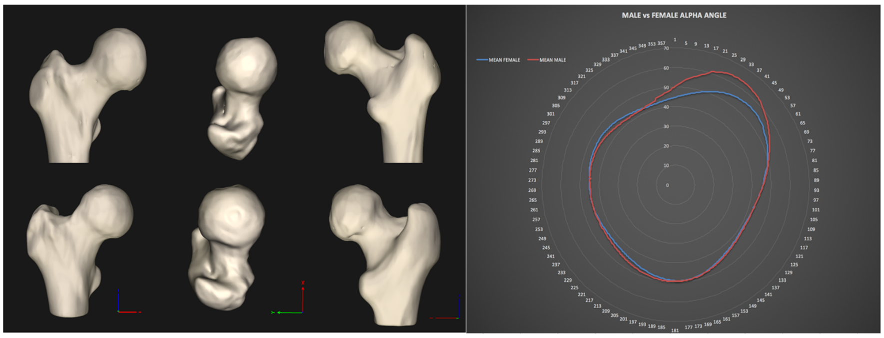

Fig. 6 Femoral head/neck (FHN) morphology by gender. Three-dimensional model in three projections: *top row* female model (left to right), anterior, superior, and posterior views; *bottom row* male model (left to right), anterior, superior, and posterior views) and corresponding 2D map of mean circumferential alpha angles (α°) at every degree (*red line* men; *blue line* women; *0* 12-o'clock position, *89°* 3-o'clock position)

and—most importantly—nonstandardized definitions of what a cam deformity is [23, 35, 50]. Although 3D imaging can identify larger α° than 2D imaging, these differences are mainly the result of measurement location [19]. Furthermore, there is an increased risk of residual impingement and vascular insult resulting from surgical treatment based on inaccurate data regarding the extent of deformities [27, 28, 51].

Intervals for the α° were significantly different between genders, coherent with results reported by Hack et al. [35] but divergent from other studies [25, 30] (Table 7). Similarly, cam location varied significantly according to sex, in agreement with Ito et al. [52] but divergent from the study by Yanke et al. [53] (in symptomatic individuals). We also found that mean magnitude, location, and the epicenter of cam morphology were significantly gender different: in men, we specifically found larger cam radial extension, higher maximal mean increased α° (63.63° vs 55.74°) and epicenter superiorly located in the anterosuperior quadrant (1 vs 1:30 o´clock). Also, Yanke et al. [53] found that cam magnitude was sex different, with deformities in men being significantly larger. Interestingly, at the posterosuperior quadrant (10/10:30 o´clock), we found surprisingly higher α°s in women. To our knowledge, this finding has not been described in the literature. Importantly, the increased span of male compared with female deformities increases the likelihood of false-negative 2D evaluations in women [53]. We hypothesize that pelvic morphology and other dynamic factors, such as distinct sports activities, increased female flexibility, pelvic rotation, or forward tilt from weaker core muscles contribute to these overall differences [53–55].

Prevalence of cam morphology using current thresholds and the width of reference intervals found in our study suggest that the currently used criteria for cam-type FAI need to be revisited. More specifically, our results stress that the α° alone is not an appropriate parameter to define cam lesions and that thresholds should be redefined according to sex and cam location. In recent CT-based studies, 3D bone reconstructions of the proximal femur have been used to evaluate femoral head sphericity using α° measurements [12, 34] and model fitting [56, 57]. However, normative data is lacking on 3D CT morphology of the femoral head in asymptomatic individuals.

Therefore, we believe that our approach improves previously described hip-imaging methods for FAI by including measures of both deformity magnitude and location [11, 14, 58]. The use of 3D CT to directly visualize and quantify 3D morphology of the FHN junction permits detailed and

Table 6 Nonparametric bivariate correlation between different quantitative variables: alpha angle at different clock-face positions and omega angle with different α° thresholds. Significant correlations are marked with an asterisk (*)

Spearman's rho (significance)	Alpha angle at 0:00 o'clock	Alpha angle at 1:00 o'clock	Alpha angle at 2:00 'clock	Alpha angle at 3:00 o'clock
Omega angle (alpha angle threshold of 50°)	0.75**	0.71**	0.76**	0.60**
Omega angle (alpha angle threshold of 55°)	0.76**	0.80**	0.77**	0.47**
Omega angle (alpha angle threshold of 60°)	0.71**	0.83**	0.66**	0.28*

*$p = 0.007$, **$p < 0.001$

Table 7 Characteristics of selected studies involving asymptomatic individuals

Ref.	Level of evidence	Population type	No. of participants	No. of hips	Demographics	Imaging type	Major findings reported
Hack et al [35]	III	Volunteers	200	400	111 women, 89 men; mean age 29.4 years (range 21.4–50.6); white 158 (79 %)	MRI	Cam prevalence: 14 %; more common in men (24.7 %) vs 5.4 % in women Mean alpha angle: anterior 40.78° ± 7.05°; anterosuperior 50.15° ± 8.13° Mean alpha angle by gender: anterior: men 44.02° ± 7.82°, women 38.19° ± 5.06°; anterosuperior: men 54.09° ± 8.54°, women 46.99° ± 6.19°
Scheidt et al [37]	III	Asymptomatic volunteers	82	164	54 women, 28 men; mean age 50.4 years (range 40–60)	CR	Mixed type: 6 (3.7 %) Cam: alpha angle >50° in 41/164 hips (one fourth of hips); average alpha angle 45° ± 8.6° (range 32–74°); mean alpha angle by gender: men 47.52°, women 43.85° ($p = 0.028$); male predominance for cam: 19/56 (34 %) male vs 12/108 (11.11 %) female
Lepage–Saucier et al [30]	III	Asymptomatic hips of patients who previously received CT	94	188	45 women, 49 men; mean age 49.0 ± 16.6 years	CT	95 % reference interval limits much higher than normally reported: upper limits for alpha angles (at 90°/45°) were 68°/83° (men) and 69°/84° (women) Cam: mean alpha angle 51° ± 9° at 90°, 59° ± 13° at 45°
Khanna et al [38]	III	Asymptomatic volunteers	170	340	93 women, 77 men; average age 29.5 years (range 25.7–54.5)	MRI	37/318 non–painful hips showed cam deformity; 170 who remained on study: mean alpha angle at 3:00, 41.1°; mean alpha angle at 1:30, 50.4°
Pollard et al [25]	III	Volunteers from general population	83		44 women, 39 men; mean age women 44 ± 11 years (range 22–67); men 48 ± 12 years (range 28–69)	AP pelvic and cross-table lateral CR	95 % reference intervals for alpha angle were higher than normally reported: 32°–62° Mean alpha angle: men 48° ± 8°; women 47° ± 8°
Van Houcke et al [39]	III	Asymptomatic	201	402	96 women, 105 men; 99 white (58 men, 41 women), 102 Chinese (47 men, 55 women)	CT	Significantly higher percentage (53 %) of hips in white participants showed ≥2 radiographic signs of FAI compared with 41 % in Chinese Significant differences: alpha angle at 1:30 in 15 % of Chinese vs 32 % of white women ($p = 0.004$)
Laborie et al [40]	III	Healthy 19–year olds; all born at Haukeland University Hospital, Norway, in 1989	1152		480 men, 672 women; age: 19 years	AP and frogleg CR	FAI detected in 35 of 480 (7.3 %) men and 32 of 672 (4.8 %) women Cam: increased alpha in men: right hips 114 (24 %), left hips 99 (21 %); women: right hips 101 (15 %), left hips 111 (16 %)
Nardo et al [41]	III	Participants from Osteoporotic Fractures in Men study	4140		All men >65 years from 6 clinics in United States; mean age 77 ± 5 years; nonwhite 395 (10 %)	AP CR	Pincer, cam, or mixed types of radiographic FAI showed prevalence of 57 % (1748/3053), 29 % (886/3053), and 14 % (419/3053), respectively; pincer and mixed type associated with hip pain; impingement angle <70° associated with less pain vs larger angles

Table 7 (continued)

Ref.	Level of evidence	Population type	No. of participants	No. of hips	Demographics	Imaging type	Major findings reported
Fraitzl et al [24]	III	Patients who lacked apparent hip problems and had X–rays due to trauma	339		169 women, 170 men; mean age men 47 ± 17 years; women 55 ± 19 years	AP and frogleg lateral CR	Significantly lower alpha angle and higher head–neck offset ratio in women; upper limit of 95 % reference interval for alpha angle 70° for men and 61° (AP) or 66° (lateral) for women; mean alpha angle: men AP 49.4° ± 10.5°, lateral 49.1° ± 10.6°; women AP 45.0° ± 8.0°, lateral 46.1° ± 9.9°
Reichenbach et al [45]	III	Sumiswald Cohort of young men being evaluated during recruitment to the Swiss Army	244		All men: mean age of those with cam 20.0 ± 0.7 years; without cam 19.9 ± 0.7 years	MRI	67/244 (27.5 %) cases of cam detected Labral lesions present in 57 (85 %) of those with cam and 118 (67 %) without cam; 2.77 odds ratio Impingement pits in 20 (30 %) with cam and 21 (12 %) without cam; odds ratio 2.91
Harris et al [43]	III	FAI vs controls	30 (15 cam, 15 normal)	30	Patients and matched controls: 26 ± 7 vs 27 ± 8 years	3D CT vs CR vs radial CT	Correlations between their 3D-model–based measurements of true femoral head asphericity to alpha angles measured on 5 radiographic and 4 radial CT views. No significant differences between alpha angles measured on radiographs and the corresponding DRRs ($p = 0.72$). Alpha angles were significantly greater in patients for all views ($p \leq 0.002$)
Masjedi et al [44]	III	FAI vs controls	47 (24 cam, 23 normal)	47	Average age of healthy participants 55 ± 21 years; female:male 13:10; average age with cam hips 54 ± 17 years; female:male 13:11	CT scans into 3D models	Normal and cam hips were significantly different: sum of head/neck ratios (HNRs) of cam hips were always smaller than normal hips ($p < 0.01$). A cutoff point of 2.55 with no overlap was found between the two groups, with HNRs larger than this being cam and smaller being normal hips

FAI femoroacetabular impingement, *AP* anteroposterior, *MRI* magnetic resonance imaging, *CT* computed tomography, *CR* conventional X-ray, *DRR* digitally reconstructed radiographs reproducible identification of cam lesions [19, 34, 43, 49, 59–61]. Clinical applications for the 3D imaging protocol reported here include the following:

(a) Accurate spatial visualization of cam deformity and hip morphology [62]
(b) Improved diagnosis and monitoring through the use of quantitative 3D morphometric assessment incorporating $\alpha°$ and $\Omega°$ measurements [63]
(c) Creation of dynamic virtual simulations for preoperative range of motion (ROM) simulation and identification of impingement areas [64]
(d) Provides a tool for standardizing and reducing variability in large-scale and clinical research [59].

This study has several limitations. First, our reference values were derived from a limited sample of 188 hips. Second, defining a normal sample population is an ambitious objective. Third, selecting a protocol for this study may be subject to several biases: Specifically, our participants were not selected from healthy volunteers. In addition, we used patient survey information to exclude hip pathology but did not perform a clinical hip examination. However, we prospectively included patients presenting for nonorthopedic pathology and excluded all patients with any reported history of hip pathology or symptoms. Additionally, we excluded any patients with signs of hip pathology on CT so that our cohort comprised asymptomatic individuals only. Fourth, this study did not include correlation of 3D $\alpha°$ measurements and traditional manual CT measurements; such comparison between 2D and 3D CT methods would be useful but was not an objective of our study, and the software used for this analysis had already been validated for this purpose.

To develop more generalizable reference intervals, larger individual cohort studies with more varied demographics are needed. Further investigations are also needed to incorporate 3D measurements of the acetabulum for a complete picture of hip biomechanics in cases of FAI.

Conclusion

Cam-type morphology is a 3D deformity. Single 2D measurements of the $\alpha°$ should be viewed with caution, as they may not provide a true estimate of the magnitude of the deformity. The $\Omega°$ obtained with 3D imaging contributes to a better understanding and characterization of the FHN junction by defining the radial extension and location of cam morphology.

Reference intervals of hip morphometric measurements in asymptomatic individuals were beyond commonly used thresholds, suggesting the need for revisiting the current parameters used in the diagnosis of cam and FAI, specifically by acknowledging that the $\alpha°$ alone is an insufficient measure by which to appreciate cam-type morphotype and that its thresholds depend on sex and measurement locations.

Acknowledgments The authors would like to thank José Roquette, João Sá, Isabel Vaz, and Pedro Patrício for their continuing and enthusiastic support toward clinical research at Hospital da Luz, and Rúben Teixeira, Ana Filipa Graça, Rogério Lopes, Diogo Corrente, João Novo, and Tiago Castela for their efforts toward optimizing technical issues and providing patient care

The scientific guarantor of this publication is Prof. Dr. José Roquette, MD PhD. The authors of this manuscript declare no relationships with any companies, whose products or services may be related to the subject matter of the article. The authors state that this work has not received any funding. One of the authors has significant statistical expertise; however no complex statistical methods were necessary for this paper. Institutional Review Board (Hospital da Luz Ethics Committee) approval was obtained and written informed consent was obtained from all participants in this study.

References

1. Tibor LM, Leunig M (2012) The pathoanatomy and arthroscopic management of femoroacetabular impingement. Bone Joint Res 1:245–257
2. Agricola R, Heijboer MP, Bierma-Zeinstra SMA et al (2013) Cam impingement causes osteoarthritis of the hip: a nationwide prospective cohort study (CHECK). Ann Rheum Dis 72:918–923
3. Glyn-Jones S, Palmer AJR, Agricola R, et al (2015) Osteoarthritis. Lancet 1–12. doi: 10.1016/S0140-6736(14)60802-3
4. Tannast M, Goricki D, Beck M et al (2008) Hip damage occurs at the zone of femoroacetabular impingement. Clin Orthop Relat Res 466:273–280
5. Frank JM, Harris JD, Erickson BJ, et al (2015) Prevalence of Femoroacetabular Impingement Imaging Findings in Asymptomatic Volunteers: A Systematic Review. YJARS 1–6. doi: 10.1016/j.arthro.2014.11.042
6. Mascarenhas VV, Rego P, Dantas P et al (2016) Imaging prevalence of femoroacetabular impingement in symptomatic patients, athletes, and asymptomatic individuals: a systematic review. Eur J Radiol 85:73–95
7. Tannast M, Siebenrock KA, Anderson SE (2007) Femoroacetabular impingement: radiographic diagnosis–what the radiologist should know. AJR Am J Roentgenol 188:1540–1552
8. Clohisy JC (2008) A systematic approach to the plain radiographic evaluation of the young adult hip. J Bone Joint Surg(Am) 90:47
9. Clohisy JC, Carlisle JC, Trousdale R et al (2008) Radiographic evaluation of the hip has limited reliability. Clin Orthop Relat Res 467:666–675
10. Barton C, Salineros MJ, Rakhra KS, Beaulé PE (2010) Validity of the alpha angle measurement on plain radiographs in the evaluation of cam-type femoroacetabular impingement. Clin Orthop Relat Res 469:464–469
11. Pfirrmann CWA, Mengiardi B, Dora C et al (2006) Cam and pincer femoroacetabular impingement: characteristic MR arthrographic findings in 50 patients. Radiology 240:778–785
12. Beaulé PE, Zaragoza EJ, Motamedi K et al (2005) Three-dimensional computed tomography of the hip in the assessment of femoroacetabular impingement. J Orthop Res 23:1286–1292
13. Domayer SE, Ziebarth K, Chan J et al (2011) Femoroacetabular cam-type impingement: diagnostic sensitivity and specificity of radiographic views compared to radial MRI. Eur J Radiol 80:805–810

14. Dudda M, Albers C, Mamisch TC et al (2008) Do normal radiographs exclude asphericity of the femoral head-neck junction? Clin Orthop Relat Res 467:651–659
15. Rakhra KS, Sheikh AM, Allen D, Beaulé PE (2008) Comparison of MRI alpha angle measurement planes in femoroacetabular impingement. Clin Orthop Relat Res 467:660–665
16. Tannast M, Kubiak-Langer M, Langlotz F et al (2006) Noninvasive three-dimensional assessment of femoroacetabular impingement. J Orthop Res 25:122–131
17. Nötzli HP, Wyss TF, Stoecklin CH et al (2002) The contour of the femoral – junction as a predictor for the risk of anterior impingement. J Bone Joint Surg- Br Vol 84:556–560
18. Nelson AE, Stiller JL, Shi XA et al (2015) Measures of hip morphology are related to development of worsening radiographic hip osteoarthritis over 6 to 13 year follow-up: the Johnston county osteoarthritis project. Osteoarthritis Cartilage / OARS, Osteoarthritis Res Soc. doi:10.1016/j.joca.2015.10.007
19. Milone MT, Bedi A, Poultsides L et al (2013) Novel CT-based three-dimensional software improves the characterization of Cam morphology. Clin Orthop Relat Res 471:2484–2491
20. Lohan DG, Seeger LL, Motamedi K, et al (2009) Cam-type femoral-acetabular impingement: is the alpha angle the best MR arthrography has to offer? Skeletal Radiol
21. Sutter R, Dietrich TJ, Zingg PO, Pfirrmann CWA (2012) How useful is the alpha angle for discriminating between symptomatic patients with cam-type femoroacetabular impingement and asymptomatic volunteers? Radiology 264:514–521
22. Nouh MR, Schweitzer ME, Rybak L, Cohen J (2008) Femoroacetabular impingement: Can the alpha angle Be estimated? Am J Roentgenol 190:1260–1262
23. Gosvig KK, Jacobsen S, Sonne-Holm S et al (2010) Prevalence of malformations of the hip joint and their relationship to sex, groin pain, and risk of osteoarthritis: a population-based survey. J Bone Joint Surg Am 92:1162–1169
24. Fraitzl CR, Kappe T, Pennekamp F et al (2012) Femoral – offset measurements in 339 subjects: distribution and implications for femoroacetabular impingement. Knee Surg Sports Traumatol Arthrosc 21:1212–1217
25. Pollard TCB, Villar RN, Norton MR et al (2010) Femoroacetabular impingement and classification of the cam deformity: the reference interval in normal hips. Acta Orthop 81:134–141
26. Ross JR, Larson CM, Adeoyo O et al (2014) Residual deformity is the most common reason for revision Hip arthroscopy: a three-dimensional CT study. Clin Orthop Relat Res 473:1388–1395
27. Rego PRA, Mascarenhas V, Oliveira FS, et al (2015) Morphologic and angular planning for cam resectionin femoro-acetabular impingement: value of the omega angle. International Orthopaedics (SICOT) 1–7. doi: 10.1007/s00264-015-3053-7
28. Cvetanovich GL, Harris JD, Erickson BJ et al (2015) Revision Hip arthroscopy: a systematic review of diagnoses, operative findings, and outcomes. Arthroscopy 31:1382–1390
29. Christensen CP, Althausen PL, Mittleman MA, et al (2003) The nonarthritic hip score: reliable and validated. Clin Orthop Relat Res 75–83. doi: 10.1097/01.blo.0000043047.84315.4b
30. Lepage-Saucier M, Thiéry C, Larbi A et al (2014) Femoroacetabular impingement: normal values of the quantitative morphometric parameters in asymptomatic hips. Eur Radiol 24:1707–1714
31. Röling MA, Visser MI, Oei EHG et al (2015) A quantitative non-invasive assessment of femoroacetabular impingement with CT-based dynamic simulation–cadaveric validation study. BMC Musculoskelet Disord 16:50
32. Klenke FM, Hoffmann DB, Cross BJ, Siebenrock KA (2014) Validation of a standardized mapping system of the hip joint for radial MRA sequencing. Skelet Radiol. doi:10.1007/s00256-014-2026-z
33. Philippon MJ, Stubbs AJ, Schenker ML et al (2007) Arthroscopic management of femoroacetabular impingement: osteoplasty technique and literature review. Am J Sports Med 35:1571–1580
34. Audenaert EA, Baelde N, Huysse W et al (2011) Development of a three-dimensional detection method of cam deformities in femoroacetabular impingement. Skelet Radiol 40:921–927
35. Hack K, Di Primio G, Rakhra K, Beaulé PE (2010) Prevalence of cam-type femoroacetabular impingement morphology in asymptomatic volunteers. J Bone Joint Surg 92:2436–2444
36. Kang ACL, Gooding AJ, Coates MH et al (2010) Computed tomography assessment of Hip joints in asymptomatic individuals in relation to femoroacetabular impingement. Am J Sports Med 38:1160–1165
37. Scheidt RB, Galia CR, Diesel CV et al (2014) Prevalence of radiographic markers of femoroacetabular impingement in asymptomatic adults. Rev Col Bras Cir 41:36–42
38. Khanna V, Caragianis A, DiPrimio G et al (2014) Incidence of Hip pain in a prospective cohort of asymptomatic volunteers: is the Cam deformity a risk factor for Hip pain? Am J Sports Med 42:793–797
39. Van Houcke J, Yau WP, Yan CH et al (2015) Prevalence of radiographic parameters predisposing to femoroacetabular impingement in young asymptomatic chinese and white subjects. J Bone Joint Surg Am 97:310–317
40. Laborie LB, Lehmann TG, Engesæter I et al (2013) Is a positive femoroacetabular impingement test a common finding in healthy young adults? Clin Orthop Relat Res 471:2267–2277
41. Osteoporotic Fractures in Men (MrOS) Research Group, Nardo L, Parimi N et al (2015) Femoroacetabular impingement: prevalent and often asymptomatic in older Men: the osteoporotic fractures in Men study. Clin Orthop Relat Res. doi:10.1007/s11999-015-4222-0
42. Reichenbach S, Leunig M, Werlen S et al (2011) Association between cam-type deformities and magnetic resonance imaging-detected structural hip damage: a cross-sectional study in young men. Arthritis Rheum 63:4023–4030
43. Harris MD, Kapron AL, Peters CL, Anderson AE (2014) Correlations between the alpha angle and femoral head asphericity: implications and recommendations for the diagnosis of cam femoroacetabular impingement. Eur J Radiol 83:788–796
44. Masjedi M, Marquardt CS, Drummond IMH et al (2012) Cam type femoro-acetabular impingement: quantifying the diagnosis using three dimensional – ratios. Skelet Radiol. doi:10.1007/s00256-012-1459-5
45. Reichenbach S, Jüni P, Werlen S et al (2010) Prevalence of cam-type deformity on hip magnetic resonance imaging in young males: a cross-sectional study. Arthritis Care Res 62:1319–1327
46. Laborie LB, Lehmann TG, Engesaeter IO et al (2011) Prevalence of radiographic findings thought to be associated with femoroacetabular impingement in a population-based cohort of 2081 healthy young adults. Radiology 260:494–502
47. de Bruin F, Reijnierse M, Farhang-Razi V, Bloem JL (2013) Radiographic signs associated with femoroacetabular impingement occur with high prevalence at all ages in a hospital population. Eur Radiol 23:3131–3139
48. Siebenrock KA, Wahab KHA, Werlen S, et al (2004) Abnormal extension of the femoral head epiphysis as a cause of cam impingement. Clin Orthop Relat Res 54–60
49. Khan O, Witt J (2014) Evaluation of the magnitude and location of Cam deformity using three dimensional CT analysis. Bone Joint J 96-B:1167–1171
50. Sutter R, Dietrich TJ, Zingg PO, Pfirrmann CWA (2012) Femoral antetorsion: comparing asymptomatic volunteers and patients with femoroacetabular impingement. Radiology 263:475–483
51. Ricciardi BF, Fields K, Kelly BT et al (2014) Causes and risk factors for revision hip preservation surgery. Am J Sports Med 42:2627–2633
52. Ito K, Minka-II MA, Leunig M et al (2001) Femoroacetabular impingement and the cam-effect. J Bone Joint Surg 83:171–176

53. Yanke AB, Khair MM, Stanley R et al (2015) Sex differences in patients with CAM deformities with femoroacetabular impingement: 3-dimensional computed tomographic quantification. Arthroscopy. doi:10.1016/j.arthro.2015.06.007
54. Tannenbaum EP, Zhang P, Maratt JD et al (2015) A computed tomography study of gender differences in acetabular version and morphology: implications for femoroacetabular impingement. Arthrosc: J Arthrosc Relat Surg 31:1247–1254
55. Ross JR, Nepple JJ, Philippon MJ et al (2014) Effect of changes in pelvic tilt on range of motion to impingement and radiographic parameters of acetabular morphologic characteristics. Am J Sports Med 42:2402–2409
56. Harris MD, Datar M, Whitaker RT et al (2013) Statistical shape modeling of cam femoroacetabular impingement. J Orthop Res 31:1620–1626
57. Masjedi M, Mandalia R, Aqil A, Cobb J (2014) Validation of the "FeMorph" software in planning cam osteochondroplasty by incorporating labral morphology. Computer Methods in Biomechanics and Biomedical Engineering 1–7. doi: 10.1080/10255842.2014.986654
58. Steppacher SD, Tannast M, Werlen S, Siebenrock KA (2008) Femoral morphology differs between deficient and excessive acetabular coverage. Clin Orthop Relat Res 466:782–790
59. Xia Y, Fripp J, Chandra SS, et al (2015) Automated 3D quantitative assessment and measurement of alpha angles from the femoral – junction using MR imaging. Physics in Medicine & Biology 7601–7616. doi: 10.1088/0031-9155/60/19/7601
60. Dandachli W, Islam SU, Liu M et al (2009) Three-dimensional CT analysis to determine acetabular retroversion and the implications for the management of femoro-acetabular impingement. J Bone Joint Surg - Bri Vol 91:1031
61. Larson CM, Moreau-Gaudry A, Kelly BT et al (2014) Are normal hips being labeled as pathologic? a CT-based method for defining normal acetabular coverage. Clin Orthop Relat Res 473:1247–1254
62. Heyworth BE, Dolan MM, Nguyen JT et al (2012) Preoperative three-dimensional CT predicts intraoperative findings in Hip arthroscopy. Clin Orthop Relat Res 470:1950–1957
63. Kang RW, Yanke AB, Orias AE et al (2012) Emerging ideas: novel 3-D quantification and classification of Cam lesions in patients with femoroacetabular impingement. Clin Orthop Relat Res 471:358–362
64. Kuhn AW, Ross JR, Bedi A (2015) Three-dimensional imaging and computer navigation in planning for hip preservation surgery. Sports Med Arthrosc 23:e31–e38

CHAPTER 4.3

This chapter is based on the following paper:

"Morphologic and angular planning for cam resection in femoroacetabular impingement: value of the omega angle".
International Orthopedics. 2016 Oct;40(10): 2011-2017.

International Orthopaedics (SICOT)
DOI 10.1007/s00264-015-3053-7

ORIGINAL PAPER

Morphologic and angular planning for cam resection in femoro-acetabular impingement: value of the omega angle

Paulo Renato Amaral Rego[1] **· Vasco Mascarenhas**[2] **· Filipe S. Oliveira**[3] **· Pedro C. Pinto**[4] **· Augusto Gaspar**[2] **· Joana Ovídio**[4] **· Diego G. Collado**[5]

Received: 11 August 2015 / Accepted: 4 November 2015

Abstract
Purpose The alpha angle is used to quantify in a single plane the head–neck junction deformity of cam femoro-acetabular impingement (FAI). When the deformity overlaps the superior retinaculum, femoral head osteoplasty in this area can jeopardise intra-articular vascular structures. This study proposes a new angular measure of the linear radial extension of cam deformity as a planning tool for bone resection and compares the accuracy of femoral head osteoplasty using open and arthroscopic surgery.
Methods Twenty-five symptomatic patients operated on for FAI were included in this study. Radial magnetic resonance imaging (MRI) was done before and after surgery. Bi-dimensional coordinates of the vascular foramina and radial extension of the deformity (omega angle) were measured. This extension was correlated with the vascular foramina location and alpha-angle value. Accuracy of resection and hip function were evaluated before and after surgery.
Results The cam lesion frequently extended posteriorly. No relation between values of alpha and omega angles was found. Cam resection was complete in 88 % of cases; there was a significant improvement in outcome score after surgery.
Conclusions This study showed that alpha angle, measured in one plane, was not a predictor of the radial extension of cam deformity. To achieve a full resection, it was frequently necessary to extend the femoral head osteoplasty over the retinacular area. Pre-operative determination of the omega angle and location of the vascular foramina helped improve cam resection safety and accuracy.

Keywords Hip arthroscopy · Femoroacetabular impingement · Cam lesion · Osteoplasty · Vascular foramina · Omega angle · Bone resection · Osteoplasty · Accuracy · Retinaculum · Surgical hip dislocation · Deformity · Angular extension

✉ Paulo Renato Amaral Rego
pauloamaralrego@gmail.com

1 Department of Orthopaedic Surgery, Hospital da Luz, Avenida Lusíada, 100, 1500-650 Lisbon, Lisbon, Portugal

2 Department of Radiology, Hospital da Luz, Lisbon, Portugal

3 Department of Orthopaedic Surgery, University Hospitals Coventry and Warwickshire, West Midlands, UK

4 Department of Orthopaedic Surgery, Hospital Beatriz Angelo, Lisbon, Portugal

5 Department of Orthopaedic Surgery, Hospital Universitari Vall d'Hebron, Universitat Autònoma de Barcelona, Barcelona, Spain

Introduction

Arthroscopic surgery is used to treat intra-articular hip deformities such as cam femoro-acetabular impingement (FAI) [22, 27]. The published short to mid-term results of this technique are good [3, 18]. There is growing interest in the development of new tools to plan the amount of head–neck junction resection and evaluate osteoplasty accuracy. Extent and shape of head–neck junction resection can be easily controlled in open surgical hip dislocation using spherical templates [8]. Conversely, in hip arthroscopy, radial extension of the cam lesion is not so clearly visible and cannot be checked with surgical instruments. Therefore, arthroscopic resection might not be as accurate as in open surgery [16, 23].

Individual head–neck junction pathomorphology is variable [12, 15, 17]. In some cases, the lesion can be located laterally, with posterior extension over superior

Published online: 18 November 2015

retinacular vessels, assuming a pistol-grip shape, which is visible [7, 21, 25] in anteroposterior (AP) pelvic X-ray. Other possible locations include a pure anterior, which is not visible in AP X-ray and—much less frequently—inferior or posterior locations. An important aspect when addressing lateral and posterior cam lesions is to ensure that resection will not place femoral head vascular supply through the posterosuperior retinacular arteries in danger [9, 11, 13, 23].

To our knowledge, there is no published study quantifying radial extension of the cam lesion and comparing the efficacy of arthroscopy versus surgical hip dislocation in cam resection over the posterosuperior retinacular foramina area. Our study aims were to: (1) identify any relation between radial extension of cam lesions and location of retinacular vascular foramina at the head–neck junction, and (2) compare the efficacy of cam resection using two different surgical techniques—open and arthroscopic—in hips with an alpha angle >80°. In addition, we propose a new measure for linear radial extension of cam lesions: the omega angle. This angle can be related to the vascular foramina location using radial magnetic resonance imaging (MRI) sequences. It can help characterise the 3D morphology of the lesion and predict the correct arc of resection in the head–neck junction area, including the lateral and posterior zone of the vascular foramina (Figs. 1 and 2).

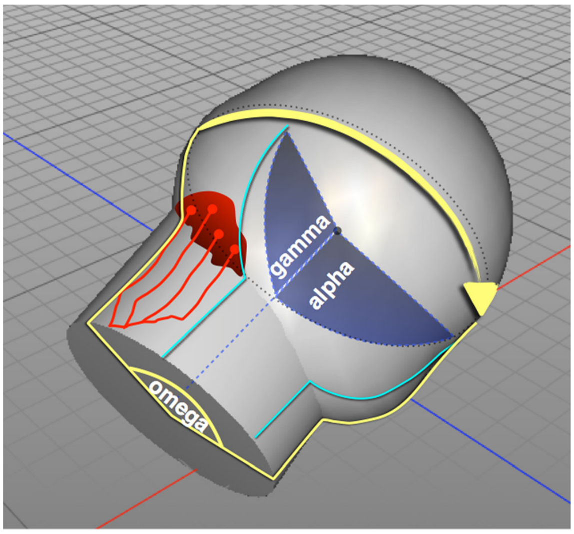

Fig. 1 Quantification of cam deformity using radial reference. The omega angle (*yellow arrow*) measures extension in the radial curved plane along the femoral head equator. The alpha and gamma angles measure elevation of the cam deformity in one radial cut. The cam lesion can extend posteriorly over the vascular foramen (*red dots*). The *blue lines* mark the deformity contour on the coronal plane expressed by the gamma angle and on the horizontal plane expressed by the alpha angle

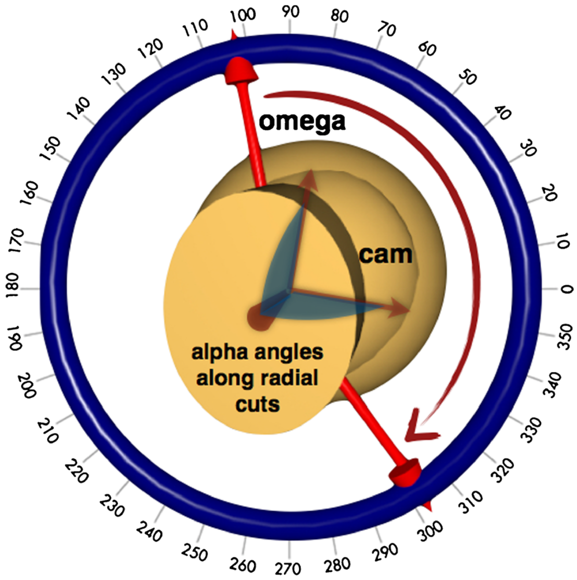

Fig. 2 Extension and location of cam lesion represented and measured using a 360° protractor ruler. The omega angle between the two *red arrows* measures the amount of linear radial extension of cam deformity with abnormal alpha angles (*blue angles*). In this case, the omega angle was 160°

Materials and methods

Patients

We selected 25 patients who had surgery for cam impingement. The only inclusion criteria was to have a preoperative alpha angle measured in cross-table view X-ray ≥80°. Fourteen patients underwent surgical hip dislocation, and 11 underwent hip arthroscopy. The same surgeon operated on all patients. Criteria for surgical hip dislocation were centre-edge angle >30° or the presence of acetabular global overcoverage. Criteria for hip arthroscopy were centre-edge angle <30° or patient preference. Average follow-up time was 40 (range 18–77) months. Patients with previous hip surgery, acetabular dysplasia, Perthes disease sequelae or slipped capital femoral epiphysis were excluded. Hips with osteoarthritis greater than grade 1 according to Tönnis [26] were also excluded. Patient age, gender, height, weight, body mass index (BMI) and sports activity prior to FAI surgical treatment were recorded. The Nonarthritic Hip Score [6] (NAHS) was used to evaluate pre- and post-operative hip function. Patients were evaluated at three, six and 12 months and then yearly. In case of a follow-up > two years, we used the score applied in the last visit. For statistic analyses we used only the outcome score from the last visit.

Head–neck junction morphology

In all cases, we obtained pre- and post-operative radial arthro-MRI, 3T, 16 radial cuts. The same protocol and the same MRI equipment (Siemens® Verio 3T) were used in all cases. The same senior radiologists did image interpretation before and after surgery. In MRI sequences perpendicular to the femoral neck axis, intercepting the head–neck junction, we found the lesser trochanter to be a constant anatomical reproducible landmark. By superimposing a protractor ruler, the tip of the lesser trochanter was located at 240° (Fig. 3). This was the most reliable reference for precise anatomic orientation (superior, anterior, inferior, posterior) of all images.

Using the Osirix® cross-reference localiser, we measured and registered alpha angle value in each of the 16 radial cuts (Fig. 4). It was considered abnormal if >45° [2, 10, 19] and was defined [20, 24] as lying between the femoral neck axis and a line drawn from the centre of the femoral head to the point where the peripheral contour of the femoral head exceeded a superimposed best-fitting circumference (radius of the subchondral bone of the femoral head).

The femoral head centre was identified by placing a circumference over its contour. The femoral neck axis was defined as a line passing through the centre of the femoral head and the centre of the femoral neck at its narrowest point.

Omega angle determination

Counterclockwise, starting inferiorly, we determined in degrees where the alpha angle exceeded the considered normal threshold value (45°) and begins to be abnormal and where it returns to a normal value. The difference between those two measurements was considered to be the radial extension of the cam lesion, which we named the omega angle (Figs. 1 and 2). This virtual angle is formed by two lines intersecting in the centre of the femoral neck at the level of the head–neck junction. The most proximal line intersects peripherally the point of the equatorial line where the alpha angle begins to be abnormal and the distal line at the point where the alpha angle returns to normal. Measurements were made before and after surgery in all cases to compare resection accuracy using surgical hip dislocation and arthroscopy approaches.

Vascular foramina location (retinacular arteries)

Using the MRI sequences intercepting the head–neck junction perpendicular to the femoral neck long axis and the protractor ruler, we divided the selected image into eight sectors (Fig. 5): 1 (90–45°), 2 (45–0°), 3 (0–315°), 4 (315–270°), 5 (270–225°), 6 (225–180°), 7 (180–135) and 8 (135–90°).

Using an X-Y axis centred on the best circle containing the head–neck junction, we measured the cartesian coordinates of all identifiable foramina [14]. To compare foramina location with radial cam extension (omega angle) and apply statistical tests, X-Y points were converted to polar (radial) coordinates using the formula r=√(*x*2+y2) and θ=tan-1y/x (where *r* = distance of the foramen to the centre of the neck and *θ* the angle formed between *r* and the *x* line). All values were represented graphically (Fig. 5).

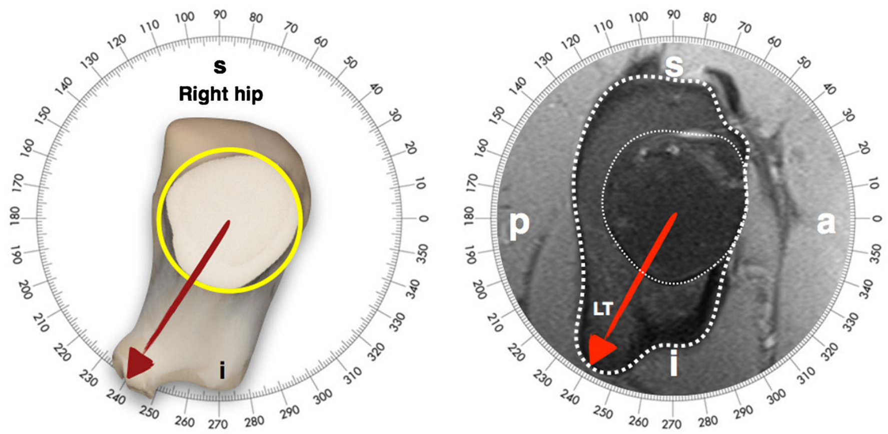

Fig. 3 Position of the lesser trochanter in a bone model simulating magnetic resonance imaging (MRI) cuts (*left*). Superimposed parallel images obtained perpendicular to the femoral neck axis (*right*); the first (*broader dotted line*) intercepts the lesser trochanter and the second (*thinner dotted line*) shows the femoral neck contour at the head–neck junction The radial position of the lesser trochanter is 240°. This anatomical reference allowed us to correctly orientate the MRI image. *s* superior, *a* anterior, *I* inferior, *p* posterior, *LT* lesser throchanter

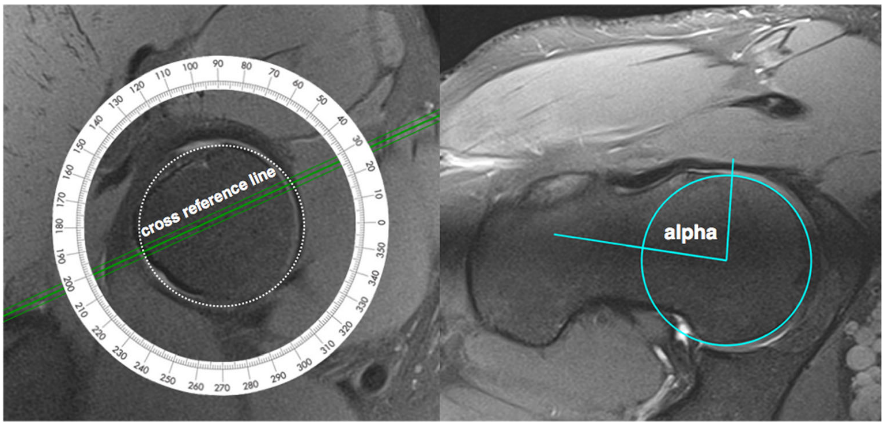

Fig. 4 Measurement of alpha angle in radial cuts. The *green line* is a cross-reference localiser tool. The radial image on the *right* corresponds to the plane represented by the *green line* on the *left*. In this case, the alpha angle at 27° of the protractor ruler was 85.3°

Statistical studies

We used AcaStat Software ® and Statviz ® to perform statistical analyses. The significance level was set at $p \leq 0.001$.

1. Analysis of variance (ANOVA) was used to analyse radial extension of cam resection in both groups and to compare absolute radial extension (omega angle) versus posterior extension of the deformity.
2. Pearson correlation test was used to analyse a possible relation of radial extension of the cam deformity (omega angle) and foramen location before surgery and a possible relation between alpha and omega angles.
3. Paired Student's *t* test was used to analyse and correlate outcome score and cam extension before and after surgery.
4. Chi-square test was used to compare surgical hip dislocation (SHD) and arthroscopy in the resection over the vessels.
5. Retinacular foramina distribution frequency was also analysed.
6. NAHS ratio of variation before and after surgery were calculated using the formula: (NAHS after – NAHS before) / NAHS before × 100.

Results

Patient cohort

Twenty-four of 25 patients were men. Mean age was 30 (range 19–56) years; mean follow-up was 40 (range 18–77) months. Fourteen patients underwent surgical hip dislocation and 11 patients arthroscopy. The average NAHS was 54 (range 18–90) points before surgery. After surgery, there was an absolute increase of 32 (range 2.5–80) points to a final score of 84 (range 50–99) points ($p < 0.001$); variation ratio was 93 % (range 3–435 %).

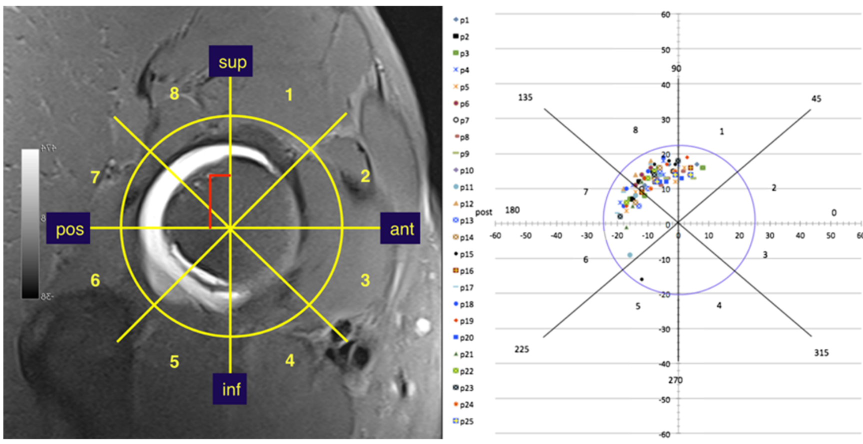

Fig. 5 Identifying and measuring X-Y coordinates of the vascular foramina in one magnetic resonance imaging sequence

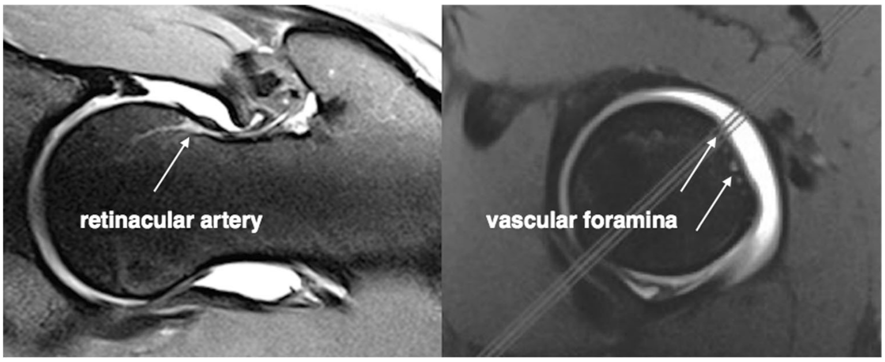

Fig. 6 Magnetic resonance imaging (3T) showing location of retinacular synovial fold at the head–neck junction (*left*) and the cross-reference perpendicular plane crossing one vascular foramen (*right*)

Head–neck junction morphology before and after surgery

We identified an average of three vascular foramina per patient. There was a higher concentration (70 %) between 90° and 150° (sectors 7 and 8) (Fig. 5). Average alpha angle was 90° before and 40° after resection ($p<0.0001$). Average radial extension of the cam lesion (omega angle) was 138° (range 90–180°); 76 % of patients presented posterior extension of the cam lesion overlapping the retinacular area (from 90–135°; sectors 7 and 8). A wider omega angle was associated with posterior extension of the cam lesion ($p=0.001$). There was no correlation of alpha and omega angle values before surgery ($p=0.3$). Radial extension of the deformity resection was 100 % and achieved in 22 (88 %) cases. In three patients, a residual posterior cam extension was not resected.

Comparison of open surgery versus arthroscopy

There was no difference in resection extent between open and arthroscopy techniques ($p=0.08$). There was also no difference in resection over the vascular area between techniques ($p=0.06$). Distribution of vascular head–neck junction foramina was similar between groups.

Discussion

Three-dimensional morphology of the cam lesion can be quantified using alpha angle (cross-table view in X-ray – anterior head–neck offset) and gamma angle (AP pelvis X-ray – lateral head neck offset) [2, 5, 19, 24]. The goal of surgery, open or arthroscopic, is to restore femoral-head spherical shape along the head–neck junction, including the critical area over the lateral retinacular fold. Less experienced arthroscopic surgeons might run an additional risk of injuring vascular supply to the femoral head while resecting bone in that area. Recent improvements in MRI resolution and image processing software allowed better identification of the posterosuperior retinacular fold [4] (Fig. 6) in radial sequences and vascular foramina in sagittal oblique sequences.

The location of these vascular structures combined with morphological characterisation of the cam lesion can be used as a pre-operative planning tool. The starting point of the omega angle can be particularly helpful to decide whether a posterior resection is necessary to accurately restore head–neck junction offset. Our results showed a clear predominance of vascular orifices on posterosuperior sectors, similar to findings of other studies [13], but there was no relation between

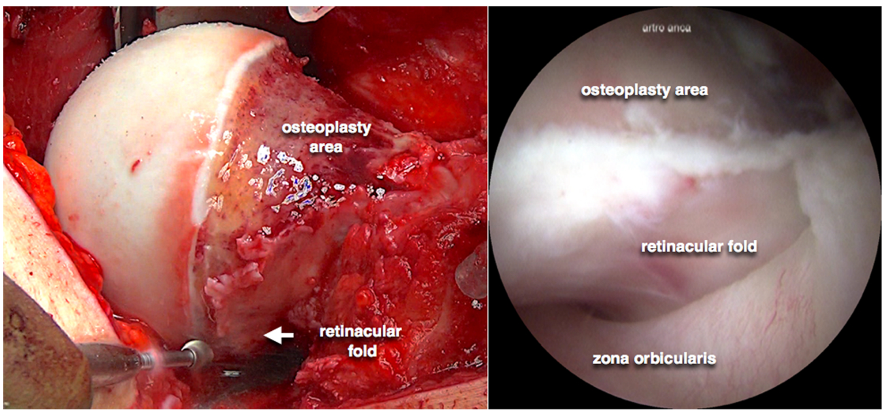

Fig. 7 Cam resection over the lateral retinaculum in a surgical hip dislocation procedure using a motorised instrument in a right hip (*right*); intraoperative arthroscopy of cam resection over superior retinacular fold (*left*). The hip capsule is open in a T shape, and traction points are used to visualise vascular structures (both patients from this study)

radial extension of the cam lesion and retinacular foramina location. We found a relation between omega angle value and posterior extension of the cam lesion. A larger omega angle was associated with a tendency for the cam lesion to overlap the lateral retinacular area.

Alpha angle value could not be related to that of the omega angle. A patient can have an important protruding cam lesion generating an aggressive intrusion mechanism [1], but in a very localised acetabular area only. The opposite is also possible: a less protuberant lesion with a broader radial extension can generate an intrusion mechanism in a wider acetabular area. We think, therefore, that the alpha angle value is not predictive of the 3D cam morphology and should not be used as a single planning tool.

We found that in 76 % of cases, in order to achieve complete cam resection, it was necessary to perform osteoplasty over the posterior vascular area. Also, in 44 % of patients, vascular foramina location extended into sector 1 (45–90°), overlapping the anterior cam lesion. Accordingly, even in pure anterior cam resection, it was necessary to remove bone over the vascular area in 44 % of cases. Previous information about those parameters allowed a more detailed pre-operative planning.

Additionally, we compared our results using surgical hip dislocation and arthroscopy to resect similar cam lesions. In surgical hip dislocation, there was a constant visual control of the retinacular area, and the resection could be accomplished using femoral head templates. In arthroscopy, references for correct cam trimming were more difficult to identify. Many surgeons, including us, use the lateral and the medial synovial fold as guides for resection. Intra- operatively, however, it can be difficult to realise whether there is an additional posterior cam extension over the lateral synovial fold. Using the omega angle and vascular area location on MRI, we achieved similar resections in both groups (Fig. 7). Overall improvement in clinical score reflects cam resection accuracy.

The main limitations of this study were the small number of patients, its retrospective nature and nonrandomisation of patients, our use of only one clinical outcome score, and the method of measuring the omega angle necessitated experienced radiologists and surgeons familiar with radial MRI sequence interpretation. Future developments in imaging software are needed to measure the omega angle in a more reproducible and practical manner.

Acknowledgments We thank the Hospital da Luz Radiology department for providing MRI equipment and all the processing software necessary for geometrical analysis

Compliance with ethical standards

Conflict of interest The authors declare that they have no conflict of interest and there was no founding involved in the preparation of this manuscript

Ethical approval This article does not include results of experimental investigations on humans, and as a retrospective study, formal consent was not required. Informed consent from all patients was obtained on a routine basis for surgical procedures. We obtained formal consent from our institutional review board to perform geometric analysis on imaging files.

References

1. Audenaert EA, Mahieu P, Pattyn C (2011) Three-dimensional assessment of cam engagement in femoroacetabular impingement. Arthroscopy 27(2):167–71. doi:10.1016/j.arthro.2010.06.031
2. Beaulé PE, Hynes K, Parker G, Kemp KA (2012) Can the alpha angle assessment of cam impingement predict acetabular cartilage delamination? Clin Orthop Relat Res 470(12):3361–7. doi:10.1007/s11999-012-2601-3
3. Beutel BG, Collins JA, Garofolo G, Youm T (2015) Hip arthroscopy outcomes, complications, and traction safety in patients with prior lower-extremity arthroplasty. Int Orthop 39(1):13–8. doi:10.1007/s00264-014-2479-7
4. Boraiah S, Dyke JP, Hettrich C, Parker RJ, Miller A, Helfet D, Lorich D (2009) Assessment of vascularity of the femoral head using gadolinium (gd-dtpa)-enhanced magnetic resonance imaging: A cadaver study. J Bone Joint Surg Br 91(1):131–7. doi:10.1302/0301-620X.91B1.21275
5. Büchler L, Neumann M, Schwab JM, Iselin L, Tannast M, Beck M (2013) Arthroscopic versus open cam resection in the treatment of femoroacetabular impingement. Arthroscopy 29(4):653–60. doi:10.1016/j.arthro.2012.12.009
6. Christensen CP, Althausen PL, Mittleman MA, Lee J-A, McCarthy JC (2003) The nonarthritic hip score: reliable and validated. Clin Orthop Relat Res 406:75–83. doi:10.1097/01.blo.0000043047.84315.4b
7. Doherty M, Courtney P, Doherty S, Jenkins W, Maciewicz RA, Muir K, Zhang W (2008) Nonspherical femoral head shape (pistol grip deformity), neck shaft angle, and risk of hip osteoarthritis: a case–control study. Arthritis Rheum 58(10):3172–82. doi:10.1002/art.23939
8. Espinosa N, Rothenfluh DA, Beck M, Ganz R, Leunig M (2006) Treatment of femoro-acetabular impingement: preliminary results of labral refixation. J Bone Joint Surg Am 88(5):925–35. doi:10.2106/JBJS.E.00290
9. Ganz R, Gill TJ, Gautier E, Ganz K, Krügel N, Berlemann U (2001) Surgical dislocation of the adult hip a technique with full access to the femoral head and acetabulum without the risk of avascular necrosis. J Bone Joint Surg Br 83(8):1119–24
10. Jamali AA, Mak W, Wang P, Tai L, Meehan JP, Lamba R (2013) What is normal femoral head/neck anatomy? An analysis of radial CT reconstructions in adolescents. Clin Orthop Relat Res 471(11):3581–7. doi:10.1007/s11999-013-3166-5
11. Kalhor M, Beck M, Huff TW, Ganz R (2009) Capsular and pericapsular contributions to acetabular and femoral head perfusion. J Bone Joint Surg Am 91(2):409–18. doi:10.2106/JBJS.G.01679
12. Kang RW, Yanke AB, Espinoza Orias AA, Orias AE, Inoue N, Nho SJ (2013) Emerging ideas: novel 3-D quantification and classification of cam lesions in patients with femoroacetabular impingement. Clin Orthop Relat Res 471(2):358–62. doi:10.1007/s11999-012-2693-9
13. Lavigne M, Kalhor M, Beck M, Ganz R, Leunig M (2005) Distribution of vascular foramina around the femoral head and neck

junction: relevance for conservative intracapsular procedures of the hip. Orthop Clin N Am 36(2):171–6. doi:10.1016/j.ocl.2005.02.002

14. Lazaro LE, Sculco PK, Pardee NC, Klinger CE, Dyke JP, Helfet DL et al (2013) Assessment of femoral head and head–neck junction perfusion following surgical hip dislocation using gadolinium-enhanced magnetic resonance imaging: a cadaveric study. J Bone Joint Surg Am 95(23):e1821–8. doi:10.2106/JBJS.L.01185
15. Lerch S, Kasperczyk A, Warnecke J, Berndt T, Rühmann O (2013) Evaluation of cam-type femoroacetabular impingement by ultrasound. Int Orthop 37(5):783–8. doi:10.1007/s00264-013-1844-2
16. Lerch S, Kasperczyk A, Berndt T, Rühmann O (2015) Ultrasonography can quantify the extent of osteochondroplasty after treatment of cam-type femoroacetabular impingement. Int Orthop 39(5):853–8. doi:10.1007/s00264-014-2588-3
17. Magerkurth O, Jacobson JA, Jax F, Morag Y, Fessell D, Lee SJ et al (2013) Femoroacetabular cam-type impingement: global assessment of the femoral head–neck junction on a single reformatted MR image. Radiology 268(3):822–30. doi:10.1148/radiol.13121961
18. Mancini D, Fontana A (2014) Five-year results of arthroscopic techniques for the treatment of acetabular chondral lesions in femoroacetabular impingement. Int Orthop 38(10):2057–64. doi:10.1007/s00264-014-2403-1
19. Neumann M, Cui Q, Siebenrock KA, Beck M (2009) Impingement-free hip motion: the 'normal" angle alpha after osteochondroplasty. Clin Orthop Relat Res 467(3):699–703. doi:10.1007/s11999-008-0616-6
20. Rakhra KS, Sheikh AM, Allen D, Beaulé PE (2009) Comparison of MRI alpha angle measurement planes in femoroacetabular impingement. Clin Orthop Relat Res 467(3):660–5. doi:10.1007/s11999-008-0627-3
21. Spencer S, Millis MB, Kim Y-J (2006) Early results of treatment of hip impingement syndrome in slipped capital femoral epiphysis and pistol grip deformity of the femoral head–neck junction using the surgical dislocation technique. J Pediatr Orthop 26(3):281–5. doi:10.1097/01.bpo.0000217726.16417.74
22. Stähelin L, Stähelin T, Jolles BM, Herzog RF (2008) Arthroscopic offset restoration in femoroacetabular cam impingement: accuracy and early clinical outcome. Arthroscopy 24(1):51–57.e1. doi:10.1016/j.arthro.2007.08.010
23. Sussmann PS, Ranawat AS, Shehaan M, Lorich D, Padgett DE, Kelly BT (2007) Vascular preservation during arthroscopic osteoplasty of the femoral head–neck junction: a cadaveric investigation. Arthroscopy 23(7):738–43. doi:10.1016/j.arthro.2007.01.025
24. Sutter R, Dietrich TJ, Zingg PO, Pfirrmann CWA (2012) How useful is the alpha angle for discriminating between symptomatic patients with cam-type femoroacetabular impingement and asymptomatic volunteers? Radiology 264(2):514–21. doi:10.1148/radiol.12112479
25. Tanzer M, Noiseux N (2004) Osseous abnormalities and early osteoarthritis: the role of hip impingement. Clin Orthop Relat Res 429:170–7
26. Tönnis D (1976) Normal values of the hip joint for the evaluation of x-rays in children and adults. Clin Orthop Relat Res 119:39–47
27. Vendittoli PA, Young DA, Stitson DJ, Wolfe R, Del Buono A, Maffulli N (2012) Acetabular rim lesions: arthroscopic assessment and clinical relevance. Int Orthop 36(11):2235–41. doi:10.1007/s00264-012-1595-5

CHAPTER 4.4

This chapter is based on the following paper:

"Arterial Topographic Anatomy Near the Femoral Head-Neck Perforation with Surgical Relevance"
The Journal of Bone and Joint 2017 99(14): 1213-1221

Arterial Topographic Anatomy Near the Femoral Head-Neck Perforation with Surgical Relevance

Paulo Rego, MD, Vasco Mascarenhas, MD, Diego Collado, MD, Ana Coelho, MD, Luis Barbosa, MD, and Reinhold Ganz, MD

Investigation performed at the Department of Orthopaedic Surgery, Hospital da Luz, Lisbon, Portugal

Background: Knowledge of the vascular supply of the femoral head is crucial for hip-preserving surgical procedures. The critical area for reshaping cam deformity is at the retinacular vessel penetration, an area with ill-defined topographic anatomy. We performed a cadaver study of the extension of the lateral retinaculum near the head-neck junction, distribution of the arterial vascular foramina, and initial intracapital course of these vessels.

Methods: In 16 fresh proximal parts of the femur without head-neck deformities, the deep branch of the medial femoral circumflex artery was injected with gadolinium for magnetic resonance imaging (MRI) sequences to identify arterial structures.

Results: We found a mean number of 4.5 arterial foramina, showing a predominance from 10 to 12 o'clock. The retinaculum extended 20 mm from 1 to 10 o'clock. The surface distance from the cartilage border to the vascular foramina under the synovial fold was 6.5 mm, and the depth from the same cartilage border to the initial intraosseous vessel pathways was 5.3 mm.

Conclusions: The data add further precision to the arterial topography at the retinacular foramina, an area that is crucial for the perfusion of the femoral head. It may overlap with the area of anterolateral cam deformity and plays a role in choosing the cuts for subcapital and intracapital osteotomies.

Clinical Relevance: The information is taken from normal hips and may not be directly applicable to the deformed hip. Nevertheless, it is a prerequisite for a surgeon to understand the normal anatomy and use those boundaries to prevent mistakes during intra-articular joint-preserving hip surgical procedures.

Peer Review: This article was reviewed by the Editor-in-Chief and one Deputy Editor, and it underwent blinded review by two or more outside experts. The Deputy Editor reviewed each revision of the article, and it underwent a final review by the Editor-in-Chief prior to publication. Final corrections and clarifications occurred during one or more exchanges between the author(s) and copyeditors.

Knowledge of the femoral-head vascular supply is crucial for hip-preserving surgical procedures[1,2]. In many cases of femoroacetabular impingement, the head-neck deformity extends over the area where retinacular vessels penetrate into bone (Fig. 1). Excessive bone trimming in this area can jeopardize vessels either where they penetrate into bone (Fig. 2) or along their intraosseous course[3,4], placing femoral-head perfusion at risk[5]. To our knowledge, the literature has been lacking studies about a safe surface distance from the lateral border of the cartilage to the vascular foramina under the retinacular synovial fold and also about the depth of the intraosseous vessels near the cartilage border. In subcapital and true neck osteotomies, the entire femoral-neck circumference is approached subperiosteally, creating a soft-tissue tube that includes the lateral and medial retinacular vessels[6,7]. In femoral-head reduction osteotomies[6], the topography and points of penetration of the medial and lateral retinacular vessels have to be identified to determine the possible size and orientation of the head segment to be resected[6]. This is relatively easy at the medial retinaculum, which runs on top of the easily visualized Weitbrecht ligament[8]. Identification of the anterior border of the lateral retinaculum is equally straightforward. However, definition of the posterior border of

Disclosure: There was no source of external funding for this study. The Hospital da Luz Radiology Department provided the MRI scan facilities for cadaver specimen imaging and all of the processing software necessary for the geometrical analysis. The Portuguese National Institute of Legal Medicine and Forensic Science, Pathology Department, supplied the cadaveric material and facilities for dissections. On the **Disclosure of Potential Conflicts of Interest** forms, *which are provided with the online version of the article*, one or more of the authors checked "yes" to indicate that the author had a relevant financial relationship in the biomedical arena outside the submitted work (http://links.lww.com/JBJS/D438).

J Bone Joint Surg Am. 2017;99:1213-21 • http://dx.doi.org/10.2106/JBJS.16.01386

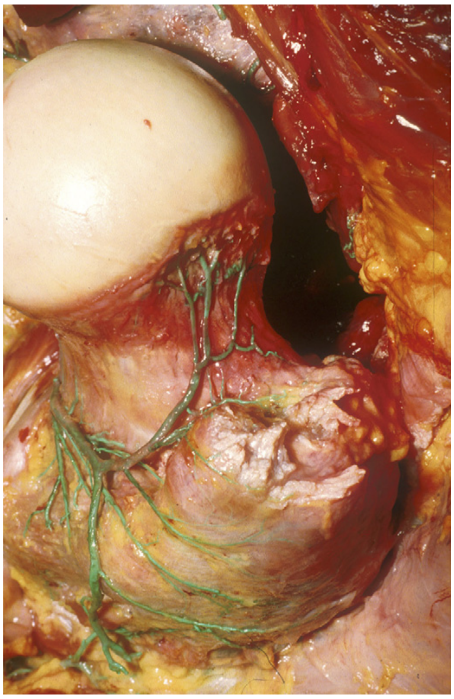

Fig. 1
Photograph showing the posterior aspect of the right hip with the deep branch of the medial femoral circumflex artery running along the greater trochanter, arborizing into the retinacular vessels at the posterosuperior neck and perforating into the bone of the head close to the superior cartilage border. Retinacular tissue was removed for better identification of the arterial vessels. (Reproduced, with permission and copyright © of the British Editorial Society of Bone and Joint Surgery, from: Gautier E, Ganz K, Krügel N, Gill T, Ganz R. Anatomy of the medial femoral circumflex artery and its surgical implications. J Bone Joint Surg Br. 2000 Jul;82-B[5]:679-83 [Fig. 1a].)

the lateral retinaculum may be troublesome, especially when gross anatomy is altered.

In current high-resolution magnetic resonance imaging (MRI), the osseous perforations for initial intraosseous pathways of the vascular structures can be seen. We hypothesize that the topography of the arterial inflow is rather uniform and an attempt at quantification may further increase and strengthen our knowledge. We performed a cadaver study of the extension of the lateral retinaculum near the head-neck junction, the distribution of the vascular foramina at the head-neck junction, and the initial course of the intracapital vessels. Gadolinium-based contrast agent was injected into the deep branch of the medial femoral circumflex artery (Fig. 3) and MRI scans of the resected specimens were performed.

Materials and Methods

Sixteen fresh hips without deformity from the Portuguese National Institute of Legal Medicine and Forensic Science were used for the study (8 male cadavers, with a mean donor age of 50 years [range, 20 to 60 years]).

In the lateral decubitus position, a 30-cm longitudinal incision was centered over the greater trochanter. The fascia was incised in line with the anterior border of the gluteus maximus muscle and the muscle was retracted posteriorly. The insertions of the gluteus medius and vastus lateralis muscles were detached from the greater trochanter and retracted anteriorly. After identification of the interval between the gluteus minimus and piriformis muscles, the gluteus minimus was resected and the capsule was exposed circumferentially except for the area of the external rotators. After careful resection of the quadratus femoris muscle, the deep branch of the medial femoral circumflex artery was found about 5 to 10 mm proximal to the base of the lesser trochanter. The remaining external rotators were divided as far as possible from their trochanteric insertions. By doing so, the vascular anastomoses between the superior and inferior gluteal arteries and the deep branch could be ligated. The capsule was resected around the femoral neck. However, the posterosuperior area including the perforation level of the deep branch of the medial femoral circumflex artery into the capsule was left pristine to protect the arterial vessels supplying the head. The deep branch was ligated and was divided close to the lesser trochanter to allow cannulation for contrast injection (Fig. 3). To determine the position of the arterial foramina at the head-neck junction, a clock-face system was used and the connecting line between the 12 and 6 o'clock positions was aligned parallel with the anatomical axes in the frontal and sagittal plane of the straight proximal third of the femur. To obtain this reference axis, the anatomical axes were marked on the bone surface. With a drill-bit pointing to the middle of the inferior neck area and held parallel to the axes, a hole was made into the head to serve as the reference for the clock orientation; the midpoint was defined with a caliper ruler (Fig. 4). The drill-bits were removed to avoid metal artifacts with the MRI scans; however, the empty drill-holes were delineated.

The femoral osteotomy was performed 1 cm below the lesser trochanter and the entire specimen was removed from the cadaver. The deep branch of the medial femoral circumflex artery was cannulated using a 22-gauge catheter. The patency of the preparation was tested by injection of 20 mL of isotonic saline solution. Leakage from the fovea capitis demonstrated adequate intraosseous saline solution perfusion. Head diameter was measured using a caliper.

The cannulated specimens were then scanned in a 3-T MRI system (Verio; Siemens) before and immediately after injection of a diluted gadolinium solution (0.5:200), Gadavist (gadobutrol). The purpose of the scan previous to gadolinium injection was to find out whether the vascular foramina and intraosseous vessels could be identified on routine MRI sequences without contrast enhancement.

Manual injection was considered completed after fluid leakage was observed at the fovea capitis. Imaging was performed in the coronal plane, the axial plane, and a plane perpendicular to the femoral-neck axis, using T1, T2, and T2-fat-saturated sequences, and volume-acquisition radial reconstructions were also performed simultaneously on both right and left proximal femoral cadaver specimens.

Image Processing, Foramen Mapping, and Distance Measurements

T1 sequences were selected for mapping. Two senior radiologists performed image interpretation before and after gadolinium injection. The drill-hole shown in Figure 4 and visible in the MRI scan was used to define the vertical axis of the neck and to mark the 6 and 12 o'clock positions of a clock face; 3 o'clock was the anterior pole and 9 o'clock was the posterior pole.

All hips were converted to the left side, mirroring the obtained MRI scans in the DICOM (Digital Imaging and Communications in Medicine) file format scans to make angular measurements easier.

Using a perpendicular x-y axis centered on the best-fit circle containing the cortical circumference, with the y axis coincident with the vertical axis of the femur, we measured the Cartesian coordinates of all identifiable

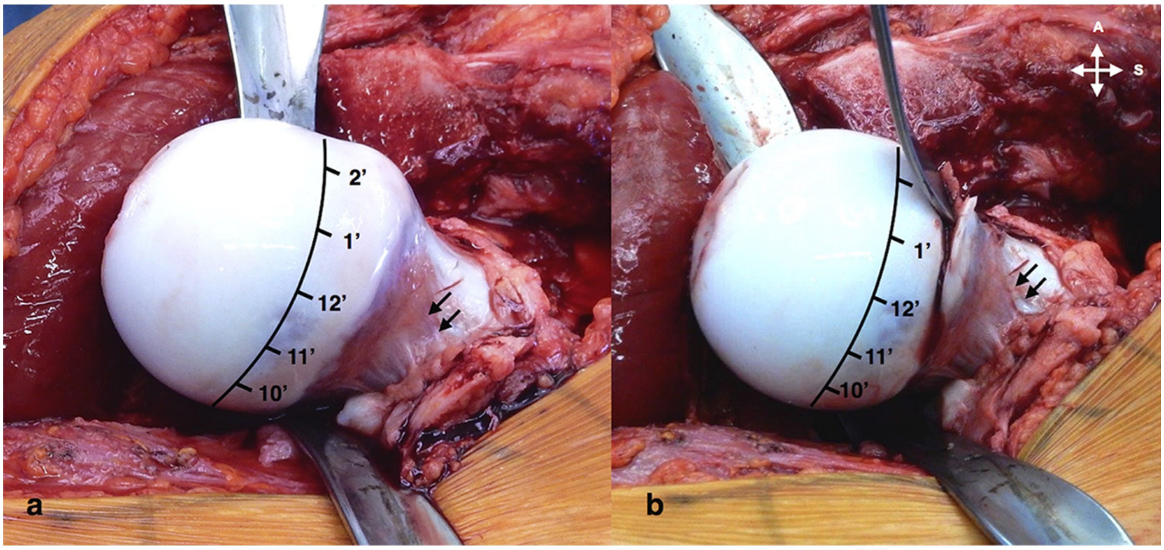

Fig. 2

Figs. 2-A and 2-B Intraoperative photographs of a right femoral head during surgical hip dislocation. The arrows indicate the anterior border of the superior retinacular fold. **Fig. 2-A** The reddish color of the cartilage outlines the extension of the anterolateral cam deformity that overlaps the anterior border of the retinaculum. The superimposed clock-face reference shows that the deformity extends from the anterior and inferior head-neck waist (below 3 o'clock) to the posterosuperior neck (10 o'clock). Retinacular arteries and perforating foramina are not clearly visible under the synovial fold. **Fig. 2-B** The part of the deformity cranial to the retinaculum has to be resected only down to the level of vessel perforation, a line that can be identified by repeated finger palpation. A = anterior and S = superior.

foramina in the head-neck junction area. These coordinates were converted to polar (radial) coordinates using the formula $r = \sqrt{(x^2 + y^2)}$ and $\theta = \tan^{-1}(y/x)$ (where r = the distance of the foramen from the center of the neck and θ = the angle formed between r and the x line) (Fig. 5). Over the same images, a digital protractor (Onde Rulers; Ondesoft Computing) was placed to create a clock face system with 12 sectors: 12 hours to 1 hour (90° to 60°), 1 to 2 hours (60° to 30°), 2 to 3 hours (30° to 0°/360°), 3 to 4 hours (0°/360° to 330°), 4 to 5 hours (330° to 300°), 5 to 6 hours (300° to 270°), 6 to 7 hours (270° to 240°), 7 to 8 hours (240° to 210°), 8 to 9 hours (210° to 180°), 9 to 10 hours (180° to 150°), 10 to 11 hours (150° to 120°) and 11 to 12 hours (120° to 90°). The positions (clock face and angles) of the most anterior and posterior vessels were determined in the MRI sequence preceding osseous entrance. The absolute distance between those 2 vessels (width of the retinaculum) was also measured in millimeters (Fig. 6).

The topographic pathway of the vessels at the extraosseous-intraosseous transition was investigated using radially reconstructed T1 sequences (Fig. 7) by measuring the distance (d1) from the entrance of the vessel into bone to the rim of the joint cartilage and the shortest distance (d2) from this cartilage rim to the intraosseous course of the contrast-filled vessels. All measurements were performed by 2 experienced radiologists. Interobserver reliability for the foraminal distribution, retinacular measurements, and distances from the cartilage border to the vascular structures were calculated using the intraclass correlation coefficient[9].

Statistical Analysis

AcaStat (AcaStat Software) was used for statistical analysis. The significance level was set at $p \leq 0.001$. Foraminal distribution was analyzed before and after gadolinium solution injection. Correlation between surface and depth and distance from the cartilage border to vascular structures was determined using Pearson correlation testing.

Results

We found a mean number (and standard deviation) of 4.5 ± 0.9 arterial foramina (range, 3 to 6 arterial foramina) per specimen. This was not dependent on age,

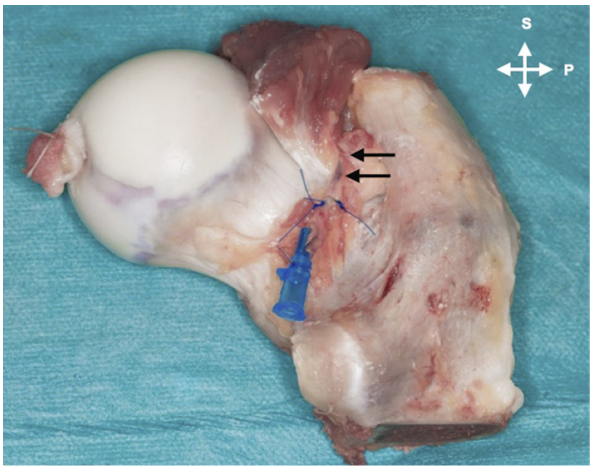

Fig. 3

A photograph showing the posterior aspect of the cadaver specimen after cannulation. We can see the terminal path and capsular penetration area of the medial femoral circumflex artery deep branch (arrows) plus the short external rotators left intact to preserve femoral-head perfusion. S = superior and P = posterior.

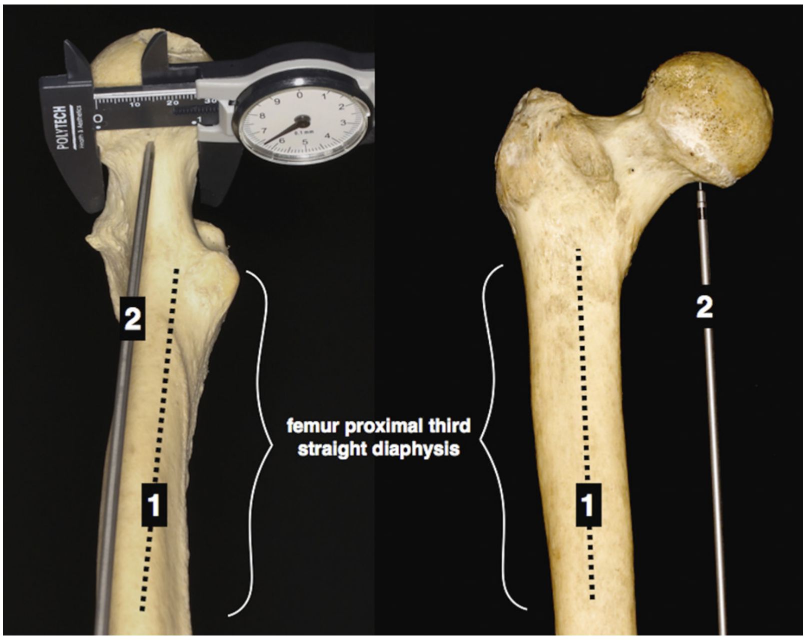

Fig. 4
A 2.5-mm drill-bit (2) is pointing to the midpoint of the undersurface of the neck and is held parallel to both anatomical axes (1); the midpoint is defined with a caliper. The drill-hole and perforation were identifiable in the MRI and served as landmarks for orientation of the clock-face positions. No marker was left in place to avoid later MRI interference.

sex, or side. After injection of the deep branch of the medial femoral circumflex artery, 80% of the 72 foramina identified on the pre-contrast MRI were filled with contrast agent.

The global foraminal distribution (before and after contrast injection) in a clock-face presentation (Table I and Fig. 8) showed a predominance in sector 11 (10 to 11 o'clock), at 32%, and sector 12 (11 to 12 o'clock), at 36%. No foramina were found from 1 to 9 o'clock (sectors 2 to 9). Between 12 and 1 o'clock, we found 16 foramina. In 60% of the hip specimens, at least 1 foramen was found in sector 1 (12 to 1 o'clock). The global percentage of foramina in sector 1 was 22%. There was a strong interobserver agreement (intraclass correlation coefficient > 0.8) in this determination.

The posterosuperior width of the retinaculum, measured from the most anterior to most posterior perforating arterial vessels, extended a mean of 20 mm (range, 13 to 26 mm). The anterior retinacular border was located at a mean of 65° or 0.82 hour on the clock face (from 40°/1.6 hours to 95°/11.80 hours). The posterior border was located at a mean of 143° or 10.3 hours (from 117°/11.10 hours to 170°/9.3 hours) (Fig. 6). Again, interobserver reliability was strong (intraclass correlation coefficient > 0.8).

In the radial reconstructions, we could clearly identify 50 arterial foramina and respective intraosseous initial vessel pathways filled with contrast agent. The mean surface

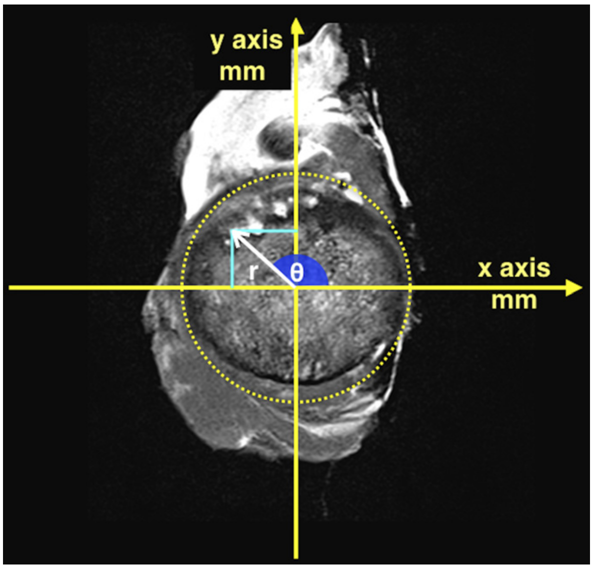

Fig. 5
T1 turbo spin echo (TSE) axial MRI showing the method of mapping the vascular foramina and retinacular borders on the MRI: drawing 2 perpendicular axes (X and Y) and determining the Cartesian (x; y) coordinates of a foramen that are later converted to a radial system in which r is the distance to the center of the neck and θ is the angle formed by axis x and r.

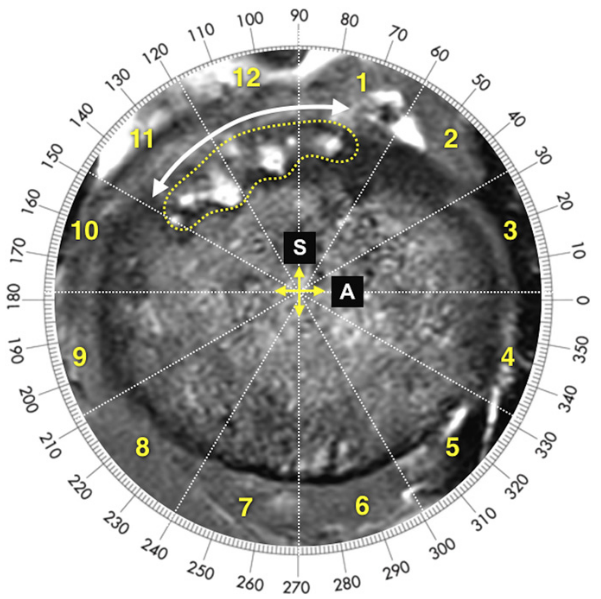

Fig. 6
The same T1 TSE axial MRI is divided like a clock face into 12 sectors of 30° each. The protractor software allowed us to directly measure the angular value θ and the distance to the neck center. Retinacular circumferential dimensions (white arrow) were measured in millimeters using this method and were delineated by the most anterior and posterior retinacular vessel locations. A = anterior and S = superior.

distance (d1) from the cartilage border to the vascular foramen under the synovial fold was 6.5 mm (range, 1.6 to 10.8 mm). The mean depth (d2) from the same cartilage

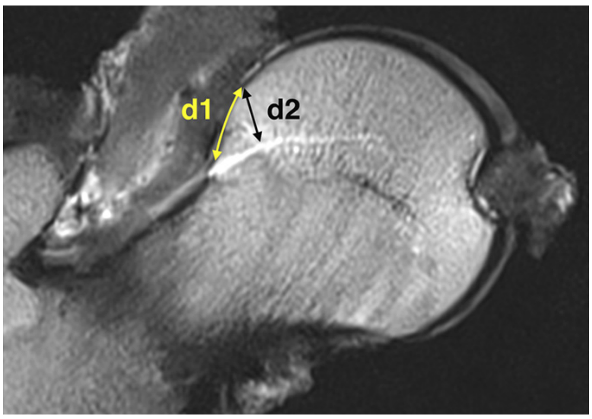

Fig. 7
T1 TSE coronal MRI representation of the surface distance from the cartilage margin to the retinacular foraminal entrance under the synovial fold (d1) and the depth from the cartilage margin to the intraosseous vessel from the same foramen (d2).

TABLE I Global Foraminal Distribution Per Clock-Face Sector

Sectors	Foramina	Percentage
1	16	22%
2	0	—
3	0	—
4	0	—
5	0	—
6	0	—
7	0	—
8	0	—
9	0	—
10	7	10%
11	23	32%
12	26	36%
Total	72	100%

border to the initial intraosseous pathway of the vessels was 5.3 mm (range, 1.7 to 9.6 mm) (Fig. 7). The interobserver reliability was also strong in these measurements (intraclass correlation coefficient > 0.8). There was moderate correlation (Pearson correlation coefficient = 0.6; $p < 0.0001$) between the 2 distances. There was no relation of those distances to femoral-head size.

Considering the pathways of the intraosseous arterial vessels, all specimens in this study would retain at least 2 arterial vessels if hypothetical bone resection depth was <2.5 mm from the cartilage margin. By increasing the resection depth to 6 mm, only 4 of the 16 specimens would keep at least 2 of the vascular structures intact. Increasing this depth to 8.5 mm would result in no specimens retaining at least 2 intact vessels. At a 10-mm depth, all vessels in all specimens would be damaged (Fig. 9).

Considering the lateral distance from the cartilage border, all specimens would retain at least 2 arterial vessels when bone resection was inferior to 2 mm lateral to the cartilage margin. If we increase the distance of resection to 6 mm, only 8 of 16 specimens would retain at least 2 vascular structures. By increasing the resection to 8 mm, no specimens would preserve 2 vessels. At 10 mm of lateral resection, all vessels in all specimens would be damaged (Fig. 10).

Discussion

Knowledge of the vascular anatomy of the proximal part of the femur is of the utmost importance for hip-preserving surgical procedures. During execution of osteochondroplasties of the femoral head-neck junction, the more lateral or even posterior portion of the neck may need to be approached in a primary or secondary cam resection as the deformity frequently extends posteriorly[10-12] (Fig. 2). Also, for subcapital realignment, for true femoral-neck osteotomy, and

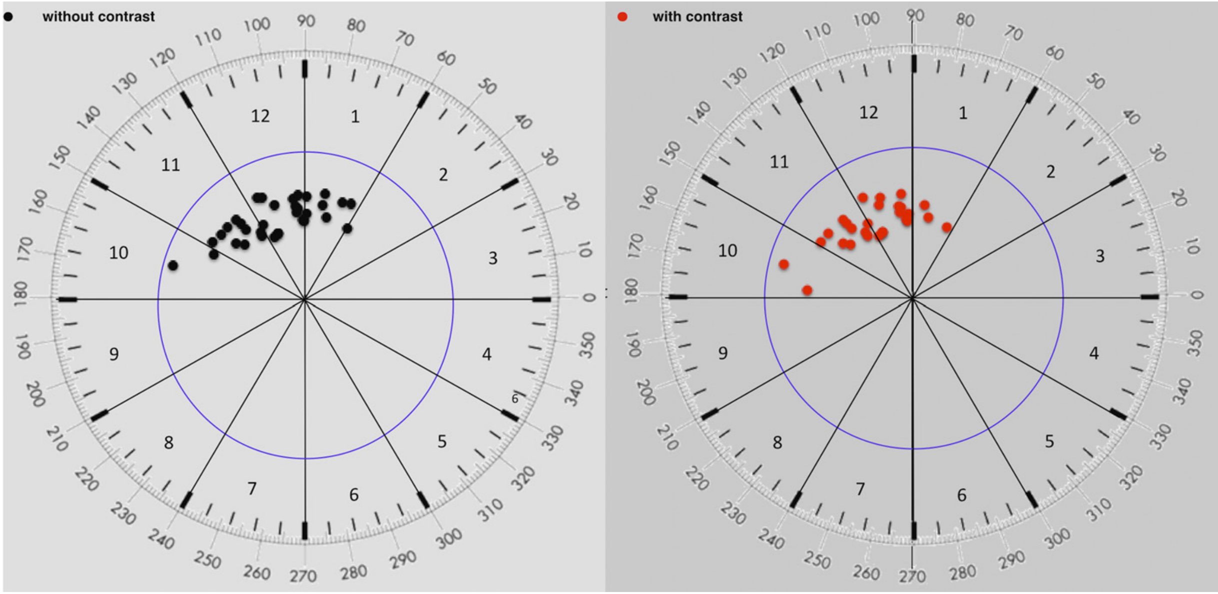

Fig. 8
Images showing the clock-face distribution of vascular foramina at the level of the head-neck junction. Black dots are the foramina before contrast injection; red dots are the foramina after contrast injection.

especially for femoral-head reduction osteotomy, a more detailed topographic understanding of the vessels feeding the epiphysis is necessary[6,7,10,12]. Spatial identification of the medial retinaculum covering the prominent Weitbrecht ligament and identification of the deep branch of the medial femoral circumflex artery are rather easy, and mobilization during subcapital and femoral-neck osteotomies can take place under direct visual control. However, resections at this part of the femoral-head circumference are rather rare. The cam lesion typically occurs from 11:30 to 3 o'clock[3,4,13], so we believe that additional information is needed about vessel perforation of the lateral retinaculum because its mobilization and nearby osseous resection occur more frequently[11,14,15].

The prevalence of osteonecrosis after treatment of femoroacetabular impingement is anecdotal[16]; minor necrotic areas may be clinically unsuspicious and may only be detectable with MRI. However, fear of risking such a complication may be responsible for inappropriate resection and residual impingement, visible in more than two-thirds of failed surgical procedures[17,18]. The fear may be bolstered by the fact that cam deformity extends to the posterior area in about 75% of the hips[3]. Necrosis occurring after an intra-articular procedure is not related to the procedure itself[19]. In the series of intracapital osteotomies performed by the senior author, no necrosis has been observed so far.

To our knowledge, literature is scarce about the detailed location and quantification of vascular foramina at the head-neck junction and is nonexistent regarding identification of arterial foramina, their locations, and the distance to the surface during the intraosseous course. Also, to our knowledge, retinaculum width and posterior extension are ill-defined in the literature. The distribution of femoral-head vascular foramina has been described[20]; however, no information was provided on the patency of vessels eventually going through the foramina and on the distribution of arterial and venous vessels. One publication focused on femoral-head vascular supply reconstruction using gadolinium-enhanced MRI[21] but did not describe the precise locations of the intraosseous vessels.

Recent improvements in MRI resolution and image-processing software have led to better identification in radial sequences of a possible vascular structure in the posterosuperior area of the femoral-neck junction and possible vascular foramina in sagittal oblique sequences[21]. However, the vessel type has remained undetermined so far. Performing an MRI on cadaver specimens before and after injection of a gadolinium solution in the medial femoral circumflex artery main branch has allowed us to demonstrate the vascular nature; contrast filling of 80% of the previously identified foramina before injection showed its arterial nature without any doubt. As previously described[2,3,8,14,20-24], we also found that the foramina were concentrated in the posterosuperior area of the femoral head. Lavigne et al. found a mean number of 15 foramina per specimen and 32% to 48% were assessed to be in an anterior location[14]. We found a mean of 4.5 foramina per specimen and only 22% of arterial foramina were located from 12 to 1 o'clock. In the study by Lavigne et al., recorded

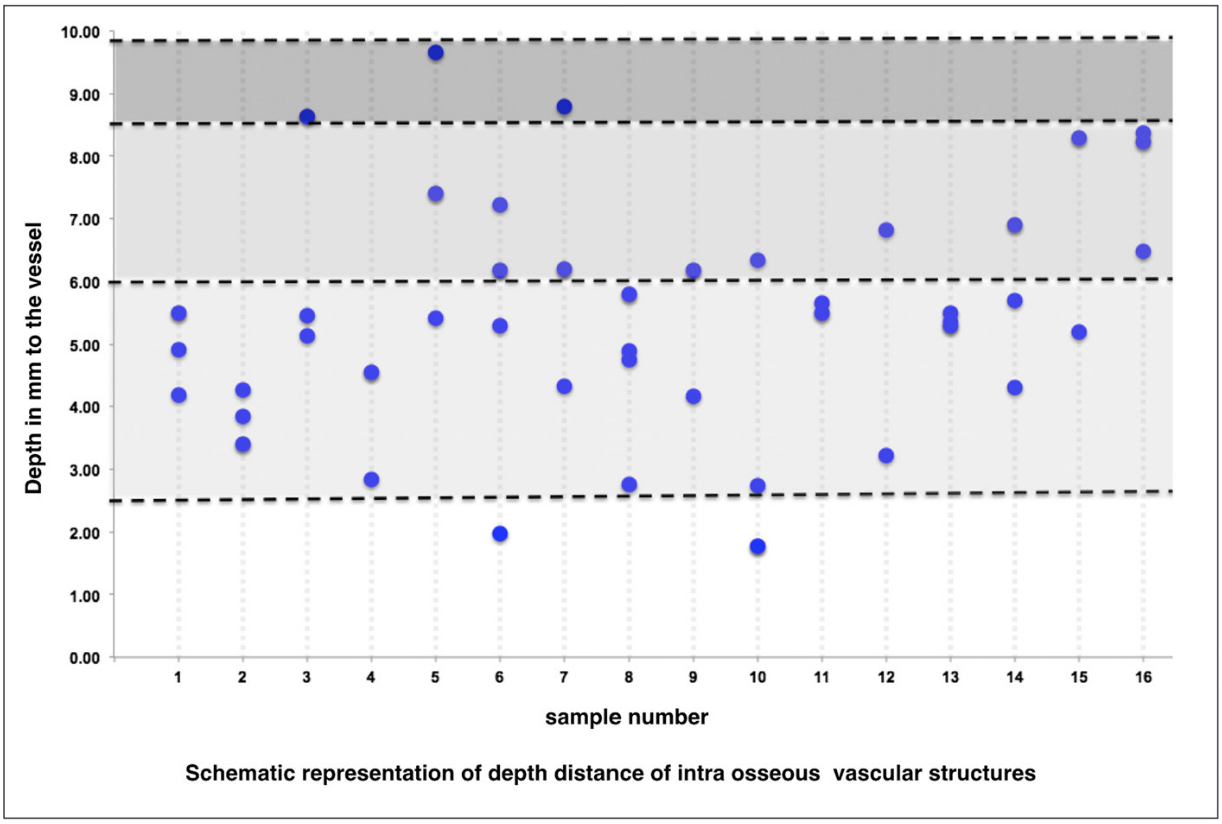

Fig. 9

Graph showing the depth from the cartilage margin to each vascular structure as identified in each specimen (blue dot). The gray areas and dotted lines represent the limits and amount of bone resection in this area. If we limit the hypothetical bone resection to 2.5 mm (the white area), all specimens in this study would preserve at least 2 vessels intact. If we increase the depth to 6 mm (lighter gray area), only 4 of 16 specimens (hip numbers 5, 6, 7, and 16) would preserve at least 2 intact vascular structures. If we increase this distance to 8.5 mm (medium gray area), no specimens would preserve at least 2 vessels intact. At 10 mm (darker gray area), all of the vessels would be damaged in all specimens.

foramina had a diameter as small as 0.5 mm, possibly overestimating the number of vessels supplying blood to the femoral head. In addition, in dry bone, their arterial or venous nature was impossible to determine. One possible explanation for the mean number of 15 dry bone foramina per femoral sample previously described, compared with our smaller number of 4.5 arterial foramina (3:1 ratio), would be the possibility that each retinacular artery is accompanied by 2 veins and that two-thirds of the dry bone foramina would correspond to venous structures.

By filling the retinacular arteries with contrast agent, it was possible to determine the circumferential extension and the anterior and posterior borders of the retinaculum. In our study, the anterior border mean location was found around 1 o'clock, but a 12 o'clock position has been mentioned[11]. Although the orientation of the clock face in that study seems to be equal to that in our study, the described anterolateral limit for resection of a protrusion might be less safe. To our knowledge, the posterior retinacular border has not been previously described; we found the mean location to be around 10 o'clock (range, 9 to 11 o'clock), clearly showing that the posterior neck between 6 and 9 o'clock is a safe area for posterior trimming or for the ending level of the posterior neck-cut in femoral-head reduction osteotomies.

The entrance of the arterial retinacular vessels into bone relative to the cartilage border and the initial intraosseous course relative to the cartilage surface are not exactly known. The measured surface distance and depth show that the margin of safe bone resection in the area is very limited and our data give an idea about the 2.5-mm minimum safe distance for bone resection in terms of depth and 2 mm in lateral extension. Increasing the resection depth also increases the probability of damaging the arterial supply to the femoral head. It is crucial to know how close the retinaculum can be detached and mobilized from

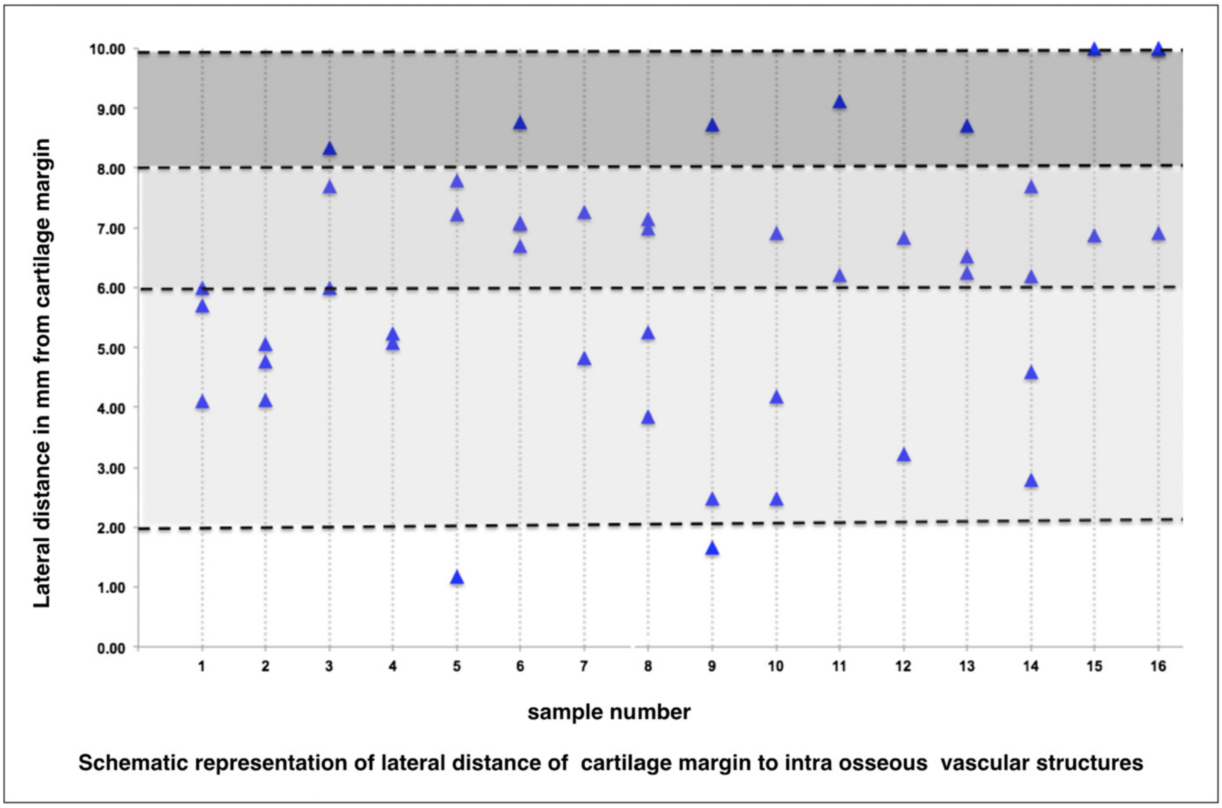

Fig. 10
Graph showing the lateral distance from the cartilage margin to each vascular foramen structure (blue triangle) identified in each specimen. The gray areas and dotted lines represent the limits and amount of bone resection in this area. If we limit the hypothetical bone resection to 2 mm (white area), all specimens in this study would preserve at least 2 vessels intact. If we increase the lateral resection to 6 mm (lighter gray area), 8 of 16 specimens (hip numbers 5, 6, 8, 11, 13, 14, 15, and 16) would preserve at least 2 intact vascular structures. If we increase this distance to 8 mm (medium gray area), no specimens would preserve at least 2 vessels intact. At 10 mm (darker gray area), all vessels would be damaged in all specimens.

the femoral neck in osteotomies when the posterior neck is very short, as in severe chronic slips or in hips with Legg-Calvé-Perthes disease.

The possible limitations of our study include the small number of specimens and the fact that the scattered range of measured data was too small to allow statistical power. Also, the injection of contrast agent was done manually, which did not guarantee a constant flow pressure; this might have contributed to the observed collapse of some structures after gadolinium injection (20%). Furthermore, it is reasonable to hypothesize that some of the foramina would not be permeable in live patients or that they were of venous origin. The width of the retinaculum was measured as the distance between the most extreme contrast permeable foraminal vessels, but the retinaculum as shown at the time of the surgical procedure may be somewhat larger. Finally, our measurements were performed on normal hips without primary or secondary deformations; therefore, it is not possible to make precise clinical recommendations for surgical procedures about the safe distance of lateral and depth resection in the retinacular area, especially with regard to cam morphology in which the location and radial extension of the deformity are very variable. Nevertheless, the information may increase attentiveness and care during intracapsular surgical procedures. ■

Paulo Rego, MD[1]
Vasco Mascarenhas, MD[1]
Diego Collado, MD[2]
Ana Coelho, MD[3]
Luis Barbosa, MD[3]
Reinhold Ganz, MD[4]

[1]Departments of Orthopaedic Surgery (P.R.) and Radiology (V.M.), Hospital da Luz, Lisbon, Portugal

[2]Department of Orthopaedic Surgery, Hospital Universitari Vall d'Hebron, Universitat Autònoma de Barcelona, Barcelona, Spain

[3]Department of Orthopaedic Surgery, Hospital Beatriz Ângelo, Lisbon, Portugal

[4]University of Berne, Berne, Switzerland

E-mail address for P. Rego: pauloamaralrego@gmail.com

ORCID iD for P. Rego: 0000-0002-8098-4526

References

1. Ganz R, Gill TJ, Gautier E, Ganz K, Krügel N, Berlemann U. Surgical dislocation of the adult hip a technique with full access to the femoral head and acetabulum without the risk of avascular necrosis. J Bone Joint Surg Br. 2001 Nov;83(8):1119-24.

2. Gautier E, Ganz K, Krügel N, Gill T, Ganz R. Anatomy of the medial femoral circumflex artery and its surgical implications. J Bone Joint Surg Br. 2000 Jul;82(5):679-83.

3. Rego PR, Mascarenhas V, Oliveira FS, Pinto PC, Gaspar A, Ovídio J, Collado DG. Morphologic and angular planning for cam resection in femoro-acetabular impingement: value of the omega angle. Int Orthop. 2016 Oct;40(10):2011-7. Epub 2015 Nov 18.

4. Mascarenhas VV, Rego P, Dantas P, Gaspar A, Soldado F, Consciência JG. Cam deformity and the omega angle, a novel quantitative measurement of femoral head-neck morphology: a 3D CT gender analysis in asymptomatic subjects. Eur Radiol. 2017 May;27(5):2011-23. Epub 2016 Aug 30.

5. Sevitt S, Thompson RG. The distribution and anastomoses of arteries supplying the head and neck of the femur. J Bone Joint Surg Br. 1965 Aug;47:560-73.

6. Ganz R, Huff TW, Leunig M. Extended retinacular soft-tissue flap for intra-articular hip surgery: surgical technique, indications, and results of application. Instr Course Lect. 2009;58:241-55.

7. Ganz R, Horowitz K, Leunig M. Algorithm for femoral and periacetabular osteotomies in complex hip deformities. Clin Orthop Relat Res. 2010 Dec;468(12):3168-80.

8. Kalhor M, Horowitz K, Gharehdaghi J, Beck M, Ganz R. Anatomic variations in femoral head circulation. Hip Int. 2012 May-Jun;22(3):307-12.

9. Barnhart HX, Haber MJ, Lin LI. An overview on assessing agreement with continuous measurements. J Biopharm Stat. 2007;17(4):529-69.

10. Leunig M, Puloski S, Beck M, Siebenrock KA, Ganz R. Proximal femoral osteotomy: current indications and techniques. Semin Arthroplasty. 2005 Mar;16(1):53-62.

11. Sussmann PS, Ranawat AS, Shehaan M, Lorich D, Padgett DE, Kelly BT. Vascular preservation during arthroscopic osteoplasty of the femoral head-neck junction: a cadaveric investigation. Arthroscopy. 2007 Jul;23(7):738-43.

12. Leunig M, Ganz R. Relative neck lengthening and intracapital osteotomy for severe Perthes and Perthes-like deformities. Bull NYU Hosp Jt Dis. 2011;69(Suppl 1):S62-7.

13. Yanke AB, Khair MM, Stanley R, Walton D, Lee S, Bush-Joseph CA, Espinoza Orías A, Inoue N, Nho SJ. Sex differences in patients with cam deformities with femoroacetabular impingement: 3-dimensional computed tomographic quantification. Arthroscopy. 2015 Dec;31(12):2301-6. Epub 2015 Jul 26.

14. Lavigne M, Kalhor M, Beck M, Ganz R, Leunig M. Distribution of vascular foramina around the femoral head and neck junction: relevance for conservative intracapsular procedures of the hip. Orthop Clin North Am. 2005 Apr;36(2):171-6, viii.

15. Büchler L, Neumann M, Schwab JM, Iselin L, Tannast M, Beck M. Arthroscopic versus open cam resection in the treatment of femoroacetabular impingement. Arthroscopy. 2013 Apr;29(4):653-60. Epub 2013 Feb 6.

16. Dietrich TJ, Dora C, Pfirrmann CWA. Postoperative imaging in femoroacetabular impingement. Semin Musculoskelet Radiol. 2013 Jul;17(3):272-8. Epub 2013 Jun 20.

17. Bogunovic L, Gottlieb M, Pashos G, Baca G, Clohisy JC. Why do hip arthroscopy procedures fail? Clin Orthop Relat Res. 2013 Aug;471(8):2523-9.

18. Ross JR, Larson CM, Adeoye O, Kelly BT, Bedi A. Residual deformity is the most common reason for revision hip arthroscopy: a three-dimensional CT study. Clin Orthop Relat Res. 2015 Apr;473(4):1388-95.

19. Ziebarth K, Leunig M, Slongo T, Kim YJ, Ganz R. Slipped capital femoral epiphysis: relevant pathophysiological findings with open surgery. Clin Orthop Relat Res. 2013 Jul;471(7):2156-62.

20. Jung A, Wurtz JP, Randrianarivo P. [Arterial circulatory modifications in aseptic necrosis of the hip and in epiphysiolysis]. Mem Acad Chir (Paris). 1965 May 12;91(15):489-506. French.

21. Boraiah S, Dyke JP, Hettrich C, Parker RJ, Miller A, Helfet D, Lorich D. Assessment of vascularity of the femoral head using gadolinium (Gd-DTPA)-enhanced magnetic resonance imaging: a cadaver study. J Bone Joint Surg Br. 2009 Jan;91(1):131-7.

22. Grose AW, Gardner MJ, Sussmann PS, Helfet DL, Lorich DG. The surgical anatomy of the blood supply to the femoral head: description of the anastomosis between the medial femoral circumflex and inferior gluteal arteries at the hip. J Bone Joint Surg Br. 2008 Oct;90(10):1298-303.

23. Dy CJ, Thompson MT, Usrey MM, Noble PC. The distribution of vascular foramina at the femoral head/neck junction: implications for resurfacing arthroplasty. J Arthroplasty. 2012 Oct;27(9):1669-75. Epub 2012 Apr 21.

24. Kalhor M, Beck M, Huff TW, Ganz R. Capsular and pericapsular contributions to acetabular and femoral head perfusion. J Bone Joint Surg Am. 2009 Feb;91(2):409-18.

chapter 5

BRIDGING THE ANATOMICAL GAP BETWEEN THE SYMPTOMATIC AND THE ASYMPTOMATIC HIP

Chapter V is based on the following publications:

"On a "Columbus' Egg": Modelling the shape of asymptomatic, dysplastic and impinged hip joints"
Medical Engineering and Physics 2018

"Can We Discriminate Symptomatic Hip Patients From Asymptomatic Volunteers Based On Anatomical Predictors? – A 3D MRI Study On Cam, Pincer And Spinopelvic Parameters"
American Journal of Sports Medicine 2018/247254

CHAPTER 5.1

This chapter is based on the following paper:

"On a "Columbus' Egg":
Modelling the shape of asymptomatic, dysplastic and impinged hip joints"
Medical Engineering and Physics 2018

Medical Engineering and Physics 59 (2018) 50–55

Contents lists available at ScienceDirect

Medical Engineering and Physics

journal homepage: www.elsevier.com/locate/medengphy

On a “Columbus’ Egg”: Modeling the shape of asymptomatic, dysplastic and impinged hip joints

Daniel Simões Lopes[a,b,*], Sara M. Pires[b], Vasco V. Mascarenhas[c], Miguel T. Silva[b], Joaquim A. Jorge[a,b]

[a] INESC-ID taguspark. Avenida Professor Cavaco Silva, Edifício IST, 2744-016 Porto Salvo, Portugal
[b] Instituto Superior Técnico, Universidade de Lisboa, Av. Rovisco Pais 1, 1049-001 Lisboa, Portugal
[c] Hospital da Luz, UIME, Av. Lusíada 100, 1500-650 Lisboa, Portugal

ARTICLE INFO

Article history:
Received 7 November 2017
Revised 12 June 2018
Accepted 9 July 2018

Keywords:
Hip joint
Femoral head
Acetabular cavity
Femoroacetabular impingement
Hip dysplasia
Surface fitting
Ellipsoid
Ovoid

ABSTRACT

Understanding morphological features that characterize normal hip joint is critical and necessary for a more comprehensive definition of pathological presentations, such as femoroacetabular impingement and hip dysplasia. Based on anatomical observations that articular surfaces of synovial joints are better represented by ovoidal shapes than by spheres, the aim of this study is to computationally test this morphological classification for the femoral head and acetabular cavity of asymptomatic, dysplastic and impinged hips by comparing spherical, ellipsoidal and ovoidal shapes. An image-based surface fitting framework was used to assess the goodness-of-fit of spherical, ellipsoidal and tapered ellipsoidal (i.e., egg-like) shapes. The framework involved image segmentation with active contour methods, mesh smoothing and decimation, and surface fitting to point clouds performed with genetic algorithms. Image data of the hip region was obtained from computed tomography and magnetic resonance imaging scans. Shape analyses were performed upon image data from 20 asymptomatic, 20 dysplastic and 20 impinged (cam, pincer, and mixed) hips of patients with ages ranging between 18 and 45 years old (28 male and 32 women). Tapered ellipsoids presented the lowest fitting errors (i.e., more oval), followed by ellipsoids and spheres which had the worst goodness-of-fit. Ovoidal geometries are also more representative of cam, pincer, mixed impinged hips when compared to spherical or ellipsoidal shapes. The statistical analysis of the surface fitting errors reveal that ovoidal shapes better represent both articular surfaces of the hip joint, revealing a greater approximation to the overall features of asymptomatic, dysplastic and impinged cases.

1. Introduction

Morphological variations of the hip joint anatomy, such as femoroacetabular impingement (FAI) and dysplasia, have been suggested to be linked to the lesion mechanism of articular cartilage and progress towards osteoarthritis (OA) [1–9]. It has been estimated that FAI morphology affects between 10% and 15% of the general adult population [10] and approximately 55% among young athletes [11]. Regarding hip dysplasia prevalence in adults, it exhibits high variability amongst different racial groups, going from approximately 6–21% [12]. Considering the young age of patients manifesting symptomatic FAI or dysplasia, they might be electable for hip conservative surgery and the application of a prosthetic device [6,13]. An early-stage intervention and appropriate diagnosis for these patients rely on the accurate morphological and geometric characterization of the underlying anatomic deformity [4]. However, consensus regarding the metrics that best identify the morphological deformities and the intervals in which they should be placed to distinguish normal from pathological hips has not been reached to date [3,6,14–17].

Regarding the shape of the hip joint, recent computational tests [18–24] are in line with medical evidence [25,26] which considers that ovoidal shapes represent the articular surface geometry better than the orthodoxal sphere [27,28]. Yet, current tools used by physicians to investigate morphological features of these structures and to guide them in the treatment of FAI and dysplasia, consider the sphere to be the shape that best fits both the femoral head and the acetabular cavity. Consequently, finding how appropriate are currently used 2D quantitative measurements and how well defined is the morphological difference between asymptomatic,

* Corresponding author at: INESC-ID taguspark. Avenida Professor Cavaco Silva, Edifício IST, 2744-016 Porto Salvo, Portugal.
E-mail addresses: daniel.lopes@inesc-id.pt (D.S. Lopes), sara.pires@tecnico.ulisboa.pt (S.M. Pires), vmascarenhas@hospitaldaluz.pt (V.V. Mascarenhas), MiguelSilva@tecnico.ulisboa.pt (M.T. Silva), jorgej@acm.org (J.A. Jorge).

https://doi.org/10.1016/j.medengphy.2018.07.001
1350-4533/

femoroacetabular impingement, and hip dysplasia are interesting questions worth addressing.

On the other hand, there seems to be high variation in the definition of the physiological values for the metrics used to describe the geometry of these surfaces, such as α angle, centre-edge angle, acetabular index of Tönnis, among others. Different authors consider different intervals for these parameters, highlighting the ambiguity associated with the classification of hip joint morphology [6,14–16]. Novel hip joint shape models, along with new sets of parameters, would allow for clear and unambiguous classification and identification of the femoral head and acetabular cavity, regardless of the form.

In order to answer these questions, a comparative study between asymptomatic and pathological hip joints was carried out to understand their underlying morphology. Surface fitting analyses of both femoral head and acetabular cavity were performed upon 20 asymptomatic hips, 20 dysplastic and 20 FAI (cam, pincer, and mixed) hips to provide quantitative evidence supporting the series of anatomical observations that the hip joint exhibits morphological features that are more consistent with ovoidal shapes than spherical ones, given that these do not contain information on global geometric characteristics such as axial asymmetry and non-homogeneous curvature.

2. Materials and methods

2.1. Medical image data

We retrospectively studied adult patients undergoing computed tomography (CT) or magnetic resonance imaging (MRI) from January and December 2015. All eligible patients had completed a questionnaire regarding their clinical history, including current or past hip/groin pain, medical or surgical hip-joint conditions, history of childhood hip pathology, and/or hip trauma. Patients who gave a positive answer to one or more of these questions were excluded from the asymptomatic group. Additionally, all patients completed the non-arthritic hip score questionnaire. Any patient with less than the maximal possible score was also excluded from the asymptomatic cohort. Images were uploaded for analysis using Articulis (ArticulisTM; Clinical Graphics, Delft, The Netherlands) and semi-automatically segmented using this software, which had been previously validated for reliability and accuracy [29].

CT scans of the asymptomatic pelvis (512 × 512 acquisition matrix, in-plane and resolutions = 0.602–0.869 mm, slice thickness = 1.5–2 mm, 262–929 slices) from 20 individuals with ages between 18 and 45 years (32.9 ± 8.5 years, 9 males and 11 females) were acquired with a Siemens Emotion 16 (Siemens Healthineers, Germany). Patients were positioned in a standard supine position with legs parallel in neutral rotation and received no additional radiation beyond that required for the CT ordered to evaluate their medical condition. The pelvis was reconstructed with 1 mm thickness from the anterosuperior iliac spine to the lesser trochanters. As for symptomatic pelves, MRI scans ((224–256)×(224–256) acquisition matrix, in-plane and resolutions = 0.703–0.804 mm, slice thickness = 0.7–0.8 mm, 96–128 slices) were acquired from 20 individuals with dysplastic hips with ages between 14 and 49 yr (34.0 ± 9.8 years, 6 males and 14 females), and of impinged hips ((224–256)×(224–256) acquisition matrix, in-plane and resolutions = 0.703–0.804 mm, slice thickness = 0.7–0.8 mm, 96–128 slices) from 20 subjects with ages between 21 and 53 yr (38.9 ± 6.8 years, 13 males and 7 females) using a T1-VIBE Fat-suppressed sequence performed by a Siemens MAGNETOM® 3T Verio (Siemens Healthineers, Germany) and an eight-channel body matrix phased-array surface coil (which was placed over the hip of the patient) and a six-channel spine matrix coil (which was integrated in the patient table) were used. As part of the routine MR protocol in patients, a three-dimensional (3D) data set of the whole pelvis was obtained with an axial water excitation true fast imaging with steady-state precession (FISP). MR was performed in standard supine position with legs parallel in neutral rotation. The pelvis was reconstructed with 1 mm thickness slices from the antero-superior iliac spine to the lesser trochanters. All data sets were anonymized. Informed consent was obtained for the use of the CT and MRI data sets from all subjects.

Cam-type deformities at the femoral head-neck junction were defined as an α angle greater than 55° at any location around the femoral neck [9,30]. Pincer type and acetabular dysplasia were considered if lateral center edge angle was greater than 40° or inferior to 20°, respectively [8,10,12]. Mixed FAI cases had both characteristics of Pincer and CAM cases.

2.2. Surface shapes

Based on results from a previous study that indicates that ellipsoids and egg-like shapes are better suited to fit the femoral head when compared to the sphere shape [23], we adopted the same assumption and considered the following shape models: sphere (S), ellipsoid (E) and tapered ellipsoid (TE). These shapes reveal an increasing degree of complexity to account for as many variations as possible within the set of subjects being considered in the study. The mathematical expressions for the considered shapes (implicit representation) are written as

$$\text{sphere } \boldsymbol{F_S}(\boldsymbol{x},\boldsymbol{y},\boldsymbol{z}) = \left(\frac{\boldsymbol{x}}{\boldsymbol{a}}\right)^2 + \left(\frac{\boldsymbol{y}}{\boldsymbol{a}}\right)^2 + \left(\frac{\boldsymbol{z}}{\boldsymbol{a}}\right)^2 \quad (1)$$

$$\text{ellipsoid } \quad \boldsymbol{F_E}(\boldsymbol{x},\boldsymbol{y},\boldsymbol{z}) = \left(\frac{\boldsymbol{x}}{\boldsymbol{a}}\right)^2 + \left(\frac{\boldsymbol{y}}{\boldsymbol{b}}\right)^2 + \left(\frac{\boldsymbol{z}}{\boldsymbol{c}}\right)^2 \quad (2)$$

$$\text{tapered ellipsoid } \quad \boldsymbol{F_{TE}}(\boldsymbol{x},\boldsymbol{y},\boldsymbol{z}) = \left(\frac{\frac{\boldsymbol{x}}{\boldsymbol{a}}}{\boldsymbol{T_x z}+1}\right)^2 + \left(\frac{\frac{\boldsymbol{y}}{\boldsymbol{b}}}{\boldsymbol{T_y z}+1}\right)^2 + \left(\frac{\boldsymbol{z}}{\boldsymbol{c}}\right)^2 \quad (3)$$

where *x, y, z* are the local coordinates of the point in space that belongs to the surface; *a, b, c* represent shape dimensions or semi-axis radii; T_x and T_y are the tapering values in the *x* and *y* directions.

2.3. Surface fitting and error analysis

The surface fitting framework presented by Lopes et al. [23] was used to reconstruct three-dimensional bone structures from the images and to fit well-defined mathematical surfaces (Fig. 1). Note that all the 3D reconstructed articular surface meshes correspond to the interface between cortical bone and cartilage (i.e., geometric modeling does not take into account soft tissues, merely the outer boundary of bony tissue and not the free surface of the articular surface).

From the medical images, each bone structure is segmented separately using a semi-automatic method that relies on active contour evolution [31] using ITK-SNAP software tools (version 3.4). Afterwards, the resulting segmented images were reconstructed into 3D surface meshes in ParaView (version 4.3.1) with the marching cubes algorithm [32,33]. Since the marching cubes meshes present a characteristic stair-step shape surface and an excessive and redundant amount of vertex information, mesh adjustment operations, namely smoothing and decimation, were then applied to the reconstructed 3D surface meshes, in order to guarantee homogeneous nodal distribution and eliminate these artifacts that result from 3D reconstruction from scanned image data. From the 3-D models, which presented non-articular bony surfaces

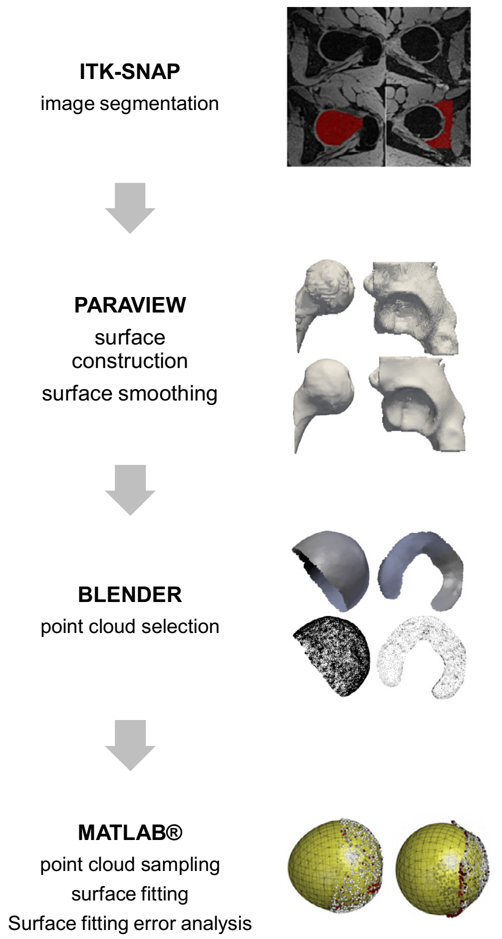

Fig. 1. Image-based surface fitting framework used to extract geometric information of spheroidal articular surfaces of the hip joint. File formats used as input in the software tools consist of DICOM medical images (*.dcm), segmented images (*.mha), triangular surface mesh (*.ply) and point cloud (*.obj).

such as the greater and lesser trochanter, we manually selected the vertices of the articular surfaces and stored them as point clouds using the brush selection tool available on Blender (version 2.75).

In order to identify and characterize the underlying morphology of the point clouds of both femoral head and acetabular cavity, implicit surface shape models (Eqs. 1–3) were adjusted to a cloud of points using a least-squares minimization approach formalized as a nonlinear optimization problem with simple boundary constraints [23]: given a set of points that belong to the outer cortical bone surface, a vector of geometric parameters (i.e., orientation, position, dimension, shape parameters) is determined to minimize the error-of-fit objective function defined as the square sum of residuals, where each residual is the difference between the shape model (Eqs. 1–3) and the corresponding point datum. Due to the non-linearity of the objective function, we approached the minimization problem with a metaheuristic Genetic Algorithm. To guarantee efficient and effective minimizations, close initial approximations in the neighborhood of the global solutions are required. Close initial approximations for sphere and ellipsoid shapes can be obtained by considering a least squares approach with a quadric surface approximation [34], which settles a close approximation of geometric parameters (i.e., position, ellipsoid orientation, sphere radius or ellipsoid radii). To provide a good initial approximation for the tapered ellipsoid, we relied on the observation that a tapered ellipsoid can be obtained by a sequence of morphing operations: an ellipsoid is a rescaled sphere and a tapered ellipsoid is an ellipsoid that lacks a symmetric axis. Thus, the surface fitting process of the tapered ellipsoid was initiated with recourse to the optimal ellipsoid parameters (i.e., position, orientation, radii). It is important to mention that several Genetic Algorithm optimization runs were then carried out to finetune the initial approximation, hence, for every surface fitting case, the optimization algorithm is constrained by boundary constraints, which are defined as simple inequalities affecting the surface parameters and are settled as a set of intervals centered at the good initial approximation and with user-defined limit constants.

Lastly, the comparison between the statistical metrics of goodness-of-fit was assessed according to the surface error, i.e., the signed Euclidean distance of each point in the point clouds to the optimally fitted surface of each shape model, which are computed according to an orthogonal distance optimization framework: points laying on the surface have zero valued distance, points inside the surface have 'negative distances' while points outside have positive valued distances In particular, a statistical analysis was then performed using first-order measures (i.e., mean, standard deviation, minimum and maximum) for each condition and joint structure, whereas paired Student's *t*-test were applied to verify if differences between the surface fitting errors were significant. Both optimization codes were implemented in Matlab® (version R2014a) using the Genetic Algorithm and Direct Search Toolbox^{TM}.

3. Results

The statistical analyses of the surface errors for each condition (asymptomatic, FAI, dysplasia) and articular surface (femoral head, acetabular cavity) was performed to quantify the goodness-of-fit of the considered shape models (S, E, TE). The resulting statistical metrics revealed which shape, along with associated shape parameters, best characterizes the general morphological features of the different hip joints.

Through visual inspection, it was possible to perform an initial assessment of the overall goodness-of-fit of the shape models to the femoral head (Fig. 2) and acetabular cavity (Fig. 3). In general, all shape models closely approximated the different anatomical structures. To assist visual inspection, a color map was designed to encode the signed Euclidean distance between each point to the closest point on the approximated surface (Figs. 2–3). Therefore, the point clouds representing the femoral head and acetabular cavity are much better approximated by primitives with less spherical geometric features, being the tapered ellipsoid the most well-adjusted shape.

Regarding the quantitative analysis of surface fitting errors for the three shape models, the statistical assessment relied on the first-order measures (i.e., mean, standard deviation, minimum and maximum) for the whole population of each condition and joint structure (Tables 1–2). The average surface fitting errors followed a similar pattern reported by Lopes et al. [23]: the sphere shape fits worse than its morphological cousins, whereas the ovoidal shape fits best (Table 1-2).

Table 1 - Surface fitting errors statistical analysis of the femoral head for each shape and total number of subjects considered in the study. All metrics are represented in millimeters (mm). The mean and standard deviation are calculated for the absolute value of the surface error. Min and Max values are represented based on the minimal signed Euclidean distances calculated between each point and the optimal fitted shape. (S - Sphere; E - Ellipsoid; TE - Tapered Ellipsoid).

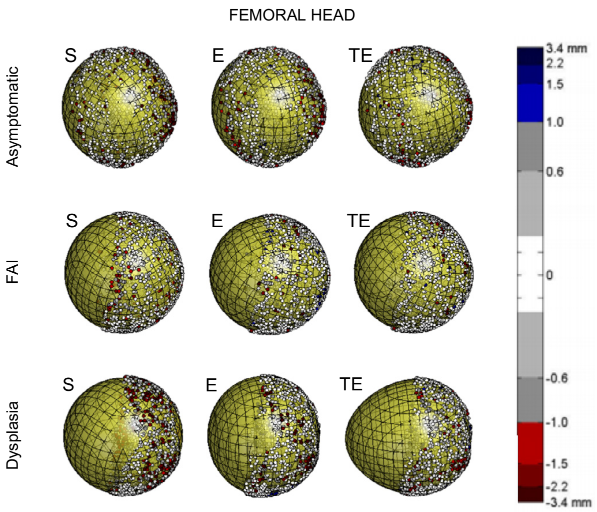

Fig. 2. 3-D view of the optimally fitted surfaces for the femoral head of asymptomatic, FAI and dysplastic hips. Each point cloud corresponds to the femoral head of the first subject of each hip population. Surface error color map: points inside the surface are represented in red; points outside the surface are colored in blue; remaining points whose distance to the surface is between −1.0 mm and 1.0 mm are represented in a gray scale; white corresponds to points with surface errors in the vicinity of 0.0 mm; maximum (+3.4 mm) and minimum (−3.4 mm) surface errors computed for all subjects, shapes, and articular surfaces delimit the color map. (For interpretation of the references to color in this figure legend, the reader is referred to the web version of this article).

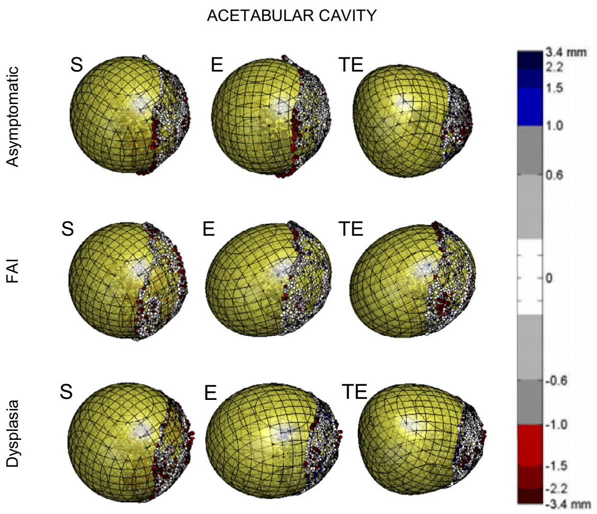

Fig. 3. Fig. 3. 3-D view of the optimally fitted surfaces for the acetabular cavity of asymptomatic, FAI and dysplastic hips. Each point cloud corresponds to the acetabular cavity of the first subject of each hip population. Surface error color map: points inside the surface are represented in red; points outside the surface are colored in blue; remaining points whose distance to the surface is between −1.0 mm and 1.0 mm are represented in a gray scale; white corresponds to points with surface errors in the vicinity of 0.0 mm; maximum (+3.4 mm) and minimum (−3.4 mm) surface errors computed for all subjects, shapes, and articular surfaces delimit the color map. (For interpretation of the references to color in this figure legend, the reader is referred to the web version of this article).

Table 1
Surface fitting errors statistical analysis of the femoral head for each shape and total number of subjects considered in the study. All metrics are represented in millimeters (mm). (S - Sphere; E - Ellipsoid; TE - Tapered Ellipsoid).

Femoral head					
Type	# Subjects		S	E	TE
Asymptomatic	20	μ	0.653	0.591	0.538
		σ	0.575	0.544	0.520
		Min	−3.464	−2.857	−2.831
		Max	1.592	3.464	3.464
FAI	20	μ	0.521	0.458	0.414
		σ	0.476	0.445	0.418
		Min	−3.464	−3.426	−2.874
		Max	-2.7×10^{-5}	2.787	2.892
FAI (cam)	7	μ	0.534	0.479	0.431
		σ	0.489	0.449	0.425
		Min	−3.461	−3.426	−2.874
		Max	-4.4×10^{-5}	2.787	2.672
FAI (pincer)	6	μ	0.515	0.478	0.429
		σ	0.450	0.443	0.415
		Min	−2.702	−2.624	−2.293
		Max	-4.1×10^{-5}	2.191	2.405
FAI (mixed)	7	μ	0.512	0.419	0.385
		σ	0.485	0.440	0.413
		Min	−3.464	−3.178	−2.718
		Max	-2.7×10^{-5}	2.525	2.892
Dysplasia	20	μ	0.578	0.459	0.449
		σ	0.485	0.434	0.430
		Min	−2.850	−2.806	−2.698
		Max	2.500	2.776	2.621

Table 2
Surface fitting errors statistical analysis of the acetabular cavity for each shape and total number of subjects considered in the study. All metrics are represented in millimeters (mm). (S - Sphere; E - Ellipsoid; TE - Tapered Ellipsoid).

Acetabular cavity					
Type	# Subjects		S	E	TE
Asymptomatic	20	μ	0.789	0.640	0.611
		σ	0.552	0.508	0.491
		Min	−3.464	−3.458	−3.449
		Max	-3.0×10^{-5}	2.789	2.943
FAI	20	μ	0.742	0.606	0.570
		σ	0.524	0.479	0.467
		Min	−3.240	−2.980	−2.726
		Max	2.301	2.612	2.600
FAI (cam)	7	μ	0.773	0.631	0.592
		σ	0.542	0.497	0.476
		Min	−3.146	−2.980	−2.684
		Max	2.301	2.612	2.600
FAI (pincer)	6	μ	0.653	0.547	0.525
		σ	0.482	0.450	0.447
		Min	−2.774	−2.711	−2.726
		Max	0.685	2.317	2.476
FAI (mixed)	7	μ	0.788	0.632	0.587
		σ	0.531	0.480	0.474
		Min	−3.240	−2.827	−2.622
		Max	-6.9×10^{-5}	2.473	2.538
Dysplasia	20	μ	0.740	0.602	0.580
		σ	0.536	0.488	0.485
		Min	−3.432	−2.921	−3.001
		Max	0.834	2.734	2.605

Table 2 - Surface fitting errors statistical analysis of the acetabular cavity for each shape and total number of subjects considered in the study. The mean and standard deviation are calculated for the absolute value of the surface error. Min and Max values are represented based on the minimal signed Euclidean distances calculated between each point and the optimal fitted shape. All metrics are represented in millimeters (mm). (S - Sphere; E - Ellipsoid; TE - Tapered Ellipsoid).

Table 3
The p-values relative to the statistical significance of the differences between fitting errors for all shape models for the femoral head and acetabular cavity, using a paired Student *t*-test with statistical significance set at $p < 0.05$. (S - Sphere; E - Ellipsoid; TE - Tapered Ellipsoid).

	Femoral head		Acetabular cavity	
Asymptomatic	S ↔ E	0.000	S ↔ E	0.000
	S ↔ TE	0.000	S ↔ TE	0.609
	E ↔ TE	0.000	E ↔ TE	0.000
FAI	S ↔ E	0.000	S ↔ E	0.000
	S ↔ TE	0.000	S ↔ TE	0.000
	E ↔ TE	0.005	E ↔ TE	0.011
Dysplasia	S ↔ E	0.000	S ↔ E	0.000
	S ↔ TE	0.000	S ↔ TE	0.000
	E ↔ TE	0.005	E ↔ TE	0.123

Relatively to the femoral head, the paired Student's *t*-test used to corroborate the significance of the statistical analysis revealed that the differences between the surface fitting parameters of all pairs of shapes for all conditions were significant ($p\text{-value} < 0.05$) between sphere ↔ ellipsoid, sphere ↔ tapered ellipsoid and also ellipsoid ↔ tapered ellipsoid shapes for all conditions (Table 3). Regarding the statistical significance of the differences in surface fitting errors for the acetabular cavity, in the asymptomatic case, these were significant for the pairs sphere ↔ ellipsoid and ellipsoid ↔ tapered ellipsoid. The pair ellipsoid ↔ tapered ellipsoid presented no statistically significant difference. For the population presenting FAI, the pairs which presented statistical significance were sphere ↔ ellipsoid and sphere ↔ tapered ellipsoid. Finally, subjects with dysplatic hips revealed statistical significance between the surface fitting errors of two pairs of shape models, sphere ↔ ellipsoid and sphere ↔ ellipsoid, while the pair of shapes ellipsoid ↔ tapered ellipsoid exhibited no statistically significant difference.

4. Discussion

The conducted morphological study revealed that the adjustment of the spherical shape to the two articular surfaces to be the worst among the hierarchy of shape models, regardless of the clinical case. On the other hand, ovoidal shapes approximated well not only to the femoral head but also to the acetabular cavity, thus validating MacConaill's assumption for synovial joint classification [25]. Results regarding the geometric parameters of the best-approximated surfaces and the surface fitting errors were considered reliable, given that their order of magnitude was identical to results from other morphological studies of the hip joint [19–23]. This work allowed the comparison of two conditions, revealing that, in general, articular surfaces of hip joints presenting femoroacetabular impingement approximated better to the tapered ellipsoidal shape than dysplastic hips.

Transversal to all three conditions and articular joint surfaces, the following pattern of decreasing surface fitting error arises (i.e., from spherical to ovoidal): $S > E > TE$. Regarding the considered hip conditions for both femoral head and acetabular cavity, asymptomatic hips have a lesser goodness-of-fit than dysplastic and impinged hips. The FAI presenting population obtained the lowest values of average values of the surface fitting errors for the sphere and tapered ellipsoid models. The lowest fitting error belonged to the fitting of the tapered ellipsoid to the FAI presenting population. The dysplastic population followed the same pattern, as did the asymptomatic, which presented the highest fitting errors of the three. A careful look into the average error values shows that dysplastic hips revealed better approximation to all the geometric primitives than the two remaining populations. In the acetabular case, the population for which the lowest fitting errors were obtained was the FAI diagnosed one, which is compliant with the results already seen for the femoral case. Similarly, the shape that fitted the point clouds better for all sets of subjects was the tapered ellipsoid. Therefore, the main novelty of this work consists of introducing shapes with axial asymmetry into morphological studies of asymptomatic, impinged and dysplastic hips. In addition, both articular surfaces of the hip joint were considered.

The major limitation of this work is that more data sets are required to provide a greater statistical significance; in particular an equitative number of FAI cases is required to promote a more fair comparison between cam, pincer, and mixed hips. Nevertheless, the surface fitting error results are at par with other morphology studies which consider non-spherical shapes to better represent femoral and acetabular joint components [19–23]. More importantly, these results question the usefulness of traditional metrics (e.g., α angle, center-edge angle, acetabular index of Tönnis), which describe hip geometry based on the bi-dimensional shapes (i.e., center-side of Wiberg assumes that the femoral head is circular), the systematic errors introduced when performing bi-dimensional measurements could be greater than errors produced by more reliable surface fitting methods based on ovoidal shapes. As future work, ovoidal shapes may also inspire software tools to support ovoidal shape metrics to fabricate personalized endoprosthesis with ovoidal shapes with subject-specific dimensions and curvatures. In addition, we expect to extend the surface fitting framework to also incorporate cartilage surface as this could lead towards new and interesting questions regarding the correlation between cartilaginous surface and bony surface, namely, If cartilage thickness compensates the lack of bony asphericity or simply follows the underlying bony shape, and if this hypothetic correlation is consistent between healthy and unhealthy hips.

Conflicts of interest

Competing interests: None declared.

Ethical approval

This study was approved by the Ethics Research Committee of the Nova Medical School | Faculdade de Ciências Médicas da Universidade Nova de Lisboa (CEFCM) under the Project entitled "DEFORMIDADES COXO-FEMURAIS E CONFLITO FEMUROACETABULAR: contributo epidemiológico, diagnóstico e prognóstico" with reference nr.61/2014/CEFCM.

Acknowledgments

All authors are thankful for the financial support given by Portuguese Foundation for Science and Technology (FCT). In particular, the first author thanks for the postdoctoral grant SFRH/BPD/97449/2013. This work was also partially supported by national funds through FCT with reference UID/CEC/50021/2013 and IT-MEDEX - PTDC/EEI-SII/6038/2014.

Reference

[1] Zeng W-N, Wang F-Y, Chen C, Zhang Y, Gong XY, Zhou K, et al. Investigation of association between hip morphology and prevalence of osteoarthritis. Sci Rep 2016;6:23477.
[2] Ganz R, Parvizi J, Beck M, Leunig M, Nötzli H, Siebenrock KA. Femoroacetabular impingement: a cause for osteoarthritis of the hip. Clin Orthop Relat Res 2003;417:112–20.
[3] Gosvig KK, Jacobsen S, Palm H, Sonne-Holm S, Magnusson E. A new radiological index for assessing asphericity of the femoral head in cam impingement. Bone Joint J 2007;89(10):1309–16.
[4] Peters CL, Erickson JA, Anderson L, Anderson AA, Weiss J. Hip-preserving surgery: understanding complex pathomorphology. J Bone Joint Surg Am 2009;91(Supplement 6):42–58.

[5] Laborie LB, IØ Engesæter, Lehmann TG, Sera F, Dezateux C, Engesæter LB, et al. Radiographic measurements of hip dysplasia at skeletal maturity—new reference intervals based on 2,038 19-year-old Norwegians. Skeletal Radiol 2013;42(7):925–35.
[6] Jorge JP, Simões FMF, Pires EB, Rego PA, Tavares DG, Lopes DS, et al. Finite element simulations of a hip joint with femoroacetabular impingement. Comput Methods Biomech Biomed Eng 2014;17(11):1275–84.
[7] Tannast M, Hanke MS, Zheng G, Steppacher SD, Siebenrock KA. What are the radiographic reference values for acetabular under-and overcoverage? Clin Orthop Relat Res 2015;473(4):1234–46.
[8] Mascarenhas VV, Rego P, Dantas P, Morais F, McWilliams J, Collado D, et al. Imaging prevalence of femoroacetabular impingement in symptomatic patients, athletes, and asymptomatic individuals: a systematic review. Eur J Radiol 2015;85(1):73–95.
[9] Mascarenhas VV, Rego P, Dantas P, Gaspar A, Soldado F, Consciência JG. Cam deformity and the omega angle, a novel quantitative measurement of femoral head-neck morphology: a 3D CT gender analysis in asymptomatic subjects. Eur Radiol 2017;27(5):2011–23.
[10] Laborie LB, Lehmann TG, Engesæter IØ, Eastwood DM, Engesæter LB, Rosendahl K. Prevalence of radiographic findings thought to be associated with femoroacetabular impingement in a population-based cohort of 2081 healthy young adults. Radiology 2011;260(2):494–502.
[11] Frank JM, Harris JD, Erickson BJ, Slikker W, Bush-Joseph CA, Salata MJ, et al. Prevalence of femoroacetabular impingement imaging findings in asymptomatic volunteers: a systematic review. Arthroscopy 2015;31(6):1199–204.
[12] Loder RT, Skopelja EN. The epidemiology and demographics of hip dysplasia. ISRN Orthop 2011;2011:238607.
[13] Clohisy JC, Carlisle JC, Beaulé PE, Kim YJ, Trousdale RT, Sierra RJ, et al. A systematic approach to the plain radiographic evaluation of the young adult hip. J Bone Joint Surg Am 2008;90(Suppl. 4):47–66.
[14] Chegini S, Beck M, Ferguson SJ. The effects of impingement and dysplasia on stress distributions in the hip joint during sitting and walking: a finite element analysis. J Orthop Res 2009;27(2):195–201.
[15] Gerhardt MB, Romero AA, Silvers HJ, Harris DJ, Watanabe D, Mandelbaum BR. The prevalence of radiographic hip abnormalities in elite soccer players. Am J Sports Med 2012;40(3):584–8.
[16] Ng KG, Lamontagne M, Labrosse MR, Beaulé PE. Hip joint stresses due to cam–type femoroacetabular impingement: a systematic review of finite element simulations. PLoS One 2016;11(1):e0147813.
[17] Rego PRA, Mascarenhas V, Oliveira FS, Pinto PC, Gaspar A, Ovídio J, et al. Morphologic and angular planning for cam resection in femoro-acetabular impingement: value of the omega angle. Int Orthop 2016;40(10):2011–17.
[18] Harris MD, Reese SP, Peters CL, Weiss JA, Anderson AE. Three-dimensional quantification of femoral head shape in controls and patients with cam-type femoroacetabular impingement. Ann Biomed Eng 2013;41(6):1162–71.
[19] Cerveri P, Manzotti A, Baroni G. Patient-specific acetabular shape modelling: comparison among sphere, ellipsoid and conchoid parameterisations. Comput Methods Biomech Biomed Eng 2014;17(5):560–7.
[20] Gu D, Chen Y, Dai K, Zhang S, Yuan J. The shape of the acetabular cartilage surface: a geometric morphometric study using three-dimensional scanning. Med Eng Phys 2008;30(8):1024–31.
[21] Liu B, Hua S, Zhang H, Liu Z, Zhao X, Zhang B, et al. A personalized ellipsoid modeling method and matching error analysis for the artificial femoral head design. Comput Aided Des 2014;56:88–103.
[22] Liu B, Zhang H, Hua S, Jiang Q, Huang R, Liu W, et al. An automatic segmentation system of acetabulum in sequential CT images for the personalized artificial femoral head design. Comput Methods Programs Biomed 2015;127:318–35.
[23] Lopes DS, Neptune RR, Gonçalves AA, Ambrósio JA, Silva MT. Shape analysis of the femoral head: a comparative study between spherical, (Super) ellipsoidal, and (Super) ovoidal shapes. J Biomech Eng 2015;137(11):114504.
[24] Menschik F. The hip joint as a conchoid shape. J Biomech 1997;30(9):971–3.
[25] MacConaill MA. A structuro-functional classification of synovial articular units. Ir J Med Sci 1973;142(1):19–26.
[26] Standring S. Gray's anatomy: the anatomical basis of clinical practice. 41st Ed. Elsevier; 2016.
[27] Rouvière H, Delmas A. Anatomía humana: descriptiva, topográfica y funcional. 11th Ed. Barcelona: Masson; 2005.
[28] Williams GM, Chan EF, Temple-Wong MM, Bae WC, Masuda K, Bugbee WD, et al. Shape, loading, and motion in the bioengineering design, fabrication, and testing of personalized synovial joints. J Biomech 2010;43(1):156–65.
[29] Röling MA, Visser MI, Oei EH, Pilot P, Kleinrensink G-J, Bloem RM. A quantitative non-invasive assessment of femoroacetabular impingement with CT-based dynamic simulation cadaveric validation study. BMC Musculoskelet Disord 2015;16:50.
[30] Sutter R, Dietrich TJ, Zingg PO, Pfirrmann CWA. How useful is the alpha angle for discriminating between symptomatic patients with cam–type femoroacetabular impingement and asymptomatic volunteers? Radiology 2012;264(2):514–21.
[31] Yushkevich PA, Piven J, Hazlett HC, Smith RG, Ho S, Gee JC, et al. User-guided 3D active contour segmentation of anatomical structures: significantly improved efficiency and reliability. Neuroimage 2006;31(3):1116–28.
[32] Lorensen WE, Cline HE. Marching cubes: a high resolution 3D surface construction algorithm. In ACM SIGGRAPH Comput Graph 1987;21(4):163–9.
[33] Ahrens J, Geveci B, Law C. 36 Paraview: An end user tool for large-data visualization. In: Hansen Charles D, Johnson Chris R, editors. The Visualization Handbook. Elsevier; 2005. p. 717–31.
[34] Dai M, Newman TS. Hyperbolic and parabolic quadric surface fitting algorithms: comparison between the least squares approach and the parameter optimization approach; 2008. UAH CS Technical Report.

CHAPTER 5.2

This chapter is based on the following paper:

"Can we discriminate symptomatic hip patients from asymptomatic volunteers based on anatomical predictors? – A 3D MRI Study On Cam, Pincer And Spinopelvic Parameters"
American Journal of Sports Medicine 2018/247254

VIDEO Abstract

Can We Discriminate Symptomatic Hip Patients From Asymptomatic Volunteers Based on Anatomic Predictors?

A 3-Dimensional Magnetic Resonance Study on Cam, Pincer, and Spinopelvic Parameters

Vasco V. Mascarenhas,*† MD, MSc, MBA, Paulo Rego,‡ MD, PhD, Pedro Dantas,§ MD, António P. Caetano,‖ MD, Lennart Jans,¶ MD, PhD, Reto Sutter,# MD, Rui Mateus Marques,** MD, PhD, Olufemi R. Ayeni,†† MD, PhD, and J. Guimarães Consciência,** MD, PhD
Investigation performed at Hospital da Luz, Lisbon, Portugal

Background: Given the high prevalence of patients with hip deformities and no ongoing hip dysfunction, understanding the anatomic factors predicting the symptomatic state is critical. One such variable is how the spinopelvic parameters (SPPs) may interplay with hip anatomic factors.

Hypothesis/Purpose: SPPs and femoral- and acetabular-specific parameters may predict which patients will become symptomatic. The purpose was to determine which anatomic characteristics with specific cutoffs were associated with hip symptom development and how these parameters relate to each other.

Study Design: Cohort study (Diagnosis); Level of evidence, 2.

Methods: 548 participants were designated either symptomatic patients (n = 176, scheduled for surgery with hip pain and/or functional limitation) or asymptomatic volunteers (n = 372, no pain) and underwent 3-dimensional magnetic resonance imaging. Multiple femoral (α angle, Ω angle, neck angle, torsion), acetabular (version, coverage), and spinopelvic (pelvic tilt, sacral slope [SS], pelvic incidence) parameters were measured semiautomatically. Normative values, optimal differentiating thresholds, and a logistic regression analysis were computed.

Results: Symptomatic patients had larger cam deformities (defined by increased Ω angle and α angle), smaller acetabular coverage, and larger pelvic incidence and SS angles compared with the asymptomatic volunteers. Discriminant receiver operating characteristic analysis confirmed that radial 2-o'clock α angle (threshold 58°-60°, sensitivity 75%-60%, specificity 80%-84%; area under the curve [AUC] = 0.831), Ω angle (threshold 43°, sensitivity 72%, specificity 70%; AUC = 0.830), acetabular inclination (threshold 6°, sensitivity 65%, specificity 70%; AUC = 0.709), and SS (threshold 44°, sensitivity 72%, specificity 75%; AUC = 0.801) ($P < .005$) were the best parameters to classify participants. When parameters were entered into a logistic regression, significant positive predictors for the symptomatic patients were achieved for SS, acetabular inclination, Ω angle, and α angle at 2-o'clock, correctly classifying 85% of cases (model sensitivity 72%, specificity 91%; AUC = 0.919).

Conclusion: Complex dynamic interplay exists between the hip and SPPs. A cam deformity, acetabular undercoverage, and increased SPP angles are predictive of a hip symptomatic state. SPPs were significant to discriminate between participants and were important in combination with other hip deformities. Symptomatic patients can be effectively differentiated from asymptomatic volunteers based on predictive anatomic factors.

Keywords: hip; femoroacetabular impingement; spinopelvic; reference values

Femoroacetabular impingement (FAI) syndrome, a motion-related hip disorder with specific symptoms, clinical signs, and imaging findings,[19] originates from contact between the acetabulum and the proximal femur. Because not all hips with cam or pincer morphology are symptomatic[32,33] or develop degenerative changes,[2] it is critical to distinguish between patients with FAI syndrome and healthy

The American Journal of Sports Medicine
2018;46(13):3097–3110
DOI: 10.1177/0363546518800825

subjects whose osseous structure is merely abnormal. The hip joints are part of the bony pelvis that moves around the bicoxofemoral axis, leading to dynamic tilting in different functional situations.[47] This suggests the need to consider the relationship between hip disease or injury and individual spinopelvic interactions.

Early diagnosis and imaging of the relevant bony structure with adequate guidance for treatment are essential, because FAI syndrome has been associated with functional impairment, irreversible cartilage damage, and premature osteoarthritis (OA).[1] High-priority issues to define the natural history of FAI syndrome include establishing morphological factors to predict who will develop hip symptoms and establishing a precise definition of FAI syndrome.[19] Concurrently, other factors are increasingly recognized as contributors to the dynamic pathological process, among which spinopelvic parameters (SPPs) are considered to be fundamental indicators of pelvic alignment and sagittal function.[47]

Several quantitative measurements for cam and pincer morphology have been proposed,[34,45,52,53] but the α angle[42] and lateral center edge angle (LCEA)[53] are most commonly used.[2] For pelvic radiographs and other modalities, an α-angle threshold of 55° to 60° is generally used,[3,42,49] although with important limitations,[32,50] underlining the need for more research to validate the presence and interchangeability of a cam deformity diagnosis between different modalities. This is particularly challenging for the acetabulum, which has many variations on its hemispherical size, shape, and structure, as well as rim contour irregularities and orientation abnormalities.[27,52] Again, the most appropriate measurements and accompanying threshold values remain to be defined.[32]

SPPs such as pelvic incidence[29] (PI) have recently been associated with specific hip morphologic features[13,23,35] and OA.[14] PI is a fixed individual angle regarded as a primary axis of spinopelvic sagittal balance.[47] Decreased PI has been associated with FAI morphology[13,47]; however, other studies reported opposite observations, namely that increased PI is associated with cam morphology.[18,39] Interestingly, increased prevalence of OA has also been linked with higher PI.[14] Therefore, it is still unknown whether and how SPPs influence hip disease and injury.

Regarding diagnostic methods, it is accepted that further research is needed to provide insight on the utility of imaging in this setting.[19] Conventional radiographs have been tested in different views[9,53]; however, characterization of the hip is more accurate with computed tomography (CT) and magnetic resonance imaging (MRI).[32] In fact, cross-sectional imaging provides a 3-dimensional (3D) perspective of the hip bone,[6,59,60] which allows for a more precise definition of the nature, location, and extent of morphological abnormalities.[6,50] Accurate assessment of the hip with quantitative imaging is critical for early diagnosis, providing a means for standardization and reducing variability.[19,34]

This study's purpose is to evaluate the morphological distinction between patients with hip pain and asymptomatic volunteers[50] by using semiautomated 3D MRI. Additionally, our study focuses on the application of this morphometric analysis for evaluating FAI and spinopelvic relations, which has not been previously described.

Using a 3D MRI technique, this study aims to (A) provide hip and spinopelvic normative measurements in asymptomatic volunteers and symptomatic patients, (B) objectively compare pathoanatomic characteristics in these populations, and (C) develop potential distinguishing threshold values to differentiate these populations by ascertaining which parameters are most useful and how they should be used to achieve best results.

METHODS

Study Population

This prospective case-control study was approved by the institutional review board (nr.61/2014/CEFCM). All individuals signed informed consent. Consecutive asymptomatic volunteers and symptomatic patients undergoing hip surgery were enrolled. All symptomatic patients were identified and matched for age and sex in a 1:2 enrollment ratio with a group of asymptomatic volunteers (Figure 1).

The asymptomatic volunteer group was recruited among consecutive adult patients undergoing MRI at multiple centers from our health group for abdominal or urogenital indications. All eligible participants completed the nonarthritic hip score questionnaire[8] and another questionnaire regarding demographics and clinical history (including current or past hip or groin pain, orthopaedic conditions, childhood hip disease and/or hip trauma). Exclusion criteria included (1) subjects older than 50 and younger than 15 years; (2) all subjects with less than the maximum possible nonarthritic hip score (100); (3) positive answer to 1 or more of the other hip-related questions; (4) MRI signs of OA or other hip pathologies (defined as the

*Address correspondence to Vasco Vogado Mascarenhas, MD, MSc, MBA, MSK Imaging Unit (UIME), Imaging Center, Hospital da Luz, Rua Artilharia Um, 71-77 Lt 6 Bloco A 3, 1250-039 Lisbon, Portugal (email: mascarenhas.vasco@gmail.com).
†MSK Imaging Unit (UIME), Imaging Center, Hospital da Luz, Lisbon, Portugal.
‡Department of Orthopaedic Surgery, Hospital da Luz, Lisbon, Portugal.
§Hospital CUF Descobertas, Lisbon, Portugal.
‖Hospital Curry Cabral, Lisbon, Portugal.
¶Department of Radiology, Ghent University Hospital, Ghent, Belgium.
#Department of Radiology, Balgrist University Hospital, University of Zurich, Zurich, Switzerland.
**NOVA Medical School, Lisbon, Portugal.
††Division of Orthopaedic Surgery, Department of Surgery, McMaster University, Hamilton, Ontario, Canada.

The authors declared that they have no conflicts of interest in the authorship and publication of this contribution. AOSSM checks author disclosures against the Open Payments Database (OPD). AOSSM has not conducted an independent investigation on the OPD and disclaims any liability or responsibility relating thereto.

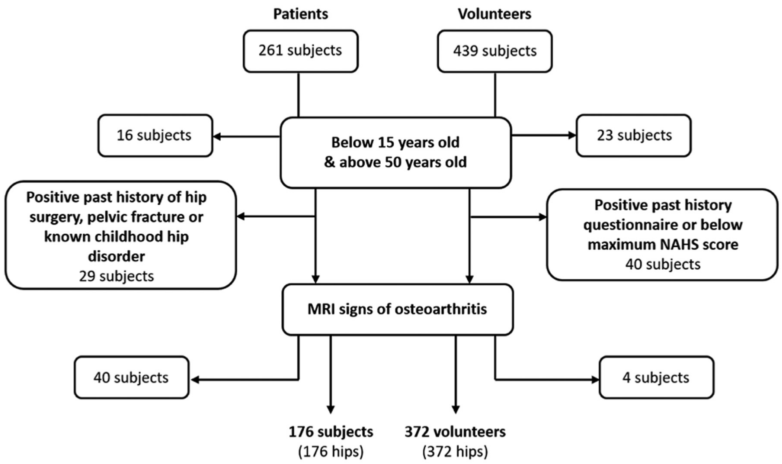

Figure 1. Flow of subjects from cohort inclusion to the final study population.

presence of at least 1 of the following findings: joint-space narrowing, osteophytes, subchondral bone changes [including sclerosis or cysts], fracture, posttraumatic deformity, Perthes disease, osteonecrosis, slipped femoral epiphysis).

The symptomatic patient group consisted of individuals who were referred for MRI of the hip by orthopaedic surgeons between 2012 and 2017 and with preliminary surgical indication. Inclusion criteria were age from 15 to 50 years, typical symptoms (persistent groin pain for >3 months in duration), and clinical signs (positive impingement test)[19] of FAI. Exclusion criteria were the same as for the asymptomatic group concerning criteria 1 and 4.

MRI and 3D Model

MRI was performed with the patients in standard supine position with legs parallel in neutral rotation. The pelvis was reconstructed with 1-mm-thick slices from the anterosuperior iliac spine to the lesser trochanters.

The assessment used a 3-T system (Magnetom Verio; Siemens Healthcare); an 8-channel, body matrix, phased-array surface coil (which was placed over the hip of the patient); and a 6-channel, spine matrix coil (which was integrated in the patient examination table). As part of the routine MRI protocol in patients, a 3D data set of the whole pelvis was obtained with a sequence consisting of axial water excitation true fast imaging with steady-state precession (this was the only sequence performed in the asymptomatic volunteer group).

Image Analysis

Images were uploaded for analysis and semiautomatically segmented by use of Articulis (Clinical Graphics), which was previously validated for reliability and accuracy.[48] One musculoskeletal radiologist (V.V.M., 10 years of experience) certified that each segmentation contained all osseous contours and accurate MRI measurements.

TABLE 1
Summary of Measured Anatomic Parameters

Variables	
Femoral	Ω angle for a 55° α-angle threshold, Ω angle for a 60° α-angle threshold (deg)
	α angle (360° around the femoral head-neck junction) (deg)
	Femoral head and neck diameter (mm)
	Cervicodiaphyseal angle (deg)
	Femoral version (deg)
Acetabular	Acetabular coverage (anterior, posterior, and total) (%)
	Acetabular version (upper, center) (deg)
	Acetabular inclination angle (deg)
	Lateral center edge (1-, 12-, 11-o'clock positions) (deg)
	Acetabular cup diameter (mm)
Spinopelvic	Pelvic incidence (deg)
	Pelvic tilt (deg)
	Sacral slope (deg)

The full workflow diagram for automated extraction of the 3D bone morphology of the hip and measurements involved (1) an active shape, model-based, bone segmentation pipeline[59] construction of a 3D local coordinate system; (2) automatic MRI reformation; and (3) variable measurements according to a previously published protocol[32] (Table 1).

Femoral Parameters

To determine the Ω angle, we calculated the clockwise 360° α angle (according to Nötzli et al[42]) by using a regression sphere fit of the femoral head-neck (FHN) junction. Next, projecting the 360° α angle in a polar plot, we determined

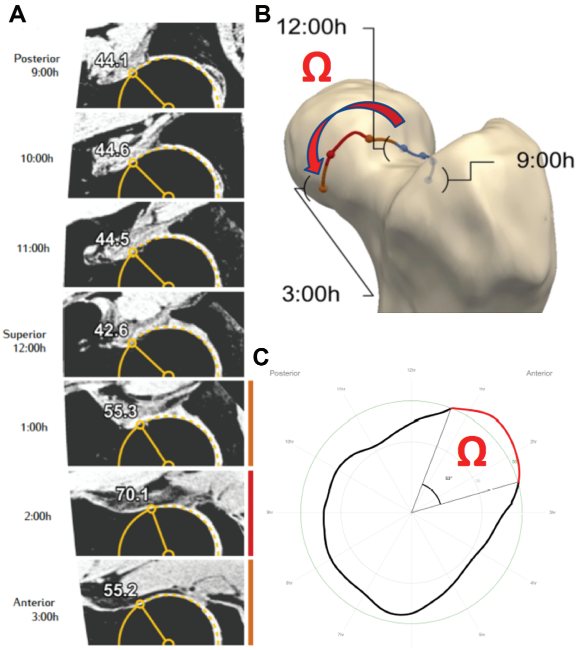

Figure 2. (A) α-angle measurements made at different points around the femoral head-neck junction starting at 9-o'clock (posterior); 10-, 11-, and 12-o'clock (superior); and 1-, 2-, and 3-o'clock (anterior). (B) 3D model representing the radial extension of the cam deformity (curved arrow corresponding to the Ω angle). (C) Polar plot of the 360° α angle, representing the Ω angle (red symbol) for an α-angle threshold of 55°. The red line represents increased α angles for a given threshold.

the Ω angle[34,45] (Figure 2). The Ω angle is formed by 2 lines intersecting the center of the femoral neck at the level of the head-neck junction. The most posterior line posteriorly intersects the point at which the α angle begins to be abnormal beyond a best-fitting circle and the anterior line at the point where the α angle returns to normal. Femoral version, head-neck femoral diameters, and the cervicodiaphyseal angle were measured semiautomatically. Malversion was defined as abnormal if less than 10° or more than 25°.[30]

Cam-type morphology was defined as an α angle greater than 55° at any location around the femoral neck,[42] although we considered additional thresholds (namely 65° and 60°).[3,49]

Acetabular Parameters

Acetabular inclination or sourcil angle (ACinc) and version at the center and upper hemisphere (center and upper ACvers) were derived from the coordinate frame by the software comparing it with the anterior pelvic plane (APP).[30] Acetabular craniocaudal coverage (ACcov) was calculated and determined as a percentage of the femoral head surface.[32]

The LCEA was measured between the plane of the y-axis of the pelvis and a line from the center of a regression sphere in the acetabulum to the osseous acetabular rim, performed in 30° steps from the 1- to 11-o'clock positions.[32]

Global pincer-type morphology was considered positive when we observed any of the following: (1) acetabular depth 3 mm or more (coxa profunda), (2) LCEA greater than 39°, (3) center ACvers less than 10°, (4) upper ACvers less than 0° (acetabular retroversion, which also defined the focal pincer subgroup). Acetabular dysplasia was defined as LCEA 20° or less; borderline dysplasia was defined as LCEA more than 20° and less than or equal to 25°.[31,40,52]

Pelvic Parameters

The measurements of interest included PI, sacral slope (SS), and spinopelvic tilt (SPT) according to a previously described method.[29] After the APP was established, the left and right hip joint centers were identified in all planes and aligned by tilting the pelvis in multiplanar reformats (a line was traced to join the 2 centers and establish the bicoxofemoral axis). PI and SS were determined, and SPT was calculated as PI minus SS (Figure 3).

Statistical Analysis

For all parameters, descriptive statistics were calculated. Quantitative parameters are described by their mean and standard deviation (SD). Qualitative parameters are described in numbers and percentages. For the mean comparisons, the Student t test was implemented to compare quantitative variables (if test conditions were not met, a nonparametric method was used, namely Mann-Whitney or Wilcoxon test). To evaluate correlation between 2 quantitative parameters, Pearson or Spearman coefficients were computed. All morphological measurements associated with the symptomatic state in the receiver operating characteristic (ROC) curve analysis and univariate analysis with $P < .1$ were included in a multivariate logistic regression, with backward selection using the likelihood ratio test to evaluate associations linking the symptomatic state to other variables.

Intertechnique (manual measurements and semiautomated analysis), interobserver, and intraobserver coefficients were identified. The data were concealed, and some anatomic parameters (SS, SPT, PI, LCEA at 12-o'clock, sourcil angle, and α angle 1:30-o'clock) were measured by 2 observers in a subset of 50 symptomatic patients, with 1 observer performing a second set of readings 2 weeks after the first. A P value of .05 was considered statistically significant for all analyses. Statistical analyses were performed by use of dedicated software (SPSS Statistics Version 24; IBM).

RESULTS

Population and Overall Morphologic Findings

The study population consisted of 548 individuals (Table 2): 176 symptomatic patients and 372 weight-, age-, and

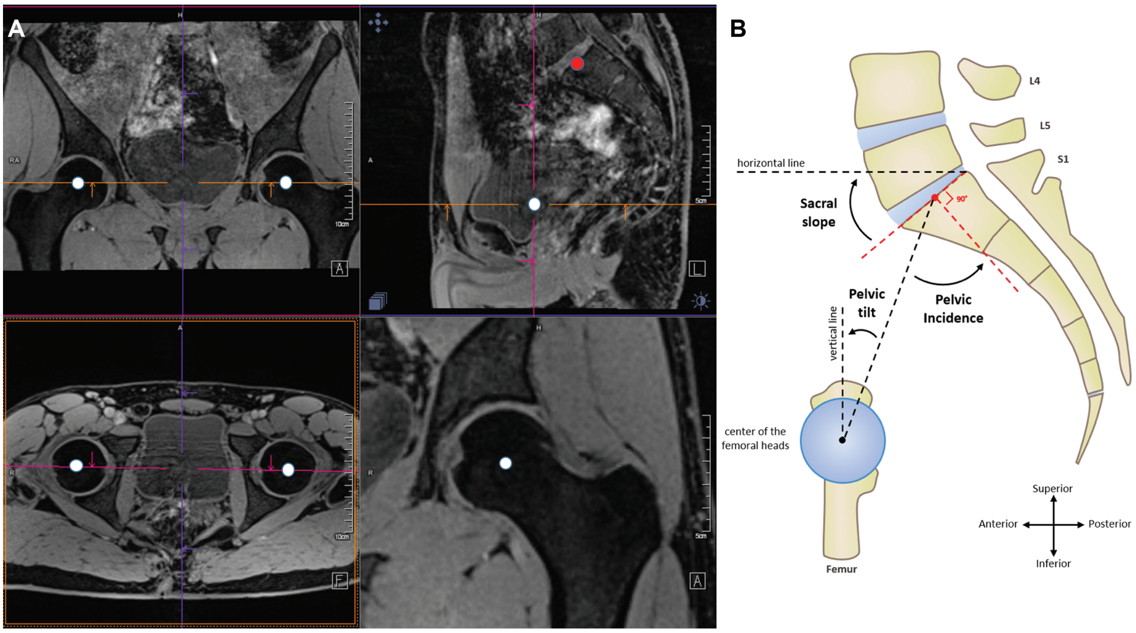

Figure 3. (A) The left hip joint center and right hip joint center (white dots) were located and aligned to determine the bicoxofemoral axis as a single point in the sagittal plane (upper right image; white dot). This point (representing the bicoxofemoral axis) was then connected to the center of the sacral endplate (shaded dot), and additional lines were joined to measure the spinopelvic tilt, sacral slope, and pelvic incidence. (B) Schematic drawing of measurements of spinopelvic parameters.

TABLE 2
Demographics of the Cohort and Subgroups

	Symptomatic Patients	Asymptomatic Volunteers	Total	*P* Value
n	176	372	548	
Age, y, mean ± SD	35.6 ± 9	33.9 ± 8	34.4 ± 8.5	.12
Male, n (%)	88 (50)	186 (50)	264 (50)	.2
Body mass index, kg/m^2, mean ± SD	25.9 ± 4.1	26 ± 4.2	26 ± 4	.9

sex-matched asymptomatic volunteers (P = .5). The patient group contained 88 men (mean age, 34.5 years; range, 18-50 years) and 88 women (mean age, 36.9 years; range, 19-50 years). The volunteer group contained 186 men (mean age, 33.8 years; range, 17-50 years) and 186 women (mean age, 34.0 years; range, 16-50 years).

Cam morphology prevalence varied between 17% and 71% in asymptomatic volunteers and between 47% and 100% in symptomatic patients according to different α-angle thresholds (65° and 55°, respectively). Conversely, 20% of all asymptomatic volunteers and 32% of symptomatic patients had pincer-type morphology (coxa profunda, 19% vs 27%; LCEA >39°, 12% vs 29%; acetabular retroversion, 3% vs 8%, respectively). About one-third of symptomatic patients had some degree of acetabular undercoverage (borderline dysplasia in 74% of those patients) in contrast to 2.6% in asymptomatic volunteers (Figure 4).

Very good intertechnique, interobserver, and intraobserver coefficients were identified (0.9-0.95, P < .001).

Femoral Parameters

Mean α angles were largest at the anterosuperior position (Table 3, Figure 5). The highest mean values of α angle in symptomatic patients were 66° ± 10° at 1:30-o'clock and 63.4° ± 9.6° at 2-o'clock; the highest mean value for the Ω angle was 66.4° ± 32.2° (considering a 55° threshold of the α angle). At the superior quadrants, α angles were significantly larger in symptomatic patients than in asymptomatic volunteers (Figure 5). The α angles in asymptomatic volunteers were 56.6° ± 7.1° at 1:30-o'clock and 53.8° ± 5.7° at 2-o'clock (P = .001, symptomatic patients vs asymptomatic volunteers). The magnitude of the mean

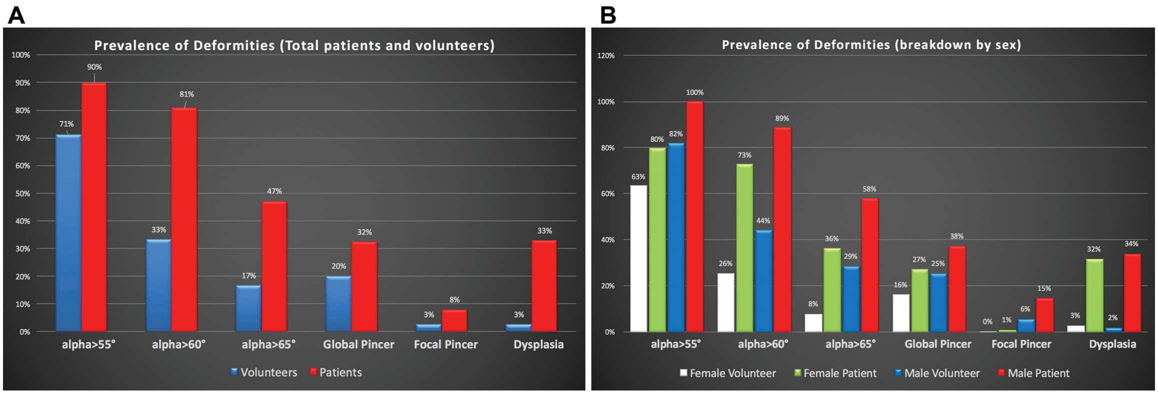

Figure 4. (A) Prevalence of cam morphology (considering α-angle thresholds of 55°, 60°, and 65°) and pincer morphology (global and focal). Breakdown by categories of abnormality (percentage of total asymptomatic volunteers or symptomatic patients). (B) Prevalence of cam morphology (considering α-angle thresholds of 55°, 60°, and 65°), pincer morphology (global and focal), and dysplasia. Breakdown by sex and categories of abnormality (percentage of total symptomatic patients and asymptomatic volunteers).

differences of α angle was higher between 1- and 2-o'clock (symptomatic patients' α angles were 8° to 10° higher than those in asymptomatic volunteers). Significant positive correlations (rho = 0.5-0.8; $P < .05$) were seen between Ω-angle and α-angle measurements at the anterosuperior quadrants, both in symptomatic patients and in asymptomatic volunteers (increasing values of the α angle significantly corresponded to higher values of the Ω angle).

Mean cam magnitude (Table 4), defined by the radial extension of the deformity, was significantly greater in symptomatic patients than in asymptomatic volunteers (from 0:30- to 2:40-o'clock vs from 0:56- to 1:52-o'clock, respectively; $P = .01$). The mean epicenter of the cam deformity was similarly located in symptomatic patients and asymptomatic volunteers (around 1:30-o'clock; $P = .5$); however, it was located significantly more superiorly in the anterosuperior quadrant for men compared with women, in both groups (1:24- vs 1:42-o'clock in symptomatic patients; $P < .001$). The mean angular range of radial extension of cam morphology was translated by a mean Ω angle. The Ω angle for a 55° α-angle threshold was 66° ± 25° and 27° ± 15° ($P = .03$) in symptomatic patients and asymptomatic volunteers, respectively.

The prevalence of decreased femoral version and increased femoral version was 15% and 25%, respectively, in the symptomatic patient group, although it was not significantly different for asymptomatic volunteers ($P = .1$).

Acetabular and Spinopelvic Parameters

Symptomatic patients had significantly less total acetabular coverage than asymptomatic volunteers, resulting in lower mean total ACcov (70.6% ± 5.2% vs 74.5% ± 4.9%, respectively), higher ACinc (7.3° ± 5.1° vs 2.9° ± 5.4°), and lower LCEA at 12-o'clock (32.7° ± 5.7° vs 35.8° ± 6.8°). Other acetabular parameters revealed significant differences although with lower mean differences (Table 5).

Concerning SPPs, symptomatic patients had significantly more anterior pelvic tilt resulting in higher SS (40.8° ± 6.2° vs 47.8° ± 6.2°, respectively; $P < .000$) and higher PI (47.2° ± 6.6° vs 51.4° ± 8°, respectively; $P = .004$).

PI and SS weakly correlated with upper acetabular anteversion (rho = –0.3 and –0.25, respectively; $P = .04$) and also with α angle at 1:30- and 2-o'clock (rho = 0.3/0.35 and 0.25/0.3, respectively; $P = .04$).

On the subgroup analysis, symptomatic hips with cam morphology had a greater amount of PI and SS (52° ± 8° and 48° ± 6°; $P = .000$) compared with individuals with asymptomatic cam morphology (45° ± 6° and 41° ± 5°) and controls, defined as asymptomatic subjects without cam morphology (48° ± 6° and 41° ± 7°). Pelvic tilt was only different between the control and cam groups (Table 6).

ROC Curve Analysis

ROC curve analysis showed that discrimination between symptomatic patients and asymptomatic volunteers was better achieved with Ω angle, α angle at 2-o'clock, sacral slope, and, to a lesser extent, ACinc, α angle at 2:30-o'clock, and α angle at 3-o'clock (Tables 3 and 5, Figure 6). The largest area under the curve (AUC) was obtained for femoral variables, specifically for the α angle at 2-o'clock position and the Ω angle (AUC = 0.831 and 0.830, respectively) and also for sacral slope (AUC = 0.801). A 55° α-angle threshold at 2-o'clock resulted in a sensitivity of 88% and a specificity of 70%. When the α-angle threshold value was increased to 58° to 60°, a sensitivity of 75% to 60% and specificity of 80% to 84% were obtained.

On the acetabular side, the only acceptable discriminating factor was ACinc with 6° as the best discriminating value, favoring specificity (Figure 6).

In males, the best discriminating factor was Ω angle and sacral slope with an AUC of 0.828 and 0.829,

TABLE 3
Femoral Side Morphometric Quantitative Measurements

	Asymptomatic Volunteers[a]	Symptomatic Patients[a]	*P* Value	Area Under the Curve
Ω angle for a 55° α-angle threshold	27.7 ± 24.5	66.4 ± 32.2	.000	0.830
Male	37.3 ± 23.8	75.2 ± 32.3	.000	0.832
Female	19.1 ± 21.9	57.6 ± 29.9	.000	0.847
Ω angle for a 60° α-angle threshold	12.2 ± 19	40 ± 35	.000	0.755
Male	19.1 ± 22.9	49.1 ± 32.7	.000	0.771
Female	6.1 ± 11.8	30.9 ± 35.2	.000	0.758
α angle 9-o'clock, deg	44.3 ± 5.1	44.4 ± 6	.583	0.515
Male	45.2 ± 4	44.2 ± 6.3	.076	0.431
Female	43.4 ± 5.8	45.5 ± 5.4	.036	0.578
α angle 12-o'clock, deg	44.9 ± 7.2	49.4 ± 13	.000	0.617
Male	48 ± 8.5	49.9 ± 12	.278	0.524
Female	42.2 ± 4.1	48.8 ± 13.9	.000	0.690
α angle 00:30-o'clock, deg	50 ± 8.9	56 ± 14	.000	0.643
Male	54.3 ± 10.2	59 ± 13.6	.005	0.610
Female	46.2 ± 5.1	52.9 ± 13.4	.000	0.676
α angle 1-o'clock, deg	54.6 ± 8.8	62.4 ± 12.8	.000	0.697
Male	59 ± 9.2	66.2 ± 12.6	.000	0.676
Female	50.7 ± 6.3	58.4 ± 11.9	.000	0.718
α angle 1:30-o'clock, deg	56.6 ± 7.1	66 ± 10	.000	0.788
Male	59.4 ± 7.2	68.2 ± 9.5	.000	0.778
Female	54.1 ± 6.1	63.8 ± 9.9	.000	0.801
α angle 2-o'clock, deg	53.8 ± 5.7	63.4 ± 9.6	.000	0.831
Male	54.7 ± 6.2	64.3 ± 9.6	.000	0.811
Female	53 ± 5.1	62.4 ± 9.5	.000	0.858
α angle 2:30-o'clock, deg	49 ± 5.6	57.6 ± 9.7	.000	0.780
Male	48.9 ± 5.8	58.4 ± 11	.000	0.797
Female	49.1 ± 5.4	56.9 ± 9.3	.000	0.755
α angle 3-o'clock, deg	46.2 ± 5.8	53.2 ± 9.2	.000	0.764
Male	44.9 ± 5.7	53.9 ± 9.9	.000	0.782
Female	45.3 ± 5.8	52.5 ± 8.6	.000	0.741
Femoral head diameter, mm	44.5 ± 4	45.7 ± 4.3	.003	0.559
Male	47.8 ± 2.6	49.2 ± 2.7	.000	0.631
Female	41.5 ± 2.2	42.1 ± 2.3	.012	0.597
Cervicodiaphyseal angle, deg	130.5 ± 5.7	129.5 ± 7.4	.004	0.432
Male	129 ± 5	129.6 ± 9.3	.545	0.500
Female	131.7 ± 5.6	129.3 ± 4.7	.000	0.360
Femoral neck version, deg	12 ± 5.8	11.1 ± 8.5	.947	0.498
Male	12.1 ± 5.7	11.1 ± 8.3	.944	0.497
Female	12 ± 5.8	11.1 ± 8.7	.948	0.499

[a]Results expressed as mean ± SD.

respectively. An Ω-angle cutoff value of 50° achieved a sensitivity and specificity of 75%. In females, the best discriminating factor was α angle at 2-o'clock position with an AUC of 0.858. A cutoff value of 57° achieved a sensitivity and specificity of 82%.

Multivariate Logistic Regression

A logistic regression was performed to ascertain the effects of sex, acetabular factors (considering ACinc, ACcov total, LCEA at 12-o'clock), femoral variables (considering femoral head diameter, Ω angle for a 55° α-angle threshold, α angle at 2-o'clock), and SPPs (sacral slope) on the likelihood that participants were symptomatic (Table 7). The model was statistically significant (χ^2 = 327.27, P < .0005), explained 64.0% (Nagelkerke R^2) of the variance in symptomatic status, and correctly classified 85% of cases. Sensitivity and specificity of the model were 72% and 91%, respectively, with an accuracy of 85% and AUC of 0.919 (range, 0.896-0.942), which accounts for an excellent discriminative model.

DISCUSSION

In this study, we assessed the usefulness of combined acetabular, femoral, and spinopelvic measurements based on 3D MRIs in distinguishing between patients with FAI syndrome and asymptomatic volunteers. Our data build on previously reported normative hip[32-34] and spinopelvic data.[18,39,47] To the best of our knowledge, our study included the largest cohort of asymptomatic volunteers

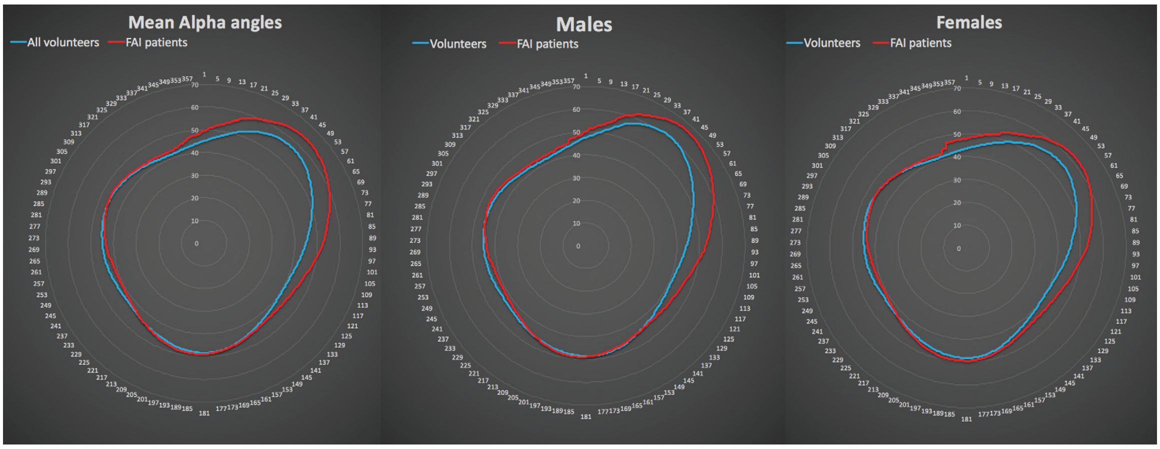

Figure 5. Radar map of mean circumferential α angles at every degree of the femoral head-neck junction. Left, all participants (blue line corresponds to asymptomatic volunteers; red line corresponds to symptomatic patients). Middle, male subjects only. Right, female subjects only. 1 corresponds to 12-o'clock position; 89 corresponds to 3-o'clock position.

TABLE 4
Asymptomatic Volunteers' and Symptomatic Patients' Mean Epicenter Position and Mean α Angle at That Point[a]

	Epicenter Position		Mean α Angles at Epicenter		Extension (Ω Angle)	
	Asymptomatic Volunteers	Symptomatic Patients	Asymptomatic Volunteers	Symptomatic Patients	Asymptomatic Volunteers	Symptomatic Patients
Mean all	1:24 (42°)	1:30 (45°)	57°	66°	0:56-1:52 (27°) 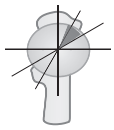	0:30-2:40 (66°) 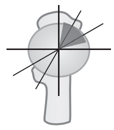
Males	1:14 (37°)	1:24 (42°)	60°	69°	0:34-1:54 (37°) 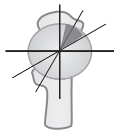	0:20-2:48 (75°) 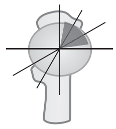
Females	1:38 (49°)	1:42 (51°)	55°	64°	1:26-1:50 (19°) 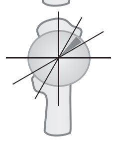	0:50-2:42 (57°) 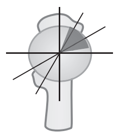

[a]The mean epicenter position is the point of the highest α angle; the position is registered in clockface position and corresponding degree location in parentheses (considering 0° the 12-o'clock position and 90° the 3-o'clock position). The Extension column provides the total mean range of cam deformity (radial extension); the values represent range in clockface positions and corresponding angular extension (Ω angle in parentheses).

and symptomatic hip patients with all FAI types and instability-related morphologies assessed by use of semiautomated 3D MRI.

Population, Method, and Controversies

Since the recent advances in knowledge regarding FAI syndrome, the real concern about overdiagnosing and overtreating of this entity closely relates to the discussion about the measurement techniques, diagnostic criteria, and case definitions.[19] A population model with a substantial overlap between the healthy and diseased group seems to be the case for FAI,[50] emphasizing that a thorough diagnostic integrated approach is critical.[19] It is paramount to recognize that the two basic mechanisms of FAI offer overly simplistic explanations of this hip condition. They often occur in addition to other complex conditions such as hip

TABLE 5
Acetabular Side and Spinopelvic Morphometric Quantitative Measurements[a]

	Asymptomatic Volunteers[b]	Symptomatic Patients[b]	*P* Value	Area Under the Curve
Acetabular coverage total, %	74.5 ± 4.9	70.6 ± 5.2	.000	0.290
Male	74.1 ± 4.6	69.8 ± 4.8	.000	0.232
Female	74.7 ± 5.2	71.4 ± 5.3	.000	0.333
Acetabular version center, deg	20.9 ± 5.2	21.9 ± 6.3	.028	0.558
Male	17.8 ± 4.6	19.8 ± 6.3	.001	0.621
Female	23.6 ± 4	24 ± 5.6	.461	0.527
Acetabular version upper, deg	21.1 ± 8	18.6 ± 9.5	.005	0.425
Male	17.9 ± 8.2	16.1 ± 11	.428	0.470
Female	23.9 ± 6.7	21 ± 6.8	.001	0.377
Acetabular cup diameter, mm	48 ± 4	49.9 ± 4.3	.000	0.614
Male	51.4 ± 2.4	53.3 ± 2.9	.000	0.683
Female	45.1 ± 2.7	46.6 ± 2.5	.000	0.665
Sourcil angle, deg	2.9 ± 5.4	7.3 ± 5.1	.000	0.715
Male	2 ± 4.8	7.6 ± 5.3	.000	0.779
Female	3.7 ± 5.8	6.9 ± 4.9	.000	0.656
LCEA at 1-o'clock, deg	26.1 ± 7.9	24.1 ± 7.4	.003	0.421
Male	28.5 ± 7.2	24.3 ± 8.4	.000	0.319
Female	23.9 ± 7.9	23.8 ± 6.3	.803	0.509
LCEA at 12-o'clock, deg	35.8 ± 6.8	32.7 ± 5.7	.000	0.347
Male	36.4 ± 5.6	32.4 ± 5.9	.000	0.283
Female	35.2 ± 7.7	32.8 ± 5.4	.009	0.403
LCEA at 11-o'clock, deg	33.4 ± 7.3	30.2 ± 6.3	.000	0.367
Male	33 ± 6.2	29 ± 5.5	.000	0.329
Female	33.8 ± 8.1	31.4 ± 6.8	.011	0.405
Sacral slope, deg	40.8 ± 6.2	47.8 ± 6.2	.000	0.801
Male	39.3 ± 7.5	48.5 ± 7	.000	0.829
Female	42.2 ± 4.1	47 ± 5.7	.000	0.777
Pelvic incidence, deg	47.2 ± 6.6	51.4 ± 8	.004	0.634
Male	45.8 ± 7	53.3 ± 8.2	.000	0.744
Female	48.5 ± 6	49.3 ± 7.8	.825	0.515
Pelvic tilt, deg	6.3 ± 6	3.7 ± 5.4	.011	0.384
Male	6.4 ± 6	4.9 ± 5.3	.417	0.449
Female	6.3 ± 6	2.2 ± 6	.006	0.313

[a]LCEA, lateral center edge angle.
[b]Results expressed as mean ± SD.

dysplasia, version abnormalities,[56] and other extra-articular factors (such as SPPs, extreme range of motion, and sports participation).[19] Thus, a comprehensive and combined analysis of hip pathomorphologic features is needed to help further our understanding of this complex 3-dimensional pathologic process.

Prior studies comparing asymptomatic volunteers and symptomatic hip patients have primarily used conventional radiographs to characterize the hip.[4,28] However, several other studies reported poor reliability for defining hip pathomorphologic features with conventional radiographs and improved accuracy with CT and MRI.[10,61] With recent developments of MRI and 3D imaging, attention has turned to the unique capability of determining bone and soft tissue abnormalities in one examination. Advantages of this specific method have been outlined in several studies,[6,32,34,60] including improved diagnosis and monitoring, accurate spatial visualization of the joint, and reduced variability in clinical research.

Logistic Regression Model

The hip should not be studied in isolation, given the value of femoral and acetabular components as well as extra-articular contributors such as SPPs.[18,23,47,57] Interestingly, our model clearly showed the complex interplay between these components. The likelihood of symptomatic disease doubled for an Ω-angle increase of 20° or an α-angle increase of 8° to 9° (measured at 2-o'clock). Accordingly, higher femoral diameters were somewhat protective against symptomatic disease, which demonstrates the importance of FHN morphologic characteristics rather than femoral head size in FAI disease.

The symptomatic state was also more associated with decreasing superior acetabular coverage (decreasing LCEA at 12-o'clock and increasing ACinc [>6°; AUC = 0.715]) than with pincer morphology (which paradoxically showed a tendency to protect against the development of the symptomatic state). Likelihood of symptomatic disease doubled with a 7° increase in ACinc in line with the findings of

TABLE 6
Spinopelvic Parameters for the Whole Cohort and as Per Group

	Mean	SD	95% Confidence Interval for Mean		*P* Value
			Lower Bound	Upper Bound	
Sacral slope					
Control[a]	40.5	6.6	38.9	42.2	
Asymptomatic cam	41.4	5.3	39.4	43.4	
Symptomatic cam	48.2	6.5	46.3	49.9	.000[b]
Total	43.4	7.2	42.2	44.5	
Pelvic incidence					
Control	48	6.7	46.3	49.6	
Asymptomatic cam	45.2	6	42.9	47.5	
Symptomatic cam	52.1	8.2	49.8	54.3	.000[b,c]
Total	48.9	7.6	47.7	50.1	
Pelvic tilt					
Control	7.5	6.3	5.9	9	
Asymptomatic cam	3.6	4	2.1	5.2	
Symptomatic cam	4.1	5.6	2.5	5.6	.06
Total	5.5	5.9	4.6	6.5	

[a]"Controls" were asymptomatic subjects without cam morphology.
[b]Between groups.
[c]Within groups (namely symptomatic cam and other groups).

dysplasia as a major factor in OA development,[2] suggesting a delicate balance regarding impingement and instability.[2,56] Undercoverage may cause higher joint contact pressures and subsequent degeneration of the articular cartilage resulting from static overload.[36] Acetabular overcoverage may lead to early pathological contact between the overcovering acetabulum and the FHN junction. This can lead to chondrolabral damage as a result of a more dynamic conflict at the acetabular rim.[51] Previous research showed an increased risk for OA with pincer morphology,[15,17] whereas other epidemiological studies found no association or even suggested a protective effect for the development of OA.[2,5,37,41,55] Conversely, recent prospective epidemiological studies have supported that even mild acetabular dysplasia is in fact associated with increased risk of OA,[2,55] concordant with our findings. Nevertheless, further prospective research with larger samples is important to further address this issue.

Concerning SPPs, a role in symptomatic hip disease is suggested by the increasing likelihood of symptomatic state with increasing SS (which is a dynamic parameter), consistent with recent reports.[18,39]

Femoral Parameters

The large prevalence (71%) of cam-type deformities in our asymptomatic population is in accordance with the previous literature[12,32-34] using an α angle greater than 55° measured with different imaging techniques (cam-type deformities were detected with CT[24] in 74% of asymptomatic volunteers and with MRI in 24%[46] to 34%[20]). This further stresses that although cam morphology is a known risk factor for OA,[1] it is not the exception but the rule in both populations.

Regarding cam morphology, distinguishing between symptomatic patients and asymptomatic volunteers was best done by measuring the α angle at 2-o'clock position (58°) and the Ω angle (43°). ROC curve analysis results also showed that the maximal α angle from 1- to 3-o'clock can be used for patient identification, with an AUC greater than 0.750. Although patient identification was also possible at other femoral positions, the AUC was less favorable at these positions.

Published reference intervals of hip morphometric measurements, in both symptomatic patients and asymptomatic volunteers, raise concerns about normal thresholds, as it becomes clear that reference standards should incorporate both higher sensitivity and specificity.[50] The use of α angle is controversial due to its moderate reproducibility, its moderate discriminative ability,[49,50] and the lack of conclusive data on ideal threshold values.[3,32,49] Reference intervals usually derive from mean values (±1 SD or ±2 SD[3,44]) and assume a normal distribution of a certain variable, often lacking specificity, which further increases the natural overlap between populations.

Examples of a conservative approach include the recently proposed α-angle upper-limit reference intervals of 60° for the 12- and 3-o'clock positions and 65° to 70° for the 1- and 1:30-o'clock positions.[32] This is in agreement with Agricola et al,[3] who used conventional radiographs (and also measured α angle at the 12-o'clock position), and Golfam et al,[16] who used MRI (and suggested increasing the thresholds to 63° at 3-o'clock and 66° at 1:30-o'clock). These results are certainly adequate for identifying a definitive pathological α angle, although with considerable loss of sensitivity. Our results show that a cam deformity extending over half the anterosuperior quadrant (corresponding to an Ω angle of 45°, AUC = 0.830) or with α-angle measurements of 57° to 60° (at the 1:30- to 2-o'clock positions; AUC = 0.788-0.831) is probably symptomatic. Sutter et al[49] found a similar AUC (0.790-0.820) for the best α-angle measurement point.

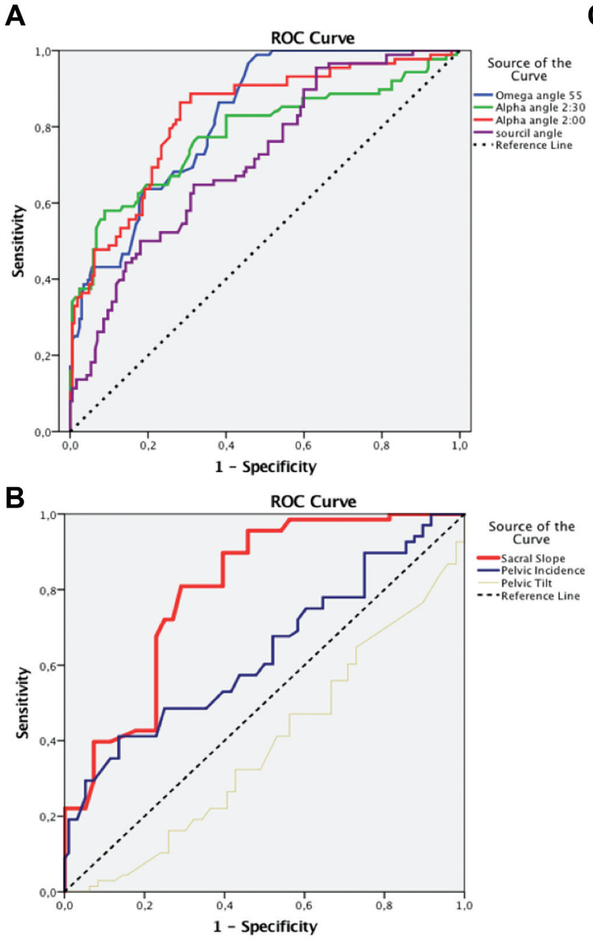

C

	OPTIMAL THRESHOLD	SENSITIVITY	SPECIFICITY	AUC
Omega 55				
Total	43°	72	70	0,830
Male	50°	75	75	0,828
Female	36°	81	76	0,847
Alpha 1:30				
Total	60°	72	75	0,788
Male	62°	70	70	0,781
Female	57°	81	70	0,801
Alpha 2:00				
Total	58°	75	80	0,831
Male	58°	77	75	0,809
Female	57°	81	82	0,858
Alpha 2:30				
Total	53°	67	80	0,780
Male	55°	68	86	0,796
Female	52	77	72	0,755
Alpha 3:00				
Total	50°	62	82	0,764
Male	50°	61	87	0,782
Female	48°	72	72	0,741
Sourcil Angle				
Total	6°	65	70	0,709
Male	5°	65	75	0,779
Female	6°	70	60	0,656
Sacral Slope				
Total	44°	72	75	0,801
Male	44°	71	80	0,829
Female	44°	73	71	0,770
Pelvic Incidence				
Total	50°	60	60	0,634
Male	50°	70	71	0,744
Female	50°	50	50	0,506

Figure 6. (A) Receiver operating characteristic (ROC) curve analysis of most significant femoral and acetabular parameters for discrimination between symptomatic patients and asymptomatic volunteers showed the largest area under the curve (AUC) for the α angle at the 2-o'clock position (red line). Discrimination power was smaller for the other positions and parameters, with decreasing AUC for the α angle at 2:30-o'clock position (green line), the Ω angle for a 55° α-angle threshold (blue line), and the sourcil angle (acetabular inclination) (purple line). (B) ROC curves for spinopelvic parameters for discrimination between symptomatic patients and asymptomatic volunteers showed the largest AUC for the sacral slope (red line). (C) Output of ROC curve analysis with AUC as an indication of predictive power. Optimum threshold is the level with highest combination of sensitivity and specificity.

Increasing the threshold for an abnormal α angle while considering its discriminative ability would improve its value as a diagnostic test. Therefore, we suggest reconsidering the threshold of abnormal α angle in the setting of a diagnostic test to incorporate higher discriminative power. An α angle of 57° to 60° measured at 1:00-, 1:30-, and 2-o'clock and 50° at 3-o'clock would optimize discriminative power while favoring specificity (Table 6).

Femoral malversion was similar to previous reported prevalence, which ranged from 13%[11] to 24%[25] for diminished version (<5°) and from 15%[25] to 34%[7] for increased version (>20°).

These results underline that (a) analyzing deformities of the femoral head with 3D imaging or at least radial images is paramount, rather than only measuring the α angle at the anterior position[32]; and (b) the α angle should be set according to specific location and sex[34] (Figure 6).

Acetabular and Spinopelvic Parameters

Dysplasia and pincer morphology are 2 distinct pathologic forms resulting in clinically different pathomechanisms, static overload or dynamic conflict.[52]

TABLE 7
Output From Multivariate Logistic Regression Analysis of Variables on the Likelihood That Participants Were Symptomatic

Variables	B	Significance	Exp(B)
Sex	–0.819	.060	0.441
Sacral slope	0.466	.000	1.252
Acetabular inclination	0.131	.001	1.141
Lateral center edge angle	–0.185	.000	0.831
Ω angle for a 55° α-angle threshold	0.054	.000	1.055
α angle at 2-o'clock	0.108	.001	1.114
Femoral head diameter	–0.458	.000	0.633
Acetabular coverage total	–0.183	.003	0.801

The goal of arthroscopy for pincer FAI is generally accepted as correcting the impingement while not causing iatrogenic dysplasia or acute instability.[26] However, there are no agreed-upon measurements to assess the location and extent of correction. LCEA is the only measurement thoroughly researched for perioperative value,[22] although pincer morphology often extends more medially and posterolaterally.[22]

The relatively high reported prevalence of pincer morphology in asymptomatic (57%-67%) and symptomatic (28%-54%) individuals may be confounded in several ways,[12,33] given that radiographic parameters such as the crossover sign and posterior wall sign have shown poor diagnostic reliability.[21,38] We observed that approximately 33% of symptomatic patients and 20% of asymptomatic volunteers had pincer morphology, which we believe is a more accurate estimate of the real prevalence given the method used.

Cranial retroversion was uncommon although significantly more prevalent in symptomatic patients (8% vs 2.6%), in agreement with radiographic differences seen in previous studies[15] although with different frequencies noted (20% among patients with hip OA vs 5% among the general population). Symptomatic males more often had cranial retroversion than did females (7% vs 1%), consistent with a previous study[27] but divergent from the report by Tannenbaum et al[54] (no sex differences noted). Males in both groups had a clear tendency for a more prominent anterosuperior wall (anteversion angles were on average 5° lower in males) in line with previous reports.[43,54]

Concerning SPPs, a definitive contribution of these parameters for a symptomatic hip is suggested by our data. Briefly, pelvic tilt and SS depend on posture (higher SS when supine and reduced when standing) and conjointly compose PI, which is an individual, position-independent angle. This dynamic "unit" may change in response to postural changes to maintain the sagittal lumbopelvic balance.[47] Decreasing values of SS may allow greater impingement-free hip flexion by effectively reducing femoral coverage anteriorly. Notably, subjects with small PI have less range to compensate through pelvic movement, as the ability to alter spinopelvic relation is reduced.[47]

The symptomatic group showed larger PI and SS angles. Recent reports with smaller cohorts examined via CT[18,39] (<70 subjects) found similar results when comparing symptomatic and asymptomatic groups (PI, 53° vs 48°; SS, 47° vs 43°[18]). Interestingly, in our study SS demonstrated higher discriminative power than PI (SS, 48° vs 41°, AUC = 0.801; PI, 51° vs 47°, AUC = 0.634). Paradoxically, these results are divergent from initial studies that reported PI to be smaller in hips with deformities (studies using lateral scout radiographs,[23] CT,[58] and cadaveric studies[13,35]). Notably, the PI and SS values in our symptomatic patients' group are similar to those studies, but our control group values are divergent (the reported average "pathological" PI of 51.4°[58] is within the range of 44°-60° reported in earlier studies[13,29,35,47]). Our control group had a 2:1 enrollment ratio, which further increases the comparative strength of our study. Furthermore, two related cadaveric studies included hips from the beginning of the previous century and with unknown symptomatic status.[13,35] Last, none of the divergent studies report body mass index, which is a critical parameter in sacral development.[39] Although it is beyond the scope of our study to prove causation between cam or pincer morphology and increased SPPs, the association can be established as a basis for prospective evaluation. Additionally, our findings are more consistent with published data on the association of higher PI and OA.[14]

A larger SS is by definition associated with both an increased anterosuperior acetabular coverage and an anteroposterior distance between hip joint centers and the sacral endplate (presumably resulting in a tighter core pelvic and iliopsoas musculature).[39] These findings have clinical significance as femoral and acetabular parameters are static parameters that are not amenable to nonoperative treatment. Conversely, SPPs may be subject to nonsurgical treatment, as increasing SPT conceptually increases posterior pelvic tilt and increases the superoanterior femoral head collision-free range of motion (manageable by nonoperative pelvic muscular-focused treatment).[18,39]

Limitations

This study has limitations. First, selecting a protocol for this study may have been subject to bias as our controls were not selected from healthy volunteers and we used patient survey information to exclude hip abnormality but did not perform a clinical hip examination. However, we prospectively included controls evaluated for nonorthopaedic disease and excluded all controls with any reported history of hip abnormality or symptoms. Additionally, we excluded any controls with signs of hip abnormality on MRI so that our cohort comprised asymptomatic individuals only. Second, this study included only partial correlation of semiautomated measurements with traditional manual measurements; such comparison between 2D and 3D MRI methods would be useful but was not an objective of our study, apart from the fact that the software used had already been validated for this purpose.

CONCLUSION AND FUTURE DIRECTIONS

These study's findings may allow clinicians to

(a) acknowledge that a cam deformity extending over half of the anterosuperior quadrant (Ω angle ranging from more than 43° to 45°), α-angle measurements of 57° to 60° (at the 1:30- to 2-o'clock positions), and undercoverage tendency (acetabular inclination >6°) are predictive factors of a symptomatic hip;
(b) identify asymptomatic populations with high PI and high SS as subjects prone to develop symptoms and conceptually benefiting from muscular strengthening (as increasing SPT may attempt to tilt the pelvis to reduce anterior acetabular coverage); and
(c) select adequate surgical indications for symptomatic hip patients by identifying the most suitable candidates who would initially benefit from nonoperative management.

Imaging-based evaluation for hip pain should include the entire pelvis to allow for determination of these parameters. Nevertheless, we acknowledge that morphologic features alone do not account for the full gamut of hip symptoms or signs. Intra-articular factors are not the only factors that lead to FAI. Extra-articular factors such as femoral torsion, pelvic morphologic features, and nonanatomic factors such as ligamentous laxity need to be considered as well.

Future research may investigate integrated risk profiling for FAI including key anatomic parameters (Ω angle, α angle, SPPs) combined with other specific biomarkers. Conceptually, patient-based imaging data can be cross-linked to population-based data available in biobanks, enabling a personalized approach.

ACKNOWLEDGMENT

The authors thank José Roquette, João Sá, Isabel Vaz, and Pedro Patrício for their continuing and enthusiastic support of clinical research at Hospital da Luz, and Rúben Teixeira, Ana Filipa Graça, João Novo, Sara Gonçalves, and Tiago Castela for their efforts to optimize technical issues and provide patient care.

REFERENCES

1. Agricola R, Heijboer MP, Bierma-Zeinstra SMA, Verhaar JAN, Weinans H, Waarsing JH. Cam impingement causes osteoarthritis of the hip: a nationwide prospective cohort study (CHECK). *Ann Rheum Dis*. 2013;72(6):918-923.
2. Agricola R, Heijboer MP, Roze RH, et al. Pincer deformity does not lead to osteoarthritis of the hip whereas acetabular dysplasia does: acetabular coverage and development of osteoarthritis in a nationwide prospective cohort study (CHECK). *Osteoarthritis Cartilage*. 2013;21(10):1514-1521.
3. Agricola R, Waarsing JH, Thomas GE, et al. Cam impingement: defining the presence of a cam deformity by the alpha angle: data from the CHECK cohort and Chingford cohort. *Osteoarthritis Cartilage*. 2014;22(2):218-225.
4. Allen D, Beaulé PE, Ramadan O, Doucette S. Prevalence of associated deformities and hip pain in patients with cam-type femoroacetabular impingement. *J Bone Joint Surg Br*. 2009;91(5):589-594.
5. Bardakos NV, Villar RN. Predictors of progression of osteoarthritis in femoroacetabular impingement: a radiological study with a minimum of ten years follow-up. *J Bone Joint Surg Br*. 2009;91(2):162-169.
6. Bittersohl B, Hosalkar HS, Hesper T, Tiderius CJ, Zilkens C, Krauspe R. Advanced imaging in femoroacetabular impingement: current state and future prospects. *Front Surg*. 2015;2(suppl 1):608.
7. Chadayammuri V, Garabekyan T, Bedi A, et al. Passive hip range of motion predicts femoral torsion and acetabular version. *J Bone Joint Surg Am*. 2016;98(2):127-134.
8. Christensen CP, Althausen PL, Mittleman MA, Lee JA, McCarthy JC. The nonarthritic hip score: reliable and validated. *Clin Orthop Relat Res*. 2003;406:75-83.
9. Clohisy JC. A systematic approach to the plain radiographic evaluation of the young adult hip. *J Bone Joint Surg Am*. 2008;90(suppl 4):47.
10. Clohisy JC, Carlisle JC, Trousdale R, et al. Radiographic evaluation of the hip has limited reliability. *Clin Orthop Relat Res*. 2008;467(3):666-675.
11. Dolan MM, Heyworth BE, Bedi A, Duke G, Kelly BT. CT Reveals a high incidence of osseous abnormalities in hips with labral tears. *Clin Orthop Relat Res*. 2010;469(3):831-838.
12. Frank JM, Harris JD, Erickson BJ, et al. Prevalence of femoroacetabular impingement imaging findings in asymptomatic volunteers: a systematic review. *Arthroscopy*. 2015;31(6):1199-1204.
13. Gebhart JJ, Streit JJ, Bedi A, Bush-Joseph CA, Nho SJ, Salata MJ. Correlation of pelvic incidence with cam and pincer lesions. *Am J Sports Med*. 2014;42(11):2649-2653.
14. Gebhart JJ, Weinberg DS, Bohl MS, Liu RW. Relationship between pelvic incidence and osteoarthritis of the hip. *Bone Joint Res*. 2016;5(2):66-72.
15. Giori NJ, Trousdale RT. Acetabular retroversion is associated with osteoarthritis of the hip. *Clin Orthop Relat Res*. 2003;417:263-269.
16. Golfam M, Di Primio LA, Beaulé PE, Hack K, Schweitzer ME. Alpha angle measurements in healthy adult volunteers vary depending on the MRI plane acquisition used. *Am J Sports Med*. 2017;45(3):620-626.
17. Gosvig KK, Jacobsen S, Sonne-Holm S, Palm H, Troelsen A. Prevalence of malformations of the hip joint and their relationship to sex, groin pain, and risk of osteoarthritis: a population-based survey. *J Bone Joint Surg Am*. 2010;92(5):1162-1169.
18. Grammatopoulos G, Speirs AD, Ng KCG, et al. The acetabular and spino-pelvic morphologies are different in subjects with symptomatic cam femoro-acetabular impingement. *J Orthop Res*. 2018;36(7):1840-1848.
19. Griffin DR, Dickenson EJ, O'Donnell J, et al. The Warwick Agreement on femoroacetabular impingement syndrome (FAI syndrome): an international consensus statement. *Br J Sports Med*. 2016;50(19):1169-1176.
20. Hack K, Di Primio G, Rakhra K, Beaulé PE. Prevalence of cam-type femoroacetabular impingement morphology in asymptomatic volunteers. *J Bone Joint Surg Am*. 2010;92(14):2436-2444.
21. Hashemi SA, Dehghani J, Vosoughi AR. Can the crossover sign be a reliable marker of global retroversion of the acetabulum? *Skeletal Radiol*. 2017;46(1):17-21.
22. Hellman MD, Gross CE, Hart M, et al. Radiographic comparison of anterior acetabular rim morphology between pincer femoroacetabular impingement and control. *Arthroscopy*. 2016;32(3):468-472.
23. Hellman MD, Haughom BD, Brown NM, Fillingham YA, Philippon MJ, Nho SJ. Femoroacetabular impingement and pelvic incidence: radiographic comparison to an asymptomatic control. *Arthroscopy*. 2017;33(3):545-550.
24. Kang ACL, Gooding AJ, Coates MH, Goh TD, Armour P, Rietveld J. Computed tomography assessment of hip joints in asymptomatic individuals in relation to femoroacetabular impingement. *Am J Sports Med*. 2010;38(6):1160-1165.
25. Kelly BT, Bedi A, Robertson CM, Torre Dela K, Giveans MR, Larson CM. Alterations in internal rotation and alpha angles are associated with arthroscopic cam decompression in the hip. *Am J Sports Med*. 2012;40(5):1107-1112.
26. Khanduja V, Villar RN. Arthroscopic surgery of the hip: current concepts and recent advances. *J Bone Joint Surg Br*. 2006;88(12):1557-1566.

27. Larson CM, Moreau-Gaudry A, Kelly BT, et al. Are normal hips being labeled as pathologic? A CT-based method for defining normal acetabular coverage. *Clin Orthop Relat Res*. 2014;473(4):1247-1254.
28. Larson CM, Sikka RS, Sardelli MC, et al. Increasing alpha angle is predictive of athletic-related ''hip'' and ''groin'' pain in collegiate National Football League prospects. *Arthroscopy*. 2013;29(3):405-410.
29. Legaye J, Duval-Beaupère G, Hecquet J, Marty C. Pelvic incidence: a fundamental pelvic parameter for three-dimensional regulation of spinal sagittal curves. *Eur Spine J*. 1998;7(2):99-103.
30. Lerch TD, Todorski IAS, Steppacher SD, et al. Prevalence of femoral and acetabular version abnormalities in patients with symptomatic hip disease: a controlled study of 538 hips. *Am J Sports Med*. 2018;46(1):122-134.
31. Leunig M, Jüni P, Werlen S, et al. Prevalence of cam and pincer-type deformities on hip MRI in an asymptomatic young Swiss female population: a cross-sectional study. *Osteoarthritis Cartilage*. 2013;21(4):544-550.
32. Mascarenhas VV, Rego P, Dantas P, et al. Hip shape is symmetric, non-dependent on limb dominance and gender-specific: implications for femoroacetabular impingement. A 3D CT analysis in asymptomatic subjects. *Eur Radiol*. 2018;28(4):1609-1624.
33. Mascarenhas VV, Rego P, Dantas P, et al. Imaging prevalence of femoroacetabular impingement in symptomatic patients, athletes, and asymptomatic individuals: a systematic review. *Eur J Radiol*. 2016;85(1):73-95.
34. Mascarenhas VV, Rego P, Dantas P, Gaspar A, Soldado F, Consciência JG. Cam deformity and the omega angle, a novel quantitative measurement of femoral head-neck morphology: a 3D CT gender analysis in asymptomatic subjects. *Eur Radiol*. 2017;27(5):2011-2023.
35. Morris WZ, Fowers CA, Yuh RT, Gebhart JJ, Salata MJ, Liu RW. Decreasing pelvic incidence is associated with greater risk of cam morphology. *Bone Joint Res*. 2016;5(9):387-392.
36. Murphy SB, Kijewski PK, Millis MB, Harless A. Acetabular dysplasia in the adolescent and young adult. *Clin Orthop Relat Res*. 1990;261:214-223.
37. Nelson AE, Stiller JL, Shi XA, et al. Measures of hip morphology are related to development of worsening radiographic hip osteoarthritis over 6 to 13 year follow-up: the Johnston County Osteoarthritis Project. *Osteoarthritis Cartilage*. 2016;24(3):443-450.
38. Nepple JJ. Coxa profunda is not a useful radiographic parameter for diagnosing pincer-type femoroacetabular impingement. *J Bone Joint Surg Am*. 2013;95(5):417.
39. Ng KCG, Lamontagne M, Jeffers JRT, Grammatopoulos G, Beaulé PE. Anatomic predictors of sagittal hip and pelvic motions in patients with a cam deformity. *Am J Sports Med*. 2018;46(6):1331-1342.
40. Nho J-H, Lee Y-K, Kim HJ, Ha Y-C, Suh Y-S, Koo K-H. Reliability and validity of measuring version of the acetabular component. *J Bone Joint Surg Br*. 2012;94(1):32-36.
41. Nicholls AS, Kiran A, Pollard TCB, et al. The association between hip morphology parameters and nineteen-year risk of end-stage osteoarthritis of the hip: a nested case-control study. *Arthritis Rheumatism*. 2011;63(11):3392-3400.
42. Nötzli HP, Wyss TF, Stoecklin CH, Schmid MR, Treiber K, Hodler J. The contour of the femoral head-neck junction as a predictor for the risk of anterior impingement. *J Bone Joint Surg Br*. 2002;84(4):556-560.
43. Peterson JB, Doan J, Bomar JD, Wenger DR, Pennock AT, Upasani VV. Sex differences in cartilage topography and orientation of the developing acetabulum: implications for hip preservation surgery. *Clin Orthop Relat Res*. 2015;473(8):2489-2494.
44. Pollard TCB, Villar RN, Norton MR, et al. Femoroacetabular impingement and classification of the cam deformity: the reference interval in normal hips. *Acta Orthop*. 2010;81(1):134-141.
45. Rego PRA, Mascarenhas V, Oliveira FS, et al. Morphologic and angular planning for cam resection in femoro-acetabular impingement: value of the omega angle. *Int Orthop (SICOT)*. 2016;40(10):2011-2017.
46. Reichenbach S, Jüni P, Werlen S, et al. Prevalence of cam-type deformity on hip magnetic resonance imaging in young males: a cross-sectional study. *Arthritis Care Res*. 2010;62(9):1319-1327.
47. Rivière C, Hardijzer A, Lazennec JY, Beaulé P, Muirhead-Allwood S, Cobb J. Spine-hip relations add understandings to the pathophysiology of femoro-acetabular impingement: a systematic review. *Orthop Traumatol Surg Res*. 2017;103(4):549-557.
48. Röling MA, Visser MI, Oei EHG, Pilot P, Kleinrensink G-J, Bloem RM. A quantitative non-invasive assessment of femoroacetabular impingement with CT-based dynamic simulation–cadaveric validation study. *BMC Musculoskelet Disord*. 2015;16:50.
49. Sutter R, Dietrich TJ, Zingg PO, Pfirrmann CWA. How useful is the alpha angle for discriminating between symptomatic patients with cam-type femoroacetabular impingement and asymptomatic volunteers? *Radiology*. 2012;264(2):514-521.
50. Sutter R, Pfirrmann CWA. Update on femoroacetabular impingement: what is new, and how should we assess it? *Semin Musculoskelet Radiol*. 2017;21(5):518-528.
51. Tannast M, Goricki D, Beck M, Murphy SB, Siebenrock KA. Hip damage occurs at the zone of femoroacetabular impingement. *Clin Orthop Relat Res*. 2008;466(2):273-280.
52. Tannast M, Hanke MS, Zheng G, Steppacher SD, Siebenrock KA. What are the radiographic reference values for acetabular under- and overcoverage? *Clin Orthop Relat Res*. 2015;473(4):1234-1246.
53. Tannast M, Siebenrock KA, Anderson SE. Femoroacetabular impingement: radiographic diagnosis—what the radiologist should know. *AJR Am J Roentgenol*. 2007;188(6):1540-1552.
54. Tannenbaum EP, Zhang P, Maratt JD, et al. A computed tomography study of gender differences in acetabular version and morphology: implications for femoroacetabular impingement. *Arthroscopy*. 2015;31(7):1247-1254.
55. Thomas GER, Palmer AJR, Batra RN, et al. Subclinical deformities of the hip are significant predictors of radiographic osteoarthritis and joint replacement in women: a 20 year longitudinal cohort study. *Osteoarthritis Cartilage*. 2014;22(10):1504-1510.
56. Tibor LM, Liebert G, Sutter R, Impellizzeri FM, Leunig M. Two or more impingement and/or instability deformities are often present in patients with hip pain. *Clin Orthop Relat Res*. 2013;471(12):3762-3773.
57. Tönnis D, Heinecke A. Acetabular and femoral anteversion: relationship with osteoarthritis of the hip. *J Bone Joint Surg Am*. 1999;81(12):1747-1770.
58. Weinberg DS, Gebhart JJ, Liu RW, Salata MJ. Radiographic signs of femoroacetabular impingement are associated with decreased pelvic incidence. *Arthroscopy*. 2016;32(5):806-813.
59. Xia Y, Fripp J, Chandra SS, Schwarz R, Engstrom C, Crozier S. Automated bone segmentation from large field of view 3D MR images of the hip joint. *Physics Med Biol*. 2013;58(20):7375-7390.
60. Xia Y, Fripp J, Chandra SS, Walker D, Crozier S, Engstrom C. Automated 3D quantitative assessment and measurement of alpha angles from the femoral head-neck junction using MR imaging. *Phys Med Biol*. 2015;60(19):7601-7616.
61. Zaltz I, Kelly BT, Hetsroni I, Bedi A. The crossover sign overestimates acetabular retroversion. *Clin Orthop Relat Res*. 2012;471(8):2463-2470.

chapter 6

TREATING THE SYMPTOMATIC HIP

Chapter 6 is based on the following publications:

"Basic concepts in hip arthroscopy."
ESSKA Instructional Course Lecture Book 2018

"Arthroscopic versus open treatment of cam-type femoroacetabular impingement: retrospective cohort clinical study."
International Orthopedics. 2018 Apr;42(4):791-797

CHAPTER 6.1

This chapter is based on the following paper:

"Basic concepts in hip arthroscopy."
ESSKA Instructional Course Lecture Book 2018

Basic Concepts in Hip Arthroscopy

4

O. Marin-Peña, B. Lund, O.R. Ayeni, P. Dantas,
D. Griffin, V. Khanduja, H.G. Said, M. Tey,
E. Dickenson, J. Kay, V. Mascarenhas,
M.A. Sadakah, K.H. Sunil Kumar, and M. Tahoun

4.1 Introduction

Hip arthroscopy has become very popular in the last decade. Numbers are increasing rapidly worldwide. More than 11,000 hip arthroscopies were performed at the English public health system from 2002 to 2013. It means an increase of more than 700%. Similar numbers were published in North America, with an increase of more than 350% in the period 2004–2009. During a similar period on the opposite side of the globe, Korean researches published a twofold increase between 2007 and 2010. In the midterm, there is a projected increase of 1388% by 2023 [1].

O. Marin-Peña (✉)
Orthopedic Surgery and Traumatology Department, University Hospital Infanta Leonor, Madrid, Spain
e-mail: olivermarin@yahoo.es

B. Lund
Orthopedic Department, Hospitalsenheden Horsens, Horsens, Denmark

O.R. Ayeni • J. Kay
Orthopedic Surgery and Traumatology Department, McMaster University, Hamilton, ON, Canada

P. Dantas
Department of Orthopaedic Surgery, Hospital CUF Descobertas, Lisbon, Portugal

D. Griffin • E. Dickenson
Department of Orthopaedic Surgery, Warwick Medical School, University of Warwick, Coventry, UK

V. Khanduja

Addenbrooke's – Cambridge University Hospital, Cambridge, UK

University of Cambridge, Cambridge, UK

The Bone & Joint Journal, Cambridge, UK

H.G. Said
Orthopaedic and Trauma Surgery Department, Assiut University Hospital, Asyut, Egypt

M. Tey • M. Tahoun
Department of Orthopaedic Surgery, Hospital del Mar, UAB, Barcelona, Spain

V. Mascarenhas
MSK imaging Unit, Imaging Center, Hospital da Luz, Lisbon, Portugal

M.A. Sadakah
Orthopaedic and Trauma Surgery Department, Tanta University Hospital, Tanta, Egypt

K.H. Sunil Kumar
Addenbrooke's – Cambridge University Hospital, Cambridge, UK

45
G.M.M.J. Kerkhoffs et al. (eds.), *ESSKA Instructional Course Lecture Book*,
https://doi.org/10.1007/978-3-662-56127-0_4

4.2 State-of-the-Art Treatment

Due to this increase of hip arthroscopy indications, it is very interesting to have a look at basic concepts that could be very useful for the beginners with this technique.

4.2.1 Good Indications for Hip Arthroscopy

The use of hip arthroscopy has recently developed and expanded more than in other joints such as the knee and shoulder. Several contributing factors are responsible for this delayed development. Anatomic constraints such as the femoral head sitting deeply recessed in the acetabulum, as well as the thick fibrocapsular and muscular envelope surrounding the hip, preclude large amounts of distension of the joint. Furthermore, the location of various neurovascular structures including the sciatic and lateral femoral cutaneous nerves makes portal placement in hip arthroscopy more complicated than in other joints. Moreover, the conditions for which hip arthroscopy is indicated such as femoroacetabular impingement (FAI), labral tears and extra-articular impingement have historically been poorly recognized and untreated [2]. Improvements in our understanding of these conditions about the hip, as well as enhanced imaging technology and arthroscopic tool development, have allowed for the recent expansion of indications for hip arthroscopic intervention. This chapter describes the common as well as emerging indications for hip arthroscopy.

4.2.1.1 Loose Body Removal

Etiologies of loose bodies within the hip joint include post-traumatic fragments of the femoral head or acetabulum, synovial chondromatosis, degenerative joint disease, avascular necrosis, osteochondritis dissecans, os acetabuli, calcium deposits inside a labral tear and foreign bodies such as bullets or pieces of surgical instruments. The diagnosis of a loose body within the hip joint involves a combination of patient history, clinical examination, diagnostic imaging and diagnostic intra-articular injections. Indications for arthroscopic removal include failure of nonoperative management after the diagnosis of a loose body within the joint. Access to the loose body may present a challenge for removal; however strategic positioning of portals such as direct anterior and posterolateral portals to access the acetabular fossa can improve access [3].

4.2.1.2 Septic Arthritis

The indications for arthroscopic management of septic arthritis of the hip include clinical, laboratory and imaging parameters. Clinical indications are pain to the anterior groin for less than 1 week, limited passive and active range of motion of the hip, inability to bear weight on the joint and/or pyrexia. Laboratory indications include leukocytosis, an elevated C-reactive protein level, an elevated erythrocyte sedimentation rate, purulent material on hip aspiration and/or a positive aspirate culture. When indicated, the arthroscopic procedure typically includes a thorough irrigation as well as debridement of any damaged or infected tissue [4].

4.2.1.3 Labral Tears

Labral tears can be traumatic or insidious in onset, and patients typically present with anterior groin pain that may radiate to the trochanteric or gluteal regions [5]. Physical examination manoeuvres that may indicate intra-articular pathology include passive log rolling of the affected leg, as well as the anterior impingement test. In terms of imaging, MRI is typically the preferred modality for labral tears as they allow for visualization of the labrum and surrounding soft tissues. A gadolinium-based contrast is added in magnetic resonance arthrography (MRA) to allow for separation of the labrum from the capsule, thereby enhancing visualization. A rigorous trial of non-surgical modalities including rest, medications, physical therapy and therapeutic injections should be completed prior to pursuing surgical intervention. The goal of surgery is to preserve the functional labral tissue with selective debridement and refixation of tissue (Fig. 4.1) [5]. A recent systematic review identified ten studies with a focus on the efficacy of hip arthroscopy for acetabular labral tears [6].

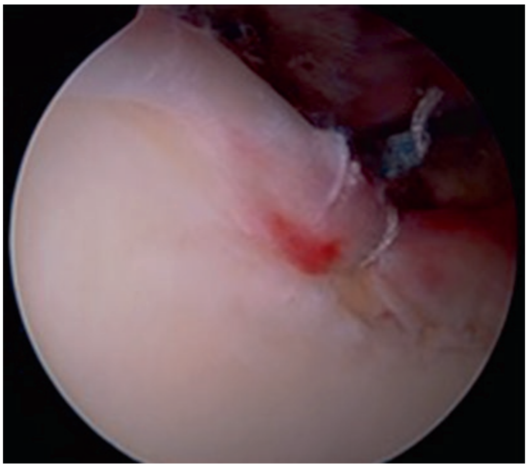

Fig. 4.1 Arthroscopic repair of a labral tear

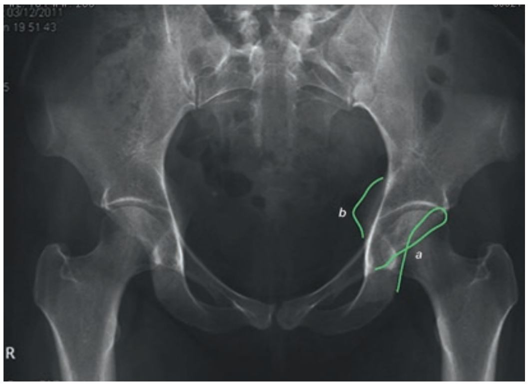

Fig. 4.2 FAI (pincer lesion) on an anteroposterior radiograph. (**a**) Crossover sign. (**b**) Medialization ischial spine

Fig. 4.3 FAI (cam lesion) on a frog-leg lateral radiograph

Good clinical outcomes have been described for patients with labral fixation and low-grade chondrolabral lesions [6]. Specific clinical hip scores should be used to evaluate the results after arthroscopic repair of hip labral injuries. Modified Harris Hip Score (mHHS), Hip Outcome Score (HOS), International Hip Outcome Tool 33 (iHOT 33) or Copenhagen Hip and Groin Outcome Score (HAGOS) are good clinical scores to measure clinical improvement after hip arthroscopy in young patients. Arthroscopic labral reconstruction may be considered in young and active patients who have undergone prior labral resection, with an irreparable or degenerative labrum, and a minimum of 2 mm joint space remaining [7].

4.2.1.4 FAI

The use of hip arthroscopy as a viable treatment option for FAI has expanded considerably in recent years. FAI is caused by a mismatch between the femoral head and acetabulum. Two subtypes of FAI, cam and pincer, involve abnormal morphologies of the femoral head and acetabular rim, respectively, with most patients presenting with a combination of these deformities (Figs. 4.2 and 4.3) [8].

The indications for arthroscopic management of FAI typically include a combination of pain, clinical examination findings, positive radiographic findings and diagnostic intra-articular injections. A positive impingement test was the commonest clinical examination manoeuvre used as an indication for surgery. Other special test manoeuvres such as FADIR (flexion, adduction and internal rotation), FABER (flexion, abduction and external rotation) (Fig. 4.4), C-sign and log roll have been reported to be involved in the decision-making process as well. Imaging modalities are important indications for arthroscopic management of FAI as well. In fact, it was found that 20% of studies that reported indications for hip arthroscopy used radiographic indications alone. The imaging modalities used include anteroposterior (AP) radiographs alone, as well as a combination of CT, MRI and MRA. Radiographic indications include, from most commonly used to least commonly used, cam or pincer lesions seen on AP radiographs, loss of sphericity of the femoral head (pistol-grip

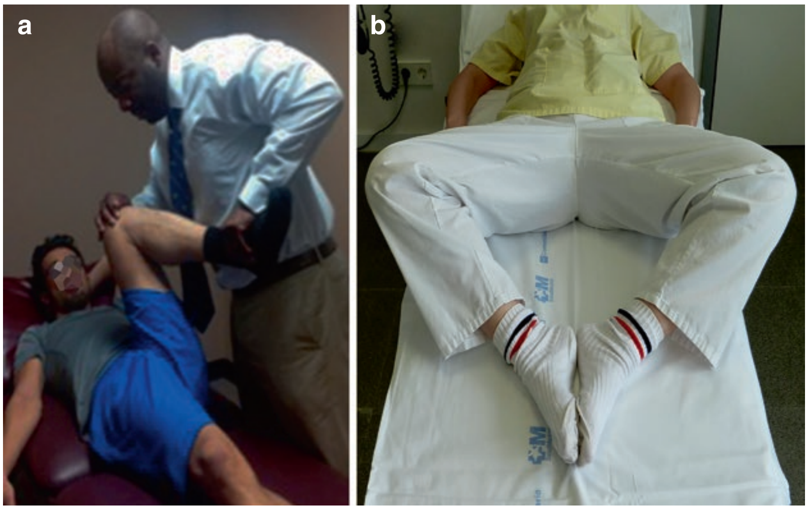

Fig. 4.4 (**a**) FADIR (flexion, adduction and internal rotation) and (**b**) FABER manoeuvres

deformity), acetabular retroversion, reduction of head-neck offset, alpha angle >50° and coxa profunda [9]. The duration of symptoms before consideration of surgical correction is typically reported as 6 months' time [9]. Arthroscopic surgical correction involves resection of the femoral head and neck, trimming of the osseous prominence on the acetabulum and repairing intra-articular damage such as cartilage and labral damage.

4.2.1.5 Extra-articular Disorders

The indications for the use of similar techniques for extra-articular pathology have continued to expand as well. Conditions include deep gluteal syndrome, internal snapping hip, external snapping hip and greater trochanteric pain syndrome [10]. In deep gluteal syndrome, entrapment of the sciatic nerve in the deep gluteal space causes pain in the buttock. Management with arthroscopic techniques involves exploration and decompression of the sciatic nerve from offending agents such as the piriformis, hamstring, obturator externus muscles or post-traumatic scar tissue. In two large series of 35 and 60 patients with deep gluteal syndrome, indications for hip arthroscopy were largely based on clinical symptoms and investigations such as imaging to rule out spinal pathology, diagnostic injections or the identification of an offending agent causing impingement on MRA [11, 12].

Sliding of the iliopsoas over the iliopectineal ridge or femoral head causes internal snapping hip. In symptomatic patients, a painful snapping sensation occurs with exercise. Indications for surgical management by means of arthroscopy involve failure of nonoperative management. First-line treatment consists of a rigorous trial of non-surgical modalities including rest, nonsteroidal anti-inflammatory drugs (NSAIDs), painkillers, physical therapy and steroid injections [13]. If patients continue to experience symptoms after nonoperative treatment, hip arthroscopy including release of the iliopsoas tendon at the pelvic brim or at its insertion to the lesser trochanter is appropriate [14]. Greater trochanteric pain syndrome includes a group of disorders at the lateral aspect of the hip including greater trochanteric bursitis, external snapping hip and gluteus medius/minimus tears. External snapping hip is caused by a thickened posterior iliotibial (IT) band, tensor fasciae latae or gluteus maximus sliding over the greater trochanter during flexion of the hip. First-line treatment for each of these conditions includes a trial of non-surgical modalities including rest, avoidance of inciting activities and anti-inflammatory medication and injections that were diagnostic and therapeutic in nature [15]. Failure of these nonoperative treatment options is the primary indication for surgical consideration [10]. Arthroscopic techniques are now more commonly used than open procedures, which include bursectomy, gluteus maximus tenotomy, IT band release, as well as abductor tendon debridement and repair [16].

4.2.1.6 Traumatic and Atraumatic Instability of the Hip

After traumatic dislocation of the hip, close reduction is the gold standard of treatment. If complete reduction is not achieved, arthroscopic surgery may be warranted to remove loose bodies or to manage accompanying labral tears and/or chondral injuries. Fractures of both the femoral head and acetabulum can be treated using arthroscopic-assisted techniques, assuming the patient is stable. Otherwise, patients with persistent pain and mechanical symptoms due to labral and/or chondral damage are suitable candidates for delayed arthroscopic management once stable [17]. Recently, hip arthroscopy has been considered for the treatment of recurrent, atraumatic instability as well. After a trial of nonoperative management, hip arthroscopy may be indicated when intra-articular injections provide significant relief in symptoms. However, patients undergoing arthroscopic management often undergo anatomic labral repair in addition to a capsule management procedure. Successful reduction in capsular volume, using either capsular plication or thermal capsulorrhaphy, is increasingly being reported. Connective tissue disorders such as Ehlers–Danlos syndrome that impact hip function can be treated with a capsular plication while addressing other concurrent lesions such as labral tears [18].

4.2.1.7 Arthroscopy in the Setting of Hip Arthroplasty

Another relatively novel indication for arthroscopic surgery of the hip involves its use after arthroplasty of the joint. The most common indication for arthroscopy in the setting of arthroplasty is in the management of patients with iliopsoas tendinopathy, commonly after a diagnostic injection of the iliopsoas tendon sheath. The second most common indication of this procedure in patients with a prior hip arthroplasty is to help with the diagnosis of persistent hip or groin pain [19].

4.2.1.8 Relative Contraindications

Although hip arthroscopy continues to expand with respect to its indications, contraindications to its use include patients with severe OA of the hip. Patients with no OA have substantially better pain and functional outcomes after hip arthroscopy than those with OA [20]. While medical history and physical examination may provide some indication as to when the extent of the OA has exceeded the allowable threshold, no definitive criteria have been established using these parameters. However, a recent systematic review has found that patients with radiographic parameters such as Tönnis grade 1 or higher or a joint space of 2 mm or less receive less benefit from hip arthroscopy and are more likely to ultimately covert to a total hip arthroplasty [21]. Other relative contraindications due to difficulties accessing the hip joint arthroscopically include obesity and significant bony deformities such as acetabular protrusio and severe heterotrophic ossification.

4.2.2 How to Best Learn Hip Arthroscopy: Dealing with the Learning Curve

Hip arthroscopy has been steadily gaining popularity since the 1970s and has seen a growth of magnanimous proportion in the last decade [22]. The concept of femoroacetabular impingement (FAI) was introduced in the late 1990s, and since then the number of publications relating to this subject has increased immensely [23]. FAI can be broadly classified into two types, cam and pincer; however, a majority of patients have a combination of both with one being a major abnormality [23]. Nonoperative measures to treat FAI include activity modification, analgesia and physiotherapy [23]. Ganz et al. proposed that early operative treatment of FAI led to slow the progression of arthritis in the hip joint [8]. Operative treatment primarily aims to treat the anatomical abnormality improving the clearance of motion of the hip joint and preventing abutment between the acetabular rim and femoral neck and secondarily to address the soft tissue damage caused by the impingement lesion [8]. The safe surgical dislocation with the trochanteric flip osteotomy was popularized by Ganz as a measure to address FAI, and of late, hip arthroscopy has become increasingly popular to achieve the same surgical goals [24]. On the other hand, in case of hip dysplasia, the surgical options available are either hip arthroscopy or periacetabular osteotomy for acetabular undercoverage. In addition to FAI and hip dysplasia, indications for hip arthroscopy include acetabular labral tears, ligamentum teres injuries, chondral defects in the hip joint, septic arthritis of the hip, loose bodies and synovial abnormalities of the hip and extra-articular indications such as snapping hip, trochanteric bursitis and gluteus medius tears, and the list keeps expanding [25]. This coupled with the fact that the risk of complications is around 3% makes the procedure attractive. However, it has a steep learning curve and is certainly not one for the inexperienced [26].

The senior author believes that one can achieve competence and become confident at performing hip arthroscopy only by having a structured approach to training. In addition to mastering the technical skills required for hip arthroscopy, understanding pathology and the decision-making process in the outpatient clinic are of utmost importance. This starts right from the assessment of a young adult with hip pain in clinic, arranging appropriate investigations and interpreting them correctly, and then finally making the decision of undertaking a hip arthroscopy if indicated. The role of a multidisciplinary team consisting of the hip surgeon, sports physician, radiologist and a physiotherapist cannot be underestimated in this regard.

Thus, not only performing the hip arthroscopic procedure safely and effectively is essential but also choosing the right patient for the procedure is paramount for a successful outcome. To progress in the technical art of arthroscopy of the hip and to become a safe and effective arthroscopist, one may consider the following avenues to master skills (Fig. 4.5):

- Simulation training
- Cadaveric skills training
- Fellowship in young adult hip surgery
- Mentored independent practice

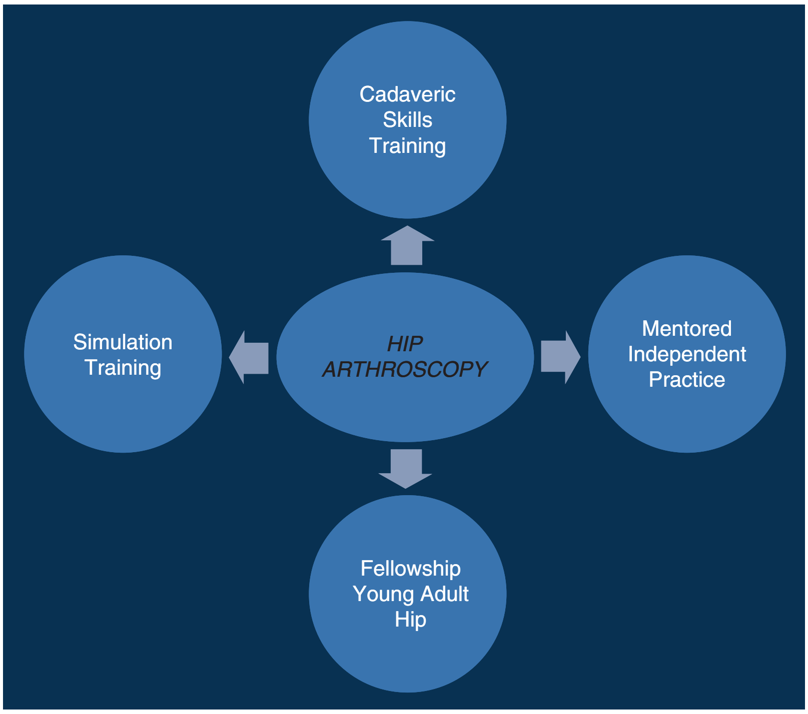

Fig. 4.5 Different aspects of a structured training in hip arthroscopy

The above is not an exhaustive list, and the surgeon may still find that his/her learning curve continues to improve throughout one's independent practice. Attending an educational meeting regularly during independent practice would give the surgeon the benefit of meeting up with their peers and discussing ideas, tips and tricks, advances in techniques and also any possible complications that one may have experienced.

4.2.2.1 Simulation Training

Virtual reality training has been shown to improve technical skills in orthopaedic surgery [27–29]. Therefore, the use of a virtual reality simulator in hip arthroscopy training has the potential to provide an additional benefit to a trainee surgeon [30]. In addition to the use of a simulator, adopting proficiency-based progression (PBP) in training has been shown to produce a superior arthroscopic skill set amongst the trainees [31]. PBP involves training to be undertaken in various key stages and several steps in each stage. A trainee then has to successfully progress through each stage. Training on an arthroscopic simulator helps with the trainee to go through a checklist making sure that one does not skip an essential step and also helps with improving hand-eye coordination [32]. In addition, simulation training can also be a useful tool to assess a trainee's judgment in a simulated setting, thereby assessing their cognitive and professional skills. This would in turn be helpful to provide a constructive feedback of both technical and non-technical skills [32]. Howells et al., in their study, showed improvement of knee arthroscopic psychomotor skills of orthopaedic trainees in theatre following a structured virtual reality knee simulator training programme [29].

4.2.2.2 Cadaveric Skills Training

With the introduction of European Working Time Directive (EWTD), there has been a significant reduction in total training time in surgical specialties in the UK from 30,000 h to around 6000 h [29]. Along with this reduction in training time, the surgical outcomes have been under public scrutiny, so one has to ensure that he/she is adequately trained in a specific procedure to provide safe and effective patient care [29]. Practicing the procedure in a cadaveric laboratory helps the trainee to experience the "feel" of the procedure in a controlled environment prior to undertaking the same procedure in a real patient [9]. Arthroscopic training in a cadaveric skills laboratory has been shown to be superior to virtual reality simulator training alone, in the case of knee arthroscopy, leading to a significantly faster progression to skill acquisition with cadaveric training [29]. The senior author chairs the Cambridge-ESSKA Hip Course, which is held in Cambridge (UK) annually and combines all the three aspects required for training in hip arthroscopy, i.e. didactic training via lectures and discussions, virtual reality hip arthroscopy simulation and alongside this state-of-the-art wet lab cadaveric training [33].

4.2.2.3 Fellowship in Young Adult Hip Surgery

Currently, the fivefold reduction in training time in Europe means that one has to undertake a specialist fellowship to consolidate clinical and surgical skills to bridge the gaps in training. In addition, hip arthroscopy is a very specialized procedure with only a select few centres and surgeons in Europe performing it in large numbers. Undertaking a specialist fellowship focused on treating hip problems in the young adult is essential for gaining adequate clinical exposure and improving surgical expertise. Travelling fellowships are invaluable, as well as in providing one with the experience from different centres of excellence, in particular a different approach to a familiar problem or tips and tricks to deal with a complex problem.

4.2.2.4 Mentored Practice During the Learning Curve

Setting up an independent surgical practice could be stressful in the beginning, especially if undertaking a highly specialized procedure like hip arthroscopy. Deitrich et al. have shown that with growing experience in performing hip arthroscopy, there was a decrease in the rate of complications [34]. At present, there is poor evidence to quantify the number of cases needed to overcome the learning curve; however some authors have reported that 30 cases are needed during this period [26, 35]. Furthermore, a newly appointed hip arthroscopy specialist may want to consider undertaking the procedure under the supervision of a senior surgeon, which has also been shown to significantly decrease the rate of complications [34]. Perez-Carro and Tey broadly classified the common pitfalls during the learning curve into three broad categories: (1) preoperative, (2) intraoperative and (3) postoperative [36]. Preoperative errors included improper or wrong patient selection and those related to improper patient positioning during hip arthroscopy [36]. Intraoperative errors included improper portal creation leading to nerve injury and/or difficult access to the hip joint and damage to intra-articular structures during introduction of instruments and those related to the total traction time [36]. These pitfalls can certainly be overcome by undertaking a structured training programme during a specialized hip arthroscopy fellowship in addition to virtual reality simulation training and cadaveric skills training which can also help with reduction in the learning curve.

4.2.2.5 Complications and Learning Curve

The rate of complications following hip arthroscopy is between 1 and 4%, for example, damage to femoral head, lateral femoral cutaneous nerve injury and neuropraxia of sciatic, femoral or pudendal nerve secondary to traction to name a few [37]. Harris et al. conducted a systematic review of 92 studies comprising of more than 6000 hip arthroscopies and found a major complication rate of 0.58% and minor complication rate of 7.5% [38]. It is therefore essential that during the initial part of the learning curve only non-complex, straightforward cases are selected to be performed via the arthroscopic route and open surgical dislocations performed for the complex cases. As the experience and the level of confidence increase, one can take on more challenging cases via the arthroscopic route. There is also evidence that with increasing experience, the rate of complications following hip arthroscopy decreases [38–40].

Adopting a structured approach to training is essential to gain an in-depth knowledge in the field of young adult hip surgery and hip arthroscopy in particular. Virtual reality simulation training and cadaveric skills training are useful adjuncts to a specialist hip arthroscopy fellowship. Finally, it would be an added benefit if one has a mentor during the initial phase of independent practice while going through the learning curve.

4.2.3 How to Get Safely into the Joint: Position and Portals

The main objective for beginners is to get a stable and comfortable setup for hip arthroscopy and obtain easy access through arthroscopic portals.

4.2.3.1 Patient Positioning

Hip arthroscopy can be effectively performed in a supine or lateral decubitus position. The position of the patient is largely dictated by the surgeon's preference and training. However, each position has its own benefits and drawbacks [41].

Supine Position

The patient is placed on a fracture table with the feet well-padded in traction boots and slightly lateralized towards the nonoperative leg, against a well-padded perineal post to limit the risk of pudendal nerve neuropraxia associated with traction. The nonoperative limb is abducted to approximately 45° with gentle traction applied to maintain the lateralized position [42, 43]. The supine position offers a familiar orientation of the joint to all orthopaedic surgeons. Also, a routine fracture table or a specialized traction table can be used [44]. Drawbacks to the supine position include difficult manoeuvrability in obese patients, and potentially decreased posterior access [45] (Fig. 4.6).

Lateral Position

A specialized traction table is usually needed. The patient must be stabilized in the decubitus position, usually with a beanbag, posts or a pegboard. Attention must be paid to padding downside bony prominences and placing an axillary roll to support the down arm. A perineal post is placed

	Recommendations
Padding of bony prominences	Foam padding, feet and ankles in traction boots, and blankets placed on ipsilateral arm
Ipsilateral upper exteremity	Placement across patient's body (flexion <90°), with pulse oximetry, papoose wrapping, and safety belt
Contralateral upper extremity	Arm board (shoulder abducted <60°, elbow flexion <20°) and IV access
Perineal post	Lateralized to operative side-contact with medial thigh (check for genital compression)
Foot and ankle	Traction boots
Fluoroscopy	45° lateral Dunn view, ROM, and vacuum crescent sign
Operative hip	15° of flexion and 0° of adduction before application of traction
Ipsilateral foot	Internal rotation of 10°-15°
Contralateral lower extremity	Delicate countertraction (10-20 lb [4.5-9 kg])

IV, intravenous; ROM, range of motion.

Fig. 4.6 Quick reference for hip arthroscopy procedure setup [43]

between the legs to allow for distraction and a lateral vector to the operative leg [44]. The lateral position is considered to have superior manoeuvrability in obese patients [46]. Also, it provides superior access to the posterior and inferior joint spaces compared with the supine position [47]. Disadvantages of lateral position include the extra time needed to position the patient and to adjust the perineal and traction posts in addition to the need to use special traction devices [41].

Most surgeons prefer general anaesthesia for hip arthroscopy because it provides adequate muscle relaxation for distraction, but regional anaesthesia can be a helpful adjunct in postoperative pain management [48]. Every effort should be made to maintain the patient's systolic blood pressure below 100 mmHg in order to optimize visualization [44].

4.2.3.2 Hip Joint Access

The hip joint space is separated into central and peripheral compartments by the acetabular labrum in addition to the extra-articular compartment around the hip joint (peritrochanteric space) [49]. So, the hip joint can be accessed either through:

1. "Central access first" is done under fluoroscopic guidance and under adequate joint distraction. This allows portal placement while minimizing the risk of injury to the labrum or cartilage [50]. However, there is a longer traction time with this technique, which leads to a higher risk of neurovascular and skin complication [51, 52].
2. "Peripheral access first", popularized by Dienst et al. [53], arthroscopic instruments are introduced along the anterior femoral neck region, which is devoid of articular cartilage and has a lower risk of injuring the labrum. This is followed by entry into the central compartment under vision without the need for fluoroscopy. No traction is needed during the arthroscopic access to the peripheral compartment. Masoud and Said [54] described anatomic surface landmarks for injection and access of the peripheral compartment that can markedly reduce or abolish the need for imaging guidance. This access is preferred by the author because it is easier and safer and involves less traction time (even acetabular recession could be started before traction) and because it is a very useful technique when central access fails.

3. "Outside-in technique", in which anterior extra-capsular space of the hip is defined under fluoroscopy, then the anterior capsule is identified under arthroscopic visualization, and capsulotomy is performed to access the peripheral compartment. However, this technique is technically demanding and can be considered extensive relative to the other techniques, and complications such as fluid extravasation and dislocation can occur [55]. This technique is most useful when intra-articular access could not be achieved as in cases with intra-articular adhesions.

4.2.3.3 Portals

For the peripheral compartment, the proximal anterolateral portal (PAL) and distal anterolateral portal (DAL) are the primary working portals (Fig. 4.7). Their direction is marked on the skin under fluoroscopy before their establishment with their intersection projecting onto the femoral head-neck junction. PAL, as described by Dienst et al. [53], is oriented 45° caudally with the entry point lying at the junction between the medial and the middle third of a line drawn between GT and ASIS (soft spot). DAL is placed on a curved line running distally from the PAL with the centre of the curve being the greater trochanter (Figs. 4.8 and 4.9).

Fig. 4.7 Demonstrates bony landmarks (GT and ASIS) with the needles denoting surface drawings (vertical line from ASIS and perpendicular line to GT). Black dotted line demonstrates the direction of PAL portal. Note position of PAL, DAL and AL portals

Fig. 4.8 Curved red line (centred over GT) from PAL portal along which DAL portal is established

Fig. 4.9 Shows the direction of PAL and DAL portals

For central compartment, the anterior (A), anterolateral (AL) and posterolateral (PL) portals are the primary working portals [41]. The AL is established first. It is placed 1 cm proximal and anterior to the tip of the GT and directed parallel to the femoral neck [56]. The superior gluteal nerve is found an average of 4.4 cm above the level of the anterolateral portal [44]. The anterior (A) portal is placed at the intersection of a longitudinal line drawn distally from the ASIS and a transverse line across the superior edge of the GT. This portal is orientated 45° cephalic and 30° towards the midline [56]. This portal is often made slightly lateral to this intersection to avoid the branches of the lateral femoral cutaneous nerve that usually branch proximal to the anterior portal, but small lateral branches may be injured. The femoral nerve is found an average of 3.2 cm medial to the location of the anterior portal. The posterolateral portal is located 1 cm superior and posterior to the tip of the GT. The sciatic nerve is most at risk as it lays approximately 2–3 cm posterior to the portal. Other described accessory portals used to access the peripheral or lateral compartments should be placed under direct visualization if needed [44].

4.2.3.4 Author's Preferred Technique

The patient is placed in the supine position. A trial traction is done under fluoroscopy to assess sufficient distraction of the hip joint (8–10 mm distraction is sufficient). The traction is done in the abducted position and then completed by adduction of the limb to lever over the post. Once achieved, the traction is then released, and the hip can be prepped and draped in the standard fashion. The leg is flexed to 30–50° to relax the anterior capsule which facilitates access to the peripheral compartment and protects the cartilage. The post is removed during work in this position and reapplied before traction.

The author prefers to initially access the joint through the DAL portal as there is more space in the distal compartment of the joint, the soft tissues are less resistant, and there is less risk of scuffing the distal part of the femoral head. A spinal needle is inserted parallel to the femoral neck towards the head-neck junction under fluoroscopic guidance. Once the intra-articular location of the needle is established, a cannulated switching stick is passed over the guide wire. A standard arthroscopic cannula is passed over the switching stick followed by introduction of a standard 70° scope. A PAL portal is established under arthroscopic vision targeting an entry point 1 cm distal to the labrum. This is followed by thinning of the anterior capsule either by a shaver or radiofrequency. It should be mentioned that capsulotomy is not preferred at this step in order to maintain the ballooning effect of the capsule. Then, a "seven-step" tour of the peripheral compartment starts. Switching of viewing portal between PAL and DAL is important to see "around the curve" for any pathology. In addition, flexion to 70° and acetabular recession of the pincer lesion are usually started in this stage. This helps further reduce the traction time. For central compartment access, the post is reapplied, the leg is extended, and traction is done. The AL portal is established under arthroscopic vision. This further minimizes the risk of lateral head cartilage scuffing or labral injury compared with setting this portal under fluoroscopy guidance. Then inter-portal capsulotomy is established between the PAL and AL portals. The instruments from the DAL are redirected through the same skin incision for further work through the central compartment.

4.2.4 Hip Arthroscopy Anatomy and Variations at Central and Peripheral Compartment

The hip has two intra-articular compartments, the central and the peripheral, separated by the acetabular labrum [57]. The central compartment (CC) includes the acetabular fossa, teres ligament, lunate surface, labrum, fovea capitis and the articular surface of the femoral head in the weight-bearing area. The peripheral compartment contains the femoral neck, the non-weight-bearing cartilage of the femoral head, the medial and lateral synovial folds, perilabral recess or paralabral sulcus, the non-articular surface of the labrum and the articular capsule [58, 59]. There are several methods to localize intra-articular lesions in hip arthroscopy. The two most commonly used mapping systems are the "clock face" system—standardized to the right hip, where 3:00 clock position is anterior, and the 6:00 position corresponds to the middle point of the transverse acetabular ligament—and the "geographic zone method" which allows for a precise and more reproducible description of a lesion's position [58, 60] (Fig. 4.10). Both systems can also be used for mapping the femoral head, and the reference lines follow the same pattern used in the acetabulum, so the femoral locations will reflect the corresponding acetabular locations. The clock face system also allows a good correlation with the radial MRI findings [58, 60].

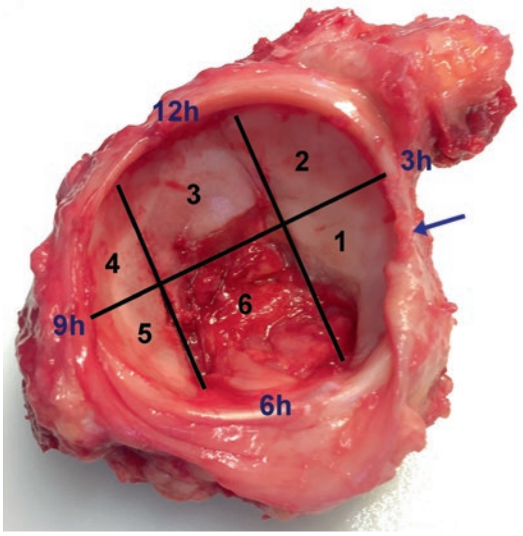

Fig. 4.10 The “clock face” system and the “geographic zone method” for the acetabular mapping. Arrow: the psoas U

4.2.4.1 Central Compartment

Acetabular Fossa

The acetabular fossa is located in the inferior region of the acetabulum and is surrounded by the horseshoe-shaped lunate surface. It is the non-articular surface of the acetabulum and is covered by synovium. The transverse ligament limits the inferior margin of the fossa and is in continuity with the anterior and the posterior labrum.

Ligamentum Teres

Arises from the transverse ligament and the ischial and pubic margins of the acetabular fossa and has a fascicular appearance with an anterior and posterior bundle. The ligamentum is trapezoidal at its base and runs to the femoral head where it becomes progressively round or oval shaped; it inserts in the fovea capitis. In the dynamic evaluation, the ligamentum is tight in hip external rotation, and head vascularity in adults is negligible [61, 62].

Fovea Capitis

The fovea capitis is a small area devoid of cartilage in the femoral head and is located slightly posterior and inferior to the centre of the femoral head cartilage. The articular cartilage thickness decreases from the centre to the periphery of the femoral head.

Labrum

The labrum is a fibrocartilage with a triangular cross section. Its base is inserted in the osseous acetabular rim, the articular or internal surface is in continuity with the acetabular cartilage, and the capsular or external surface is attached to the articular capsule. The labrum is in continuity with the transverse ligament antero-inferiorly and postero-inferiorly. The labral vascular supply arises from a periacetabular vascular ring with radial branches that course over the capsular surface of the labrum, terminating in its free edge [63]. This study did not show vessels entering the labrum from the adjacent subchondral bone. The clinical relevance of this fact is that the majority of the labral lesions are located in the chondrolabral junction with preservation of the vascularity, and the surgical labral detachment may interfere with its blood supply. The sublabral sulcus is an anatomic variant that should not be confused with a labral tear. In arthroscopy, it is a well-defined cleft between the labrum and the acetabular hyaline cartilage with smooth edges, with no signs of inflammation and no labral displacement or instability on probing. In the hips with a sublabral sulcus, the most frequent location is the postero-inferior (48%) and anterosuperior (44%) quadrant [64]. There is a normal concavity in the anterior acetabular rim in relation to the iliopsoas tendon (psoas U). It is universally present, and its superior aspect is a reliable arthroscopic landmark for the 3:00 clock position [58].

Physeal Scars

The ilio-pubic and the ilio-ischial physeal scars are remnants of the triradiate physis and can be found in the anterior and posterior lunate surfaces, respectively.

Stellate Crease and Supra-acetabular Fossa

The stellate crease is an anatomic variant and represents a focal fibrocartilaginous slitlike structure.

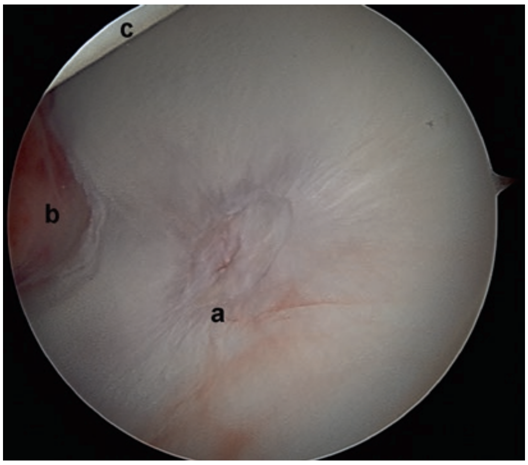

Fig. 4.11 Arthroscopic image of the left hip. The supra-acetabular fossa (**a**) separated from the acetabular fossa (**b**) and the femoral head (**c**)

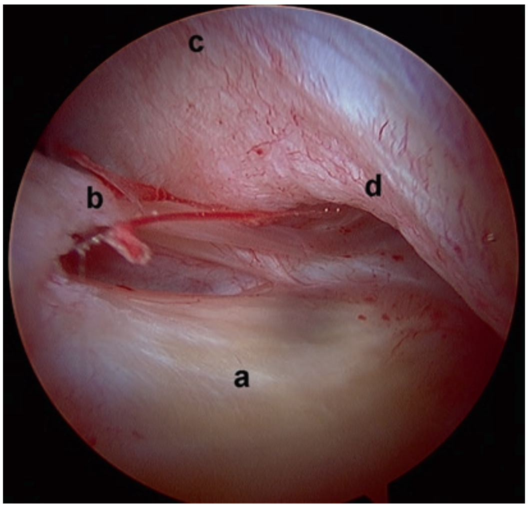

Fig. 4.12 Arthroscopic image of the peripheral compartment of a right hip. The anterior femoral neck (**a**), the medial synovial fold (**b**), the anterior capsule (**c**) and the zona orbicularis (**d**)

Its location is variable but is usually found above the apex of the acetabular fossa at the 12:30 position. Another anatomic variant, more frequent in younger patients, is the supra-acetabular fossa located in the roof of the acetabulum at the 12:00 position on coronal and sagittal imaging. It can be detected in high-resolution hip MRI scans with normal marrow signal intensity and should not be confused with an osteochondral lesion (Fig. 4.11). The stellate crease is in continuity with the acetabular fossa, while supra-acetabular fossa is completely separated from it, but the former might be a residual scar left after obliteration of the supra-acetabular fossa [65, 66].

4.2.4.2 Peripheral Compartment

The peripheral compartment (PC) consists of the unloaded cartilage of the femoral head (FH); the femoral neck with the medial, anterior and posterolateral synovial folds (Weitbrecht's ligaments); the articular capsule with its intrinsic ligaments, including the zona orbicularis (ZO); the non-articular surface of the labrum and the perilabral recess or paralabral sulcus. PC of the hip can be divided routinely into the following areas: anterior neck area, medial neck area, medial head area, anterior head area, lateral head area, lateral neck area and posterior area (Fig. 4.12). Access to the CC can be undertaken by, initially, approaching the PC and, afterwards, accessing the CC under arthroscopic control [67]. Another technique to access the PC is an outside-in approach. The access to the PC is also important because loose bodies are commonly located here, and ultimately femoral osteoplasty is performed in the PC.

Labrum

The external surface of the labrum is observed from the PC enclosing the femoral head. At labral insertion lays the synovial membrane responsible for some of the labrum vascularization. In turn, the congruency of the labrum and the FH creates a perfect sealing mechanism. The acetabular labrum exhibits variability in shape, symmetry and dimensions. Labral shape can vary between triangular (66–69% of asymptomatic hips), round (11–16%) and flat (9–13%). It is thickest in the superior and posterior aspects and widest in the anterior and superior portions [68]. At the anterior and posterior margins, the hip joint capsule inserts directly at the base of the labrum. On the superior aspect of the PC, the anatomic space created between the joint capsule and labrum is the perilabral sulcus which is larger in this zone and also might be subject to dimensional variability [69].

Synovial Folds

Synovial folds are sheetlike structures of synovial and connective tissue that run longitudinally in various zones of the peripheral compartment and serve as important landmarks. The *medial synovial fold* ("iliopectineal fold") is located at the antero-medial aspect of the femoral neck but usually is not stuck to it. This structure is a very helpful landmark (guide to the 6:00 position), especially when visibility within the PC is limited by synovial disease. This fold passes proximally from the medial border of the femoral head, distal to the lesser trochanter [67]. The anterior synovial fold is adherent to the neck and only recognizable by its single fibres covering the bone of the neck. The lateral synovial fold is located at the junction between the lateral and the posterior femoral neck being a common landmark to the 12:00 position [58]. It runs from the greater trochanter upwards along the lateral side of the neck to the lateral margin of the head. It is often posteriorly stuck to the neck and forms a small pouch. It contains the lateral retinaculum and the intracapsular penetrating arteries from the lateral epiphyseal vessels arising from the terminal branches of the deep medial circumflex artery (the major responsible of femoral head blood supply). This fold usually marks the endpoint of trimming of the femoral head-neck junction in femoroacetabular impingement. Thus, preservation of these vessels is of primary importance, although cam deformities frequently extend beyond this point [70, 71].

Capsule

The anatomical structure that most influences the peripheral space is the joint capsule. It is a thick and tense fibrous sleeve extending from the outer neck to the acetabular rim. The inner surface is entirely covered with synovium. Some portions of the capsule have an increased thickness or are reinforced. Namely, (a) the superolateral part is reinforced by the reflected tendon of the rectus femoris, (b) the anterolateral part by the ilio-femoral ligament (y-shaped ligament of Bigelow), (c) the antero-medial part by the pubofemoral ligament and (d) the posterior capsule by the ischio-femoral ligament.

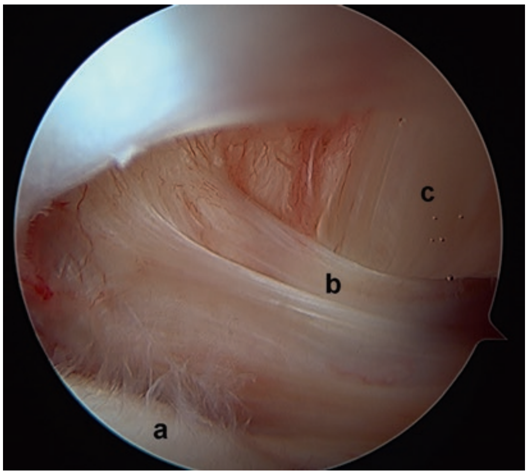

Fig. 4.13 Arthroscopic image of the peripheral compartment of a right hip with an articular communication with the iliopsoas tendon. The femoral head (**a**), the anterior capsule (**b**) and the iliopsoas tendon (**c**)

The zona orbicularis (ZO) is a major hip stabilizer and represents a circumferential thickening of the hip capsule forming a ring around the femoral neck. It consists of a thicker layer of annular fibres crossing the above-mentioned longitudinal ligaments and thus strengthening the capsule. Just cranial to the ZO, close to the anterior capsular recess, lies the psoas tendon. The iliopsoas bursa is located beneath the musculotendinous portion of the iliopsoas muscle, anterior to the hip joint capsule and lateral to the femoral vessels. The bursa separates the iliopsoas tendon from the articular capsule of the hip joint, and it may directly communicate with the PC in 15–20% of cases [69]. This finding may bear clinical relevance and can increase the risk of fluid extravasation during hip arthroscopy (Fig. 4.13).

4.2.5 How to Treat Cam Deformity: Tips and Tricks

Femoroacetabular impingement syndrome is most often associated with cam morphology. Successful treatment depends on precise reshaping of the proximal femur, whether done arthroscopically or by open surgery. We present ten steps to help get arthroscopic surgery right.

4.2.5.1 Be Sure of the Diagnosis

Not all patients with cam morphology have FAI syndrome, and coexisting diagnosis are common [72]. Be certain that this is the correct diagnosis before embarking on surgery. Local anaesthetic test injections and image intensifier examination under sedation, performed by the surgeon, and with pre- and postinjection exercise testing are very helpful. Be cautious of operating on patients with a negative injection test, and use the examination under sedation to inform the preoperative planning [73].

4.2.5.2 Preoperative Planning

We always perform CT with 3D reconstruction before surgery to reshape a cam. Modern CT protocols allow a low dose of radiation, without compromising the image quality. The 3D reconstruction acts as a map that can guide you around the hip (Fig. 4.14). Measurements from the scans allow accurate reshaping by quantifying depth and extent of bone resection. These scans should also include the distal femur so that femoral torsion can be measured and taken into account in planning the depth of resection.

Fig. 4.14 3D reconstruction of CT. A planned cam resection margin is marked

4.2.5.3 Setup

Surgery can be performed in supine or lateral positions. We prefer the lateral position as it is easy to achieve posterolateral access to the hip, the scrub nurse can work from other side of the patient, and the instruments do not fall out. Whichever approach is preferred, a range of motion from hyperextension to 100° flexion, abduction and internal and external rotation in flexion must be achievable. The foot must be easily detachable and reattachable from the traction system so that traction can be used where required while also allowing a wide range of motion (Fig. 4.15). We use a fully transparent drape with adhesive to allow visualization of the hip. An image intensifier, that can provide AP and lateral views, is required without interfering with the surgeon's position.

4.2.5.4 Portals

Most cases will need two to four portals depending on the technique and the shape and location of the cam. We typically use three portals: postero-superior, antero-superior and superior-lateral. Inject local anaesthetic with adrenaline into the skin before each incision to minimize bleeding. Avoid crowding by spacing out the entry points, and think carefully about where they penetrate the capsule more than the exact position of the skin

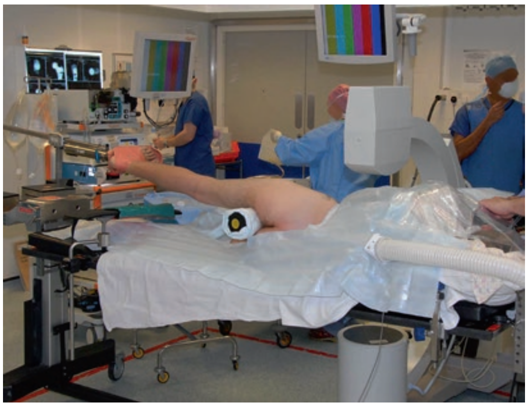

Fig. 4.15 Operating theatre set up with the patient in the lateral position. The surgeon stands behind the patient with the scrub nurse opposite. The C-arm, of the image intensifier, is under the radiolucent table, providing an AP view of the hip. The C-arm can rotate to provide a lateral view. When not in use the image intensifier moves to the distal end of the table

incision. Optimize triangulation by aiming for an angle of approximately 60° between each portal.

4.2.5.5 Capsulotomy

It is possible to reshape a cam without performing a capsulotomy, but for most cases a capsulotomy will improve visibility and access. We use an "L"-shaped capsulotomy extending from 11 to 1 o'clock, parallel to the labrum and from 1 o'clock towards the capsular insertion on the intertrochanteric line parallel to the femoral neck. This avoids dividing the ilio-femoral ligament and ensures postoperative stability of the hip. Only when the cam is large and extends well laterally does the second limb of the capsulotomy need to traverse the zona orbicularis. We control the capsulotomy flap with traction sutures and retractors inserted through the third portal.

4.2.5.6 Step-by-Step Reshaping

With the hip in traction, a 70° arthroscope in the postero-superior portal and a profile view of the postero-superior and superior head-neck junction, we begin resection just in front of the retinacular vessels. If the cam is very superior and lateral, then you may need to dissect these vessels as bone is removed, protecting them from injury. This is made easier by slightly abducting and extending the hip. Extend the intended line of the head-neck junction across the anterior aspect of the cam towards the inferior aspect of the neck, reducing traction and flexing the hip off traction to achieve a good view. Refer the 3D reconstruction of the CT to ensure the new head-neck junction is neither too medial nor too lateral. With various combinations of flexion and internal rotation of the hip, expose the more lateral aspect of the cam, and resect this right out to the normal neck surface. Make sure the resection extends all the way inferiorly by visualizing the medial synovial fold (Fig. 4.16). Frequently move the arthroscope, and change portals to properly appreciate the three-dimensional shape of the resection.

4.2.5.7 Create a Smooth Head-Neck Transition

Avoid a sharp edge at the junction between the femoral neck cartilage and the femoral neck, which might catch on the labrum during extension from a flexed position. Ideally, the profile should be an "S" shape with convexity at the edge of the femoral head and a concavity further lateral on the neck (Fig. 4.17). This will keep the labrum in contact

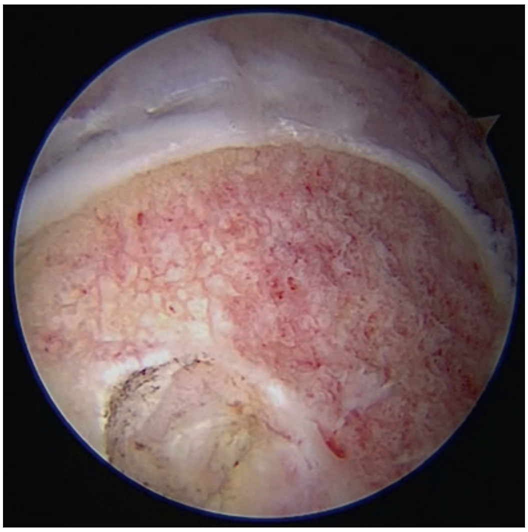

Fig. 4.16 View of antero-superior femoral head-neck junction following a cam resection

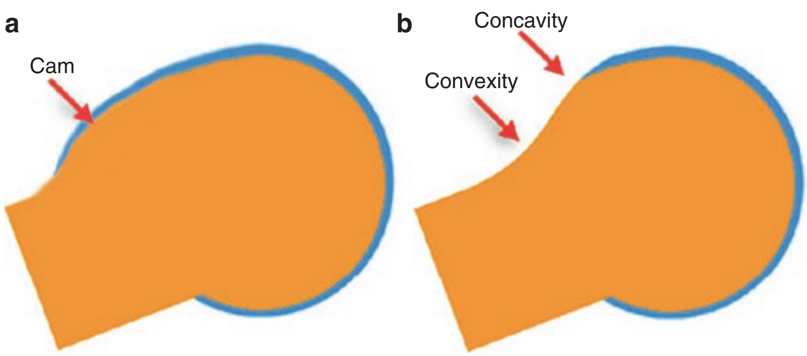

Fig. 4.17 Diagrammatic representation of cam morphology before (**a**) and after (**b**) resection. Note the "S"-shaped resection

with the head-neck junction throughout movement and help to maintain suction seal and stability.

4.2.5.8 Be Sure that the Shape Is Correct

Use an image intensifier to monitor progress of the resection, especially in the early part of your surgical experience. Always perform a dynamic impingement test observing the labrum and the head-neck junction through the arthroscope. Check in particular that the resection is adequate during flexion, adduction and internal rotation: flexion abduction and internal rotation and pure abduction.

4.2.5.9 Be Prepared to Close the Capsule

Hip instability is a devastating complication of hip arthroscopy, so we always consider whether to close the capsule. It may not be necessary in every patient, but we are more likely to do it if the patient has ligamentous laxity, a relatively shallow acetabulum, labral or ligamentum teres deficiency, performs a flexibility sport, has needed a more extensive capsulotomy dividing the zona orbicularis or has had a large resection. We close with several sutures including the corner of the "L" shape and the zona orbicularis.

4.2.5.10 Recovery and Rehabilitation

Use cryotherapy and CPM to facilitate early mobilization. Almost all patients can be fully weight bearing after surgery and can start exercising with a physiotherapist on the same day. We prefer to keep patients in the hospital for a day or two, so that they can begin with an intensive course of rehabilitation. Subsequent recovery is driven by milestones, which include a quiet hip with a full range of motion, normal core and hip muscle control and normal strength in dynamic movements. Most patients can return to full activity including sports training within 3 months.

Open surgery to correct cam morphology in FAI syndrome has been very successful where surgeons have been careful to achieve very accurate reshaping to a spherical head with a smooth head-neck transition [74]. Sometimes this is still the best approach. However, cam reshaping can be successfully performed in many patients by arthroscopic surgery [75]. Despite the extra challenges of a limited view and difficult access, arthroscopic surgery needs to achieve the same precision as an open approach. Only then does the less invasive technique provide an advantage. These ten steps provide a framework, but the best way to learn the surgical technique is in a hip preservation fellowship with a high-volume expert surgeon.

4.2.6 How to Manage a Chondro-Labral Lesion

The normal movement of the hip is purely rotatory due to the spherical congruency of the joint surfaces, so any change in this strict configuration will produce mechanical dysfunction and abnormal stresses on the articular cartilage. Cam deformity was described as a bony morphological change in the head-neck junction, mainly in the anterolateral area, that produces outside-in shear stress on the corresponding acetabular rim during the terminal flexion and internal rotation resulting in chondro-labral damage, usually labral detachment and chondral delamination (Fig. 4.18). On the other side, acetabular overcoverage may produce a pincer effect against the femoral neck on the terminal range of flexion.

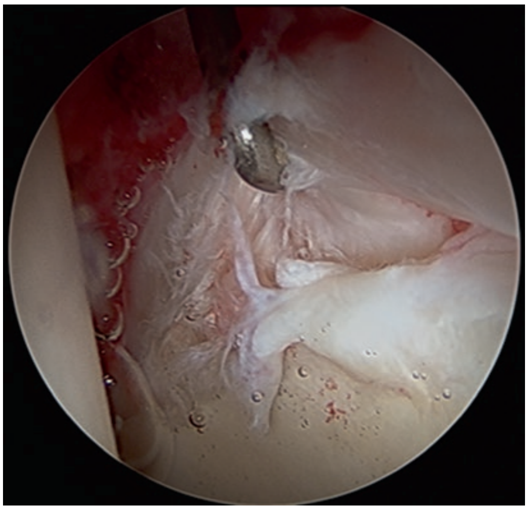

Fig. 4.18 Arthroscopic view of left hip with mixed type of FAI from anterolateral portal. The probe is showing labral detachment associated with a peripheral acetabular cartilage lesion

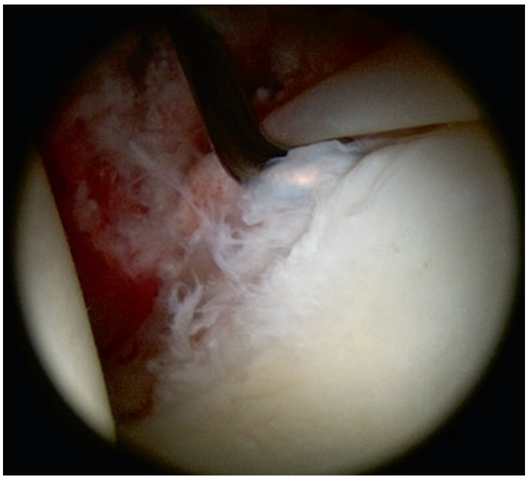

Fig. 4.19 Arthroscopic view of left hip with pincer type of FAI from anterolateral portal. A small labrum is typical in those cases, and detachment and degeneration due to impact at anterolateral zone are usually found

This compression mechanism against the labrum can lead to contusion and degeneration of it (Fig. 4.19). Secondarily, a levering mechanism of the head against the postero-inferior acetabular cartilage produces a contrecoup cartilage lesion [76, 77]. Instability is a wide term that includes the gross subluxation and dislocation caused by significant bony dysplasia as well as the new concept of microinstability caused by traumatic or atraumatic dysfunction of the soft tissues stabilizing the hip as the labrum, capsule, ligaments and muscles. In case of instability, there are abnormal translation movements of the femoral head producing inside-out shearing forces (mainly anterior to lateral) and causing chondrolabral injuries [78, 79] leading to detachment of the labrum in a similar way that cam lesion does.

4.2.6.1 Diagnosis

Chondro-labral lesions should be suspected in a young athletic patient presenting with groin pain during activity. As initial assessment, plain radiographs are used for detecting the underlying pathologies that predispose to chondro-labral lesions. Measurements of the centre-edge angle of Wiberg, acetabular index angle of Tönnis, alpha angle, head-neck offset and crossover sign of acetabular retroversion are reliable radiological findings for evaluating the bony morphology before and after any kind of hip preservative surgery [79].

Although the Tönnis classification is widely used for grading osteoarthritis based on specific radiographs, it cannot be used as an accurate predictor for condition of the cartilage in the early stages of the joint disease [80]. After development of magnetic resonance techniques, MRA with intra-articular injection of gadolinium has become the investigation of choice for detection of chondro-labral lesions with high sensitivity (71–100%) compared with standard MRI [81]. Nowadays, quantitative MRI techniques can map the concentration of glycosaminoglycans (GAGs) in the cartilage. Delayed gadolinium-enhanced MRI of cartilage (dGEMRIC) or T2 mapping is used for detecting early damage and for follow-up of patients after preservative hip surgeries [82].

4.2.6.2 Classification

Clinical interest towards hip pathologies produced many classification systems to describe the chondro-labral lesions. According to Beck et al. [76], labral condition is classified as (1) normal, (2) degeneration, (3) full-thickness tear, (4) detachment or (5) ossification, while articular cartilage is classified as (1) normal, (2) malacia, (3) debonding, (4) cleavage or (5) defect. Although most of these classification systems depend on the visual inspection of the lesion, the geographic description (Fig. 4.10) based on the six anatomical zones done by Ilizaliturri et al. [60] provides a simple and reproducible method with implications for prognosis and is commonly used for medical reporting.

4.2.6.3 Approach for Treatment

Since it was first described by Ganz et al. [83] in the early 2000s, surgical hip dislocation gained a worldwide popularity as a safe method for treatment of intra-articular hip lesions. However the evolution of arthroscopic techniques attracted the attention of hip surgeons, and today hip arthroscopy is a commonly performed procedure for intra-articular lesions and achieved favourable clinical outcomes compared with other surgical methods [84]. Cam deformity and acetabular overcoverage, if present, should be properly corrected as a first step of treatment to protect the repaired chondro-labral tissues and avoid further damage. Labral debridement was reported with satisfactory short-term clinical results in a few literature reports, but recent studies demonstrate better clinical outcomes in hip scores with labral preservation, becoming this option as the gold standard for labral damage repair. Biomechanical studies show that labral reattachment restores normal biomechanics. Labral preservation is the actual standard of care, so reattachment is performed when possible, and labral replacement should be considered when it is strongly degenerated or absent. The articular cartilage has poor intrinsic healing capacity, so the aim of treatment is to potentiate the cartilage healing and reproduce a new tissue with structural and biomechanical properties similar to the normal cartilage. Labral repair can be considered only in stable pocket lesions (Fig. 4.20), where viable chondrocytes can be demonstrated at the delaminated flaps of acetabular cartilage.

Debridement and bone marrow stimulation techniques are considered standard methods for small, focal full-thickness defect <2 cm^2 at the acetabular rim (Fig. 4.21), with improvement in the functional outcomes [85]. The microfracture technique depends on stimulation of subchondral bone marrow by penetrations that liberate undifferentiated stem cells, and then the blood clot formed in the defect provides a supporting environment for the cartilage progenitor cells and finally differentiates into stable fibrocartilage. Enhanced bone marrow stimulation techniques (EBMST) have been developed to improve the results of surgical standard methods of cartilage repair. For instance, AMIC technique adds membranes to the microfractured area, and chitosan-glycerol phosphate works as a scaffold material. These techniques augmented the biomechanical properties of clot formed in the microfractured area and provided more stable environment for growth and differentiation of hyaline cartilage. Both are recommended for full-thickness defect >2 cm^2 after adequate debridement and microfracture [86].

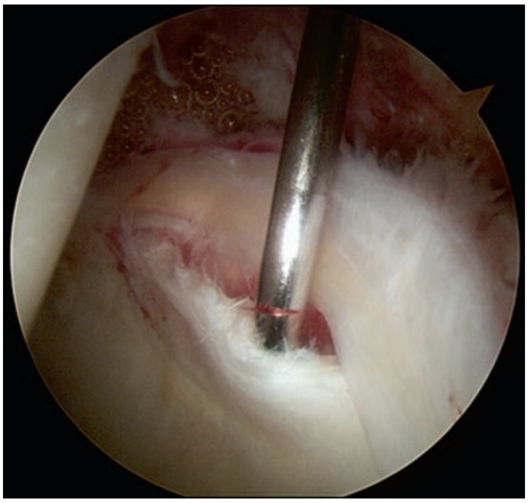

Fig. 4.20 Arthroscopic view of left hip with cam type of FAI from anterolateral portal. Cartilage delamination due to shear force named pocket lesion. Cartilage repair may be an option in these cases

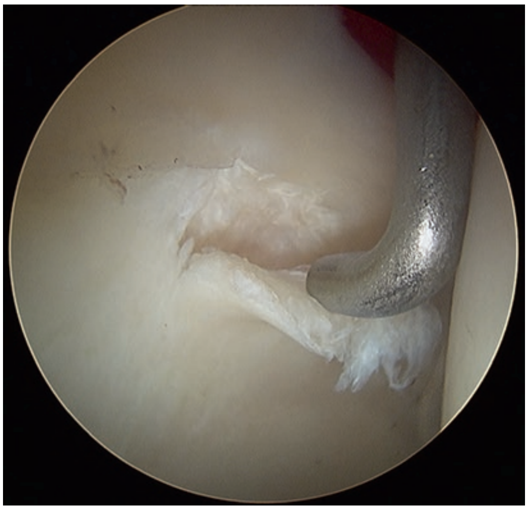

Fig. 4.21 Arthroscopic view of the right hip with cam type of FAI from anterolateral portal. Cartilage delamination has evolved to an unstable flap

4.3 Take-Home Message

Hip arthroscopy is an evolving technique that is expanding its indications. We should be very cautious during the learning curve period, and we must be very careful with the small details mentioned in this chapter. Special care should be taken to get a stable and comfortable initial setup of the patient. Knowledge of arthroscopic anatomy and its normal variants could facilitate identification of the anatomical deformities and its proper correction.

References

1. Maradit Kremers H, Schilz SR, Van Houten HK, Herrin J, Koenig KM, Bozic KJ, et al. Trends in utilization and outcomes of hip arthroscopy in the united states between 2005 and 2013. J Arthroplast. 2017;32(3):750–5.
2. Kelly BT, Williams RJ, Philippon MJ. Hip arthroscopy: current indications, treatment options, and management issues. Am J Sports Med. 2003;31(6):1020–37. http://www.ncbi.nlm.nih.gov/pubmed/14623676
3. Domb B, Botser I. Loose bodies: tips and pearls. In: Thomas Byrd JW, editor. Operative hip arthroscopy. New York: Springer; 2013. p. 161–9. https://doi.org/10.1007/978-1-4419-7925-4_12.
4. De Sa D, Cargnelli S, Catapano M, et al. Efficacy of hip arthroscopy for the management of septic arthritis: a systematic review. Arthrosc J Arthrosc Relat Surg. 2015;31(7):1358–70. https://doi.org/10.1016/j.arthro.2014.12.028.
5. Lynch TS, Terry MA, Bedi A, Kelly BT. Hip arthroscopic surgery: patient evaluation, current indications, and outcomes. Am J Sports Med. 2013;41(5):1174–89. https://doi.org/10.1177/0363546513476281.
6. Stevens MS, LeGay DA, Glazebrook MA, Amirault D. The evidence for hip arthroscopy: grading the current indications. Arthrosc J Arthrosc Relat Surg. 2010;26(10):1370–83. https://doi.org/10.1016/j.arthro.2010.07.016.
7. Ayeni OR, Alradwan H, de Sa D, Philippon MJ. The hip labrum reconstruction: indications and outcomes-a systematic review. Knee Surg Sport Traumatol Arthrosc. 2014;22(4):737–43. https://doi.org/10.1007/s00167-013-2804-5.
8. Ganz R, Parvizi J, Beck M, Leunig M, Nötzli H, Siebenrock KA. Femoroacetabular impingement: a cause for osteoarthritis of the hip. Clin Orthop Relat Res. 2003;417:112–20. https://doi.org/10.1097/01.blo.0000096804.78689.c2.
9. Ayeni OR, Wong I, Chien T, Musahl V, Kelly BT, Bhandari M. Surgical indications for arthroscopic management of femoroacetabular impingement. Anthroscopy. 2012;28:1170–9. https://doi.org/10.1016/j.arthro.2012.01.010.
10. Reich MS, Shannon C, Tsai E, Salata MJ. Hip arthroscopy for extra-articular hip disease. Curr Rev Musculoskelet Med. 2013;6(3):250–7. https://doi.org/10.1007/s12178-013-9177-8.
11. Park M, Yoon S-J, Jung S, Kim S-H. Clinical results of endoscopic sciatic nerve decompression for deep gluteal syndrome: mean 2-year follow-up. BMC Musculoskelet Disord. 2016;17(1):218. https://doi.org/10.1186/s12891-016-1062-3.
12. Martin HD, Shears SA, Johnson JC, Smathers AM, Palmer IJ. The endoscopic treatment of sciatic nerve entrapment/deep gluteal syndrome. Arthrosc J Arthrosc Relat Surg. 2011;27(2):172–81. https://doi.org/10.1016/j.arthro.2010.07.008.
13. Allen W, Cope R. Coxa saltans: the snapping hip revisited. J Am Acad Orthop Surg. 1995;3(5):303–8. http://www.ncbi.nlm.nih.gov/pubmed/10790668
14. Byrd JWT. Snapping hip. Oper Tech Sports Med. 2005;13(1):46–54. https://doi.org/10.1053/j.otsm.2004.09.003.
15. Shbeeb MI, O'Duffy JD, Michet CJ, O'Fallon WM, Matteson EL. Evaluation of glucocorticosteroid injection for the treatment of trochanteric bursitis. J Rheumatol. 1996;23(12):2104–6.
16. Domb BG, Nasser RM, Botser IB. Partial-thickness tears of the gluteus medius: rationale and technique for trans-tendinous endoscopic repair. Arthrosc J Arthrosc Relat Surg. 2010;26(12):1697–705. https://doi.org/10.1016/j.arthro.2010.06.002.
17. Newman JT, Saroki AJ, Philippon MJ. Hip arthroscopy for the management of trauma: a literature review. J Hip Preserv Surg. 2015;2(3):242–8. https://doi.org/10.1093/jhps/hnv047.
18. Shindle MK, Ranawat AS, Kelly BT. Diagnosis and management of traumatic and atraumatic hip instability in the athletic patient. Clin Sports Med. 2006;25(2):309–26. https://doi.org/10.1016/j.csm.2005.12.003.
19. Heaven S, Simunovic N, Williams DS, Naudie D, Ayeni OR. Hip arthroscopy in the setting of hip arthroplasty. Knee Surg Sport Traumatol Arthrosc. 2016;24(1):287–94. https://doi.org/10.1007/s00167-014-3379-5.
20. Kemp JL, MacDonald D, Collins NJ, Hatton AL, Crossley KM. Hip arthroscopy in the setting of hip osteoarthritis: systematic review of outcomes and progression to hip arthroplasty. Clin Orthop Relat Res. 2014;473(3):1055–73. https://doi.org/10.1007/s11999-014-3943-9.
21. Domb BG, Gui C, Lodhia P. How much arthritis is too much for hip arthroscopy: a systematic review. Arthrosc J Arthrosc Relat Surg. 2015;31(3):520–9. https://doi.org/10.1016/j.arthro.2014.11.008.
22. Palmer A, Malak TT, Broomfield J, Holton J, Majkowski L, Thomas GE, Taylor A, Andrade AJ, Collins G, Watson K, Carr AJ, Glyn-Jones S. Past and projected temporal trends in arthroscopic hip surgery in England between 2002 and 2013. BMJ Open Sport Exerc Med. 2016;2(1):e000082. eCollection 2016
23. Leunig M, Ganz R. The evolution and concepts of joint-preserving surgery of the hip. Bone Joint J. 2014;96-b(1):5–18.

24. Imam S, Khanduja V. Current concepts in the diagnosis and management of femoroacetabular impingement. Int Orthop. 2011;35(10):1427–35.
25. Bedi AK, Kelly BT, Khanduja V. Arthroscopic hip preservation surgery: current concepts and perspective. Bone Joint J. 2013;95-B(1):10.
26. Konan S, Rhee SJ, Haddad FS. Hip arthroscopy: analysis of a single surgeon's learning experience. J Bone Joint Surg Am. 2011;93(Suppl 2):52–6.
27. Aim F, Lonjon G, Hannouche D, Nizard R. Effectiveness of virtual reality training in orthopaedic surgery. Arthroscopy. 2016;32(1):224–32.
28. Boutefnouchet T, Laios T. Transfer of arthroscopic skills from computer simulation training to the operating theatre: a review of evidence from two randomised controlled studies. SICOT-J. 2016;2:4.
29. Howells NR, Gill HS, Carr AJ, Price AJ, Rees JL. Transferring simulated arthroscopic skills to the operating theatre: a randomised blinded study. J Bone Joint Surg Br Vol. 2008;90(4):494–9.
30. Khanduja VL, Lawrence JE, Audenaert E. Testing the construct validity of a virtual reality hip arthroscopy simulator. Arthroscopy. 2017;33(3):566–71.
31. Angelo RL, Ryu RK, Pedowitz RA, Beach W, Burns J, Dodds J, et al. A proficiency-based progression training curriculum coupled with a model simulator results in the acquisition of a superior arthroscopic Bankart skill set. Arthroscopy. 2015;31(10):1854–71.
32. Cannon WD, Garrett WE Jr, Hunter RE, Sweeney HJ, Eckhoff DG, Nicandri GT, et al. Improving residency training in arthroscopic knee surgery with use of a virtual-reality simulator. A randomized blinded study. J Bone Joint Surg Am. 2014;96(21):1798–806.
33. Sunil Kumar KL, Lawrence JE, Khanduja V. Training young adult hip surgeons for the future: the Cambridge vision. Bone Joint 360. 2016;5(6):8–12.
34. Dietrich F, Ries C, Eiermann C, Miehlke W, Sobau C. Complications in hip arthroscopy: necessity of supervision during the learning curve. Knee Surg Sports Traumatol Arthrosc. 2014;22(4):953–8.
35. Hoppe DJ, de Sa D, Simunovic N, Bhandari M, Safran MR, Larson CM, et al. The learning curve for hip arthroscopy: a systematic review. Arthroscopy. 2014;30(3):389–97.
36. Perez-Carro L, Tey M. What goes on during the learning curve? In: Marín-Peña O, editor. Femoroacetabular impingement. Berlin Heidelberg: Springer; 2012. p. 123–30.
37. Griffiths EJ, Khanduja V. Hip arthroscopy: evolution, current practice and future developments. Int Orthop. 2012;36(6):1115–21.
38. Harris JD, McCormick FM, Abrams GD, Gupta AK, Ellis TJ, Bach BR Jr, et al. Complications and reoperations during and after hip arthroscopy: a systematic review of 92 studies and more than 6,000 patients. Arthroscopy. 2013;29(3):589–95.
39. de Amorim Cabrita HA, de Castro Trindade CA, de Campos Gurgel HM, Leal RD, de Souza Marques RDF. Hip arthroscopy. Rev Bras Ortop. 2015;50(3):245–53.
40. Souza BG, Dani WS, Honda EK, Ricioli W Jr, Guimaraes RP, Ono NK, et al. Do complications in hip arthroscopy change with experience? Arthroscopy. 2010;26(8):1053–7.
41. Smart LR, Oetgen M, Noonan B, Medvecky M. Beginning hip arthroscopy: indications, positioning, portals, basic techniques, and complications. Arthroscopy. 2007;23(12):1348–53.
42. Vaughn ZD, Safran MR. Arthroscopic femoral osteoplasty/chielectomy for cam-type femoroacetabular impingement in the athlete. Sports Med Arthrosc Rev. 2010;18(2):90–9.
43. Mannava S, Howse EA, Stone AV, Stubbs AJ. Basic hip arthroscopy: supine patient positioning and dynamic fluoroscopic evaluation. Arthrosc Tech. 2015;4(4):e391–6.
44. Boyle JR, Silva JA, Mc Millan S, Busconi BD. Mechanics of hip arthroscopy. Clin Sports Med. 2011;30(2):285–92.
45. Byrd JW. Hip arthroscopy. J Am Acad Orthop Surg. 2006;14(7):433–44.
46. Shetty VD, Villar RN. Hip arthroscopy: current concepts and review of literature. Br J Sports Med. 2007;41(2):64–8. discussion 8
47. Mason JB, McCarthy JC, O'Donnell J, Barsoum W, Mayor MB, Busconi BD, et al. Hip arthroscopy: surgical approach, positioning, and distraction. Clin Orthop Relat Res. 2003;406:29–37.
48. Bond JL, Knutson ZA, Ebert A, Guanche CA. The 23-point arthroscopic examination of the hip: basic setup, portal placement, and surgical technique. Arthrosc J Arthrosc Relat Surg. 2009;25(4):416–29.
49. Dorfmann H, Boyer T, De Bie B. Arthroscopy of the hip. Rev Rhum Mal Osteoartic. 1988;55(1):33–6.
50. Cuellar Gutierrez R, Ruiz Iban MA, Cuellar Ayestaran A, Sanchez Sobrino A, Oteo-Alvaro A. Peripheral compartment as the initial access for hip arthroscopy in complex cases: technical note. Orthopedics. 2013;36(6):456–62.
51. Rupp R, Duggan B. Peripheral versus central compartment starting point in hip arthroscopy for femoroacetabular impingement. Orthopedics. 2012;35(2):e148–53.
52. Said HG, Steimer O, Kohn D, Dienst M. Vascular obstruction at the level of the ankle joint as a complication of hip arthroscopy. Arthrosc J Arthrosc Relat Surg. 2011;27(11):1594–6.
53. Dienst M, Seil R, Kohn DM. Safe arthroscopic access to the central compartment of the hip. Arthrosc J Arthrosc Relat Surg. 2005;21(12):1510–4.
54. Masoud MA, Said HG. Intra-articular hip injection using anatomic surface landmarks. Arthrosc Tech. 2013;2(2):e147–9.
55. Thaunat M, Murphy CG, Chatellard R, Sonnery-Cottet B, Graveleau N, Meyer A, et al. Capsulotomy first: a novel concept for hip arthroscopy. Arthrosc Tech. 2014;3(5):e599–603.

56. Thorey F, Ezechieli M, Ettinger M, Albrecht U-V, Budde S. Access to the hip joint from standard arthroscopic portals: a cadaveric study. Arthrosc J Arthrosc Relat Surg. 2013;29(8):1297–307.
57. Dorfmann H, Boyer T. Hip arthroscopy utilizing the supine position. YJARS. 1996;12(2):264–7.
58. Philippon MJ, Stubbs AJ, Schenker ML, Maxwell RB, Ganz R, Leunig M. Arthroscopic management of femoroacetabular impingement: osteoplasty technique and literature review. Am J Sports Med. 2007;35(9):1571–80.
59. Marín-Peña O, Fernández-Tormos E, Dantas P, Rego P, Pérez-Carro L. Anatomía y función de la articulación coxofemoral. Anatomía artroscópica de la cadera. Rev Esp Artrosc Cir Artic. 2016;23(1):3–10.
60. Ilizaliturri VM, Byrd JWT, Sampson TG, Guanche CA, Philippon MJ, Kelly BT, et al. A geographic zone method to describe intra-articular pathology in hip arthroscopy: cadaveric study and preliminary report. Arthroscopy. 2008;24(5):534–9.
61. Rao J, Zhou YX, Villar RN. Injury to the ligamentum teres. Mechanism, findings, and results of treatment. Clin Sports Med. 2001;20(4):791–9–vii.
62. Cerezal L, Kassarjian A, Canga A, Dobado MC, Montero JA, Llopis E, et al. Anatomy, biomechanics, imaging, and management of ligamentum teres injuries. Radiographics. 2010;30(6):1637–51.
63. Kalhor M, Horowitz K, Beck M, Nazparvar B, Ganz R. Vascular supply to the acetabular labrum. J Bone Joint Surg Am. 2010;92(15):2570–5.
64. Saddik D, Troupis J, Tirman P, O'Donnell J, Howells R. Prevalence and location of acetabular sublabral sulci at hip arthroscopy with retrospective MRI review. Am J Roentgenol. 2006;187(5):W507–11.
65. Dietrich TJ, Suter A, Pfirrmann C, Dora C. Supraacetabular fossa (pseudodefect of acetabular cartilage): frequency at MR arthrography and comparison of findings at MR arthrography and arthroscopy. Radiology. 2012;263(2):484–91.
66. Byrd JWT. Supraacetabular fossa. Radiology 2012;265(2):648–8.
67. Dienst M. Hip arthroscopy: technique and anatomy. Oper Tech Sports Med. 2005;13(1):13–23.
68. Nguyen MS, Kheyfits V, Giordano BD, Dieudonne G, Monu JUV. Hip anatomic variants that may mimic abnormalities at MRI: labral variants. Am J Roentgenol. 2013;201(3):W394–400.
69. Nguyen MS, Kheyfits V, Giordano BD, Dieudonne G, Monu JUV. Hip anatomic variants that may mimic pathologic entities on MRI: nonlabral variants. Am J Roentgenol. 2013;201(3):W401–8.
70. Mascarenhas VV, Rego P, Dantas P, Gaspar A, Soldado F, Consciência JG. Cam deformity and the omega angle, a novel quantitative measurement of femoral head-neck morphology: a 3D CT gender analysis in asymptomatic subjects. Eur Radiol. 2017; 27(5):2011–23. Epub 2016 Aug 30.
71. Rego PRA, Mascarenhas V, Oliveira FS, Pinto PC, Gaspar A, Ovídio J, et al. Morphologic and angular planning for cam resection in femoro-acetabular impingement: value of the omega angle. Int Orthop. 2016;40(10):2011–7. Epub 2015 Nov 18.
72. Griffin DR, Dickenson EJ, Agricola R, Awan T, Beck M, Dijkstra P, et al. The 2016 Warwick agreement on femoroacetabular impingement. Br J Sports Med. 2016;50(19):1169–76.
73. Khan W, Khan M, Alradwan H, Williams R, Simunovic N, Ayeni OR. Utility of intra-articular hip injections for femoroacetabular impingement: a systematic review. Orthop J Sports Med. 2015;3(9):2325967115601030.
74. Steppacher SD, Anwander H, Zurmühle CA, Tannast M, Siebenrock KA. Eighty percent of patients with surgical hip dislocation for femoroacetabular impingement have a good clinical result without osteoarthritis progression at 10 years. Clin Orthop Relat Res. 2015;473(4):1333–41.
75. Philippon M, Briggs K, Yen Y-M, Kuppersmith D. Outcomes following hip arthroscopy for femoroacetabular impingement with associated chondrolabral dysfunction. J Bone Joint Surg Br Vol. 2009;91(1):16–23.
76. Beck M, Kalhor M, Leunig M, Ganz R, Surgeon O. Hip morphology influences the pattern of damage to the acetabular cartilage femoroacetabular impingement as a cause of early osteoarthritis of the hip. J Bone Joint Surg Br. 2005;87:1012–8. https://doi.org/10.1302/0301-620X.87B7.
77. Martin DE, Tashman S. The biomechanics of femoroacetabular impingement. Oper Tech Orthop. 2010;20(4):248–54. https://doi.org/10.1053/j.oto.2010.09.015.
78. Shibata KR, Matsuda S, Safran MR. Is there a distinct pattern to the acetabular labrum and articular cartilage damage in the non-dysplastic hip with instability? Knee Surg Sport Traumatol Arthrosc. 2016:1–10. https://doi.org/10.1007/s00167-016-4342-4.
79. Philippon MJ. Microinstability of the hip: a previously unrecognized pathology. 2016;6(3):354–60.
80. Valera M, Ibañez N, Sancho R, Tey M. Reliability of Tonnis classification in early hip arthritis: a useless reference for hip-preserving surgery. Arch Orthop Trauma Surg. 2016;136(1):27–33. https://doi.org/10.1007/s00402-015-2356-x.
81. McCarthy JC, Glassner PJ. Correlation of magnetic resonance arthrography with revision hip arthroscopy. Clin Orthop Relat Res. 2013;471(12):4006–11. https://doi.org/10.1007/s11999-013-3202-5.
82. Lattanzi R, Petchprapa C, Glaser C, et al. A new method to analyze dGEMRIC measurements in femoroacetabular impingement: preliminary validation against arthroscopic findings. Osteoarthr Cartil. 2012;20(10):1127–33. https://doi.org/10.1016/j.joca.2012.06.012.
83. Ganz R, Gill TJ, Gautier E, Ganz K, Krügel N, Berlemann U. Surgical dislocation of the adult hip: A technique with full access to the femoral head and acetabulum without the risk of avascular necrosis. J Bone Joint Surg Br. 2001;83-B:1119–24.

84. Botser IB, Smith TW, Nasser R, Domb BG. Open surgical dislocation versus arthroscopy for femoroacetabular impingement: a comparison of clinical outcomes. Arthrosc J Arthrosc Relat Surg. 2011;27(2):270–8. https://doi.org/10.1016/j.arthro.2010.11.008.
85. MacDonald AE, Bedi A, Horner NS, et al. Indications and outcomes for microfracture as an adjunct to hip arthroscopy for treatment of chondral defects in patients with femoroacetabular impingement: a systematic review. Arthroscopy. 2016;32(1):190–200. https://doi.org/10.1016/j.arthro.2015.06.041.
86. Tey M, Mas J, Pelfort X, Monllau JC. Arthroscopic treatment of hip chondral defects with bone marrow stimulation and BST-CarGel. Arthrosc Tech. 2015;4(1):e29–33. https://doi.org/10.1016/j.eats.2014.10.002.

CHAPTER 6.2

This chapter is based on the following paper:

"Arthroscopic versus open treatment of cam-type femoroacetabular impingement: retrospective cohort clinical study."
International Orthopedics. 2018 Apr;42(4):791-797

International Orthopaedics
https://doi.org/10.1007/s00264-017-3735-4

ORIGINAL PAPER

Arthroscopic versus open treatment of cam-type femoro-acetabular impingement: retrospective cohort clinical study

Paulo A. Rego [1] · Vasco Mascarenhas [2] · Filipe S. Oliveira [1] · Pedro C. Pinto [1] · Eduardo Sampaio [3] · Jacinto Monteiro [4]

Received: 4 December 2017 / Accepted: 12 December 2017

Abstract

Purpose The purpose of this study was to determine if there were significant differences between patients submitted to hip arthroscopy (HA) and surgical hip dislocation (SHD) to treat femoro-acetabular impingement (FAI), which variables were significantly associated with hip function before surgery and those predictive of the applied functional outcome scale and its variation rate after surgery.

Methods We selected 198 patients treated with HA or SHD with a mean follow-up of 59 months. Inclusion criteria were ages 18–50 years, isolated FAI cam morphology and complete clinical and radiologic documentation. The subjective outcome measure used was the nonarthritic hip score (NAHS). We compared pre-operative and post-operative NAHS, alpha angles and complication rates. Multiple linear regression analyses were performed to find which variables could influence NAHS values.

Results The mean alpha-angle value improved from 71.5° to 40.8°, and mean NAHS improved from 50 to 83 points, with no difference between groups (HA/SHD). We found only a 16.9% influence rate on the pre-operative score, explained by variables of gender/pre-operative alpha angle and presence of degenerative changes/age. The influence rate on the NAHS variation ratio after surgery was 62.8%, explained by the variables of pre-operative score, type of surgery and type of surgery/alpha angle. The complication rate was 7%.

Conclusions FAI surgery can be considered effective in improving patient symptoms. There were no differences in clinical or radiographic results between techniques. We could more accurately predict the variation ratio of NAHS after surgery than its pre-operative value.

Keywords Femoro-acetabular impingement · Hip arthroscopy · Surgical hip dislocation · Cam · Nonarthritic hip score · Results

Introduction

Cam-type femoro-acetabular impingement (FAI) is considered one of the main causes of painful hips in young adults. Surgical hip dislocation (SHD), as described by Ganz et al. [1], led to a major breakthrough in understanding the pathology by allowing direct visualisation of the impingement mechanism. The femoral head can easily be reshaped and concomitant labral or cartilaginous lesions treated at the same time. Additionally, if necessary, it is possible to progress intra-operatively to more complex techniques of periarticular realignment of both the proximal femur and the acetabulum [2–4]. In the last decade, the increasingly detailed knowledge of hip anatomy and intraosseous vascular supply [5–8] has made hip arthroscopy (HA) a safer and more precise option. HA has evolved from a difficult-access technique (indicated only in the treatment of mild cam deformities) to a reproducible procedure that can be used successfully to treat all cam lesions, including those overlapping the arterial perforation area of the femoral head (Fig. 1) [9]. In the last few years, we have seen a substantial increase in the number of published studies showing promising midterm results in the arthroscopic treatment of FAI. However, studies comparing open and

✉ Paulo A. Rego
pauloamaralrego@gmail.com

1 Department of Orthopaedic Surgery, Hospital da Luz, Avenida Lusíada n 100, 1500-650 Lisbon, Portugal

2 Department of Radiology, Hospital da Luz, Lisbon, Portugal

3 Department of Orthopaedic Surgery, Klinikum Ingolstadt, Ingolstadt, Germany

4 Department of Orthopaedic Surgery, Hospital de Santa Maria, Lisbon, Portugal

Published online: 03 January 2018

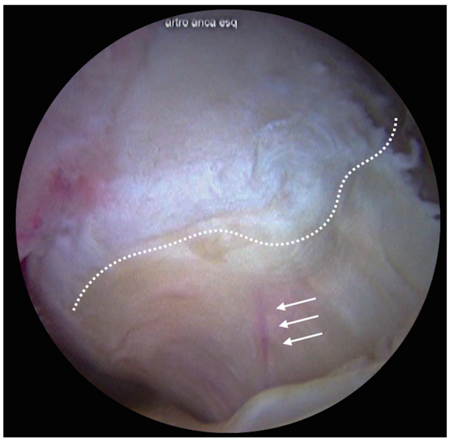

Fig. 1 Arthroscopic view prior to bone resection showing a cam lesion on the posterosuperior femoral head (*dotted line*) and anterior limit of the vascular synovial folds defined by the most anterior arterial structure (*white arrows*). Note the large cartilage ulcers in this area, indicating the presence of an impingement mechanism. In this case, it was necessary to resect bone over the vascular area

arthroscopic surgeries, particularly using the same outcome measures, are less frequently found in the literature.

At our centre, we have gained experience in FAI surgery using both SHD and HA. By increasing our knowledge of the intra-articular vascular anatomy [8], we have changed our preferred approach to treating cam FAI from an open to a fully arthroscopic approach, even where there are extensive cam deformities. The purpose of this retrospective study was to evaluate and compare clinical and radiographic results of cam FAI surgery using both HA and SHD techniques in patients operated upon by the same surgeon, with an average follow-up time of 59 months (24–132). With this study, we intended to find: (a) which patient variables were significantly associated with the value of the functional pre-operative score; (b) if there were significant differences in the results from HA and SHD; (c) which variables were predictive of the functional outcome scale and its variation rate after surgery.

Materials and methods

Patients

Our institutional review board approved this study. From the FAI surgical treatment database started in 2005 (that in 2015 included a total of 400 patients all operated upon by the same surgeon), we selected cases with >24 months of follow-up for a total of 300 patients. From those 300, we excluded all who had more complex intra-articular procedures, those with pincer or mixed-type impingement, those <18 or >50 years and those requiring conversion to total hip replacement (three cases). We obtained a final sample of 198 patients, all exhibiting chronic FAI symptoms, with an average age of 33 years (18–49): 112 men and 86 women. Patients were divided into two groups: One group, with 102 patients, underwent HA; the other, with 96 patients, were submitted to SHD. The mean follow-up time was 59 months (24–132). All patients were informed and gave signed consent authorising data review. Table 1 summarises demographic and clinical data of all included cases. The preoperative evaluation included a detailed physical examination in which we emphasised the importance of a positive impingement test triggering pain that reproduced the daily complaints that motivated the visit to the doctor.

Before surgery, all patients had a standardised anteroposterior (AP) pelvis radiograph, a cross-table lateral view (CTV) radiograph and radial magnetic resonance imaging (MRI) of the hip. The degenerative changes present in the AP radiograph were qualified as present ($T_{>0}$) or absent (T_0) and graded according the Tönnis (T) classification [10]. Alpha angle was measured in the CTV radiograph before and after surgery by an independent surgeon and by a radiologist (Fig. 2). Each patient completed the functional assessment scale Nonarthritic Hip Score (NAHS) [11], validated for the Portuguese language [12], before and after surgery, at three, six and 12 months, and then yearly. For practical purposes only, the last evaluation after surgery was considered. Return to previous sports and job activities were also assessed. We calculated the difference between the initial and the latest available NAHS values and their variation rate (%) using the formula [(final NAHS − initial NAHS) / initial NAHS] × 100. We recorded all cases in which the labrum was repaired for clear instability at the bone–rim interface. Complications were recorded using the modified Clavien–Dindo classification [13] (Table 4).

Statistical analysis

Statistical analysis was carried out by a statistics consultant using the commercial software package IBM SPSS ® version 23 for MAC OS X®. Student's t test was used to compare the means of two continuous variables with normal distribution. Mann–Whitney U test was used to compare the means of two independent nonnormal variables. Pearson (r) and Spearman (s) correlation coefficient tests were used to associate two continuous variables. We also ran a multiple linear regression analysis using the automatic linear modeling (ALM) test (IBM SPSS ® software) to quantify the rate of influence that independent variables could have on the value of the applied outcome scale. All statistical tests were performed with a significance level of 5%.

Table 1 Patient demographic, clinical and radiographic data. The statistical significance of some variables is referred to in Table 2

Characteristic		All patients	Group 1 (arthroscopy)	Group 2 (surgical hip dislocation)
Gender	Male	112 (56%)	54 (53%)	58 (60%)
	Female	86 (44%)	48 (47%)	38 (40%)
Age		33	34	31
Side	Right		57%	61%
	Left		43%	39%
Follow-up time (months)		59 (24–132)	44 (24–80)	76 (25–132)
Alpha angle	Preop	71.5° (50°–108°)	68° (49°–100°)	75° (50°–108°)
	Postop	40.8° (25°–65°)	42.4° (34°–56°)	39° (25°–65°)
NAHS	Preop	50 (10–96)	53 (12–93)	48 (10–94)
	Postop	83 (30–100)	82 (30–100)	83 (35–100)
Tönnis grade	T_0	53%	51%	55%
	T_1	26%	31%	21%
	T_2	19%	17%	21%
	T_3	2%	1%	3%

NAHS nonarthritic hip score, *Preop* pre-operatively, *Postop* post-operatively

Results

All patient demographics and pre- and post-operative clinical and radiographic results are summarised in Tables 1 and 2.

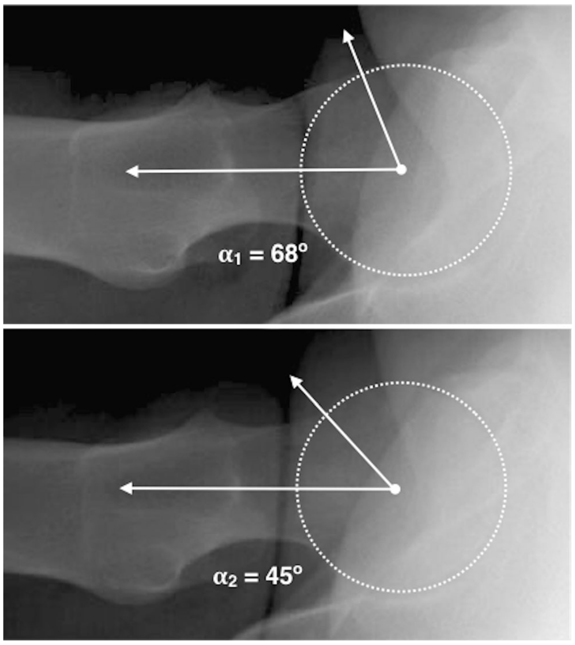

Fig. 2 Pre-operative and post-operative radiographs of a right hip with cam impingement treated with hip arthroscopy. Alpha angles (anterior femoral neck offset) were measured on a lateral cross-table view radiograph of the hip. Alpha angle is defined as the angle between the midline of the femoral neck and a line connecting the centre of the femoral head to the point at which the head–neck junction first deviates from a circle approximating the shape of the femoral head. In this patient, alpha angle diminished from 68° ($_1$) to 45° ($_2$) after surgery

Pre-operative

The mean alpha angle value before surgery was 71.5° (50–108°) and was significantly higher in men and in the open surgery group. Mean NAHS score before surgery was 50 points (10–96) (Fig. 3). The difference between groups was not significant. Male patients had a significantly higher pre-operative score than female patients. Correlation of the pre-operative NAHS scale with the alpha angle value and patient age was weak.

An ALM test analysis was carried out on all variables significantly associated with pre-operative NAHS functional score. The maximum explained possible influence rate on the pre-operative score (16.9%) was dependent on the following association of variables: (a) gender/pre-operative alpha angle (influence rate of 84.6% and positive association with being male and having a larger alpha angle); (b) presence of degenerative changes/age (influence rate of 15.4% and positive association with younger age and absence of degenerative changes).

Post-operative

Mean post-operative NAHS score was 83 points (35–100) (Fig. 3). Twenty-nine percent of patients presented with a score <70 points, 15% varying from 71 to 80 points, 17% varying from 81 to 90 points and 39% >91 points. The absolute difference of 33 points (25–82.5) in the NAHS before and after surgery was strongly significant ($p < 0.0001$). The absolute NAHS value after surgery did not differ between SHD (83 points) and HA (82 points) groups.

Table 2 Statistic significance of several variables individually tested

	Dependent variable	Independent variable		Statistical test	*p* value	Variable mean values
Pre-operative studied variables	Alpha angle	Gender		Student's *t* test	<0.001	F = 65° / M = 76°
		Type of surgery			<0.001	A = 68° / SHD = 75°
		T_0 / $T_{>0}$			0.06	T_0 = 70 / $T_{>0}$ = 73.3
	NAHS	Gender		Student's *t* test	<0.001	F = 40.8 / M = 57.5
		Type of surgery			0.16	A = 53 / SHD = 48
		Age		Pearson's correlation	<0.05	Negative and weak correlation (*r* = − 0.17)
		Alpha angle			< 0.001	Weak correlation (*r* = 0.22)
		Labral repair	SHD	Student's *t* test	0.9	Yes = 83 / No = 83
			HA		0.1	Yes = 80 / No = 84
Postoperative studied variables	Alpha angle	Type of surgery		Student's *t* test	<0.001	A = 42,4° / SHD = 39°
	NAHS variation ratio (%)	Gender		Mann-Whitney *U*	<0.0001	F = 178% / M = 64%
		Type of surgery			<0.05	A = 107% / SHD = 123%
		T_0 / $T_{>0}$			<0.0001	T_0 = 127% / $T_{>0}$ = 100%
		Labral repair	SHD		0.5	Yes = 125% / No = 100%
			HA		0.2	Yes = 140% / No = 80%
		Age		Spearman's correlation	0.7	No correlation
		Alpha angle postop			<0.01	Negative and weak correlation (*s* = − 0.2)
		Preoperative NAHS			<0.001	Negative and strong correlation (*s* = − 0.9)

T_0 without degenerative changes, *$T_{>0}$* with degenerative changes, *F* female, *M* male, *HA* hip arthroscopy, *SHD* surgical hip dislocation, *r* Pearson's correlation coefficient, *s* Spearman's correlation coefficient, *postop* postoperatively, *NAHS* nonarthritic hip score

Considering all patients, mean NAHS variation rate after surgery was 98% (26–675%). Values achieved for specific subgroups according to their pre-operative score values are presented in Table 3.

Alpha-angle value decreased significantly ($p < 0.0001$) after surgery to a mean value of 40.8° (25–65°), and the observed difference between SHD and HA groups was 3.3° ($p < 0.001$). We individually analysed the statistical significance that some variables could have on the post-operative NAHS and those variation rates after surgery. The following were tested: gender, type of surgery, presence or absence of degenerative changes, whether the labrum was repaired, age, post-operative alpha-angle value and NAHS pre-operative value. The absolute value of the post-operative NAHS showed a moderately significant correlation with the initial value ($r = 0.4$; $p < 0.01$) and a weak and negative correlation with age ($r = -0.2$; $p < 0.01$). No other variables showed statistical significance.

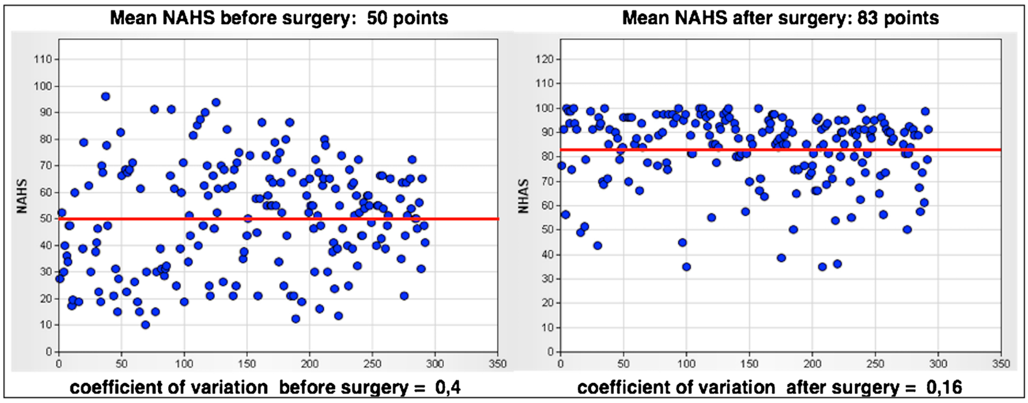

Fig. 3 Nonarthritic hip score (NAHS) per patient before and after surgery. The *red line* shows the mean score before and after surgery. The coefficient of variation was considered the ratio of the standard deviation (SD) to the mean. After surgery, the mean value of the NAHS increased significantly and the coefficient of variation decreased, showing the tendency to improve and converge the outcome measures after surgery

Table 3 Division of patients into four groups according to their pre-operative nonarthritic hip score (NAHS) value and respective variation rate in score achieved after surgery for each group. The higher variation rate (%) occurs in groups were the initial score value was lower. This explains the negative correlation of the pre-operative NAHS with its own variation ratio achieved with surgery (Table 2)

Group	Preop NAHS	Number of patients	Average postop NAHS	Average postop NAHS variation rate
a	0–20	14 (7%)	69	394%
b	21–40	51 (26%)	76	154%
c	41–60	63 (32%)	86	66%
d	> 60	70 (35%)	88	27%

NAHS nonarthritic hip score

The variation rate of the NAHS was significantly higher in female patients, in the absence of degenerative changes, in the SHD group and in patients with a lower pre-operative NAHS value (Table 2). Correlation with the post-operative alpha angle value was weak and negative. Labral repair did not influence the NAHS variation rate in either the open or arthroscopic surgery groups. The remaining variables were also not significant. We again ran an ALM test on post-operative data. The maximum explained possible influence on the NAHS variation rate after surgery (62.8%) was reached with the variables: (a) pre-operative score (influence rate of 92.4%) with negative association; (b) type of surgery (influence rate of 4.5%); (c) variable association type of surgery/alpha angle (influence rate of 3.2%). Our complication rate was 7% without a significant difference between groups (Table 4). The incidence of complications was no higher in patients with a longer follow-up period.

After surgery, 14% of patients still mentioned having some residual pain, although with different pain characteristics than before surgery. Those cases occurred more frequently in women and in $T_{>0}$ patients. Post-operative alpha angle did not correlate significantly with post-operative pain persistence ($p = 0.4$). Ninety-eight percent of patients resumed their professional activities without limitations, and 80% considered that their noncompetitive sports activities improved.

Discussion

Cam-type FAI has recently been recognised as a risk factor for osteoarthritis in young symptomatic patients [14]. Many authors consider hip arthroscopy the technique of choice for treatment of cam deformities that do not need acetabular or proximal femur realignment procedures. SHD, however, maximises hip exposure and allows treatment of more complex, extra-articular deformities or impingement mechanisms. At our institution, cam FAI was initially treated exclusively via open surgery. We believe that detailed knowledge of periarticular anatomy and impingent mechanism—acquired from dynamic joint inspection during SHD procedures—was a crucial step towards changing over to a fully arthroscopic procedure.

However, it was very important not to jeopardise clinical results or accuracy of the osseous resection when changing over to a less-invasive approach. Upon initial indication for arthroscopic surgery, certain factors besides patient

Table 4 Complications from surgery in both groups

Complication	Artrhoscopy	SHD	Modified Clavien–Dindo classification	Treatment
Adhesive capsulitis	1	1	Grade III	Surgical
TO delayed consolidation	–	2	Grade II	No treatment
TO pseudarthrosis	–	1	Grade III	Surgical
Deep venous thrombosis	–	2	Grade II	Medical
Superficial wound infection	–	1	Grade II	Surgical
Reversible pudendal nerve paresis	2	–	Grade I	No treatment
Perineal cutaneous necrosis	1	–	Grade II	Medical
Compartment syndrome	1	–	Grade III	Surgical
Haematoma	1	–	Grade II	Medical
Heterotopic ossification	1	–	Grade I	No treatment

TO trochanteric osteotomy

preference, or those related to the learning curve, were also important: the dimension and radial extension of the cam protuberance and the absence of deformity overlapping the retinacular area. For these reasons, patients submitting to open surgery presented with a significantly higher pre-operative alpha-angle value when compared with the arthroscopy group (11° difference). As in our institution, arthroscopic surgery followed open surgery by about three years; the average follow-up time for patients included in the HA group differed 46 months in relation to the SHD group (Table 1).

Correlation between preoperative alpha-angle and NAHS values was weak, showing the limited value of a single uniplanar measurement of the deformity as being predictive of hip function. [9, 15]. As in other series [16, 17], we also found a significantly higher alpha angle in male patients.

Even though gender and the presence of degenerative changes were the only significant correlations with pre-operative functional NAHS in the ALM approach, it was not possible to identify either variable as a single predictive factor. Female patients showed a significantly lower mean pre-operative score and alpha-angle value when compared to male patients. Other series [18–20] refer to this variation between genders in the pre-operative functional evaluation. One possible explanation for the occurrence of a lower alpha angle with more symptoms in women may be related to a wider range of motion allowed by smaller deformities, which could trigger more symptoms.

After surgery, positive variation of the NAHS and its variation rate were consistent with significant clinical improvement of symptoms. Pain disappeared in 86% of cases; sports activity improved in 80% of patients. Results obtained with these two surgical techniques did not differ significantly, showing that both were effective in the treatment of cam-type FAI. The highest NAHS variation rate, obtained in open surgery patients (Table 2), resulted from a lower initial functional score in this group.

The significant decrease in the alpha-angle value attained by surgery also reflects its efficiency in correcting bone morphology. Despite the existing 3.3° difference between the two techniques, the clinical relevance of this finding is debatable, since the possible error when measuring the alpha angle in CTV radiographs ranges from 2.1° to 6° [21].

The 7% complication rate does not seem to differ from that described in other studies [22–25]. None of the complications were irreversible. There were no cases of avascular necrosis of the femoral head, deep infection or femoral-neck fracture related to bone resection. The open surgery group had more complications requiring reintervention but without significant statistical difference. We also found no significant statistical difference in the incidence of complications related to the surgeon's learning curve.

In our series, before surgery, there was a large dispersion of NAHS values (Fig. 3), which reflected the heterogeneity of the sample. After surgery, this dispersion diminished significantly. The positive variation and convergence of NAHS values reflect the overall improvement of the patients' conditions and, once again, effectiveness of the surgery.

We found 56% of patients with post-operative score values >80 points. Even though this result seems less favourable at first glance, pre-operative values and their respective variation rates to properly evaluate the final post-operative result must be considered. When considering, for example, patients with an initial score <20 points (group a, Table 3), they attained an average post-operative absolute value of 69 points, which we can consider poor. However, in this group, the average NAHS variation rate was 394%. It seems, therefore, that in patients with a poorer final result, the fact that they almost quadrupled the initial value shows the effectiveness of the surgery. The ALM analysis explains 62.8% of the variation ratio of NAHS after surgery. It assigns a greater importance (92.4%) for pre-operative NAHS value. The higher the patient's initial NAHS value, the lower the increment rate. This negative association explained the convergence of absolute score values after surgery (Fig. 3). Although gender was statistically significant in individual associations of variables with the NAHS variation rate (Table 2), this finding had no expression in the ALM analysis, probably because female patients also had a lower initial functional score.

In some published studies [26, 27], improvement in outcome measures seems to be significantly higher after labral repair when compared with labral resection, but with questionable clinical importance. We found a higher variation rate in NAHS score for patients in whom a labrum avulsion was reattached with suture anchors, but that was not statistically significant (Table 2). This might be because we did not resect the labrum; our impingement cases were exclusively of the cam type, and our mean follow-up was shorter. In our current approach to cam impingement, we considered that labral detachment and bone–rim trimming (bone exposure is needed for suture anchor placement) in the presence of intrasubstance degeneration only, without bony avulsion or pincer type impingement, is of questionable value.

The limitations of this study are its retrospective design and that patients were not randomised for each surgical technique. The use of a single functional assessment scale may have been limiting, although this score was used in ~30% of published series regarding FAI treatment [28].

The statistical model developed did not allow us to define isolated predictive factors regarding the evolution of post-operative functional scores but allowed us to conclude that FAI surgery is effective and safe using both arthroscopic and open techniques. Furthermore, it seems that women benefited more from this surgery and that the absence of degenerative changes was associated with a significantly higher increment rate in the post-operative outcome scale.

Acknowledgments We wish to thank to Dr. Vasco Mascarenhas (Hospital da Luz Radiology department) for the collaboration in the alpha angle measurements and the Tönnis grading of all AP pelvis radiographs. We wish to thank to Dr. Teresa Rodrigues (biostatistics department of the the Faculty of Medicine, University of Lisbon) for support in all statistical analysis presented in this manuscript.

Compliance with ethical standards This article does not include results of experimental investigations on humans, and as a retrospective study, formal consent was not required. Informed consent from all patients was obtained on a routine basis for surgical procedures. We obtained formal consent from our institutional review board.

Conflict of interest The authors declare that they have no conflict of interest and there was no funding involved in the preparation of this manuscript.

References

1. Ganz R, Gill TJ, Gautier E, Ganz K, Krügel N, Berlemann U (2001) Surgical dislocation of the adult hip a technique with full access to the femoral head and acetabulum without the risk of avascular necrosis. J Bone Joint Surg Br 83(8):1119–1124
2. Leunig M, Puloski S, Beck M, Siebenrock K-A, Ganz R (2005) Proximal femoral osteotomy: current indications and techniques. Semin Arthroplast 16(1):53–62. https://doi.org/10.1053/j.sart.2004.12.006
3. Ganz R, Huff TW, Leunig M (2009) Extended retinacular soft-tissue flap for intra-articular hip surgery: surgical technique, indications, and results of application. Instr Course Lect 58:241–255
4. Schoenecker PL, Clohisy JC, Millis MB, Wenger DR (2011) Surgical management of the problematic hip in adolescent and young adult patients. J Am Acad Orthop Surg 19(5):275–286
5. Sussmann PS, Ranawat AS, Shehaan M, Lorich D, Padgett DE, Kelly BT (2007) Vascular preservation during arthroscopic osteoplasty of the femoral head-neck junction: a cadaveric investigation. Arthroscopy 23(7):738–743. https://doi.org/10.1016/j.arthro.2007.01.025
6. Grose AW, Gardner MJ, Sussmann PS, Helfet DL, Lorich DG (2008) The surgical anatomy of the blood supply to the femoral head: description of the anastomosis between the medial femoral circumflex and inferior gluteal arteries at the hip. J Bone Joint Surg Br 90(10):1298–1303. https://doi.org/10.1302/0301-620X.90B10.20983
7. Kalhor M, Horowitz K, Gharehdaghi J, Beck M, Ganz R (2012) Anatomic variations in femoral head circulation. Hip Int 22(3):307–312. https://doi.org/10.5301/HIP.2012.9242
8. Rego P, Mascarenhas V, Collado D, Coelho A, Barbosa L, Ganz R (2017) Arterial topographic anatomy near the femoral head-neck perforation with surgical relevance. J Bone Joint Surg Am 99(14):1213–1221. https://doi.org/10.2106/jbjs.16.01386
9. Rego PRA, Mascarenhas V, Oliveira FS, Pinto PC, Gaspar A, Ovídio J, Collado DG (2015) Morphologic and angular planning for cam resection in femoro-acetabular impingement: value of the omega angle. Int Orthop. https://doi.org/10.1007/s00264-015-3053-7
10. Busse J, Gasteiger W, Tönnis D (1972) Significance of the "summarized hip factor" in the diagnosis and prognosis deformed hip joints. Arch Orthop Unfallchir 72(3):245–252
11. Christensen CP, Althausen PL, Mittleman MA, Lee J-A, McCarthy JC (2003) The nonarthritic hip score: reliable and validated. Clin Orthop Relat Res 406:75–83. https://doi.org/10.1097/01.blo.0000043047.84315.4b
12. Del Castillo LNC, Leporace G, Cardinot TM, Levy RA, de Oliveira LP (2013) Translation, cross-cultural adaptation and validation of the brazilian version of the nonarthritic hip score. Sao Paulo Med J 131(4):244–251. https://doi.org/10.1590/1516-3180.2013.1314487
13. Sink EL, Leunig M, Zaltz I, Gilbert JC, Clohisy J (2012) Reliability of a complication classification system for orthopaedic surgery. Clin Orthop Relat Res 470(8):2220–2226. https://doi.org/10.1007/s11999-012-2343-2
14. Ganz R, Leunig M, Leunig-Ganz K, Harris WH (2008) The etiology of osteoarthritis of the hip: an integrated mechanical concept. Clin Orthop Relat Res 466(2):264–272. https://doi.org/10.1007/s11999-007-0060-z
15. Mascarenhas VV, Rego P, Dantas P, Gaspar A, Soldado F, Consciência JG (2016) Cam deformity and the omega angle, a novel quantitative measurement of femoral head-neck morphology: a 3D CT gender analysis in asymptomatic subjects. Eur Radiol. https://doi.org/10.1007/s00330-016-4530-0
16. Jamali AA, Mak W, Wang P, Tai L, Meehan JP, Lamba R (2013) What is normal femoral head/neck anatomy? An analysis of radial CT reconstructions in adolescents. Clin Orthop Relat Res 471(11):3581–3587. https://doi.org/10.1007/s11999-013-3166-5
17. Yanke AB, Khair MM, Stanley R, Walton D, Lee S, Bush-Joseph CA et al (2015) Sex differences in patients with CAM deformities with femoroacetabular impingement: 3-dimensional computed tomographic quantification. Arthroscopy 31(12):2301–2306. https://doi.org/10.1016/j.arthro.2015.06.007
18. Hetsroni I, Dela Torre K, Duke G, Lyman S, Kelly BT (2013) Sex differences of hip morphology in young adults with hip pain and labral tears. Arthroscopy 29(1):54–63. https://doi.org/10.1016/j.arthro.2012.07.008
19. Halim A, Badrinath R, Carter CW (2015) The importance of sex of patient in the management of femoroacetabular impingement. Am J Orthop (Belle Mead NJ) 44(4):172–175
20. Joseph R, Pan X, Cenkus K, Brown L, Ellis T, Di Stasi S (2016) Sex differences in self-reported hip function up to 2 years after arthroscopic surgery for femoroacetabular impingement. Am J Sports Med 44(1):54–59. https://doi.org/10.1177/0363546515610535
21. Mast NH, Impellizzeri F, Keller S, Leunig M (2010) Reliability and agreement of measures used in radiographic evaluation of the adult hip. Clin Orthop Relat Res 469(1):188–199. https://doi.org/10.1007/s11999-010-1447-9
22. McCarthy JC, Lee J-A (2006) Hip arthroscopy: indications, outcomes, and complications. Instr Course Lect 55:301–308
23. Sink EL, Beaulé PE, Sucato D, Kim Y-J, Millis MB, Dayton M et al (2011) Multicenter study of complications following surgical dislocation of the hip. J Bone Joint Surg Am 93(12):1132–1136. https://doi.org/10.2106/JBJS.J.00794
24. Papavasiliou AV, Bardakos NV (2012) Complications of arthroscopic surgery of the hip. Bone Joint Res 1(7):131–144. https://doi.org/10.1302/2046-3758.17.2000108
25. Harris JD, McCormick FM, Abrams GD, Gupta AK, Ellis TJ, Bach BR et al (2013) Complications and reoperations during and after hip arthroscopy: a systematic review of 92 studies and more than 6,000 patients. Arthroscopy 29(3):589–595. https://doi.org/10.1016/j.arthro.2012.11.003
26. Walker JA, Pagnotto M, Trousdale RT, Sierra RJ (2012) Preliminary pain and function after labral reconstruction during femoroacetabular impingement surgery. Clin Orthop Relat Res 470(12):3414–3420. https://doi.org/10.1007/s11999-012-2506-1
27. Anwander H, Siebenrock KA, Tannast M, Steppacher SD (2016) Labral reattachment in femoroacetabular impingement surgery results in increased 10-year survivorship compared with resection. Clin Orthop Relat Res 475(4):1178–1188. https://doi.org/10.1007/s11999-016-5114-7
28. Hetaimish BM, Khan M, Crouch S, Simunovic N, Bedi A, Mohtadi N et al (2013) Consistency of reported outcomes after arthroscopic management of femoroacetabular impingement. Arthroscopy 29(4):780–787. https://doi.org/10.1016/j.arthro.2012.11.011

part IV

DISCUSSION, CONCLUSIONS and FUTURE PROSPECTS

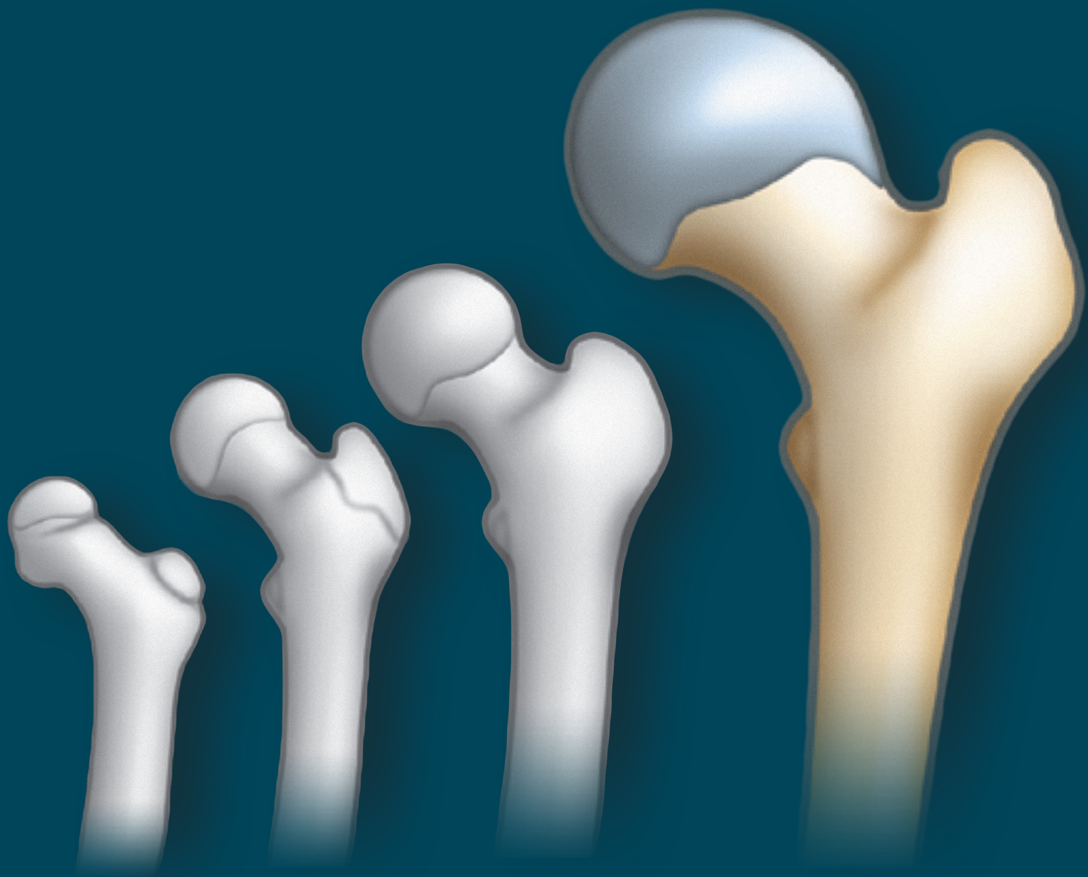

DISCUSSION

All the research developed during this dissertation, more precisely in imaging, was based on the clinical motivation and accumulated experience in the analysis of registries as our clinical knowledge evolved. While every research has limitations, we designed solid prospective studies that we believe may contribute to the development of this emerging field and respond to multiple shortcomings in our clinical practice and gaps in knowledge.

The four parts and six chapters of this thesis covered the spectrum from the analysis of the asymptomatic hip to the treatment of the symptomatic hip.

From standard conventional imaging to 3D imaging

We first introduced the topics that are relevant to understand the full scope of our thesis. Keeping in mind that imaging-related research is the cornerstone for the current dissertation, we believe that we have set the basis to enhance the methodology to further investigate hip and pelvis related topics.

Prior studies have primarily used CR parameters to characterise the acetabulum, femur and pelvis[215-220]. However, several other studies reported poor reliability for defining hip pathomorphology with CR and improved accuracy with CT scans, raising concerns on defining hip disorders and anatomy based on CR alone[215,220-222]. It is possible that clinicians are not only over diagnosing and over treating these conditions, but also paradoxically missing the diagnosis entirely[222]. Prevalence of FAI morphology using current thresholds and the width of reference intervals found in our research suggest that the commonly used criteria for Pincer and Cam-type FAI need to be revisited. More specifically, our results stress that the $\alpha°$ alone is not an appropriate parameter to define Cam morphology and that thresholds should be redefined according to sex and Cam location.

In recent CT-based studies, 3D bone reconstructions of the acetabulum and the proximal femur have been used to evaluate femoral head sphericity using α° measurements[176,223], model fitting[224,225] and 3D volumetric quantification[209,226]. However, normative data is lacking on 3D morphology of the femoral head in asymptomatic individuals. With recent developments of MRI and 3D imaging, attention has turned to the unique capability of determining bone and soft tissue abnormalities in an all-in-one examination. 3D-MR imaging can be used to accurately diagnose and quantify the typical osseous pathological conditions in FAI and has the potential to eliminate the need for 3D-CT imaging and its associated radiation exposure[209].

Clinically, our results stress the magnitude of applications for the 3D imaging protocol reported here, including the following:

- **I.** Accurate spatial visualization of Cam deformity, hip morphology[227] and spinopelvic parameters[34,62];
- **II.** Improved diagnosis and monitoring through the use of quantitative 3D morphometric assessment, incorporating acetabular and femoral measurements[228];
- **III.** Creation of dynamic virtual simulations for preoperative ROM simulations and identification of impingement areas[229];
- **IV.** Provides a tool for standardizing and reducing variability in large-scale and clinical research[230,231].

There is currently established support for advanced 3D hip modelling for research and for potential use in more challenging FAI cases such as revision FAI surgery[232]. However, we believe and proved that the use of 3D imaging to directly visualize and quantify the 3D morphology of the hip and pelvis (namely with MRI) permits detailed and reproducible identification of Cam lesions' magnitude/location[91,233-235]. Furthermore, it significantly improves previously described hip-imaging methods for evaluating acetabular orientation/coverage[169,236,237] and spinopelvic parameters. With respect to clinical outcomes, future research can help to determine if adding advanced 3D hip imaging for pre-surgical planning can improve surgical outcomes for FAI patients compared with using 2D imaging and CR.

What does the literature say?

We performed a systematic review of the literature regarding asymptomatic and symptomatic FAI morphology prevalence. This paper highlighted the gap in knowledge regarding hip morphology prevalence and its role in the pathogenesis of FAI.

Imaging FAI-like morphology was detected in all populations. However, there was a substantial variability in the prevalence of Cam, Pincer, and mixed-type FAI among the populations included in this review. Imaging detected at least one sign of FAI in the majority of symptomatic patients and athletes, whereas asymptomatic subjects showed the lowest prevalence of radiographic signs of FAI, as expected.

Few of the included studies used the same case definitions for Cam or Pincer morphology, and additionally, others used a different case definition for males and females. Despite clinicians becoming increasingly familiar with the concept of FAI, there does not appear to be any consensus on how best to define it[138], how to best image it[209] and what in fact is a definite FAI case[238]. The included studies used a variety of imaging modalities including CR, CT and MRI and measured α° at different positions on the FHN junction. Amazingly, other studies[167,239,240] demonstrated how FAI prevalence estimates changed based on the case definition used.

FAI must be regarded as a syndrome and thus a clinical diagnosis, with patient history and physical examination being the cornerstone of hip evaluation. Overall, imaging becomes an indispensable tool for evaluating morphology, especially among athletes and patients reporting pain. However, reliance on imaging diagnosis of FAI is definitely inappropriate and discouraged.

There is currently insufficient high-quality data to determine the true prevalence of Cam and Pincer morphology in the general population or selected subgroups. Well-designed population--based epidemiological studies that use homogenous case definitions are required to determine the true prevalence of these morphologies and their relationship to hip pain. Most importantly, criteria to define and correctly classify Pincer and Cam hip shape morphology needs to be agreed upon and the diagnostic utility delineated prior to conducting such research.

Characterisation of Hip Morphology

We presented the body of our work, focusing on the original research described by initially performing a detailed characterisation of hip morphology in an asymptomatic cohort. We aimed to develop the imaging approach of hip morphology and FAI by characterising femoral and acetabular anatomy using quantitative measurements taken from 3D-CT (a reproducible method for evaluating the largest reported population using cross-sectional imaging). Furthermore, bony hip morphology was quantified using a semi-automated software, which allowed the in-detail study of, shape variants and their relationship with sex, side and limb dominance.

Hip morphometric measurements in this cohort of asymptomatic individuals extended beyond current thresholds used for the clinical diagnosis of FAI, which was especially true for Cam-type parameters, suggesting that symptomatic FAI reflects a complex dynamic interaction of morphology and other factors and thus is hardly explained by differences in hip shape alone. We must stress that often we confuse reference intervals of a certain parameter, which reflects the normal variation in a certain population (within 95% reference intervals), with a pathological threshold that can differentiate those populations. As stated in the introduction, the reality of hip morphology better resembles an overlapping population model[94]. As such, the measurements and thresholds applied will result in a large number of false-positive and false-negative findings[241].

Some variation between our results and previously reported values might be explained by the heterogeneity of imaging methods employed, different locations of measurements, and – most importantly – nonstandardised definitions of what a Cam/Pincer deformity really is[93,148,167]. Although 3D imaging can identify larger α° than 2D imaging, these differences are mainly the result of measurement location[234].

There is a need for improved techniques and criteria to identify and treat FAI. Considering the strong association between Cam FAI and OA[124], the ongoing debate in the literature on criteria for an imaging diagnosis of FAI is of paramount importance. Additionally, there is an increased risk of residual impingement and vascular insult resulting from surgical treatment based on inaccurate data regarding the extent of these deformities[242,243].

The femoral side

The Reference Intervals (RefInt) limits were beyond abnormal thresholds found in the literature for Cam morphology, providing additional insights into the evolving understanding of the α° and its associated reference standards. It also suggested the need for revisiting the current parameters used in the diagnosis of Cam and FAI, specifically by acknowledging that the α° alone is an insufficient measure by which to appreciate Cam-type morphotype and that its thresholds depend on sex and measurement locations. Conceptually, increasing the threshold of abnormal α° would improve its specificity, prevent overdiagnosis of FAI and consequently decrease the number of unneeded surgeries.

Prior studies have used different cut-off values for morphometric parameters of Cam FAI[80,87,88,91,93,98,148,167,168,244-251]. Accordingly, recent studies have pointed out the high prevalence of radiographic findings that are suggestive of FAI in asymptomatic populations[214] when applying currently used diagnostic thresholds, emphasizing the need for re-evaluation of these cut-offs[88,251-253]. Based on our large cohort, we suggest the need to rethink the threshold of an abnormal α°. We propose an α° upper-limit RefInt of 60° for the 12:00/3:00 positions and 65–70° for the 1:00/1:30 o'clock positions. Although higher than the previously published threshold of 50° to 55°[87,167], the results are in agreement with several authors, namely with Agricola et al.[92], who also measured α° at the 12:00 position, and similar to a recent report using MRI[90] that suggested increasing the threshold to 63°/66° at 3:00/1:30 o'clock, respectively. Importantly, the sample size used in our study was significantly larger than that of previous studies, demonstrating higher statistical power.

In regard to Cam location and magnitude, our study confirms that in an asymptomatic cohort, the deformity was most prominent in the anterosuperior FHN junction and extended around a significant radial extent. The most common position in which we found the largest α° and a raised α° coincided with 1 and 1:30 o'clock on the clock face. These results are generally consistent with findings of other studies[96,169].

In our systematic review, Cam-type morphology was found in 22.4±6.2% of all asymptomatic individuals[214]. In contrast, in our cohorts, we found a higher prevalence of Cam morphology, reaching 79%/33% for 55°/60° α° thresholds, respectively.

The acetabular side

Regarding the acetabulum, the mean values found for LCEA (35°±6°), ACinc (3°±5°) and craniocaudal coverage (74% ± 5) were in accordance with the results of large-scale studies[246], namely regarding the upper thresholds for the LCEA[88,246,254,255] and discordant with other studies[113] on small observational groups. Conversely, 20% of all subjects had Pincer-type morphology (*coxa profunda*: 18.5%; LCEA > 39°: 12.2%; acetabular retroversion: 3%) and 2.6% DHD morphology. Interestingly, Pincer-type morphology was found in 57–76% of individuals in two systematic reviews[36,214].

Sex-related hip differences

At the femoral side, in males, we noticed lower mean CCD and higher mean Ω° and α° at the antero-superior quadrants. Magnitudes of Cam morphology and RefInt for α° were significantly sex-different, consistent with the majority of previous results[167,256,257] but divergent from some studies[244,245]. Mean α° was significantly sex-different at 1:00/1:30 (more 8–10° in males).

Similarly, Cam location varied significantly according to sex, in agreement with Ito et al.[97] but divergent from the study by Yanke et al.[258] (in symptomatic individuals). We also found that mean magnitude, location, and the epicentre of Cam morphology were significantly gender different. In men, we specifically found larger Cam radial extension, higher maximal mean increased α° (63.63° vs 55.74°) and epicentre superiorly located in the anterosuperior quadrant (1 vs 1:30 o'clock), which is also in accordance with previous reports[258]. Importantly, the increased span in males compared with female Cam deformities increases the likelihood of false-negative 2D evaluations in women[258]. Pelvic morphology and other dynamic factors such as distinct sports activities, increased female flexibility, pelvic rotation or forward tilt from weaker core muscles surely contribute to these overall differences[112,258,259].

For the Pincer morphotype, there is also controversy as prior studies have shown that women have more acetabular anteversion and a greater prevalence of global acetabular overcoverage [257,260,261]. Sex differences arise in the natural physiological growth, namely in the development of the FHN junction[262] but also in joint orientation, including acetabular anteversion and coverage[263]. Interestingly, other studies found sex-dependent disease patterns in patients with symptomatic FAI. Females had milder morphological abnormalities, while males had larger morphological abnormalities and more extensive joint disease[154,264-267]. We found that acetabular retroversion and anterior overcoverage were not more prevalent in women in the anterosuperior acetabulum, consistent with some previous reports[259]. In fact, males had a higher prevalence of retroversion with a clear tendency to have a more prominent antero-superior wall (anteversion angles were on average 5° lower in males). Women had more Accov and a smaller anterior wall, also in line with previous reports[255,259,268].

Age related hip morphology

Femoral parameters were stable after physeal maturity, meaning that no further significant development occurs in adult life (at least until the upper age limit studied in our cohorts (50 y.o.)).

In contrast, on the acetabular side LCEA, Accov and Acvers increased with age. This finding to the best of our knowledge has not been well addressed in the literature and suggests that pelvic orientation and version change during adulthood. LCEA increased with age (approximately 5–7° between 15 to 45 y.o.), coherent with previous reports that estimated that the LCEA was positively correlated with age, increasing annually by 0.07° in adults[254]. Similarly, anterior Accov and Acvers increased with age (respectively 4% and 6-7° between 15–45 y.o.) in accordance with Stem et al.[269], who estimated an increase of 0.7° in anteversion for every 10-year age increase.

We hypothesise that osseous apposition, cumulative degenerative changes and pregnancy might contribute to this upward coverage and anteversion tendency. An all-in-one explanation comes from the fact that increasing anterior pelvic tilt associated with osseous acetabular apposition results in this re-orientation of the acetabular cavity and thus changes imaging parameters with increasing age.

Relationship between hip shape and side, limb dominance

Concerning member dominance, dominant/non-dominant limbs hip shapes were globally symmetric. Given that more than 85% of individuals are right-handed, we sought to investigate the association between dominance side and hip shape as in the development of OA one is significantly more likely to require hip arthroplasty on their dominant side[270]. This predisposition cannot be explained by differences in hip shape alone and may be functionally related. Conceptually, as varying tasks are attributed to each of the lower limbs, the dominant limb for forward propulsion and non-dominant limb for postural stabilisation, this may influence the dominant hip in the progression of degenerative disease.

Similarly, there were no differences between sides' shapes, which is comparable with previous reports[245,252,271]. Interestingly, also in a symptomatic cohort, there were no differences in Cam deformity parameters, femoral torsion, acetabular version and LCEA between affected/unaffected hips. In this setting, a decreased CCD was hypothesised as the only diagnostic predictor to determine which hip may be at a greater risk of developing early symptoms[191,213] or OA[151]. These findings have important associated implications. First, hip symmetry in the asymptomatic population questions the concept that only some morphological variations, namely the CCD and ACinc, could alter the interplay between the femoral and acetabular side. Second, questions remain about the aetiology of hip OA, which may be more prevalent on the dominant side, and as such we hypothesise that causation might be related to other dynamic causes (non--morphological). Third, for study design and clinical trial purposes, one can safely assume that both hips are alike.

The omega angle

Cam morphology was further defined by developing a novel quantitative measure with diagnostic and treatment planning capabilities. The importance of this parameter was additionally outlined by our arterial topographic study of the proximal femur. Cam-type morphology is a 3D deformity and, as we have proved in this dissertation, single 2D α°-based measurements should be viewed with caution, as they may not provide a true estimate of the magnitude of the deformity.

Additionally, in our everyday practice, we felt the need to step up to a 3D perception of the morphology of the Cam deformity, determining its radial extension expressed by the Ω° and originally described by our group[272]. The correlation of this new angular measure with the patient reported "non arthritic hip score" (NAHS) before surgery seemed to be significant and presenting a negative variation. Patients with a more extensive deformity presented an inferior

NAHS score before surgery (more symptomatic). We think that these results were relevant, although we recognize their important limitations, namely that the manual measurement of the Ω° is complex and that only 25 patients were used to validate this imaging parameter. Clinical validation of this angle was undoubtedly a need. Building from this initial approach, we moved to larger patient samples and more practical methods of measurement.
Accordingly, we further developed the Ω° by using 3D imaging and a specific software, contributing to a better understanding and characterisation of the FHN junction by semi--automatically defining the radial extension and location of Cam morphology in asymptomatic subjects. Interestingly, we proved that greater α° correlates with increasing Ω°, meaning that a larger Cam is indeed larger in all 3 dimensions. Additionally, we found a mean increase in α° measurements of 60.5° (50.1–80.3°) in our asymptomatic cohort compared with 64.6° (50.8–86°) in a symptomatic cohort using a similar methodology[233]. In the latter study the "arc" of Cam deformity ranged between 60° and 90°, in contrast to our study which found lower magnitudes (mean Ω° of 65°) as it would be expected[233] in an asymptomatic cohort. These findings resulted as an area for further application of the Ω° technique, enabling the detailed subgroup analysis in Chapter 5.

Accordingly, we also found that symptomatic participants had larger Cam deformities (defined by increased Ω° and α°) than asymptomatic participants. Discriminant receiver operating characteristic (ROC) analysis confirmed that the Ω° angle (threshold 43°, sensitivity 72%, specificity 70%; AUC: 0.830) was one of the best parameters to classify participants. When parameters were entered into a logistic regression, significant positive predictors for the symptomatic group were achieved (including the Ω° angle), correctly classifying 85% of cases (model sensitivity 72%, specificity 91%; AUC: 0.919).

Currently, there is no magic imaging tool that facilitates the reliable allocation of all patients into the correct diagnostic group or confidently rules out the diagnosis. Nevertheless, imaging can be used to describe the various morphological characteristics of the hip and can be beneficial in confirming or precluding the diagnosis of FAI in many patients. Based on these results, we further developed insights in finding the "key" to differentiate asymptomatic and symptomatic hips, i.e. identifying "at-risk" joints.

Bridging the Anatomical Gap

In order to find the anatomical "key" that could bridge the mentioned gap, a comprehensive and combined analysis of hip pathomorphology is needed to help our understanding of this complex, 3D-pathologic dynamic process. We also tested multiple parameters and their associated shape variants to find which ones allowed the identification of a risk-increased joint in various populations. To this end, we used advanced computing for both shape modelling and 3D-MRI. In our opinion, these studies specifically added to existing knowledge by allowing:

1) In-depth assessment of hip morphology with advanced computational shape modelling, revealing that ovoid shapes better represent both articular surfaces of the hip joint. On the other hand, ovoid geometries are also more representative of Cam, Pincer and mixed--impinged hips when compared to spherical or ellipsoidal shapes.

This finding greatly questions the accuracy of 2D-based imaging measurements that assume that the femoral head is a sphere and/or use the hip joint centres as the basis of its measurement methodology. In fact, the most used Cam and Pincer surrogate measurements (α° and LCEA) are examples of such parameters.

2) Establishing normative reference values and differentiating thresholds on spinopelvic, Cam and Pincer parameters with reproducible methodology using 3D-MRI.

Our results show that a Cam deformity extending over half the anterosuperior quadrant (corresponding to Ω°: 45°; AUC: 0.830) or with α° measurements of 57–60° (at the 1:30 to 2:00 positions; AUC: 0.788-0.831) is probably symptomatic. Similarly, Sutter et al.[93] found identical AUC (0.790–0.820) for the best α° measurement point. As earlier stated, increasing an α° upper-limit RefInt to 60° for the 12:00/3:00 positions and 65–70° for the 1:00/1:30 o'clock positions are certainly accurate to establish upper thresholds for this parameter. However, increasing the threshold of abnormal α° while considering its discriminative ability would additionally improve its value as a diagnostic test. Therefore, we suggest rethinking the threshold of abnormal α° in the setting of a diagnostic test to incorporate higher discriminative power. An α° of 57–60° measured at 1:00/1:30/2:00 and 50° at 3:00 would optimize discriminative power while favouring specificity.

On the acetabular side, dysplasia and Pincer morphology are two distinct pathologic forms resulting in clinically different pathomechanisms, static overload or dynamic conflict[126]. The relatively high reported prevalence of Pincer morphology in asymptomatic (57–67%) and symptomatic (28–54%) individuals may be confounded in several ways[36,214], given that radiographic parameters such as the *coxa profunda*, COS and PWS have shown poor diagnostic reliability[220,273-275]. We observed that approximately 33% of symptomatic patients and 20% of volunteers have Pincer morphology, which we believe is a more accurate estimate of its real prevalence, given the methodology used. More symptomatic males have cranial retroversion than females (7% vs 1%), coherent with a previous study[276]. Males in both groups had a clear tendency to have a more prominent anterosuperior wall (anteversion angles were on average 5° lower in males), in line with previous reports[259,268].

Concerning SPP, a definitive contribution of these parameters for a symptomatic hip is suggested by our data. The symptomatic group showed larger PI and SS angles, coherent with more recent reports with smaller cohorts performed with CT[34,62]. A larger SS and PI are associated with both an increased anterosuperior acetabular coverage and an increased anteroposterior distance between hip joint centres and the sacral endplate. Although beyond the scope of this research to prove causation between Cam/Pincer morphology and increased SPP, the association can be established as the basis for prospective evaluation. Additionally, our findings are more coherent with published data on the association of higher PI and OA[277].

3) Knowledge of useful independent predictive factors in identifying "risk-increased" joints, both in asymptomatic populations and symptomatic individuals.

The likelihood of symptomatic disease doubled for an Ω° increase of 20° or an α° increase of 8–9° (measured at 2:00 o'clock). Accordingly, higher femoral head diameters were somewhat protective against symptomatic disease, which demonstrates the importance of FHN morphology rather than femoral head size in FAI disease. The symptomatic state was also more associated with decreasing superior acetabular coverage (decreasing LCEA 12:00 and increasing ACinc (> 6°; AUC: 0.715)) than with Pincer morphology (which, paradoxically, showed a tendency to protect against the development of the symptomatic state). The likelihood of symptomatic disease doubled with a 7° increase in ACinc, in line with the findings of dysplasia as a major factor in OA development[102,126], suggesting delicate balancing regarding impingement and instability[42,278]. Previous research showed an increased risk for OA with Pincer morphology[148,149], where other epidemiological studies found no association or even suggested a protective effect for the development of OA[126,150,151,199,279]. Furthermore, recent prospective epidemiological studies have supported that even mild acetabular dysplasia is, in fact, associated with increased risk of OA[126,199], indirectly concordant with our findings.

4) Improve patient selection for FAI surgery vs conservative treatment by identifying the most suitable candidates that would primarily benefit from nonsurgical management.

Femoral and acetabular parameters are static variables that are not amenable to conservative treatment. Conversely, SPP may be subject to non-surgical treatment as increasing posterior pelvic tilt also increases the superoanterior femoral head collision-free ROM (manageable by conservative pelvic muscular-focused treatment). Proper patient selection would be important to identify the most suitable candidates who would benefit from nonsurgical management and strength conditioning to delay or avoid unnecessary HPS. In some circumstances, patients likely do not benefit from surgery or, worse, they may experience iatrogenic instability.[280,281]

Regarding clinical relevance, not only were SPP significant to discriminate between participants, but were also important in combination with other hip deformities, allowing to effectively differentiate these populations based on predictive anatomical factors. Patients with FAIS may show a higher SS and PI, perhaps changing the core pelvic musculature and contributing to functional impairment. Applying diagnostic imaging thresholds in combination with thorough clinical examinations allow for an early and accurate diagnosis, helping clinicians to improve patient selection for surgery by ascertaining which athletes/patients could benefit from a conservative approach. Overall, complex dynamic interplay exists between the hip and SPP. A Cam deformity, along with acetabular undercoverage and increased SPP angles, all are predictive of a hip symptomatic state.

On the basis of this work, it is adequate to consider that some symptomatic patients could extend their nonsurgical treatment, focusing more on core stability and muscle strengthening (psoas, flexors, gluteal muscles) to alter sagittal-plane moment arms and assess if symptoms cease. Similarly, asymptomatic patients with a higher pelvic incidence may also start benefiting from early targeted muscle strengthening. To our knowledge, these original findings further strengthen the biomechanical concept behind physical therapy in FAI and in asymptomatic populations.

Treating the Symptomatic Hip

Furthermore, we closed the loop from improving diagnosis and bridging gaps in knowledge, to describing treatment options and outcomes in a cohort clinical study.

The perception that there was often a deformity on the posterior-superior retinacular region led us to progressively interpret the location of structures that we considered vascular in radial MRI images more carefully. We observed that in many cases, they assumed a much higher and anterior position than was described in the scarce publications on arterial perfusion of the proximal femoral epiphysis[282-284]. In fact, to the best of our knowledge, we haven't found any reference about the vascular origin of those "vascular" structures and, for that reason, we planned the study presented in Chapter 4.4 of this dissertation. Despite the limitations already mentioned, we believe that the arterial origin of these structures was adequately clarified. This study also allowed us to determine i) the safety distances in depth and laterality of the initial interosseous path of the nourishing arteries in relation to the cartilage margin of the FHN junction; ii) the radial extension of the retinacular fold and; iii) its precise location.

The practical importance of this contribution relates to the information that can be used, in performing osteoplasty of the Cam deformity and in others HPS procedures that involve the mobilization of the deep branch of the MCFA[63,285]. Treating more complex deformities is challenging and the detailed knowledge acquired from this research has led to its improvement.

In the treatment cohort, which we consider sufficient for statistical analysis[286], we included only Cam-type FAI cases because there is no definite evidence to date that other mechanisms (other than DHD), although symptomatic, are truly detrimental to cartilage[126]. The most relevant fact was that, although surgical techniques with different approaches were used at different times of the surgeon's learning curve, the final outcome did not differ significantly. In both samples, the functional scores and the final bone resection (evaluated by the measurement of the radiographic α°), did not present a statistically significant difference (concordant with other authors[287-289]).

Adequate resection of the deformity has probably been the determining factor in the overall symptomatic and functional improvement experienced by our patients. Supporting this assumption, some reviews after failed primary osteoplasty[290,291] clearly showed that the most frequent cause of failure is insufficient bone resection, particularly over the vascular area of the FHN[291]. The exposure of the retinacular folds is not problematic in open surgery with SHD[63], but the same is not the case where the deformity extends to the vascular area of the FHN[292,293]. In these cases, there is the additional risk that resection may be insufficient, which may be potentially detrimental to joint cartilage, especially if there are sharp bone edges within the resection limits.

In our cohort, an unexpected result was the weak or non-existent correlation between functional assessment before surgery and the value of the α° measured (cross table view). Clinical evidence, so far, emphasizes scarce correlation between the magnitude of the deformity and function before surgery. In most cases, surgery outcomes are assessed by taking into account functional score variation and α° correction, without considering the correlation between these two parameters. Our study revealed that the correlation between the α° and the initial NAHS score was poor. As we previously pointed out, the explanation for this observation is that the α°, measured on CR, is not representative of the real size of the deformity.
Regarding the parameters evaluated after surgery (patients with a minimum follow-up time of two years), we did not seek to find predictive factors of conversion to total hip arthroplasty. We sought, in a more rational way, variables that were independently associated with the absolute value of the applied scale of evaluation and its variation after surgery. In the case of the absolute postoperative value of the NAHS score, our statistical model failed to identify independent variables but found associations of variables that, on the whole, explained only 16% of their variation. Conversely, when analysing variables and the NAHS score percentage variation we found that preoperative NAHS value explained 62.8% of its variation. These results are unexpected, although they reflect the difficulty in determining independent prognostic factors in this type of surgery in accordance to other authors[267]. Gender and degenerative changes were variables (not independent), to consider as they were strongly associated with the NAHS score percentage variation. Accordingly, a lower preoperative functional score and the female gender seem to be associated with a greater clinical improvement (reflected as a higher NAHS score variation). In the statistical impossibility of determining prognostic factors, the inclusion of these

variables in the rationale decision of surgical indication, even with the mentioned shortcomings, may help to improve patient selection.

Interestingly, patients who had a very low baseline NAHS score improved significantly but seldom achieved a good or excellent outcome. On the other hand, most patients with a high baseline score reached an equally high assessment value after surgery at the expense of a lesser variability.

CONCLUSIONS AND PROSPECTS FOR FUTURE RESEARCH

General considerations

The formulation of the theory of FAI by Ganz was an important step in understanding the pathophysiology of FAI[118]. Since then, the diagnosis and treatment of nonarthritic hip pathology is arguably the fastest-growing field within orthopedics[294].

Accordingly, advances in our understanding of hip pathology, better imaging, improved equipment and surgical technique have all incremented this exponential rise in arthroscopic and open hip procedures[182,294]. Along with this increase in the number of surgical cases, however, comes an increased responsibility to make sure that we make the correct diagnosis and also build accurate clinical decisions.

Despite the increase in FAI literature, the level of evidence has generally remained low. As such, the ability for clinicians to make evidence-based treatment decisions is still limited[295]. Now, there is a need for high-level evidence to supplement this theory and enable clinicians to diagnose and direct treatment when appropriate. Accordingly, the key to safe adoption of emerging technologies is guidance by well-conducted studies. Through-high level studies, the potential for safe dissemination of good practices in both imaging and FAI surgery may be increased[294,296].

In efforts to further understand FAI diagnosis and treatment, this research program was structured to investigate the pathoanatomical differences between asymptomatic and symptomatic cohorts. To help delineate focal sub-studies and improve the understanding of FAI, this dissertation initially identified gaps in the literature. From the systematic review of imaging prevalence of FAI morphology, specific gaps in the literature and three main areas for development were identified. They are as follows:

- I. No consideration for a clinical case definition of FAI, FAIS, Pincer, Cam and other morphologies;
- II. No consideration for imaging criteria to define such cases;

III. No consideration for imaging technique specificities, regarding reference intervals, thresholds and cut-offs to differentiate cases and asymptomatic populations.

Therefore, the basis of this doctoral research was to formulate more population-based specific criteria and thresholds in order to bridge the gap between symptomatic and asymptomatic populations. Concurrently, one specific focus was the increasingly complex analysis and understanding of hip joint deformities. Hip morphology analysis became more complex when we included torsional deformities of the femur and the acetabulum, as well as malorientation of the femur into the 3D concept of joint instability and impingement. Presently, it is clear that hip morphology should not be appreciated in isolation, illustrating the value of femoral and acetabular components as well as extra-articular contributors such as SPP[33,34,297].

Summary of Research

In efforts to preserve the natural hip joint, understanding that hip morphology variants are the rule in all populations and that anatomical parameters can play an important role in the onset of hip symptomatology, it is critical to help identify those who are at a greater risk of earlier onset of irreversible damage. Since not all hips with Cam morphology are symptomatic, it would be important to note: i) what "static" morphological features (in addition to the Cam deformity) may differentiate between symptomatic and asymptomatic hips and ii) whether "dynamic" differences exist between symptomatic and asymptomatic hips with distinct morphologies.
Furthermore, in the process of doing so with the aforementioned studies, we have set forth the basic tenets of i) screening in order to identify the population at risk of developing hip symptoms and ii) holistic patient imaging assessment in order to address the pathology prior to symptoms development in a timely manner.

With the ultimate goal of understanding the pathomorphology of the hip, the collective sub-studies presented a modelling approach to the analysis of hip pain by integrating more subject-specific data to investigate which parameters could predict the "at-risk" joint.

Upon closer observation, hip pain was less likely due to increased acetabular coverage but more likely due to the combination of a Cam deformity and increased pelvic anteflexion, which could affect the resultant mechanical loading directions and contact mechanics. With this in mind, anatomical and functional parameters will be crucial to help distinguish asymptomatic individuals and could be implemented towards developing screening programs – in efforts to predict hips that will be at risk of early symptoms. The combined effects of the Cam morphology and dysplastic-prone hips may induce higher stresses into the subchondral bone during larger hip motions, increasing the likelihood of early pain associated with FAI. Although it is possible that an asymptomatic hip deformity can remain subclinical, while predisposing to early subchondral bone stiffening, hips with an asymptomatic Cam morphology may be at greater risks of labral tears and degeneration. Additional research will examine the functional outcomes of asymptomatic participants, to observe how different natural histories and the role of soft tissues (i.e., capsular ligaments and muscles) will influence the progression of symptoms. Ultimately, with the goal of delaying surgery and preserve the inherent stability of the native hip, physical examinations and additional anatomical parameters (i.e., pelvic tilt and Cam morphology parameters) should be observed early, prior to the onset of symptoms. With these parameters in mind, other treatment options such as physiotherapy, abductors and psoas muscle training and recruitment strategies should be considered.

Although the research question of "what hip morphologies benefit from early treatment?" is still elusive, the overall benefit taken from the present research work is the characterisation of the population-specific prevalence of hip-deformities and the pathoanatomical aspects associated with hip pain. Further understanding of the interaction between the joint morphology, function and mechanical *stimuli* could possibly lead to an improved screening process to detect the progression of FAI and provide clinicians with indications of where initial chondrolabral or cartilage damage could occur. Conceptually, early recognition could help reduce hip OA cases and, thus, the number of hip arthroplasty surgeries.

In short, having in mind the natural history of the hip, our research contributed to the development of both the imaging identification of individuals at risk (prevention and diagnosis) and the characterisation of subclinical and clinical disease (diagnosis and treatment) (Figure 31).

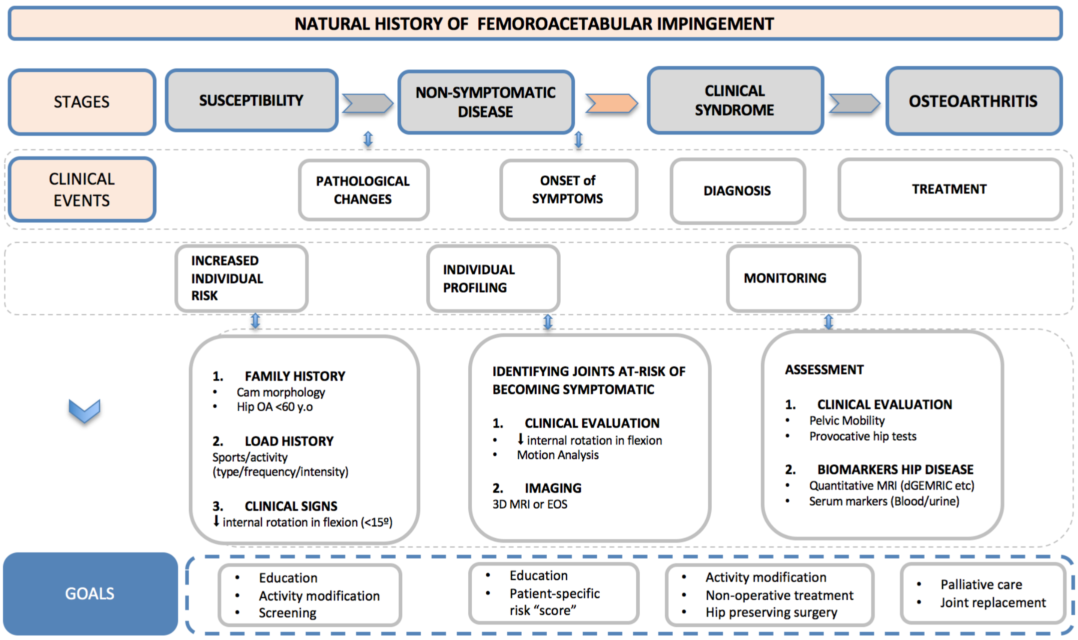

FIGURE 31 – The natural history of femoroacetabular impingement disorders. EOS – low dose radiography-based 3D imaging; dGEMRIC – delayed gadolinium-enhanced MRI of cartilage.

Clinical applications

We believe that some of the aspects described in this dissertation may be of immediate application in daily clinical practice, namely in many steps of the clinical decision algorithm:

1) Case diagnosis: In clinical practice, it is often questioned whether a specific patient with hip pain is an instability or an impingement case. Although a case definition is not yet consensually established, the basis for clinical diagnosis often results from the combined information derived from clinical signs/symptoms, imaging and diagnostic injections. By incorporating these "anatomic imaging predictors" into the clinical decision process (case diagnosis) we can safely state that significant diagnostic improvements were set forth.

2) Treatment decision: By incorporating the variables and parameters discussed in the clinical study into the treatment algorithm decision, we can, on the one hand, contribute to improve the selection of surgical candidates and, on the other hand, adequately measure the expectations of the patient and surgeon with regards to functional outcomes. One of the most relevant research questions has not been answered yet, and certainly will not be in the next few years: "Is there any indication for the Cam deformity prophylactic surgery in asymptomatic patients?". The results presented in this thesis show that, in the current era, treatment should be directed only to symptomatic patients with an established deformity and few degenerative changes. Even in those patients, a conservative approach trial might be adequate. It is our responsibility to continue validating some of the parameters and ideas introduced here and continue to contribute to deepen our knowledge in this specific medical area.

3) Imaging protocol: Case diagnosis, treatment decision, preoperative planning and postoperative assessment can be improved using our 3D comprehensive protocol. In fact, measuring SPP and the radial extent of the Cam deformity (and its relationship with the vascular structures), will improve treatment decisions (conservative vs surgical) and, in surgical cases, determine the extension of osteoplasty without significant risk of iatrogenic injury to the postero-superior vascular fold.

Future prospects

There is a gap in well-conducted research addressing the best strategies for diagnosing and treating FAI. Areas of research that need further evaluation include diagnostic strategy, efficacy of surgical intervention and relationship between FAI and OA[138]. Literature suggest that the current management of FAI is limited by the lack of awareness of high-level evidence[294].

Therefore, we believe that the continuity of the research presented in this dissertation should be based on three pillars:

1) Epidemiological analysis: The characterisation of the Portuguese hip morphotype can be safely and easily performed building on the data hereby presented. With little additional effort, it would feasible to build a Portuguese imaging "biobank" as far as hip shape/ /morphotype is concerned. Having in mind that, in the near future, individualized, tailored clinical approaches will certainly be the rule, we believe that this would be a promising endeavour. In order to develop more generalizable RefInt, larger individual cohort studies with more varied demographics are needed.

2) Clinical studies:

a. Diagnostic and treatment algorithm: There is a need for more reliable diagnostic and treatment guidelines beyond differentiation into pure Cam, Pincer, or mixed FAI and a simple definition of a hip dysplasia. The largely unknown natural course both in hips with asymptomatic Cam/Pincer morphology and symptomatic FAI continues to be unknown. Future research should focus on the development of reliable validated outcome measures and international collaborations to conduct high-quality research. The current treatment paradigms for FAI are evolving along with the clinical evidence evaluating this condition. Several ongoing randomized controlled trials, including the FAI Trial[298] (FAIT) and the FAI Randomized Controlled Trial[299] (FIRST), will provide critical information in terms of the diagnosis, management and prognosis of patients undergoing arthroscopic management of FAI.

b. Prognostic factors: In the continuity of clinical studies, dilating the sample analysed in Chapter 6.2, including more patients as the follow-up time increases. Within five years, we may be able to determine predictive factors with a stronger association and, if appropriate, describe the survival analysis of the joints, with the end point being the conversion to total hip arthroplasty. The relatively short follow-up time of this cohort does not allow us to base surgical indication beyond the existence of symptoms and simultaneous imaging diagnosis of Cam morphology. Long term prospective studies are needed to help us determine which abnormalities are most important to correct, and which ones can be safely left alone.

3) Morphological studies:

a. Further clinically validating the concept of the Ω°. Radial measurement of the extent of Cam deformity is a parameter that can be used clinically as a planning tool for surgery, especially to evaluate the posterior extent of deformity where resection is more critical in terms of joint preservation. Its clinical validation cannot be accomplished in a small number of cases. It needs a larger sample of symptomatic individuals to be able to infer its usefulness as an imaging parameter with definite influence in the selection of candidates for surgery.

b. Hip-specific morphological MRI is considered the gold standard for detecting cartilage and labral lesions. A standardized method for diagnosing and monitoring joint shapes and joint damage in the long-term, after either nonsurgical or surgical treatment of impinging or unstable hips, is yet to be established. We must continue refining our evaluation of hip joint pathomorphologies including through the use of 3D analysis. Further investigations are also needed to incorporate 3D measurements of the symptomatic hip for a complete comparison between these populations to get a better picture of hip biomechanics in FAI cases.

On this regard, in each of these work pillars, Artificial Intelligence (AI) will certainly pave the way for better and comprehensive assessment. In the medical context, AI refers to devices or systems that can perceive some element of their environment and use this information to achieve a predefined goal.

It has been heralded as the next big wave in the computing revolution and touted as a transformative technology for many industries including healthcare. Radiology has often served as the gateway for medical technological advancements, and AI will likely be no different. Although beyond the scope of this thesis, future research may explore deep learning techniques focusing on automated hip segmentation and enabling large-scale radiomic analysis with the potential to identify disease characteristics based on imaging patterns that may not be readily apparent to the human eye. "Big data" techniques, consisting of both deep learning and other machine learning strategies, may also allow for better identification of "at-risk" subgroups and prediction of response to therapy, by providing information on which patients may benefit from conservative care as opposed to surgery.

Looking ahead, imaging, AI and HPS will continue to evolve hand-in-hand, with new problems and greater challenges. The increasing number of analytic parameters describing hip joint pathomorphologies, as well as new sophisticated MRI and 3D CT-analysis, have carried us beyond the point of simple classification systems. We need more reliable treatment guidelines beyond differentiation into pure FAI and dysplasia. It is time to refine the diagnostic algorithm. The largely unknown natural course, especially in hips with symptomatic FAI and asymptomatic population, continues to be a problem as far as diagnosis, treatment and prognosis are concerned.

Limitations

We acknowledge that study heterogeneity is the most striking feature in FAI literature. Hence, a systematic review on FAI imaging certainly incorporates the limitations of the analysed studies, introducing selection and information bias reflected by the variability in the threshold values used to detect radiographic FAI, participants' age, sex, geography, activity level, race and sports engaged. Assignment of FAI morphologic features were made by both radiography and MRI on different radiographic views or MRI protocols and with different threshold values to determine pathological and non-pathological conditions. Further research, with general population-based studies and strict classifying criterion is paramount. Tools such as the modified risk of bias tool for prevalence studies can assist in ensuring methodological rigour and valid conclusions.

Selecting a protocol for some of the prospective cohort studies included in this thesis, may have been also subjected to bias as our controls were not selected from healthy volunteers and we used patient survey information to exclude hip abnormality but did not perform a clinical hip examination. However, we prospectively included controls evaluated for nonorthopaedic disease and excluded all controls with any reported history of hip abnormality or symptoms. Additionally, we excluded any controls with signs of hip abnormality on CT/MRI so that our cohorts comprised asymptomatic individuals only. Second, these studies included only partial correlation of semi-automated measurements with traditional manual measurements; such comparisons between 2D and 3D MRI methods would be useful but were not an objective of our study, apart from the fact that the software used had already been validated.
Despite the inherent limitations and other biases specifically referenced in our published papers, our studies were methodologically well conducted and had a low risk of bias, providing several Level 2 evidence papers (according to the "Oxford Centre for Evidence-based Medicine"; OCEBM Levels of Evidence Working Group. "The Oxford 2011 Levels of Evidence").

part V

REFER-
ENCES

REFERENCES

References hereby listed are numbered in order of appearance throughout the thesis according to the format of the "American Medical Association" (excluding published papers). Published papers are embedded in the thesis, although retaining their original referencing style and numbering (in accordance to the guidelines of the corresponding journal). For clarity sake, references of the published papers are only listed in the corresponding section and not repeated here.

1. Hogervorst T, Bouma H, de Boer SF, de Vos J. Human hip impingement morphology: AN EVOLUTIONARY EXPLANATION. *Journal of Bone and Joint Surgery – British Volume*. 2011;93(6):769. doi:10.1302/0301.

2. Bowman KF, Fox J, Sekiya JK. A clinically relevant review of hip biomechanics. *Arthroscopy*. 2010;26(8):1118–1129. doi:10.1016/j.arthro.2010.01.027.

3. Hogervorst T, Eilander W, Fikkers JT, Meulenbelt I. Hip Ontogenesis: How Evolution, Genes, and Load History Shape Hip Morphotype and Cartilotype. *Clin Orthop Relat Res*. 2012;470(12):3284–3296. doi:10.1007/s11999-012-2511-4.

4. Ranawat AS, Kelly BT. Anatomy of the hip: Open and arthroscopic structure and function. *Operative Techniques in Orthopaedics*. 2005;15:160–174. doi:10.1053/j.oto.2005.06.010.

5. Sandell LJ. Etiology of osteoarthritis: genetics and synovial joint development. *Nature Publishing Group*. 2012;8(2):77–89. doi:10.1038/nrrheum.2011.199.

6. Davidson EH, Erwin DH. Evolutionary innovation and stability in animal gene networks. *J Exp Zool B Mol Dev Evol*. 2010;314(3):182–186. doi:10.1002/jez.b.21329.

7. Hogervorst T, Vereecke EE. Evolution of the human hip. Part 1: the osseous framework. *Journal of Hip Preservation Surgery*. 2014;1(2):39–45. doi:10.1126/science.6849136.

8. Singh A, Beaulé PE. Development Anatomy and Its Impact on Hip Function. *Hip Joint Restoration*. 2017. doi:10.1007/978-1-4614-0694-5_99.

9. Hogervorst T, Vereecke EE. Evolution of the human hip. Part 2: muscling the double extension. *Journal of Hip Preservation Surgery*. 2015;2(1):3–14. doi:10.1136/ard.2004.021188.

10. Wagner DO, Aspenberg P. Where did bone come from? *Acta Orthop*. 2011;82(4):393–398. doi:10.3109/17453674.2011.588861.

11. Fikkers JT, Bouma HW, de Boer SF, Toogood PA, van Kampen PM, Hogervorst T. What ape proximal femora tell us about femoroacetabular impingement: a comparison. *Clin Orthop Relat Res*. 2015;473(4):1204–1211. doi:10.1007/s11999-014-3754-z.

12. McCarthy JC, Noble PC, Villar RN. *Hip Joint Restoration*. Springer; 2016. doi:10.1007/978-1-4614-0694-5_1.

13. Hogervorst T, Bouma HW. Coxa recta (cam-type) proximal femoral morphology: what causes it. *HIP*. 2011;21(3):383–384. doi:10.5301/HIP.2011.8394.

14. Anwander H, Beck M, Büchler L. The Influence of Evolution on Cam Deformity and its Impact on Biomechanics of the Human Hip Joint. *J Orthop Res*. February 2018. doi:10.1002/jor.23863.

15. van Klij P, Heerey J, Waarsing JH, Agricola R. The Prevalence of Cam and Pincer Morphology and Its Association With Development of Hip Osteoarthritis. *J Orthop Sports Phys Ther*. 2018;48(4):230–238. doi:10.2519/jospt.2018.7816.

16. Connolly P, Weinstein SL. [The natural history of acetabular development in developmental dysplasia of the hip]. *Acta Orthop Traumatol Turc*. 2007;41 Suppl 1:1–5.

17. Walker JM, Goldsmith CH. Morphometric study of the fetal development of the human hip joint: significance for congenital hip disease. *Yale J Biol Med*. 1981;54(6):411–437.

18. Masłoń A, Sibiński M, Topol M, Krajewski K, Grzegorzewski A. Development of human hip joint in the second and the third trimester of pregnancy; a cadaveric study. *BMC Dev Biol*. 2013;13:19. doi:10.1186/1471-213X-13-19.

19. Lee MC, Eberson CP. Growth and development of the child's hip. *Orthop Clin North Am*. 2006;37(2):119–32–v. doi:10.1016/j.ocl.2005.12.001.

20. Philippon MJ, Michalski MP, Campbell KJ, et al. An anatomical study of the acetabulum with clinical applications to hip arthroscopy. *The Journal of Bone and Joint Surgery*. 2014;96(20): 1673–1682. doi:10.2106/JBJS.M.01502.

21. Morris WZ, Chen JY, Cooperman DR, Liu RW. Characterization of ossification of the posterior rim of acetabulum in the developing hip and its impact on the assessment of femoroacetabular impingement. *J Bone Joint Surg Am*. 2015;97(3):e11. doi:10.2106/JBJS.N.00553.

22. Kienle K-P, Keck J, Werlen S, Kim Y-J, Siebenrock KA, Mamisch TC. Femoral morphology and epiphyseal growth plate changes of the hip during maturation: MR assessments in a 1-year follow-up on a cross-sectional asymptomatic cohort in the age range of 9-17 years. *Skeletal Radiol*. 2012;41(11):1381–1390. doi:10.1007/s00256-012-1358-9.

23. Agricola R, Heijboer MP, Ginai AZ, et al. A Cam Deformity Is Gradually Acquired During Skeletal Maturation in Adolescent and Young Male Soccer Players: A Prospective Study With Minimum 2-Year Follow-up. *The American Journal of Sports Medicine*. 2014;42(4):798–806. doi:10.1177/0363546514524364.

24. Roels P, Agricola R, Oei E, Weinans H, Campoli G, Zadpoor AA. Mechanical factors explain development of cam-type deformity. *Osteoarthritis and Cartilage*. October 2014:1–9. doi:10.1016/j.joca.2014.09.011.

25. McCarthy JC, Noble PC, Villar RN. *Hip Joint Restoration*. Springer; 2016.

26. Evangelou E, Kerkhof HJ, Styrkarsdottir U, et al. A meta-analysis of genome-wide association studies identifies novel variants associated with osteoarthritis of the hip. *Ann Rheum Dis*. 2014;73(12):2130–2136. doi:10.1136/annrheumdis-2012-203114.

27. Pollard TCB, Batra RN, Judge A, et al. The hereditary predisposition to hip osteoarthritis and its association with abnormal joint morphology. *Osteoarthritis and cartilage / OARS, Osteoarthritis Research Society*. 2013;21(2):314–321. doi:10.1016/j.joca.2012.10.015.

28. Huiskes R, Ruimerman R, van Lenthe GH, Janssen JD. Effects of mechanical forces on maintenance and adaptation of form in trabecular bone. *Nature*. 2000;405(6787):704–706. doi:10.1038/35015116.

29. Agricola R, Bessems JHJM, Ginai AZ, et al. The Development of Cam-Type Deformity in Adolescent and Young Male Soccer Players. *The American Journal of Sports Medicine*. 2012;40(5):1099–1106. doi:10.1177/0363546512438381.

30. Philippon MJ, Ho CP, Briggs KK, Stull J, LaPrade RF. Prevalence of Increased Alpha Angles as a Measure of Cam-Type Femoroacetabular Impingement in Youth Ice Hockey Players. *The American Journal of Sports Medicine*. 2013;41(6):1357–1362. doi:10.1177/0363546513483448.

31. MacKelvie KJ, Khan KM, McKay HA. Is there a critical period for bone response to weight-bearing exercise in children and adolescents? a systematic review. *British Journal of Sports Medicine*. 2002;36(4):250–7–discussion257.

32. Tak I, Weir A, Langhout R, et al. The relationship between the frequency of football practice during skeletal growth and the presence of a cam deformity in adult elite football players. *British Journal of Sports Medicine*. 2015;49(9):630–634. doi:10.1136/bjsports-2014-094130.

33. Rivière C, Hardijzer A, Lazennec JY, Beaulé P, Muirhead-Allwood S, Cobb J. Spine-hip relations add understandings to the pathophysiology of femoro-acetabular impingement: A systematic review. *Orthopaedics \& traumatology, surgery \& research : OTSR*. 2017;103(4):549–557. doi:10.1016/j.otsr.2017.03.010.

34. Grammatopoulos G, Speirs AD, Ng KCG, et al. Acetabular and spino-pelvic morphologies are different in subjects with symptomatic cam femoro-acetabular impingement. *J Orthop Res*. 2018;36(7):1840–1848. doi:10.1002/jor.22375.

35. Rivière C, Lazennec JY, Van Der Straeten C, Auvinet E, Cobb J, Muirhead-Allwood S. The influence of spine-hip relations on total hip replacement: A systematic review. *Orthopaedics \& traumatology, surgery \& research : OTSR*. 2017;103(4):559–568. doi:10.1016/j.otsr.2017.02.014.

36. Frank JM, Harris JD, Erickson BJ, et al. Prevalence of Femoroacetabular Impingement Imaging Findings in Asymptomatic Volunteers: A Systematic Review. *Arthroscopy*. 2015;31(6):1199–1204. doi:10.1016/j.arthro.2014.11.042.

37. Kalhor M, Horowitz K, Beck M, Nazparvar B, Ganz R. Vascular supply to the acetabular labrum. *J Bone Joint Surg Am*. 2010;92(15):2570–2575. doi:10.2106/JBJS.I.01719.

38. Seldes RM, Tan V, Hunt J, Katz M, Winiarsky R, Fitzgerald RH. Anatomy, histologic features, and vascularity of the adult acetabular labrum. *Clin Orthop Relat Res*. 2001;(382):232–240.

39. Dienst M. Hip arthroscopy: Technique and anatomy. *Operative Techniques in Sports Medicine*. 2005;13(1):13–23. doi:10.1053/j.otsm.2004.09.009.

40. Kelly BT, Buly RL. Hip Arthroscopy Update. *HSS Jrnl*. 2005;1(1):40–48. doi:10.1007/s11420-005-0105-3.

41. Leunig M, Podeszwa D, Beck M, Werlen S, Ganz R. Magnetic resonance arthrography of labral disorders in hips with dysplasia and impingement. *Clin Orthop Relat Res*. 2004;(418):74–80.

42. Tibor LM, Liebert G, Sutter R, Impellizzeri FM, Leunig M. Two or more impingement and/or instability deformities are often present in patients with hip pain. *Clin Orthop Relat Res*. 2013;471(12):3762–3773. doi:10.1007/s11999-013-2918-6.

43. Saddik D, Troupis J, Tirman P, O'Donnell J, Howells R. Prevalence and Location of Acetabular Sublabral Sulci at Hip Arthroscopy with Retrospective MRI Review. *American Journal of Roentgenology*. 2006;187(5):W507–W511. doi:10.2214/AJR.05.1465.

44. Philippon MJ, Stubbs AJ, Schenker ML, Maxwell RB, Ganz R, Leunig M. Arthroscopic Management of Femoroacetabular Impingement: Osteoplasty Technique and Literature Review. *The American Journal of Sports Medicine*. 2007;35(9):1571–1580. doi:10.1177/0363546507300258.

45. Hartig-Andreasen C, Søballe K, Troelsen A. The role of the acetabular labrum in hip dysplasia. A literature overview. *Acta Orthop*. 2013;84(1):60–64. doi:10.3109/17453674.2013.765626.

46. Nepple JJ, Philippon MJ, Campbell KJ, et al. The hip fluid seal--Part II: The effect of an acetabular labral tear, repair, resection, and reconstruction on hip stability to distraction. *Knee Surg Sports Traumatol Arthrosc*. 2014;22(4):730–736. doi:10.1007/s00167-014-2875-y.

47. Bsat S, Frei H, Beaulé PE. The acetabular labrum: a review of its function. *The Bone & Joint Journal*. 2016;98-B(6):730–735. doi:10.1302/0301-620X.98B6.37099.

48. Ollivier M, Parratte S, Lecorroller T, Reggiori A, Champsaur P, Argenson J-N. Anatomy of the proximal femur at the time of total hip arthroplasty is a matter of morphotype and etiology but not gender. *Surg Radiol Anat*. May 2015:1–8. doi:10.1007/s00276-014-1368-5.

49. Dietrich TJ, Grob K, Kim C-HO. Postoperative Imaging after Impingement Surgery. *Semin Musculoskelet Radiol*. 2017;21(5):529–538. doi:10.1055/s-0037-1606131.

50. Cerezal L, Kassarjian A, Canga A, et al. Anatomy, Biomechanics, Imaging, and Management of Ligamentum Teres Injuries. *Radiographics*. 2010;30(6):1637–1651. doi:10.1148/rg.306105516.

51. Cerezal L, Arnaiz J, Canga A, et al. European Journal of Radiology. *European Journal of Radiology*. 2012;81(12):3745–3754. doi:10.1016/j.ejrad.2011.04.001.

52. Rao J, Zhou YX, Villar RN. Injury to the ligamentum teres. Mechanism, findings, and results of treatment. *Clin Sports Med*. 2001;20(4):791–9–vii.

53. Chahla J, Soares EAM, Devitt BM, et al. Ligamentum Teres Tears and Femoroacetabular Impingement: Prevalence and Preoperative Findings. *Arthroscopy*. 2016;32(7):1293–1297. doi:10.1016/j.arthro.2016.01.045.

54. Aprato A, Giachino M, Massè A. Arthroscopic approach and anatomy of the hip. *Muscles Ligaments Tendons J*. 2016;6(3):309–316. doi:10.11138/mltj/2016.6.3.309.

55. Beck M, Sledge JB, Gautier E, Dora CF, Ganz R. The anatomy and function of the gluteus minimus muscle. *Journal of Bone and Joint Surgery – British Volume*. 2000;82(3):358–363.

56. Inan M, Mahar A, Swimmer T, Tomlinson T, Wenger DR. [Changes in the lengths of the gluteus medius and gluteus minimus muscles with trochanteric transfer following pelvic support osteotomy: a biomechanical study]. *Acta Orthop Traumatol Turc*. 2004;38(1):67–70.

57. Lieberman DE. The human gluteus maximus and its role in running. *Journal of Experimental Biology*. 2006;209(11):2143–2155. doi:10.1242/jeb.02255.

58. Domb BG, Shindle MK, McArthur B, Voos JE, Magennis EM, Kelly BT. Iliopsoas impingement: a newly identified cause of labral pathology in the hip. *HSS Jrnl*. 2011;7(2):145–150. doi:10.1007/s11420-011-9198-z.

59. de Sa D, Alradwan H, Cargnelli S, et al. Extra-articular hip impingement: a systematic review examining operative treatment of psoas, subspine, ischiofemoral, and greater trochanteric/pelvic impingement. *Arthroscopy*. 2014;30(8):1026–1041. doi:10.1016/j.arthro.2014.02.042.

60. Thorborg K, Reiman MP, Weir A, et al. Clinical Examination, Diagnostic Imaging, and Testing of Athletes With Groin Pain: An Evidence-Based Approach to Effective Management. *J Orthop Sports Phys Ther*. 2018;48(4):239–249. doi:10.2519/jospt.2018.7850.

61. Cruz J, Mascarenhas V. Adult thigh muscle injuries-from diagnosis to treatment: what the radiologist should know. *Skeletal Radiol*. March 2018. doi:10.1007/s00256-018-2929-1.

62. Ng KCG, Lamontagne M, Jeffers JRT, Grammatopoulos G, Beaulé PE. Anatomic Predictors of Sagittal Hip and Pelvic Motions in Patients With a Cam Deformity. *The American Journal of Sports Medicine*. 2018;2014:036354651875515. doi:10.1016/j.arthro.2016.01.011.

63. Ganz R, Gill TJ, Gautier E, Ganz K, Krügel N, Berlemann U. Surgical dislocation of the adult hip a technique with full access to the femoral head and acetabulum without the risk of avascular necrosis. *Journal of Bone and Joint Surgery – British Volume*. 2001;83(8):1119–1124.

64. Leunig M, Ganz R. Evolution of technique and indications for the Bernese periacetabular osteotomy. *Bull NYU Hosp Jt Dis*. 2011;69 Suppl 1:S42–S46.

65. Sussmann PS, Ranawat AS, Shehaan M, Lorich D, Padgett DE, Kelly BT. Vascular Preservation During Arthroscopic Osteoplasty of the Femoral Head-Neck Junction: A Cadaveric Investigation. *Arthroscopy: The Journal of Arthroscopic & Related Surgery*. 2007;23(7):738–743. doi:10.1016/j.arthro.2007.01.025.

66. Kalhor M, Horowitz K, Gharehdaghi J, Beck M, Ganz R. Anatomic variations in femoral head circulation. *HIP*. 2012;22(3):307–312. doi:10.5301/HIP.2012.9242.

67. Gautier E, Ganz K, Krügel N, Gill T, Ganz R. Anatomy of the medial femoral circumflex artery and its surgical implications. *Journal of Bone and Joint Surgery – British Volume*. 2000;82(5):679–683.

68. Nötzli HP, Siebenrock KA, Hempfing A, Ramseier LE, Ganz R. Perfusion of the femoral head during surgical dislocation of the hip. Monitoring by laser Doppler flowmetry. *Journal of Bone and Joint Surgery – British Volume*. 2002;84(2):300–304.

69. Kalhor M. Capsular and Pericapsular Contributions to Acetabular and Femoral Head Perfusion. *The Journal of Bone and Joint Surgery (American)*. 2009;91(2):409. doi:10.2106/JBJS.G.01679.

70. Beck M, Leunig M, Ellis T, Sledge JB, Ganz R. The acetabular blood supply: implications for periacetabular osteotomies. *Surg Radiol Anat*. 2003;25(5-6):361–367. doi:10.1007/s00276-003-0149-3.

71. Siebenrock KA, Kalbermatten DF, Ganz R. Effect of pelvic tilt on acetabular retroversion: a study of pelves from cadavers. *Clin Orthop Relat Res*. 2003;(407):241–248. doi:10.1097/01.blo.0000030508.43495.79.

72. Kalberer F, Sierra RJ, Madan SS, Ganz R, Leunig M. Ischial spine projection into the pelvis : a new sign for acetabular retroversion. *Clin Orthop Relat Res*. 2008;466(3):677–683. doi:10.1007/s11999-007-0058-6.

73. Tannenbaum E, Kopydlowski N, Smith M, Bedi A, Sekiya JK. Gender and Racial Differences in Focal and Global Acetabular Version. *The Journal of Arthroplasty*. 2014;29(2):373–376. doi:10.1016/j.arth.2013.05.015.

74. van der Bom MJ, Groote ME, Vincken KL, Beek FJ, Bartels LW. Pelvic Rotation and Tilt Can Cause Misinterpretation of the Acetabular Index Measured on Radiographs. *Clin Orthop Relat Res*. 2011;469(6):1743–1749. doi:10.1007/s11999-011-1781-6.

75. Pedersen DR, Lamb CA, Dolan LA, Ralston HM, Weinstein SL, Morcuende JA. Radiographic measurements in developmental dysplasia of the hip: reliability and validity of a digitizing program. *Journal of Pediatric Orthopaedics*. 2004;24(2):156–160.

76. Hellman MD, Gross CE, Hart M, et al. Radiographic Comparison of Anterior Acetabular Rim Morphology Between Pincer Femoroacetabular Impingement and Control. *Arthroscopy*. 2016;32(3):468–472. doi:10.1016/j.arthro.2015.08.035.

77. Tönnis D. *Congenital Dysplasia and Dislocation of the Hip in Children and Adults. Berlin. Springer*. 1987.

78. Tönnis D. Normal values of the hip joint for the evaluation of X-rays in children and adults. *Clin Orthop Relat Res*. 1976:39–47. doi:10.1097/00003086-197609000-00007.

79. Tannast M, Fritsch S, Zheng G, Siebenrock KA, Steppacher SD. Which Radiographic Hip Parameters Do Not Have to Be Corrected for Pelvic Rotation and Tilt? *Clin Orthop Relat Res*. 2014. doi:10.1007/s11999-014-3936-8.

80. Tannast M, Siebenrock KA, Anderson SE. Femoroacetabular impingement: radiographic diagnosis--what the radiologist should know. *AJR Am J Roentgenol*. 2007;188(6):1540–1552. doi:10.2214/AJR.06.0921.

81. Clohisy JC. A Systematic Approach to the Plain Radiographic Evaluation of the Young Adult Hip. *The Journal of Bone and Joint Surgery (American)*. 2008;90(Supplement_4):47. doi:10.2106/JBJS.H.00756.

82. Jackson TJ, Estess AA, Adamson GJ. Supine and Standing AP Pelvis Radiographs in the Evaluation of Pincer Femoroacetabular Impingement. *Clin Orthop Relat Res*. 2016;474(7):1692–1696. doi:10.1007/s11999-016-4766-7.

83. Welton KL, Jesse MK, Kraeutler MJ, Garabekyan T, Mei-Dan O. The Anteroposterior Pelvic Radiograph. *The Journal of Bone and Joint Surgery*. 2018;100(1):76–85. doi:10.2106/JBJS.17.00500.

84. Boese CK, Dargel J, Oppermann J, et al. The femoral neck-shaft angle on plain radiographs: a systematic review. *Skeletal Radiol*. 2015;45(1):19–28. doi:10.1007/s00256-015-2236-z.

85. Toogood PA, Skalak A, Cooperman DR. Proximal femoral anatomy in the normal human population. *Clin Orthop Relat Res*. 2009;467(4):876–885. doi:10.1007/s11999-008-0473-3.

86. Botser IB, Ozoude GC, Martin DE, Siddiqi AJ, Kuppuswami S, Domb BG. Femoral anteversion in the hip: comparison of measurement by computed tomography, magnetic resonance imaging, and physical examination. *Arthroscopy*. 2012;28(5):619–627. doi:10.1016/j.arthro.2011.10.021.

87. Nötzli HP, Wyss TF, Stoecklin CH, Schmid MR, Treiber K, Hodler J. The contour of the femoral head-neck junction as a predictor for the risk of anterior impingement. *Journal of Bone and Joint Surgery – British Volume*. 2002;84(4):556–560.

88. Kang ACL, Gooding AJ, Coates MH, Goh TD, Armour P, Rietveld J. Computed Tomography Assessment of Hip Joints in Asymptomatic Individuals in Relation to Femoroacetabular Impingement. *The American Journal of Sports Medicine*. 2010;38(6):1160–1165. doi:10.1177/0363546509358320.

89. Bouma HW, Hogervorst T, Audenaert E, Krekel P, van Kampen PM. Can Combining Femoral and Acetabular Morphology Parameters Improve the Characterization of Femoroacetabular Impingement? *Clin Orthop Relat Res*. 2014;473(4):1396–1403. doi:10.1007/s11999-014-4037-4.

90. Golfam M, Di Primio LA, Beaulé PE, Hack K, Schweitzer ME. Alpha Angle Measurements in Healthy Adult Volunteers Vary Depending on the MRI Plane Acquisition Used. *The American Journal of Sports Medicine*. 2017;45(3):620–626. doi:10.2214/AJR.06.0921.

91. Harris MD, Kapron AL, Peters CL, Anderson AE. Correlations between the alpha angle and femoral head asphericity: Implications and recommendations for the diagnosis of cam femoroacetabular impingement. *European Journal of Radiology*. 2014;83(5):788–796. doi:10.1016/j.ejrad.2014.02.005.

92. Agricola R, Waarsing JH, Thomas GE, et al. Cam impingement: defining the presence of a cam deformity by the alpha angle: data from the CHECK cohort and Chingford cohort. *Osteoarthritis and cartilage / OARS, Osteoarthritis Research Society*. 2014;22(2):218–225. doi:10.1016/j.joca.2013.11.007.

93. Sutter R, Dietrich TJ, Zingg PO, Pfirrmann CWA. How useful is the alpha angle for discriminating between symptomatic patients with cam-type femoroacetabular impingement and asymptomatic volunteers? *Radiology*. 2012;264(2):514–521. doi:10.1148/radiol.12112479.

94. Sutter R, Pfirrmann CWA. Update on Femoroacetabular Impingement: What Is New, and How Should We Assess It? *Semin Musculoskelet Radiol*. 2017;21(5):518–528. doi:10.1055/s-0037-1606141.

95. Harris WH. Etiology of osteoarthritis of the hip. *Clin Orthop Relat Res*. 1986;(213):20–33.

96. Siebenrock KA, Wahab KHA, Werlen S, Kalhor M, Leunig M, Ganz R. Abnormal extension of the femoral head epiphysis as a cause of cam impingement. *Clin Orthop Relat Res*. 2004;(418):54–60.

97. Ito K, Minka-II MA, Leunig M, Werlen S, Ganz R. Femoroacetabular impingement and the cam-effect. *The Journal of Bone and Joint Surgery*. 2001;83(2):171–176. doi:10.1302/0301-620X.83B2.11092.

98. Fraitzl CR, Kappe T, Pennekamp F, Reichel H, Billich C. Femoral head-neck offset measurements in 339 subjects: distribution and implications for femoroacetabular impingement. *Knee Surg Sports Traumatol Arthrosc*. 2012;21(5):1212–1217. doi:10.1007/s00167-012-2042-2.

99. Ehrmann C, Rosskopf AB, Pfirrmann CWA, Sutter R. Beyond the alpha angle: Alternative measurements for quantifying cam-type deformities in femoroacetabular impingement. *J Magn Reson Imaging*. February 2015:n/a–n/a. doi:10.1002/jmri.24861.

100. Gosvig KK, Jacobsen S, Palm H, Sonne-Holm S, Magnusson E. A new radiological index for assessing asphericity of the femoral head in cam impingement. *Journal of Bone and Joint Surgery – British Volume*. 2007;89(10):1309–1316. doi:10.1302/0301-620X.89B10.19405.

101. Cooperman DR, Wallensten R, Stulberg SD. Acetabular dysplasia in the adult. *Clin Orthop Relat Res*. 1983;(175):79–85.

102. Jacobsen S, Sonne-Holm S. Hip dysplasia: a significant risk factor for the development of hip osteoarthritis. A cross-sectional survey. *Rheumatology (Oxford)*. 2005;44(2):211–218. doi:10.1093/rheumtology/keh436.

103. Tönnis D, Heinecke A. Current concepts review-Acetabular and femoral anteversion: relationship with osteoarthritis of the hip. *J Bone Joint Surg Am*. 1999.

104. Govsa F, Ozer MA, Ozgur Z. Morphologic features of the acetabulum. *Arch Orthop Trauma Surg*. 2005;125(7):453–461. doi:10.1007/s00402-005-0020-6.

105. Wiberg G. Studies on dysplastic acetabula and congenital subluxation of the hip joint. With special reference to the complication of osteoarthritis. *Acta Chir Scand*. 1939;83(Suppl 5:1939; 83(Suppl58):28–38.

106. Ogata S, Moriya H, Tsuchiya K, Akita T, Kamegaya M, Someya M. Acetabular cover in congenital dislocation of the hip. *Journal of Bone and Joint Surgery – British Volume*. 1990;72(2):190–196.

107. Dandachli W, Kannan V, Richards R, Shah Z, Hall-Craggs M, Witt J. Analysis of cover of the femoral head in normal and dysplastic hips: new CT-based technique. *Journal of Bone and Joint Surgery – British Volume*. 2008;90(11):1428–1434. doi:10.1302/0301-620X.90B11.20073.

108. Anda S, Svenningsen S, Dale LG, Benum P. The acetabular sector angle of the adult hip determined by computed tomography. *Acta Radiol Diagn (Stockh)*. 1986;27(4):443–447.

109. Lerch TD, Todorski IAS, Steppacher SD, et al. Prevalence of Femoral and Acetabular Version Abnormalities in Patients With Symptomatic Hip Disease: A Controlled Study of 538 Hips. *The American Journal of Sports Medicine*. 2017;417(1):036354651772698. doi:10.1016/j.cmpb.2007.02.010.

110. Sutter R, Dietrich TJ, Zingg PO, Pfirrmann CWA. Femoral antetorsion: comparing asymptomatic volunteers and patients with femoroacetabular impingement. *Radiology*. 2012;263(2):475–483. doi:10.1148/radiol.12111903.

111. Chen H-F, Zhao C-Q. Pelvic incidence variation among individuals: functional influence versus genetic determinism. March 2018:1–6. doi:10.1186/s13018-018-0762-9.

112. Ross JR, Nepple JJ, Philippon MJ, Kelly BT, Larson CM, Bedi A. Effect of Changes in Pelvic Tilt on Range of Motion to Impingement and Radiographic Parameters of Acetabular Morphologic Characteristics. *The American Journal of Sports Medicine*. 2014;42(10):2402–2409. doi:10.1177/0363546514541229.

113. Tannast M, Hanke MS, Zheng G, Steppacher SD, Siebenrock KA. What are the radiographic reference values for acetabular under- and overcoverage? *Clin Orthop Relat Res*. 2015;473(4): 1234–1246. doi:10.1007/s11999-014-4038-3.

114. Smith-Petersen MN. The classic: Treatment of malum coxae senilis, old slipped upper femoral epiphysis, intrapelvic protrusion of the acetabulum, and coxa plana by means of acetabuloplasty. 1936. *Clin Orthop Relat Res*. 2009;467(3):608–615. doi:10.1007/s11999-008-0670-0.

115. Murray RO. The aetiology of primary osteoarthritis of the hip. *British Journal of Radiology*. 1965;38(455):810–824. doi:10.1259/0007-1285-38-455-810.

116. Doherty M, Courtney P, Doherty S, et al. Nonspherical femoral head shape (pistol grip deformity), neck shaft angle, and risk of hip osteoarthritis: A case-control study. *Arthritis & Rheumatism*. 2008;58(10):3172–3182. doi:10.1002/art.23939.

117. Goodman DA, Feighan JE, Smith AD, Latimer B, Buly RL, Cooperman DR. Subclinical slipped capital femoral epiphysis. Relationship to osteoarthrosis of the hip. *The Journal of Bone and Joint Surgery*. 1997;79(10):1489–1497.

118. Ganz R, Parvizi J, Beck M, Leunig M, Nötzli H, Siebenrock KA. Femoroacetabular impingement: a cause for osteoarthritis of the hip. *Clin Orthop Relat Res*. 2003;(417):112–120. doi:10.1097/01.blo.0000096804.78689.c2.

119. Klaue K, Durnin CW, Ganz R. The acetabular rim syndrome. A clinical presentation of dysplasia of the hip. *J Bone Joint Surg Br*. 1991;73:423–429.

120. Myers SR, Eijer H, Ganz R. Anterior femoroacetabular impingement after periacetabular osteotomy. *Clin Orthop Relat Res*. 1999;(363):93–99.

121. Eijer H, Myers SR, Ganz R. Anterior femoroacetabular impingement after femoral neck fractures. *J Orthop Trauma*. 2001;15(7):475–481.

122. Leunig M, Ganz R. The evolution and concepts of joint-preserving surgery of the hip. *The Bone & Joint Journal*. 2014;96-B(1):5–18. doi:10.1302/0301-620X.96B1.32823.

123. Beck M, Kalhor M, Leunig M, Ganz R. Hip morphology influences the pattern of damage to the acetabular cartilage. *Journal of Bone and Joint Surgery – British Volume*. 2005;87(7):1012–1018. doi:10.1302/0301-620X.87B7.

124. Agricola R, Heijboer MP, Bierma-Zeinstra SMA, Verhaar JAN, Weinans H, Waarsing JH. Cam impingement causes osteoarthritis of the hip: a nationwide prospective cohort study (CHECK). *Ann Rheum Dis*. 2013;72(6):918–923. doi:10.1136/annrheumdis-2012-201643.

125. Agricola R, Waarsing JH, Arden NK, et al. Cam impingement of the hip: a risk factor for hip osteoarthritis. *Nature Publishing Group*. 2013;9(10):630–634. doi:10.1038/nrrheum.2013.114.

126. Agricola R, Heijboer MP, Roze RH, et al. Pincer deformity does not lead to osteoarthritis of the hip whereas acetabular dysplasia does: acetabular coverage and development of osteoarthritis in a nationwide prospective cohort study (CHECK). *Osteoarthritis and Cartilage*. 2013;21(10): 1514–1521. doi:10.1016/j.joca.2013.07.004.

127. Clohisy JC, St John LC, Schutz AL. Surgical Treatment of Femoroacetabular Impingement: A Systematic Review of the Literature. *Clin Orthop Relat Res*. 2009;468(2):555–564. doi:10.1007/s11999-009-1138-6.

128. Ilizaliturri VM, Nossa-Barrera JM, Acosta-Rodriguez E, Camacho-Galindo J. Arthroscopic treatment of femoroacetabular impingement secondary to paediatric hip disorders. *Journal of Bone and Joint Surgery – British Volume*. 2007;89(8):1025–1030. doi:10.1302/0301-620X.89B8.19152.

129. Larson CM, Giveans MR. Arthroscopic Management of Femoroacetabular Impingement: Early Outcomes Measures. *Arthroscopy: The Journal of Arthroscopic & Related Surgery*. 2008;24(5):540–546. doi:10.1016/j.arthro.2007.11.007.

130. Larson CM, Stone RM. Current concepts and trends for operative treatment of FAI: hip arthroscopy. *Curr Rev Musculoskelet Med*. 2013;6(3):242–249. doi:10.1007/s12178-013-9170-2.

131. Beaulé PE, Hynes K, Parker G, Kemp KA. Can the Alpha Angle Assessment of Cam Impingement Predict Acetabular Cartilage Delamination? *Clin Orthop Relat Res*. 2012;470(12):3361–3367. doi:10.1007/s11999-012-2601-3.

132. Beck M, Leunig M, Parvizi J, Boutier V, Wyss D, Ganz R. Anterior femoroacetabular impingement: part II. Midterm results of surgical treatment. *Clin Orthop Relat Res*. 2004;(418):67–73.

133. Clohisy JC, Baca G, Beaulé PE, et al. Descriptive Epidemiology of Femoroacetabular Impingement: A North American Cohort of Patients Undergoing Surgery. *The American Journal of Sports Medicine*. 2013;41(6):1348–1356. doi:10.1177/0363546513488861.

134. Beaulé PE, Grammatopoulos G, Speirs A, et al. Unravelling the Hip Pistol Grip / CAM Deformity: Origins to Joint Degeneration. *J Orthop Res*. September 2018. doi:10.1002/jor.24137.

135. Wilkin GP, Ibrahim MM, Smit KM, Beaulé PE. A Contemporary Definition of Hip Dysplasia and Structural Instability: Toward a Comprehensive Classification for Acetabular Dysplasia. *Journal of Arthroplasty*. 2017;32(9S):S20–S27. doi:10.1016/j.arth.2017.02.067.

136. Morvan J, Bouttier R, Mazieres B, et al. Relationship between hip dysplasia, pain, and osteoarthritis in a cohort of patients with hip symptoms. *J Rheumatol*. 2013;40(9):1583–1589. doi:10.3899/jrheum.121544.

137. Kraeutler MJ, Garabekyan T, Pascual-Garrido C, Mei-Dan O. Hip instability: a review of hip dysplasia and other contributing factors. *Muscles Ligaments Tendons J*. 2016;6(3):343–353. doi:10.11138/mltj/2016.6.3.343.

138. Griffin DR, Dickenson EJ, O'Donnell J, et al. The Warwick Agreement on femoroacetabular impingement syndrome (FAI syndrome): an international consensus statement. *British Journal of Sports Medicine*. 2016;50(19):1169–1176. doi:10.1136/bjsports-2016-096743.

139. Matheney T, Sandell L, Foucher K, Lamontagne M, Grodzinsky AJ, Peters CL. Motion analysis, cartilage mechanics, and biology in femoroacetabular impingement: current understanding and areas of future research. *J Am Acad Orthop Surg*. 2013;21 Suppl 1:S27–S32. doi:10.5435/JAAOS-21-07-S27.

140. Czuppon S, Prather H, Hunt DM, et al. Gender-Dependent Differences in Hip Range of Motion and Impingement Testing in Asymptomatic College Freshman Athletes. *PM R*. November 2016. doi:10.1016/j.pmrj.2016.10.022.

141. Bedi A, Chen N, Robertson W, Kelly BT. The Management of Labral Tears and Femoroacetabular Impingement of the Hip in the Young, Active Patient. *Arthroscopy: The Journal of Arthroscopic & Related Surgery*. 2008;24(10):1135–1145.

142. Bittersohl B, Steppacher S, Haamberg T, et al. Cartilage damage in femoroacetabular impingement (FAI): preliminary results on comparison of standard diagnostic vs delayed gadolinium-enhanced magnetic resonance imaging of cartilage (dGEMRIC). *Osteoarthritis and Cartilage*. 2009;17(10):1297–1306. doi:10.1016/j.joca.2009.04.016.

143. Allen D, Beaulé PE, Ramadan O, Doucette S. Prevalence of associated deformities and hip pain in patients with cam-type femoroacetabular impingement. *Journal of Bone and Joint Surgery – British Volume*. 2009;91(5):589–594. doi:10.1302/0301-620X.91B5.22028.

144. Kim HKW, Kaste S, Dempsey M, Wilkes D. A comparison of non-contrast and contrast-enhanced MRI in the initial stage of Legg-Calvé-Perthes disease. *Pediatr Radiol*. 2013;43(9):1166–1173. doi:10.1007/s00247-013-2664-7.

145. Wagner S, Hofstetter W, Chiquet M, et al. Early osteoarthritic changes of human femoral head cartilage subsequent to femoro-acetabular impingement. *Osteoarthritis and Cartilage*. 2003;11:508–518. doi:10.1016/S1063-4584(03)00075-X.

146. Anderson LA, Peters CL, Park BB, Stoddard GJ, Erickson JA, Crim JR. Acetabular cartilage delamination in femoroacetabular impingement. Risk factors and magnetic resonance imaging diagnosis. *The Journal of Bone and Joint Surgery*. 2009;91(2):305–313. doi:10.2106/JBJS.G.01198.

147. Leunig M, Jüni P, Werlen S, et al. Prevalence of cam and pincer-type deformities on hip MRI in an asymptomatic young Swiss female population: a cross-sectional study. *Osteoarthritis and Cartilage*. 2013;21(4):544–550. doi:10.1016/j.joca.2013.01.003.

148. Gosvig KK, Jacobsen S, Sonne-Holm S, Palm H, Troelsen A. Prevalence of malformations of the hip joint and their relationship to sex, groin pain, and risk of osteoarthritis: a population-based survey. *J Bone Joint Surg Am*. 2010;92(5):1162–1169. doi:10.2106/JBJS.H.01674.

149. Giori NJ, Trousdale RT. Acetabular retroversion is associated with osteoarthritis of the hip. *Clin Orthop Relat Res*. 2003;(417):263–269. doi:10.1097/01.blo.0000093014.90435.64.

150. Nicholls AS, Kiran A, Pollard TCB, et al. The association between hip morphology parameters and nineteen-year risk of end-stage osteoarthritis of the hip: A nested case-control study. *Arthritis & Rheumatism*. 2011;63(11):3392–3400. doi:10.1002/art.30523.

151. Bardakos NV, Villar RN. Predictors of progression of osteoarthritis in femoroacetabular impingement A RADIOLOGICAL STUDY WITH A MINIMUM OF TEN YEARS FOLLOW-UP. *Journal of Bone and Joint Surgery – British Volume*. 2009;91(2):162–169. doi:10.1302/0301-620X.91B2.

152. Sankar WN, Nevitt M, Parvizi J, Felson DT, Agricola R, Leunig M. Femoroacetabular Impingement: Defining the Condition and its Role in the Pathophysiology of Osteoarthritis. *J Am Acad Orthop Surg*. 2013;21(suppl):S7–S15. doi:10.5435/JAAOS-21-07-S7.

153. Sankar WN, Matheney TH, Zaltz I. Femoroacetabular impingement: current concepts and controversies. *Orthop Clin North Am*. 2013;44(4):575–589. doi:10.1016/j.ocl.2013.07.003.

154. Nepple JJ, Riggs CN, Ross JR, Clohisy JC. Clinical Presentation and Disease Characteristics of Femoroacetabular Impingement Are Sex-Dependent. *The Journal of Bone and Joint Surgery*. 2014;96(20):1683–1689. doi:10.2106/JBJS.M.01320.

155. Philippon MJ, Maxwell RB, Johnston TL, Schenker M, Briggs KK. Clinical presentation of femoroacetabular impingement. *Knee Surg Sports Traumatol Arthrosc*. 2007;15(8):1041–1047. doi:10.1007/s00167-007-0348-2.

156. Ayeni OR, Wong I, Chien T, Musahl V, Kelly BT, Bhandari M. Surgical Indications for Arthroscopic Management of Femoroacetabular Impingement. *Arthroscopy: The Journal of Arthroscopic & Related Surgery*. 2012;28(8):1170–1179. doi:10.1016/j.arthro.2012.01.010.

157. Reiman MP, Goode AP, Cook CE, Hölmich P, Thorborg K. Diagnostic accuracy of clinical tests for the diagnosis of hip femoroacetabular impingement/labral tear: a systematic review with meta-analysis. *British Journal of Sports Medicine*. 2015;49(12):811. doi:10.1136/bjsports-2014-094302.

158. Shanmugaraj A, Shell JR, Horner NS, et al. How Useful Is the Flexion–Adduction–Internal Rotation Test for Diagnosing Femoroacetabular Impingement. *Clinical Journal of Sport Medicine*. March 2018:1. doi:10.1097/JSM.0000000000000575.

159. Freke MD, Kemp J, Svege I, Risberg MA, Semciw A, Crossley KM. Physical impairments in symptomatic femoroacetabular impingement: a systematic review of the evidence. *British Journal of Sports Medicine*. 2016;50(19):1180–1180. doi:10.1136/bjsports-2016-096152.

160. Kivlan BR, Martin RL, Sekiya JK. Response to diagnostic injection in patients with femoroacetabular impingement, labral tears, chondral lesions, and extra-articular pathology. *Arthroscopy*. 2011;27(5):619–627. doi:10.1016/j.arthro.2010.12.009.

161. Khan W, Khan M, Alradwan H, Williams R, Simunovic N, Ayeni OR. Utility of Intra-articular Hip Injections for Femoroacetabular Impingement: A Systematic Review. *Orthopaedic Journal of Sports Medicine*. 2015;3(9). doi:10.1177/2325967115601030.

162. Byrd JWT, Jones KS. Diagnostic accuracy of clinical assessment, magnetic resonance imaging, magnetic resonance arthrography, and intra-articular injection in hip arthroscopy patients. *The American Journal of Sports Medicine*. 2004;32(7):1668–1674. doi:10.1177/0363546504266480.

163. Ayeni OR, Farrokhyar F, Crouch S, Chan K, Sprague S, Bhandari M. Pre-operative intra-articular hip injection as a predictor of short-term outcome following arthroscopic management of femoroacetabular impingement. *Knee Surg Sports Traumatol Arthrosc*. 2014;22(4):801–805. doi:10.1007/s00167-014-2883-y.

164. Griffin DR, Dickenson EJ, Wall PDH, et al. Hip arthroscopy versus best conservative care for the treatment of femoroacetabular impingement syndrome (UK FASHIoN): a multicentre randomised controlled trial. *Lancet*. 2018;391(10136):2225–2235. doi:10.1016/S0140-6736(18)31202-9.

165. Kassarjian A, Cerezal L, Llopis E. Femoroacetabular impingement. *Top Magn Reson Imaging*. 2006;17(5):337–345. doi:10.1097/rmr.0b013e3180421caf.

166. Barton C, Salineros MJ, Rakhra KS, Beaulé PE. Validity of the Alpha Angle Measurement on Plain Radiographs in the Evaluation of Cam-type Femoroacetabular Impingement. *Clin Orthop Relat Res*. 2010;469(2):464–469. doi:10.1007/s11999-010-1624-x.

167. Hack K, Di Primio G, Rakhra K, Beaulé PE. Prevalence of cam-type femoroacetabular impingement morphology in asymptomatic volunteers. *The Journal of Bone and Joint Surgery*. 2010;92(14):2436–2444. doi:10.2106/JBJS.J.01280.

168. Khanna V, Caragianis A, DiPrimio G, Rakhra K, Beaulé PE. Incidence of Hip Pain in a Prospective Cohort of Asymptomatic Volunteers: Is the Cam Deformity a Risk Factor for Hip Pain? *The American Journal of Sports Medicine*. 2014;42(4):793–797. doi:10.1177/0363546513518417.

169. Pfirrmann CWA, Mengiardi B, Dora C, Kalberer F, Zanetti M, Hodler J. Cam and Pincer Femoroacetabular Impingement: Characteristic MR Arthrographic Findings in 50 Patients. *Radiology*. 2006;240(3):778–785. doi:10.1148/radiol.2403050767.

170. Rakhra KS, Sheikh AM, Allen D, Beaulé PE. Comparison of MRI Alpha Angle Measurement Planes in Femoroacetabular Impingement. *Clin Orthop Relat Res*. 2008;467(3):660–665. doi:10.1007/s11999-008-0627-3.

171. Kaya M, Suzuki T, Emori M, Yamashita T. Hip morphology in uences the pattern of articular cartilage damage. *Knee Surg Sports Traumatol Arthrosc*. 2016;24(6):2016–2023. doi:10.1007/s00167-014-3297-6.

172. Tannast M, Goricki D, Beck M, Murphy SB, Siebenrock KA. Hip Damage Occurs at the Zone of Femoroacetabular Impingement. *Clin Orthop Relat Res*. 2008;466(2):273–280. doi:10.1007/s11999-007-0061-y.

173. Lohan DG, Seeger LL, Motamedi K, Hame SL, al E. Cam-type femoral-acetabular impingement: is the alpha angle the best MR arthrography has to offer? *Skeletal Radiol*. 2009.

174. Konan S, Rayan F, Haddad FS. Is the frog lateral plain radiograph a reliable predictor of the alpha angle in femoroacetabular impingement? *Journal of Bone and Joint Surgery – British Volume*. 2010;92(1):47. doi:10.1302/0301-620X.92B1.

175. Meyer DC, Beck M, Ellis T, Ganz R, Leunig M. Comparison of Six Radiographic Projections to Assess Femoral Head/Neck Asphericity. *Clin Orthop Relat Res*. 2006;PAP. doi:10.1097/01.blo.0000201168.72388.24.

176. Beaulé PE, Zaragoza EJ, Motamedi K, Copelan N, Dorey FJ. Three-dimensional computed tomography of the hip in the assessment of femoroacetabular impingement. *J Orthop Res*. 2005;23(6):1286–1292. doi:10.1016/j.orthres.2005.03.011.

177. Wall PDH, Brown JS, Parsons N, Buchbinder R, Costa ML, Griffin D. Surgery for treating hip impingement (femoroacetabular impingement) (Review). *Cochrane Database Syst Rev*. 2014;9:CD010796. doi:10.1002/14651858.CD010796.pub2.

178. Fairley J, Wang Y, Teichtahl AJ, et al. Management options for femoroacetabular impingement: a systematic review of symptom and structural outcomes. *Osteoarthritis and Cartilage*. May 2016:1–15. doi:10.1016/j.joca.2016.04.014.

179. Alonso-Coello P, Schünemann HJ, Moberg J, et al. GRADE Evidence to Decision (EtD) frameworks: a systematic and transparent approach to making well informed healthcare choices. 1: Introduction. *BMJ*. 2016;353:i2016. doi:10.1136/bmj.i2016.

180. Wall PDH, Fernandez M, Griffin DR, Foster NE. Nonoperative treatment for femoroacetabular impingement: a systematic review of the literature. *PM R*. 2013;5(5):418–426. doi:10.1016/j.pmrj.2013.02.005.

181. Fernandes L, Hagen KB, Bijlsma JWJ, et al. EULAR recommendations for the non-pharmacological core management of hip and knee osteoarthritis. In:Vol 72. 2013:1125–1135. doi:10.1136/annrheumdis-2012-202745.

182. Khan M, Habib A, de Sa D, et al. Arthroscopy Up to Date: Hip Femoroacetabular Impingement. *Arthroscopy: The Journal of Arthroscopic & Related Surgery*. 2016;32(1):177–189. doi:10.1016/j.arthro.2015.10.010.

183. Wall PDH, Brown JS, Karthikeyan S, Griffin D. An introduction to hip arthroscopy. Part two: indications, outcomes and complications. *Orthopaedics and Trauma*. 2012;26(1):38–43. doi:10.1016/j.mporth.2011.10.004.

184. Harris JD, Erickson BJ, Bush-Joseph CA, Nho SJ. Treatment of femoroacetabular impingement: a systematic review. *Curr Rev Musculoskelet Med*. 2013;6(3):207–218. doi:10.1007/s12178-013-9172-0.

185. de Sa D, Horner NS, MacDonald A, et al. Evaluating healthcare resource utilization and outcomes for surgical hip dislocation and hip arthroscopy for femoroacetabular impingement. *Knee Surg Sports Traumatol Arthrosc*. 2016;24(12):3943–3954. doi:10.1007/s00167-015-3722-5.

186. Ng VY, Arora N, Best TM, Pan X, Ellis TJ. Efficacy of Surgery for Femoroacetabular Impingement: A Systematic Review. *The American Journal of Sports Medicine*. 2010;38(11):2337–2345. doi:10.1177/0363546510365530.

187. Grzybowski JS, Malloy P, Stegemann C, Bush-Joseph C, Harris JD, Nho SJ. Rehabilitation Following Hip Arthroscopy – A Systematic Review. *Front Surg*. 2015;2:21. doi:10.3389/fsurg.2015.00021.

188. Bennell KL, O'Donnell JM, Takla A, et al. Efficacy of a physiotherapy rehabilitation program for individuals undergoing arthroscopic management of femoroacetabular impingement – the FAIR trial: a randomised controlled trial protocol. *BMC Musculoskelet Disord*. 2014;15:58. doi:10.1186/1471-2474-15-58.

189. Spencer-Gardner L, Eischen JJ, Levy BA, Sierra RJ, Engasser WM, Krych AJ. A comprehensive five-phase rehabilitation programme after hip arthroscopy for femoroacetabular impingement. *Knee Surg Sports Traumatol Arthrosc*. 2013;22(4):848–859. doi:10.1007/s00167-013-2664-z.

190. Lahner M, Walter PA, Schulze Pellengahr von C, Hagen M, Engelhardt von LV, Lukas C. Comparative study of the femoroacetabular impingement (FAI) prevalence in male semiprofessional and amateur soccer players. *Arch Orthop Trauma Surg*. 2014;134(8):1135–1141. doi:10.1007/s00402-014-2008-6.

191. Ng KCG, Lamontagne M, Beaulé PE. Differences in anatomical parameters between the affected and unaffected hip in patients with bilateral cam-type deformities. *Clin Biomech (Bristol, Avon)*. 2016;33:13–19. doi:10.1016/j.clinbiomech.2016.01.007.

192. Amstutz HC, Le Duff MJ. The Natural History of Osteoarthritis: What Happens to the Other Hip? *Clin Orthop Relat Res*. May 2016:1–8. doi:10.1007/s11999-016-4888-y.

193. Philippon M, Schenker M, Briggs K, Kuppersmith D. Femoroacetabular impingement in 45 professional athletes: associated pathologies and return to sport following arthroscopic decompression. *Knee Surg Sports Traumatol Arthrosc*. 2007;15(7):908–914. doi:10.1007/s00167-007-0332-x.

194. Philippon MJ, Yen Y-M, Briggs KK, Kuppersmith DA, Maxwell RB. Early outcomes after hip arthroscopy for femoroacetabular impingement in the athletic adolescent patient: a preliminary report. *J Pediatr Orthop*. 2008;28(7):705–710. doi:10.1097/BPO.0b013e318186eb2e.

195. Philippon MJ, Briggs KK, Yen Y-M, Kuppersmith DA. Outcomes following hip arthroscopy for femoroacetabular impingement with associated chondrolabral dysfunction: minimum two-year follow-up. *Journal of Bone and Joint Surgery – British Volume*. 2009;91(1):16–23. doi:10.1302/0301-620X.91B1.21329.

196. Palmer DH, Ganesh V, Comfort T, Tatman P. Midterm outcomes in patients with cam femoroacetabular impingement treated arthroscopically. *Arthroscopy*. 2012;28(11):1671–1681. doi:10.1016/j.arthro.2012.04.154.

197. Meftah M, Rodriguez JA, Panagopoulos G, Alexiades MM. Long-term Results of Arthroscopic Labral Debridement: Predictors of Outcomes. *Orthopedics*. October 2011. doi:10.3928/01477447-20110826-04.

198. Steppacher SD, Anwander H, Zurmühle CA, Tannast M, Siebenrock KA. Eighty Percent of Patients With Surgical Hip Dislocation for Femoroacetabular Impingement Have a Good Clinical Result Without Osteoarthritis Progression at 10 Years. *Clin Orthop Relat Res*. 2014;473(4):1333–1341. doi:10.1007/s11999-014-4025-8.

199. Thomas GER, Palmer AJR, Batra RN, et al. Subclinical deformities of the hip are significant predictors of radiographic osteoarthritis and joint replacement in women. A 20 year longitudinal cohort study. *Osteoarthritis and cartilage / OARS, Osteoarthritis Research Society*. 2014;22(10):1504–1510. doi:10.1016/j.joca.2014.06.038.

200. Hosnijeh FS, Zuiderwijk ME, Versteeg M, et al. Cam deformity and acetabular dysplasia as risk factors for hip osteoarthritis. *Arthritis & Rheumatology*. September 2016. doi:10.1002/art.39929.

201. Hawker GA, Stanaitis I. Osteoarthritis Year in Review 2014: clinical. *Osteoarthritis and Cartilage*. 2014;22(12):1953–1957. doi:10.1016/j.joca.2014.06.018.

202. Wang Y, Teichtahl AJ, Cicuttini FM. Osteoarthritis year in review 2015: imaging. *Osteoarthritis and Cartilage*. 2016;24(1):49–57. doi:10.1016/j.joca.2015.07.027.

203. Turkiewicz A, Petersson IF, Björk J, et al. Current and future impact of osteoarthritis on health care: a population-based study with projections to year 2032. *Osteoarthritis and Cartilage*. 2014;22(11):1826–1832. doi:10.1016/j.joca.2014.07.015.

204. Hunter DJ, Arden N, Conaghan PG, et al. nition of osteoarthritis on MRI: results of a Delphi exercise. *Osteoarthritis and Cartilage*. 2011;19(8):963–969. doi:10.1016/j.joca.2011.04.017.

205. Kellgren JH, Jeffrey MR, Ball J. *The Epidemiology of Chronic Rheumatism: a Symposium*. 1963.

206. Hoaglund FT, Steinbach LS. Primary osteoarthritis of the hip: etiology and epidemiology. *Journal of the American Academy of Orthopaedic Surgeons*. 2001;9(5):320–327.

207. Nho SJ, Kymes SM, Callaghan JJ, Felson DT. The burden of hip osteoarthritis in the United States: epidemiologic and economic considerations. *J Am Acad Orthop Surg*. 2013;21 Suppl 1:S1–S6. doi:10.5435/JAAOS-21-07-S1.

208. Kahlenberg CA, Han B, Patel RM, Deshmane PP, Terry MA. Time and Cost of Diagnosis for Symptomatic Femoroacetabular Impingement. *Orthopaedic Journal of Sports Medicine*. 2014;2(3):2325967114523916. doi:10.1177/2325967114523916.

209. Samim M, Eftekhary N, Vigdorchik JM, et al. 3D-MRI versus 3D-CT in the evaluation of osseous anatomyin femoroacetabular impingement using Dixon 3D FLASH sequence. September 2018:1–8. doi:10.1007/s00256-018-3049-7.

210. Hanke MS, Steppacher SD, Anwander H, Werlen S, Siebenrock KA, Tannast M. What MRI Findings Predict Failure 10 Years After Surgery for Femoroacetabular Impingement? *Clin Orthop Relat Res*. August 2016:1–16. doi:10.1007/s11999-016-5040-8.

211. Lamontagne M, Ng K, Mantovani G, Catelli DS. Biomechanics of femoroacetabular impingement. *Sports Injuries*. 2015. doi:10.1007/978-3-642-36801-1_289-1.

212. Lamontagne M, Kennedy MJ, Beaulé PE. The effect of cam FAI on hip and pelvic motion during maximum squat. *Clin Orthop Relat Res*. 2009;467(3):645–650. doi:10.1007/s11999-008-0620-x.

213. Ranawat AS, Schulz B, Baumbach SF, Meftah M, Ganz R, Leunig M. Radiographic Predictors of Hip Pain in Femoroacetabular Impingement. *HSS Jrnl*. 2011;7(2):115–119. doi:10.1007/s11420-010-9192-x.

214. Mascarenhas VV, rego P, Dantas P, et al. Imaging prevalence of femoroacetabular impingement in symptomatic patients, athletes, and asymptomatic individuals: A systematic review. *European Journal of Radiology*. 2016;85(1):73–95. doi:10.1016/j.ejrad.2015.10.016.

215. Clohisy JC, Carlisle JC, Trousdale R, et al. Radiographic Evaluation of the Hip has Limited Reliability. *Clin Orthop Relat Res*. 2008;467(3):666–675. doi:10.1007/s11999-008-0626-4.

216. Jamali AA, Mak W, Wang P, Tai L, Meehan JP, Lamba R. What Is Normal Femoral Head/Neck Anatomy? An Analysis of Radial CT Reconstructions in Adolescents. *Clin Orthop Relat Res*. 2013;471(11):3581–3587. doi:10.1007/s11999-013-3166-5.

217. Monazzam S, Bomar JD, Agashe M, Hosalkar HS. Does Femoral Rotation Influence Anteroposterior Alpha Angle, Lateral Center-edge Angle, and Medial Proximal Femoral Angle? A Pilot Study. *Clin Orthop Relat Res*. 2012;471(5):1639–1645. doi:10.1007/s11999-012-2708-6.

218. Nepple JJ, Brophy RH, Matava MJ, Wright RW, Clohisy JC. Radiographic findings of femoroacetabular impingement in National Football League Combine athletes undergoing radiographs for previous hip or groin pain. *Arthroscopy*. 2012;28(10):1396–1403. doi:10.1016/j.arthro.2012.03.005.

219. Siebenrock KA, Schoeniger R, Ganz R. Anterior femoro-acetabular impingement due to acetabular retroversion. Treatment with periacetabular osteotomy. *J Bone Joint Surg Am*. 2003;85-A(2):278–286.

220. Zaltz I, Kelly BT, Hetsroni I, Bedi A. The Crossover Sign Overestimates Acetabular Retroversion. *Clin Orthop Relat Res*. 2012;471(8):2463–2470. doi:10.1007/s11999-012-2689-5.

221. Wassilew GI, Heller MO, Diederichs G, Janz V, Wenzl M, Perka C. Standardized AP radiographs do not provide reliable diagnostic measures for the assessment of acetabular retroversion. *J Orthop Res*. 2012;30(9):1369–1376. doi:10.1016/j.gaitpost.2010.05.005.

222. Ayeni OR, Chan K, Whelan DB, et al. Diagnosing Femoroacetabular Impingement From Plain Radiographs: Do Radiologists and Orthopaedic Surgeons Differ? *Orthopaedic Journal of Sports Medicine*. 2014;2(7):2325967114541414. doi:10.1177/2325967114541414.

223. Audenaert EA, Baelde N, Huysse W, Vigneron L, Pattyn C. Development of a three-dimensional detection method of cam deformities in femoroacetabular impingement. *Skeletal Radiol*. 2011;40(7):921–927. doi:10.1007/s00256-010-1021-2.

224. Harris MD, Datar M, Whitaker RT, Jurrus ER, Peters CL, Anderson AE. Statistical shape modeling of cam femoroacetabular impingement. *J Orthop Res*. 2013;31(10):1620–1626. doi:10.1002/jor.22389.

225. Masjedi M, Mandalia R, Aqil A, Cobb J. Validation of the "FeMorph" software in planning cam osteochondroplasty by incorporating labral morphology. *Computer Methods in Biomechanics and Biomedical Engineering*. December 2014:1–7. doi:10.1080/10255842.2014.986654.

226. Zhang L, Wells J, Dessouky R, et al. 3d CT segmentation of CAM type femoroacetabular impingement – Reliability and Relationship of CAM lesion with Anthropomorphic Features. *Br J Radiol*. August 2018:20180371. doi:10.1259/bjr.20180371.

227. Heyworth BE, Dolan MM, Nguyen JT, Chen NC, Kelly BT. Preoperative Three-dimensional CT Predicts Intraoperative Findings in Hip Arthroscopy. *Clin Orthop Relat Res*. 2012;470(7):1950–1957. doi:10.1007/s11999-012-2331-6.

228. Kang RW, Yanke AB, Orias AE, Inoue N, Nho SJ. Emerging Ideas: Novel 3-D Quantification and Classification of Cam Lesions in Patients With Femoroacetabular Impingement. *Clin Orthop Relat Res*. 2012;471(2):358–362. doi:10.1007/s11999-012-2693-9.

229. Kuhn AW, Ross JR, Bedi A. Three-dimensional Imaging and Computer Navigation in Planning for Hip Preservation Surgery. *Sports Med Arthrosc*. 2015;23(4):e31–e38. doi:10.1097/JSA.0000000000000094.

230. Xia Y, Fripp J, Chandra SS, Walker D, Crozier S, Engstrom C. Automated 3D quantitative assessment and measurement of alpha angles from the femoral head-neck junction using MR imaging. *Physics in Medicine & Biology*. September 2015:7601–7616. doi:10.1088/0031-9155/60/19/7601.

231. Xia Y, Fripp J, Chandra SS, Schwarz R, Engstrom C, Crozier S. Automated bone segmentation from large field of view 3D MR images of the hip joint. *Physics in Medicine & Biology*. 2013;58(20):7375–7390. doi:10.1088/0031-9155/58/20/7375.

232. Cadet ER, Babatunde OM, Gorroochurn P, et al. Inter- and intra-observer agreement of femoroacetabular impingement (FAI) parameters comparing plain radiographs and advanced, 3D computed tomographic (CT)-generated hip models in a surgical patient cohort. *Knee Surg Sports Traumatol Arthrosc*. 2014;24(7):2324–2331. doi:10.1007/s00167-014-3315-8.

233. Khan O, Witt J. Evaluation of the magnitude and location of Cam deformity using three dimensional CT analysis. *The Bone & Joint Journal*. 2014;96-B(9):1167–1171. doi:10.1302/0301-620X.96B9.33555.

234. Milone MT, Bedi A, Poultsides L, et al. Novel CT-based Three-dimensional Software Improves the Characterization of Cam Morphology. *Clin Orthop Relat Res*. 2013;471(8):2484–2491. doi:10.1007/s11999-013-2809-x.

235. Masjedi M, Nightingale CL, Azimi DY, Cobb JP. The three-dimensional relationship between acetabular rim morphology and the severity of femoral cam lesions. *The Bone & Joint Journal*. 2013;95-B(3):314–319. doi:10.1302/0301-620X.95B3.30901.

236. Dudda M, Albers C, Mamisch TC, Werlen S, Beck M. Do Normal Radiographs Exclude Asphericity of the Femoral Head-Neck Junction? *Clin Orthop Relat Res*. 2008;467(3):651–659. doi:10.1007/s11999-008-0617-5.

237. Steppacher SD, Tannast M, Werlen S, Siebenrock KA. Femoral Morphology Differs Between Deficient and Excessive Acetabular Coverage. *Clin Orthop Relat Res*. 2008;466(4):782–790. doi:10.1007/s11999-008-0141-7.

238. Dickenson E, Wall PDH, Robinson B, et al. Prevalence of cam hip shape morphology: a systematic review. *Osteoarthritis and Cartilage*. January 2016:1–13. doi:10.1016/j.joca.2015.12.020.

239. Mariconda M, Cozzolino A, Di Pietto F, Ribas M, Bellotti V, Soldati A. Radiographic findings of femoroacetabular impingement in capoeira players. *Knee Surg Sports Traumatol Arthrosc*. 2014;22(4):874–881. doi:10.1007/s00167-014-2850-7.

240. Omoumi P, Thiéry C, Michoux N, Malghem J, Lecouvet FE, Vande Berg BC. Anatomic Features Associated With Femoroacetabular Impingement Are Equally Common in Hips of Old and Young Asymptomatic Individuals Without CT Signs of Osteoarthritis. *AJR Am J Roentgenol*. 2014;202(5):1078–1086. doi:10.2214/AJR.12.10083.

241. Bennett PH, Wood P. *Population Studies of the Rheumatic Diseases*. Amsterdam: Excerpta Medica Foundation; 1968.

242. Cvetanovich GL, Harris JD, Erickson BJ, Bach BR Jr., Bush-Joseph CA, Nho SJ. Revision Hip Arthroscopy: A Systematic Review of Diagnoses, Operative Findings, and Outcomes. *Arthroscopy*. 2015;31(7):1382–1390. doi:10.1016/j.arthro.2014.12.027.

243. Ricciardi BF, Fields K, Kelly BT, Ranawat AS, Coleman SH, Sink EL. Causes and Risk Factors for Revision Hip Preservation Surgery. *The American Journal of Sports Medicine*. 2014;42(11):2627–2633. doi:10.1177/0363546514545855.

244. Pollard TCB, Villar RN, Norton MR, et al. Femoroacetabular impingement and classification of the cam deformity: the reference interval in normal hips. *Acta Orthop*. 2010;81(1):134–141. doi:10.3109/17453671003619011.

245. Lepage-Saucier M, Thiéry C, Larbi A, Lecouvet FE, Vande Berg BC, Omoumi P. Femoroacetabular impingement: normal values of the quantitative morphometric parameters in asymptomatic hips. *Eur Radiol*. 2014;24(7):1707–1714. doi:10.1007/s00330-014-3171-4.

246. Scheidt RB, Galia CR, Diesel CV, Rosito R, Macedo CA de S. Prevalence of radiographic markers of femoroacetabular impingement in asymptomatic adults. *Rev Col Bras Cir*. 2014;41(1):36–42.

247. Van Houcke J, Yau WP, Yan CH, et al. Prevalence of radiographic parameters predisposing to femoroacetabular impingement in young asymptomatic chinese and white subjects. *J Bone Joint Surg Am*. 2015;97(4):310–317. doi:10.2106/JBJS.M.01538.

248. Laborie LB, Lehmann TG, Engesæter IØ, Engesæter LB, Rosendahl K. Is a Positive Femoroacetabular Impingement Test a Common Finding in Healthy Young Adults? *Clin Orthop Relat Res*. 2013;471(7):2267–2277. doi:10.1007/s11999-013-2850-9.

249. Osteoporotic Fractures in Men (MrOS) Research Group, Nardo L, Parimi N, et al. Femoroacetabular Impingement: Prevalent and Often Asymptomatic in Older Men: The Osteoporotic Fractures in Men Study. *Clin Orthop Relat Res*. March 2015. doi:10.1007/s11999-015-4222-0.

250. Reichenbach S, Leunig M, Werlen S, et al. Association between cam-type deformities and magnetic resonance imaging-detected structural hip damage: A cross-sectional study in young men. *Arthritis & Rheumatism*. 2011;63(12):4023–4030. doi:10.1002/art.30589.

251. Reichenbach S, Jüni P, Werlen S, et al. Prevalence of cam-type deformity on hip magnetic resonance imaging in young males: A cross-sectional study. *Arthritis Care Res*. 2010;62(9):1319–1327. doi:10.1002/acr.20198.

252. Laborie LB, Lehmann TG, Engesaeter IO, Eastwood DM, Engesaeter LB, Rosendahl K. Prevalence of Radiographic Findings Thought to Be Associated with Femoroacetabular Impingement in a Population-based Cohort of 2081 Healthy Young Adults. *Radiology*. 2011;260(2):494–502. doi:10.1148/radiol.11102354.

253. de Bruin F, Reijnierse M, Farhang-Razi V, Bloem JL. Radiographic signs associated with femoroacetabular impingement occur with high prevalence at all ages in a hospital population. *Eur Radiol*. 2013;23(11):3131–3139. doi:10.1007/s00330-013-2912-0.

254. Shi YY, Liu TJ, Zhao Q, Zhang LJ, Ji SJ, Wang EB. The normal centre-edge angle of Wiberg in the Chinese population: a population-based cross-sectional study. *Journal of Bone and Joint Surgery – British Volume*. 2010;92(8):1144–1147. doi:10.1302/0301-620X.92B8.23993.

255. Fowkes LA, Petridou E, Zagorski C, Karuppiah A, Toms AP. Defining a reference range of acetabular inclination and center-edge angle of the hip in asymptomatic individuals. *Skeletal Radiol*. 2011;40(11):1427–1434. doi:10.1007/s00256-011-1109-3.

256. Gosvig KK, Jacobsen S, Sonne-Holm S, Gebuhr P. The Prevalence of Cam-Type Deformity of the Hip Joint: A Survey of 4151 Subjects of the Copenhagen Osteoarthritis Study. *Acta Radiol*. 2008;49(4):436–441. doi:10.1080/02841850801935567.

257. Hetsroni I, Torre Dela K, Duke G, Lyman S, Kelly BT. Sex differences of hip morphology in young adults with hip pain and labral tears. *Arthroscopy*. 2013;29(1):54–63. doi:10.1016/j.arthro.2012.07.008.

258. Yanke AB, Khair MM, Stanley R, et al. Sex Differences in Patients With CAM Deformities With Femoroacetabular Impingement: 3-Dimensional Computed Tomographic Quantification. *Arthroscopy*. July 2015. doi:10.1016/j.arthro.2015.06.007.

259. Tannenbaum EP, Zhang P, Maratt JD, et al. A Computed Tomography Study of Gender Differences in Acetabular Version and Morphology: Implications for Femoroacetabular Impingement. *Arthroscopy: The Journal of Arthroscopic & Related Surgery*. 2015;31(7):1247–1254. doi:10.1016/j.arthro.2015.02.007.

260. Hildebrand F, Shin H-O, Flötotto L, Krettek C, Gerich T. [The prevalence of reduced acetabular anteversion in asymptomatic patients: a retrospective analysis]. *Z Orthop Unfall*. 2012;150(6):601–606. doi:10.1055/s-0032-1327795.

261. Atkinson HD, Johal KS, Willis-Owen C, Zadow S, Oakeshott RD. Differences in hip morphology between the sexes in patients undergoing hip resurfacing. *J Orthop Surg Res*. 2010;5:76. doi:10.1186/1749-799X-5-76.

262. Vo A, Beaulé PE, Sampaio ML, Rotaru C, Rakhra KS. The femoral head-neck contour varies as a function of physeal development. *Bone and Joint Research*. 2015;4(2):17–22. doi:10.1302/2046-3758.42.2000356.

263. Nakahara I, Takao M, Sakai T, Nishii T, Yoshikawa H, Sugano N. Gender differences in 3D morphology and bony impingement of human hips. *J Orthop Res*. 2010;29(3):333–339. doi:10.1002/jor.21265.

264. Lindner D, Bitar El YF, Jackson TJ, Sadik AY, Stake CE, Domb BG. Sex-Based Differences in the Clinical Presentation of Patients With Symptomatic Hip Labral Tears. *The American Journal of Sports Medicine*. 2014;42(6):1365–1369. doi:10.1177/0363546514532226.

265. Joseph R, Pan X, Cenkus K, Brown L, Ellis T, Di Stasi S. Sex Differences in Self-Reported Hip Function Up to 2 Years After Arthroscopic Surgery for Femoroacetabular Impingement. *The American Journal of Sports Medicine*. 2016;44(1):54–59. doi:10.1177/0363546515610535.

266. Frank RM, Lee S, Bush-Joseph CA, Salata MJ, Mather RC, Nho SJ. Outcomes for Hip Arthroscopy According to Sex and Age: A Comparative Matched-Group Analysis. *The Journal of Bone and Joint Surgery*. 2016;98(10):797–804. doi:10.2106/JBJS.15.00445.

267. Malviya A, Raza A, Jameson S, James P, Reed MR, Partington PF. Complications and Survival Analyses of Hip Arthroscopies Performed in the National Health Service in England: A Review of 6,395 Cases. *Arthroscopy*. February 2015. doi:10.1016/j.arthro.2014.12.013.

268. Peterson JB, Doan J, Bomar JD, Wenger DR, Pennock AT, Upasani VV. Sex Differences in Cartilage Topography and Orientation of the Developing Acetabulum: Implications for Hip Preservation Surgery. *Clin Orthop Relat Res*. December 2014. doi:10.1007/s11999-014-4109-5.

269. Stem ES, O'Connor MI, Kransdorf MJ, Crook J. Computed tomography analysis of acetabular anteversion and abduction. *Skeletal Radiol*. 2006;35(6):385–389. doi:10.1007/s00256-006-0086-4.

270. Cawley DT, Guerin SJ, Walsh J, Simpkin A, Masterson EL. The significance of hand dominance in hip osteoarthritis. *Seminars in Arthritis and Rheumatism*. 2015;44(5):527–530. doi:10.1016/j.semarthrit.2014.11.001.

271. Laborie LB, Lehmann TG, Engesaeter IO, Sera F, Engesaeter LB, Rosendahl K. The alpha angle in cam-type femoroacetabular impingement: new reference intervals based on 2038 healthy young adults. *The Bone & Joint Journal*. 2014;96-B(4):449–454. doi:10.1302/0301-620X.96B4.32194.

272. Rego PRA, Mascarenhas V, Oliveira FS, et al. Morphologic and angular planning for cam resection in femoro-acetabular impingement: value of the omega angle. *International Orthopaedics (SICOT)*. 2016;40(10):2011–2017. doi:10.1007/s00264-015-3053-7.

273. Wassilew GI, Heller MO, Janz V, Perka C, Müller M, Renner L. High prevalence of acetabular retroversion in asymptomatic adults: a 3D CT-based study. *The Bone & Joint Journal*. 2017;99-B(12):1584–1589. doi:10.1302/0301-620X.99B12.37081.

274. Hashemi SA, Dehghani J, Vosoughi AR. Can the crossover sign be a reliable marker of global retroversion of the acetabulum? *Skeletal Radiol*. October 2016:1–5. doi:10.1007/s00256-016-2497-1.

275. Nepple JJ. Coxa Profunda Is Not a Useful Radiographic Parameter for Diagnosing Pincer-Type Femoroacetabular Impingement. *The Journal of Bone and Joint Surgery (American)*. 2013;95(5):417. doi:10.2106/JBJS.K.01664.

276. Larson CM, Moreau-Gaudry A, Kelly BT, et al. Are Normal Hips Being Labeled as Pathologic? A CT-based Method for Defining Normal Acetabular Coverage. *Clin Orthop Relat Res*. 2014;473(4):1247–1254. doi:10.1007/s11999-014-4055-2.

277. Gebhart JJ, Weinberg DS, Bohl MS, Liu RW. Relationship between pelvic incidence and osteoarthritis of the hip. *Bone and Joint Research*. 2016;5(2):66–72. doi:10.1302/2046-3758.52.2000552.

278. Canham CD, Yen YM, Giordano BD. Does Femoroacetabular Impingement Cause Hip Instability? A Systematic Review. *YJARS*. September 2015:1–7. doi:10.1016/j.arthro.2015.07.021.

279. Nelson AE, Stiller JL, Shi XA, et al. Measures of hip morphology are related to development of worsening radiographic hip osteoarthritis over 6 to 13 year follow-up: the Johnston County Osteoarthritis Project. *Osteoarthritis and Cartilage*. November 2015:1–8. doi:10.1016/j.joca.2015.10.007.

280. Levy DM, Hellman MD, Haughom B, Stover MD, Nho SJ. Techniques and Results for Open Hip Preservation. *Front Surg*. 2015;2(6):112. doi:10.1007/s11999-008-0687-4.

281. Yeung M, Khan M, Schreiber VM, et al. Global Discrepancies in the Diagnosis, Surgical Management, and Investigation of Femoroacetabular Impingement. *Arthroscopy: The Journal of Arthroscopic & Related Surgery*. August 2014. doi:10.1016/j.arthro.2014.06.008.

282. Boraiah S, Dyke JP, Hettrich C, et al. Assessment of vascularity of the femoral head using gadolinium (Gd-DTPA)-enhanced magnetic resonance imaging: a cadaver study. *Journal of Bone and Joint Surgery – British Volume*. 2009;91(1):131–137. doi:10.1302/0301-620X.91B1.21275.

283. Dy CJ, Thompson MT, Usrey MM, Noble PC. The distribution of vascular foramina at the femoral head/neck junction: implications for resurfacing arthroplasty. *Journal of Arthroplasty*. 2012;27(9):1669–1675. doi:10.1016/j.arth.2012.02.029.

284. Lavigne M, Kalhor M, Beck M, Ganz R, Leunig M. Distribution of Vascular Foramina Around the Femoral Head and Neck Junction: Relevance for Conservative Intracapsular Procedures of the Hip. *Orthopedic Clinics of North America*. 2005;36(2):171–176. doi:10.1016/j.ocl.2005.02.002.

285. Leunig M, Ganz R. Relative neck lengthening and intracapital osteotomy for severe Perthes and Perthes-like deformities. *Bull NYU Hosp Jt Dis*. 2011;69 Suppl 1:S62–S67.

286. Obuchowski NA, Subhas N, Polster J. Statistics for Radiology Research. *Semin Musculoskelet Radiol*. 2017;21(1):23–31. doi:10.1055/s-0036-1597252.

287. Botser IB, Smith TW, Nasser R, Domb BG. Open Surgical Dislocation Versus Arthroscopy for Femoroacetabular Impingement: A Comparison of Clinical Outcomes. *YJARS*. 2011;27(2):270–278. doi:10.1016/j.arthro.2010.11.008.

288. Zingg PO, Ulbrich EJ, Buehler TC, Kalberer F, Poutawera VR, Dora C. Surgical hip dislocation versus hip arthroscopy for femoroacetabular impingement: clinical and morphological short-term results. *Arch Orthop Trauma Surg*. 2012;133(1):69–79. doi:10.1007/s00402-012-1616-2.

289. Büchler L, Neumann M, Schwab JM, Iselin L, Tannast M, Beck M. Arthroscopic Versus Open Cam Resection in the Treatment of Femoroacetabular Impingement. *YJARS*. 2013;29(4):653–660. doi:10.1016/j.arthro.2012.12.009.

290. Bogunovic L, Gottlieb M, Pashos G, Baca G, Clohisy JC. Why Do Hip Arthroscopy Procedures Fail? *Clin Orthop Relat Res*. 2013;471(8):2523–2529. doi:10.1007/s11999-013-3015-6.

291. Ross JR, Larson CM, Adeoyo O, Kelly BT, Bedi A. Residual Deformity Is the Most Common Reason for Revision Hip Arthroscopy: A Three-dimensional CT Study. *Clin Orthop Relat Res*. 2014;473(4):1388–1395. doi:10.1007/s11999-014-4069-9.

292. Mardones R, Lara J, Donndorff A, et al. Surgical Correction of "Cam-Type" Femoroacetabular Impingement: A Cadaveric Comparison of Open Versus Arthroscopic Debridement. *YJARS*. 2009;25(2):175–182. doi:10.1016/j.arthro.2008.09.011.

293. Haefeli PC, Albers CE, Steppacher SD, Tannast M, Büchler L. What Are the Risk Factors for Revision Surgery After Hip Arthroscopy for Femoroacetabular Impingement at 7-year Followup? *Clin Orthop Relat Res*. October 2016:1–9. doi:10.1007/s11999-016-5115-6.

294. Khan M, Ayeni OR, Madden K, et al. Femoroacetabular Impingement: Have We Hit a Global Tipping Point in Diagnosis and Treatment? Results From the InterNational Femoroacetabular Impingement Optimal Care Update Survey (IN FOCUS). *Arthroscopy: The Journal of Arthroscopic & Related Surgery*. January 2016. doi:10.1016/j.arthro.2015.10.011.

295. Ayeni OR, Chan K, Al-Asiri J, et al. Sources and quality of literature addressing femoroacetabular impingement. *Knee Surg Sports Traumatol Arthrosc*. 2012;21(2):415–419. doi:10.1007/s00167-012-2236-7.

296. Khan M, Bedi A, Fu F, Karlsson J, Ayeni OR, Bhandari M. New perspectives on femoroacetabular impingement syndrome. *Nature Publishing Group*. March 2016:1–8. doi:10.1038/nrrheum.2016.17.

297. Hellman MD, Haughom BD, Brown NM, Fillingham YA, Philippon MJ, Nho SJ. Femoroacetabular Impingement and Pelvic Incidence: Radiographic Comparison to an Asymptomatic Control. *Arthroscopy*. 2017;33(3):545–550. doi:10.1016/j.arthro.2016.08.033.

298. Palmer AJR, Ayyar-Gupta V, Dutton SJ, et al. Protocol for the Femoroacetabular Impingement Trial (FAIT): a multi-centre randomised controlled trial comparing surgical and non-surgical management of femoroacetabular impingement. *Bone and Joint Research*. 2014;3(11):321–327. doi:10.1302/2046-3758.311.2000336.

299. Simunovic N, Heels-Ansdell D, Thabane L, Ayeni OR. Femoroacetabular ImpingementRandomised controlled Trial (FIRST) – a multi-centre randomized controlled trial comparing arthroscopic lavage and arthroscopic osteochondroplasty on patient important outcomes and quality of life inthe treatment of young adult (18–50 years) femoroacetabular impingement: a statistical analysis plan. October 2018:1–11. doi:10.1186/s13063-018-2965-0.